Mukhtar Ahmed *Editor*

Systems Modeling

Springer

Systems Modeling

Mukhtar Ahmed
Editor

Systems Modeling

Springer

Editor
Mukhtar Ahmed
Department of Agricultural Research for
Northern Sweden
Swedish University of
Agricultural Sciences
Umeå, Sweden

Department of Agronomy
Pir Mehr Ali Shah Arid Agriculture University
Rawalpindi, Pakistan

ISBN 978-981-15-4727-0 ISBN 978-981-15-4728-7 (eBook)
https://doi.org/10.1007/978-981-15-4728-7

This Springer imprint is published by the registered company Springer Nature Singapore Pte Ltd.
The registered company address is: 152 Beach Road, #21-01/04 Gateway East, Singapore 189721, Singapore

Preface

Artificial intelligence (AI) or machine intelligence is helping mankind to solve different problems at a faster pace. Similarly, qualitative and quantitative knowledge is increasing at a rapid pace with the invention of modern tools. These tools help to generate big data sets that can be used by different decision support tools. Knowledge is meagre and unsatisfactory if it is not in the numerical form. Thus, artificial intelligence is playing a role to generate big data sets in numerical form. Sustainable agricultural production requires new methods and techniques under challenges like climate change, market globalization, and increased population. Field-based approaches (e.g., agronomic diagnosis and prototyping) have been used successfully, but these approaches are too slow to provide timely responses to such rapid contextual changes. Similarly, a large number of systems could not be easily explored by using such techniques. Current social, political, and environmental concerns could be easily tackled by the use of in silico approaches. These approaches can help study a broader range of possible systems through modeling and simulation, and can offer the possibility of identifying more quickly new sustainable systems. The goals of agroecosystems models can be sorted into the following groups: (i) models as representative of knowledge, concepts, and methods for scientists, (ii) models as communication tools, (iii) models as tools to manage or run systems (iv), models as tools to assist debates, and (v) models to design crop management systems. Models have been used as an excellent tool to develop new cropping systems. Steps to design new cropping systems include (i) defining goals and constraints of new cropping systems, (ii) designing of new compatible systems with the set of constraints, (iii) evaluation of new systems, and (iv) testing and transfer of new innovative systems to the practitioners. Simulation models can be instrumental in determining recommendations for various agro-technology packages. Crop models help us to understand complex and nonlinear crop responses to management at different spatio-temporal scales (e.g., different soil and climate). Similarly, innumerable interactions among weather, soil, crop, and management factors throughout the growing season could be easily explored through modeling. Models can predict crop productivity under various climate change scenarios that are even not possible through field experimentation. Simulated outputs can be delivered to the policymakers at local, national, regional, and global levels to help implement appropriate measures. Computer applications in the field of agriculture can help to understand the interactions between the system and its variables. Models, which are mainly mathematical representations of the biological system, can generate answers to the problems. Most people think that models are complicated and complex thus need time to be implemented on the ground scale. However, no special mathematics are necessary for big or complex models. They come from small bits and pieces. There is a prosperous future for systems modeling, and it can open new frontiers, and it helps in the agroecological transitions of agriculture. Similarly, it's essential to understand belowground processes, roots, soil, and their complex abiotic and biotic interactions. We need to consider plants or crops as holobionts (individual host and its microbial community). Such consideration can account for their extended phenotypes and (phyllosphere and rhizosphere) microbiomes. Simulation is a good substitute for experiments, and it has been shown by different researchers and technologists that models work with a higher degree of accuracy. Thus, we should include simulation at all levels of system understandings. The system can be soil, plant, and atmosphere. This book with title "System Modeling" is useful for undergraduate and post-graduate students from different disciplines of Data Science, Agronomy, Crop Physiology, Plant Breeding, Plant Pathology, Entomology, Soil Science, Remote Sensing, Agricultural Meteorology, and Environmental Science. It can be used by policymakers and administrators to direct teaching, research, and extension activities.

Chapter 1 presents a fundamental description of Systems Modeling in which the focus is agricultural systems that have complex interactions with their surrounding environments and soil, and in which a better understanding is possible through computer applications. Solar radiation, temperature, photoperiod, humidity, ozone, and wind are some of the important environmental variables which interact with the agricultural system that are discussed in this chapter. These variables are important considerations for the development of understanding of the agricultural system on a scientific basis. Similarly, the application of different models at different scales is presented, which could help one to understand the mechanisms in qualitative and quantitative ways. Finally, the concept of digital agriculture and its linkage with modeling is elaborated. In general, the chapter discusses in detail the type, methods of measurement along with mathematical representation, terminologies and their impacts on the various processes of plants. Chapter 2 summarizes crop phenotyping and elaborates on different techniques/approaches used in the process of phenotyping. Corresponding to genotypic, the phenotypic form of the plant is more important for high yield. The selection of germplasm based on phenotype has been of great interest of breeders and farmers. Considering the importance of phenotyping, Tuberosa (2012) referred to phenotyping as "king" and heritability as "queen." Chapter 3 discusses the role of statistics and modeling for the analysis of experimental data. Also discussed is the data that should be collected to address our research questions and what should be our experimental design. All these aspects are discussed in this chapter with the description about Completely Randomized Design (CRD), Randomized Complete Block Design (RCBD), Latin Square Design, Nested and Split Plot Design, Strip-Plot/Split-Block Design, Split-Split plot Design, factorial experiments, fractional factorial design, multivariate analysis of variance (MANOVA), Analysis of Covariance (ANCOVA), Principal component analysis, regression, correlation, and different analytical tools/softwares. Chapter 4 focuses on different dynamic modeling approaches and description of different dynamic models in practical use. Similarly, a general description of modeling with a history of dynamic modeling from the eighteenth century until today is presented. Calibration of crop model as standard practice and the estimation of crop parameters based upon observed field data are discussed in Chap. 5.

Calibration is the process of the estimation of unknown parameters using practical observations. It is generally carried out manually by adjusting the settings of the model. It consists of choosing the accurate coefficients that play a significant role in the adjustment of soil nitrogen, soil organic carbon, soil phosphorus, crop growth, phenological development, biomass accumulation, dry matter partitioning, nutrient uptake, grain dry weight, grain numbers, grain yield, grain nitrogen (N) at maturity, and protein contents. Chapter 6 presents the application of crop models for wheat production. Potential and limitation of wheat crop models to assist breeders, researchers, agronomists, and decision-makers are discussed in this chapter. Chapter 7 is about genetic analysis that requires phenotyping and genotyping, followed by the application of statistical principles. Chapter 8 elaborates the contribution of process-based models in sugarcane research. Climate characterization of the leading sugarcane producing countries with the influence of main weather variables on sugarcane growth, development, and yields are presented in this chapter. Chapter 9 presents the forecasting of rainfed wheat yield using Landsat 8 satellite imagery and DSSAT. Methane (CH_4) is a potent greenhouse gas that is produced in many sectors, and is discussed in Chap. 10. Measurements of methane are impossible in some cases, thus in vitro techniques together with modeling approaches are presented in this chapter to predict methane emissions. Chapter 11 is a review of sunflower modeling with a description of different models used in the improvement of sunflower. Disease modeling is discussed in Chap. 12. DSSAT-CROPGRO-Chickpea model is presented in Chap. 13.

Chapter 14 focuses on potatoes, which is one of the important crops in the world after rice and wheat. This crop is under threat due to climate variability; thus, different adaptation strategies are needed through simulation modeling to mitigate the impacts of climate change. Different process-based models such as Decision Support System for Agrotechnology Transfer (DSSAT), Agricultural Production Systems Simulator (APSIM), CropSyst (CropSyst VB – Simpotato), and STICS (Simulateur multidisciplinaire pour les Cultures Standard) are presented in this chapter as they have shown great potential to develop sustainable agronomic practices as well as virtual potato cultivars to have good potato cultivars for the future. Finally, in Chap. 15, application of a generalized additive model for rainfall forecasting is presented with the aim to predict the most suitable sowing time for rainfed wheat.

It is my hope that knowledge about system modeling presented in this book will enhance the understanding and catalyze the application of artificial intelligence, phenotyping, and modeling at different scales.

Rawalpindi, Pakistan Mukhtar Ahmed

Contents

About the Editor

Mukhtar Ahmed's research focuses on the impact of climate change on crop ecology, crop physiology, cropping system and rain-fed ecosystem management. He has been involved in teaching and research since 2005. During his PhD and visit to Sydney University, Australia, he worked on the application of APSIM as a decision support tool, and rainfall forecasting using generalised additive models. He was awarded a young scientist fellowship by APCC South Korea. He also won a research productivity award from Pakistan Council of Science and Technology (PCST), and a Publons reviewer award in 2018 and 2019. He was part of the Regional Approaches for Climate Change (REACCH) project in the USA, which developed multi-model ensemble approaches to minimize the uncertainties. He is involved in the use of statistical and dynamic models as risk management tools to mitigate the challenges of climate change. His current research includes agroecosystems modelling, precision agriculture, modelling the nutrient use efficiency of legume-based cropping systems, forage agronomy and physiological responses to climate variability and its modelling. He is a Project co-leader in the Model Calibration Group of the Agricultural Model Intercomparison and Improvement Project (AGMIP) Wheat and Maize Evapotranspiration.

Systems Modeling

1

Mukhtar Ahmed and Shakeel Ahmad

Abstract

The agricultural systems have complex interactions with the surrounding environment and soil, and better understanding is possible through computer application. The interactions between systems and environment are so complex that one cannot quantify their cumulative affects without application of latest computing tools. The solar radiations, temperature, photoperiod, humidity, and wind are some of the important environmental variables which interact with agricultural system. These variables should be considered with importance for understanding the agricultural system on scientific basis. The light required is for photosynthesis and photoperiod, humidity for determination of water loss, and wind to transfer water vapors and gases to and from plants. The model converts qualitative data into quantitative to give out quantitative predictions to the theories which can be compared very easily in the real world. There is rich future for systems modeling, and it can open new frontiers and helps in the agroecological transitions of agriculture. Plants and crops should be considered as holobionts (individual host and its microbial community). In system modeling, the environmental variables are linked to various physiological processes to predict the crop responses with a given set of environmental conditions. The increased ozone concentration in the environment also damages the crop, and these impacts should be considered during model development. Similarly, application of

M. Ahmed (✉)
Department of Agricultural Research for Northern Sweden, Swedish University of Agricultural Sciences, Umeå, Sweden

Department of Agronomy, Pir Mehr Ali Shah Arid Agriculture University, Rawalpindi, Pakistan
e-mail: mukhtar.ahmed@slu.se; ahmadmukhtar@uaar.edu.pk

S. Ahmad
Department of Agronomy, Faculty of Agricultural Sciences and Technology, Bahauddin Zakariya University, Multan, Pakistan

M. Ahmed (ed.), *Systems Modeling*, https://doi.org/10.1007/978-981-15-4728-7_1

different models at different scales is presented which could help to understand the mechanisms in qualitative and quantitative way. Last but not least, the concept of digital agriculture and its linkage with modeling were elaborated. In general the chapter discusses in detail the type, methods of measurement along with mathematical representation, terminologies, and their impact on the various processes of the plants.

Keywords

Agricultural systems · System modeling · Holobionts · Environmental variables · Solar radiations · Temperature · Photoperiod · Humidity · Wind ozone

1.1 Introduction

System is anything under observation. Here in this chapter, we will be mainly focusing on the system related to the agricultural sector, so it could be an agricultural system or cropping system or farming system. System is the complex combination of various components. Since agricultural disciplines are changing at rapid pace, thus quantitative experimentations are very important to understand the system. An accurate description of the system such as photosynthesis to light, water, and carbon dioxide (CO_2); crop phenology to temperature; crop biomass to radiation use efficiency (RUE); and crop yield to fertilizer is no doubt very important, but these responses will be more useful if we also understand the mechanisms behind all these responses. Thus, the working hypothesis is required to explain and predict responses in the agricultural science. The progress in this sector is only due to the continuous interaction between experiment and hypothesis, observation and theory, and day-by-day precision in the techniques used to understand the problem first and then suggest appropriate solution. Computer application in the field of agriculture can help to understand the interactions between system and its variables. Models, which are mainly mathematical representation of the biological system, could generate answers to the problems. Most people think that models are difficult and complex thus need time to be implemented on the ground scale. However, no special mathematics is needed for big or complex models. They come from small bits and pieces. There is a rich future for systems modeling, and it can open new frontiers and helps in the agroecological transitions of agriculture. Similarly, it is essential to understand belowground processes, roots, soil, and their complex abiotic and biotic interactions. Plants or crops should be considered as holobionts (individual host and its microbial community). This can account for their extended phenotypes and (phyllosphere and rhizosphere) microbiomes (Fig. 1.1). Agriculture deals with the activities that take place on the farm, and it results in the production of food, fuel, and energy. It is the interaction of environment, crop, soil, and animal among each other. The environment consists of abiotic variables such as light/solar radiation, temperature, water, CO_2, wind speed, and humidity. Thus, agriculture is the interaction of farm and ecology.

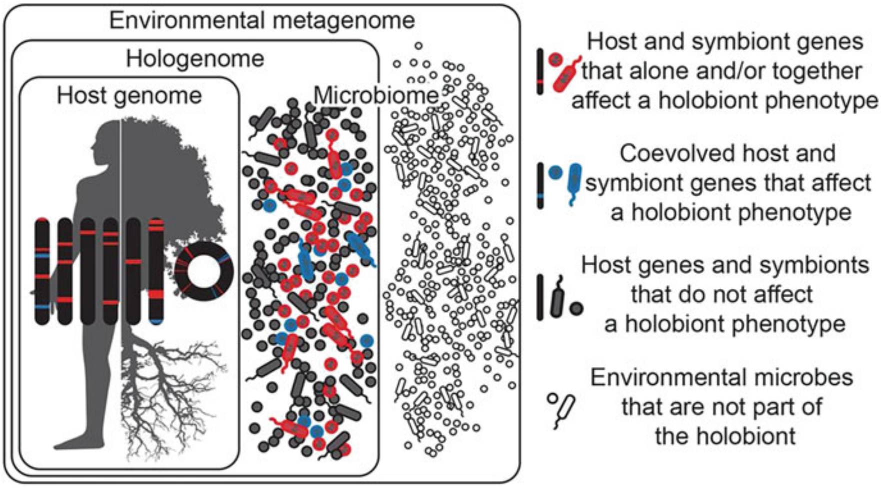

Fig. 1.1 Holobionts (host (blue) and all its symbiotic microbes, red; one that affects the holobiont's phenotype, gray; one that do not affect the holobiont's phenotype)

Light is one of the important variables in the agricultural sector. Plants convert light energy to the biochemical energy through the process of photosynthesis. Biomass production through the action of light could be elaborated by considering the Planck's quantum (PQ) theory of radiation:

$$E_{\mathrm{PQ}} = hv \tag{1.1}$$

where E is energy according to the Planck's quantum theory of radiation, h is Planck's constant ($6.62607004 \times 10^{-34}$ joule· second), and v is frequency.

Since frequency is inversely proportional to wavelength (λ), thus

$$v \, \alpha \frac{1}{\lambda} \tag{1.2}$$

$$v = \frac{C}{\lambda} \tag{1.3}$$

where C is speed of light $= 3 \times 10^8$ m s^{-1}.

Putting value of v in Eq. (1.1) results to the following equation:

$$E_{\mathrm{PQ}} = h \; {}^{c}\!/_{\lambda} \tag{1.4}$$

Furthermore, Einstein equation will be required to convert light energy into mass (m).

$$E_{\mathrm{einstein}} = mc^2 \tag{1.5}$$

Comparing both equations of energy:

$$E_{PQ} = E_{einstein} \tag{1.6}$$

$$h\ {}^{c}\!/\!_{\lambda} = mc^2 \tag{1.7}$$

$$\frac{h}{\lambda} = mc \tag{1.8}$$

$$m = \frac{hc}{\lambda} \tag{1.9}$$

Thus, we can find the mass by putting values of λ as h and c which are constants. Therefore, this is the simple model of light energy conversion to mass energy, and is the law of thermodynamics in the field of crop production.

1.2 Photosynthesis

Photosynthesis is the capture of light by grana of chloroplast, and it results to the fixation of carbon dioxide (CO_2) into simple sugar ($C_6H_{12}O_6$). Different environmental variables have significant impact on the rate of photosynthesis as shown in Fig. 1.2. This process is strongly dependent on photon flux density (PFD) and intracellular CO_2 concentration (C_i). The simple model equation for this reaction can be expressed as

$$6CO_2 + 6H_2O \frac{\text{Light}}{\text{Chloroplast}} > C_6H_{12}O_6 + 6O_2$$

Light reaction is the primary photochemical reaction initiated by the PAR absorbed by the photosynthetic pigment, which results in the activation of chlorophyll molecules to an excited sate. Electron carriers take the electrons and move down through the electron transport chain (ETC) resulting in the formation of ATP (adenosine triphosphate). This light-initiated process is known photophosphorylation. Furthermore, reduced form of nicotinamide adenine dinucleotide phosphate (NADPH) and oxygen was released in this process (Fig. 1.3). Light reaction is the photolysis of water, and in this process, ATP (adenosine triphosphate), NADPH (nicotinamide dinucleotide phosphate hydrogenase), and O_2 are produced. This reaction takes place at grana of chloroplast which is the green pigment in leaf (Fig. 1.3). Afterward in dark reaction C is fixed to three-carbon compounds known as PGA (phosphoglyceraldehyde) or G3P (glyceraldehyde-3-phosphate). The enzyme which plays a role in this reaction is RUBISCO (ribulose bisphosphate carboxylase) which is dual in nature (carboxylase as well as oxidase) as it can combine with both CO_2 and Oxygen (O_2). If O_2 is in excess in the mesophyll cell of leaf, it will combine with G3P and lead to the process of photorespiration which is a typical feature of C3 plants. In this reaction, most of the photosynthates are lost. There are other types of plants which can fix CO_2 more efficiently and are known as

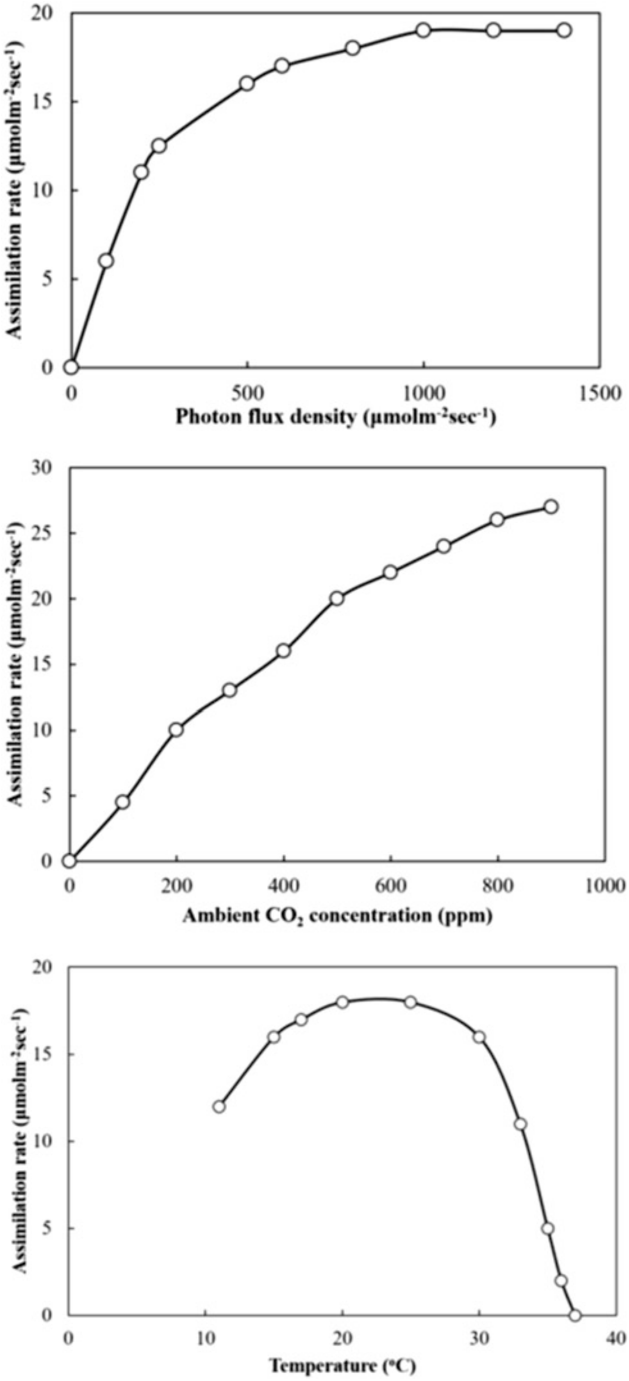

Fig. 1.2 Photosynthesis as function of different environmental variables (Landsberg and Sands 2011a)

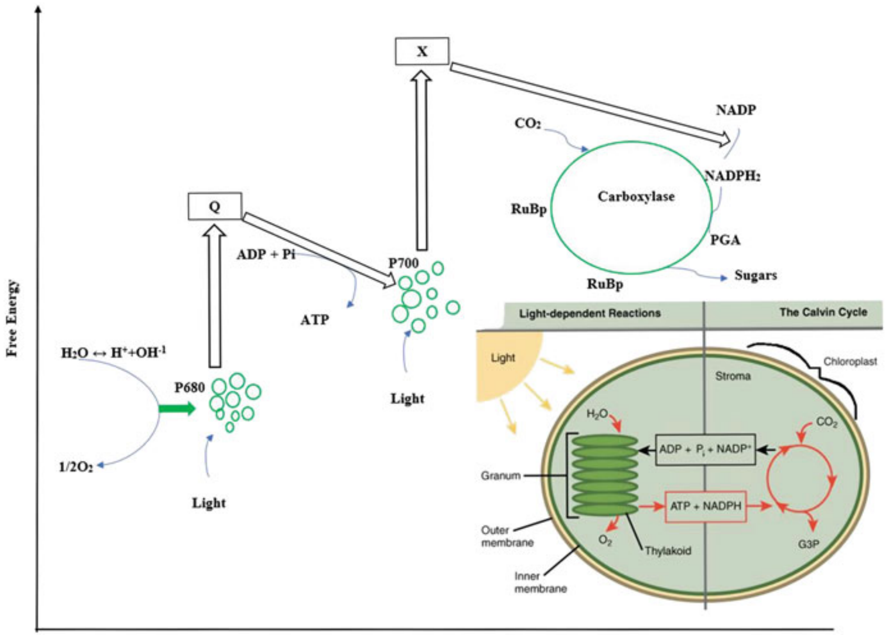

Fig. 1.3 Photosynthetic reactions in plants showing the role of multiple actors. (Source: Landsberg and Sands 2011a, b)

C4 plants. These plants can avoid O_2 due to their leaf anatomy (bundle sheath cell surrounded with mesophyll cell) and, thus, do not show any process of photorespiration. In the bundle sheet cell, CO_2 combines with three carbon molecules, i.e., PEP (phosphoenolpyruvate or phosphoenolpyruvic acid) in the presence of enzyme PEPCO (phosphoenol pyruvate carboxylase) resulting to 4-C compound (Fig. 1.12). This is the efficient way of producing sugars. Thus, plants can be classified into C3, C4, and CAM (Crassulacean acid metabolism) plants based upon PCR cycle. CAM plants are a subset of C4 plants, but they open stomata at night as they have to conserve water due to their presence in hot desert climate (Fig. 1.3).

The rate of light reaction depends on the quality and intensity of light alone, and it is not affected by temperature or CO_2 concentration. Excessive photon other than excitation of chlorophyll acceptors results in fluorescence or heat. Dark reaction doesn't require light energy; it uses energy produced in the light reaction to do the reduction of CO_2 to carbohydrate (CH_2O). Ribulose bisphosphate (RuBP) will be the initial acceptor for CO_2, and it will be catalyzed by the enzyme ribulose bisphosphate (RuBP) or RUBISCO (ribulose bisphosphate carboxylase). The first product of dark reaction is 3-phosphoglyceric acid (3-PGA), a three-carbon compound in C_3 plant species. ATP and NADPH then reduce this molecule in a complex

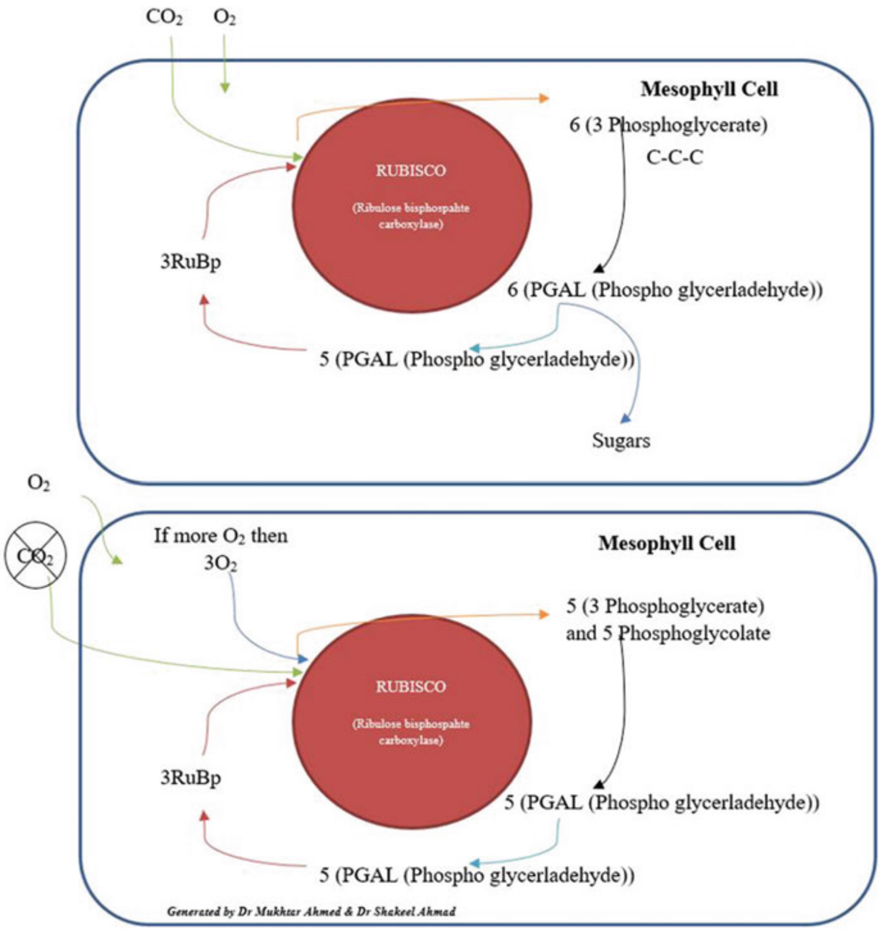

Fig. 1.3 (continued)

sequence of reactions to produce sugars. Temperature and CO_2 concentration are necessary to model this reaction, as it is dependent upon them. In general, we can say that this reaction is the function of temperature and CO_2 concentration. Photosynthesis as the function of environmental variables was explained by Wang et al. (2001) and presented in Fig. 1.2, which showed nonlinear response to different environmental variables. However, there are crops (e.g., maize and sugar cane) where first carbon reduction product is a four-carbon compound called as C_4 plants. Furthermore, there are plants, which can do carboxylation at night by opening stomata, thus called as water-conserving plants following crassulacean acid metabo lism (CAM). Photosynthetic parameters, i.e., stomatal conductance (g_s) (mol m^{-2} s^{-1}), net photosynthetic rate (A_n) (mol m^{-2} s^{-1}), and intercellular and

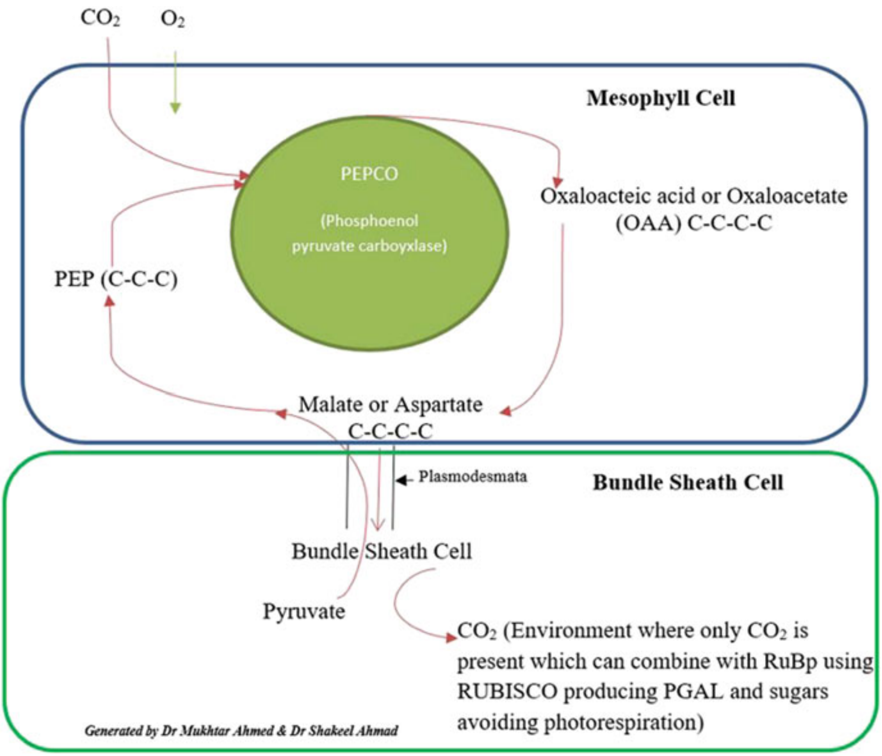

Fig. 1.3 (continued)

leaf surface concentrations of CO_2 (C_i and C_s, mol mol^{-1}, respectively), are interlinked with each other and can be expressed by the following equation:

$$g_s = \frac{A_n}{(C_a - C_i)}$$

However, this simple model equation can be transformed to the complex model if we consider the number of different factors which affect the availability of light to the leaves in a plant canopy. Light response curve depicts how availability of light (irradiance or photon flux density) is related to the rate of photosynthesis (Fig. 1.4).

The portion of light spectrum utilized by the plant called PAR (photosynthetically active radiation) and PPFD (photosynthetic photon flux density) is defined as the photon flux density of PAR. Accurate modeling of PAR is essential to predict the crop behavior under different systems. Nowadays light is measured as the rate at which moles (Avogadro's number, 6.02×10^{23} quanta) of PAR land on a unit area of leaves (μmol quanta m^{-2} s^{-1}). However, there are different other units also available to measure light (Table 1.1).

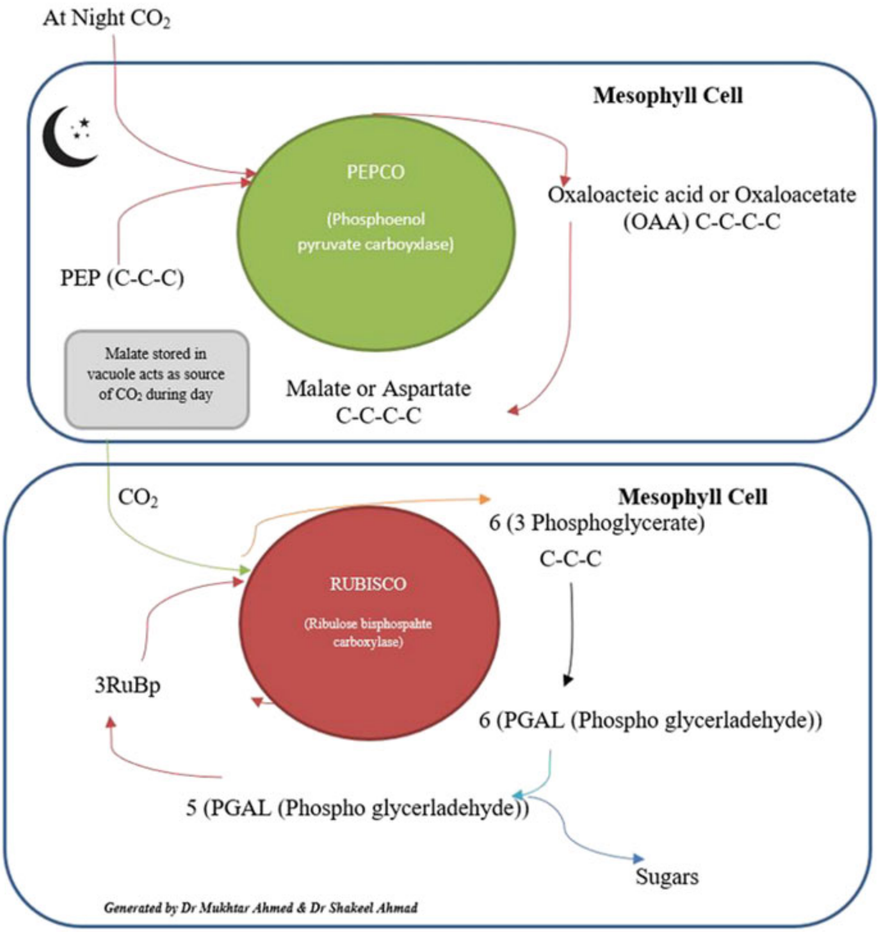

Fig. 1.3 (continued)

1.3 Solar Radiation

Photosynthesis at canopy level is a key driver of crop growth in most of available crop models, e.g., APSIM (Agricultural Production Systems Simulator) (Holzworth et al. 2014), CropSyst (StÖckle et al. 2003), DSSAT (Decision Support Systems for Agrotechnology Transfer) (Jones et al. 2003), GECROS (Yin and van Laar 2005), and STICS (Simulateur multidiscplinaire pour les Cultures Standard) (Brisson et al. 1998; Coucheney et al. 2015). It can be either (i) photosynthesis of individual leaves

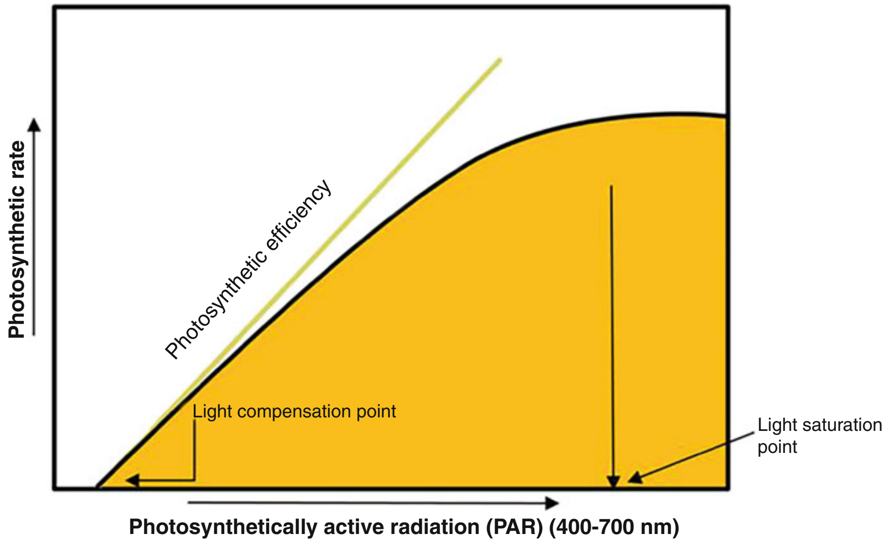

Fig. 1.4 Generalized photosynthetic response model to photosynthetic active radiation (PAR)

Table 1.1 Conversion factors for different light (400–700 nm) measuring units (Carruthers et al. 2001)

(a) Sunlight	**Measure**	**Units**	**Conversion**
	Photosynthetic photon flux density (PPFD)	μmol quanta m^{-2} s^{-1}	1
	Irradiance	Langley h^{-1}	0.0187
		Watts m^{-2}	0.217
	Luminosity	Lux = lumens m^{-2}	51.2
		Ft candles	4.78
	Other unit conversions	1 Langley	1 g cal m^{-2}
		1 Watts	10^7 ergs s^{-1}
		1 lux	1 lm m^{-2}
(b) Artificial light	**klux (= 1 × 10^3lux)**	**Wm^{-2}**	**μmol quanta m^{-2} s^{-1}**
Metal halide	1	3.1	14
Sodium/mercury	1	2.9	14
White fluorescent	1	2.7	12
Incandescent	1	4	20

Table 1.2 Photosynthesis as function of light intensity elaborated by light response models

Type of model	Generic function	References
Linear	$A_n = \begin{cases} \propto I, I \leq A_{\max} \div \propto \\ A_{\max}, I > A_{\max} \div \propto \end{cases}$, where $A_{\max}$ is the maximum rate of photosynthesis, I is the light intensity, and $\propto$ is the maximum quantum yield	Blackman (1905)
Rectangular hyperbola	$A_n = {}^{\propto IA_{\max}}/_{aI + A_{\max}}$	Maskell (1928)
Non-rectangular hyperbola	$\theta A_n{}^2 - (\propto I + A_{\max})A_n + \propto IA_{\max} = 0$	Thornley (1976, 1998)
Exponential equation	$A_n = A_{\max}\left\{1 - e^{-\propto I/_{A_{\max}}}\right\}$	Hammer and Wright (1994) and Hammer et al. (2006)
Rectangular hyperbola (modified)	$A_n = \delta \frac{1 - \beta I}{1 + \gamma I}\,(I - I_c)$, where δ, β, and γ are coefficients and I_c is the compensation irradiance	Ye (2007)

in the canopy or (ii) linear relationship between accumulated crop canopy biomass and intercepted solar radiation known as radiation use efficiency (RUE, g MJ^{-1}).

Light intensity (I)/radiation is the main environmental factor of photosynthesis. Modeling the response of net photosynthesis (An) to I or the A_n/I curve is the main focus of modeling of photosynthesis. The response of "A_n" to "I" increases linearly with a slope α (maximum quantum yield) until it reaches to the maximum rate of photosynthesis ($A_{\max}$) where CO_2 supply becomes limited. The maximum efficiency of light which can be converted to chemical energy is represented by α (Table 1.2).

Solar radiations can be direct and diffuse. Both of these are important for canopy photosynthesis and are an essential part of canopy photosynthesis modeling in plant. Canopy level photosynthesis was first described by Boysen Jensen (1932), which stated that canopy photosynthesis light response is different from individual leaf. This difference could be because leaves in a canopy exposed to different light environment in a day due to their spatial arrangements (leaf angle and leaf position in the canopy), location of the sun during diurnal, and seasonal cycle and solar radiation intensity. Thus, canopy photosynthesis is a complicated process due to heterogeneity of radiation in the canopy. First model is used to quantify how sunlight is intercepted by leaves when it moves from top to bottom and was named as 1D canopy model (Monsi and Saeki 1953). They showed that the light attenuation in the canopies is exponential and can be modeled by the Beer-Lambert equation:

$$I = I_o e^{-k * \mathrm{LAI}}$$

where I is the light intensity at point of interest, I_o is the light intensity at the top of the canopy, K is the light extinction coefficient, and LAI is the leaf area index.

Multilayer canopy models were further developed by dividing the canopy into layers specified by the respective LAI. The intensity of solar radiations reaching each fraction (sunlit and shaded leaf fractions) was specified by the Beer-Lambert equation. It was assumed that diffuse solar radiation was intercepted by shaded fraction, while direct solar radiation could be intercepted by sunlit fraction. Different *K* values were used to incorporate attenuation of different types of radiation in canopy models. De Pury and Farquhar (1997) reported that single-layer sunshade modeling approach agrees with multilayer modeling approach as well as with 3D plant architecture model in simulating canopy photosynthesis. This confirms the robustness of the sunshade modeling approach. It has been proven that *K* has significant effect on crop growth, and it can be influenced by crop developmental stage, canopy configurations, and canopy architectural traits (leaf shape, angle, and internode length). However, earlier researchers like deWit (1959) and Loomis and Williams (1963) in their work reported crop productivity as the function of radiation instead of leaf photosynthesis. Many other researchers showed that dry-matter production and intercepted radiation have linear relationship among each other. This resulted to the term of RUE (Sinclair and Muchow 1999). The simplicity of RUE approach resulted to its widespread use in quantification of crop growth in different crop models (e.g., Hammer et al. 2010). The RUE values vary among crop species as it is higher in C_4 than in C_3. The reported RUE of C_4 crops like maize is 1.6–1.9 g MJ^{-1}; for pearl millet, it is 2.0 g MJ^{-1}; for sorghum it is 1.2–1.4 g MJ^{-1} (dwarf species), while for Indian dwarf sorghum hybrid, it is 1.6–1.8 g MJ^{-1}. However, in C_3 plants like wheat, RUE is 1.2 g MJ^{-1}, while for dicotyledonous legume crop like soybean, it is 1.0 g MJ^{-1} (Lindquist et al. 2005; Hammer et al. 2010; Sinclair and Muchow 1999). The RUE also has relationship with specific leaf nitrogen (SLN); e.g., in C_4 crop species, RUE increases from SLN of 0.3 g m^{-2} and reaches to plateau when SLN = 1.0 g m^{-2}. SLN is a key driver of leaf level photosynthesis and RUE. However, for C_3 crops like wheat, SLN is in the range of 0.3–2.0 g m^{-2} showing higher values than C_4 crops. Other factors like vertical profile of SLN and environmental variables (air temperature, partial pressure of atmospheric CO_2, and plant water status) also affect the RUE. Higher RUE was reported under diffuse solar radiation (Sinclair et al. 1992). Different indices as multipliers were used to incorporate the impacts of change in air temperature, CO_2 concentrations, and plant water status on RUE. However, in APSIM-Wheat, RUE is not affected in the temperature range of 10–25 °C, while in CERES-Maize model, it is 17–33 °C. Similarly, for CO_2, RUE is increased with elevated CO_2 in C_3 plants but not in C_4 (Lobell et al. 2015).

Photosynthesis depends nonlinearly on the rate of absorption of solar energy by the leaves. The solar constant (flux of radiant energy from the sun exterior to the earth atmosphere) varies from 1321 W m^{-2} to 1412 W m^{-2}. Radiation emitted from material bodies such as the sun, atmosphere, ground, and plant parts are called as thermal radiation. It is determined by the absolute temperature T (k) and total flux $\varphi(T)$ (W m^{-2}). Solar radiations from the sun (direct and diffused) are called as short-wave radiation, while radiation that originates from earth is called long-wave radiation.

1.3.1 Photosynthetically Active Solar Radiation (PAR)

Photosynthetically active solar radiation (PAR) or visible radiation or visible radiation lies in the spectral band of 0.4–0.7 μm (400–700 nm), while full solar spectrum or total solar radiation lie in the range of 0.15–3.2 μm. Outside earth atmosphere, the ratio of PAR to total solar radiation is 0.44, while if we consider atmospheric effects, it is in the range of 0.4–0.6; thus generally used value is 0.5. Energy flux density (W m^{-2}) is used to consider the process of transpiration (energy balance of bodies). Since the actual number of photons is important in photochemical processes (e.g., photosynthesis), thus PAR is expressed in mole, and one mole of photon is called Einstein (E). PAR can be expressed as energy flux density or photon flux density (mol m^{-2} s^{-1}) but has great advantage to express as number of moles of CO_2 fixed/ mole of photons in the visible band which activates photosynthesis (1 J_{PAR} = 4.6 μmol, i.e., for solar radiation 1000 W m^{-2} ≈ 2300 μmol m^{-2} s^{-1} PAR).

1.3.2 Irradiance (I, W m^{-2}, or J m^{-2} s^{-1})

The irradiance (I)/flux density of radiant energy is the power incident on a unit area (W m^{-2} or J m^{-2} s^{-1}). It can be of two types I_{dir} (direct beam solar irradiance) and I_{dif} (diffuse irradiance). I_{dif} is measured on horizontal plane, while I_{dir} is measured on a plane perpendicular to the beam.

1.3.3 Insolation (Q, MJ m^{-2} day^{-1})

The amount of solar radiation on a given surface in a given time period is called insolation. It is the solar radiation in a day on a horizontal surface, and it varies throughout the year. Total energy comes at various sites across the globe ranging from 6 MJ m^{-2} day^{-1} to 30 MJ m^{-2} day^{-1} (Monteith and Unsworth 2013) (Fig. 1.5). Different units have been used to express radiation (Table 1.3), and the standard unit used is megajoule per square meter and per day (MJ m^{-2} day^{-1}) or as equivalent evaporation in mm per day (mm day^{-1}).

1.3.4 Radiant Energy

Radiant energy is the total energy that comprises of short-wave (from the sun) and long-wave radiations (from the sky, the ground, and other bodies). Stefan-Boltzman law could be used to determine long-wave radiation. The term net radiation (φn) could be used to represent the sum of short-wave and long-wave radiation:

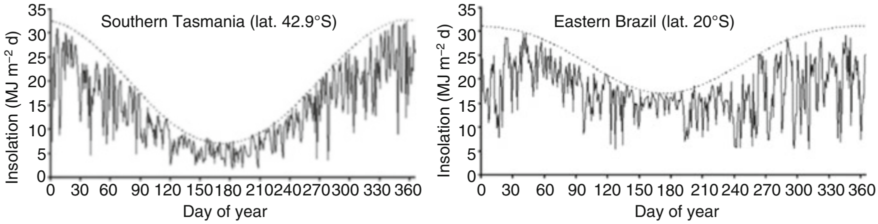

Fig. 1.5 Insolation at Tasmania (total annual energy = 5200 MJ m^{-2}) and Brazil (total annual energy = 6400 MJ m^{-2}) predicted by Bird and Hulstrom (1981) model). (Source: Landsberg and Sands 2011a, b; reproduced by permission of Elsevier)

Table 1.3 Units for radiation expression

Units	Equivalence to MJ m^{-2} day^{-1}
Equivalent evaporation (mm day^{-1})	1 mm day^{-1} = 2.45 MJ m^{-2} day^{-1}
Joule per cm^2 per day (J cm^{-2} day^{-1})	1 J cm^{-2} day^{-1} = 0.01 MJ m^{-2} day^{-1}
Calorie per cm^2 per day (cal cm^{-2} day^{-1})	1 cal = 4.1868 J = 4.1868 × 10^{-6} MJ, 1 cal cm^{-2} day^{-1} = 4.1868 × 10^{-2} MJ m^{-2} day^{-1}
Watt per m^2 (W m^{-2})	1 W = 1 J s^{-1}, 1 W m-2 = 0.0864 MJ m^{-2} day^{-1}

$$\varphi n = \varphi \mathrm{SWR} + \varphi \mathrm{LWR} \downarrow - \varphi \mathrm{LWR} \uparrow$$

where φSWR is the short-wave radiation (direct and diffuse radiation sum), φLWR↓ is the incoming long-wave radiation, and φLWR↑ is the outgoing long-wave radiation. The value of φLWR↑ on clear skies is 100 W m^{-2}, while on cloudy skies it is 10 W m^{-2}. At night φSWR = 0, and so on clear skies net radiation will be −100 W m^{-2}. Net radiation for bodies like leaves or canopies which absorbs radiation it is balance between incoming short-wave and long-wave radiation, reflected radiation, and thermal radiation from the body depending on its surface temperature (T_s). Thus the equation would be

$$\varphi n = (1 - \alpha)\varphi \mathrm{SWR} + \varphi \mathrm{LWR} \downarrow - \varphi \mathrm{LWR} \uparrow (T_s)$$

where α is albedo or refection coefficient of the surface. The net radiation absorbed by the body could be used to drive metabolic process such as evapotranspiration.

1.3.5 Albedo

The albedo (α) or reflectivity is measures of how much light that hits surface is reflected by the body without being absorbed. It can be the main drivers of land surface temperature. Heat is less absorbed by snow and ice (higher albedo) and more

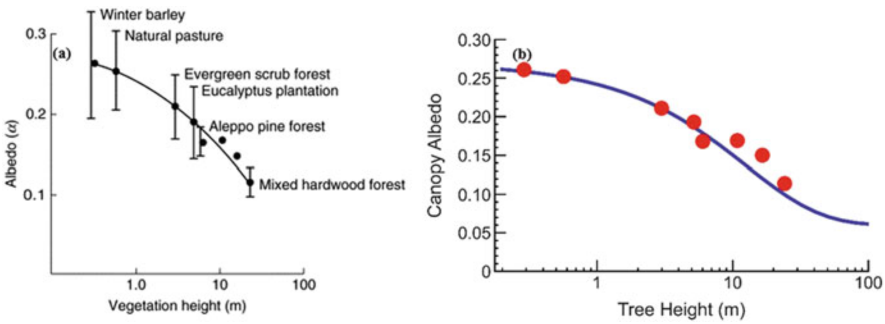

Fig. 1.6 Albedo and height of the canopy. (Source (**a**): Landsberg and Sands 2011a, b; (**b**): Kempes et al. (2011))

absorbed by vegetation, soil, and water bodies (lower albedo). It also varies with the surface roughness and height of the canopy as shown in Fig. 1.6.

1.4 Temperature

Temperature is the key determinant abiotic factor which controls the rate of metabolic processes in plants. Thus, it has major impact on plant growth, development, and yield through its influence on photosynthesis and respiration. It controls evaporation, transpiration, and water balance in plants. Temperature can be air temperature (T_{air}) measured at a standard height of 1.4 m, tissue temperature (T_{tis}), leaf temperature (T_L), canopy temperature (T_{canopy}), stem temperature (T_{stem}), and soil temperature (T_{soil}). In general, most of the time, Ta is in focus as it determines the temperature environment of the plant. It has been also reported earlier that sometimes Ta around plants is very low, but they have very high T_{tis} due to the higher radiation loads. It can be further divided into daily maximum and minimum temperatures. Generally, the average of maximum and minimum temperatures has been used to study the impacts on plant growth (Fig. 1.7).

1.4.1 Leaf Temperatures (T_L)

Leaf is the main photosynthesizing machinery; thus T_L has significant impacts on the physiological process related to the photosynthesis and respiration. It also governs energy balance and transpiration rate. Leaf temperatures are generally determined by the radiation load instead of T_{air}. It can be higher than T_{air} when radiation loads are high and wind speed is low (Fig. 1.8).

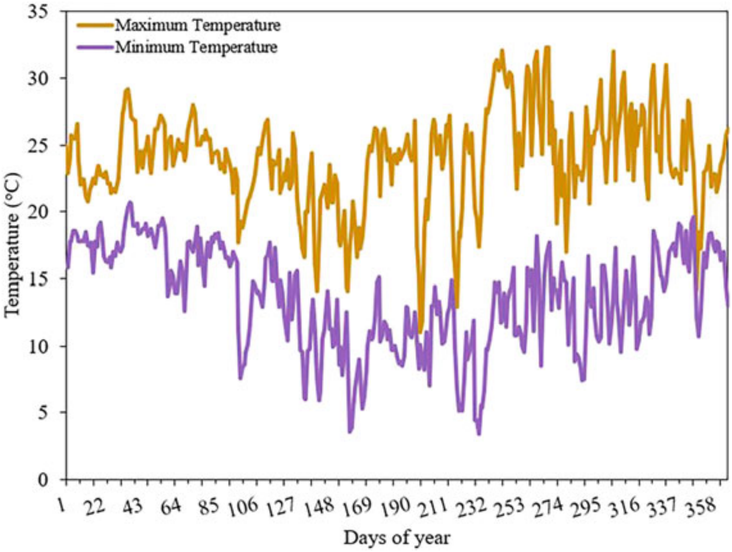

Fig. 1.7 Annual maximum and minimum air temperatures

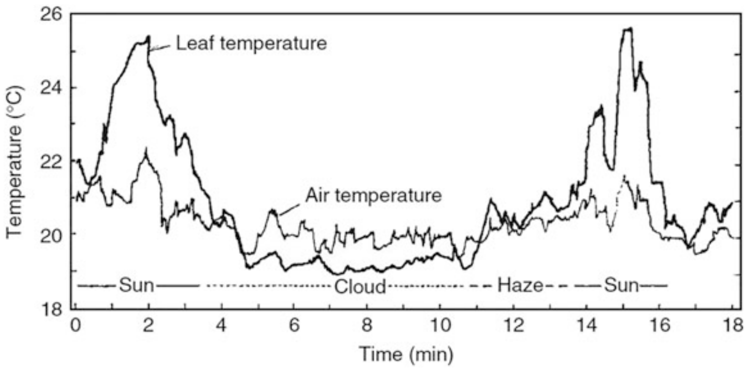

Fig. 1.8 Variation in the T_L and T_{air} in response to changing solar radiation. (Source: Landsberg and Sands 2011a, b; reproduced by permission of Elsevier)

1.4.2 Cardinal Temperature

Cardinal temperature includes minimum, maximum, and optimum temperatures. Minimum and maximum temperatures define the growth and development of an organism, while optimum temperature (T_{opt}) is the one in which growth proceeds with a great pace (temperature at which rate is maximum (99%)). Cardinal temperature components include T_{base} (base temperature below which development rate = 0), T_{opt1} (first optimum temperature at which development rate is most rapid), T_{opt2} (second optimum temperature; highest temperature at which rate is still at its

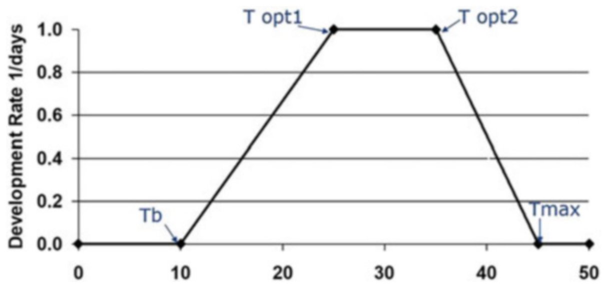

Fig. 1.9 Cardinal temperature

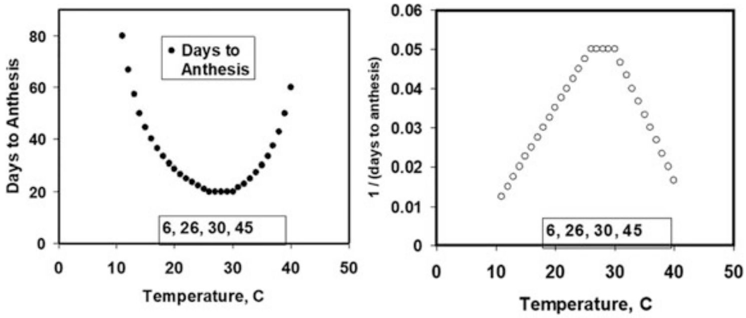

Fig. 1.10 Calculation of T_{base} (the x-axis intercept) and T_{opt} from field data

maximum), and T_{max} (maximum temperature at which development rate = 0) (Fig. 1.9). T_{base} (the x-axis intercept), and T_{opt} from field data can be calculated by plotting reciprocal of days to anthesis to temperature as shown in Fig. 1.10. However, this relationship between temperature and rate of development can be nonlinear as revealed in Fig. 1.11.

Yan and Hunt (1999) presented simple generalized equation to simulate the temperature impacts on plant's daily rate of growth (r) or development. According to them plant response to temperature can be summarized by three cardinal temperature base or minimum (T_{min}), the optimum (T_{opt}), and the maximum (T_{max}) temperatures. In earlier linear model, it has been found that the rate of development (r) is the linear function of the temperature. Thus, commonly accepted concepts of growing degree days (GDD) or thermal time and leaf unit or phyllochron interval were used. However, this approach is good if the temperature does not exceed T_{opt} which is not possible under natural conditions. Therefore, *bilinear model* was used to describe the response to suboptimum and supra-optimum temperatures:

$$r = a_1 + b_1 T \qquad \left(T < T_{opt}\right)$$

$$r = a_2 + b_2 T \qquad \left(T > T_{opt}\right)$$

Fig. 1.11 Nonlinear relationship between temperature and rate of development. (Source: Yin et al. 1995; reproduced by permission of Elsevier)

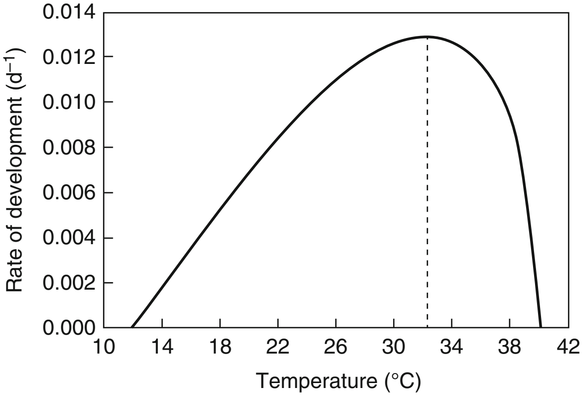

where a_1, a_2, b_1, and b_2 are the ones from where cardinal temperatures were determined. However, this model also has issues in the prediction of T_{min} and T_{max}. Thus, a multilinear model was constructed to minimize this issue and has been used in most process-based crop models. Furthermore, it has been stated that temperature response of a given process should be smooth and suggested implementation of exponential and polynomial equations. Yan et al. (1996) and Yan and Wallace (1998) proposed quadratic equation to incorporate reduced rate of development at high temperature.

$$r = R_{\text{max}} - b\left(T - T_{\text{opt}}\right)^2$$

However, the application of quadratic equation at low and high temperature can generate inaccurate results. Yin et al. (1995) introduces beta-distribution (unimodal response to an independent variable x in the range of 0–1). The function density $= 0$ if $x \leq 0$ or $x \geq 1$, and it will be maximum if x is between 0 and 1. Replacing "x" with "T" between base temperatures (T_{min}) and T_{max} leads to an expression that can be used to describe a T response:

$$r = R_{\text{max}}\left[\left(\frac{T - T_{\text{min}}}{T_{\text{opt}} - T_{\text{min}}}\right)\left(\frac{T_{\text{max}} - T}{T_{\text{max}} - T_{\text{opt}}}\right)^{\frac{T_{\text{max}} - T_{\text{opt}}}{T_{\text{opt}} - T_{\text{min}}}}\right]^c$$

where R_{max} is the maximum rate at T_{opt} and c is the parameter that determines the shape of the curve. Yin et al. (1995) equation depicted a reasonably good result as it produces smooth and realistic curve. In order to make equation biologically meaningful, Yan and Hunt (1999) replaced "c". Thus, the new suggested equation is

$$r = R_{\text{max}}\left(\frac{T_{\text{max}} - T}{T_{\text{max}} - T_{\text{opt}}}\right)\left(\frac{T - T_{\text{min}}}{T_{\text{opt}} - T_{\text{min}}}\right)^{\frac{T_{\text{opt}} - T_{\text{min}}}{T_{\text{max}} - T_{\text{opt}}}}$$

where $R_{\max}$ is the maximum rate at T_{opt}, r is 0 (if $T = T_{\min}$ or if $T = T_{\max}$), and r is $R_{\max}$ (if $T = T_{\mathrm{opt}}$). Here $c = \frac{T_{\mathrm{opt}} - T_{\min}}{T_{\max} - T_{\mathrm{opt}}} = 1$ (Reed et al. 1976). If the rate of growth or development is presented relative to the $R_{\max}$, the new equation would be

$$\frac{r}{R_{\max}} = \left(\frac{T_{\max} - T}{T_{\max} - T_{\mathrm{opt}}}\right)\left(\frac{T - T_{\min}}{T_{\mathrm{opt}} - T_{\min}}\right)^{\frac{T_{\mathrm{opt}} - T_{\min}}{T_{\max} - T_{\mathrm{opt}}}}$$

This equation has three parameters (minimum, optimum, and maximum temperatures), but it cannot be used in curve fitting unless $R_{\max}$ is well established. To simplify further they assumed $T_{\min} = 0$ for growth and development. Thus, new equations are

$$r = R_{\max}\left(\frac{T_{\max} - T}{T_{\max} - T_{\mathrm{opt}}}\right)\left(\frac{T}{T_{\mathrm{opt}}}\right)^{\frac{T_{\mathrm{opt}}}{T_{\max} - T_{\mathrm{opt}}}}$$

$$\frac{r}{R_{\max}} = \left(\frac{T_{\max} - T}{T_{\max} - T_{\mathrm{opt}}}\right)\left(\frac{T}{T_{\mathrm{opt}}}\right)^{\frac{T_{\mathrm{opt}}}{T_{\max} - T_{\mathrm{opt}}}}$$

The work of Yan and Hunt (1999) showed that beta-distribution equation could be used to describe temperature response of different plant processes (Fig. 1.12).

1.4.3 Crown Temperature

Crown temperature is the temperature that resides near crown tissues. These tissues are the most important organ for regeneration after overwintering. This temperature is important as it determines whether the plant will suffer from frost kill during winter or not (Fig. 1.13). Crown temperature in response to air temperature used by APSIM-Wheat model has been elaborated by Zheng et al. (2014).

1.4.4 Growing Degree Day Approach

Temperature impacts on organism growth, and development can be expressed by using growing degree day (GDD) approach. This approach has been used in most of the cropping systems models. According to GDD approach, if

$$T_{\mathrm{air}} > T_{\mathrm{base}}$$

then

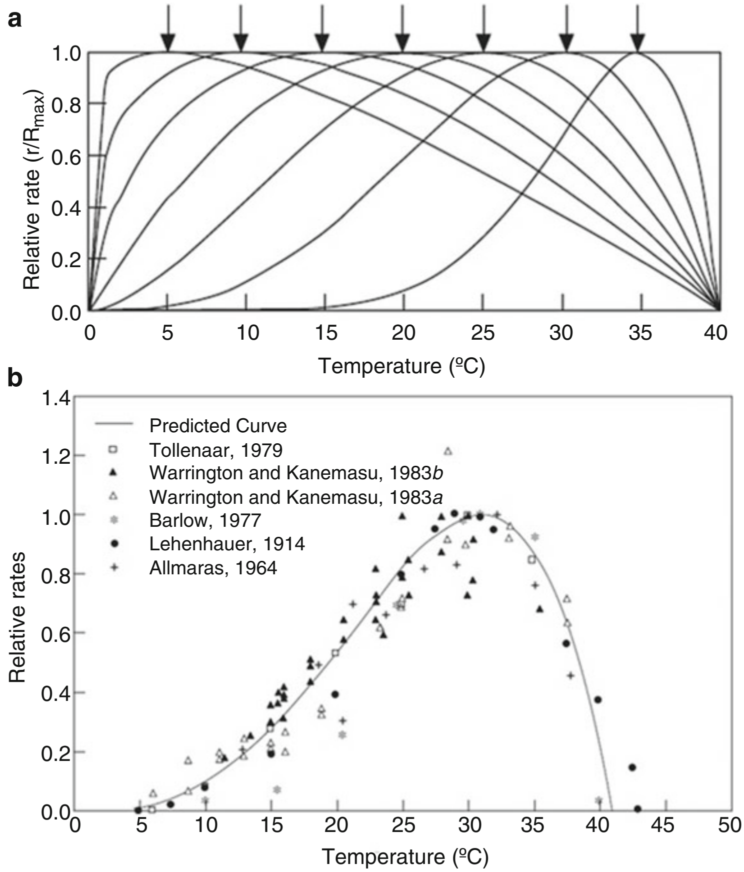

Fig. 1.12 (**a**) Application of beta distribution function (Fixed $T_{min} = 0$, $T_{max} = 40$ °C and $T_{opt} = 5{-}35$ °C). (**b**) Predicated relative rate of maize with measured values with single curve only ($T_{max} = 41$ °C and $T_{opt} = 31$ °C). (Source: Yan and Hunt 1999)

$$\mathrm{GDD} = T_{\text{average}} - T_{\text{base}}$$

if

$$T_{\text{air}} < T_{\text{base}}$$

then

$$\mathrm{GDD} = 0$$

if

$$T_{\text{air}} > T_{\text{opt}}$$

then

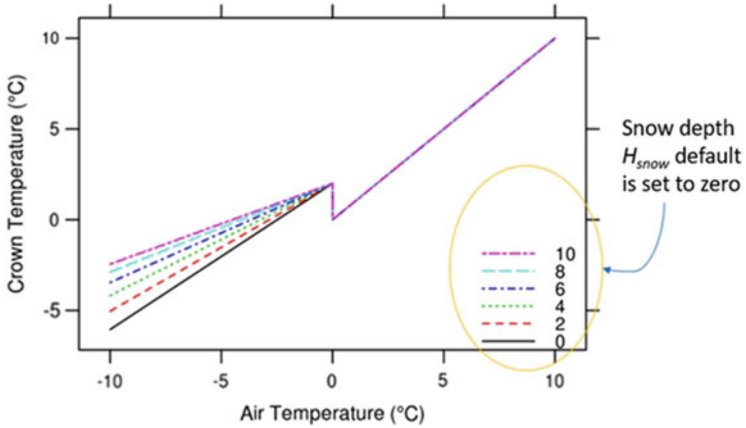

Fig. 1.13 Crown temperature in response to air temperature used by APSIM-Wheat model. (Source: Zheng et al. 2014)

Table 1.4 Average temperature and growing degree day calculations

Average temperature (°C)	Growing degree days (°C)
7	0
15	7
30	22
40	22

$$\mathrm{GDD} = T_{\mathrm{opt}} - T_{\mathrm{base}}$$

For example, if $T_{\mathrm{base}} = 8$ and $T_{\mathrm{opt}} = 30$, then GDD can be calculated as shown in Table 1.4.

1.4.4.1 Growing Degree Day Calculation: Nonlinear Approach

Crop model's accuracy to simulate crop growth, development, and yield depends upon accurate calculation of growing degree days (GDD). Since traditional method of GDD calculation assumes linear response to temperature, thus it generates inaccuracy above the T_{opt}. Zhou and Wang (2018) suggested new nonlinear method which addresses this issue of prediction of crop response at higher temperature (Fig. 1.14).

GDD = $\sum$ DTT (cumulative daily thermal time (DTT)).

Method 1

$$\mathrm{DTT} = \begin{cases} 0 & T_{\mathrm{avg}} < T_{\mathrm{b}} \\ T_{\mathrm{avg}} - T_{\mathrm{b}} & T_{\mathrm{b}} < T_{\mathrm{avg}} < T_{\mathrm{u}} \\ T_{\mathrm{u}} - T_{\mathrm{b}} & T_{\mathrm{avg}} > T_{\mathrm{u}} \end{cases}$$

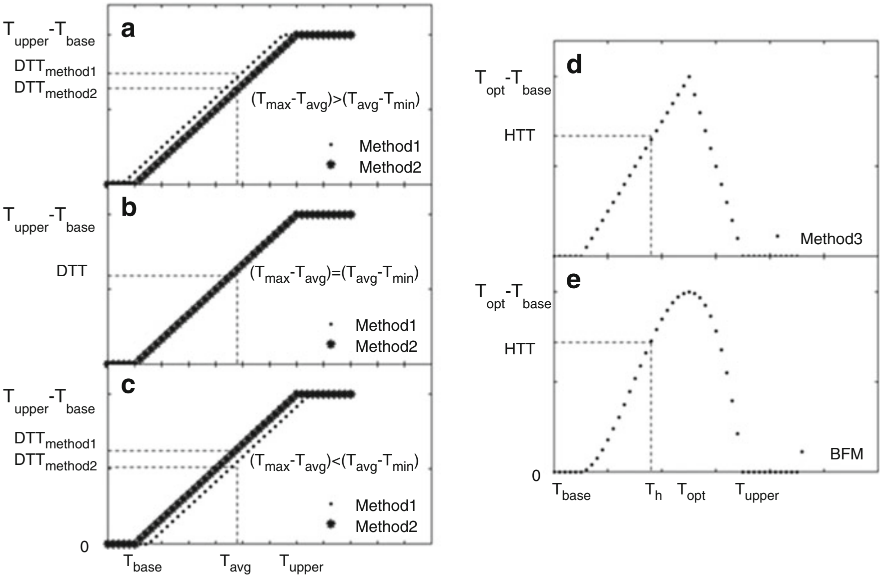

Fig. 1.14 Comparison of thermal time (DTT and HTT) calculation methods. (Source: Zhou and Wang 2018)

where $T_{\max}$ is the maximum temperature, $T_{\min}$ is the minimum temperature, T_{avg} is $(T_{\max} + T_{\min})/2$, T_{b} is the base temperature, and T_{u} is the upper threshold temperature.

Method 2

$$\text{DTT} = \begin{cases} 0 & T_{\text{avg}} < T_{\text{b}} \\ T_{\text{avg}}{}' - T_{\text{b}} & T_{\text{b}} < T_{\text{avg}} < T_{\text{u}} \\ T_{\text{u}} - T_{\text{b}} & T_{\text{avg}} > T_{\text{u}} \end{cases}$$

where $T_{\text{m}} = \min(T_{\max}, T_{\text{u}})$, $T_{\text{n}} = \max(T_{\text{m}}, T_{\text{b}})$, and $T_{\text{avg}}{}' = (T_{\text{m}} + T_{\text{n}})/2$.

T_{b} is compared with T_{u} before the average temperature ($T_{\text{avg}}{}'$) is calculated. T_{m} and T_{n} are adjusted if they are $< T_{\text{b}}$ or $> T_{\text{u}}$. In this method, DTT is given by

Method 3

$$\text{HTT} = \begin{cases} 0 & T_{\text{h}} < T_{\text{b}} \\ T_{\text{h}} - T & T_{\text{b}} \leq T_{\text{h}} \leq T_{\text{opt}} \\ \dfrac{T_{\text{opt}} - T_{\text{b}}}{T_{\text{u}} - T_{\text{opt}}} (T_{\text{u}} - T_{\text{h}}) & T_{\text{opt}} < T_{\text{h}} \leq T_{\text{u}} \\ 0 & T_{\text{u}} < T_{\text{h}} \end{cases}$$

$$\mathrm{DTT} = \frac{\left(\sum_{1}^{24} \mathrm{HTT_i}\right)}{24}$$

Method 4

$$r = R_{\max} \begin{cases} 0 & T_{\mathrm{h}} < T_{\mathrm{b}} \\ \left(\dfrac{T_{\mathrm{h}} - T_{\mathrm{b}}}{T_{\mathrm{opt}} - T_{\mathrm{b}}}\right)\left(\dfrac{T_{\mathrm{u}} - T_{\mathrm{h}}}{T_{\mathrm{u}} - T_{\mathrm{opt}}}\right)^{\frac{T_{\mathrm{u}} - T_{\mathrm{opt}}}{T_{\mathrm{opt}} - T_{\mathrm{b}}}} & T_{\mathrm{b}} \le T_{\mathrm{h}} \le T_{\mathrm{u}} \\ 0 & T_{\mathrm{u}} < T_{\mathrm{h}} \end{cases}$$

1.5 Photoperiod

Photoperiod is the time in each day in which plants receives illumination (day length). It can be called exposure of plants to light in a 24-h period. According to the Oxford Dictionary of English (2010), it is day length or the period of illumination received by an organism and remains constant between years at any given geographical location. It controls many developmental processes (e.g., flowering, tuberization, and bud set) in plants. This is due to the entertainment of circadian rhythms (biological clock) in the plant due to the detection of light signals. This sensing mechanism in plants helps them to do flowering/reproduction under favorable conditions and avoid harsh weather.

The reason for this photoperiod response in plants is due to the influence of latitude, since the axis of the earth remains tilted in the same direction throughout the year. Therefore, one hemisphere will be directed away from the sun at one side of the orbit, and after half a year, it will be directed toward the sun. Thus, latitude has great effect on day length at different times of the year. At the equator day length is equal to night length and remains constants throughout the year, while if we move away from the equator toward the poles, the days becomes shorter in winter and longer in summer. Photoperiodism response to changes in day length enables plants to adapt to seasonal changes in the surrounding environment. However, the rate of change of day length is linked with latitude (Figs. 1.15 and 1.16). Garner and Allard (American physiologist) were the first scientists to explore the flowering responses in plants linked with long days (LD) or short days (SD) and introduce the term photoperiod and photoperiodism. However, these things were mentioned clearly in the verses of the Holy book Quran, dating around 1400 years back. It has been stated in the Quran that the night and day are signs of the great power of Allah. Allah reminds us of the great signs that He created, including the alternation of the night and day, so that people may rest at night and go out and earn a living, do their work, and travel during the day, and so that they may know the number of days, weeks, months, and years, so they will know the appointed times for paying debts, doing acts of worship, dealing with transactions, paying rents, and so on. Garner and Allard classified plants into short-day plants (SDP) (day length < critical day length), long-day plants (LDP)

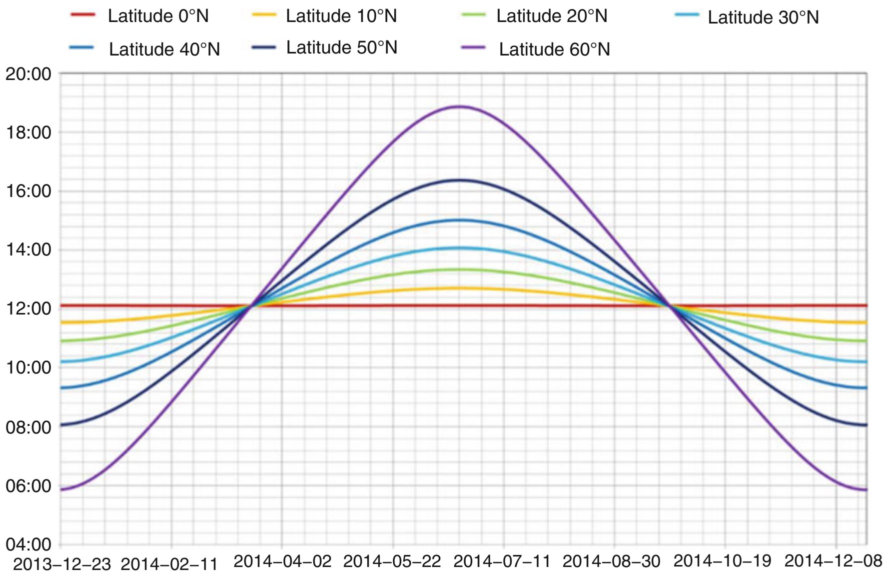

Fig. 1.15 Change in day length with latitude. (Source: http://wordpress.mrreid.org/)

(day length > critical day length), and day-neutral plants (DNP). Furthermore, it has been concluded that flowering only occurred if the night length was greater than 8.5 h. Particularly in SDP, the night length is the decisive factor. If night period is disturbed even for short period of time, it will eventually affect the process of flowering. If response to day length depends on dark period length, plants are called dark dominant, and if not, plants are called as light dominant. Generally, LDP are light dominant, while SDP are dark dominant (Fig. 1.17).

Flowering is a highly complex response linked with biological clock through environmental signals (day length and temperature). Different types of receptors called as photoreceptors are present in plants to detect light. They can be categorized into the phytochromes (PHY) and the cryptochromes. Phytochromes are family of chromoproteins sensitive to the red and far-red parts of the spectrum. There are five different PHY (PHYA to PHYE). Two common forms of phytochromes are red (Pr) and far-red (Pfr), and they are interconvertible due to the action of light as shown in Fig. 1.18.

The application of the concept of the photoperiod in models (CERES-sorghum and STICS) was implemented by Folliard et al. (2004). Alagarswamy and Ritchie's (1991) linear relationship concept was employed by considering P_{2O} as threshold. If photoperiod (P) is below P_{2O} ($P < P_{2O}$) than the duration of vegetative phase, "*fp*" is a constant/minimum and equals to the duration of juvenile phase (P_1) (f_p = constant, minimum, P_1). Above P_{2O}, the f_p increases as linear function of day length with slope P2R. Thomas and Vince-Prue (1997) reported that this model matches to the quantitative plants that will finally flower even if photoperiod remains

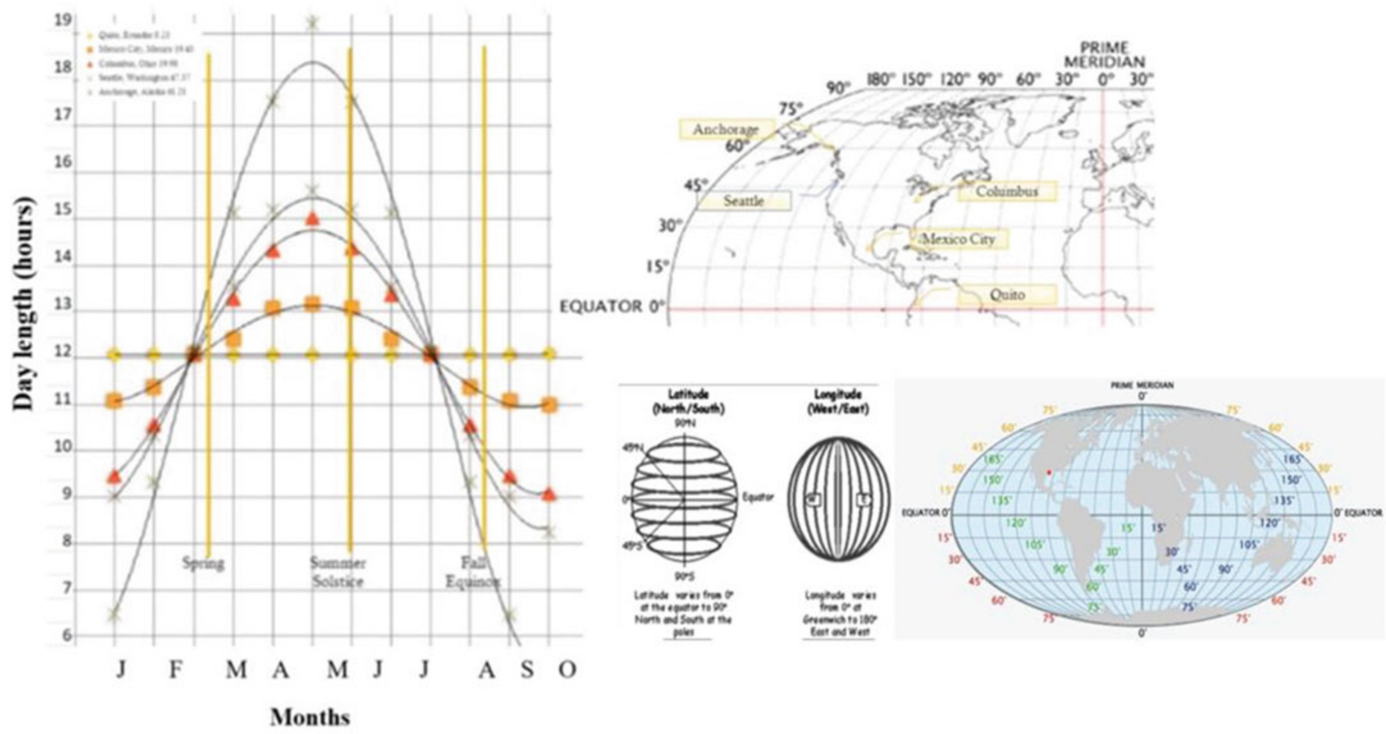

Fig. 1.16 Effect of latitude on photoperiod at four sites (Quito (Ecuador), Mexico city (Mexico), Columbus (Ohio), Seattle (Washington), and Anchorage (Alaska)) during different times of the year with description about latitude longitude and world map. (Source: http://www.timeanddate.com/sun/; http://www.theflatearthsociety.org)

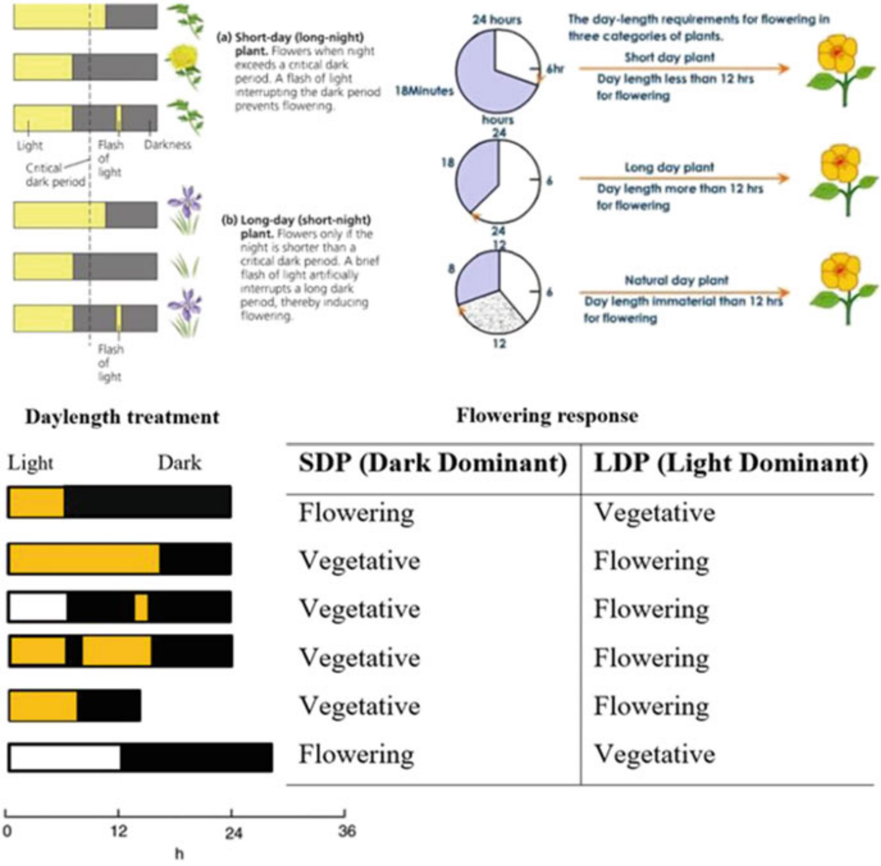

Fig. 1.17 Flowering response of plants to the combinations of different length of light and dark periods. (Source: Thomas 2003; reproduced by permission of Elsevier)

high. Brisson et al. (2003) employed hyperbolic relationship in crop model STICS by considering vegetative stage f_p constant, minimum, and equals to the duration of juvenile phase P_1 below threshold photoperiod P_{sat}. However, above P_{sat}, the f_p increases as a hyperbolic function of day length until an asymptote is reached for $P = P_{\text{base}}$. Flowering is not possible if $P > P_{\text{base}}$ and development are stopped. This model is applicable for qualitative plants as vegetative phase continues until day length conditions were not met.

Daily developmental rate (DR_j) was calculated as function of thermal time and photoperiod, and if $DR_j = 1$, panicle initiation occurs. Following two approaches (cumulative and *threshold*) could be used for the calculation of DR_j:

$DR_j = \sum i = 1jdtt_i(fP_i)$ (cumulative method, $dtti = daily\ thermal\ time$ and $(fP_i) =$ thermal time required for panicle initiation)

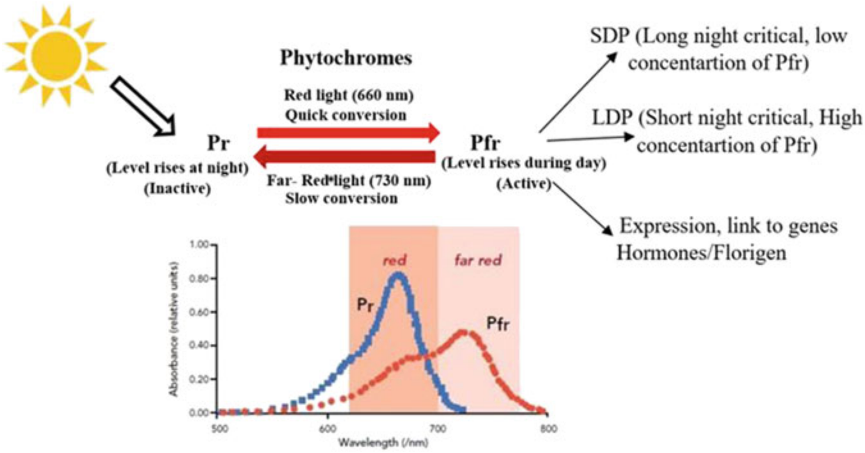

Fig. 1.18 Phytochromes photoconversion for physiological responses (e.g., germination, flowering, and photomorphogenesis) in plants

$DR_j = 1f(P_j) \sum i = 1jdtt_i$ (*threshold* method, panicle initiation occurs when the sum of temperatures $\sum dtt_i$ *meets the demand expressed by* $f(P_j)$).

These two methods have different meanings as in cumulative method plant progress every day toward flowering as function of temperature and photoperiod at variable rate. However, in threshold method, flowering is only possible if day length conditions are met.

Alagarswamy and Ritchie (1991) stated that in *cumulative linear case* $f(P_i)$ is calculated by following ways with the assumptions that phenological stage starts at the end of the juvenile phase.

If

$$P_i > P2O$$

then

$$f(P_i) = 102 + P2R(P_i - P2O)$$

Otherwise

$$f(P_i) = 102$$

For the *cumulative hyperbolic case* (as in STICS), phenological stage is assumed to start at emergence, and $f(P_i)$ is computed as follows (Brisson et al. 2003):

According to the Brisson et al. (2003), $f(P_i)$ in *cumulative hyperbolic case* is computed with assumptions that phenological stage starts at emergence. The suggested equation will be

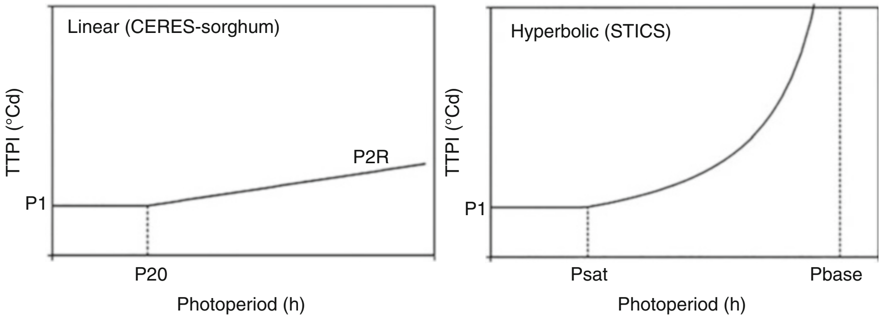

Fig. 1.19 Linear and hyperbolic relationship between the duration of vegetative stage f_p expressed as TTPI (thermal time to panicle initiation) (°C days) and photoperiod. (Source: Folliard et al. 2004; reproduced by permission of Elsevier)

if

$$P_i > P_{\text{sat}}$$

then

$$f(P_i) = P1P_{\text{sat}} - P_{\text{base}}P_i - P_{\text{base}}$$

Otherwise

$$f(P_i) = P1$$

Like the threshold concept, trigger effect has been also used to explain the concept of photoperiodicity in plants. It has been concluded by Folliard et al. (2004) that hyperbolic response to photoperiod and a daily threshold iteration procedure could be used to monitor the development of crops (Figs. 1.19 and 1.20).

APSIM model calculates photoperiod from day of year and latitude using the parameter twilight (interval between sunrise or sunset and the time when the true center of the sun is 6° below the horizon). Photoperiod affects phenology between emergence and floral initiation as elaborated by Zheng et al. (2014). Thermal time during this period (between emergence and floral initiation) is affected by photoperiod factor (f_D):

$$f_D = 1 - 0.002R_p(20 - L_p)^2$$

where L_p is the day length (h) and R_P is the sensitivities to photoperiod which is cultivar-specific and is specified by photop_sens (default value of $R_P = 3$) (Fig. 1.21).

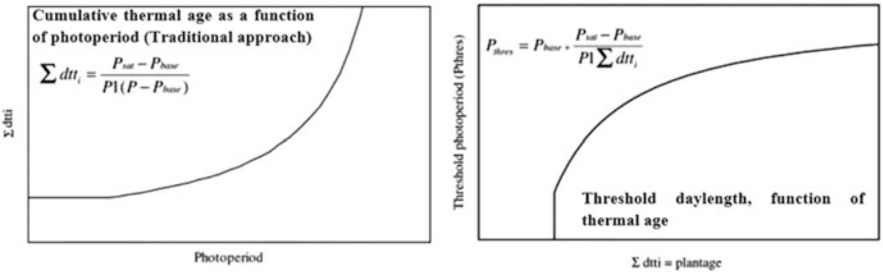

Fig. 1.20 Reversing traditional approach of cumulative thermal age as function of photoperiod to determine threshold day length as function of thermal age. (Source: Folliard et al. 2004; reproduced by permission of Elsevier)

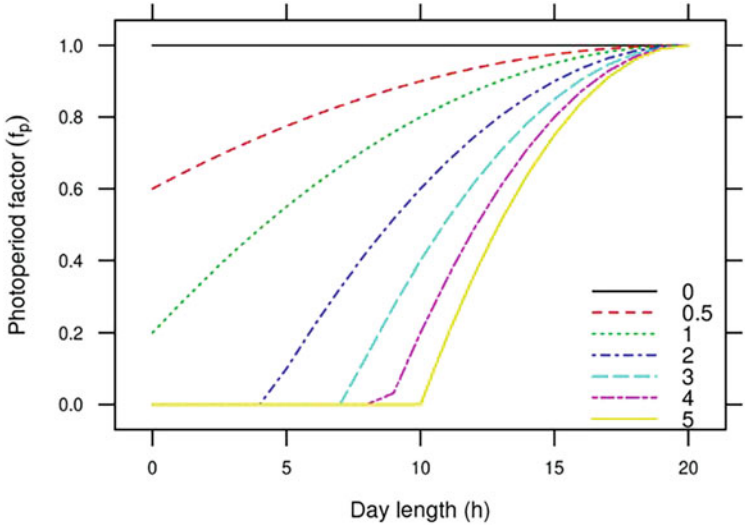

Fig. 1.21 Photoperiod approach used by APSIM. (Source: Zheng et al. 2014)

1.5.1 Photo Growing Degree Days (PGDD)

The combination of GDD with photoperiod gives another concept called as photo growing degree days (PGDD). This concept was presented by Aslam et al. (2017b) in their work to monitor wheat development between emergence and floral initiation. Firstly, the Wang and Engel (1998) degree day (WEDD) equation was used to calculate GDD with assumption that if $T_{av} < T_{min}$ or $T_{av} > T_{max}$, then WEDD $= 0$. Two different cardinal temperatures were used which includes pre-anthesis ($T_{min} = 0.00$, $T_{opt} = 27.70$, and $T_{max} = 40.00$) and post anthesis ($T_{min} = 0.00$, $T_{opt} = 32.75$, and $T_{max} = 44.00$) cardinal temperatures.

$$\alpha = {}^{\ln 2}\!/_{\ln\left(\frac{T_{\max}-T_{\min}}{T_{\mathrm{opt}}-T_{\min}}\right)}$$

$$\text{Numerator} = 2(T_{\mathrm{av}} - T_{\min})^{\alpha}\left(T_{\mathrm{opt}} - T_{\min}\right)^{\alpha} - (T_{\mathrm{av}} - T_{\min})^{2\alpha}$$

$$\text{Denominator} = \left(T_{\mathrm{opt}} - T_{\min}\right)^{2\alpha}$$

$$\text{Wang and Engel degree days (WEDD)} = \left[\frac{\text{Numerator}}{\text{Denominator}}\right]\left(T_{\mathrm{opt}} - T_{\min}\right)$$

Zheng et al. (2014) APSIM-Wheat approach was used to calculate photoperiod.

$$\text{Photoperiod} = 1 - 0.002(\text{Photoperiod coefficient}) \times (20 - \text{day length})^2$$

After combining Wang and Engel (1998) equation and Zheng et al. (2014) photoperiod approach, the new equation of photo growing degree days (PGDD) has been presented below:

$$\text{PGDD} = (\text{WEDD})(\text{Photoperiod})$$

1.6 Humidity and Vapor Pressure Deficit

Water vapor in the air is important to be considered for modeling as it can determine water lost from the leaves through the process of transpiration. Transpiration is mainly driven by water vapor pressure gradient between leaves and air through the sensing mechanism of stomata. Partial pressure of water vapor in the atmosphere is called as vapor pressure (e). The vapor pressure can be saturated $e_s(T)$ at a particular temperature (T), and relative humidity (H_r) is the ratio of vapor pressure of unsaturated air to saturated air at the same temperature and expressed in percentage (%).

The vapor pressure difference (Δe) between the inside of the leaves and the ambient air is an important variable. It depends on the foliage temperature (T_f) and vapor pressure of the air (e_a).

$$\Delta e = e_s\left(T_f\right) - e_a$$

The drying power of air is determined by the vapor pressure deficit (D):

$$D = e_s(T) - e_a = e_s(T)\left(1 - \frac{H_r}{100}\right)$$

where $e_s(T)$ is the saturated vapor pressure at T, e_a is the unsaturated vapor pressure, and H_r is the relative humidity.

According to Campbell and Norman (2012), D could be determined by following equation:

$$D = a \times e^{\frac{b \times T_{\text{air}}}{T_{\text{air}} + c}} \times \langle 1 - RH \rangle$$

where T_{air} is the air temperature (°C); RH is the relative humidity (%); and a, b, and c are constants.

Vapor pressure could be used to calculated potential evapotranspiration (PET, mm day−1) as proposed by Shuttleworth (2007):

$$\text{PET} = {}^{(mR_n + g \times 6.13 \times (1 - 0.31U) \times D}\!\big/_{L \times (m+g)}$$

where m is the slope of the saturation vapor pressure curve (kPa K^{-1}), R_n is the net irradiance (MJ m^{-2} day^{-1}), g is the psychrometric constant = 0.0016286, D is the vapor pressure deficit (kPa), U is the wind speed (m s^{-1}), and L is the latent heat of vaporization (MJ kg^{-1}).

Similarly, transpiration efficiency (TE) can also be calculated by considering "D" given below:

$$TE = {}^{BM \times D}\!\big/_{TE_n}$$

where BM is biomass, D is vapor pressure deficit, and TE_n is the normalized transpiration efficiency.

Plants have developed several adaptive strategies to survive under drought stress/ water-deficit environments. One top strategy is to limit transpiration rate under high D. Since high D usually occurs in the midday to end of day thus limiting transpiration, this situation is the best option to conserve water (Devi and Reddy 2018).

1.7 Wind

Wind affects plant growth by influencing on the transfer of water vapor, heat, and CO_2 to and from leaf and plant canopies. Thus, it has significant effects on the energy balance and transpiration of whole canopies.

1.8 Canopy Transpiration

Penman-Monteith equation is generally used to determine canopy transpiration, and in this equation canopy conductance was considered as stomatal conductance. Granier et al. (1996) concept of Penman-Monteith equation to determine stomatal conductance and canopy transpiration is

$$g_s = {}^{y\lambda T_r}/_{\rho_a C_p D}$$

where g_s is canopy stomatal conductance (m s^{-1}), y is psychrometric constant (kPa K^{-1}), λ is the latent heat of vaporization (J g^{-1}), ρ_a is dry air density (kg m^{-3}), C_p is the specific heat of air at constant pressure (J kg^{-1} K^{-1}), and D is atmospheric vapor pressure deficit (kPa).

1.9 Eddy Correlation

It is the standard technique used for the production of continuous data on the fluxes of CO_2, water vapor, and heat from extensive vegetated surfaces. Since forest occupies a major portion of land, it is mostly used to collect data from forest surfaces. Under the FLUXNET program (https://daac.ornl.gov/cgi-bin/dataset_lister.pl?p=9), large number of stations has been established to monitor CO_2 and water vapor fluxes worldwide.

1.10 Ozone Effects on Crop Modeling

The changes in ozone concentrations may harm the plants at canopy level which further affects the internal physiological processes and overall crop responses to the environment. It should be considered for the development of crop model to incorporate ozone effects to improve model performance. The observation ozone data is absent in the world, and ozone damage assessment for crop is only made through crop modeling approach (Emberson et al. 2018). It was reported by Van Dingenen et al. (2009) and Avnery et al. (2011) that worldwide ozone may reduce yield of maize (2–5%), wheat (4–15%), rice (3–4%), and soybean (5–15%). In the past, empirical concentration-based modeling was used for the assessment of yield losses due to ozone. It was followed by semiempirical ozone effects modeling, and because of certain limitations, flux-based approach was used. It accounts the statistical relationship between ozone effects and crop yield. However, dynamic process-based modeling was introduced to overcome the shortcoming of previous modeling approaches. These are most appropriate as these also consider the effective ozone flux. The effective ozone flux represents the stomatal ozone flux which is above the detoxification capacity of the plants. There large-scale application is limited by unavailability of ozone flux data.

The plants have the ability to detoxify a certain amount of ozone and remaining results damages to crop pants. The incorporation of different types of the damages to plants from ozone is necessary in model development. For generating such information, the in-depth studies must be carried out to find out the damages at various plant processes at cellular processes. Some important considerations for modeling the ozone effects on plants are necessary. These include time step, carbon assimilation, canopy development, assimilate partitioning, and water uptake and stomatal ozone uptake. The time step of 1 day is appropriate to overcome the co-variations in ozone concentration with various physiological processes. The carbon assimilation is used to assess the zone damage to photosynthesis. The canopy measurement is necessary for estimating ozone damages to leaves. Assimilate partitioning is used for incorporating the effects of ozone on leaf senescence. The water uptake and transpiration help the models to estimate the ozone effects on roots and interception of radiations on the leaves (Emberson et al. 2018). For modeling the ozone damages to the plants, the experimental datasets would be required for testing and calibration of the models. These datasets include daily, ideally hourly, ozone values and meteorological conditions during the course of the crop development and yield. The availability of such datasets is the main limitation for such studies. The development of varieties to avoid the adverse effects of the ozone on crop is also the need of the day.

1.11 Agriculture, Science, and Systems Modeling

Agriculture (cultivation of fields) consists of activities which took place at farms and results in the production of food, fuel, and fiber. The farm work involves wider ecological context; thus, agriculture and ecology interact, so agriculture could be a science that deals with the interaction of ecology/environment, soil, crops, and animals. All variables discussed in the above headings are thus most important in understanding the agricultural system on a scientific basis. Since science is the systematic study of knowledge, thus agriculture involves all important components of science. Agricultural practices involve three components, i.e., traditional, scientific, and estimation. Scientific knowledge is very important for the progress of agriculture as it involves proper steps to get answers to the problems (Fig. 1.22). In every field of life and particularly in agriculture, numbers matter; thus hypothesis needs to be expressed numerically, and in order to do this, we need to apply concepts of modeling. Thus, modeling converts qualitative data into quantitative, and it can be statistical modeling or mathematical modeling. It gives quantitative predictions to the theories which can be compared very easily in the real world (Fig. 1.23).

System is anything under observation, and it has a set of components which interacts with each other. Agricultural systems which involve crops mainly have interactions with crop, soil, environment, and management. To understand this system effectively, we need to use the concept of modeling (Fig. 1.24).

1.12 Mathematical Modeling

Modeling by the use of mathematical equations which represent the behavior of a system is called mathematical modeling. It represents the relationship between dependent and independent variables. Growth curve between applications of fertilizer and dry-matter produced by the crops could be represented by the mathematical

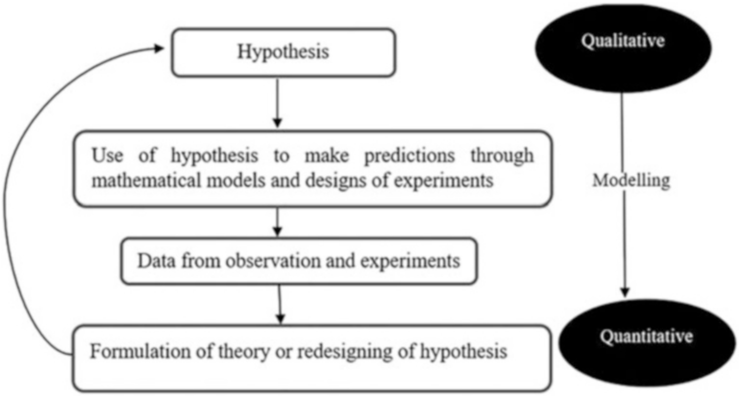

Fig. 1.22 Cycle of scientific enquiry and application of modeling

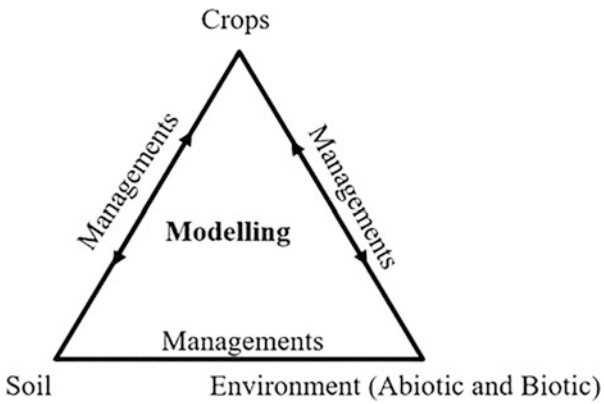

Fig. 1.23 Crops as an example of agricultural systems modeling and its interactions with different components

equations. Thornley and France (2007) describe the application of mathematical model by considering relationship between growth (G) and food intake (F) (Fig. 1.24) which is an example of static model as there is no time variable:

$$G = G_1 \frac{F}{K + F} - G_2$$

where G_1 andG_2 are growth rate, F is food intake, and K is the steepness of curve.

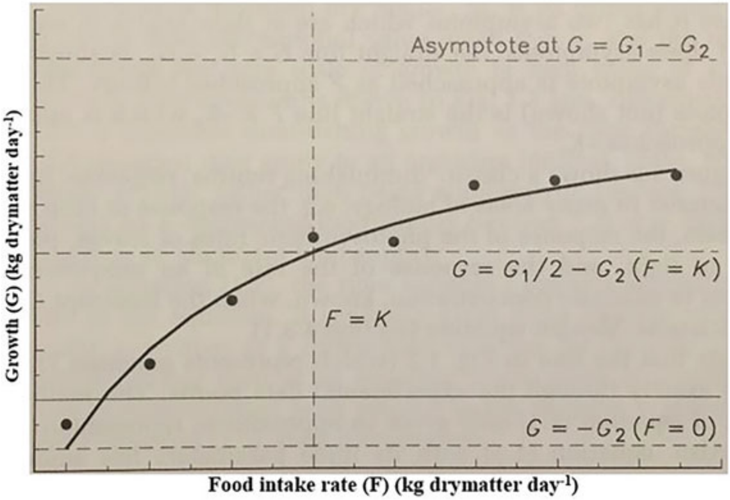

Fig. 1.24 Application of mathematical model to show relationship between animal growth and food intake. (Source: Thornley and France 2007)

1.13 Dynamic Model

Dynamic model is the model in which time is involved, and it describes time-dependent relationship. Consider the following equation,

$$DM = DM_0 + \left(DM_f - DM_0\right)\left(1 - e^{-kt}\right)$$

where DM is dry matter, DM_0 is the initial value of dry matter at $t = 0$, DM_f is the final (asymptotic) value when $t \to \infty$, and k is the rate constant that determines the time scale of growth, higher value of k means higher growth. This equation can give more practical answer when converted to the differential form, i.e., rate of change of dry matter. Thus, the equation is

$$\frac{\Delta DM}{\Delta t} = k\left(DM_f - DM\right)$$

1.14 Deterministic Models

These are models which give predictions for quantities (e.g., plant dry matter) without any associated probability distribution (Fig. 1.25).

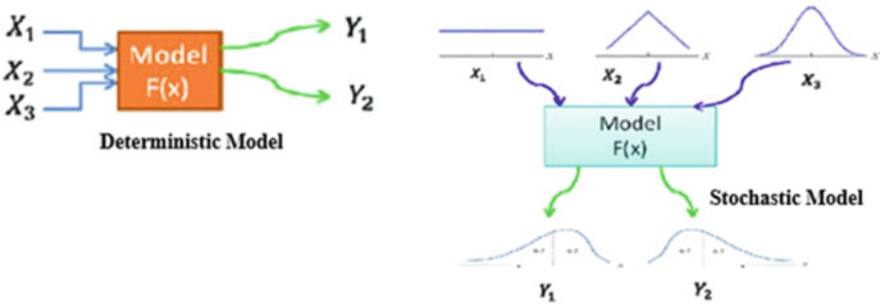

Fig. 1.25 Comparison between deterministic and stochastic models

1.15 Stochastic Models

These are models which give predictions for quantities (e.g., plant dry matter) with associated probability distribution. It involves random variables (Fig. 1.25).

1.16 Empirical Models

These are models which describe the relationship among two variables often using mathematical or statistical equation without considering scientific principles.

1.17 Mechanistic Models

These are models which can describe relationship from lower hierarchy of one variable to higher hierarchy by considering different factors and incorporate the understanding of the phenomenon which are going to be predicted. For example, crop growth rate (higher hierarchy) could be considered as function of photosynthesis, respiration, transpiration, and nutrients uptake (lower hierarchy). Mechanistic models are more research oriented than application oriented. Many models with different levels of abstraction have been presented in Table 1.5. Application of these models at different scales could help to understand the mechanisms in qualitative and quantitative way (Ijaz et al. 2017; Jabeen et al. 2017; Aslam et al. 2017a; Ahmed et al. 2014, 2016, 2017, 2018, 2019; Ahmad et al. 2017, 2019). Therefore, they can boost system efficiencies, e.g., agricultural production or agronomic activities, which might lead to the transformation of agriculture to digital agriculture. Future agronomists will be digital agronomist having strong link with data and crops. Digital technologies help to monitor soil quality, weather patterns, and crop productivity and quality. These technologies and analytical tools help to optimize key

Table 1.5 Models with different levels of abstraction

Scale	**Cell-Cm^2 (minutes day^{-1})**	**Organs (minutes day^{-1})**	**Plant or Canopy (minutes to weeks)**	**Canopy in a range of environments (Weeks to months)**
Genetic complexity				Genome wide allelic composition
Mechanisms	Transcripts/ Ion Channels/ Biophysics	Hydraulics/ Metabolism/ Hormones	Coordination/ Hormones/ Nutrients	Feedbacks, Water/C/N balances, coordination
Models	Networks Boolean and differential equation	Differential equation, gradients, Conserved fluxes	Functional structural plant model (FSPM)	Regression Models Crop Models
Abstraction	Explicit genes/Metabolites/No Explicit Organs	No explicit genes/No explicit organs/Explicit fluxes (m^2 Sec^{-1})	No explicit genes/ Explicit organs (x,y,z)/ No explicit fluxes	No explicit genes/ No explicit organs/ No explicit fluxes
Total number of parameters	100	50	100	150
Trait	Simple			Complex
Trait	Stomatal	Leaf growth rate	Radiation	Grain number

Table 1.5 (continued)

	conductance		interception efficiency	
Phenotypic distribution	Few alleles			Many alleles
Heritability	High			Low
QTLs for explaining 30% genetic variation	Few			many
References	Vialet-Chabrand et al. (2017)	Caldeira et al. (2014)	Mairhofer et al. (2012) Pradal et al. (2015)	Hammer et al. (2010); Millet et al. (2019); Tardieu et al. (2018); Louca et al. (2019); Wu et al. (2019)

component of food systems and increase productivity and profitability by giving options to reduce environmental impacts. Furthermore, digital agriculture revolution provides new means and methods for farmers to optimize management and improve crop quality and quantity even under changing climate. Traditional method of fertilizer application and other managements will be replaced by digital agricultural system which can gather data more frequently and accurately in combination with external factors. This collected data is analyzed and interpreted so that farmers can have accurate information and appropriate decisions. These decisions then can be implemented with greater accuracy through technologies (e.g., sensors, communication networks, unmanned aviation system, artificial intelligence, robotics, and advanced machinery), and afterward farmers can get real benefits. Thus, our system of agriculture will be more productive, consistent, and higher in efficiency. Many of the sustainable development goals (SDGs) can be easily achieved by adopting digital agriculture (Figs. 1.26 and 1.27).

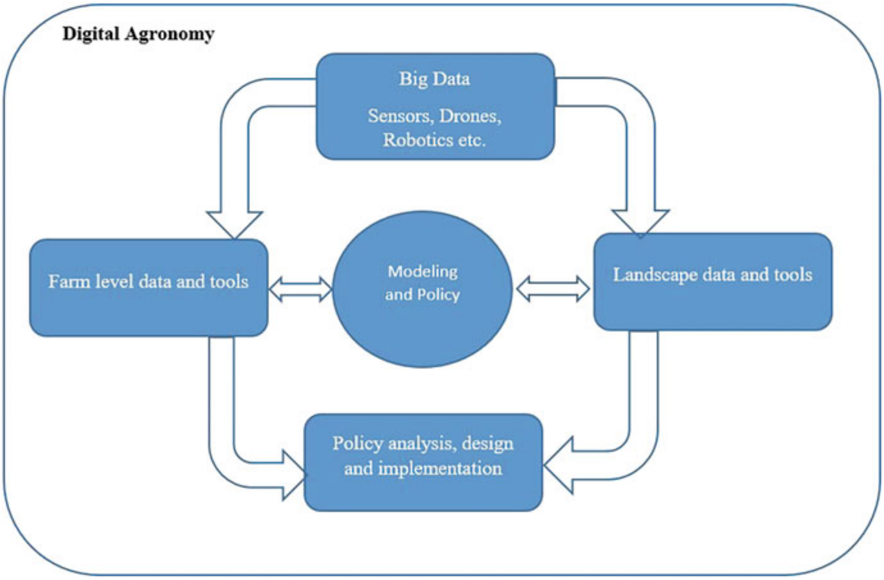

Fig. 1.26 Digital agronomy

1.18 Conclusion

Anything under observation is referred as system. The agricultural systems (farming systems and cropping systems) basically interact with the environment. In the past, the better understanding of these systems were made through quantitative experimentation and now various crop models are used for the purpose. The models are mathematical representation of the biological system. The main types of modeling include mathematical, dynamic, deterministic, stochastic, empirical, and mechanistic models. These are used to represent the relationship between dependent and independent factor, the time-dependent relation, predictions for quantities without probability distribution, predictions with associated probability, relationship between two variables through mathematical and statistical equations, and relationship of lower hierarchy of one variable to higher hierarchy, respectively. Such models can be successfully applied to estimate the impact of environmental variables on various growth processes. The impact of changes in ozone layers on crop growth may influence the model performance, since these impacts should be considered to improve model performance.

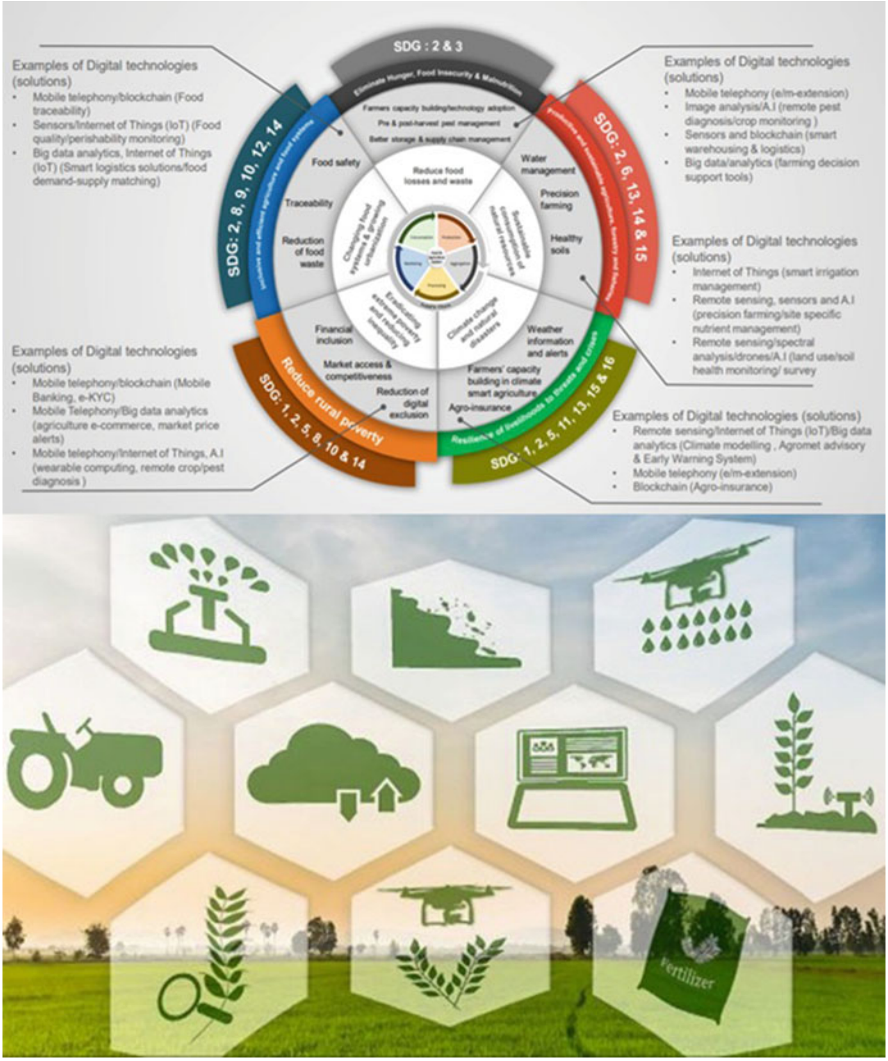

Fig. 1.27 Digital agriculture: feeding the future. (Source: ©PA Knowledge limited: https://www.paconsulting.com/ and FAO 2020: http://www.fao.org/3/nb844en/nb844en.pdf)

References

Ahmad S, Abbas G, Fatima Z, Khan RJ, Anjum MA, Ahmed M, Khan MA, Porter CH, Hoogenboom G (2017) Quantification of the impacts of climate warming and crop management on canola phenology in Punjab, Pakistan. J Agron Crop Sci 203(5):442–452. https://doi.org/10.1111/jac.12206

Ahmad S, Abbas G, Ahmed M, Fatima Z, Anjum MA, Rasul G, Khan MA, Hoogenboom G (2019) Climate warming and management impact on the change of phenology of the rice-wheat cropping system in Punjab, Pakistan. Field Crop Res 230:46–61. https://doi.org/10.1016/j.fcr.2018.10.008

Ahmed M, Aslam MA, Hassan FU, Asif M, Hayat R (2014) Use of APSIM to model nitrogen use efficiency of rain-fed wheat. Int J Agric Biol 16:461–470

Ahmed M, Akram MN, Asim M, Aslam M, F-u H, Higgins S, Stöckle CO, Hoogenboom G (2016) Calibration and validation of APSIM-wheat and CERES-wheat for spring wheat under rainfed conditions: models evaluation and application. Comput Electron Agric 123:384–401. https://doi.org/10.1016/j.compag.2016.03.015

Ahmed M, Stöckle CO, Nelson R, Higgins S (2017) Assessment of climate change and atmospheric CO_2 impact on winter wheat in the Pacific northwest using a multimodel ensemble. Front Ecol Evol 5(51). https://doi.org/10.3389/fevo.2017.00051

Ahmed M, Ijaz W, Ahmad S (2018) Adapting and evaluating APSIM-SoilP-wheat model for response to phosphorus under rainfed conditions of Pakistan. J Plant Nutr 41(16):2069–2084. https://doi.org/10.1080/01904167.2018.1485933

Ahmed M, Stöckle CO, Nelson R, Higgins S, Ahmad S, Raza MA (2019) Novel multimodel ensemble approach to evaluate the sole effect of elevated CO_2 on winter wheat productivity. Sci Rep 9(1):7813. https://doi.org/10.1038/s41598-019-44251-x

Alagarswamy G, Ritchie JT (1991) Phasic development in CERES-sorghum model. In: Hodges T (ed) Predicting crop phenology. CRC Press, Boca Raton, pp 143–152

Aslam MA, Ahmed M, Hayat R (2017a) Modeling nitrogen use efficiency under changing climate. In: Ahmed M, Stockle CO (eds) Quantification of climate variability, adaptation and mitigation for agricultural sustainability. Springer International Publishing, Cham, pp 71–90. https://doi.org/10.1007/978-3-319-32059-5_4

Aslam MA, Ahmed M, Stöckle CO, Higgins SS, Hassan FU, Hayat R (2017b) Can growing degree days and photoperiod predict spring wheat phenology? Front Environ Sci 5

Avnery S, Mauzerall DL, Liu J, Horowitz LW (2011) Global crop yield reductions due to surface ozone exposure: 2. Year 2030 potential crop production losses and economic damage under two scenarios of O3 pollution. Atmos Environ 45(13):2297–2309. https://doi.org/10.1016/j.atmosenv.2011.01.002

Bird R, Hulstrom R (1981) A simplified clear sky model for direct and diffuse insolation on horizontal surfaces, SERI. TR. Solar Energy Research Institute, Golden, CO, pp 642–761

Blackman FF (1905) Optima and limiting factors. Ann Bot 19:281–296

Boysen Jensen P (1932) Die Stoffproduktion der Pflanzen. Gustav Fischer, Jena

Brisson N, Mary B, Ripoche D, Jeuffroy MH, Ruget F, Nicoullaud B, Gate P, Devienne-barret F, Antonioletti R, Durr C, Richard G, Beaudoin N, Recous S, Tayot X, Plenet D, Cellier P, Machet J-M, Meynard JM, Delécolle R (1998) STICS: a generic model for the simulation of crops and their water and nitrogen balances. I. Theory and parameterization applied to wheat and corn. Agronomie 18:311–346

Brisson N, Gary C, Justes E, Roche R, Mary B, Ripoche D, Zimmer D, Sierra J, Bertuzzi P, Burger P, Bussière F, Cabidoche YM, Cellier P, Debaeke P, Gaudillère JP, Hénault C, Maraux F, Seguin B, Sinoquet H (2003) An overview of the crop model stics. Eur J Agron 18:309–332

Caldeira CF, Jeanguenin L, Chaumont F, Tardieu F (2014) Circadian rhythms of hydraulic conductance and growth are enhanced by drought and improve plant performance. Nat Commun 5(1):5365. https://doi.org/10.1038/ncomms6365

Campbell GS, Norman JM (2012) An introduction to environmental biophysics. Springer, New York

Carruthers TJB, Longstaff BJ, Dennison WC, Abal EG, Aioi K (2001) Chapter 19: Measurement of light penetration in relation to seagrass. In: Short FT, Coles RG (eds) Global seagrass research methods. Elsevier Science, Amsterdam

Coucheney E, Buis S, Launay M, Constantin J, Mary B, García de Cortázar-Atauri I, Ripoche D, Beaudoin N, Ruget F, Andrianarisoa KS, Le Bas C, Justes E, Léonard J (2015) Accuracy, robustness and behavior of the STICS soil–crop model for plant, water and nitrogen outputs: evaluation over a wide range of agro-environmental conditions in France. Environ Model Softw 64:177–190
De Pury DGG, Farquhar GD (1997) Simple scaling of photosynthesis from leaves to canopies without the errors of big-leaf models. Plant Cell Environ 20:537–557
Devi MJ, Reddy VR (2018) Transpiration response of cotton to vapor pressure deficit and its relationship with stomatal traits. Front Plant Sci 9
Emberson LD, Pleijel H, Ainsworth EA, van den Berg M, Ren W, Osborne S, Mills G, Pandey D, Dentener F, Büker P, Ewert F, Koeble R, Van Dingenen R (2018) Ozone effects on crops and consideration in crop models. Eur J Agron 100:19–34. https://doi.org/10.1016/j.eja.2018.06.002
Folliard A, Traoré PCS, Vaksmann M, Kouressy M (2004) Modeling of sorghum response to photoperiod: a threshold–hyperbolic approach. Field Crop Res 89:59–70
Granier A, Huc R, Barigah S (1996) Transpiration of natural rain forest and its dependence on climatic factors. Agric For Meteorol 78:19–29
Hammer G, Wright G (1994) A theoretical analysis of nitrogen and radiation effects on radiation use efficiency in peanut. Aust J Agric Res 45:575–589
Hammer G, Cooper M, Tardieu F, Welch S, Walsh B, Van Eeuwijk F, Chapman S, Podlich D (2006) Models for navigating biological complexity in breeding improved crop plants. Trends Plant Sci 11:587–593
Hammer GL, Van Oosterom E, Mclean G, Chapman SC, Broad I, Harland P, Muchow RC (2010) Adapting APSIM to model the physiology and genetics of complex adaptive traits in field crops. J Exp Bot 61:2185–2202
Holzworth DP, Huth NI, Devoil PG, Zurcher EJ, Herrmann NI, Mclean G, Chenu K, Van Oosterom EJ, Snow V, Murphy C, Moore AD, Brown H, Whish JPM, Verrall S, Fainges J, Bell LW, Peake AS, Poulton PL, Hochman Z, Thorburn PJ, Gaydon DS, Dalgliesh NP, Rodriguez D, Cox H, Chapman S, Doherty A, Teixeira E, Sharp J, Cichota R, Vogeler I, Li FY, Wang E, Hammer GL, Robertson MJ, Dimes JP, Whitbread AM, Hunt J, Van Rees H, Mcclelland T, Carberry PS, Hargreaves JNG, Macleod N, Mcdonald C, Harsdorf J, Wedgwood S, Keating BA (2014) APSIM – evolution towards a new generation of agricultural systems simulation. Environ Model Softw 62:327–350
Ijaz W, Ahmed M, Asim M, Aslam M (2017) Models to study phosphorous dynamics under changing climate. In: Ahmed M, Stockle CO (eds) Quantification of climate variability, adaptation and mitigation for agricultural sustainability. Springer International Publishing, Cham, pp 371–386. https://doi.org/10.1007/978-3-319-32059-5_15
Jabeen M, Gabriel HF, Ahmed M, Mahboob MA, Iqbal J (2017) Studying impact of climate change on wheat yield by using DSSAT and GIS: a case study of Pothwar region. In: Ahmed M, Stockle CO (eds) Quantification of climate variability, adaptation and mitigation for agricultural sustainability. Springer International Publishing, Cham, pp 387–411. https://doi.org/10.1007/978-3-319-32059-5_16
Jones JW, Hoogenboom G, Porter CH, Boote KJ, Batchelor WD, Hunt LA, Wilkens PW, Singh U, Gijsman AJ, Ritchie JT (2003) The DSSAT cropping system model. Eur J Agron 18:235–265
Kempes CP, West GB, Crowell K, Girvan M (2011) Predicting maximum tree heights and other traits from allometric scaling and resource limitations. PLoS One 6:e20551
Landsberg J, Sands P (2011a) Chapter 2: Weather and energy balance. Elsevier, Terrestrial Ecology
Landsberg J, Sands P (2011b) Chapter 3: Physiological processes. In: Terrestrial ecology. Elsevier, Oxford
Lindquist JL, Arkebauer TJ, Walters DT, Cassman KG, Dobermann A (2005) Maize radiation use efficiency under optimal growth conditions. Agron J 97:72–78
Lobell DB, Hammer GL, Chenu K, Zheng B, Mclean G, Chapman SC (2015) The shifting influence of drought and heat stress for crops in Northeast Australia. Glob Chang Biol 21:4115–4127

Loomis RS, Williams WA (1963) Maximum crop productivity: an Extimate1. Crop Sci 3(1): cropsci1963.0011183X000300010021x. https://doi.org/10.2135/cropsci1963.0011183X000300010021x

Louca S, Scranton MI, Taylor GT, Astor YM, Crowe SA, Doebeli M (2019) Circumventing kinetics in biogeochemical modeling. Proc Natl Acad Sci 116(23):11329–11338. https://doi.org/10.1073/pnas.1819883116

Mairhofer S, Zappala S, Tracy SR, Sturrock C, Bennett M, Mooney SJ, Pridmore T (2012) RooTrak: automated recovery of three-dimensional plant root architecture in soil from X-ray microcomputed tomography images using visual tracking. Plant Physiol 158(2):561–569. https://doi.org/10.1104/pp.111.186221

Maskell EJ (1928) Experimental researches on vegetable assimilation and respiration. XVIII.—the relation between stomatal opening and assimilation.—a critical study of assimilation rates and porometer rates in leaves of Cherry Laurel. Proc R Soc Lond Ser B 102:488–533

Millet EJ, Kruijer W, Coupel-Ledru A, Alvarez Prado S, Cabrera-Bosquet L, Lacube S, Charcosset A, Welcker C, van Eeuwijk F, Tardieu F (2019) Genomic prediction of maize yield across European environmental conditions. Nat Genet 51(6):952–956. https://doi.org/10.1038/s41588-019-0414-y

Monsi M, Saeki T (1953) Über den Lichtfaktor in den Pflanzengesellschaften und seine Bedeutung für die Stoffproduktion. Jpn J Bot 14:22–52

Monteith JL, Unsworth MH (2013) Chapter 13 – steady-state heat balance: (i) Water surfaces, soil, and vegetation. In: Monteith JL, Unsworth MH (eds) Principles of environmental physics, 4th edn. Academic Press, Boston, pp 217–247. https://doi.org/10.1016/B978-0-12-386910-4.00013-5

Oxford Dictionary of English (2010) Oxford University Press. ISBN: 9780199571123. https://doi.org/10.1093/acref/9780199571123.001.0001

Pradal C, Fournier C, Valduriez P, Cohen-Boulakia S (2015) OpenAlea: scientific workflows combining data analysis and simulation. Paper presented at the Proceedings of the 27th international conference on Scientific and Statistical Database Management, La Jolla, CA

Reed K, Hamerly E, Dinger B, Jarvis P (1976) An analytical model for field measurement of photosynthesis. J Appl Ecol 13:925–942

Shuttleworth WJ (2007) Putting the ‘vap’ into evaporation. Hydrol Earth Syst Sci 11:1–35

Sinclair TR, Muchow RC (1999) Radiation use efficiency. In: SPARKS DL (ed) Advances in agronomy. Academic, New York

Sinclair TR, Shiraiwa T, Hammer GL (1992) Variation in crop radiation-use efficiency with increased diffuse radiation. Crop Sci 32:1281–1284

StÖckle CO, Donatelli M, Nelson R (2003) CropSyst, a cropping systems simulation model. Eur J Agron 18:289–307

Tardieu F, Simonneau T, Muller B (2018) The physiological basis of drought tolerance in crop plants: a scenario-dependent probabilistic approach. Annu Rev Plant Biol 69(1):733–759. https://doi.org/10.1146/annurev-arplant-042817-040218

Thomas B (2003) Regulators of growth photoperiodism. In: Thomas B (ed) Encyclopedia of applied plant sciences. Elsevier, Oxford

Thomas B, Vince-Prue D (1997) Photoperiodism in plants. Academic, San Diego

Thornley JH (1976) Mathematical models in plant physiology. Academic, London

Thornley JHM (1998) Dynamic model of leaf photosynthesis with acclimation to light and nitrogen. Ann Bot 81:421–430

Thornley JH, France J (2007) Mathematical models in agriculture: quantitative methods for the plant, animal and ecological sciences. CABI, Cambridge, MA

Van Dingenen R, Dentener FJ, Raes F, Krol MC, Emberson L, Cofala J (2009) The global impact of ozone on agricultural crop yields under current and future air quality legislation. Atmos Environ 43(3):604–618. https://doi.org/10.1016/j.atmosenv.2008.10.033

Vialet-Chabrand SRM, Matthews JSA, McAusland L, Blatt MR, Griffiths H, Lawson T (2017) Temporal dynamics of stomatal behavior: modeling and implications for photosynthesis and water use. Plant Physiol 174(2):603–613. https://doi.org/10.1104/pp.17.00125
Wang E, Engel T (1998) Simulation of phenological development of wheat crops. Agric Syst 58 (1):1–24. https://doi.org/10.1016/S0308-521X(98)00028-6
Wang S, Grant RF, Verseghy DL, Black TA (2001) Modelling plant carbon and nitrogen dynamics of a boreal aspen forest in CLASS – the Canadian Land Surface Scheme. Ecol Model 142:135–154
Wu S, Wang X, Reddy U, Sun H, Bao K, Gao L, Mao L, Patel T, Ortiz C, Abburi VL (2019) Genome of 'Charleston Gray', the principal American watermelon cultivar, and genetic characterization of 1,365 accessions in the US National Plant Germplasm System watermelon collection. Plant Biotechnol J 17(12):2246–2258
Yan W, Hunt LA (1999) An equation for modelling the temperature response of plants using only the cardinal temperatures. Ann Bot 84:607–614
Yan W, Wallace DH, Ross J (1996) A model of photoperiod × Temperature interaction effects on plant development. Crit Rev Plant Sci 15(1):63–96. https://doi.org/10.1080/07352689609701936
Yan W, Wallace DH (1998) Simulation and prediction of plant phenology for five crops based on photoperiod × temperature interaction. Ann Bot 81:705–716
Ye Z-P (2007) A new model for relationship between irradiance and the rate of photosynthesis in Oryza sativa. Photosynthetica 45:637–640
Yin X, van Laar HH (2005) Crop systems dynamics: an ecophysiological simulation model for genotype-by-environment interactions. Wageningen Academic Publishers, Wageningen
Yin X, Kropff MJ, Mclaren G, Visperas RM (1995) A nonlinear model for crop development as a function of temperature. Agric For Meteorol 77:1–16
Zheng B, Chenu K, Doherty A, Doherty T, Chapman L (2014) The APSIM-wheat module (7.5 R3008). In: APSRU Toowoomba, Australia
Zhou G, Wang Q (2018) A new nonlinear method for calculating growing degree days. Sci Rep 8:10149

Crop Phenotyping

2

Muhammad Tariq, Mukhtar Ahmed, Pakeeza Iqbal, Zartash Fatima, and Shakeel Ahmad

Abstract

The visible form of an organism is the result of its genotype, environment and complex interaction and is referred to as phenotype. Quick, precise and non-destructive measurement of phenotypic traits has been of key importance in the field of plant breeding and crop production. The image-based non-destructive phenotyping started in early twenty-first century, and these techniques are based on spectra, canopy temperature and visible light. Initially, such approaches were used for phenotyping the plants in a controlled environment, where the influence of the environment could not be considered for phenotypic expression. Hence, the need for the development of high-throughput phenotyping (HTPPs) was realized to get the required information. This chapter provides an overview of advanced phenotyping techniques with special focus on field phenotyping. These techniques have the ability to evaluate multiple traits of interest from mixed populations, monitoring of crop growth and development, and health, and also provide key information on various physiological processes. The range of plant phenotyping techniques starts from phenotyping the whole plant canopy to organ and tissue.

M. Tariq
Central Cotton Research Institute, Multan, Pakistan

M. Ahmed
Department of Agricultural Research for Northern Sweden, Swedish University of Agricultural Sciences, Umeå, Sweden

Department of Agronomy, Pir Mehr Ali Shah Arid Agriculture University, Rawalpindi, Pakistan

P. Iqbal
Department of Botany, University of Agriculture, Faisalabad, Pakistan

Z. Fatima · S. Ahmad (✉)
Department of Agronomy, Bahauddin Zakariya University, Multan, Pakistan
e-mail: shakeelahmad@bzu.edu.pk

M. Ahmed (ed.), *Systems Modeling*, https://doi.org/10.1007/978-981-15-4728-7_2

Keywords

Phenotype · Non-destructive measurement · High-throughput phenotyping (HTPPs) · Phenotyping technique

2.1 Definition and Introduction

The description of plant anatomical, biochemical, physiological and ontogenetical properties of plants in quantitative term is called plant phenotyping (Walter et al. 2015), and producing such description is the basic objective of phenotyping (Guo and Zhu 2014). The phenotype may be described as the functional plant body, which is formed during growth and development by interaction of the genotypes with the physical environment. The term phenotype was initially known during the 1960s. The study of phenotypes at a large-scale level is termed phenomics. Besides genetic (G) and environmental factors (E), management practices (M) also influence the phenotypic expression, thus phenotype is the result of G × E × M (Porter and Christensen 2013). Because of complex interactions, it is difficult to estimate the individual contribution of these factors in phenotypic expression. Mathematically, it would be expressed according to the following proposed formula

$$Phenotype = G \times E \times M$$

The visible plant shape that we observe is the expression of genotypes in a given environment. The cob size and colour in Fig. 2.1 are phenotypic characters that resulted from genetic and environmental influence. The selection of the best genotypes based on phenotypic characters has been in practice since a long time ago. In this conventional system, one or few traits act as a basis of selection without considering the functional analysis of constituent traits. Moreover, the system is labor-intensive, time-consuming and expensive, which is a bottleneck for efficient breeding (Fig. 2.2). Various disciplines like agronomy, information technology, math, engineering and modern image analysis technologies are integrated together in the field of phenotyping. Many advanced phenotypic platforms have been made by realizing the need for phenotyping multiple traits in a short time. The major focus of the latest phenotyping techniques in literature has been non-destructive optical analysis through imaging techniques.

Such platforms are based on various imaging techniques to estimate the plant morphology, biomass, health, plant water contents, photosynthesis etc. The modern high-throughput plant phenotyping platforms (HTPPP) are low-cost, automated, precise and have the ability to analyze images (Pratap et al. 2019). The non-destructive image-based identification of traits to a field level has gained popularity since the beginning of the twenty-first century. Now, new techniques have been developed that are not only helpful for trait identification but also are very important for monitoring overall crop growth and development.

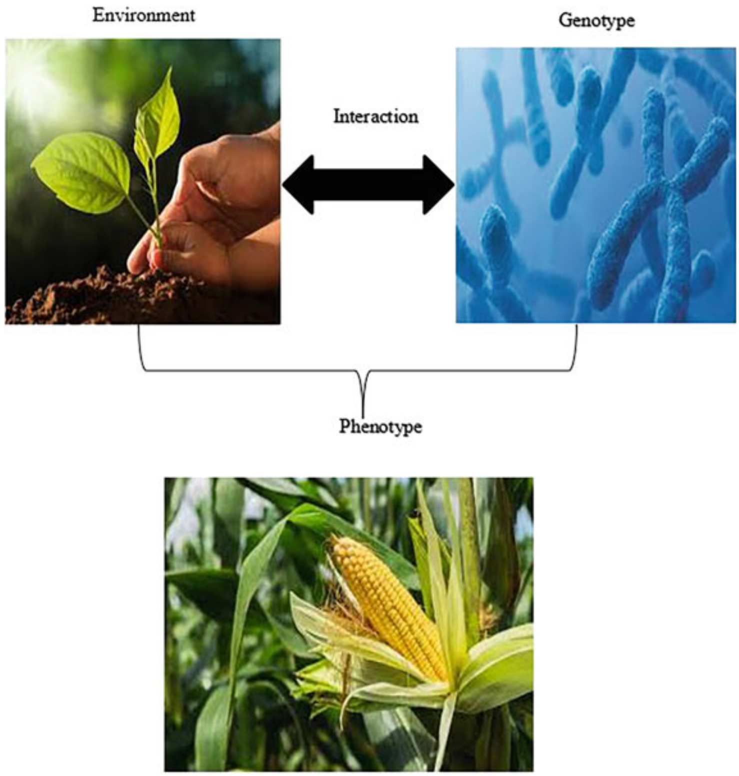

Fig. 2.1 Phenotype is the outcome of genotype and environment

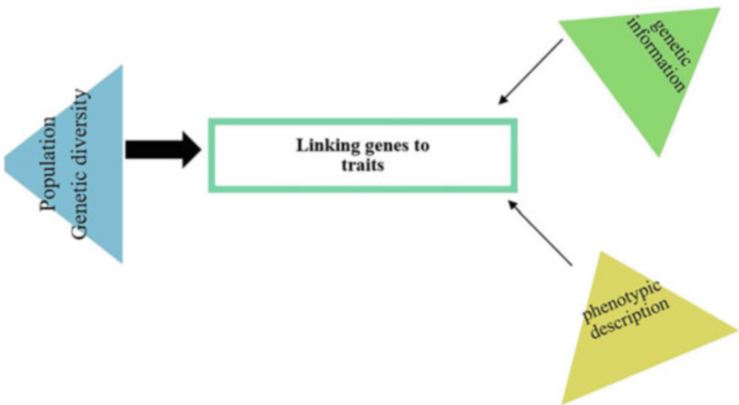

Fig. 2.2 Phenotyping as a bottleneck in developing genetic information

Agriculture is the main source of food, fibre, fuel and raw materials, which are vital components for human livelihood. In this era of climate change, it is very important to uplift the agricultural sector in such a way that it can ensure environmental sustainability and food security (Ahmed et al. 2013; Ahmed and Ahmad 2019; Ahmed and Stockle 2016; Ahmed 2020). Thus, to ensure food for billions of people in future it is very important to adopt modern tools in agricultural production. Remote sensing (RS) has the potential to support the adaptive evolution of agricultural practices to face the future challenges by providing information throughout the seasons at different spatio-temporal scales. It is the collection of information about the phenomenon or an object without making any physical contact. Different agronomical variables and plant traits e.g. canopy height and green area index (Primary variables) and grain yield (Secondary variables) can be estimated by RS. Different empirical and deterministic approaches could be used to retrieve information. Application of RS is gaining attention in different agricultural disciplines such as crop breeding, crop yield forecasting, crop damage assessment, cropping systems analysis, stress detection in crop, evaluation of **pests and disease infestation, soil moisture estimation, drought monitoring and nutrient deficiency detection.**

Sensors are devices that detect and respond to input from physical environment. The resultant outputs are signals, which are subjected to further process to make them readable for humans. These are actually a part of a bigger system; a few classes of sensors include temperature sensors, light sensors, colour sensors and humidity sensors. Sensor use has become so common that we are living in the world of sensors. The arrangement of light according to wavelength of visible, ultraviolet and infrared light is called as spectrum. The term was first used by Isaac Newton in the seventeenth century to describe the range of colours when light passes through a prism or drop of water.

Remote sensing is an important phenotyping technique, and the term remote sensing was first introduced by Ms. Evelyn Pruitt in the U.S. Office of Naval Research during the 1950s. As the word “remote” indicates, it is a technique of obtaining information from long distances. Remote sensing uses various active and passive sensors, which are mostly deployed on satellites and other related platforms. Radio detection and ranging (RADAR), optical sensor and near-infrared sensors are the main sensors used in remote sensing. The data recorded by sensors fall in the range of electromagnetic spectrum, and these datasets are further subjected to processing techniques for image and signal analysis.

The Yara N-Sensor ALS 2 (active light source) is used for monitoring crop nitrogen requirement through measuring light reflectance from canopy. Crop identification, land use systems, land cover, monitoring of crop health and field phenotyping are a few applications of remote sensing in agriculture. The SPAD reading is based on the light transmission through the leaf, which is emitted from light-emitting diodes at 650 and 940 nm. The reflected light from the canopy is measured with sensors, and technology is used for non-destructive measurement of the leaf area (Kim et al. 2012).

The choices of phenotyping tool vary with scale of measurement, as phenotyping in controlled environment is carried out with automated phenotyping platform.

Fig. 2.3 Pictorial view of various phenotypic approaches developed by Australian Phenotypic Facility

While high-throughput phenotyping is used at field scale level, in-depth and high resolution is used for organ, tissue and cell characterization. Generally, a complex micro-phenotyping is recommended for studying the phenotypes at cellular and tissue level (Ahmed et al. 2020; Zhao et al. 2019). Phenotyping is equally important particularly for precision farming like its basic role in plant breeding. It is being applied for irrigation, fertilizer application, weeds detection and overall monitoring of plant health, and the key aim is to improve crop management practices. The physical crop damage from different biotic and abiotic stresses is assessed with the help of satellite imaging. The tools developed from Australian Plant Phenomics Facility are presented in Fig. 2.3. The future success of plant phenotyping lies in synergy between national and international organizations working in this particular field (Coppens et al. 2017).

2.2 Field Phenotyping

High-throughput phenotyping devices were initially developed to study phenotypes in growth chambers and green houses and mainly used to characterize individual plant characters. These technologies do not fulfill the requirement of field phenotyping, as plant phenotypes in controlled environments do not fully depict the environment and genotype interactions. Phenotyping at field scale is very important because visible characters express the role of genetic factors. High-throughput field phenotyping (HTPPs) is classified into two types, namely based and aerial HTPPs. Ground-based HTPPs are mostly used for phenotyping at plot level, while aerial HTPPs are made for entire fields. Ground-based HTPPs are driven by cart, tractor etc., and aerial HTPPs use small airplanes, drones, unmanned small aerial platforms etc. The important pillars of field phenotyping are trait of interest, sensors for measurement, positioning of sensors mounted on the system, experimental sites and environmental monitoring (Muller et al. 2018). The current phenotyping platform uses spectral imaging and sensor technologies in the form of ground wheels, aerial vehicles and robotics, equipped with high-quality sensors, cameras and computing devices (Fritsche-Neto and Borém 2015; Pratap et al. 2019). However, the proper working of these platforms depends on a set of conditions. For example, ground-based field phenotyping platform is unsuitable for large crops like maize (Montes et al. 2011), and the use of aerial vehicles is a better alternative.

The phenotypic characterization of various plant parts (root, stem and leaves), physiological processes (leaf water and chlorophyll contents) and detection of abiotic stresses through canopy temperature measurement and stomatal conductance have been successfully carried out through these modern imaging technologies (Pratap et al. 2019). Morphological plant phenotyping is carried out at three levels including plant and canopy scale in the fields, plant and organ scale and microscale laboratory (Wang et al. 2019). Roots are important plant parts, and studies on root variations are very important particularly for nutrient and water uptake. Root architecture was conventionally studied through excavating roots followed by washing with water. It was very difficult to study the genetic control of roots due to laborious root excavation processes. Following the roots, phenotyping seedling vigor and shoot growth is another important study to quantify the genetic impact. The estimation of genetic variations with respect to plant height, leaf area, canopy, number and angle of branches in necessary for field conditions.

Light reflection from the leaves is related to the concentration of various pigments in the leaves. Light reflection in visible light is associated with chlorophyll, lutein and carotenoids in the palisade tissues. Meanwhile, light reflection in the range of near-infrared band is used for cell composition (Yang et al. 2017). Yield prediction is made in an indirect way like measuring canopy temperature, leaf chlorophyll and nitrogen status and various growth and development indicators.

The collection of phenotypic data from field population is the first step, which is followed by phenotypic extraction based on image analysis. The image is extracted on the basis of geometry, texture, quantity and colour. The use of clustering algorithm, support vector machines and neutral network are some important techniques for image analysis of field-based phenotyping (Singh et al. 2016). The conversion of image into quantitative data is relatively more tedious in field phenotyping. The advanced non-destructive imaging techniques used in literature for phenotyping plant traits are listed in Table 2.1.

Table 2.1 Description of a few examples of modern phenotypic techniques in crop sciences

Sr. No.	Crop	Parameters	Technique	Reference
1	Rapeseed	Biomass and nitrogen	Laser-induced chlorophyll florescence	Thoren and Schmidhalter (2009)
2	Maize	Crosssection, cortex and steel studies	Laser Ablation Tomography (LAT)	Burton et al. (2012)
3	Sorghum	Plant architecture, height and stem diameter	Phenobot 1.0	Fernandez et al. (2017)
4	Sorghum	Shoot height, leaf area	Microsoft Kinect cameras	McCormick et al. (2016)
5	Maize	Biomass	Spectral reflectance sensors and light curtains	Montes et al. (2011)
6	Cotton	Plant height, canopy temperature and NDVI	Infrared thermometer, sonar proximity sensor and multispectral crop canopy sensor	Andrade-Sanchez et al. (2014)
7	Maize	Water stress	Thermography	Romano et al. (2011)
8	Grapevine	Water status	Near-infrared spectroscopy	De Bei et al. (2011)
9	Wheat	Canopy temperature	Airborne thermography	Deery et al. (2016)
10	Barley and sugar beet	Laser scanning	Crop height	Hoffmeister et al. (2016)

Table 2.2 Randomized Complete Block Design (RCBD) for evaluation of the cotton genotypes yield performance

R1	**V1**	**V2**	**V3**	**V4**
R2	V2	V3	V4	V1
R3	V4	V1	V2	V3

Note: No. of replications: 3; Plant-to-plant distance: 22.5 cm; Row-to-row distance: 75 cm; Net plot size: 600 cm × 1000 cm; Plant population: 355

2.3 Experimental Designs

The details of randomization and layout Randomized Complete Block Design (RCBD) for cotton genotypes are presented in Table 2.2. The historical weather trends of the experimental site (at latitude 30°12′N, longitude 71°28′E and altitude 123 m a.s.l.) are given in Fig. 2.4. For modelling purposes, the meteorological data (Tmax, Tmin, solar radiation and precipitation), soil data (texture, structure and fertility profile) and crop management data (date and method of sowing, time,

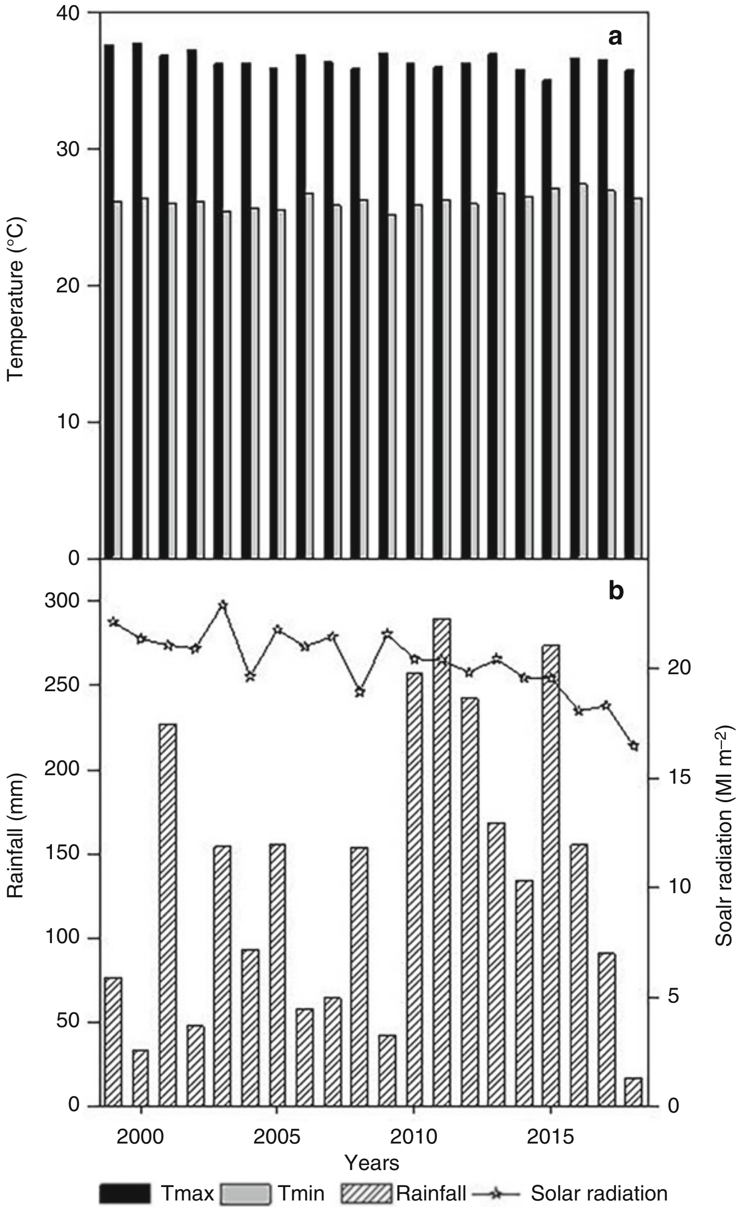

Fig. 2.4 Historical seasonal weather data (Tmax, Tmin, rainfall and solar radiation) from 1999–2018 during cotton season at Multan, Pakistan

amount and method of nutrient application and irrigation) would be required (Ahmed et al. 2014, 2016, 2017, 2018, 2019; Ahmad et al. 2017, 2019. The time to events like days to emergence, squaring, flowering and first boll split would describe the phenology data. The quantitative measurement of total dry matter, leaf area index (LAI) and seedcotton yield will be made through destructive and non-destructive means (Ahmad and Hasanuzzaman 2020). The plants are harvested from field for destructive sampling and rows allocated for destructive sampling are not used for yield measurement. In non-destructive samplings, advanced tools are used, which have the ability to quantitatively measure the various traits in the field. The non-destructive measurement of leaf area index of row crops is carried out with allometric methods, AccuPAR, Li-cor's LAI-2000 Plant Canopy Analyzer, Decagon Devices and Delta T Devices' SunScan. The Digital Vegetation Charting Techniques (DVCT), visual obstruction and light penetration, terrestrial laser scanning and attenuated total reflection (ATR)-fourier transform infrared (FTIR) spectroscopy are helpful for non-destructive biomass measurement. However, the accuracy of non-destructive method often falls below the destructive measurement because it provides estimated values.

2.4 Phenotyping Types

2.4.1 3D Laser Scanner

2D phenotyping systems lack the in-depth structural information and influence of plant structure (Großkinsky et al. 2015). These are especially designed to record the 3D view of plant shoot and branching pattern to monitor the geometric development. 3D systems are applied for measurement of biomass and other morphological traits in the field, while in a controlled environment, it is applicable for the measurement of leaf angles and growth rates. The 3D measuring techniques are described by active and passive sensors (Paulus 2019). Active sensors are light emitters and passive sensors utilize the sunlight for recording phenotypic parameters. The time of flight measurement and triangulation-based systems are categorized under active sensors, and structure from motion and light field camera use passive sensors. Although 3D imaging techniques are being used as important tools for phenotyping, they cannot evaluate the hidden plant organs like roots, and their performance is negatively affected by sunlight and plant movement. The detailed processes used in 3D phenotyping are shown in Fig. 2.5.

2.4.2 X-Ray Tomography

It is a part of electromagnetic spectrum but uses short wavelength than ultraviolet (UV) imaging. The tomography technique is used as a 3D phenotyping method, and it is the best approach to investigate the internal plant structure for in vivo phenotyping. Computerized tomography (CT) is being combined with other imaging techniques to extend its utilization. For example, combining with inflorescence imaging and positron emission tomography (PET) has been done for determining the metal concentration in the tissue and to trace the positron-emitting

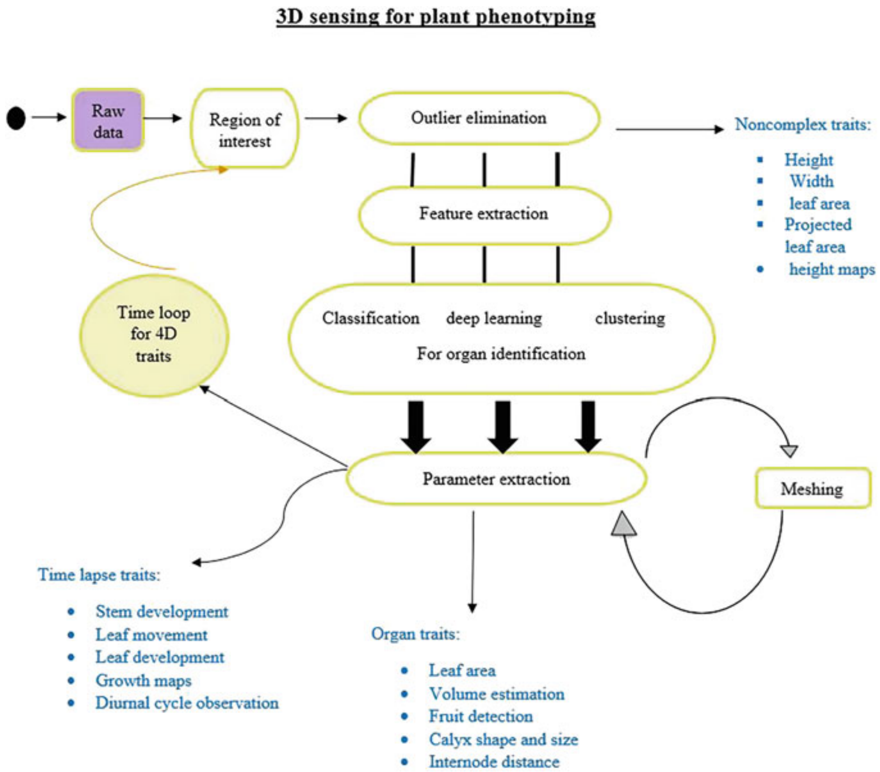

Fig. 2.5 The detail of 3D phenotyping

radionucleotides, respectively (Punshon et al. 2013; Garbout et al. 2012). Tracing of positron-emitting radionucleotides has been an important application for the quantification of real-time soil–plant interaction. Photoacoustic tomography (PAT) is used for recording anatomical and functional readings of organelles to organs (Wang and Hu 2012).

2.5 Phenomics

The term phenomics was derived from the word "phenome" indicating phenotype, and the study of phenotype is referred as phenomics. Furthermore, Furbank and Tester (2011) defined plant phenomics as the study of plant growth, performance and composition. The systematic study of physical and biochemical traits of an organism with the concerns of efficient measurement and analysis of the phenotypic traits at various levels of organization (Houle et al. 2010). Therefore, it may be called as a link between genomics and environment. Analogous to genomics, the concept of phenomics was introduced by Nicholas Schork in 1997. The overall concept of phenomics is given in Fig. 2.6. The importance of the phenomics can be judged by

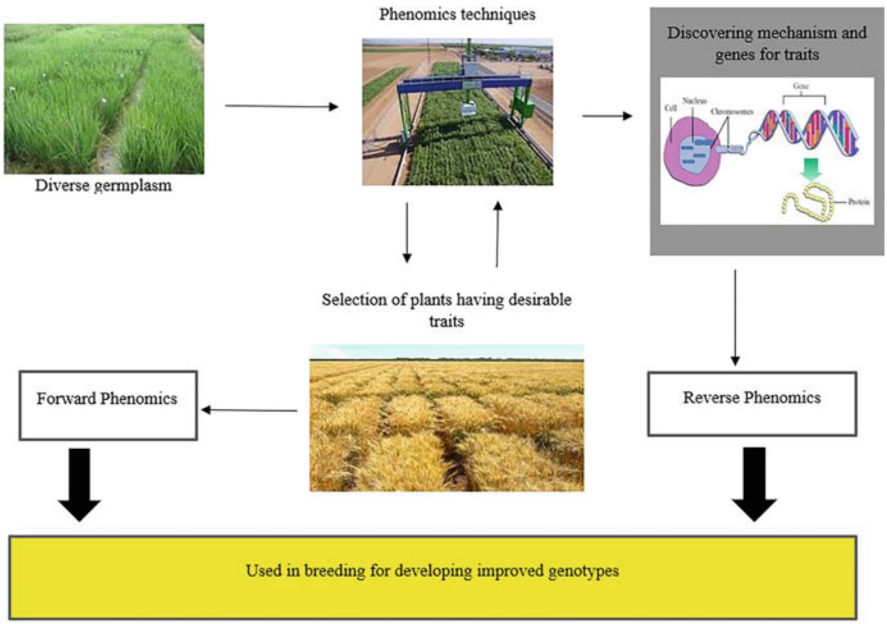

Fig. 2.6 Diagrammatic concept of phenomics

the fact that the phenotype of an organism is of great importance for agronomists as well as biologists than the corresponding genotypes. There are two types of phenomics i.e. forward phenomics and reverse phenomics. In the first type, the germplasm is screened out for valuable traits, and in the second type, a detailed dissection of these traits is performed to understand the mechanism and its exploitation in new approaches. Fig. 2.7 represents the different steps of phenomics**.**

2.6 Plant Phenotyping Techniques

The following high-throughput field phenotyping techniques were proposed by Chawade et al. (2019).

2.6.1 Satellite Imaging

Satellites are objects that revolve around other objects; moon is a satellite (natural satellite) of the Earth (object). Medium-resolution satellite data is free, while high-resolution data is provided commercially. High-resolution satellite imaging is required for phenotyping for breeding because plots are relatively small. A few examples of satellite imaging technologies are WorldView-3, WorldView-4, Digital Globe WorldView-2 and CBERS-2. WorldView-3 is the most advanced form of

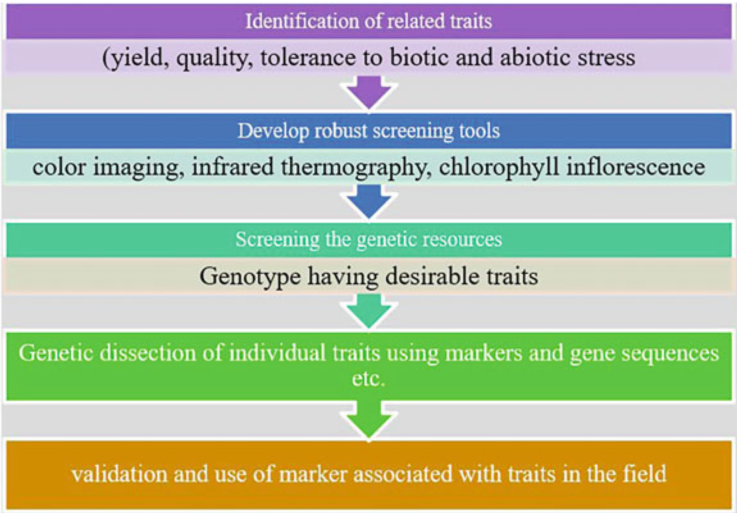

Fig. 2.7 Steps in plant phenomics

satellite imaging with spatial sensor resolution of 0.31 m GSD (ground sample distance) and multispectral resolution of 1.24 m (Chawade et al. 2019). Satellite imaging is not very useful for phenotyping small plots, for which remote sensing and proximal phenotyping are recommended. Satellite imaging is performed for phenotyping large plots and multilocation trials. It has been applied for monitoring growth (Nandibewoor et al. 2015) and vegetation height (Petroua et al. 2012). The sensors have no direct contact with the object, and carry information from object to sensors through physical career in intervening medium. The remote sensing data ranges between visible and reflective infrared regions, hence reflectance from the object determines the range of spectrum.

2.6.2 Unmanned Aerial Vehicles (UAVs)

These are flown at relatively low height, thus have least GSD and provide better spatial, spectral and temporal resolution than satellite imaging. Hence, it provides better trait identification, and chances of data losses due to clouds, smog and raining are very rare (Su et al. 2019). There are four different types of UAVs, which include parachute, blimps, rotocopter and fixed wing (Sankaran et al. 2015). Their respective payload and flight time values are 1.5, >3.0, 0.8–8.0, 1.0–10 kg and 10–30, ~600, 8–120, 30–240 min. The parachutes and blimps are simple in operation but performance is affected by winds, mainly due to light weight. The main advantages of rotocopters are navigation facility, flying and carrying capacity of multiple sensors. However, its battery and flight timing are limited by high payload. Just like rotocopters, the fixed wings UAVs also have waypoint navigation systems, better flight and hold multiple sensors. At the same time, their working is limited by low hovering capacity and high velocity. The technique was applied for measuring plant height of sorghum and vegetation cover and leaf area index of wheat; strong correlations were observed between UAVs and ground truth values (Shi et al. 2016).

2.6.3 Proximal Phenotyping

Phenotyping with ground-based vehicles equipped with sensor is referred to as proximal phenotyping (Chawade et al. 2019). The sensors may be mounted on vehicles or may be handheld. The handheld devices can evaluate small number of plots, while sophisticated mobile vehicles should be used for phenotyping large fields. Few examples of ground-based vehicles are Phenocart, Proximal sensing cart, Phenomobiles, PhenoTrac 4 and GPhenoVision. These crafts or vehicles are advantageous over the handheld devices because of their ability to move and evaluate multiple traits over multiple rows in a single pass. The screening of cotton genotypes for drought tolerance has been carried out through proximal sensing cart (Thompson et al. 2018).

2.6.4 Thermography or Thermal Imaging

Thermography is basically a remote sensing technique that integrates canopy temperature approach to make the selection process speedier for drought tolerance. It records the surface temperature by evaluating the long-wave radiations which are being emitted from the surface of the leaves. More infrared radiations are discharged from the canopy of stressed plants due to low water content. The thermal camera is highly temperature sensitive and detects minor fluctuations in temperature. It is placed at a certain distance to record leaf information on large canopies. The leaves temperature is used to measure transpiration rate because of their close association. Hence, this technology is used for plant water status to monitor irrigation requirement and to detect drought tolerance trait in a population. The temperature differences are indicated by variations of image colour. It was observed that the image colour for maize was blue, light blue, green, yellow, red and light red at 25.7 °C, 27.0 °C, 29.0 °C, 30.5 °C, 32 °C and 33 °C, respectively (Siddiqui et al. 2019). The technique has been successfully applied to screen out salt-tolerant cereal germplasm on the basis of variations in stomatal traits (Sirault et al. 2009). The microclimate due to difference in plant density, variations in genotypes development rate, radiations, wind speed and cloudy conditions may mislead the results.

2.7 Summary

Corresponding to genotypic, the phenotypic form of plant is more important for high yield. The selection of germplasm based on phenotype has been of great interest for breeders and farmers. Keeping in view the importance of the phenotyping, Tuberosa

(2012) referred to phenotyping as "king" and heritability as "queen". The modern phenotyping techniques are based on image science and are used as non-destructive tools for trait measurement. To extend the application of these techniques in the field, high-throughput field phenotypic platform was designed and equipped with different sensors. However, the type of sensors varies according to the trait of interest; thermography is suitable for drought tolerance and x-ray tomography is used for 3D phenotyping and investigation of internal plant structure.

References

Ahmad S, Hasanuzzaman M (2020) Cotton production and uses. Springer Nature Singapore Pvt. Ltd., Singapore, 641 pp. https://doi.org/10.1007/978-981-15-1472-2

Ahmad S, Abbas G, Fatima Z, Khan RJ, Anjum MA, Ahmed M, Khan MA, Porter CH, Hoogenboom G (2017) Quantification of the impacts of climate warming and crop management on canola phenology in Punjab, Pakistan. J Agron Crop Sci 203(5):442–452. https://doi.org/10.1111/jac.12206

Ahmad S, Abbas G, Ahmed M, Fatima Z, Anjum MA, Rasul G, Khan MA, Hoogenboom G (2019) Climate warming and management impact on the change of phenology of the rice-wheat cropping system in Punjab, Pakistan. Field Crop Res 230:46–61. https://doi.org/10.1016/j.fcr.2018.10.008

Ahmed M (2020) Introduction to modern climate change. Andrew E. Dessler: Cambridge University Press, 2011, 252 pp, ISBN-10: 0521173159. Sci Total Environ 734:139397. https://doi.org/10.1016/j.scitotenv.2020.139397

Ahmed M, Ahmad S (2019) Carbon dioxide enrichment and crop productivity. In: Hasanuzzaman M (ed) Agronomic crops. Management practices, vol 2. Springer Singapore, Singapore, pp 31–46. https://doi.org/10.1007/978-981-32-9783-8_3

Ahmed M, Stockle CO (2016) Quantification of climate variability, adaptation and mitigation for agricultural sustainability. Springer Nature Singapore Pvt. Ltd., Singapore, 437 pp. https://doi.org/10.1007/978-3-319-32059-5

Ahmed M, Asif M, Hirani AH, Akram MN, Goyal A (2013) Modeling for agricultural sustainability: a review. In: Bhullar GS, Bhullar NK (eds) Agricultural sustainability progress and prospects in crop research. Elsevier, London

Ahmed M, Aslam MA, Hassan FU, Asif M, Hayat R (2014) Use of APSIM to model nitrogen use efficiency of rain-fed wheat. Int J Agric Biol 16:461–470

Ahmed M, Akram MN, Asim M, Aslam M, Hassan F-u, Higgins S, Stöckle CO, Hoogenboom G (2016) Calibration and validation of APSIM-wheat and CERES-wheat for spring wheat under rainfed conditions: models evaluation and application. Comput Electron Agric 123:384–401. https://doi.org/10.1016/j.compag.2016.03.015

Ahmed M, Stöckle CO, Nelson R, Higgins S (2017) Assessment of climate change and atmospheric CO_2 impact on winter wheat in the pacific northwest using a multimodel ensemble. Front Ecol Evol 5(51). https://doi.org/10.3389/fevo.2017.00051

Ahmed M, Ijaz W, Ahmad S (2018) Adapting and evaluating APSIM-SoilP-wheat model for response to phosphorus under rainfed conditions of Pakistan. J Plant Nutr 41(16):2069–2084. https://doi.org/10.1080/01904167.2018.1485933

Ahmed M, Stöckle CO, Nelson R, Higgins S, Ahmad S, Raza MA (2019) Novel multimodel ensemble approach to evaluate the sole effect of elevated CO_2 on winter wheat productivity. Sci Rep 9(1):7813. https://doi.org/10.1038/s41598-019-44251-x

Ahmed K, Shabbir G, Ahmed M, Shah KN (2020) Phenotyping for drought resistance in bread wheat using physiological and biochemical traits. Sci Total Environ 729:139082. https://doi.org/10.1016/j.scitotenv.2020.139082

Andrade-Sanchez P, Gore M, Heun JT, Thorp KR, Carmo-Silva AE, French AN, Salvucci ME, White JW (2014) Development and evaluation of a field-based high throughput phenotyping platform. Funct Plant Biol 41:68–79

Burton AL, Williams M, Lynch JP, Brown KM (2012) Rootscan: software for high-throughput analysis of root anatomical traits. Plant Soil 357:189–203

Chawade A, van Ham J, Blomquist H, Bagge O, Alexandersson E, Ortiz R (2019) High-throughput field-phenotyping tools for plant breeding and precision agriculture. Agronomy 9(5):258

Coppens F, Wuyts N, Inzé D, Dhondt S (2017) Unlocking the potential of plant phenotyping data through integration and data-driven approaches. Curr Opin Syst Biol 4:58–63

De Bei R, Cozzolino D, Sullivan W, Cynkar W, Fuentes S, Dambergs R, Pech J, Tyerman S (2011) Non-destructive measurement of grapevine water potential using near infrared spectroscopy. Aust J Grape Wine Res 17(1):62–71

Deery DM, Rebetzke GJ, Jimenez-Berni JA, James RA, Condon AG, Bovill WD, Furbank RT (2016) Methodology for high-throughput field phenotyping of canopy temperature using airborne thermography. Front Plant Sci 7:1808

Fernandez MGS, Bao Y, Tang L, Schnable PS (2017) A high-throughput, field-based phenotyping technology for tall biomass crops. Plant Physiol 174:2008–2022

Fritsche-Neto R, Borém A (2015) Phenomics how next-generation phenotyping is revolutionizing plant breeding. Springer Press, Cham

Furbank RT, Tester M (2011) Phenomics – technologies to relieve the phenotyping bottleneck. Trends Plant Sci 16(12):635–644

Garbout A, Munkholm LJ, Hansen SB, Petersen BM, Munk OL, Pajor R (2012) The use of PET/CT scanning technique for 3D visualization and quantification of real-time soil/plant interactions. Plant Soil 352:113–127

Großkinsky DK, Svensgaard J, Christensen S, Roitsch T (2015) Plant phenomics and the need for physiological phenotyping across scales to narrow the genotype-to-phenotype knowledge gap. J Exp Bot 66(18):5429–5440

Guo, Zhu (2014) Phenotyping of plants. Encyclopedia of analytical chemistry. Published online: http://onlinelibrary.wiley.com/doi/10.1002/9780470027318.a9934/full

Hoffmeister D, Waldhoff G, Korres W, Curdt C, Bareth G (2016) Crop height variability detection in a single field by multi-temporal terrestrial laser scanning. Precis Agric 17(3):296–312

Houle D, Govindaraju DR, Omholt S (2010) Phenomics: the next challenge. Nat Rev Genet 11:855–866

Kim Y, Glenn DM, Park J, Ngugi HK, Lehman BL (2012) Characteristics of active spectral sensor for plant sensing. American Society of Agricultural and Biological Engineers 55(1):293–301

McCormick RF, Truong SK, Mullet JE (2016) 3D sorghum reconstructions from depth images identify QTL regulating shoot architecture. Plant Physiol 172:823–834

Montes JM, Technow F, Dhillon B, Mauch F, Melchinger A (2011) High-throughput non-destructive biomass determination during early plant development in maize under field conditions. Field Crops Res 121:268–273

Muller O, Keller B, Zimmermann L, Jedmowski C, Pingle V, Acebron K, Zendonadi NS, Steier A, Pieruschka R, Kraska T, Schurr U, Rascher U (2018) Field phenotyping and an example of proximal sensing of photosynthesis. In: Proceedings of the 14th International Conference on Precision Agriculture June 24–June 27, 2018, Montreal, Quebec, Canada

Nandibewoor A, Hebbal SB, Hegadi R (2015) Remote monitoring of maize crop through satellite multispectral imagery. Procedia Computer Science 45:344–353

Paulus S (2019) Measuring crops in 3D: using geometry for plant phenotyping. Paulus Plant Methods 15:103

Petroua ZI, Tarantinoc C, Adamoc M, Blondac P, Petrou M (2012) Estimation of vegetation height through satellite image texture analysis. In: International Archives of the Photogrammetry, Remote Sensing and Spatial Information Sciences, Volume XXXIX-B8, 2012 XXII ISPRS Congress, 25 August–01 September 2012, Melbourne, Australia

Porter JR, Christensen S (2013) Deconstructing crop processes and models via identities. Plant Cell Environ 36:1919–1925

Pratap A, Gupta S, Nair RM, Gupta SK, Schafleitner R, Basu PS, Singh CM, Prajapati U, Gupta AK, Nayyar H, Mishra AK, Baek K-H (2019) Using plant phenomics to exploit the gains of genomics. Agronomy 9:126

Punshon T, Ricachenevsky F, Hindt M, Socha A, Zuber H (2013) Methodological approaches for using synchrotron X-ray fluorescence (SXRF) imaging as a tool in ionomics: examples from Arabidipsis thaliana. Metallomics 5:1133

Romano G, Zia S, Spreer W, Sanchez C, Cairns J, Araus JL, Müller J (2011) Use of thermography for high throughput phenotyping of tropical maize adaptation in water stress. Comput Electron Agric 79:67–74

Sankaran S, Khot LR, Espinoza CZ, Jarolmasjed S, Sathuvalli VR, Vandemark GJ, Pavek MJ (2015) Low-altitude, high-resolution aerial imaging systems for row and field crop phenotyping: a review. Eur J Agron 70:112–123

Schork NJ (1997) Genetics of complex disease: approaches, problem, and solutions. Am J Respir Crit Care Med 156:S103–S109

Shi Y, Thomasson JA, Murray SC, Pugh NA, Rooney WL, Shafian S, Rajan N, Rouze G, Morgan CLS, Neely HL, Rana A, Bagavathiannan M, Henrickson J, Bowden E, Valasek J, Olsenholler J, Bishop MP, Sheridan R, Putman EB, Popescu S, Burks T, Cope D, Ibrahim A, McCutchen BF, Baltensperger DD, Avant RV Jr, Vidrine M, Yang C (2016) Unmanned aerial vehicles for high-throughput phenotyping and agronomic research. PLoS One 11(7):e0159781

Siddiqui ZS, Umar M, Kwon TR, Park SC (2019) Phenotyping through infrared thermography in stress environment. In: Gul B et al (eds) Sabkha ecosystems, tasks for vegetation science. Springer Nature Switzerland AG, Cham

Singh A, Ganapathysubramanian B, Singh AK, Sarkar S (2016) Machine learning for high-throughput stress phenotyping in plants. Trends Plant Sci 21:110

Sirault XR, James RA, Furbank RT (2009) A new screening method for osmotic component of salinity tolerance in cereals using infrared thermography. Funct Plant Biol 36(11):970–977

Su W, Zhang M, Bian D, Liu Z, Huang J, Wang W, Wu J, Guo H (2019) Phenotyping of corn plants using unmanned aerial vehicle (UAV) images. Remote Sens 11:2021

Thompson AL, Thorp KR, Conley M, Andrade-Sanchez P, Heun JT, Dyer JM, White JW (2018) Deploying a proximal sensing cart to identify drought-adaptive traits in upland cotton for high-throughput phenotyping. Front Plant Sci 9:507

Thoren D, Schmidhalter U (2009) Nitrogen status and biomass determination of oil seed rape by laser-induced chlorophyll fluorescence. Eur J Agron 30:238–242

Tuberosa R (2012) Phenotyping for drought tolerance of crops in the genomics era. Front Physiol 3:347

Walter A, Liebisch F, Hund A (2015) Plant phenotyping: from bean weighing to image analysis. Plant Methods 11:14

Wang LH, Hu S (2012) Photoacoustic tomography: in vivo imaging from organelles to organs. Science 335:1458–1462

Wang Y, Wen W, Wu S, Wang C, Yu Z, Guo X, Zhao C (2019) Maize plant phenotyping: comparing 3D laser scanning, multi-view stereo reconstruction, and 3D digitizing estimates. Remote Sens 11:63

Yang G, Liu J, Zhao C, Li Z, Huang Y, Yu H, Xu B, Yang X, Zhu D, Zhang X, Zhang R, Feng H, Zhao X, Li Z, Li H, Yang H (2017) Unmanned aerial vehicle remote sensing for field-based crop phenotyping: current status and perspectives. Front Plant Sci 8:1111

Zhao C, Zhang Y, DuJ GX, En W, Gu S, Wang J, Fan J (2019) Crop phenomics: current status and perspectives. Front Plant Sci 10:714

Statistics and Modeling

3

Mukhtar Ahmed

Abstract

This chapter describes the application of statistical concepts with illustration about statistical models, probability, normal distribution, and analysis of variance (ANOVA). Statistical analysis is an important action process in research that deals with data. It follows well-defined, systematic, and mathematical procedures and rules. Data is information obtained to answer questions related to how much, how many, how long, how fast and how related. Statistics main objective is the analysis of data from generated experiment, but how should this data be collected to address our research questions and what should be our experimental design? Thus, in order to address question of interest clearly and efficiently, we need to organize experiment accurately so that we can have right type and amount of data. This is only possible using experimental design which has been elaborated in this chapter. The designs discussed here are completely randomized design (CRD), randomized complete block design (RCBD), Latin square design, nested and split plot design, strip-plot/split-block design, and split-split plot design. Similarly, factorial experiments have been discussed in detail with description about the interaction. The concept about fractional factorial design, multivariate analysis of variance (MANOVA), and analysis of covariance (ANCOVA) has been presented. Principal component analysis which is the method of multivariate statistics and used to check variation and patterns in a data set was also presented. It is easy way to visualize and explore data. The relationship between one or more variables to generate model which could be used for the prediction analysis has been discussed using concept of regression. Finally, association between two or more variables was presented using correlation. At the end different analytical

M. Ahmed (✉)
Department of Agricultural Research for Northern Sweden, Swedish University of Agricultural Sciences, Umeå, Sweden

Department of Agronomy, Pir Mehr Ali Shah Arid Agriculture University, Rawalpindi, Pakistan
e-mail: mukhtar.ahmed@slu.se; ahmadmukhtar@uaar.edu.pk

M. Ahmed (ed.), *Systems Modeling*, https://doi.org/10.1007/978-981-15-4728-7_3

tools/software were listed which can be used to do different kind of statistical analysis.

Keywords

Statistics · Probability · Normal distribution · Analysis of variance · Experimental designs · Factorial experiments · Regression · Correlation

3.1 Basic Statistics

Statistics is the science (pure and applied) dealing with creating, developing, and applying techniques to evaluate uncertainty of inductive inferences. It helps to answer the question about different hypothesis. It can model the role of chance in our experiments in a quantitative way and gives estimates with errors. Propagation of error in input values could also be determined by the statistics. History of statistics goes back to the experience of gambling (seventeenth century) which leads to the concept of probability. Afterwards concepts of normal curve/normal curve of error were introduced. Charles Darwin (1809–1882) work was largely biostatistical in nature. Karle Pearson (1857–1936) founded the journal *Biometrika* and school of statistics. Pearson was mainly concerned with large data, and his student W. S. Gosset (Pseudonym, Student) (1876–1937) presented Student's *t-test* which is a basic tool of statistician and experimenters throughout the globe. Genichi Taguchi (1924–2012) promoted the use of experimental designs.

Observations in the form of numbers are very important to perform different kind of statistical analysis. In case of crop production, observation can be phenology, leaf area, crop biomass, and yield. These numbers then constitute data, and its common characteristics include variability or variation. Variables may be quantitative or qualitative. Observations on quantitative variables may be further classified as discrete or continuous. Furthermore, probability of occurrence of value such as blondeness may be measured by probability function or probability density function (PDF). Chance and random variable terms are generally used for the variables possessing PDF. Population is all possible values of a variable, while part of population is called a sample. The concept of randomness is used to have true representative data sample from the population. Collected data could be characterized using tables, charts (pie chart, bars, etc.), and pictures (histogram). Afterwards data are presented in frequency tables, and measure of central tendency is used to locate center. This can help to find measure of spreading of the observation. Mean or average (μ) is the most common method to use the measure of central tendency. In case of dice, μ can be calculated by using following equation

$$\mu = \frac{1 + 2 + 3 + 4 + 5 + 6}{6} = 3\frac{1}{2} \tag{3.1}$$

If a sample is taken from the population having four observation, then $\overline{Y}$ (sample mean) for the four observation (3, 5,7,9) is

$$\overline{Y} = \frac{3+5+7+9}{4} = 6 \tag{3.2}$$

This can be further symbolized by

$$\overline{Y} = \frac{Y_1 + Y_2 + Y_3 + Y_4}{4} \tag{3.3}$$

where $Y_1 = \textit{value of first observation}$, $Y_2 = \textit{value of second observation}$, $Y_3 = \textit{value of third observation}$, $\textit{and } Y_4 = \textit{value of fourth observation}$. For the nth observations, Y_i is used to represent the ith observation and ⍰Y is given by

$$\overline{Y} = \frac{Y_1 + Y_2 + Y_3 + Y_4 + \ldots + Y_i + \ldots. + Y_n}{n} \tag{3.4}$$

This equation can be further shortened to

$$\overline{Y} = \frac{\sum_{i=1}^{n} Y_i}{n} \tag{3.5}$$

Difference between observations (Y_i) and sample mean $(\overline{Y})$ is called sample deviation (Y_i– $\overline{Y}$), and its sum is equal to zero $\sum\left(Y_i - \overline{Y}\right) = 0$.

For the different number of observations, it's better to use weights that depend on the number of observations in each mean called weighted mean. A weighted mean is defined as follows:

$$\overline{Y}_w = \frac{\sum w_i Y_i}{\sum w_i} \tag{3.6}$$

Another term supplement to the mean is median and it is value for which 50% of the observations lie on each side. However, if values are even, then median is average of the two middle values, e.g., 3, 6, 8, and 11 median is 7 (6 + 8)/2. If data is nonsymmetrical in that case, mean and median could be different, and data might be skewed in one direction; thus arithmetic mean may not be a good criteria to measure central value. Mode (most frequent value) is another measure to calculate central tendency. Central tendency provides summary about the data but does not provide information about variation. Standard deviation or variance or square root $(Y_i - \mu)^2$ is used to measure variation or dispersion from the mean. It can be represented by two symbols: (i) σ^2 (sigma square for the population) and (ii) S^2 (sample). Population variance is defined as sum of squared deviations divided with total number, and it can be elaborated by the following equation if we intent to sample this population with replacement:

$$\sigma^2 = \frac{(Y_1 - \mu)^2 + (Y_2 - \mu)^2 + (Y_3 - \mu)^2 + \ldots + (Y_N - \mu)^2}{N} \tag{3.7}$$

$$= \frac{\sum_i (Y_i - \mu)^2}{N} \tag{3.8}$$

However, when sampling is without replacement, then divisor is $N-1$, and it could be represented by the equation as follows:

$$S^2 = \frac{(Y_1 - \mu)^2 + (Y_2 - \mu)^2 + (Y_3 - \mu)^2 + \ldots + (Y_N - \mu)^2}{N - 1} \tag{3.9}$$

$$= \frac{\sum_i (Y_i - \mu)^2}{N - 1} \tag{3.10}$$

The sample variance/mean square can be computed by using following formulas:

$$s^2 = \frac{\left(Y_1 - \overline{Y}\right)^2 + \left(Y_2 - \overline{Y}\right)^2 + \left(Y_3 - \overline{Y}\right)^2 + \ldots + \left(Y_N - \overline{Y}\right)^2}{n - 1} \tag{3.11}$$

$$s^2 = \frac{\sum_i \left(Y_i - \overline{Y}\right)^2}{n - 1} \tag{3.12}$$

$$(n - 1)s^2 = \sum_i \left(Y_i - \overline{Y}\right)^2 \tag{3.13}$$

$s^2 = SS$ (sum of squares). For example, for the numbers 3, 5, 7, and 9, the SS is

$$\begin{aligned}(3-6)^2 + (5-6)^2 + (7-6)^2 + (9-6)^2 &= (-3)^2 + (-1)^2 + (1)^2 + (3)^2 \\ &= 9 + 1 + 1 + 9 = 20\end{aligned}$$

The variance for this data set will be 20/3 = 6.66, and the square root of the sample variance is called the standard deviation (s). For the above example, it can be calculated by the following method:

$$s = \sqrt{\frac{20}{3}} = 2.58$$

Thus Eq. (3.12) can be represented as follows:

$$SS = \sum_i \left(Y_i - \overline{Y}\right)^2 \tag{3.14}$$

This Eq. (3.14) could be further modified to a computing formula as follow:

$$\sum_i \left(Y_i - \overline{Y}\right)^2 = \sum_i Y_i^2 - \left(\textstyle\sum_i Y_i\right)^2 \!/ n \tag{3.15}$$

Table 3.1 Data set for the validation of sum of squares equation

	Y_i	Y_i^2	$Y_i - \overline{Y}$	$\lvert Y_i - \overline{Y} \rvert$	$(Y_i - \overline{Y})^2$
	3	9	$3–6 = -3$	3	9
	5	25	$5–6 = -1$	1	1
	7	49	$7–6 = 1$	1	1
	9	81	$9–6 = 3$	3	9
$\sum_i$:	24	164	**0**	**8**	**20**
$\overline{Y}$	6				

The term $\left(\sum_i Y_i\right)^2 / n$ is called the correction factor (CF) or correction term or adjustment for the mean. The Eq. (3.15) could be easily validated by using following data set in the Table 3.1.

Thus, $SS = \sum_i \left(Y_i - \overline{Y}\right)^2 = 20$ and by the $\sum_i Y_i^2 - \left(\sum_i Y_i\right)^2 / n = 164 - \frac{(24)^2}{4} = 20$ (Table 3.1). Another term which is generally used is called degree of freedom (df) (number of values in the calculation that are free to vary), and it is equal to $n-1$. The absolute mean deviation or average deviation is calculated as:

$$\text{Average deviation or Absolute mean deviation} = \frac{\sum_i \left|Y_i - \overline{Y}\right|}{n} \tag{3.16}$$

The absolute mean deviation or average deviation for the values 3, 5, 7, and 9 is 2 as vertical bars tell us consider all deviations as positive. The variance of the population $\left(\sigma^2{}_{\overline{Y}}\right)$ of $\overline{Y}$ can be calculated by the following equation:

$$\sigma^2{}_{\overline{Y}} = \frac{\sigma^2}{n} \tag{3.17}$$

However, $\sigma_{\overline{Y}}$ for the population can be computed by the following expression:

$$\sigma_{\overline{Y}} = \sqrt{\frac{\sigma^2}{n}} \tag{3.18}$$

$$\sigma_{\overline{Y}} = \frac{\sigma}{\sqrt{n}} \tag{3.19}$$

Standard deviation of sample mean is called standard error (SE). Variance for the sample $(s^2{}_{\overline{Y}})$ can be calculated by the following equations:

$$s^2{}_{\overline{Y}} = \frac{s^2}{n} \tag{3.20}$$

$$\mathrm{SE}_{\overline{Y}} = \sqrt{\frac{s^2}{n}} \tag{3.21}$$

Table 3.2 Example of the data set for the calculation of above concepts

Number of observations = i	Yield (kg ha^{-1}) = Y_i	$\overline{Y}$= Mean	$Y_i - \overline{Y}$	
1	1500	1536		−36
2	1850	1536	314	
3	1300	1536		−236
4	1730	1536	194	
5	1300	1536		−236
Total	7680		508	−508

$$\mathrm{SE}_{\overline{Y}} = \frac{s}{\sqrt{n}} \tag{3.22}$$

SE can be calculated by using following equation for the numbers 3, 5, 7, and 9 as used above to calculate standard deviation.

$$\mathrm{SE} = \sqrt{\frac{s^2}{n}} = \sqrt{\frac{6.66}{4}} = \sqrt{1.66} = 1.29$$

Variation can also be measured using coefficient of variability (CV) or relative standard deviation (RSD) which is widely used as a well-known indicator as described in Table 3.2. It is a measure of relative variability. It is the ratio of standard deviation (σ) to the mean (μ) and can be calculated by the following expression:

$$\text{coefficient of variation (CV)} = \frac{\sigma}{\mu} \tag{3.23}$$

$$\overline{Y} = \frac{\sum Y_i}{5} = \frac{7680}{5} = 1536\,\mathrm{kg\ ha}^{-1}$$

$$s^2 = \frac{\sum Y_i^{\,2} - \left(\sum Y_i\right)^2/5}{4} = \frac{12,045,400 - (7680)^2/5}{4} = 62,230$$

$$s = \sqrt{62,230} = 249.45\,\mathrm{kg\ ha}^{-1}$$

$$s^2{}_{\overline{Y}} = \frac{s^2}{5} = \frac{62,230}{5} = 12,446$$

$$\mathrm{SE}_{\overline{Y}} = \sqrt{\frac{s^2}{5}} = \sqrt{\frac{62,230}{5} = 12,446} = 111.56\,\mathrm{kg\ ha}^{-1}$$

$$\mathrm{CV} = \frac{249.45}{1536} \times 100 = 16\%$$

3.2 Statistical Models

A model is an abstract representation of a system in a quantitative way. It is a way of describing a real system in mathematical functions or diagrams. It can also be used to represent the simplification in different process trying to represent biological systems. A model can summarize factors affecting different process in a system. Mathematical models use different notation and expressions from mathematics to describe process, while statistical model is a mathematical model that allows variability in the process. This variability might be due to the number of reasons such as sampling, biological, and inaccuracies in measurements or due to the influential variables being omitted from the model. Thus, statistical models have potential to measure uncertainty associated with it. Statistical models come in the category of empirical models where principle of correlation was used to build a simple equation to describe relationship with different explanatory variables. Furthermore, if the explanatory variables are in numbers (quantitative), they were referred as variates, while if they are qualitative, then they were considered as factors and distinct groups as factor levels. For example, qualitative trait height can be classified as short, medium, or tall. Linear models are most importantly used statistical model.

3.3 The Linear Additive Model

Natural phenomenon in science such as earth rotation could be explained by the models. Linear additive model (LAM) is a commonly used model to describe the observation which has mean and error. Assumption for the application of this model includes that population of Y should be selected at random as well as errors are at random. This model could be used to make inferences about population means and variance. The simple LAM could be represented by the following equation:

$$Y_i = \mu + \varepsilon_i$$

where μ = mean and ε_i= sampling error.

The sampling error for the population having mean zero could be calculated by the following procedure in which sample from the population is drawn in a random manner. The steps include

$$\overline{Y} = \frac{\sum_i Y_i}{n} = \frac{\sum_i (\mu + \varepsilon_i)}{n} = \mu + \frac{\sum_i \varepsilon_i}{n}$$

For random sampling the equation will be $= \frac{\left(\sum_i \varepsilon_i\right)}{n}$, and it is expected to be smaller as sample size increases and positive and negative epsilon will cancel. Generally variance of mean of large samples are usually small. Epsilon could be calculated by using $\left(Y_i - \overline{Y}\right)$.

3.4 Probability

Probability is a numerical description of how likely an event is to occur or how likely it is that a proposition is true. Probability is a number between 0 and 1, where 0 indicates impossibility and 1 indicates certainty. The best example for understanding probability is flipping a coin: There are two possible outcomes—heads (H) or tails (T). What's the probability of the coin landing on heads? We can find out using the equation

$$\text{probability of head } P_H = \frac{1}{2}$$

or

$$\text{Probability of an event} = \frac{\text{number of ways it can happen}}{\text{total number of outcomes}}$$

Similarly, in case of dice rolling, there are six different outcomes (1, 2, 3, 4, 5, and 6), and probability of getting a one will be:

$$P_1 = \frac{1}{6}$$

The probability of getting 1 or 6 can be calculated by following way:

$$P_{1 \text{ or } 6} = \frac{2}{6} = \frac{1}{3}$$

The probability of rolling an even number (2, 4, and 6) will be:

$$P_{2,4 \text{ or } 6} = \frac{3}{6} = \frac{1}{2}$$

For many experiments there are only two possible outcomes, for example, a tossed coin falls heads or tails or student fail or pass or plant could be tall or short. Such outcomes are referred as binomial, and sample space will consist of two points only. Thus, sample space is made up of sample points (represented with E and, if event does not occur, represented with $-E$ or $\bar{E}$ or $\not{E}$) as shown in the following Fig. 3.1. Probability associated with each value of the random variable is called as

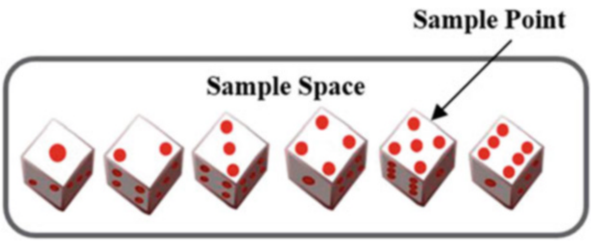

Fig. 3.1 Illustration of sample space and sample point

binomial probability function or binomial distribution. Formula that can gives the probability associated with each chance event e.g. for a fair coin if we consider $Y = 0$ for tail and $Y = 1$ for head will be:

$$P_{Y=Y_i} = \frac{1}{2}\ Y_i = 0 \text{ and } 1$$

For tossing a fair dice, probability distribution would be:

$$P_{Y=Y_i} = \frac{1}{6}\ Y_i = 1, 2, 3, 4, 5 \text{ and } 6$$

Ten thousand random digit tables are a very large sample for a population, and probability distribution for this table would be

$$P_{Y=Y_i} = \frac{1}{10}\ Y_i = 0, 1, 2, 3, 4, 5 \ldots 9$$

If we consider only odd and even numbers, then we can relate ten thousand random digit tables with $P_{Y=Y_i} = \frac{1}{2}\ Y_i = 0$ and 1, $P_{Y=Y_i} = \frac{1}{6} Y_i = 1$, 2, 3, 4, 5 and 6 and $P_{Y=Y_i} = \frac{1}{10} Y_i = 0$, 1, 2, 3, 4, 5. . .9, but it would not be binomial now, it will be multinomial. Probabilities of binomial distribution in single statement can be elaborated by generating single equation. Consider an experiment that contains n independent trials. Let $P_E = P_1 = p$ then $P_{\neg E} = P_0 = 1 - p$ as we know that $p = \frac{\text{number of successes}}{\text{total number of events (Successes+Failures)}}$ and probability of an event (E_i) *l*ies between 0 and 1 $(0 \le P_{E_i} \le 1)$ and sum of the probabilities of events in a mutually exclusive set is 1 $\left(\sum_i P_{E_i} = 1\right)$. Five tosses of coins could result in (0, 0, 1, 1, 0), that is, two tails followed by two heads and final tail. Since trial is independent, thus probability of this outcome can be found by multiplying probabilities in each stage, i.e., $(1-p)(1-p)pp(1-p) = p^2(1-p)^3$. If $p = 0.5$ then $(0.5)^5 = 0.03125$ or 3 % . The random variable Y associates a unique value with each sample point, e.g., for sample vector (0, 0, 1, 1, 0), we have $Y = 2$, and there are possibilities of 10 sequences with $Y = 2$. Thus $Y = 2$ is $10p^2(1-p)^3$. The equatin which can be used to calculate this value directly will be:

$$\binom{n}{Y} = \frac{n!}{Y!(n-Y)!}$$

where $n! = n$ factorial $= n(n-1)(n-2)\ldots0.1$. Thus, for $Y = 2$, i.e., two 1 s in $n = 5$ trials, the equation would be:

$$\binom{5}{2} = \frac{5.4.3.2.1}{2.1.3.2.1} = 10$$

One formula which can be used to count sample points with the same Y and one that assigns probability to each sample point in the binomial probability distribution can be represented as:

$P(Y = Y_i|n) = \binom{n}{Y_i} p^{Y_i}(1-p)^{n-Y_i}$ (In this equation the probability that the random variable Y takes the particular value Y_i in a random experiment with n trials). For the coin above illustration, this equation will be:

$$P(Y = 2|5) = \binom{5}{2}\left(\frac{1}{2}\right)^2\left(\frac{1}{2}\right)^3$$

The mean and variance of a random variable with a binomial distribution could be calculated by using following equations:

$$\text{Mean} : \mu = np$$

$$\text{Variance} : \sigma^2 = np(1-p)$$

3.5 Normal Distribution

Normal distribution is the most important widely used probability distribution as it fits with many natural processes such as heights, blood pressure, IQ score, and measurement error. It is also called as bell curve or Gaussian distribution. It is a standard reference for probability-related problems. The normal distribution has two parameters, i.e., mean (μ) and standard deviation (σ) (Fig. 3.2). The characteristics of normal distributions are as follows: (i) X lies between $-\infty$ and ∞ ($-\infty \leq X \leq \infty$); (ii) symmetric; (iii) normal density function rule, $f(x; \mu, \sigma^2) = \frac{1}{\sqrt{2\pi\sigma^2}} e^{-(x-\mu)^2/2\sigma^2}$; (iv) 2/3 of the most cases lies with one σ of μ, i.e., $P(\mu - \sigma \leq X \leq \mu + \sigma) = 0.6826$; and (iv) 95% of cases lies two σ of μ, i.e., $P(\mu - 2\sigma \leq X \leq \mu + 2\sigma) = 0.9544$.

3.6 Comparison of Means

Statistical concepts are used everywhere in daily life, e.g., while purchasing honey bottle from market, it may be labelled as 500 g, but to confirm this claim, we need to take random sample from the population. We could report the probability of obtaining a sample at least this uncommon if true mean is 500 g. This can be the problem of hypothesis testing. In such cases testing is done by using Student's t-test or F-Test. If means are more than two, the analysis of variance (ANOVA) F-test is to

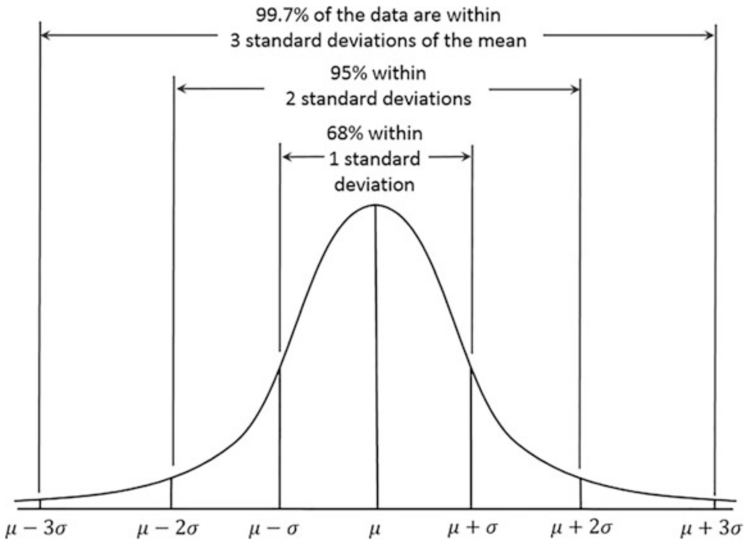

Fig. 3.2 Normal distribution curve

be used. Thus, sample size should be considered while selecting a test. Hypothesis test and confidence interval (CI) are interlinked. The formula to apply Student's *t*-test is

$$t = \frac{\overline{Y} - \mu}{S_{\overline{Y}}}$$

$$t = \frac{\overline{Y} - \mu}{\sqrt{\frac{s}{n}}}$$

$$t = \frac{\overline{Y} - \mu}{\frac{s}{\sqrt{n}}}$$

For the data having two means, *t*-test equation will be:

$$t = \frac{\overline{Y_1} - \overline{Y_2}}{S_{\overline{Y_1}} - S_{\overline{Y_2}}}$$

where $\overline{Y} = \text{sample mean}$, s is the sample standard deviation, and n is the sample size.

Consider a null hypothesis $H_o : \mu = \mu_o$ and alternative hypothesis $H_1 : \mu \neq \mu_o$, if t exceeds critical value $t_{0.025}$, then H_o is rejected, but if null hypothesis is true and still, it has been rejected and is called type I error. However, if H_1 is true and we accept H_o anyway, this type of error is called type II error.

3.7 Analysis of Variance (ANOVA)

It is an undeniable fact that agronomic research resulted to the improved quality of life and sustainability of the planet earth. The principles and procedures of analysis of variance (ANOVA) have been considered as fundamental tools in all agronomic research. ANOVA is an established statistical procedure that can be used to test the hypothesis by partitioning the sources of variation (SOV), variance components estimation, explanation and reduction of residual variation, and determination of the significance of effects. ANOVA history of application in agronomic field research and plant breeding trials goes back to the early twentieth century in which the main goal of research work was to have a better understanding of the effects of treatments, e.g., fertilizer, cultivars, planting dates, soil amendments, and their interactions. Earlier, trials main focus was on yield and thus to have better scientific understanding of the effects of treatments and guidance to the farmers; ANOVA was used widely. ANOVA helped in the early twentieth century to have good credibility of field agronomic trials. Furthermore, significant differences between treatment and check plots could be evaluated by ANOVA; however, there were issues between years as random effects of years could not be replicated (Loughin 2006). Fisher was a pioneer in the introduction of ANOVA, and he applied this concept in the 1920s on long-term wheat yield experiments (>half century) in response to the soil amendments (Fisher 1921). Fisher used ANOVA to disentangle large variability in average yield from other changes and evaluate significant difference between treatments. The basis of ANOVA was described as the variance (mean σ of variate from its mean thus square of its standard deviation) produced by all the causes at once in an operation is the sum of the values produced by each cause individually. Thus, with ANOVA we can partition the total variation into separate and independent SOV. To implement ANOVA accurately, it is important that treatment plots (experimental units) must be replicated and randomized. The basic assumptions to apply ANOVA are (i) Treatments and environment effects are additive and (ii) Experimental errors are random, independently and normally distributed about zero mean and with a common variance. Fisher in his experimental design work documented that the systematic arrangement of treatments resulted in the biased estimates of treatment averages, overestimation, and underestimation of error variation and correlated errors. Thus, replication is needed to estimate experimental error and randomization to have correct probability or level of significance. Generally, ANOVA divides total variation into two independent sources: (i) variation among treatments and (ii) variation within treatments (experimental error/residual error/error mean square/error variance). After considering that data is normally and independently distributed, F-ratio $\left(F = {}^{\text{variation between sample means}}\!/_{\text{variation within the samples}}\right)$ is used to test the null hypothesis that treatment means are equal or not. One-way ANOVA example could be best way to understand this ratio. Firstly, ANOVA was used for the fixed effect models (Model I, specific treatments or level of treatments of interest) but later used also for the random effect models (Model II). Afterwards it has been proposed that ANOVA should also be used for the mixed effect models (both fixed

Table 3.3 One-way analysis of variance with equal replication

SOV	df	Sum of squares (SS)	Mean squares (MS)	F
Treatments	$t-1$	$r\sum_i(\overline{X}_i. - \overline{X}..)^2 = \sum_i \frac{X_i^2}{r} - \frac{X^2..}{rt}$	$\frac{SS_{treatments}}{df_{treatments}}$	$\frac{MS_{treatments}}{MS_{error}}$
Error	$t(r-1)$	$\sum_{i,j}(\overline{X}_{ij} - \overline{X}.)^2$	$\frac{SS_{error}}{df_{error}}$	
Total	$rt-1$	$\sum_{i,j}(\overline{X}_{ij} - \overline{X}..)^2 = \sum_{i,j} X_{ij}{}^2 - \frac{X^2..}{rt}$		

Table 3.4 Analysis of variance in randomized complete block

SOV	df	Sum of squares (SS)	Mean squares (MS)	F
Blocks	$r-1$	$t\sum_j(\overline{X}_{.j} - \overline{X}..)^2 = \frac{\sum_j X^2{}_{.j}}{t} - C$	$\frac{SS_{blocks}}{df_{blocks}}$	
Treatments	$t-1$	$r\sum_i(\overline{X}_i. - \overline{X}..)^2 = \sum_i \frac{X_i^2}{r} - C$	$\frac{SS_{treatments}}{df_{treatments}}$	$\frac{MS_{treatments}}{MS_{error}}$
Error	$(r-1)$ $(t-1)$	$\sum_{i,j}(X_{ij} - \overline{X}_{.J} - \overline{X}_i. + \overline{X}..)^2$ $=SS_{total} - SS_{blocks} - SS_{treatments}$	$\frac{SS_{error}}{df_{error}}$	
Total	$rt-1$	$\sum_{i,j}(X_{ij} - \overline{X}..)^2 = \sum_{i,j} X_{ij}{}^2 - C$		

and random treatment factors) (Gbur et al. 2012; West and Galecki 2012). The importance of mixed effect models was shown in some of experiments where use of fixed model instead of mixed models resulted to the misleading results (Acutis et al. 2012; Bolker et al. 2009; Moore and Dixon 2015; Yang 2010). Fisher's ANOVA is the most frequently used method to determine if differences among means are significant or not. His preference was to declare significance when $P \leq 0.05$ (P value) by considering F table also. The components of ANOVA include sources of variations (SOV), degrees of freedom, sum of squares, mean squares, F values, and P values (Tables 3.3, 3.4 and 3.5). The ANOVA importance and applications in different earlier work have been presented in Table 3.6. Meantime as Fisher was working on his ANOVA framework, Neyman and Pearson presented the concept of type of errors (type I (true null hypothesis rejection) and type II errors (failing to reject false null hypothesis)) (McIntosh 2015).

3.7.1 Calculation of the *F*-Test

F-ratio calculation for one-way ANOVA is possible by using following equations and is reported in the representative Table 3.7.

Table 3.5 Analysis of variance for Latin square

SOV	df	Sum of squares (SS)	Mean squares (MS)	F
Rows	$r-1$	$r\sum_{i}(\overline{X}_{i\cdot}-\overline{X}_{\cdot\cdot})^2=\frac{\sum_{i}X^2{}_{i\cdot}}{r}-C$	$\frac{SS_{blocks}}{df_{blocks}}$	
Columns	$r-1$	$r\sum_{j}(\overline{X}_{\cdot j}-\overline{X}_{\cdot\cdot})^2=\frac{\sum_{j}X^2{}_{\cdot j}}{r}-C$		
Treatments	$r-1$	$r\sum_{t}(\overline{X}_{t}-\overline{X}_{\cdot\cdot})^2=\sum_{t}\frac{X_t{}^2}{r}-C$	$\frac{SS_{treatments}}{df_{treatments}}$	$\frac{MS_{treatments}}{MS_{error}}$
Error	$(r-1)(r-2)$	$\sum_{i,j}(X_{ij}-\overline{X}_{i\cdot}-\overline{X}_{\cdot j}-\overline{X}\,\overline{X}_{\cdot\cdot})^2$ $=SS_{total}-SS_{blocks}-SS_{treatments}$	$\frac{SS_{error}}{df_{error}}$	
Total	$rt-1$	$\sum_{i,j}(X_{ij}-\overline{X}_{\cdot\cdot})^2=\sum_{i,j}X_{ij}{}^2-C$		

Table 3.6 ANOVA importance and applications in different earlier work

S. no	Applications	References
1.	Statistical guidelines for authors	Nature Publishing Group (2005) and (2013a, b)
2.	Raising of data analysis standards	McNutt (2014)
3.	Improvement in the accuracy of the statistical analyses	Acutis et al. (2012)
4.	ANOVA is a commonly used technique, but selection of factors as fixed or random can be complex	Bennington and Thayne (1994)
5.	Mixed model analysis	Yang (2010)
6.	Inclusion/exclusion of fixed by random effects in mixed model	Blouin et al. (2011)
7.	Analysis of combined experiments	McIntosh (1983)
8.	Combined experiment analysis	Moore and Dixon (2015)
9.	Choice of models	Lencina et al. (2005)
10.	Mixed models controversy	Nelder (2008)
11.	Accurate selection of analysis	Nelder and Lane (1995)
12.	Mixed models controversy	Voss (1999)
13.	Two-way factorial ANOVA with mixed effects and interactions	Wang and DeVogel (2019)
14.	ANOVA to show relationship between sources of variation (SOV) and terms in the general linear model (GLM)	Gomez and Gomez (1984)
15.	Explanation of statistical ideas	Mead (2017)
16.	Tests of significance	Snedecor (1942)
17.	Application of statistics principles and procedures	Steel and Torrie (1980)
18.	SAS application in experimental design and analysis	Lawson (2010)

Table 3.7 Representative table for F-test calculation

SOV	SS	Df	MS	F
Factor of interest (between groups)	$\mathrm{SS}_B = \sum\left(\overline{x_j} - \overline{x}\right)^2 = \sum_j n_j\left(x_j^{\,2}\right) = \frac{\left(\sum x_{ij}\right)^2}{n}$	$\mathrm{df}_B = j - 1$	$\mathrm{MS}_B = \frac{\mathrm{SS}_B}{\mathrm{df}_B}$	$F = \frac{\mathrm{MS}_B}{\mathrm{MS}_W}$
Error (within groups)	$\mathrm{SS}_W = \sum_j\sum_i\left(x_{ij} - \overline{x}_j\right)^2$	$\mathrm{df}_W = (n-1) - (j-1)$	$\mathrm{MS}_W = \frac{\mathrm{SS}_W}{\mathrm{df}_W}$	
Total	$\mathrm{SS}_T = \sum\left(x_{ij} - \overline{x}\right)^2 = \sum\left(x_{ij}^2\right) - \frac{\left(\sum x_{ij}\right)^2}{n}$	$\mathrm{df} = n - 1$		

$$\sigma^2 = \frac{\sum (x_i - \overline{x})^2}{n - 1}$$

where σ^2 = vraince, x_i = observation, $\overline{\mathrm{x}}$ = sample population mean, and n = obsevtaion number.

Sum of squares (SS) in ANOVA is sum of the squared deviations of observation from the mean. Total sum of squares ($\mathrm{SS_T}$) can be calculated by using following equation:

$$\mathrm{SS_T} = \sum \left(x_{ij} - \overline{x}\right)^2$$

where x_{ij} = ith observation in the jth group. The formulae can be rewritten as:

$$\mathrm{SS_T} = \sum \left(x_{ij} - \overline{x}\right)^2 = \sum \left(x_{ij}^2\right) - \frac{\left(\sum x_{ij}\right)^2}{n}$$

The total SS between group ($\mathrm{SS_B}$) and within group ($\mathrm{SS_w}$) can be calculated by using following equations:

$$\mathrm{SS_B} = \sum \left(\overline{x_j} - \overline{x}\right)^2 = \sum_j n_j \left(x_j{}^2\right) = \frac{\left(\sum x_{ij}\right)^2}{n}$$

$$\mathrm{SS_W} = \sum_j \sum_i \left(x_{ij} - \overline{x}_j\right)^2$$

Total SS in the model can be calculated by following equation which can be further used to get $\mathrm{SS_w}$:

$$\mathrm{SS_T} = \mathrm{SS_B} + \mathrm{SS_W}$$

$$\mathrm{SS_W} = \mathrm{SS_{TT}} + \mathrm{SS_B}$$

The mean square (MS) (mean of entire sample population or average squared deviation of observation from grand mean) is calculated next which is sum of squares ($\mathrm{SS_T}$) by the total number of *degrees of freedom* (df) or n–1. The mean square between groups ($\mathrm{MS_B}$) can be calculated by using following equation:

$$\mathrm{MS_B} = \frac{\mathrm{SS_B}}{\mathrm{df_B}}$$

Finally, R ratio is calculated by using following equation:

$$F = \frac{\mathrm{MS_B}}{\mathrm{MS_W}}$$

3.8 Experimental Design and Its Principles

New knowledge can be easily obtained by careful planning, analysis, and interpretation of data. Designing of an efficient experiment needs consultation with statistician as they can help to have appropriate design which can enable researchers to have unbiased estimates of treatment means and experimental error. An experiment is planned inquiry to obtain new facts or to confirm earlier findings. Experiments are generally designed to answer the questions or test the hypothesis. Before designing an experiment, it is important that objectives of the experiment should be clear. The unit of material or place where one application of treatment is applied is called experimental unit or experimental plot. Variation is the characteristics of all experimental material and experimental error is used to measure the variation among experimental unit. Variation could be due to number of reasons. It can be due to inherent variability or lack of uniformity in the physical conduction of experiment. Replication is another important component of experimental design. The main functions of replication are to (i) estimate experimental error, (ii) improve precision of the experiment by minimizing standard deviation of treatments, (iii) control error variance, and (iv) increase the scope of inference of the experiment. Error in the experiments could be controlled by the selection of appropriate experimental design, use of parallel observations, and choice of size and shape of the experimental units. Furthermore, unbiased estimate of experimental error is possible by the application of randomization.

3.8.1 Completely Randomized Design (CRD)

Completely randomized design is used when experimental units are homogeneous and less to be gained by putting them into blocks due to similarity of response. For example, variety trial in greenhouse will be subjected to CRD because of uniformity of soil. Similarly, laboratory experiments where it's easy to control variability and experimental units are homogenous; CRD is used. The advantages of CRD are as follows: number of replicates can vary from treatment to treatment, and loss of information due to missing data is small. The precision of experiment is high due to maximum degree of freedom (df) for estimating experimental error. In this design treatments are assigned at random so that each experimental unit receives same chance of getting treatment. The randomization procedure and layout for the pot experiment having four treatments (A, B, C, and D) replicated four times have following steps:

1. Determination of total number of plots or experimental unit (n): Determine the total number of plots or experimental unit by multiplying treatments (t) with the number of replications (R); $n = Rt = 4 \times 4 = 16$. However, if replications are not the same, then "n" can be calculated by getting sum of the replications of each treatment.
2. Assigning of plot number

Table 3.8 Random ranking of experimental unit

Random number	Experimental unit	Ranking	Treatments
0.07	1	4	A
0.842	2	15	B
0.502	3	10	C
0.174	4	5	D
0.426	5	8	A
0.699	6	14	B
0.926	7	16	C
0.039	8	2	D
0.244	9	6	A
0.663	10	13	B
0.045	11	3	C
0.305	12	7	D
0.503	13	11	A
0.429	14	9	B
0.583	15	12	C
0.025	16	1	D

Table 3.9 Group numbers based on random numbers ranking

Treatments	Group number	Ranks in the group			
A	1	4	8	6	11
B	2	15	14	13	9
C	3	10	16	3	12
D	4	5	2	7	1

Fig. 3.3 A layout of completely randomized design with four treatments (A, B, C, and D) replicated four times

Plot/Experimental unit Number	1	2	3	4
Treatment	D	D	C	A
	5	6	7	8
	D	A	D	A
	9	10	11	12
	B	C	A	C
	13	14	15	16
	B	B	B	C

3. Assigning of treatments into plots using random number method and further its ranking as shown in the Table 3.8. Afterwards group number assigned based on random number ranking (Table 3.9) and treatments was placed in the experimental units as shown in the layout (Fig. 3.3).

In order to have ANOVA for the treatments mentioned in Table 3.10, we need to obtain $X_i.$ and $\sum_j X^2 ij$ as mentioned in Table 3.10 (points 1 and 2). Afterwards each treatment total is squared and divided by $r = 5$ to get $(X_{i\cdot})^2/_r$ named as treatments sum of square. Correction factor (CF) is calculated afterwards by dividing total sum of squares of all observations with total numbers (rt). The equation to calculate CF is:

$$\mathrm{CF} = \frac{X^2..}{rt} = \frac{\left(\sum_{i,j} X_{ij}\right)^2}{rt} = \frac{(670.6)^2}{(5)(6)} = 14,990.15$$

$$\mathrm{SS}\ (\mathrm{total}) = \sum_{i,j} X^2 ij - \mathrm{CF} = 16,093.56 - 14,990.15 = 1103.41$$

$$\begin{aligned}
\mathrm{SS}\,(\mathrm{treatment})\,(\mathrm{between\ \ or\ \ among\ \ groups}) &= \frac{X^2 1. + \cdots + X^2 t.}{r} - \mathrm{CF} \\
&= \frac{(148.1)^2 + (132.8)^2 + \cdots + (100.9)^2}{5} \\
&= \frac{7,788,008.00}{5} - 14,990.15 \\
&= 15,576.02 - 14,990.15 \\
&= 585.87
\end{aligned}$$

The sum of squares (SS) among individuals is called within group SS, residual SS, error SS, or discrepancy SS, and it can be obtained by following equation:

$$\begin{aligned}
\mathrm{SS}_{\mathrm{error}} &= \mathrm{SS}_{\mathrm{Total}} - \mathrm{SS}_{\mathrm{Treatment}} \\
&= 1103.41 - 585.87 \\
&= 517.54
\end{aligned}$$

The error SS ($\mathrm{SS}_{\mathrm{error}}$) can also be calculated by pooling the within treatments SS as shown below:

$$\begin{aligned}
\mathrm{SS}_{\mathrm{error}} &= \sum_i \left(\sum_j X^2 ij - \frac{X^2 i.}{r} \right) \\
&= \left(4593.45 - \frac{148.1^2}{5}\right) + \left(3623.34 - \frac{132.8^2}{5}\right) + \left(1980.28 - \frac{95.8^2}{5}\right) \\
&\quad + \left(2406.37 - \frac{109.3^2}{5}\right) + \left(1435.61 - \frac{83.7^2}{5}\right) + \left(2054.51 - \frac{100.9^2}{5}\right) \\
&= 517.54
\end{aligned}$$

Table 3.10 Nitrogen contents of Lucerne plants inoculated with *Rhizobium trifolii* strains (RTS) (mg)

Calculation	RTS1	RTS2	RTS3	RTS4	RTS5	Composite	Total
1. $\sum_j X_{ij} = X_i.$	17.4	18.1	19.1	21.2	15.3	19.3	
	33.7	27.8	22.4	24	17.4	22.4	
	29.0	30.9	12.1	23.5	14.8	22.1	
	33.0	28.2	14.9	21.8	14.6	19.9	
	35.0	27.8	27.3	18.8	21.6	17.2	
	148.1	132.8	95.8	109.3	83.7	100.9	$670.6 = X..$
2. $\sum_j X^2 ij$	4593.45	3623.34	1980.28	2406.37	1435.61	2054.51	16093.56
3. $(X_i.)^2/r$	4386.72	3527.17	1835.53	2389.30	1401.14	2036.16	15,576.02
4. $\sum_j (X_{ij} - \overline{X}_i.)^2$	206.73	96.17	144.75	17.07	34.47	18.35	517.54
5. $\overline{X}_i.$	29.62	26.56	19.16	21.86	16.74	20.18	$22.4 =$ mean

Note: $X_{ij} = j$th observation on the ith treatment ($i = 1, 2, 3. \ldots t$ and $j = 1, 2, \ldots\ldots r.$), $X_i =$ individual observation, and $X_i. =$ sum of all observation for the ith treatment

Table 3.11 Analysis of variance for data of Table 3.10

SOV	df	SS	Mean squares (MS)	$F_{\text{calulated}}$	$F_{\text{tablulated}}$
Among treatments	6–1 = 5	585.87	$\frac{585.87}{5}$ $= 117.17$	$\frac{117.17}{21.56} = 5.43^{**}$ Since $F_{\text{cal}} > F_{\text{tab}}$ at 0.05 and 0.01 thus there are highly significant (∗∗) differences among treatments	2.62 (0.05) 3.90 (0.01)
Error	6 (5–1) = 24	517.54	$\frac{517.54}{24}$ $= 21.56$		
Total	(5)(6)− 1 = 29	1103.41			

These generated numerical results are presented in an AONVA (Table 3.11), and it shows that there is significant difference among treatments. The standard error of treatment mean ($SE_{\overline{X}}$) and differences between treatment, CV, and least significance difference (LSD) are calculated by using the following equations:

$$SE_{\overline{X}} = \sqrt{\frac{s^2}{r}} = \sqrt{\frac{21.56}{5}}\text{mg} = \sqrt{4.312} = 2.07 \text{ mg}$$

$$SE_{\overline{X}_{i.}-\overline{X}_{i.}\cdot\cdot} = \sqrt{\frac{2s^2}{r}} = \sqrt{\frac{2(21.56)}{5}} = \sqrt{\frac{43.12}{5}} = \sqrt{8.62} = 2.93 \text{ mg}$$

$$\text{CV (Coefficient of variability)} = \frac{\sqrt{S^2}}{\overline{X}} \times 100 = \frac{\sqrt{21.56}}{22.4} \times 100 = \frac{4.64}{22.4} \times 100$$
$$= 20.7\%$$

$$\text{LSD} = t_{\alpha/2} S_{\overline{X}i.-\overline{X}i.\cdot\cdot} = t_{\alpha/2} S\sqrt{\frac{2}{r}} \text{ (for equal } r)$$

$$\text{LSD}_{0.05} = t_{0.025} S_{\overline{X}i.-\overline{X}i.\cdot\cdot} = 2.064\sqrt{\frac{2(21.56)}{5}} = 2.064\sqrt{8.62} = 2.064 \times 2.93$$
$$= 6.06 \text{ mg}$$

$$\text{LSD}_{0.01} = t_{0.005} S_{\overline{X}i.-\overline{X}i.\cdot\cdot} = 2.797\sqrt{\frac{2(21.56)}{5}} = 8.21 \text{ mg}$$

The observed differences are $\overline{X}1. - \overline{X}2. = 29.62–26.56 = 3.06$; $\overline{X}3. - \overline{X}4. = 19.16–21.86 = -2.7$; and $\overline{X}5. - \overline{X}6. = 16.74–20.18 = -3.44$. Now rank the means from the smallest to largest as shown below:

RTS1	RTS2	RTS3	RTS4	RTS5	Composite
29.62 (6)	26.56 (5)	19.16 (2)	21.86 (4)	16.74 (1)	20.18 (3)

Next is to calculate the difference and test significance level using LSD test at 5%.

6–1 = 29.62–16.74 = 12.88 > 6.06 = significant
6–2 = 29.62–19.16 = 10.46 > 6.06 = significant
6–3 = 29.62–20.18 = 9.44 > 6.06 = significant
6–4 = 29.62–21.86 = 7.76 > 6.06 = significant
6–5 = 29.62–26.56 = 3.06 < 6.06 = nonsignificant
5–1 = 26.56–16.74 = 9.82 > 6.06 = significant
5–2 = 26.56–19.16 = 7.4 > 6.06 = significant
5–3 = 26.56–20.18 = 6.38 > 6.06 = significant
5–4 = 26.56–21.86 = 4.70 < 6.06 = nonsignificant
4–1 = 21.86–16.74 = 5.12 < 6.06 = nonsignificant
4–2 = 21.86–19.16 = 2.70 < 6.06 = nonsignificant
4–3 = 21.86–20.18 = 1.68 < 6.06 = nonsignificant
3–1 = 20.18–16.74 = 3.44 < 6.06 = nonsignificant
3–2 = 20.18–19.16 = 1.02 < 6.06 = nonsignificant
2–1 = 19.16–16.74 = 2.42 < 6.06 = nonsignificant

3.8.2 Randomized Complete Block Design (RCBD)

The randomized complete block design (RCBD) is one of the most widely used designs in an agronomic field research. In this design experimental unit can be meaningfully grouped, and number of units in a group is equal to the number of treatments. These groups are called block or replication. The objective to have groups in blocks is to minimize error and ensure that observed differences will be due to treatments only. The RCBD has more advantages than the CRD due to blocking and further randomization which results to the more precision. The main purpose of blocking is to have higher accuracy by minimizing the experimental error due to the known sources of variation (SOV) among the experimental units. Grouping is done in such a way that variability within each block is minimized, while among block it is maximized. Variation within a block will be part of the experimental error; thus blocking is most effective when experimental area has a predictable pattern of variability. An ideal known SOV which can be used as basis for the blocking includes soil heterogeneity in nitrogen fertilizer experiments or varietal trials at multiple sites or sowing date experiments.

Thus, basis of blocking depends on the main SOV. The size and shape of blocks are selected in such a way so that there should be maximum variability among blocks. To do blocking, firstly, identify the gradient and do blocking vertical to the gradients, and if gradient occurs in two directions (one strong and other weak), then consider that gradient which is stronger, e.g., in case of fertility gradient. If fertility gradient is strong on both sides and perpendicular to each other, then use square blocks and choose Latin square design as elaborated by Gomez and Gomez (1980). Furthermore, whenever blocking is done, blocks identity and purpose should be clear. Similarly, if SOV is beyond the control, then ensure that such variation occurs among blocks as compared to within blocks. For example, in case of application of herbicides or data collection which might not be possible to complete in one day. In such scenario, it is recommended that it should be completed firstly for all plots of the same block. In this way, variation due to collection of data by multiple observers or application of treatments in more than one day becomes part of block variation and excluded from the experimental error. Following steps should be followed to design layout for RCBD.

1. Division of experimental area into "R" equal blocks (R = replications). The experimental area is divided into four blocks as shown in Fig. 3.4.
2. Subdivision of blocks into experimental plots based on number of treatments. For example, here if we suppose there are six treatments, i.e. A, B, C, D, E, and F, then divide each block into six subplots and assign each treatment into subplot using the random numbers (Fig. 3.5).
3. Repetition of step 2 for the remaining blocks (Fig. 3.6).

Let's apply the concept of RCBD on the data provided in Table 3.12 to generate ANOVA table and see significant difference among different oil contents of different canola cultivars. Step 1 includes arranging of raw data in ways as shown in Table 3.4. Calculate $\sum X^2$ and treatment ($X_{i.}$) and blocks ($X_{.j}$) totals, i. e. , $\sum_j X^2{}_{ij}$; $i = 1, 2...t$, and $\sum_i X^2{}_{ij}; j = 1, 2...r$. Step 2 is to calculate sum of squares using following formulas:

Fig. 3.4 Layout for the RCBD (division of experimental area into four blocks)

A
B
E
F
D
C
Block 1

Fig. 3.5 Subdivision of blocks into experimental plots based on number of treatments and randomization of treatments (A, B, C, D, E, and F)

A	B	E	A
B	D	B	E
E	C	A	F
F	F	C	C
D	E	D	B
C	A	F	D
Block 1	Block 2	Block 3	Block 4

Fig. 3.6 A randomized layout for the RCBD (six treatments and four replications)

$$\text{Correction factor} = \text{CF} = \frac{Y^2_{..}}{rt} = \frac{(1085.5)^2}{24} = \frac{(1085.5)^2}{24} = \frac{1,178,310.25}{24}$$
$$= 49,096.26$$

$$\text{SS}_{\text{total}} = \sum_{i,j} X^2 ij - \text{CF}$$

$$\text{SS}_{\text{total}} = 49,150.77 - 49,096.26 = 54.51$$

$$\text{SS}_{\text{block}} = \frac{\sum_j Y^2{}_{.j}}{t} - \text{CF}$$

$$\text{SS}_{\text{block}} = \frac{(269.8)^2 + (268.8)^2 + (274.2)^2 + (272.7)^2}{6} - 49,096.26$$

Table 3.12 Oil content (%) data of different canola cultivars with analysis of variance table

Cultivars		**Block**				**Treatments totals**		
		1	2	3	4	$Y_{i.}$	$\sum_j X^2_{ij}$	$\overline{Y}_i$
Can1		44.1	45.6	45.7	43.8	179.2	8031.1	44.8
Can2		43.0	41.6	44.6	46.8	176.0	7759.0	44.0
Can3		46.5	46.3	46.7	46.1	185.6	8612.0	46.4
Can4		44.1	43.7	44.2	42.8	174.8	7640.0	43.7
Can5		46.0	44.6	45.6	46.8	183.0	8374.8	45.8
Can6		46.1	47.0	47.4	46.4	186.9	8733.9	46.7
Block totals	$X_{.j}$	269.8	268.8	274.2	272.7	1085.5		
	$\sum_i X^2_{ij}$	12,142.08	12,061.46	12,538.3	12,408.93		49,150.77	

Analysis of variance (ANOVA)

SOV	**df**	**Sum of squares (SS)**	**Mean squares (MS)**	***F***
Blocks	$r-1 = 4-1 = 3$	3.14	1.05	
Treatments	$t-1 = 6-1 = 5$	31.65	6.33	4.83**
Error	$(r-1)(t-1) = 15$	19.72	1.31	
Total	$rt-1 = 24-1 = 23$	54.51		

** $P < 0.05$

$$SS_{\text{block}} = 49,099.4 - 49,096.26 = 3.14$$

$$SS_{\text{treatment}} = \frac{\sum_i Y^2{}_{i.}}{r} - CF$$

$$SS_{\text{treatment}} = \frac{(179.2)^2 + (176.0)^2 + (185.6)^2 + (174.8)^2 + (183.0)^2 + (186.9)^2}{4} - 49,096.26$$

$$SS_{\text{treatment}} = \frac{196,511.70}{4} - 49,096.26$$

$$SS_{\text{treatment}} = 49,127.91 - 49,096.26 = 31.65$$

$$SS_{\text{error}} = SS_{\text{total}} - SS_{\text{block}} - SS_{\text{treatment}}$$

$$SS_{\text{error}} = 54.51 - 3.14 - 31.65 = 19.72$$

3.8.3 Missing Values Estimation

Sometimes due to poor germination or due to climatic conditions, etc., data might be missing from the experimental unit. This missing data can be calculated by using following equation:

$$y = \frac{rB_o + tT_o - G_o}{(r-1)(t-1)}$$

where y = missing value estimation; t = number of treatments; r = number of replications; B_o = replication total that contains missing value; T_o = treatments total that contains missing value; and G_o = total of all observed values.

3.8.4 Latin Square Design

Treatments are arranged in rows and columns in Latin square design. Treatments (t) are repeated "t" times in such a way that t appear exactly one time in each column and row and denoted by Roman characters, thus called as Latin square design. The main purpose of this design is to reduce systematic error due to columns and rows (treatments) ($n \times$ n). The advantage in the use of this design is in the field experiment where two major SOVs exist, e.g., in case of soil difference in two directions, this design will help to remove variation. The disadvantage of this design is that number of rows, columns, and treatments should be equal. Latin square design for six treatments, i.e., A, B, C, D, E, and F, will be like as shown in Fig. 3.7. Analysis of

A	B	C	D	E	F
F	E	D	C	B	A
D	A	B	F	C	E
E	C	F	A	D	B
B	D	A	E	F	C
C	F	E	B	A	D

Fig. 3.7 Layout for Latin square design

variance for an $r \times r$ (6×6) Latin square data set oil yield (kg ha^{-1}) of canola cultivars is given in Table 3.13. The calculation involves following steps:

1. Calculation of row totals ($X_i.$), column totals ($X._j$), treatment totals (X_t), and grand total ($Y..$). Similarly, calculate $\sum_j X^2{}_{ij}$ and $\sum_i X^2{}_{ij}$ for each value of rows and columns (Table 3.13).
2. Calculation of correction factor and sum of squares (SS):

$$\mathrm{CF} = \frac{X^2..}{r^2} = \frac{(40,380)^2}{6^2} = 452,92,900$$

$$\mathrm{SS}_{\mathrm{total}} = \sum_{i,j} X^2{}_{ij} - \mathrm{CF} = 459,82,806 - 452,92,900 = 689,906$$

$$\begin{aligned}\mathrm{SS}_{\mathrm{row}} &= \frac{\sum_i X^2{}_{i.}}{r} - \mathrm{CF}\\ &= \frac{(6669)^2 + (6732)^2 + (6781)^2 + (6757)^2 + (6718)^2 + (6723)^2}{6}\\ &- 452,92,900 = 452,94,108 - 45,292,900 = 1208\end{aligned}$$

$$\begin{aligned}\mathrm{SS}_{\mathrm{column}} &= \frac{\sum_j X^2{}_{.j}}{r} - \mathrm{CF}\\ &= \frac{(6592)^2 + (6839)^2 + (6750)^2 + (6749)^2 + (6680)^2 + (6770)^2}{6}\\ &- 452,92,900 = 452,98,864 - 452,92,900 = 5964\end{aligned}$$

Table 3.13 Oil yield (kg ha^{-1}) of different canola cultivars with analysis of variance table under Latin square design

Rows	**Columns**						**Row totals**	
	1	2	3	4	5	6	$X_{i.}$	$\sum_j X^2 ij$
1	1329 (A)	950 (B)	980 (C)	1130 (D)	1060 (E)	1220 (F)	6669	7,518,041
2	1237 (F)	1070 (E)	1150 (D)	990 (C)	965 (B)	1320 (A)	6732	7,651,294
3	1126 (D)	1380 (A)	970 (B)	1240 (F)	985 (C)	1080 (E)	6781	7,787,401
4	1022 (E)	990 (C)	1250 (F)	1370 (A)	1140 (D)	985 (B)	6757	7,733,809
5	923 (B)	1170 (D)	1350 (A)	1040 (E)	1230 (F)	1005 (C)	6718	7,647,854
6	955 (C)	1279 (F)	1050 (E)	979 (B)	1300 (A)	1160 (D)	6723	7,644,407
Column totals $X_{.j}$	6592	6839	6750	6749	6680	6770	$\sum_{i,j} X_{ij}$ 40,380	$\sum_{i,j} X^2 ij$
$\sum_i X^2 ij$	7,372,724	7,936,641	7,711,300	7,711,541	7,527,550	7,723,050		45,982,806
Cultivar totals and means								
	A	**B**	**C**	**D**	**E**	**F**		
Total $= X_t$	8049	5772	5905	6876	6322	7456		
Mean $= \overline{X}_t$	1341.5	962	984.1667	1146	1053.667	1242.667		
Analysis of variance								
SOV	**df**	**SS**	**MS**	***F***				
Rows	$r-1 = 5$	1208	241.6	0.66				
Columns	$r-1 = 5$	5964	1192.8	3.29				
Cultivars	$r-1 = 5$	675,501	135,100.2	373.61** (highly significant difference among cultivars for oil yield since F calculated is greater than F tabulated at 1 and 5%)				
Error	$(r-1)(r-2) = 20$	7233	361.6					
Total	$r^2 - 1 = 35$	689,906	19,711.6					

$$\mathrm{SS_{treatment}} = \frac{\sum_t X^2{}_t}{r} - \mathrm{CF}$$
$$= \frac{(8049)^2 + (5772)^2 + (5905)^2 + (6876)^2 + (6322)^2 + (7456)^2}{6}$$
$$- 452,92,900 = 459,68,401 - 452,92,900 = 675,501$$

$$\begin{aligned}\mathrm{SS_{error}} &= \mathrm{SS_{total}} - \mathrm{SS_{row}} - \mathrm{SS_{column}} - \mathrm{SS_{treatment}} \\ &= 689,906 - 1208 - 5964 - 675,501 = 7233\end{aligned}$$

$$\text{Standard error of treatment means} = S_{\overline{X}} = \sqrt{\frac{S^2}{r}} = \sqrt{\frac{361.6}{6}} = 7.76\ \mathrm{kg}$$

$$\text{Sample standard error of difference between two treatment means} = S_{\overline{X}i-\overline{X}it}$$
$$= \sqrt{\frac{2S^2}{r}} = \sqrt{\frac{2S^2}{r}} = 10.97\ \mathrm{kg}$$

3.8.5 Factorial Experiments

Factorial experiments consist of number of factors as treatment with all possible combinations with different levels of equal importance. For example, an experiment involves temperature as treatment (factor) will have different levels of temperature. Similarly, if silicon (Si) fertilization is used as factor in pot experiment, several levels will be used to evaluate the experiment. For example, if we use two sources of Si (potassium silicate and sodium silicate) each at two different concentrations, it will be referred as a 2 × 2 or 2^2 factorial experiment. The possible combinations of two levels in each of the two factors will be four as shown in Table 3.14. Similarly, if Si fertilization experiment is conducted by using only potassium silicate with its two levels (no application as Si_0 and 200 mg L^{-1} of potassium silicate as Si_{200}) under

Table 3.14 2 × 2 or 2^2 factorial treatment combinations

Treatment combinations		
Treatment number	**Source (factor A)**	**Concentrations (factor B)**
1	Potassium silicate	100 mg L^{-1}
2	Potassium silicate	200 mg L^{-1}
3	Sodium silicate	100 mg L^{-1}
4	Sodium silicate	200 mg L^{-1}
Treatment number	**Water regimes**	**Concentrations**
1	W+	Si_o
2	W−	Si_{200}
3	W+	Si_o
4	W−	Si_{200}

Table 3.15 Symbolic representation of 3 × 3 or 3^2 factorial treatment combinations

Factors	*A*			
B	Levels	a_0	a_1	a_2
	b_0	a_0b_0	a_1b_0	a_2b_0
	b_1	a_0b_1	a_1b_1	a_2b_1
	b_2	a_0b_2	a_1b_2	a_2b_2

Table 3.16 Shoot dry weight (*g*) of sorghum plant under different silicon source as factor *A* and silicon concentration as factor *B* to illustrate simple effects, main effects, and interactions

Factor	***A* = Si source (case I)**				
B = Si concentrations	Level	a_1	a_2	Mean	$a_2 - a_1$ (simple effects)
	b_1	32.13	34.13	33.13	2
	b_2	38.13	44.13	41.13	6
	Mean	35.13	39.13	37.13	4 (main effect)
	$b_2 - b_1$ (simple effects)	6	10	8 (main effect)	
Factor	***A* = Si source (case II)**				
B = Si concentrations	Level	a_1	a_2	Mean	$a_2 - a_1$ (simple effects)
	b_1	34.13	37.13	35.63	3
	b_2	43.13	33.13	38.13	−10
	Mean	38.63	35.13	36.88	−3.5 (main effect)
	$b_2 - b_1$ (simple effects)	9	−4	2.5 (main effect)	
Factor	***A* = Si source (case III)**				
B = Si concentrations	Level	a_1	a_2	Mean	$a_2 - a_1$ (simple effects)
	b_1	30.13	32.13	31.13	2
	b_2	38.13	40.13	39.13	2
	Mean	34.13	36.13	35.13	2 (main effect)
	$b_2 - b_1$ (simple effects)	8	8	8 (main effect)	

two water regimes, i.e., with water (W+) and without water (W−), the design should be factorial with 2 × 2 or 2^2 as shown in Table 3.14. In factorial experiment, term *level* represents several treatments within any factor. The capital letters are used to represent factors, while levels (treatment combinations and means) were represented with small letters and numerical subscripts, e.g., a_1b_2 may refer to treatment combination consists of first level of A and second level of factor B with the mean of corresponding treatment. The df and SS for the variance among four treatment means in a 2^2 can be divided into single df and SS. Symbolic representation of 3 × 3 or 3^2 factorial treatment combinations has been shown in Table 3.15. The principles involved in the partitioning can be elaborated by Table 3.16. The four differences $a_2 - a_1$ at each level of *B* and $b_2 - b_1$ at each level of *A* are called simple effects. Average of simple effects is called main effect denoted by capital letters, e.g., A and B. The A and B for 2^2 factorial experiment can be calculated by using following equations:

$$A = \frac{1}{2}\ [(a_2b_2 - a_1b_2) + (a_2b_2 - a_1b_1)] = \frac{1}{2}\ [(a_2b_2 + a_2b_1) - (a_1b_2 + a_1b_1)]$$

$$B = \frac{1}{2}\ [(a_2b_2 - a_2b_1) + (a_1b_2 - a_1b_1)] = \frac{1}{2}\ [(a_2b_2 + a_1b_2) - (a_2b_1 + a_1b_1)]$$

Main effects in factorial experiment are averaged in number of ways same as other treatment. Different conditions might prevail within blocks and among blocks for factorial experiment in RCBD, and Latin square design thus in Table 3.16 factor A is replicated within every block as it is present at both levels for each level of factor B. In case of factorially arrangement treatment, hypothesis that is usually tested is "there is no interaction among factors." Data presented in Table 3.16 have shown that simple effects under I and II for Si sources (A) and concentrations (B) are different, while for III the simple effects for A and B as well as main effect are the same. The differential response obtained between the simple effects of a factor is called interaction as seen in cases I and II of Table 3.16. However, interaction is not present in case III of Table 3.16. This is the major advantage of application of factorial experiment as it provides information about the interaction between factors. The interaction of A and B can be defined by using following equations:

$$AB = \frac{1}{2}\ [(a_2b_2 - a_1b_2) - (a_2b_1 - a_1b_1)] = \frac{1}{2}\ [(a_2b_2 + a_1b_1) - (a_1b_2 + a_2b_1)]$$

The interaction for the data in Table 3.16:

$$AB = \frac{1}{2}\ (6 - 2) = 2\ (\text{simple effects of } A \text{ for Case I})$$

$$AB = \frac{1}{2}\ (10 - 6) = 2\ (\text{simple effects of } B \text{ for Case I})$$

The interaction for case II in Table 3.16:

$$AB = \frac{1}{2}\ [(33.13 - 43.13) - (37.13 - 34.13)]$$

$$AB = \frac{1}{2}\ [33.13 - 43.13 - 37.13 + 34.13]$$

$$AB = \frac{1}{2}\ [-13]$$

Fig. 3.8 Graphical illustration of interaction

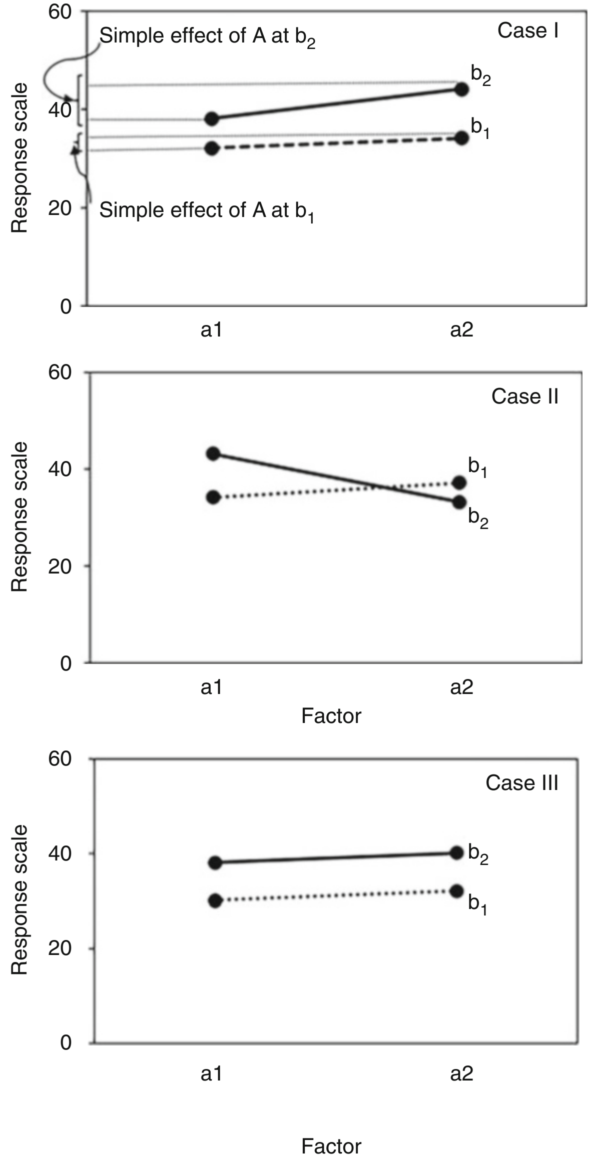

$$AB = -6.5$$

The interaction for case III in Table 3.16:

Table 3.17 Three factor ($3 \times 2 \times 3$ or $3^2 \times 2$) factorial experiments

Factor C (sorghum cultivars)	Factor B (Si fertilizer)	Factor A (locations)		
		a_1	a_2	a_3
c_1	b_1	$a_1b_1c_1$	$a_2b_1c_1$	$a_3b_1c_1$
	b_2	$a_1b_2c_1$	$a_2b_2c_1$	$a_3b_2c_1$
c_2	b_1	$a_1b_1c_2$	$a_2b_1c_2$	$a_3b_1c_2$
	b_2	$a_1b_2c_2$	$a_2b_2c_2$	$a_3b_2c_2$
c_3	b_1	$a_1b_1c_3$	$a_2b_1c_3$	$a_3b_1c_3$
	b_2	$a_1b_2c_3$	$a_2b_2c_3$	$a_3b_2c_3$

Table 3.18 Analysis of variance table for $3^2 \times 2$ factorial experiment in RCBD

SOV	df	SS	MS	F
Replication	$r-1 = 2$	61.65	30.83	8.96
A = locations	$a-1 = 2$	687.75	343.88	99.96**
B = Si fertilizer	$b-1 = 1$	149.25	149.25	43.39**
C = sorghum cultivars	$c-1 = 2$	1438.93	719.46	209.15**
AB	$(a-1)(b-1) = 2$	2.47	1.24	0.36
AC	$(a-1)(c-1) = 4$	6.35	1.59	0.46
BC	$(b-1)(c-1) = 2$	1.38	0.69	0.20
ABC	$(a-1)(b-1)(c-1) = 4$	0.024	0.006	0.001744
Error	$(r-1)(abc-1) = 34$	116.98	3.44	
Total	$abcr-1 = 53$	2464.78		

** P < 0.05

$$AB = \frac{1}{2}\left[(40.13 - 38.13) - (32.13 - 30.13)\right]$$

$$AB = \frac{1}{2}\left[40.13 - 38.13 - 32.13 + 30.13\right]$$

$$AB = \frac{1}{2}\left[0\right] = 0 \text{ (no intearction)}$$

Interaction concept is further elaborated by using graph as shown in Fig. 3.8. It should be noted that presence or absence of main effects does not tell anything about interaction presences or absence and vice versa. If interaction is nonsignificant, we can conclude that factors act independently. However, if interaction is large and significant, then main effects have little meaning. For large factorial experiments, it has been suggested to use confounded designs as described by Das and Giri (1979).

Factorial experiment other case includes e.g. if we have actor A as three locations and factor B as Si fertilizer with two levels, while factor C consists of three sorghum cultivars; such kind of factorial experiment will be referred as $3 \times 2 \times 3$ or $3^2 \times 2$ (Table 3.17).

ANOVA calculation for the $3 \times 3 \times 2$ or $3^2 \times 2$ factorial experiments involves following steps with results presented in ANOVA Table 3.18:

1. Calculation of correction factor, total sum of square, block SS, treatment SS and error SS

$$\text{Correction factor} = \text{CF} = \frac{X^2_{..}}{rabc} = \frac{(2903)^2}{54} = 156,038.77$$

$$\text{SS}_{\text{total}} = \sum_{i,j,k,r} X^2{}_{ijkr} - \text{CF} = 158,503.56 - 156,038.77 = 2464.78$$

$$\text{SS}_{\text{replication}} = \frac{\sum_{k=1}^{r} R^2{}_k}{abc} - \text{CF}$$

$$\text{SS}_{\text{repliaction}} = \frac{(968)^2 + (983)^2 + (953)^2}{18} - 156,038.77$$
$$= 156,100.43 - 156,038.77 = 61.65$$

$$\text{SS}_{\text{treatment}} = \frac{\sum_{j=1}^{a} \sum_{k=1}^{b} \sum_{i=1}^{c} Tr^2{}_{ijk}}{R} - \text{CF}$$

$$\text{SS}_{\text{treatment}} = \frac{(187)^2 + \ldots + (134)^2}{3} - 156,038.77 = 158,324.90 - 156,038.77$$
$$= 2286.15$$

$$\text{SS}_{\text{error}} = \text{SS}_{\text{total}} - \text{SS}_{\text{repliaction}} - \text{SS}_{\text{treatment}} = 2464.78 - 61.65 - 2286.15 = 116.98$$

2. Partitioning of treatments sum of squares into main effects and interactions

$$\text{SS}_A = \frac{\sum_j (a_j)^2}{rbc} - \text{CF}$$

$$\text{SS}_A = \frac{(1053)^2 + (952)^2 + (898)^2}{18} - 156,038.77 = 156,726.5 - 156,038.77$$
$$= 687.75$$

$$\text{SS}_B = \frac{\sum_k (b_k)^2}{rac} - \text{CF}$$

$$\mathrm{SS}_B = \frac{(1406)^2 + (1496)^2}{27} - 156,038.77 = 156,188 - 156,038.77 = 149.25$$

$$\mathrm{SS}_C = \frac{\sum_i (c_i)^2}{rab} - \mathrm{CF}$$

$$\mathrm{SS}_C = \frac{(1067)^2 + (992)^2 + (843)^2}{18} - 156,038.77 = 157,477.7 - 156,038.77$$
$$= 1438.93$$

$$\mathrm{SS}_{AB} = \frac{\sum_{j,k} \left(a_j b_k\right)^2}{rc} - \mathrm{CF} - (\mathrm{SS}_A + \mathrm{SS}_B)$$

$$\mathrm{SS}_{AB} = \frac{(509)^2 + (544)^2 + (462)^2 + (490)^2 + (435)^2 + (462)^2}{9}$$
$$- 156,038.77 - 687.75 - 149.25 = 2.47$$

$$\mathrm{SS}_{AC} = \frac{\sum_{j,i} \left(a_j c_i\right)^2}{rb} - \mathrm{CF} - (\mathrm{SS}_A + \mathrm{SS}_C)$$

$$\mathrm{SS}_{AC} = \frac{(387)^2 + (360)^2 + (306)^2 + (350)^2 + (326)^2 + (277)^2 + (330)^2 + (307)^2 + (261)^2}{6}$$
$$- 156,038.77 - (687.75 + 1438.93) = 6.35$$

$$\mathrm{SS}_{BC} = \frac{\sum_{k,i} (b_k c_i)^2}{ra} - CF - (\mathrm{SS}_B + \mathrm{SS}_C)$$

$$\mathrm{SS}_{BC} = \frac{(517)^2 + (550)^2 + (481)^2 + (512)^2 + (409)^2 + (435)^2}{9}$$
$$- 156,038.77 - (149.25 + 1438.93) = 1.38$$

$$\mathrm{SS}_{ABC} = \frac{\sum_{i,j,k} \left(a_j b_k c_i\right)^2}{r} - \mathrm{CF} - \mathrm{SS}_A - \mathrm{SS}_B - \mathrm{SS}_C - \mathrm{SS}_{AB} - \mathrm{SS}_{AC} - \mathrm{SS}_{BC}$$

$$\mathrm{SS}_{ABC} = \frac{(187)^2 + \ldots (134)^2}{3} - 156,038.77$$
$$- (\ \mathrm{SS}_A + \mathrm{SS}_B + \mathrm{SS}_C + \mathrm{SS}_{AB} + \mathrm{SS}_{AC} + \mathrm{SS}_{BC})$$

$$\mathrm{SS}_{ABC} = \frac{(187)^2 + \ldots (134)^2}{3} - 156,038.77 - 2286.3 = 0.024$$

Cultivars	Main Plot				Main Plot				Main Plot			
(Subplot)	N_0	N_1	N_2	N_3	N_1	N_0	N_3	N_2	N_3	N_2	N_1	N_0
C_1	C_1	C_2	C_3	C_2	C_2	C_3	C_2	C_1	C_2	C_1	C_2	C_3
C_2	C_2	C_1	C_1	C_3	C_3	C_1	C_1	C_2	C_1	C_2	C_3	C_1
C_3	C_3	C_3	C_2	C_1	C_1	C_2	C_3	C_3	C_3	C_3	C_1	C_2
	Replication 1				Replication II				Replication III			

Fig. 3.9 Layout for the split plot design

3.8.6 Fractional Factorial Design

Fractional factorial design is used when large number of factors needs to be tested. In this case, only fraction of total number of treatments is going to be tested based upon the systematic selection.

3.8.7 Nested and Split Plot Design

Nested and split plot experiments are multifactor experiments. Split plot design is used for factorial experiment with a principle that whole plots are divided into subplots or subunits. The factors which need more importance, greater precision, and smaller experimental material and expected to exhibit smaller differences are placed in the subunits. Consider an experiment to test factor *A* (nitrogen fertilizer) at four levels of RCBD and second factor *B* (sorghum cultivars) at three levels which can be placed by dividing each A units into subunits. Thus, layout for the split plot includes factor *A* which will be in the main plot while factor *B* in the subplot as shown in Fig. 3.9.

Layout design steps for the split plot includes (i) Division of experimental area into three blocks or replication with further division into four main plots for the nitrogen fertilizer application (ii) Two separate randomization is needed, firstly for the main plot (*N* treatments) and then for the subplots (cultivars). Split plot design in figure showed that size of the main plot is "*c*" times greater than subplot. Since in this experiment $c = 3$ (cultivars in subplot), thus the size of main plot is three times greater than subplot. However, each main plot treatment is tested, e.g., 3 times, while subplot treatment will be tested 12 times which leads to more precision in subplot treatments as compared to the main plot. Partitioning of degree of freedom for the split plot design under different arrangements has been presented in Table 3.19.

3.8.8 Strip Plot/Split-Block Design

Experiments in which both factors (e.g., *A* and *B* with multiple levels of *a* and *b*) require larger plot area strip plot design are used. In this design, whole area is divided into "*a*" horizontal and "*b*" vertical strips. One level of factor *A* is applied in

Table 3.19 Degree of freedom for split plot design under different arrangements

Completely randomized (r replications)		RCBD		Latin square	
SOV	df	SOV	df	SOV	df
Main unit or main plot					
				Rows	$a-1$
		Blocks	$r-1$	Columns	$a-1$
A	$a-1$	A	$a-1$	A	$a-1$
Error (a)	$a(r-1)$	Error (a)	$(a-1)(r-1)$	Error (a)	$(a-1)(a-2)$
Total	$ar-1$	Total	$ar-1$	Total	a^2-1
Subunit or subplot					
B	$b-1$	B	$b-1$	B	$b-1$
AB	$(a-1)(b-1)$	AB	$(a-1)(b-1)$	AB	$(a-1)(b-1)$
Error (b)	$a(r-1)(b-1)$	Error (b)	$a(r-1)(b-1)$	Error (b)	$a(a-1)(b-1)$
Subtotal	$ar(b-1)$	Subtotal	$ar(b-1)$	Subtotal	$a^2(b-1)$
Total	$abr-1$	Total	$abr-1$	Total	a^2b-1

Table 3.20 Analysis of variance for split-split plot design

SOV	df
(Main plot)	
Block	$r-1$
Factor A	$a-1$
Whole plot error	$(r-1)(a-1)$
(Subplots)	
Factor B	$b-1$
$A \times B$	$(a-1)(b-1)$
Subplot error	$a(r-1)(b-1)$
(Sub-subplots)	
Factor C	$c-1$
$A \times C$	$(a-1)(c-1)$
$B \times C$	$(b-1)(c-1)$
$A \times B \times C$	$(a-1)(b-1)(c-1)$
Sub-subplot error	$ab(r-1)(c-1)$
Total	$(rabc)-1$

horizontal strips while level of B in vertical strips. Strip plot main difference from split plot is to have second factor as strip.

3.8.9 Split-Split Plot Design

Split-split plot designs are applicable when there are three-factor factorial experiments with factor A assign to whole plots while factor B to subplot and factor C to sub-subplot. The ANOVA for split-split plot design with r blocks, a levels of factor A, b levels of factor B, and c levels of factor C has been shown in Table 3.20.

3.8.10 MANOVA (Multivariate Analysis of Variance)

Multivariate analysis of variance (MANOVA) is ANOVA with several dependent variables. It tests the difference in two or more vectors of means, e.g., evaluation of student's improvements in Physics and Chemistry using different syllabus. In this case, response variable (students' improvements) is altered by the observer manipulation of the independent variables. The assumptions to use MANOVA are:

1. The dependent variable should be normally distributed.
2. Linear relationship among all pairs of dependent variables.
3. Homogeneity of variances.

3.9 ANCOVA (Analysis of Covariance)

Analysis of covariance (ANCOVA) uses concepts of both analysis of variance and regression, and it is used when one independent variable is not at predetermined level. The uses of ANCOVA includes (i) increase of precision and control of error, (ii) estimation of missing data, (iii) adjustment of treatment means of dependent variables for corresponding independent variables, (iv) assistance in the data interpretation, and (v) partitioning of total covariance into parts.

3.10 Principal Component Analysis (PCA)

Principal component analysis is the method of multivariate statistics used to check variation and patterns in a data set. It is an easy way to visualize and explore data (Ahmed et al. 2020). Consider a data in two dimensions first (e.g., height and weight). The data can be plotted using scatter plot, but if we want to see variation, we must use PCA with new coordinate system. The axes don't have any physical meaning. Thus, PCA is a statistical procedure that uses orthogonal transformation to convert set of observation of correlated variables into values of linearly uncorrelated variables. It is the most common form of factor analysis applied to analyze interrelationship among variables (Fig. 3.10). The main objective of PCA is to cluster variables into manageable groups. These groups are known as the components (factors). Steps involved for the PCA are:

1. Standardization of the data $\left(z = {}^{\text{Variable value}-\text{Mean}}\!/_{\text{Standard deviation}}\right)$
2. Computing the covariance matrix (identification of correlation and dependence among features in a data set)
3. Eigenvectors and eigenvalues calculation
4. Commuting the principal components
5. Reducing the dimension of data set

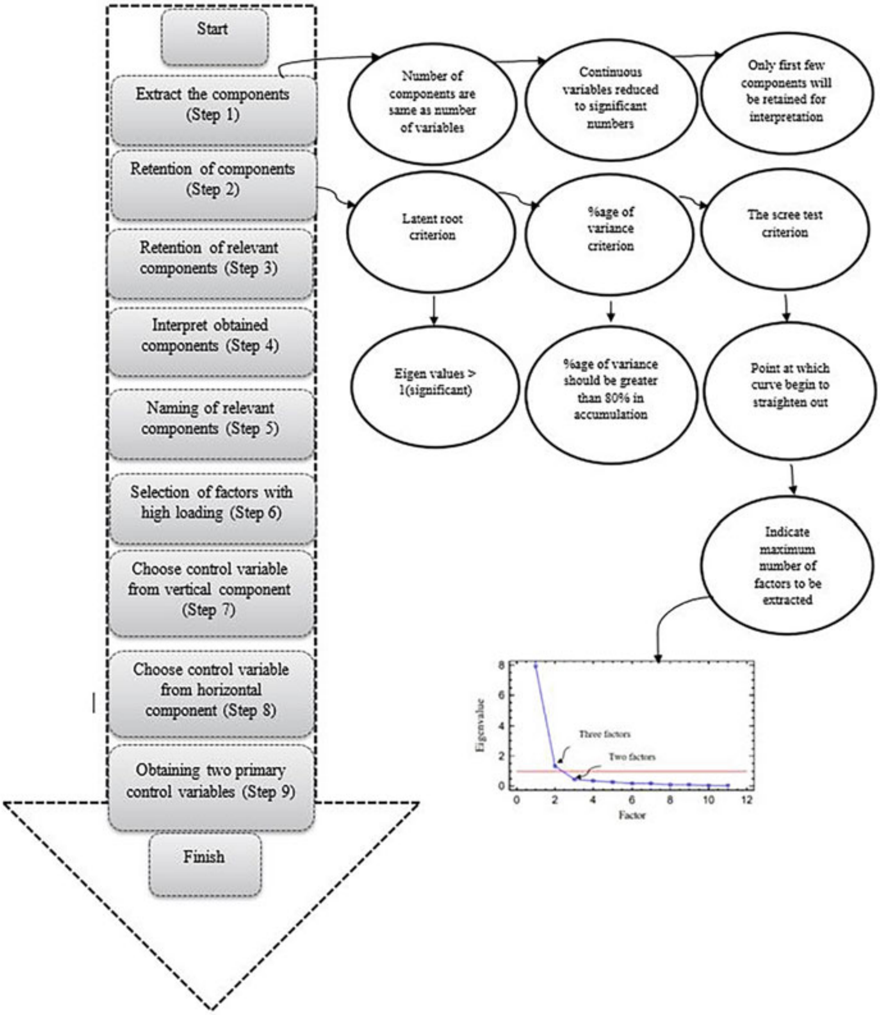

Fig. 3.10 PCA flow diagram

3.11 Regression

Consider a random sample of n observations in which Y values are determined from the corresponding X values, i.e., (X_1, Y_1), (X_2, Y_2), (X_3, Y_3). . . . (X_n, Y_n). In this case, Y is a dependent variable while X is an independent variable. First descriptive technique which can be used to determine the relationship between X and Y is the scatter diagram. This diagram is drawn by plotting the X and Y in Cartesian coordinates. The plotting pattern of points obtained between variables tells the relationship which can be either linear or nonlinear (Fig. 3.11). If relationship is

Fig. 3.11 Scatter plot to show relationship between two variables X and Y

linear, then we need to fit model that fits with the given data. Mathematically, the relation between X and Y can be elaborated by the following equation:

$$Y \propto X$$

This shows that there is relationship present between the two variables and drawn straight line between the points can serve as moving average of the Y values. The equation of straight line can be:

$$Y = a + bX$$

Any point (X, Y) on this line has a X coordinate (abscissa) and a Y coordinate (ordinate) whose values satisfy this equation. When $X = 0$ or minimum, $Y = a$ (intercept, value of Y X is minimum or zero). When intercept (a) is zero, the line passes through the origin. A unit change in Y due to unit change in X is called slope of the line and represented with b. Thus $b = \frac{\Delta Y}{\Delta X} = \frac{\text{Unit change in } Y}{\text{Unit Change in } X}$. If b is positive, both values increase or decrease together, but if b is negative, then one value increases while other decreases. This is an example of simple linear regression equation (Ahmed et al. 2011). However, if we increase number of X variables called as predictor variable (X_1 to X_n) against Y, it will be called multiple linear regression. The form of equation for the multiple linear regression will be:

$$Y = a + \beta_o X_1 + \beta_1 X_2 + \beta_2 X_3 + \ldots \beta_n X_n + \varepsilon$$

where $X_1 \ldots X_n$ = independent non-random variable; β_0, β_1, $\beta_2 \ldots \beta_n$ = slope; and ε = random varible represnting error term and genearlly equal to zero.

Let's consider the data set presented in Table 3.21 to describe the method of least square in order to fit a straight line and calculate simple regression equation and coefficient of determination (R^2). The calculation involves determination of SS_{xx}, SS_{xy}, $\overline{X}$, $\overline{Y}$, and β_1 as shown in the following equations:

$$SS_{xx} = \sum_{i=1}^{n} X^2{}_i - \frac{\left(\sum_{i=1}^{n} X_i\right)^2}{n} = 639 - \frac{(45)^2}{10} = 436.5$$

Table 3.21 Data set to illustrate method of least squares to fit a straight line

X_i	Y_i	X_iY_i	X_i^2
−2	−7	14	4
0	−3	0	0
4	3	12	16
−4	−9	36	16
7	8	56	49
8	11	88	64
10	15	150	100
13	23	299	169
14	25	350	196
−5	−11	55	25
$\sum X_i$=45	$\sum Y_i$=55	$\sum X_iY_i$=1060	$\sum X_i^2$=639

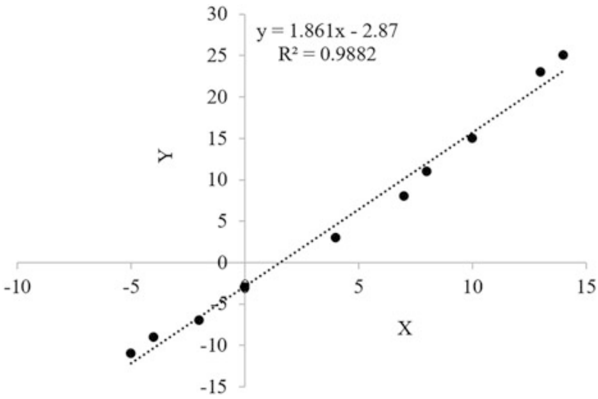

Fig. 3.12 Simple linear regression line with regression equation and coefficient of determination (R^2)

$$\mathrm{SS}_{xy} = \sum\nolimits_{i=1}^{n} X_iY_i - \frac{\left(\sum_{i=1}^{n} X_i\right)\left(\sum_{i=1}^{n} Y_i\right)}{n} = 1060 - \frac{(45)(55)}{10} = 812.5$$

$$\overline{X} = 4.5 \text{ and } \overline{Y} = 5.5.$$

$$\beta_1 = \frac{\mathrm{SS}_{XX}}{\mathrm{SS}_X} = \frac{812.5}{436.5} = 1.86$$

and

$$\overline{Y} = a + \beta_1\overline{X}$$

$$a = \overline{Y} - \beta_1\overline{X} = 5.5 - (1.86)(4.5) = 5.5 - 8.37 = -2.87.$$

Hence simple regression equation for this data is:

Table 3.22 ANOVA table for simple regression

SOV	df	Sum of squares (SS)	Mean squares (MS)	F
Regression (model)	1	$SS_R = \sum_{i=1}^{n} (\hat{y}_i - \bar{y})^2$	$\frac{SS_R}{df_R}$	$\frac{MS_R}{MS_{error}}$
Error (residuals)	$n-2$	$SS_E = \sum_{i=1}^{n} (y_i - \hat{y}_i)^2$	$\frac{SS_{error}}{df_{error}}$	
Total	$n-1$	$SS_T = \sum_{i=1}^{n} (y_i - \bar{y})^2$		

$$\hat{Y} = a + \beta_1 X = -2.87 + (1.86)\mathrm{X}.$$

The plot for this least square line is shown in Fig. 3.12. The quality of this fit can be measured quantitatively by using coefficient of determination (R^2). The equation for R^2 calculation is:

$$R^2 = \frac{SS_{yy} - SS_{error}}{SS_{yy}} = 1 - \frac{\sum_{i=1}^{n} (y_i - \hat{y}_i)^2}{\sum_{i=1}^{n} (y_i - \bar{y})^2}$$

$$SS_{error} = \sum_{i=1}^{n} (y_i - \hat{y}_i)^2 = \sum_{i=1}^{n} \left(y_i - (a + \beta_1 X)^2 = \sum_{i=1}^{n} (y_i - a - \beta_1 X)^2 \right.$$

Other approach which could be used to test hypothesis is use of ANOVA table as presented in earlier section. The ANOVA table for regression analysis is presented in Table 3.22. Furthermore, application of concept of multiple linear stepwise regression models has been elaborated using spring wheat grain yield data with respective R^2 (Table 3.23).

3.12 Correlation

Correlation is used to measure intensity or degree of association between variables. It is the same as covariance. It is a bivariate statistical technique. The simple linear correlation coefficient or simple correlation (total correlation and product-moment correlation) is sued for descriptive purposes and can be calculated by using following equations:

$$\boldsymbol{r} = \frac{\sum (X - \bar{X})(Y - \bar{Y}) / n - 1}{\sqrt{\sum (X - \bar{X})^2 / n - 1} \sqrt{\sum (Y - \bar{Y})^2 / n - 1}}$$

Table 3.23 Multiple linear stepwise regression models for spring wheat grain yield with environmental variables (E = environments (2008–09 and 2009–10), PW = planting windows, SR1 = solar radiation at anthesis, SR1 = solar radiation at maturity, T1 = mean average temperature at anthesis, T2 = mean average temperature at anthesis, PTQ1 = photothermal quotient at anthesis, PTQ2 = photothermal quotient at maturity) using stepwise method developed to predict wheat grain yield under changing climate

Regression models	
GY = β0 + β1X1	R^2
GY = 4495.18–872.517∗E	69.13
GY = 4115.66–309.75∗PW	69.28
GY = −1516.48 + 3.95491∗SR1	92.63
GY = −1575.85 + 2.57179∗SR2	93.43
GY = 3284.76–5.97019∗T1	51.02
GY = 4542.37–57.863∗T2	52.15
GY = −3814.55 + 49.8777∗PTQ1	87.77
GY = −2582.32 + 31.8736∗PTQ2	93.34
GY = β0 + β1X1 + β2X2	R^2
GY = 5424.43–872.517∗E − 309.75∗PW	87.41
GY = −2440.37 + 224.118∗E + 4.44915∗SR1	93.18
GY = −2366.93 + 193.912∗E + 2.84192∗SR2	93.86
GY = 5196.35–901.852∗E − 39.8932∗T1	69.85
GY = 1594.13–1225.4∗E + 146.385∗T2	73.54
GY = −2465.19 − 302.166∗E + 43.4934∗PTQ1	89.34
GY = −3268.13 + 149.999∗E + 34.4196∗PTQ2	93.61
GY = −836.161 − 80.6277∗PW + 3.5862∗SR1	93.51
GY = −820.636 − 92.5138∗PW + 2.31383∗SR2	94.63
GY = 1995.01–443.928∗PW + 153.171∗T1	76.77
GY = 5347.72–308.175∗PW − 52.7775∗T2	70.24
GY = −3453.92 − 26.2988∗PW + 47.8705∗PTQ1	87.84
GY = −2399.35 − 16.9782∗PW + 31.144∗PTQ2	93.38
GY = −1667.97 + 1.65868∗SR1 + 1.55638∗SR2	94.14
GY = −1241.88 + 3.96355∗SR1–17.2937∗T1	92.77
GY = −4931.17 + 27.4934∗SR1–519.678∗T2	93.91
GY = −1411.9 + 4.0845∗SR1–1.84298∗PTQ1	92.64
GY = −2262.19 + 1.62354∗SR1 + 19.4378∗PTQ2	93.91
GY = −945.844 + 2.61657∗SR2–43.2789∗T1	94.29
GY = −2612.93 + 2.64662∗SR2 + 38.3422∗T2	93.90
GY = −1808.8 + 2.39643∗SR2 + 3.97299∗PTQ1	93.46
GY = −2133.2 + 1.35065∗SR2 + 15.5732∗PTQ2	93.97
GY = 4550.48–0.599316∗T1–57.7877∗T2	52.15
GY = −3680.6 − 8.23152∗T1 + 49.8894∗PTQ1	87.80
GY = −2804.74 + 12.603∗T1 + 31.9554∗PTQ2	93.42
GY = −4063.73 + 8.96602∗T2 + 50.156∗PTQ1	87.80
GY = −4661.87 + 71.4527∗T2 + 34.112∗PTQ2	94.89
GY = −2572.68 − 0.241837∗PTQ1 + 32.0078∗PTQ2	93.34
GY = β0 + β1X1 + β2X2 + β3X3	R^2

(continued)

Table 3.23 (continued)

Regression models	
GY = −1121.59 + 49.1956∗E − 70.8354∗PW + 3.73947∗SR1	93.52
GY = −740.097 − 14.575∗E − 95.0961∗PW + 2.28633∗SR2	94.63
GY = 3783.86–791.812∗E − 405.893∗PW + 109.752∗T1	91.10
GY = 2365.39–1246.31∗E − 314.376∗PW + 155.057∗T2	92.36
GY = 305.873–494.994∗E − 139.285∗PW + 28.7889∗PTQ1	90.73
GY = −4950.36 + 342.09∗E + 74.6∗PW + 40.8858∗PTQ2	93.81
GY = −2778.85 + 266.679∗E + 2.0718∗SR1 + 1.67498∗SR2	94.90
GY = −2210.96 + 209.746∗E + 4.42281∗SR1–10.7162∗T1	93.23
GY = −3512.62 + 0.220823∗E + 4.23482∗SR1 + 70.9633∗T2	94.16
GY = −1752.91 + 564.722∗E + 7.79189∗SR1–36.8568∗PTQ1	94.12
GY = −3220.65 + 230.332∗E + 2.10348∗SR1 + 19.6712∗PTQ2	94.49
GY = −1660.51 + 164.599∗E + 2.8428∗SR2–40.3133∗T1	94.59
GY = −2686.81 + 105.353∗E + 2.7677∗SR2 + 25.1835∗T2	93.97
GY = −2248.81 + 223.19∗E + 3.06154∗SR2–4.05167∗PTQ1	93.88
GY = −2985.38 + 203.511∗E + 1.58608∗SR2 + 16.1864∗PTQ2	94.44
GY = 2279.55–1352.58∗E − 73.2781∗T1 + 176.787∗T2	75.78
GY = −2050.44 − 322.027∗E − 20.0369∗T1 + 43.1024∗PTQ1	89.52
GY = −3836.52 + 190.605∗E + 21.6873∗T1 + 35.2497∗PTQ2	93.81
GY = −3818.53 − 545.453∗E + 87.7865∗T2 + 41.0788∗PTQ1	90.87
GY = −4546.3 − 96.9147∗E + 82.7066∗T2 + 32.8195∗PTQ2	94.97
GY = −3189.3 + 212.106∗E − 9.10147∗PTQ1 + 40.5279∗PTQ2	93.72
GY = −981.556 − 81.4573∗PW + 1.27236∗SR1 + 1.56575∗SR2	95.03
GY = −959.051 − 111.806∗PW + 3.43148∗SR1 + 24.3069∗T1	93.65
GY = −2758.03 − 61.055∗PW + 3.92173∗SR1 + 62.4805∗T2	94.64
GY = 881.792–127.627∗PW + 5.00859∗SR1–23.2851∗PTQ1	94.09
GY = −1734.58 − 43.2957∗PW + 1.93291∗SR1 + 15.2077∗PTQ2	94.11
GY = −772.826 − 75.9091∗PW + 2.37316∗SR2–12.596∗T1	94.67
GY = −1696.5 − 86.1818∗PW + 2.39096∗SR2 + 30.4708∗T2	94.92
GY = 365.25–128.985∗PW + 2.88071∗SR2–15.1477∗PTQ1	94.97
GY = −765.837 − 95.1082∗PW + 2.38026∗SR2–0.939409∗PTQ2	94.63
GY = 3529.35–449.248∗PW + 161.654∗T1–70.7574∗T2	78.47
GY = −3435.79 − 31.2956∗PW + 3.09644∗T1 + 47.4847∗PTQ1	87.85
GY = −2497.58 − 63.0856∗PW + 33.7223∗T1 + 29.3817∗PTQ2	93.66
GY = −3669.07 − 24.3883∗PW + 6.79871∗T2 + 48.2274∗PTQ1	87.86
GY = −4910.46 + 15.9228∗PW + 74.0978∗T2 + 34.879∗PTQ2	94.92
GY = −2318.27 − 18.7935∗PW − 1.54335∗PTQ1 + 31.923∗PTQ2	93.38
GY = −1128.05 + 1.28052∗SR1 + 1.82477∗SR2–35.6472∗T1	94.68
GY = −3287.84 + 2.29884∗SR1 + 1.27881∗SR2 + 58.5742∗T2	95.13
GY = −1166.99 + 2.14204∗SR1 + 1.65779∗SR2–9.00197∗PTQ1	94.26
GY = −1975.86 + 1.25311∗SR1 + 1.08073∗SR2 + 9.23233∗PTQ2	94.29
GY = −4391.49 + 1.78814∗SR1 + 74.2775∗T2 + 20.5039∗PTQ2	95.58
GY = −1715.88 + 2.1342∗SR1–11.1793∗PTQ1 + 21.734∗PTQ2	94.10
GY = −2132.17 + 2.71418∗SR2–49.035∗T1 + 46.9579∗T2	94.98

(continued)

Table 3.23 (continued)

Regression models	
GY = −860.582 + 2.6733∗SR2–44.0303∗T1–1.2676∗PTQ1	94.29
GY = −987.816 + 2.5613∗SR2–42.0901∗T1 + 0.689252∗PTQ2	94.29
GY = −2736.16 + 2.53799∗SR2 + 37.6309∗T2 + 2.42991∗PTQ1	93.91
GY = −4176.79 + 0.754416∗SR2 + 63.405∗T2 + 24.7552∗PTQ2	95.07
GY = −2003.58 + 1.38361∗SR2–2.97666∗PTQ1 + 16.8284∗PTQ2	93.99
GY = −3948.13 − 9.1929∗T1 + 10.189∗T2 + 50.2071∗PTQ1	87.84
GY = −4766.43 + 7.30566∗T1 + 70.6152∗T2 + 34.1332∗PTQ2	94.92
GY = −4497.06 + 81.5281∗T2–11.4913∗PTQ1 + 40.8087∗PTQ2	95.12
GY = β0 + β1X1 + β2X2 + β3X3 + β4X4	R^2
GY = −1717.12 + 125.93∗E − 56.4191∗PW + 1.58618∗SR1 + 1.61888∗SR2	95.12
GY = −668.395 − 53.9363∗E − 128.193∗PW + 3.2354∗SR1 + 28.713∗T1	93.66
GY = −1479.49 − 418.451∗E − 132.643∗PW + 2.81869∗SR1 + 99.8435∗T2	95.20
GY = −117.991 + 382.545∗E − 84.8503∗PW + 7.21027∗SR1–39.8168∗PTQ1	94.61
GY = −4412.45 + 362.263∗E + 52.7493∗PW + 2.00147∗SR1 + 24.9586∗PTQ2	94.59
GY = −1029.59 + 50.4408∗E − 59.3438∗PW + 2.49561∗SR2–18.383∗T1	94.68
GY = −818.424 − 375.193∗E − 144.014∗PW + 1.78818∗SR2 + 72.0508∗T2	95.36
GY = 211.56 + 35.3623∗E − 124.003∗PW + 2.96738∗SR2–15.6806∗PTQ1	94.98
GY = 17.1993–84.1002∗E − 125.078∗PW + 2.60741∗SR2–6.39615∗PTQ2	94.65
GY = 1809.0–1117.23∗E − 380.863∗PW + 76.9233∗T1 + 124.976∗T2	93.99
GY = 1727.51–626.402∗E − 285.99∗PW + 72.3236∗T1 + 14.7125∗PTQ1	91.54
GY = −4499.41 + 276.811∗E + 40.3019∗PW + 12.304∗T1 + 38.3838∗PTQ2	93.83
GY = −345.954 − 932.419∗E − 203.84∗PW + 125.59∗T2 + 18.5194∗PTQ1	93.55
GY = −4041.76 − 179.645∗E − 25.9982∗PW + 87.9945∗T2 + 30.4637∗PTQ2	94.98
GY = −5519.16 + 522.302∗E + 105.491∗PW − 14.7528∗PTQ1 + 53.4642∗PTQ2	94.07
GY = −2201.79 + 233.107∗E + 1.71356∗SR1 + 1.87739∗SR2–28.8663∗T1	95.25
GY = −3381.18 + 122.646∗E + 2.32382∗SR1 + 1.40491∗SR2 + 43.4754∗T2	95.23
GY = −1594.43 + 1002.58∗E + 7.31229∗SR1 + 2.8626∗SR2–76.3668∗PTQ1	98.07
GY = −3001.23 + 259.019∗E + 1.72496∗SR1 + 1.27873∗SR2 + 7.62509∗PTQ2	95.00
GY = −2118.36 − 13.347∗E + 2.69947∗SR2–49.4896∗T1 + 48.7048∗T2	94.98
GY = −1298.82 + 231.246∗E + 3.36756∗SR2–44.8499∗T1–9.67945∗PTQ1	94.74
GY = −1996.51 + 173.71∗E + 2.46492∗SR2–31.7531∗T1 + 4.86799∗PTQ2	94.61
GY = −3250.19 − 640.28∗E − 41.8047∗T1 + 107.051∗T2 + 39.7331∗PTQ1	91.58
GY = −4587.11 − 89.3775∗E + 2.22363∗T1 + 81.5764∗T2 + 32.9265∗PTQ2	94.97
GY = −4475.23 − 28.2616∗E + 84.084∗T2–10.6634∗PTQ1 + 39.9494∗PTQ2	95.12
GY = −955.007 − 73.689∗PW + 1.24475∗SR1 + 1.61059∗SR2–6.07485∗T1	95.04
GY = −2462.56 − 66.0303∗PW + 1.87942∗SR1 + 1.33248∗SR2 + 48.8522∗T2	95.69
GY = 1674.45–155.41∗PW + 2.88299∗SR1 + 1.98577∗SR2–36.528∗PTQ1	96.35
GY = −312.752 − 112.05∗PW + 1.66867∗SR1 + 2.20423∗SR2–12.3245∗PTQ2	95.17
GY = −1843.34 − 44.634∗PW + 2.55566∗SR2–30.0858∗T1 + 39.5518∗T2	95.09
GY = 363.669–128.524∗PW + 2.88078∗SR2–0.28732∗T1–15.1136∗PTQ1	94.97
GY = −408.71 − 81.9211∗PW + 2.81537∗SR2–20.0906∗T1–5.75433∗PTQ2	94.69
GY = −3670.93 − 24.1757∗PW − 0.12556∗T1 + 6.83431∗T2 + 48.2449∗PTQ1	87.86
GY = −4874.7 + 10.215∗PW + 3.72791∗T1 + 72.7223∗T2 + 34.6149∗PTQ2	94.92

(continued)

Table 3.23 (continued)

Regression models	
GY = −4602.61 + 6.44894∗PW + 82.3013∗T2–11.1513∗PTQ1 + 40.9213∗PTQ2	95.12
GY = −2789.6 + 1.91952∗SR1 + 1.55887∗SR2–39.4595∗T1 + 62.1691∗T2	95.80
GY = −396.329 + 1.89706∗SR1 + 1.98872∗SR2–39.1942∗T1–12.183∗PTQ1	94.91
GY = −480.841 + 1.59121∗SR1 + 2.54324∗SR2–53.3785∗T1–11.3543∗PTQ2	94.77
GY = −1893.98 + 2.90465∗SR2–51.719∗T1 + 48.6524∗T2–4.17775∗PTQ1	95.01
GY = −3391.81 + 1.46283∗SR2–23.0213∗T1 + 58.4869∗T2 + 15.9022∗PTQ2	95.16
GY = −3981.32 + 0.791952∗SR2 + 73.4787∗T2–11.9459∗PTQ1 + 31.2513∗PTQ2	95.31
Y = β0 + β1X1 + β2X2 + β3X3 + β4X4 + β5X5	R^2
GY = −2348.68 + 258.764∗E + 12.2235∗PW + 1.76716∗SR1 + 1.9187∗SR2–33.0254∗T1	95.25
GY = −1792.68 − 234.418∗E − 105.354∗PW + 1.58191∗SR1 + 1.12343∗SR2 + 71.9212∗T2	95.84
GY = −184.511 + 838.766∗E − 73.2942∗PW + 6.81694∗SR1 + 2.82043∗SR2–78.3416∗PTQ1	98.43
GY = −289.506 − 2.53508∗E − 112.94∗PW + 1.66736∗SR1 + 2.21121∗SR2–12.48∗PTQ2	95.17
GY = −2589.5 − 27.4556∗PW + 1.85404∗SR1 + 1.50077∗SR2–28.13∗T1 + 57.0945∗T2	95.84
GY = 2202.57–231.216∗PW + 3.51711∗SR1 + 1.77738∗SR2 + 43.6298∗T1–46.4137∗PTQ1	96.65
GY = 245.489–93.855∗PW + 1.78851∗SR1 + 2.83208∗SR2–29.5739∗T1–20.2299∗PTQ2	95.30
GY = −746.366 − 94.1724∗PW + 3.00058∗SR2–17.8032∗T1 + 36.8552∗T2–13.6174∗PTQ1	95.34
GY = −3009.02 − 20.8459∗PW + 1.63506∗SR2–19.2907∗T1 + 52.7591∗T2 + 12.7727∗PTQ2	95.18
GY = −4266.05 − 32.9476∗PW + 23.4955∗T1 + 76.5957∗T2–15.1799∗PTQ1 + 41.4392∗PTQ2	95.21
GY = −1819.0 + 3.50132∗SR1 + 1.81621∗SR2–48.6106∗T1 + 85.463∗T2–26.5257∗PTQ1	96.70
GY = −3031.46 + 1.8465∗SR1 + 1.33771∗SR2–34.3125∗T1 + 64.033∗T2 + 3.36904∗PTQ2	95.80
GY = −3461.14 + 1.27339∗SR2–15.7506∗T1 + 69.2434∗T2–10.9138∗PTQ1 + 24.633∗PTQ2	95.32
Y = β0 + β1X1 + β2X2 + β3X3 + β4X4 + β5X5 + β6X6	R^2
GY = −2115.22 − 148.483∗E − 67.5486∗PW + 1.67558∗SR1 + 1.30211∗SR2–17.0565∗T1 + 68.4621∗T2	95.88
GY = −517.057 + 898.256∗E − 38.6623∗PW + 6.85498∗SR1 + 2.95882∗SR2–16.5802∗T1–77.5504∗PTQ1	98.47
GY = −738.307 + 118.975∗E − 48.5922∗PW + 1.87334∗SR1 + 2.62473∗SR2–35.251∗T1–14.4497∗PTQ2	95.32
GY = −1178.05 + 899.602∗E + 6.8455∗SR1 + 2.96831∗SR2–31.9094∗T1 + 13.5518∗T2–74.1903∗PTQ1	98.46
GY = −3028.67 + 21.7114∗E + 1.86749∗SR1 + 1.38125∗SR2–34.1386∗T1 + 61.0605∗T2 + 2.95928∗PTQ2	95.80

(continued)

Table 3.23 (continued)

Regression models	
GY = −3486.29 + 92.9008∗E + 1.41235∗SR2–12.406∗T1 + 59.2894∗T2–13.9926∗PTQ1 + 25.9524∗PTQ2	95.38
GY = 594.397–196.044∗PW + 4.63831∗SR1 + 1.66246∗SR2 + 23.0033∗T1 + 72.8577∗T2–53.4338∗PTQ1	97.91
GY = −2481.28 − 29.6402∗PW + 1.8767∗SR1 + 1.58055∗SR2–29.1928∗T1 + 55.9794∗T2–1.28573∗PTQ2	95.84
GY = −2227.94 − 68.9646∗PW + 1.75248∗SR2 + 0.0719391∗T1 + 55.4433∗T2–16.1384∗PTQ1 + 18.4592∗PTQ2	95.50
GY = −2930.65 + 3.35027∗SR1 + 0.709417∗SR2–23.3052∗T1 + 98.4384∗T2–30.3258∗PTQ1 + 17.4223∗PTQ2	96.86
Y = β0 + β1X1 + β2X2 + β3X3 + β4X4 + β5X5 + β6X6 + β7X7	R^2
GY = −522.117 + 734.207∗E − 62.8549∗PW + 6.59519∗SR1 + 2.7072∗SR2–12.0194∗T1 + 22.7315∗T2–74.0542∗PTQ1	99.53
GY = −1202.83 − 216.846∗E − 100.018∗PW + 1.73874∗SR1 + 1.72226∗SR2–18.7737∗T1 + 66.5448∗T2–8.24543∗PTQ2	96.90
GY = 905.486–202.513∗PW + 4.70728∗SR1 + 1.88784∗SR2 + 20.0973∗T1 + 69.7402∗T2–53.5304∗PTQ1–3.62754∗PTQ2	98.92
Y = β0 + β1X1 + β2X2 + β3X3 + β4X4 + β5X5 + β6X6 + β7X7 + β8X8	R^2
GY = −3670.28 + 1097.09∗E + 56.959∗PW + 6.98681∗SR1 + 1.34258∗SR2–5.07598∗T1 + 23.9757∗T2–83.4396∗PTQ1 + 30.2752∗PTQ2	99.78

$$r = \frac{\sum\left(X-\overline{X}\right)\left(Y-\overline{Y}\right)}{\sqrt{\sum\left(X-\overline{X}\right)^2\sum\left(Y-\overline{Y}\right)^2}}$$

Correlation coefficient ranges from +1 to −1. If $r = +1$, then it shows positive covariance, while if $r = -1$, it means negative correlation, and if $r = 0$, it means no correlation at all. Correlation measures co-relation a joint property of two variables, while regression deals with the change of one variable in relation to change of another variable. In correlation, random pair of observation was obtained, while in regression, only the dependent variable needs to be randomly and normally distributed. The application of concept of correlation has been illustrated in Fig. 3.13 (Ahmed 2011).

3.13 Analytical Tools/Software

Analytical tools which can be used for the statistical analysis are listed below:

1. R
2. SAS
3. Sigma plot

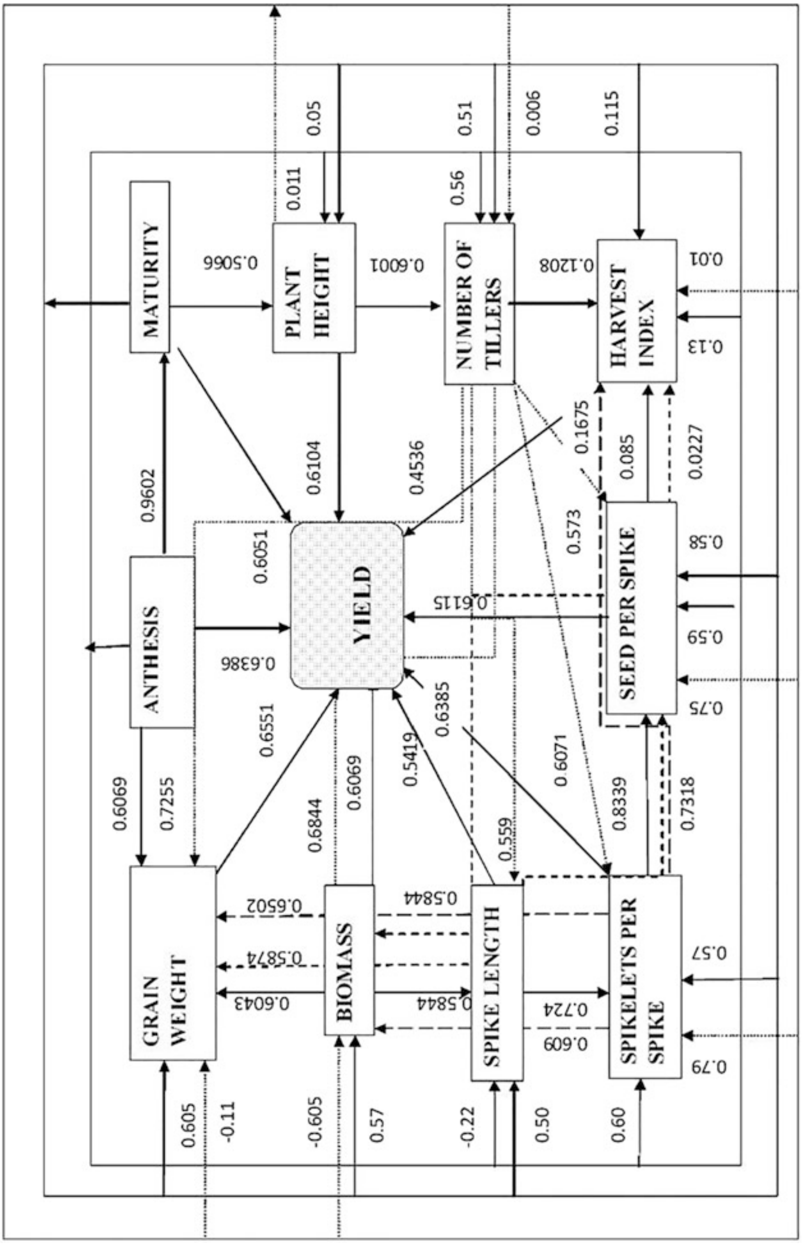

Fig. 3.13 Correlation analysis between spring wheat yield and yield components

4. Stat graphics
5. Minitab
6. SPSS
7. MS Excel
8. MATLAB
9. GraphPad Prism
10. GenStat
11. SigmaStat
12. Stata
13. Statistica

References

Acutis M, Scaglia B, Confalonieri R (2012) Perfunctory analysis of variance in agronomy, and its consequences in experimental results interpretation. Eur J Agron 43:129–135. https://doi.org/10.1016/j.eja.2012.06.006

Ahmed M (2011) Climatic resilience of wheat using simulation modeling in Pothwar. PhD thesis. Arid Agriculture University, Rawalpindi

Ahmed M, Hassan FU, Aslam MA, Akram MN, Akmal M (2011) Regression model for the study of sole and cumulative effect of temperature and solar radiation on wheat yield. Afr J Biotechnol 10(45):9114–9121. https://doi.org/10.5897/AJB11.1318

Ahmed K, Shabbir G, Ahmed M, Shah KN (2020) Phenotyping for drought resistance in bread wheat using physiological and biochemical traits. Sci Total Environ 729:139082. https://doi.org/10.1016/j.scitotenv.2020.139082

Bennington CC, Thayne WV (1994) Use and misuse of mixed model analysis of variance in ecological studies. Ecology 75(3):717–722. https://doi.org/10.2307/1941729

Blouin DC, Webster EP, Bond JA (2011) On the analysis of combined experiments. Weed Technol 25(1):165–169

Bolker BM, Brooks ME, Clark CJ, Geange SW, Poulsen JR, Stevens MHH, White J-SS (2009) Generalized linear mixed models: a practical guide for ecology and evolution. Trends Ecol Evol 24(3):127–135. https://doi.org/10.1016/j.tree.2008.10.008

Das MN, Giri NC (1979) Design and analysis of experiments. Wiley Eastern, New Delhi, 295 p

Fisher RA (1921) Studies in crop variation. I. An examination of the yield of dressed grain from Broadbalk. J Agric Sci 11(2):107–135. https://doi.org/10.1017/S0021859600003750

Gbur EE, Stroup WW, KS MC, Durham S, Young LJ, Christman M, West M, Kramer M (eds) (2012) Analysis of generalized linear mixed models in the agricultural and natural resources sciences. American Society of Agronomy, Crop Science Society of America, Soil Science Society of America, Madison. https://doi.org/10.2134/2012.generalized-linear-mixed-models.frontmatter

Gomez KA, Gomez AA (1984) Statistical procedures for agricultural research. Wiley, New York, 680 p

Lawson J (2010) Design and analysis of experiments with SAS. Chapman and Hall/CRC

Lencina VB, Singer JM, Stanek EJ III (2005) Much ado about nothing: the mixed models controversy revisited. Int Stat Rev 73(1):9–20. https://doi.org/10.1111/j.1751-5823.2005.tb00248.x

Loughin TM (2006) Improved experimental design and analysis for long-term experiments this work was done while the author was on faculty in the Department of Statistics at Kansas State University. Crop Sci 46(6):2492–2502. https://doi.org/10.2135/cropsci2006.04.0271

McIntosh MS (1983) Analysis of combined Experiments1. Agron J 75(1):153–155. https://doi.org/10.2134/agronj1983.00021962007500010041x

McIntosh MS (2015) Can analysis of variance be more significant? Agron J 107(2):706–717. https://doi.org/10.2134/agronj14.0177

McNutt M (2014) Raising the bar. Science 345(6192):9–9. https://doi.org/10.1126/science.1257891

Mead R (2017) Statistical methods in agriculture and experimental biology. Chapman and Hall/CRC

Moore KJ, Dixon PM (2015) Analysis of combined experiments revisited. Agron J 107(2):763–771. https://doi.org/10.2134/agronj13.0485

Nature Publishing Group (2005) Statistically significant. Nat Med 11(1):1–1. https://doi.org/10.1038/nm0105-1

Nature Publishing Group (2013a) Nature. Medicine 19(5):508–508. https://doi.org/10.1038/nm0513-508

Nature Publishing Group (2013b) Reporting life sciences research. Nature Publishing Group, London. http://www.nature.com/authors/policies/reporting.pdf

Nelder JA (2008) What is the mixed-models controversy? Int Stat Rev 76(1):134–135. https://doi.org/10.1111/j.1751-5823.2007.00022_1.x

Nelder JA, Lane PW (1995) The computer analysis of factorial experiments: in memoriam—Frank Yates. Am Stat 49(4):382–385. https://doi.org/10.1080/00031305.1995.10476189

Snedecor GW (1942) The use of tests of significance in an agricultural experiment station. J Am Stat Assoc 37(219):383–386. https://doi.org/10.2307/2279007

Steel R, Torrie J (1980) Principles and procedures of statistics, 2nd edn. McGraw-Hill Book Co., New York

Voss DT (1999) Resolving the mixed models controversy. Am Stat 53(4):352–356. https://doi.org/10.2307/2686056

Wang T, DeVogel N (2019) A revisit to two-way factorial ANOVA with mixed effects and interactions. Commun Stat Theory Method:1–18. https://doi.org/10.1080/03610926.2019.1604961

West BT, Galecki AT (2012) An overview of current software procedures for fitting linear mixed models. Am Stat 65(4):274–282. https://doi.org/10.1198/tas.2011.11077

Yang RC (2010) Towards understanding and use of mixed-model analysis of agricultural experiments. Can J Plant Sci 90(5):605–627. https://doi.org/10.4141/CJPS10049

Dynamic Modeling

4

Mukhtar Ahmed, Muhammad Ali Raza, and Taimoor Hussain

Abstract

Dynamic modeling is a valuable technique used to understand different systems on a temporal basis. This approach resulted in a more practical, intuitive endeavor modeling. The main objective of this chapter is to elaborate on different modeling approaches with more emphasis on dynamic modeling. Firstly mathematical modeling was discussed and defined as the quantitative expression of the biological system from the lower hierarchy to the higher. It is a description of a system using mathematical concepts and language to facilitate the process of explanation of a system. The mathematical model can be further classified into static or dynamic, deterministic or stochastic, and continuous or discrete. A model that uses large numbers of theoretical information to predict what happens at one level by considering processes at lower levels of the system is known as mechanistic models. In this book chapter, we present a general description of modeling with a history of dynamic modeling from the eighteenth century to today. Furthermore, the application of dynamic process-based crop growth model in different fields of studies was discussed. Outcomes of the reviewed studies confirmed that process-based dynamic crop simulation models are valuable tools for the understanding of the system and giving options and solutions to the what-if questions under different sets of scenarios and managements.

M. Ahmed (✉)
Department of Agricultural Research for Northern Sweden, Swedish University of Agricultural Sciences, Umeå, Sweden

Department of Agronomy, Pir Mehr Ali Shah Arid Agriculture University, Rawalpindi, Pakistan
e-mail: mukhtar.ahmed@slu.se; ahmadmukhtar@uaar.edu.pk

M. A. Raza
College of Agronomy, Sichuan Agricultural University, Chengdu, Sichuan, China

T. Hussain
Department of Agronomy, Pir Mehr Ali Shah Arid Agriculture University, Rawalpindi, Pakistan

M. Ahmed (ed.), *Systems Modeling*, https://doi.org/10.1007/978-981-15-4728-7_4

Keywords

Dynamic modeling · Modeling approaches · Mathematical modeling · Static or dynamic · Deterministic or stochastic · Continuous or discrete · Mechanistic models

4.1 Introduction

Modeling is the mathematical expression of the biological system starting from the lower to the higher hierarchy, e.g., cell, tissues, organ, organ system, and complete plant as a system. However, the system can also be anything under observation that could be soil organic carbon, soil water and temperature, nutrients, erosion, runoff, and drainage, etc. A mathematical model is a description of a system using mathematical concepts and language to facilitate the process of explanation of a system. It can also be used to check the relationship between different variables. The relationship can be linear, i.e., $y = a+bx$, or it can be nonlinear. Mathematical concepts and languages are used to describe all kinds of systems. It can be systems belonging to the social sciences, engineering, natural sciences, and agricultural sciences. The process of developing a mathematical model is called mathematical modeling which can further help to solve different what-if scenarios. The typical mathematical modeling process has been elaborated in Fig. 4.1. For example, how long the pasture will last in a field depends on the numbers of cows. If there are nine cows, then it might last for 3 days, and if there are three, it might last for 7. However, how long it will last if there is only one cow? This can be a good example of a task for the students to think mathematically and apply linear or nonlinear models to get answers to the problem. Application tools like GeoGebra (https://www.geogebra.org/?

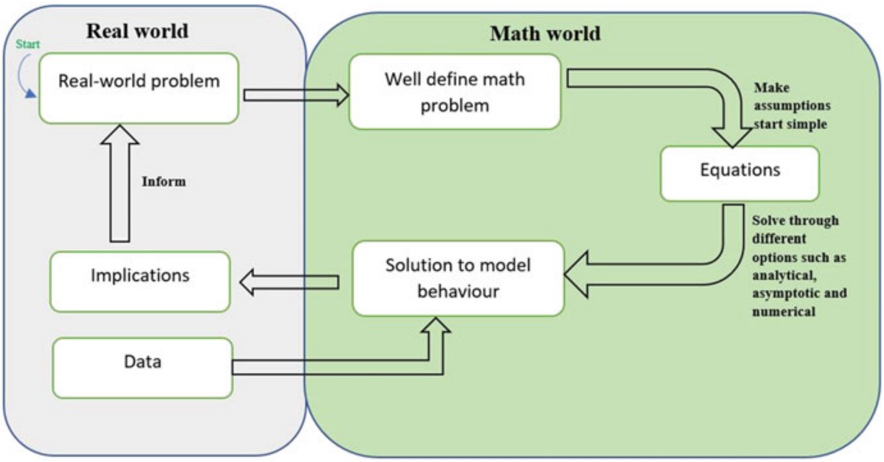

Fig. 4.1 Typical mathematical modeling process

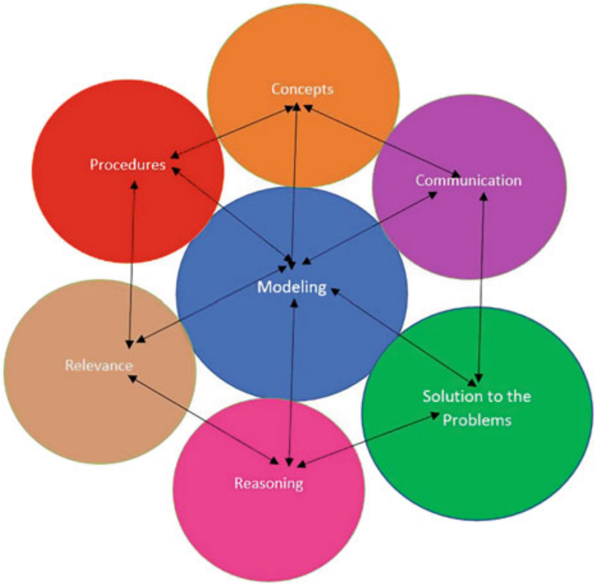

Fig. 4.2 Modeling interaction and linkage with different components

lang=en) have been mainly used to develop simple mathematical models and proposed solutions to different issues. The interaction and linkage of modeling with various components such as procedures, concepts, communication, relevance, reasoning, and solution to the problem have been shown in Fig. 4.2.Thus a model helps to explain systems under different sets of scenarios and give answers to the issues.

Mathematical modeling has been used due to different reasons such as building a scientific understanding through the quantitative expression of a system, testing of a system through different variables, and aiding in decision-making powers of policymakers. The mathematical model can be further classified into static or dynamic, deterministic or stochastic, and continuous or discrete. Deterministic models ignore random variation and all the time produce the same output (fixed outputs against fixed inputs). A model that can predict the distribution of possible outcomes is called stochastic (different outputs against fixed inputs by considering random variation). The distinction between different types of models can also be made by considering the hierarchy of organizational structures that have been used to model the system (Fig. 4.3). A model that employs large numbers of theoretical information to predict what happens at one level by considering processes at lower levels of the system is called mechanistic models. These models consider a mechanism to describe the changes occur at any level of the systems. However, in the case of empirical models, mechanisms were not considered. These two-division models (deterministic/stochastic and mechanistic/empirical) represent a wide range of model types. Furthermore, two other methods of classification are complementary, e.g., a deterministic model can be either be empirical or mechanistic but can never be

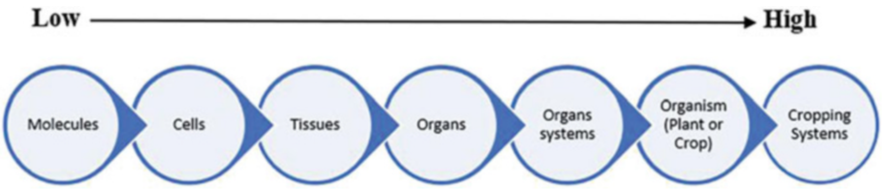

Fig. 4.3 Hierarchy of system

Table 4.1 Four briad categories of models

	Deterministic	Stochastic
Mechanistic	Differential equation (Newtonian mechanics based on planetary motion)	Probabilistic equations
Empirical	Regression relationship (Predicting cattle growth with feed intake)	Analysis of variance (ANOVA) of crop yields over sites, sowing dates and years

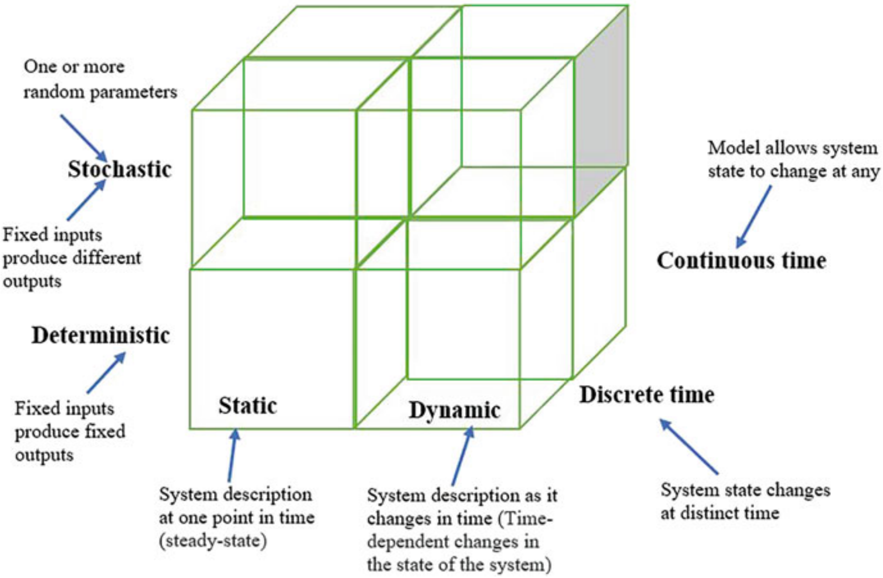

Fig. 4.4 Type of modeling

stochastic as presented in Table 4.1. Further elaboration of the classification of mathematical models has been displayed in Fig. 4.4.

Chew et al. (2014) reported that nowadays it is complementary to use mathematical modeling as a tool with experimental approaches to have a clear understanding of different biological mechanisms from lower hierarchy to higher at different spatio-temporal scale. Different time-based dynamic models have been used to elaborate events at a wide range of biological levels. These models were able to answer specific biological questions and help to facilitate the investigation of several phenomena in the plant system, e.g., light signaling and environmental responses. Models could be classified into three categories: (i) molecular-level modeling, which can be (a) oscillating system (time-dependent) and (b) non-oscillating system (time-independent constant/steady state); (ii) cellular-level modeling; and (iii) phenology-level modeling. The circadian clock (a sensor of time) is the best example of an oscillating system, while activation of phytochrome by red light comes under the non-oscillating system. Examples of circadian-regulated processes include hypocotyl elongation, stomatal activity, photosynthetic rate, cold acclimation, signaling of hormones, and starch turnover (Dodd et al. 2005; Dong et al. 2011; Graf et al. 2010; Keily et al. 2013; Nomoto et al. 2012). Similarly, the circadian clock enables plants to recognize day length necessary to have flowering and complete reproduction in favorable climatic conditions. Thus, flowering is induced by photoperiod in many species (Corbesier et al. 1996, 2007).

Models can help in the building, testing, and refining of the hypothesis. Roeder et al. (2010) conducted a modeling study of cell growth and division with the question of how cell size distribution in the sepal epidermis is regulated by endoreduplication or endo-cycling (nuclear genome replication in the absence of mitosis) patterns. The epidermal cell growth and development model was developed with integration to the stochastic model of the cell cycle. This helps to switch between endoreduplication and mitotic states. The model was able to generate sepal epidermis with proper distribution of cell sizes, and its linkage with endoreduplication observed patterns with the size of individual cells in tissues. Finally, it provides a simple mechanistic explanation for the complex observed phenotype. Peng et al. (2020) reported that prediction of manipulation of genotype (G) and agronomic management (M) on agricultural ecosystem performances under future environmental (E) conditions remains a challenge that can be solved by process based modelling. They also suggested multiscale crop modelling framework that can design gene to farm level resilient systems from regional to global scale.

Dupuy et al. (2010) used similar techniques to study the coupling of growth and development to determine cell shape. Biomechanical modeling was further used by Hamant et al. (2008) and Kierzkowski et al. (2012), in which they demonstrated how cell growth is regulated by mechanical forces by using mathematical modeling of the tissue mechanics. Similarly, modeling helps to connect tissue- and organ-level phenomena to molecular mechanisms. Furthermore, there are models with a long history that can stimulate growth and development at the organismal level. These models have been used practically in the simulation of crop growth and development. Simulation models can be a useful helping tool for crop management (Ahmed et al. 2013; Asseng et al. 2019; Aslam et al. 2017a; Ahmed and Stockle 2016; van Keulen and Asseng 2019). Nowadays, these models are trying to be merged with genetics to have gene-based modeling, which will improve their predictive power.

4.2 History of Dynamic Models

The history of the dynamic model goes back to the eighteenth century when developmental events (e.g., flowering) in plants were modeled in relation to cumulative daily temperature (Robertson 1968). A positive correlation between temperature and plant development was observed in this model, but later studies showed that above a critical temperature, plant development is impaired (Summerfield et al. 1992). The photothermal time model concept was further introduced in crop modeling after the discovery of photoperiodism (Brisson et al. 2003; Stöckle et al. 2003; Dingkuhn et al. 2008). Additionally, the concept of vernalization (winter chilling) was incorporated in the thermal time models. Crop growth modeling was further improved by Farquhar et al. (1980). They were able to simulate photosynthesis by considering kinetic details of light-dependent and light-independent reactions. A number of key events and drivers that led to the development of a dynamic agricultural systems model have been presented in Table 4.2 (Jones et al. 2017).

4.3 Examples of Dynamic Agricultural Systems Models

4.3.1 AquaCrop

AquaCrop is developed by the Food and Agriculture Organization (FAO) to simulate the effect of management and environment on crop production under conditions where water is the limiting factor (Fig. 4.5). Zeleke (2019) calibrated and validated AquaCrop for faba bean under supplemental irrigation, sowing time, and sowing rate and concluded that this model could be used as a decision support tool for different agronomic managements. Drought frequency and severity are increasing day by day, and there is dire need to determine water productivity and total evaporation (ET). This will help manage water resource in an effective way. Mbangiwa et al. (2019) used the FAO AquaCrop model to measure water productivity and ET for soybean (*Glycine max* L.) crop. Application of AquaCrop for cotton production under film-mulched drip irrigation in salt-affected soil was conducted by Tan et al. (2018) using a 4-year dataset. One-year data was used for model calibration, while the remaining 3 years of data was used for validation. The model was able to simulate canopy cover, soil water content, and dry matter with good accuracy. Thus this model can be a good tool to simulate cotton growth under film-mulched drip irrigation. The irrigation schedule for good crop production can be designed by the use of the AquaCrop model. Ran et al. (2018) conducted maize simulation under plastic film-mulch using default parameters initially. Afterward, model parameters which include soil water content, canopy cover, biomass, and yield were parameterized using field data. The results showed that the parameterized model was better compared to the default model. However, model behavior was very sensitive to water stress conditions. Traditional leafy vegetables (TLV) are a good source of nutrients to combat micronutrient deficiency, but they are not utilized properly due to lack of information related to TLV water and fertilizer management. Nyathi et al.

Table 4.2 Historical prospective of dynamic models in the agricultural systems

S. No	Year	Event	References
1.	1940–50	Computational analysis of soil and plant process for the optimization of plant soil system research	de Wit (1958), van Bavel (1953)
2.	1940–50	Dairy cattle nutritional requirement and modeling animal response to nutrients	NRC (1945)
3.	1950–70	Policy analysis of rural development by modeling agricultural production through linear programming methods	Heady and students at Iowa State University
4.	1960–70	Soil-water balance modeling (WATBAL)	Slatyer (1960, 1964), Keig and McAlpine (1969), Ritchie (1972), McCown (1973)
5.	1964–74	Development of grassland ecosystem models by International Biological Program	–
6.	1965	Europe feeding systems models	ARC (Agricultural Research Council (Great Britain)) (1965)
7.	1965–70	Development of photosynthesis and growth models	de Wit (1958, 1965), de Wit et al. (1970, 1978), Duncan et al. (1967)
8.	1969–75	Cotton models by Cotton Systems Analysis Project	Jones et al. (1974, 1980), Stapleton et al. (1974), Baker et al. (1983)
9.	1970	Development of insect and disease models through Integrated Pest Management (IPM) Project	–
10.	1971	Biological System Simulation Group (BSSG)	–
11.	1970–80	Herd dynamics simulation models	IADB (Inter-American Development Bank) (1975), Konandreas and Anderson (1982)
12.	1970	Modeling predator-prey, host-disease interactions	May (1976)
13.	1972–74	Crop forecasts through crop models and remote sensing	Pinter Jr et al. (2003)
14.	1974–78	Agro-ecological zoning (AEZ) for land evaluation on a global basis by FAO	Higgins et al. (1978)
15.	1975–82	First crop and pest model in the hands of Australian farmers for decision support by the Australian cotton modeling	CSIRO (1980)
16.	1975–82	SOYGRO and GLYCIM (soybean models)	Wilkerson et al. (1983), Acock et al. (1985)
17.	1976	Agricultural system journal to publish about agricultural systems modeling	Spedding (1976)

(continued)

Table 4.2 (continued)

S. No	Year	Event	References
18.	1979	Feed degradability in the rumen by dacron bag technique (Animal Model)	Orskov and McDonald (1979)
19.	1980	EPIC (Environmental Policy Integrated Climate) model to predict impacts of soil erosion on crop productivity	Williams et al. (1984)
20.	1981	First soil nitrogen (N) model	Seligman and Keulen (1980)
21.	1982–86	CERES (maize and wheat) and GRO (SOYGRO and PNUTGRO) models	Boote et al. (1986)
22.	1980–90	Pasture modeling (Hurley and the SAVANNA models)	Johnson and Thornley (1983), Coughenour et al. (1984)
23.	1983–93	USAID-funded IBSNAT (International Benchmark Sites Network for Agrotechnology Transfer) project and development of DSSAT	IBSNAT (1984), Uehara and Tsuji (1998)
24.	1991	ORYZA dynamic rice model	Penning de Vries et al. (1991)
25.	1985–92	APSIM (Agricultural Production Systems Simulator) evolution	McCown et al. (1992), Keating et al. (1991)
26.	1986	IGBP (International Geosphere-Biosphere Program) by the ICSU (International Council for Science) about ecosystem modeling to give attention to the planet under pressure	–
27.	1990	Application of carbon dynamics and economic models for assessing impacts of climate change on agriculture (Intergovernmental Panel on Climate Change (IPCC) First Assessment Report)	IPCC (1990)
28.	1990–continue	Livestock systems model integration	Herrero et al. (1996), Freer et al. (1997)
29.	1990–94	First modeling work about potential climate change global impacts on agricultural systems	Rosenzweig and Parry (1994)
30.	1991–continue	Development of APSRU (Agricultural Production Systems Research Unit) for agricultural systems modeling	Keating et al. (2003), Holzworth et al. (2014)
31.	1992	Model-based scenario analysis	Netherlands Scientific Council for Government Policy (1992)
32.	1992	CNCPS (Cornell Net Carbohydrate and Protein System) dynamic model of digestion in ruminants	Russell et al. (1992)
33.	1993–11	ICASA (International Consortium for Agricultural Systems	Hunt et al. (1994), White et al. (2013)

(continued)

Table 4.2 (continued)

S. No	Year	Event	References
		Applications) consortium to help crop modelers to develop standards for input data for crop models. This leads to the ICASA data dictionary and data standards used nowadays in AgMIP project.	
34.	1998	Open-source software availability (e.g., APSIM and DSSAT)	–
35.	1999	Projected growth of livestock sector	Delgado (1999)
36.	1990–10	Crop modeling and breeding	White and Hoogenboom (1996), Hoogenboom and White (2003), Hammer et al. (2006), Messina et al. (2006).
37.	2001–03	Special session on modeling cropping systems by the European Society for Agronomy. published in the *European Journal of Agronomy*	–
38.	2006	Modeling CO_2 effects in crop model	Long et al. (2006)
39.	2005–09	SEAMLESS (System for Environmental and Agricultural Modeling: Linking European Science and Society)	–
40.	2005–10	GCMs (general circulation models)	Challinor et al. (2004)
41.	2006	Livestock footprint	Steinfeld et al. (2006)
42.	2005–contiue	Global livestock models	Bouwman et al. (2005), FAO (2013), Havlík et al. (2014), Herrero et al. (2013)
43.	2010–continue	The AgMIP (Agricultural Model Intercomparison and Improvement Project)	Asseng et al. (2013), Rosenzweig et al. (2013, 2014),
44.	2010–continue	Private sector in agricultural system models and public-private collaborations	–
45.	2010–continue	Developments of new ICT tools (e.g., UAVs for agricultural management, smart phones app stores, cloud and mobile computing)	–

(2018) used the AquaCrop model to better assess TLV response to water stress. The model was able to simulate soil water content, canopy cover, biomass, actual evapotranspiration, and water productivity with good accuracy under well-watered treatment as compared to the water-stressed treatment. Similarly, the authors pointed out that it was cumbersome to run each harvest separately as the model was unable to do sequential harvests run at one time. Thus they suggested that vegetables should be included in the model with the facility of subsequent harvesting.

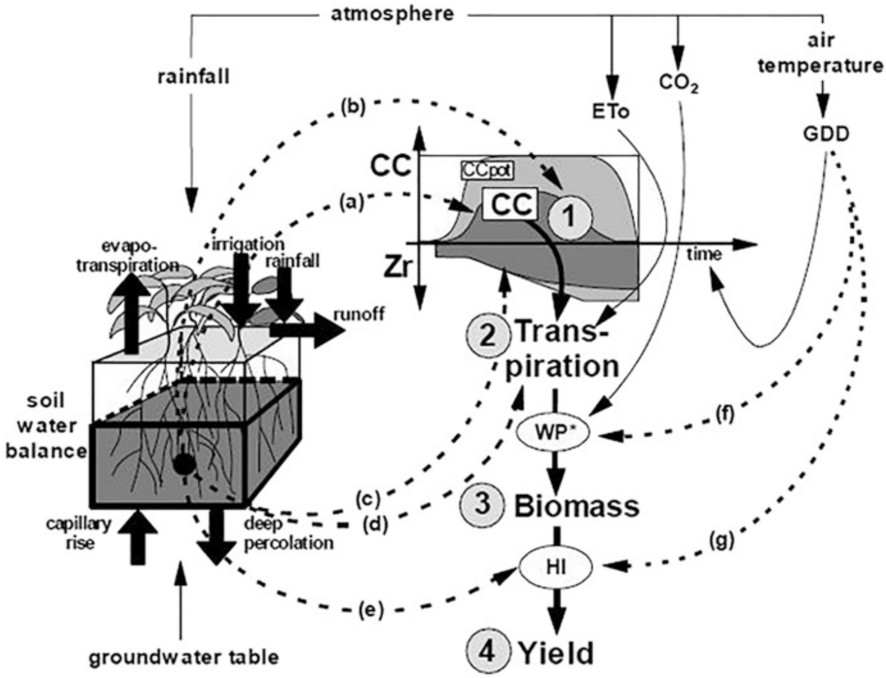

Fig. 4.5 AquaCrop four-step working mechanism. (Source: Foster et al. 2017)

Potato (*Solanum tuberosum* L.), a crop highly sensitive to water stress, ranks 4th in production across the globe after rice, wheat, and maize. The effect of water stress on potato production could be minimized by the implementation of irrigation management strategies through crop modeling.

Razzaghi et al. (2017) used the AquaCrop model to simulate potato soil water content, dry matter, and yield under different water stress regimes. Treatments include I_f (full irrigated), I_d (deficit irrigated), and I_0 (not irrigated). Complete irrigated treatment data in 2014 was used for model calibration, while 3 years of data from 2013–2015 for all treatments (I_f, I_d, and I_0) was used for model validation. The sensitivity analysis results showed that specific parameters such as K_{cTr}, HI_0, CCX, calendar day from sowing to start of senescence, and WP have a significant effect on tuber yield. The model was able to predict results with good accuracy but not performed well under I_0. Groundnut (*Arachis hypogaea* L.) canopy cover (CC), biomass, yield, and evapotranspiration (ET) were simulated for water stress conditions after calibration of AquaCrop by Chibarabada et al. (2020). The model was able to simulate CC, biomass, yield, and ET with good accuracy. Thus AquaCrop can be a useful tool to support a decision on when and how much to irrigate. Further details about the AquaCrop model are available at www.fao.org/aquacrop.

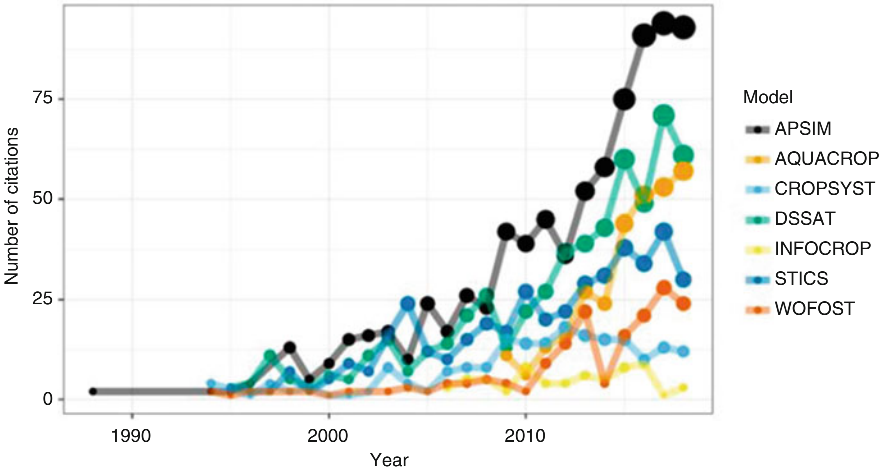

Fig. 4.6 Number of citations for different models

4.3.2 APSIM Next Generation

Agricultural Production Systems Simulator (APSIM) has grown from a farming system framework to a collection of models with a large number of users across the globe. APSIM is the top cited model among other crop models, as shown in Fig. 4.6. APSIM consists of 100–1000 lines of codes and runs in 6 different programming languages. In order to meet new computing challenges, APSIM Initiative developed APSIM Next Gen (APSIM 7.x Framework). It is a new modern rewrite of APSIM. The aim behind the development of APSIM Next Generation is to have a model that can run faster on multiple operating systems and under multiple spatiotemporal scales (Holzworth et al. 2018). APSIM Next Generation has a range of tools in a single-user interface to help modelers. It ensures model reliability and accessibility with updates as it uses a modern control system. Brown et al. (2018) used the APSIM Next Generation wheat model as a case study to describe the model development process. Simulation models (CLEM, barley, chicory, controlled environment, eucalyptus, EucalyptusRotation, factorial, fodder beet, maize, oats, oil palm, plantain, potato, red clover, SCRUM, SLURP, sugarcane, wheat, and white clover) available yet in the APSIM Next Generation have been shown in Fig. 4.7. Further details about APSIM Next Generation usage, development, and documentation are available at https://apsimnextgeneration.netlify.com/.

4.3.3 APSIM (Agricultural Production Systems Simulator)

APSIM is one of the well-known modeling frameworks to model crop and pasture production, cropping systems, decomposition of residues, soil water and nutrient dynamics, agronomic management, and climate change impact assessments (Osman

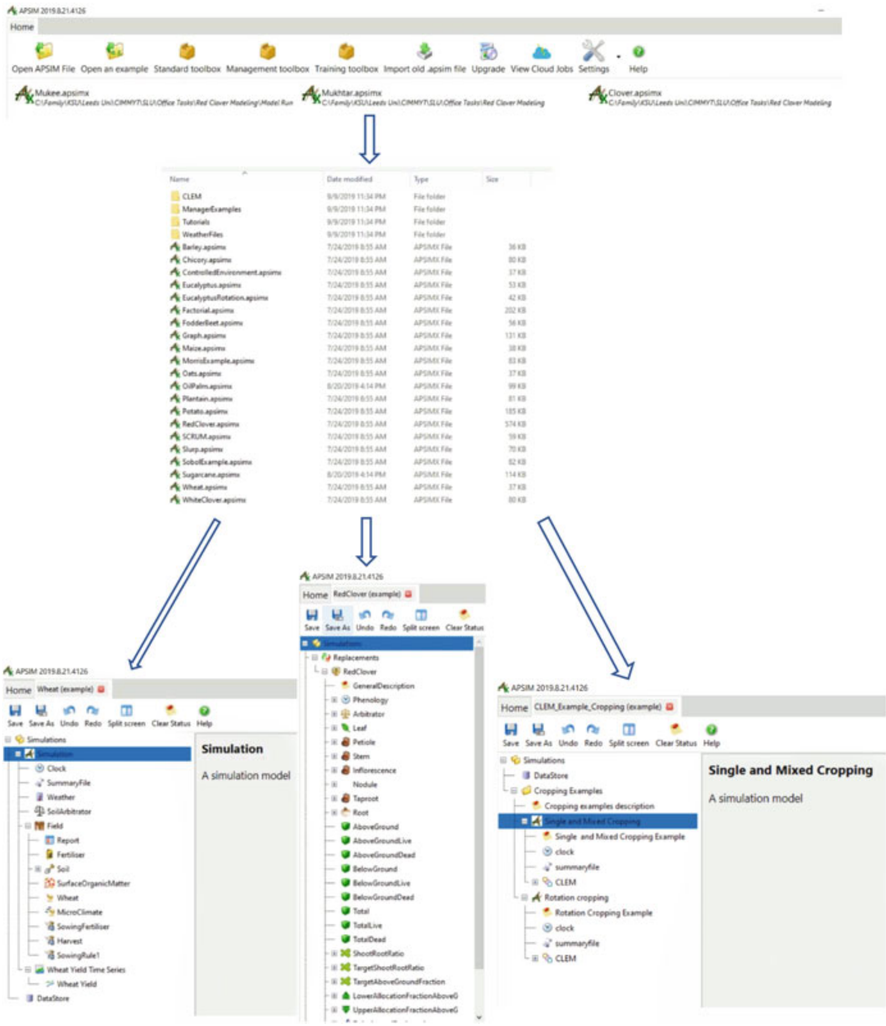

Fig. 4.7 Overview of APSIM Next Generation

et al. 2020; Ijaz et al. 2017). The model was well elaborated by McCown et al. (1996) and tested by Meinke et al. (1998a, b). System components of APSIM include atmosphere, plant, soil, and management as shown in Fig. 4.8. Furthermore, its working mechanism has been elaborated in Fig. 4.9, and key features of APSIM have been displayed in Table 4.3. APSIM is a powerful tool for agricultural system research such as crop rotation, intercropping, farming systems, tree windbreak, crop-weed associations, genetic trait identification, seasonal climate forecasting, drought policy formation, environmental impacts, and on-farm trial analyses (Schepen et al.

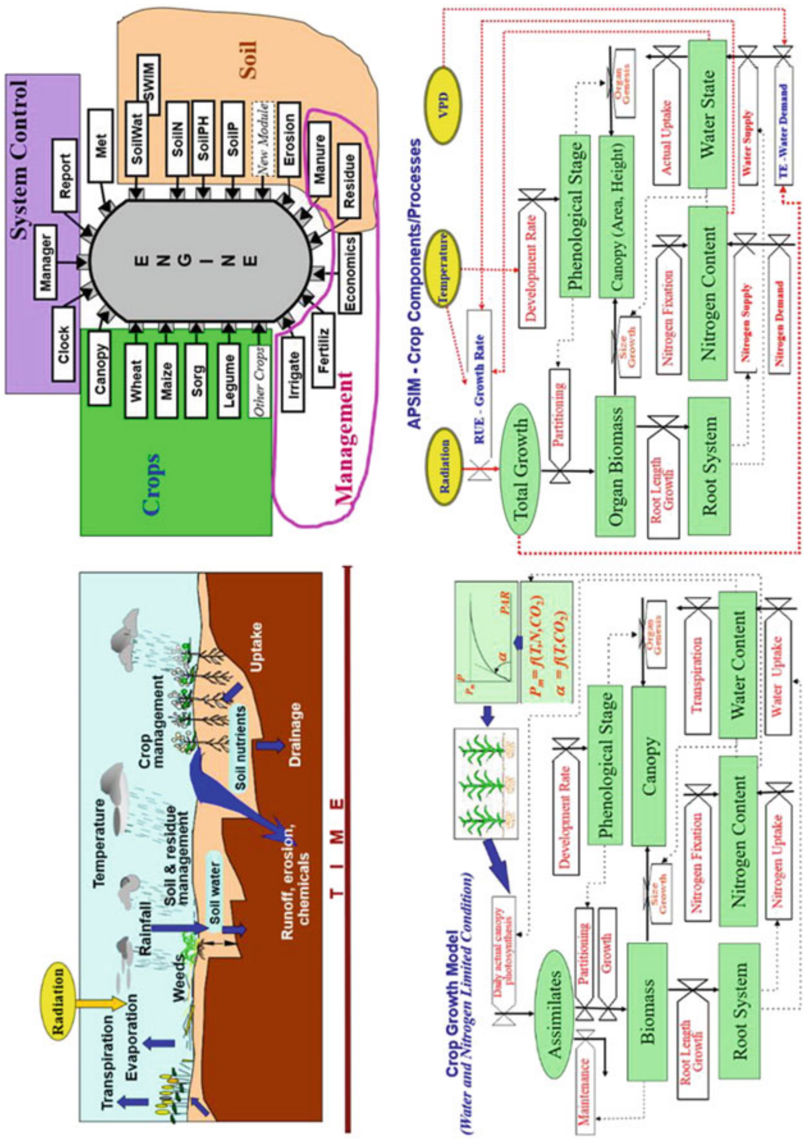

Fig. 4.8 APSIM working mechanism with details about crop component only. (Source: APSRU Toowoomba)

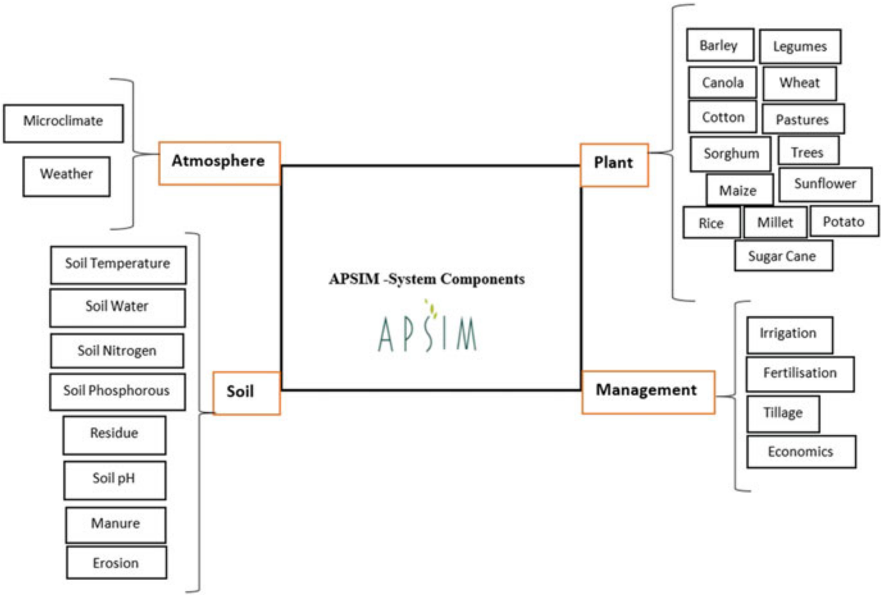

Fig. 4.9 APSIM -System Components

Table 4.3 Key features of APSIM (Source: APSIM)

Key features	
Soil	Availability and dynamics of water and nutrients
Plant	Growth and development of crops, seeds, trees
Weather	Changes of radiation, temperature, rainfall, CO_2
Management	Tillage, sowing, irrigation, fertilization
Residue	Decomposition of crop residues
Erosion	Soil loss through erosion

2020; Xin and Tao 2019). The main application of APSIM in different fields has been reviewed and presented in Table 4.4.

4.3.4 CropSyst

CropSyst is a comprehensive cropping system model that can analyze management practices of water and nitrogen on a wide range of crops. CropSyst's ability to simulate ET, crop N content, leaf area, biomass, and grain yield was tested in a Mediterranean type of environment by Stockle et al. (1994). The results showed that the model was able to simulate these parameters with good accuracy. Pala et al. (1996) evaluated CropSyst to simulate water and nitrogen use, growth, and yield of wheat. Crop coefficients related to the crop growth named as growth parameters

Table 4.4 Application of APSIM in different fields

S. no	Research applications	References
1.	Modeling forage chicory	Cichota et al. (2020)
2.	Simulation of sorghum yield under different management practices	Akinseye et al. (2020)
3.	Water use and crop production of different cropping systems under three irrigation strategies	Yan et al. (2020)
4.	Modeling crop-livestock system and agricultural sustainability	Smith and Moore (2020), Ahmed et al. (2013)
5.	Hypothetical crop production modeling under three rotations: (i) continuous wheat (ii), wheat-chickpea, and (iii) wheat-fallow	Cann et al. (2020)
6.	Climate impact projections	Tao et al. (2020)
7.	Modeling annual crop mixtures	Gaudio et al. (2019)
8.	Modeling N release from *Brassica* catch crop residues	Vogeler et al. (2019)
9.	Genotype to phenotype (G2P) modeling approaches	Bustos-Korts et al. (2019)
10.	Adoption of conservation agriculture	Bahri et al. (2019)
11.	Precision cost-benefit analysis of variable seeding and nitrogen application rates	McNunn et al. (2019)
12.	Moisture and root growth	Ebrahimi-Mollabashi et al. (2019)
13.	Double cropping system modeling	Gao et al. (2019)
14.	Modeling yield potential of near isogenic lines of barley	Ibrahim et al. (2019)
15.	APSIM-sugar	Dias et al. (2019)
16.	Elevated CO_2 and winter wheat productivity	Ahmed et al. (2019)
17.	Modeling water and heat stress patterns on sorghum	Carcedo and Gambin (2019)
18.	Optimization of the genotype (G) × environment (E) × management (M) interactions	
19.	APSIM-soilP-wheat model	Ahmed et al. (2018)
20.	Simulation of fertilizer management of hypothetical dairy farm under different scenarios	Cichota et al. (2018)
21.	Modeling cropping systems of Asia	Gaydon et al. (2017)
22.	APSIM-wheat under rainfed conditions	Ahmed et al. (2016)
23.	Agronomic management of zero tillage wheat	Balwinder et al. (2016)
24.	Canola (*Brassica napus*) simulation	Robertson and Lilley (2016)
25.	Climate change benefits on crop productivity	Yang et al. (2015)
26.	Flowering time of wheat and future wheat varieties	Wang et al. (2015)
27.	Ideotype designing of cereal	Rötter et al. (2015)
28.	APSIM-*Oryza*	Nissanka et al. (2015)
29.	APSIM to model nitrogen use efficiency	Ahmed et al. (2014), Aslam et al. (2017b)
30.	SWIM3(Soil Water Infiltration and Movement 3) model for soil water and solute dynamics	Huth et al. (2012)
31.	Soybean-wheat cropping system	Mohanty et al. (2012)
32.	Modeling mulch and irrigation management	Balwinder et al. (2011)

(continued)

Table 4.4 (continued)

S. no	Research applications	References
33.	Modeling nitrous oxide emissions from sugarcane production systems	Thorburn et al. (2010)
34.	Genotype (G) × environment (E) interactions	Chapman (2008), Wallach et al. (2018)
35.	APSIM-SWIM	Connolly et al. (2002)
36.	G × E and grain sorghum	Chapman et al. (2000a, b, c)
37.	Modeling dynamics of nitrogen and water in fallow system	Probert et al. (1998)
38.	Simulation of legume-ley farming system	Carberry et al. (1996)

(e.g., biomass transpiration coefficient, light to aboveground biomass conversion, ratio of actual to potential transpiration, maximum water uptake, critical leaf water potential, wilting leaf water potential, unstressed harvest index (HI), HI sensitivity to water stress during flowering and grain filling, and translocation factor) were adjusted to have accurate calibration. Similarly, crop phenology parameters such as growing degree days (GDD) to emergence, GDD to flowering, GDD to grain filling, GDD to physiological maturity, base temperature, cutoff temperature, phenological sensitivity to water stress, photoperiod (day length) insensitivity, and photoperiod (day length) to inhibit flowering were also adjusted. Crop parameters that affect crop morphology include maximum rooting depth, maximum leaf area index (LAI), a fraction of maximum LAI at physiological maturity, specific leaf area, leaf stem partition, leaf duration, extinction coefficient for solar radiation, leaf duration sensitivity to water stress, and ET crop coefficients were calibrated. Similarly, nitrogen parameters, i.e., maximum plant N content at early linear growth, minimum plant N content at rapid linear growth, maximum plant N content at maturity, and maximum N content at standing stubble, were also adjusted to have accurate calibration of the model. Model results showed that crop phenology (e.g., anthesis, grain filling, and physiological maturity) was predicted very well. However, the underwater stress model resulted in accelerated phenology. The model was able to simulate LAI, ET, crop N content, and aboveground biomass and grain yield, but extreme conditions (e.g., water stress, frost, and heat) created discrepancies between observed and simulated grain yield. Donatelli et al. (1997) did an evaluation of CropSyst as a cropping system model by using field-based crop rotation data. The model was able to simulate a number of cropping systems, but they suggested further improvement in the model so that it can be considered a promising tool in agricultural systems research. An improved version of CropSyst (daily time step, multi-year, and multi-crop) was released to capture actual field impacts on the cropping system by Stöckle et al. (2003). Components of CropSyst include CropSyst parameter editor, cropping system simulator, ClimGen (weather generator), ArcCS (GIS-CropSyst simulation co-operator), and CropSyst Watershed. CropSyst mainly runs by considering two important folders, (i) database and (ii) scenario. The database folder consists of six further sub-components, i.e., crop, soil, weather,

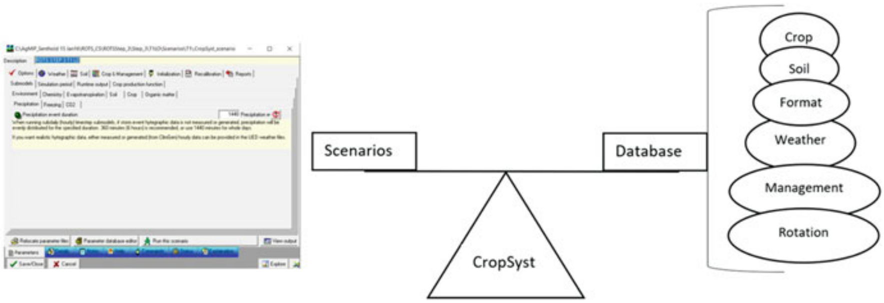

Fig. 4.10 CropSyst components

rotation, management, and output format, as shown in Fig. 4.10. Further details of CropSyst are available at http://modeling.bsyse.wsu.edu/CS_Suite_4/CropSyst/index.html, and a flowchart of biomass growth calculations in CropSyst has been elaborated in Fig. 4.11.

CropSyst was used to assess the impact of climate change on economically important crops using historical and future climate sequences, and it was concluded that climate change impact will be mild for the next two decades but could be detrimental at the end of the century (Stöckle et al. 2010). Maize crop yield and water footprint (green, rainfall water stored in soil, and blue, water other than rainfall during the cropping season or extracted from underground or water flowing in rivers and lakes, water footprint) in response to future climate change scenarios were simulated by using CropSyst. Results depicted that under extreme scenarios (increased temperature and decreased precipitation), blue water footprint increases, which could be due to increased ET and higher irrigation demand. This resulted in lower crop yield (Bocchiola et al. 2013). Jalota et al. (2014) used the CropSyst model to evaluate location-specific climate change scenarios (mid-century and end-century) impact on rice-wheat cropping system with delaying of trans-/planting date of crops as adaptation measures. The simulation parameters included crop duration, yield, water and N balance, and use efficiency of the system. Results showed that crop duration might be shortened at mid-century, while ET, transpiration, irrigation, and drainage could be decreased at both the mid- and end-century. Delayed sowing of 15–21 days in wheat and 15 days in rice could be the best adaptation measures to have sustainable crop yield in rice-wheat cropping systems. CropSyst to predict water use and crop coefficients (K_c) in Japanese plum trees was examined by Samperio et al. (2014). CropSyst crop parameters, i.e., $K_{c\cdot Fc}$ (crop coefficient at full canopy) and C_{max} (maximum plant hydraulic conductance), were parameterized using one season data but validated with the other two seasons dataset. The results showed that different sets of CropSyst parameters ($K_{c\cdot Fc}$, and C_{max}) are required to have accurate crop evapotranspiration, water potential, and Kc. AquaCrop and CropSyst modeling approaches were compared to simulate barley growth and yield under different water and N regimes (Abi Saab et al. 2015). The results showed that both models could be calibrated with data of any of the 1 year and validated with

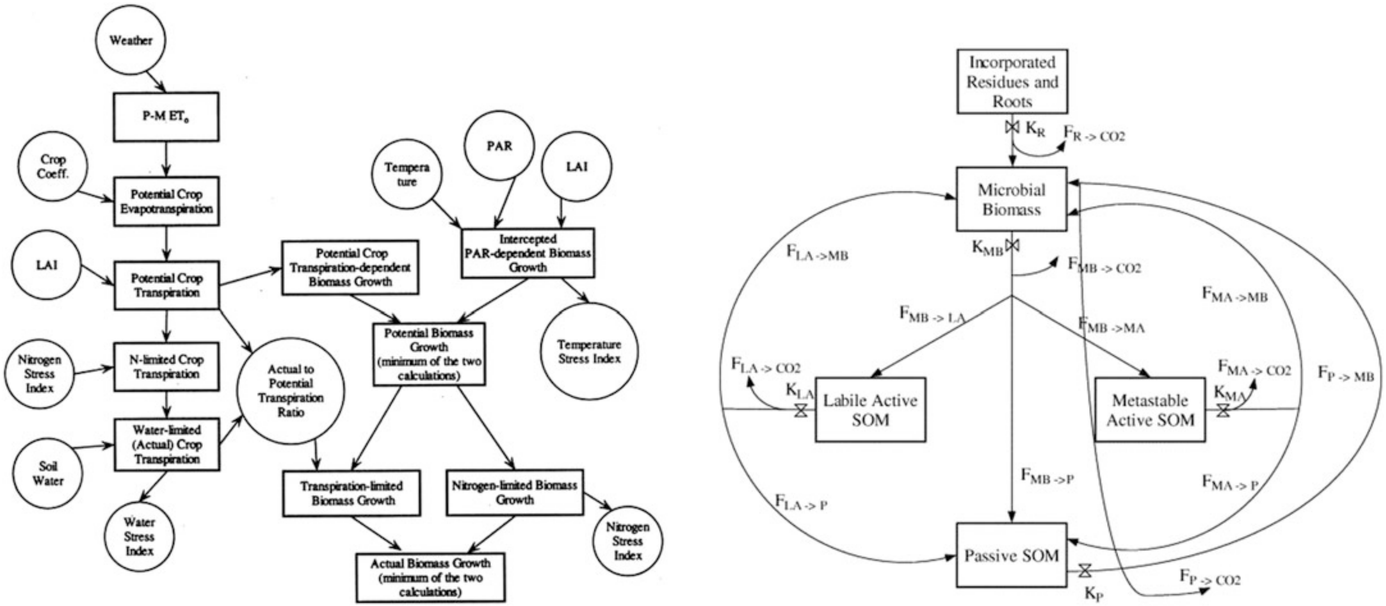

Fig. 4.11 CropSyst flowchart for biomass growth calculations. (Source: Stöckle et al. 2003 with permission from Elsevier) and conceptual carbon flow model. (Source: Badini et al. 2007 with permission from Elsevier)

all other year's data. Furthermore, CropSyst was also used as a risk assessment tool in comparison with other growth models which could help to design adaptation strategies like crop insurance (Castañeda-Vera et al. 2015). The transparency (number of input parameters) and robustness (validation) of four wheat models (CropSyst, SSM, APSIM, and DSSAT) were evaluated by using a wide range of environmental and growth conditions dataset from Iran by Soltani and Sinclair (2015). The results showed that CropSyst and SSM were robust, while APSIM and DSSAT had higher transparency. This is because transparency is gauged by a number of input parameters that were higher in APSIM (292 parameters), followed by DSSAT (211 parameters), SSM (55 parameters), and CropSyst (50 parameters). Karimi et al. (2017) simulated shifts in the dry land cropping system of the Pacific Northwest in response to climate change using CropSyst. The results showed that climate change due to the direct effect of atmospheric CO_2 would be positive for transpiration use efficiency and grain yield of crops. Regional opportunities for agricultural diversification and intensification are possible for the Pacific Northwest of the USA due to warming with an increase in rainfall and atmospheric CO_2, as evaluated by Stöckle et al. (2018). The model could help to design crop diversification with the introduction of new winter crops. Nasrallah et al. (2020) use the CropSyst biophysical simulation model to have optimum rotations and managements for a wheat-based cropping system. The study was designed with the aim to have low-risk, sustainable farming systems. The data from four rotations (wheat-fallow, wheat-wheat, wheat-potato, and wheat-fava bean) and four management systems, i.e., (i) full fertilization and full irrigation, (ii) full fertilization and zero irrigation, (iii) zero fertilization and full irrigation, and (iv) zero fertilization and irrigation, were used for model calibration and evaluation. The results showed that wheat-fava bean rotation with no fertilization could be a better substitute for wheat-wheat rotation in terms of protein production. This system showed a higher net profit and high resource-use efficiency and to be less risky for farmers. Similarly, a very high profit is possible with wheat-potato rotation but with low input efficiency and higher risk.

4.3.5 DSSAT

The Decision Support System for Agrotechnology Transfer (DSSAT) is a model with a long history and has been used all around the world by researchers as a decision support tool. DSSAT was developed by the IBSNAT project to facilitate agronomic research. It was designed to improve decisions about production technologies of crops and for the analysis of complex alternative choices. Although crop models like CERES models for maize and wheat, SOYGRO soybean, and PNUTGRO peanut were available already, to make these models compatible, the DSSAT model was designed with the addition of new crops. The first version of DSSAT was released in 1989 (v2.1), then v3.0 in 1994, and v3.5 in 1998. There were 16 different crops in v3.5, but now, in v4.7, there are 42 different crops available. A further detailed description of DSSAT is available in the work of Jones et al. (2003) and also at https://dssat.net/about. The potential effects of climate change on wheat production were explored by Luo et al. (2003) using the DSSAT 3.5 CERES-Wheat model. The results showed that wheat yield was increased under all levels of CO_2 but crop quality was decreased. CROPGRO-soybean model's ability to predict canopy and leaf photosynthesis to photosynthetic photon flux under different concentrations of CO_2 was evaluated by Alagarswamy et al. (2006). Net leaf photosynthesis was simulated well by the CROPGRO default photosynthesis equations. Cropping system model (CSM)-CERES-maize model was used with the objectives to evaluate the impacts of different planting dates on maize yield under rainfed and irrigated conditions and to do yield forecasting (Soler et al. 2007). The model was able to simulate crop phenology and grain yield with reasonable accuracy. Thus, it can be used in the practical decisions related to the management of maize. Soltani and Hoogenboom (2007) assessed crop management options for maize, wheat, and soybean using DSSAT based on observed (30 years) and weather generated data (90 years) through WGEN and SIMMETEO. Their results showed that DSSAT is a useful complement to experimental research. Apollo, a prototype decision support system, was developed by Thorp et al. (2008) to analyze the precision farming system dataset using DSSAT.

The pattern recognition approach was used by Bannayan and Hoogenboom (2008) to estimate cultivar coefficients to be used in the crop models. This approach classifies data based on statistical information or prior knowledge obtained from the patterns. K-nearest neighbor (k-NN) approach is one of the well-known most attractive similarity-based techniques or attractive pattern classification algorithms in different scientific disciplines (Bannayan and Hoogenboom 2008). Six cultivar coefficients (P1, °C day, thermal time from seedling emergence to the end of the juvenile phase (expressed in degree days, °C day, above a base temperature of 8 °C) during which the plant is not responsive to changes in photoperiod; P2, days, extent to which development (expressed as days) is delayed for each hour increase in photoperiod above the longest photoperiod at which development proceeds at a maximum rate (which is considered to be 12.5 h); P5, °C day, thermal time from silking to physiological maturity (expressed in degree days above a base temperature of 8 °C); G2, number, maximum possible number of kernels per plant; G3, mg day^{-1}, kernel filling rate during the linear grain filling stage and under optimum conditions; and PHINT, °C day, phyllochron interval, the interval in thermal time (degree days) between successive leaf tip appearances) of the DSSAT-CSM-CERES-maize were used using pattern recognition approach to construct 27,789 hypothetical cultivars, and then model was run for the potential production of all cultivars. Afterward, outputs of all simulations were used as feature databases. Furthermore, this approach was evaluated by utilizing maize cultivars (29) of the DSSAT database and additional 4 cultivars from three study sites that have not been used anywhere earlier. The simulation outcome showed that the pattern recognition approach was able to estimate cultivar coefficients with good accuracy. MANIHOT, a new mechanistic cassava simulation model version 4.7 of DSSAT (Hoogenboom et al. 2019), was evaluated by Moreno-Cadena et al. (2020). The objective of their study was to identify the most sensitive genotype-specific parameters (GSPs) and their contribution to the uncertainty of the model. Global sensitivity and uncertainty analysis (GSUA) was applied to see performance of GSPs. The results showed that about 80% of the GSPs contributed to the variation in crop parameters like LAI, yield and biomass at harvest. However, importance of GSPs was variable between warm and cool temperatures. The most important GSPs they reported were individual node weight, radiation use efficiency, and maximum individual leaf area. Under cool conditions base temperature for leaf development was more important. Further application of DSSAT in different fields has been reviewed and presented in Table 4.5.

4.3.6 STICS

STICS (Simulateur multidisciplinaire pour Les Cultures Standard) is a dynamic, generic, and robust model to simulate the soil-crop-atmosphere system. It was developed by INRA (Institut national de la recherche Agronomique). STICS model was created by combining pieces of GOA (plant), BYM (water) and LIXIM (nitrogen) models. Earlier, the STICS model was used for the simulation of two main crops, but with the passage of time, it was able to simulate new crops and other agronomic practices (Yin et al. 2020). Now the model is well-recognized all over the globe and is part of the inter-model comparison projects of AgMIP (Agricultural Model Intercomparison and Improvement Project) and MACSUR (Modelling European Agriculture with Climate Change for Food Security). The developmental time period of STICS has been shown in Fig. 4.12. Strullu et al. (2020) used the STICS model to simulate the effects of cultivation practices on alfalfa crop biomass production and N accumulation. Since alfalfa is a perennial crop that undergoes regular defoliation, thus, establishment and regrowth phases were simulated with the hypothesis that crop growth is controlled by the interaction between abiotic stresses and crop development stage. The model was able to simulate total and aboveground biomass with good accuracy and performed well during the evaluation process. Soil water and nitrate contents were simulated accurately during the cropping period and after crop harvesting. STICS soil crop model was used to quantify ecosystem functions (EF) and ecosystem services (ES) to ensure maximum productivity of apple orchards. The conceptual scheme of the study of the apple orchard system with EF (yellow boxes) and ES (red boxes) has been presented in Fig. 4.13 as elaborated by Demestihas et al. (2018). These two services, EF and ES, were impacted by agricultural practices, e.g., cropping system (green boxes). Thus STICS could be used to simulate EF and ES under different sets of soil and climatic conditions. Mesbah et al. (2017) applied the STICS model in Canada to find the ecophysiological optimum rate of N application to have maximum achievable corn yield and minimum N losses.

Table 4.5 Application of DSSAT in different fields

S. No	Research applications	Refrences
1.	Pasture growth modeling	Bosi et al. (2020)
2.	Modeling N losses	Malik and Dechmi (2020)
3.	Conservation tillage (CT) and N modeling	Liben et al. (2020)
4.	Alfalfa (*Medicago sativa* L.) regrowth and biomass modeling	Jing et al. (2020)
5.	Phenology modeling of the rice-wheat cropping system under climate warming and management	Ahmad et al. (2019)
6.	Model evaluation under a set of agronomic practices	Mehrabi and Sepaskhah (2019)
7.	Climate change (rising temperature and elevated CO_2)	Kheir et al. (2019)
8.	Modeling climate change impact on water and nitrogen use efficiencies using DSSAT-CERES-maize and sorghum	Amouzou et al. (2019)
9.	Elevated CO_2 and winter wheat productivity	Ahmed et al. (2019)
10.	Optimization of sowing window	Jahan et al. (2018)
11.	Climate change	Hussain et al. (2018), Jabeen et al. (2017)
12.	Application of cropping system model (CSM)-SUBSTOR-potato	Woli and Hoogenboom (2018)
13.	Canegro model improvement with revised algorithms for tillering, respiration, and crop-water relations.	Jones and Singels (2018)
14.	Climate change	Ahmed et al. (2017)
15.	Cropping system modeling	Araya et al. (2017)
16.	Irrigation management	Dar et al. (2017)
17.	Modeling canola phenology under climate warming and crop management	Ahmad et al. (2017)
18.	Hybrid modeling (coupling of DSSAT and SWAP models)	Dokoohaki et al. (2016)
19.	Review about DSSAT models (CERES-wheat, CERES-maize and CERES-rice)	Basso et al. (2016)
20.	Heat stress modeling	Liu et al. (2016)
21.	DSSAT-Nwheat evaluation	Kassie et al. (2016)
22.	Irrigation scheduling	Jiang et al. (2016), Attia et al. (2016)
23.	Climatic variability	Singh et al. (2015), Liu et al. (2019)
24.	Modeling soil organic carbon, N dynamics, and grain yield	Li et al. (2015)
25.	Aerobic rice-maize cropping systems management for the improvement of water and nitrogen use efficiencies	Kadiyala et al. (2015)
26.	SALUS (System Approach to Land Use Sustainability)	Dzotsi et al. (2015)
27.	Modeling water saving irrigation and conservation agriculture practices	Devkota et al. (2015)
28.	Evaluation of CERES-maize and IXIM models	Ban et al. (2015)
29.	Climate change and future maize yield	Araya et al. (2015)
30.	Conservation agriculture and climate change	Ngwira et al. (2014)
31.	Application of DRAINMOD-DSSAT model	Negm et al. (2014)

(continued)

Table 4.5 (continued)

S. No	Research applications	Refrences
32.	Yield variability and yield gaps analysis	Kassie et al. (2014)
33.	CROPGRO-groundnut model to simulate drought and heat tolerance and yield-enhancing traits	Singh et al. (2014a)
34.	CROPGRO-chickpea model to simulate benefits of incorporation of drought and heat tolerance traits in Chickpea	Singh et al. (2014b)
35.	Modeling rice-wheat system productivity	Subash and Ram Mohan (2012)
36.	Modeling spring barley yield in Europe	Rötter et al. (2012)
37.	Estimation of cultivar coefficient	Bannayan and Hoogenboom (2009)
38.	Precision agriculture and improving soil fertility recommendations	Thorp et al. (2008), Ahmed (2012)
39.	Simulation of photosynthesis to CO_2 levels (CROPGRO-soybean model)	Alagarswamy et al. (2006)
40.	Linking field performance to genomics	Boote et al. (2003)

4.4 List of Other Dynamic Models

Other process-based models used across the globe includes APEX (Agricultural Policy/Environmental eXtender Model) (https://epicapex.tamu.edu/apex/), AFRCWHEAT2 (Porter 1993), CLM (http://www.cgd.ucar.edu/projects/chsp/research/crop-modeling.html), DAISY (https://soil-modeling.org/resources-links/model-portal/daisy) (Gyldengren et al. 2020), DNDC (http://www.dndc.sr.unh.edu/), EPIC (https://epicapex.tamu.edu/epic/), ECOSYS (https://ecosys.ualberta.ca/model-development-01/), FASSET (https://www.fasset.dk/), GLAM (Droutsas et al. 2019), HERMES (http://www.zalf.de/de/forschung_lehre/software_downloads/Seiten/default.aspx) (Hlavinka et al. 2013), INFOCROP (Aggarwal et al. 2006), LINTUL3 (Shibu et al. 2010), LPJmL (https://www.pik-potsdam.de/research/projects/activities/biosphere-water-modelling/lpjml/lpjml) (Sitch et al. 2003), LPJmL4 (Schaphoff et al. 2018a, b), LPJmL5 (von Bloh et al. 2018), MCWLA (Tao et al. 2009), MONICA (Nendel et al. 2011), OLEARY (O'Leary and Connor 1996), RZWQM2 (https://www.ars.usda.gov/plains-area/fort-collins-co/center-for-agricultural-resources-research/rangeland-resources-systems-research/docs/system/rzwqm/), SIRIUS (http://resources.rothamsted.ac.uk/mas-models/sirius), SALUS (Dzotsi et al. 2013), SIRIUSQUALITY (http://www1.clermont.inra.fr/siriusquality/), and WOFOST (de Wit et al. 2019).

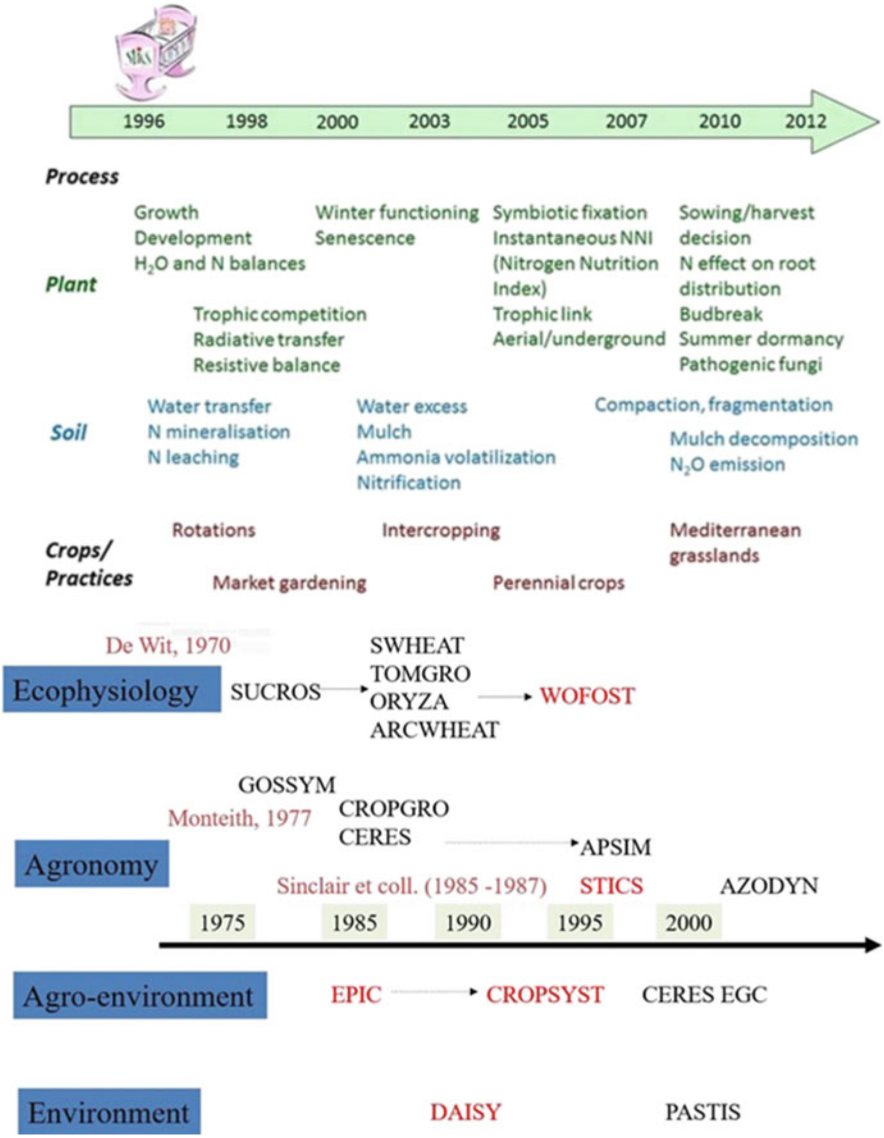

Fig. 4.12 STICS developmental time period. (Source: https://www6.paca.inra.fr/stics_eng/About-us/Stics-model-overview)

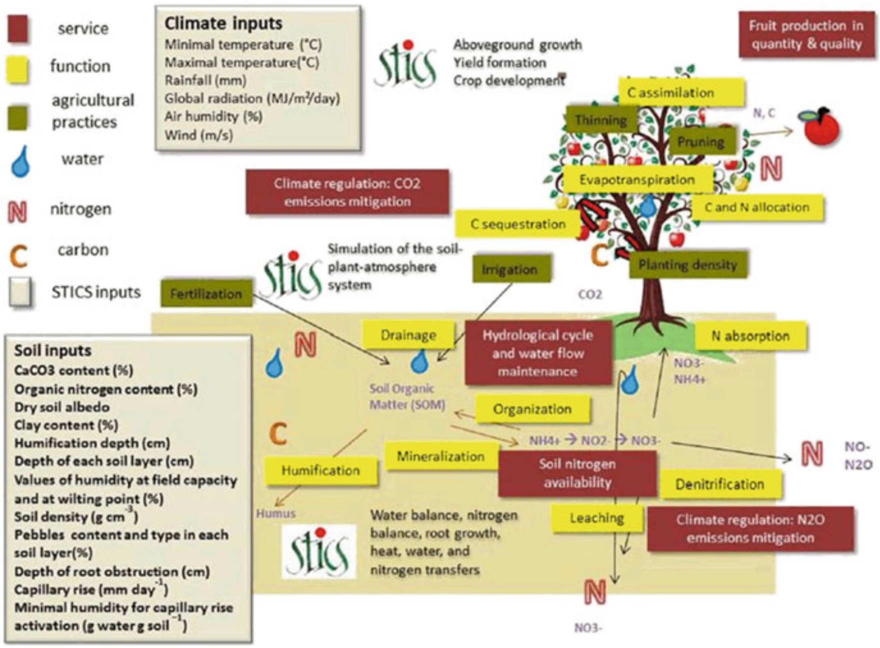

Fig. 4.13 Conceptual scheme of STICS crop-soil model. (Source: Demestihas et al. 2018 with permission from Elsevier)

4.5 Conclusion

Dynamic models are considered perfect tools that can be used from a lower to a higher hierarchy of a system to have good decision power under a different set of management scenarios. However, the performance of the model depends upon the availability of good-quality dataset. Thus, real-time field experiments complemented with the modeling approaches can lead to improve answering capability of what-if questions. Dynamic model as the whole farm could further help to monitor plant, animal, and market interactions by considering different climate shocks (Ahmed et al. 2020). Modeling annual and perennial crop mixtures and intercropping would be future thrust to design different agroecosystems. Since most of the earlier modeling studies were mainly on the evaluation of sole crop models, thus a mixture of crops would be new avenues for the modeling community. Therefore, identification of crop parameters, platform, and multiple datasets for the evaluation of models for the crop mixture is needed. Similarly, designing of plant x environment x managements interactions is possible through the use of different process-based models (Stöckle and Kemanian 2020). Furthermore, models could be used for the problem situation analysis, optimization of management practices, gene-based studies, QTL modeling (Aslam et al. 2017c), crop yield potential analysis, farming system evaluation, environmental sustainability evaluation, yield gap assessment, climate impact projections (Ahmed 2020), and economic risk analysis of different systems.

References

Abi Saab MT, Todorovic M, Albrizio R (2015) Comparing AquaCrop and CropSyst models in simulating barley growth and yield under different water and nitrogen regimes. Does calibration year influence the performance of crop growth models? Agric Water Manag 147(0):21–33. https://doi.org/10.1016/j.agwat.2014.08.001

Acock B, Reddy V, Whisler F, Baker D, McKinion J, Hodges H, Boote K (1985) The soybean crop simulator GLYCIM. Model documentation 1982. PB85171163/AS. US Dept Agric, Washington, DC (available from NTIS Springfield, Virginia)

Aggarwal PK, Banerjee B, Daryaei MG, Bhatia A, Bala A, Rani S, Chander S, Pathak H, Kalra N (2006) InfoCrop: a dynamic simulation model for the assessment of crop yields, losses due to pests, and environmental impact of agro-ecosystems in tropical environments. II. Performance of the model. Agric Syst 89(1):47–67. https://doi.org/10.1016/j.agsy.2005.08.003

Ahmad S, Abbas G, Fatima Z, Khan RJ, Anjum MA, Ahmed M, Khan MA, Porter CH, Hoogenboom G (2017) Quantification of the impacts of climate warming and crop management on canola phenology in Punjab, Pakistan. J Agron Crop Sci 203(5):442–452. https://doi.org/10.1111/jac.12206

Ahmad S, Abbas G, Ahmed M, Fatima Z, Anjum MA, Rasul G, Khan MA, Hoogenboom G (2019) Climate warming and management impact on the change of phenology of the rice-wheat cropping system in Punjab, Pakistan. Field Crop Res 230:46–61. https://doi.org/10.1016/j.fcr.2018.10.008

Ahmed M (2012) Improving soil fertility recommendations in Africa using the decision support system for Agrotechnology transfer (DSSAT); a book review. Exp Agric 48(4):602–603

Ahmed M (2020) Introduction to modern climate change. Andrew E. Dessler: Cambridge University Press, 2011, 252 pp, ISBN-10: 0521173159. Sci Total Environ 734:139397. https://doi.org/10.1016/j.scitotenv.2020.139397

Ahmed M, Stockle CO (2016) Quantification of climate variability, adaptation and mitigation for agricultural sustainability. Springer Nature Singapore Pvt. Ltd., Singapore, 437 pp. https://doi.org/10.1007/978-3-319-32059-5

Ahmed M, Asif M, Hirani AH, Akram MN, Goyal A (2013) Modeling for agricultural sustainability: a review. In: Bhullar GS, Bhullar NK (eds) Agricultural sustainability progress and prospects in crop research. Elsevier, London

Ahmed M, Aslam MA, Hassan FU, Asif M, Hayat R (2014) Use of APSIM to model nitrogen use efficiency of rain-fed wheat. Int J Agric Biol 16:461–470

Ahmed M, Akram MN, Asim M, Aslam M, F-u H, Higgins S, Stöckle CO, Hoogenboom G (2016) Calibration and validation of APSIM-Wheat and CERES-Wheat for spring wheat under rainfed conditions: models evaluation and application. Comput Electron Agric 123:384–401. https://doi.org/10.1016/j.compag.2016.03.015

Ahmed M, Stöckle CO, Nelson R, Higgins S (2017) Assessment of climate change and atmospheric CO_2 impact on winter wheat in the Pacific northwest using a multimodel ensemble. Front Ecol Evol 5(51). https://doi.org/10.3389/fevo.2017.00051

Ahmed M, Ijaz W, Ahmad S (2018) Adapting and evaluating APSIM-SoilP-Wheat model for response to phosphorus under rainfed conditions of Pakistan. J Plant Nutr 41(16):2069–2084. https://doi.org/10.1080/01904167.2018.1485933

Ahmed M, Stöckle CO, Nelson R, Higgins S, Ahmad S, Raza MA (2019) Novel multimodel ensemble approach to evaluate the sole effect of elevated CO2 on winter wheat productivity. Sci Rep 9(1):7813. https://doi.org/10.1038/s41598-019-44251-x

Ahmed M, Ahmad S, Waldrip HM, Ramin M, Raza MA (2020) Whole farm modeling: a systems approach to understanding and managing livestock for greenhouse gas mitigation, economic viability and environmental quality. Anim Manure 67:345–371

Akinseye FM, Ajeigbe HA, Traore PCS, Agele SO, Zemadim B, Whitbread A (2020) Improving sorghum productivity under changing climatic conditions: a modelling approach. Field Crop Res 246:107685. https://doi.org/10.1016/j.fcr.2019.107685

Alagarswamy G, Boote KJ, Allen LH, Jones JW (2006) Evaluating the CROPGRO–soybean model ability to simulate photosynthesis response to carbon dioxide levels. Agron J 98(1):34–42. https://doi.org/10.2134/agronj2004-0298

Amouzou KA, Lamers JPA, Naab JB, Borgemeister C, Vlek PLG, Becker M (2019) Climate change impact on water- and nitrogen-use efficiencies and yields of maize and sorghum in the northern Benin dry savanna, West Africa. Field Crop Res 235:104–117. https://doi.org/10.1016/j.fcr.2019.02.021

Araya A, Hoogenboom G, Luedeling E, Hadgu KM, Kisekka I, Martorano LG (2015) Assessment of maize growth and yield using crop models under present and future climate in southwestern Ethiopia. Agric For Meteorol 214–215:252–265. https://doi.org/10.1016/j.agrformet.2015.08.259

Araya A, Kisekka I, Gowda PH, Prasad PVV (2017) Evaluation of water-limited cropping systems in a semi-arid climate using DSSAT-CSM. Agric Syst 150:86–98. https://doi.org/10.1016/j.agsy.2016.10.007

ARC (1965) The nutrient requirements of farm livestock. No. 2, ruminants. HMSO, London

Aslam MA, Ahmed M, Hayat R (2017a) Modeling nitrogen use efficiency under changing climate. In: Ahmed M, Stockle CO (eds) Quantification of climate variability, adaptation and mitigation for agricultural sustainability. Springer International Publishing, Cham, pp 71–90. https://doi.org/10.1007/978-3-319-32059-5_4

Aslam MA, Ahmed M, Stöckle CO, Higgins SS, Hassan FU, Hayat R (2017b) Can growing degree days and photoperiod predict spring wheat phenology? Front Environ Sci 5:57. https://doi.org/10.3389/fenvs.2017.00057

Aslam MU, Shehzad A, Ahmed M, Iqbal M, Asim M, Aslam M (2017c) QTL modelling: an adaptation option in spring wheat for drought stress. In: Ahmed M, Stockle CO (eds) Quantification of climate variability, adaptation and mitigation for agricultural sustainability. Springer International Publishing, Cham, pp 113–136. https://doi.org/10.1007/978-3-319-32059-5_6

Asseng S, Ewert F, Rosenzweig C, Jones JW, Hatfield JL, Ruane AC, Boote KJ, Thorburn PJ, Rotter RP, Cammarano D, Brisson N, Basso B, Martre P, Aggarwal PK, Angulo C, Bertuzzi P, Biernath C, Challinor AJ, Doltra J, Gayler S, Goldberg R, Grant R, Heng L, Hooker J, Hunt LA, Ingwersen J, Izaurralde RC, Kersebaum KC, Muller C, Naresh Kumar S, Nendel C, O'Leary G, Olesen JE, Osborne TM, Palosuo T, Priesack E, Ripoche D, Semenov MA, Shcherbak I, Steduto P, Stockle C, Stratonovitch P, Streck T, Supit I, Tao F, Travasso M, Waha K, Wallach D, White JW, Williams JR, Wolf J (2013) Uncertainty in simulating wheat yields under climate change. Nat Clim Chang 3(9):827–832. https://doi.org/10.1038/nclimate1916. http://www.nature.com/nclimate/journal/v3/n9/abs/nclimate1916.html#supplementary-information

Asseng S, Martre P, Maiorano A, Rötter RP, O'Leary GJ, Fitzgerald GJ, Girousse C, Motzo R, Giunta F, Babar MA, Reynolds MP, Kheir AMS, Thorburn PJ, Waha K, Ruane AC, Aggarwal PK, Ahmed M, Balkovič J, Basso B, Biernath C, Bindi M, Cammarano D, Challinor AJ, De Sanctis G, Dumont B, Eyshi Rezaei E, Fereres E, Ferrise R, Garcia-Vila M, Gayler S, Gao Y, Horan H, Hoogenboom G, Izaurralde RC, Jabloun M, Jones CD, Kassie BT, Kersebaum K-C, Klein C, Koehler A-K, Liu B, Minoli S, Montesino San Martin M, Müller C, Naresh Kumar S, Nendel C, Olesen JE, Palosuo T, Porter JR, Priesack E, Ripoche D, Semenov MA, Stöckle C, Stratonovitch P, Streck T, Supit I, Tao F, Van der Velde M, Wallach D, Wang E, Webber H, Wolf J, Xiao L, Zhang Z, Zhao Z, Zhu Y, Ewert F (2019) Climate change impact and adaptation for wheat protein. Glob Chang Biol 25(1):155–173. https://doi.org/10.1111/gcb.14481

Attia A, Rajan N, Xue Q, Nair S, Ibrahim A, Hays D (2016) Application of DSSAT-CERES-Wheat model to simulate winter wheat response to irrigation management in the Texas High Plains. Agric Water Manag 165:50–60. https://doi.org/10.1016/j.agwat.2015.11.002

Badini O, Stöckle CO, Jones JW, Nelson R, Kodio A, Keita M (2007) A simulation-based analysis of productivity and soil carbon in response to time-controlled rotational grazing in the West African Sahel region. Agric Syst 94(1):87–96. https://doi.org/10.1016/j.agsy.2005.09.010

Bahri H, Annabi M, Cheikh M'Hamed H, Frija A (2019) Assessing the long-term impact of conservation agriculture on wheat-based systems in Tunisia using APSIM simulations under a climate change context. Sci Total Environ 692:1223–1233. https://doi.org/10.1016/j.scitotenv.2019.07.307

Baker DN, Lambert JR, McKinion JM (1983) GOSSYM: a simulator of cotton crop growth and yield. South Carolina Agricultural Experiment Station Technical bulletin (USA)

Balwinder S, Gaydon DS, Humphreys E, Eberbach PL (2011) The effects of mulch and irrigation management on wheat in Punjab, India—evaluation of the APSIM model. Field Crop Res 124 (1):1–13. https://doi.org/10.1016/j.fcr.2011.04.016

Balwinder S, Humphreys E, Gaydon DS, Eberbach PL (2016) Evaluation of the effects of mulch on optimum sowing date and irrigation management of zero till wheat in central Punjab, India using APSIM. Field Crop Res 197:83–96. https://doi.org/10.1016/j.fcr.2016.08.016

Ban H-Y, Sim D, Lee K-J, Kim J, Kim KS, Lee B-W (2015) Evaluating maize growth models "CERES-Maize" and "IXIM-Maize" under elevated temperature conditions. J Crop Sci Biotechnol 18(4):265–272. https://doi.org/10.1007/s12892-015-0071-3

Bannayan M, Hoogenboom G (2008) Predicting realizations of daily weather data for climate forecasts using the non-parametric nearest-neighbour re-sampling technique. Int J Climatol 28 (10):1357–1368. https://doi.org/10.1002/joc.1637

Bannayan M, Hoogenboom G (2009) Using pattern recognition for estimating cultivar coefficients of a crop simulation model. Field Crop Res 111(3):290–302. https://doi.org/10.1016/j.fcr.2009.01.007

Basso B, Liu L, Ritchie JT (2016) A comprehensive review of the CERES-wheat, -maize and -rice models' performances. In: Sparks DL (ed) Advances in agronomy, vol 136. Academic Press, Burlington, pp 27–132. https://doi.org/10.1016/bs.agron.2015.11.004

Bocchiola D, Nana E, Soncini A (2013) Impact of climate change scenarios on crop yield and water footprint of maize in the Po valley of Italy. Agric Water Manag 116(0):50–61. https://doi.org/10.1016/j.agwat.2012.10.009

Boote KJ, Jones JW, Mishoe JW, Wilkerson GG (1986) Modeling growth and yield of groundnut. Agrometeorology of groundnut. In: Proceedings of an International Symposium, 21–26 Aug 1985, ICRISAT Sahelian Center, Niamey, Niger. ICRISAT, Patancheru, pp 243–254

Boote KJ, Jones JW, Batchelor WD, Nafziger ED, Myers O (2003) Genetic coefficients in the CROPGRO–soybean model. Agron J 95(1):32–51. https://doi.org/10.2134/agronj2003.3200

Bosi C, Sentelhas PC, Pezzopane JRM, Santos PM (2020) CROPGRO-Perennial Forage model parameterization for simulating Piatã palisade grass growth in monoculture and in a silvopastoral system. Agric Syst 177:102724. https://doi.org/10.1016/j.agsy.2019.102724

Bouwman AF, Van Der Hoek KW, Eickhout B, Soenario I (2005) Exploring changes in world ruminant production systems. Agric Syst 84(2):121–153. https://doi.org/10.1016/j.agsy.2004.05.006

Brisson N, Gary C, Justes E, Roche R, Mary B, Ripoche D, Zimmer D, Sierra J, Bertuzzi P, Burger P, Bussière F, Cabidoche YM, Cellier P, Debaeke P, Gaudillère JP, Hénault C, Maraux F, Seguin B, Sinoquet H (2003) An overview of the crop model STICS. Eur J Agron 18(3–4):309–332. https://doi.org/10.1016/S1161-0301(02)00110-7

Brown H, Huth N, Holzworth D (2018) Crop model improvement in APSIM: using wheat as a case study. Eur J Agron 100:141–150. https://doi.org/10.1016/j.eja.2018.02.002

Bustos-Korts D, Malosetti M, Chenu K, Chapman S, Boer MP, Zheng B, van Eeuwijk FA (2019) From QTLs to adaptation landscapes: using genotype-to-phenotype models to characterize G×E over time. Front Plant Sci 10(1540). https://doi.org/10.3389/fpls.2019.01540

Cann DJ, Hunt JR, Malcolm B (2020) Long fallows can maintain whole-farm profit and reduce risk in semi-arid south-eastern Australia. Agric Syst 178:102721. https://doi.org/10.1016/j.agsy.2019.102721

Carberry P, McCown R, Muchow R, Dimes J, Probert M, Poulton P, Dalgliesh N (1996) Simulation of a legume ley farming system in northern Australia using the Agricultural Production Systems Simulator. Aust J Exp Agric 36(8):1037–1048. https://doi.org/10.1071/EA9961037

Carcedo AJP, Gambin BL (2019) Sorghum drought and heat stress patterns across the Argentinean temperate central region. Field Crop Res 241:107552. https://doi.org/10.1016/j.fcr.2019.06.009

Castañeda-Vera A, Leffelaar PA, Álvaro-Fuentes J, Cantero-Martínez C, Mínguez MI (2015) Selecting crop models for decision making in wheat insurance. Eur J Agron 68:97–116. https://doi.org/10.1016/j.eja.2015.04.008

Challinor AJ, Wheeler TR, Craufurd PQ, Slingo JM, Grimes DIF (2004) Design and optimisation of a large-area process-based model for annual crops. Agric For Meteorol 124(1–2):99–120. https://doi.org/10.1016/j.agrformet.2004.01.002

Chapman SC (2008) Use of crop models to understand genotype by environment interactions for drought in real-world and simulated plant breeding trials. Euphytica 161(1):195–208. https://doi.org/10.1007/s10681-007-9623-z

Chapman SC, Cooper M, Butler DG, Henzell RG (2000a) Genotype by environment interactions affecting grain sorghum. I. Characteristics that confound interpretation of hybrid yield. Aust J Agric Res 51(2):197–208. https://doi.org/10.1071/AR99020

Chapman SC, Cooper M, Hammer GL, Butler DG (2000b) Genotype by environment interactions affecting grain sorghum. II. Frequencies of different seasonal patterns of drought stress are related to location effects on hybrid yields. Aust J Agric Res 51(2):209–222. https://doi.org/10.1071/AR99021

Chapman SC, Hammer GL, Butler DG, Cooper M (2000c) Genotype by environment interactions affecting grain sorghum. III. Temporal sequences and spatial patterns in the target population of environments. Aust J Agric Res 51(2):223–234. https://doi.org/10.1071/AR99022

Chew YH, Smith RW, Jones HJ, Seaton DD, Grima R, Halliday KJ (2014) Mathematical models light up plant signaling. Plant Cell 26(1):5–20. https://doi.org/10.1105/tpc.113.120006

Chibarabada TP, Modi AT, Mabhaudhi T (2020) Calibration and evaluation of AquaCrop for groundnut (Arachis hypogaea) under water deficit conditions. Agric For Meteorol 281:107850. https://doi.org/10.1016/j.agrformet.2019.107850

Cichota R, Vogeler I, Werner A, Wigley K, Paton B (2018) Performance of a fertiliser management algorithm to balance yield and nitrogen losses in dairy systems. Agric Syst 162:56–65. https://doi.org/10.1016/j.agsy.2018.01.017

Cichota R, McAuliffe R, Lee J, Minnee E, Martin K, Brown HE, Moot DJ, Snow VO (2020) Forage chicory model: development and evaluation. Field Crop Res 246:107633. https://doi.org/10.1016/j.fcr.2019.107633

Connolly RD, Bell M, Huth N, Freebairn DM, Thomas G (2002) Simulating infiltration and the water balance in cropping systems with APSIM-SWIM. Aust J Soil Res 40(2):221–242. https://doi.org/10.1071/SR01007

Corbesier L, Gadisseur I, Silvestre G, Jacqmard A, Bernier G (1996) Design in Arabidopsis thaliana of a synchronous system of floral induction by one long day. Plant J 9(6):947–952

Corbesier L, Vincent C, Jang S, Fornara F, Fan Q, Searle I, Giakountis A, Farrona S, Gissot L, Turnbull C, Coupland G (2007) FT protein movement contributes to long-distance signaling in floral induction of Arabidopsis. Science 316(5827):1030–1033. https://doi.org/10.1126/science.1141752

Coughenour MB, McNaughton SJ, Wallace LL (1984) Modelling primary production of perennial graminoids 3 $ uniting physiological processes and morphometric traits. Ecol Model 23 (1–2):101–134. https://doi.org/10.1016/0304-3800(84)90121-2

CSIRO (1980) SIROTAC — cotton by computer. http://www.scienceimage.csiro.au/library/plants/v/12312/cotton-by-computer/

Dar EA, Brar AS, Mishra SK, Singh KB (2017) Simulating response of wheat to timing and depth of irrigation water in drip irrigation system using CERES-wheat model. Field Crop Res 214:149–163. https://doi.org/10.1016/j.fcr.2017.09.010

de Wit CT (1958) Transpiration and crop yields. Volume 64 of Agricultural research report/ Netherlands Volume 59 of Mededeling (Instituut voor Biologisch en Scheikundig Onderzoek va Landbouwgewasses) Verslagen van landbouwkundige

de Wit CT (1965) Photosynthesis of leaf canopies. Agric Res Rep 663:57

de Wit CT, Brouwer R, Penning de Vries FWT (1970) The simulation of photosynthetic systems. In: Setlik I (ed) Prediction and measurement of photosynthetic productivity. proceedings IBP/PP technical symposium, Trebon, 14–21 September 1969, Pudoc, Wageningen, The Netherlands, pp 47–70

de Wit CT et al (1978) Simulation of assimilation, respiration and transpiration of crops. Simulation monographs. Pudoc, Wageningen, The Netherlands, pp 141

de Wit A, Boogaard H, Fumagalli D, Janssen S, Knapen R, van Kraalingen D, Supit I, van der Wijngaart R, van Diepen K (2019) 25 years of the WOFOST cropping systems model. Agric Syst 168:154–167. https://doi.org/10.1016/j.agsy.2018.06.018

Delgado M (1999) Lifesaving 101: how a veteran teacher can help a beginner. Educ Leadersh 56 (8):27–29

Demestihas C, Plénet D, Génard M, Garcia de Cortazar-Atauri I, Launay M, Ripoche D, Beaudoin N, Simon S, Charreyron M, Raynal C, Lescourret F (2018) Analyzing ecosystem services in apple orchards using the STICS model. Eur J Agron 94:108–119. https://doi.org/10.1016/j.eja.2018.01.009

Devkota KP, Hoogenboom G, Boote KJ, Singh U, Lamers JPA, Devkota M, Vlek PLG (2015) Simulating the impact of water saving irrigation and conservation agriculture practices for rice–wheat systems in the irrigated semi-arid drylands of Central Asia. Agric For Meteorol 214–215 (Supplement C):266–280. https://doi.org/10.1016/j.agrformet.2015.08.264

Dias HB, Inman-Bamber G, Bermejo R, Sentelhas PC, Christodoulou D (2019) New APSIM-Sugar features and parameters required to account for high sugarcane yields in tropical environments. Field Crop Res 235:38–53. https://doi.org/10.1016/j.fcr.2019.02.002

Dingkuhn M, Kouressy M, Vaksmann M, Clerget B, Chantereau J (2008) A model of sorghum photoperiodism using the concept of threshold-lowering during prolonged appetence. Eur J Agron 28(2):74–89. https://doi.org/10.1016/j.eja.2007.05.005

Dodd AN, Salathia N, Hall A, Kévei E, Tóth R, Nagy F, Hibberd JM, Millar AJ, Webb AAR (2005) Plant circadian clocks increase photosynthesis, growth, survival, and competitive advantage. Science 309(5734):630–633. https://doi.org/10.1126/science.1115581

Dokoohaki H, Gheysari M, Mousavi S-F, Zand-Parsa S, Miguez FE, Archontoulis SV, Hoogenboom G (2016) Coupling and testing a new soil water module in DSSAT CERES-Maize model for maize production under semi-arid condition. Agric Water Manag 163:90–99. https://doi.org/10.1016/j.agwat.2015.09.002

Donatelli M, Stöckle C, Ceotto E, Rinaldi M (1997) Evaluation of CropSyst for cropping systems at two locations of northern and southern Italy. Eur J Agron 6(1–2):35–45. https://doi.org/10.1016/S1161-0301(96)02029-1

Dong MA, Farré EM, Thomashow MF (2011) Circadian clock-associated 1 and late elongated hypocotyl regulate expression of the C-repeat binding factor (CBF) pathway in arabidopsis. Proc Natl Acad Sci 108(17):7241–7246. https://doi.org/10.1073/pnas.1103741108

Droutsas I, Challinor AJ, Swiderski M, Semenov MA (2019) New modelling technique for improving crop model performance – application to the GLAM model. Environ Model Softw 118:187–200. https://doi.org/10.1016/j.envsoft.2019.05.005

Duncan WG, Loomis RS, Williams WA, Hanau R (1967) A model for simulating photosynthesis in plant communities. Hilgardia 38:181–205

Dupuy L, Mackenzie J, Haseloff J (2010) Coordination of plant cell division and expansion in a simple morphogenetic system. Proc Natl Acad Sci 107(6):2711–2716. https://doi.org/10.1073/pnas.0906322107

Dzotsi KA, Basso B, Jones JW (2013) Development, uncertainty and sensitivity analysis of the simple SALUS crop model in DSSAT. Ecol Model 260:62–76. https://doi.org/10.1016/j.ecolmodel.2013.03.017

Dzotsi KA, Basso B, Jones JW (2015) Parameter and uncertainty estimation for maize, peanut and cotton using the SALUS crop model. Agric Syst 135(0):31–47. https://doi.org/10.1016/j.agsy.2014.12.003

Ebrahimi-Mollabashi E, Huth NI, Holzwoth DP, Ordóñez RA, Hatfield JL, Huber I, Castellano MJ, Archontoulis SV (2019) Enhancing APSIM to simulate excessive moisture effects on root growth. Field Crop Res 236:58–67. https://doi.org/10.1016/j.fcr.2019.03.014

FAO (2013) Greenhouse gas emissions from ruminant supply chains. A global life cycle Assessment. Food and Agriculture Organization of the United Nations, Rome

Farquhar GD, von Caemmerer S, Berry JA (1980) A biochemical model of photosynthetic CO_2 assimilation in leaves of C3 species. Planta 149(1):78–90. https://doi.org/10.1007/bf00386231

Foster T, Brozović N, Butler AP, Neale CMU, Raes D, Steduto P, Fereres E, Hsiao TC (2017) AquaCrop-OS: an open source version of FAO's crop water productivity model. Agric Water Manag 181:18–22. https://doi.org/10.1016/j.agwat.2016.11.015

Freer M, Moore AD, Donnelly JR (1997) GRAZPLAN: decision support systems for Australian grazing enterprises. I. Overview of the GRAZPLAN project and a description of the MetAccess and LambAlive DSS. Agric Syst 54:57–76

Gao J, Yang X, Zheng B, Liu Z, Zhao J, Sun S, Li K, Dong C (2019) Effects of climate change on the extension of the potential double cropping region and crop water requirements in Northern China. Agric For Meteorol 268:146–155. https://doi.org/10.1016/j.agrformet.2019.01.009

Gaudio N, Escobar-Gutiérrez AJ, Casadebaig P, Evers JB, Gérard F, Louarn G, Colbach N, Munz S, Launay M, Marrou H, Barillot R, Hinsinger P, Bergez J-E, Combes D, Durand J-L, Frak E, Pagès L, Pradal C, Saint-Jean S, Van Der Werf W, Justes E (2019) Current knowledge and future research opportunities for modeling annual crop mixtures. A review. Agron Sustain Dev 39(2):20. https://doi.org/10.1007/s13593-019-0562-6

Gaydon DS, Balwinder S, Wang E, Poulton PL, Ahmad B, Ahmed F, Akhter S, Ali I, Amarasingha R, Chaki AK, Chen C, Choudhury BU, Darai R, Das A, Hochman Z, Horan H, Hosang EY, Kumar PV, Khan ASMMR, Laing AM, Liu L, Malaviachichi MAPWK, Mohapatra KP, Muttaleb MA, Power B, Radanielson AM, Rai GS, Rashid MH, Rathanayake WMUK, Sarker MMR, Sena DR, Shamim M, Subash N, Suriadi A, Suriyagoda LDB, Wang G, Wang J, Yadav RK, Roth CH (2017) Evaluation of the APSIM model in cropping systems of Asia. Field Crop Res 204:52–75. https://doi.org/10.1016/j.fcr.2016.12.015

Graf A, Schlereth A, Stitt M, Smith AM (2010) Circadian control of carbohydrate availability for growth in Arabidopsis plants at night. Proc Natl Acad Sci 107(20):9458–9463. https://doi.org/10.1073/pnas.0914299107

Gyldengren JG, Abrahamsen P, Olesen JE, Styczen M, Hansen S, Gislum R (2020) Effects of winter wheat N status on assimilate and N partitioning in the mechanistic agroecosystem model DAISY. J Agro Crop Sci:1–22. https://doi.org/10.1111/jac.12412

Hamant O, Heisler MG, Jönsson H, Krupinski P, Uyttewaal M, Bokov P, Corson F, Sahlin P, Boudaoud A, Meyerowitz EM, Couder Y, Traas J (2008) Developmental Patterning by Mechanical Signals in Arabidopsis. Science 322(5908):1650–1655. https://doi.org/10.1126/science.1165594

Hammer G, Cooper M, Tardieu F, Welch S, Walsh B, van Eeuwijk F, Chapman S, Podlich D (2006) Models for navigating biological complexity in breeding improved crop plants. Trends Plant Sci 11(12):587–593. https://doi.org/10.1016/j.tplants.2006.10.006

Havlík P, Valin H, Herrero M, Obersteiner M, Schmid E, Rufino MC, Mosnier A, Thornton PK, Böttcher H, Conant RT, Frank S, Fritz S, Fuss S, Kraxner F, Notenbaert A (2014) Climate change mitigation through livestock system transitions. Proc Natl Acad Sci U S A 111 (10):3709–3714. https://doi.org/10.1073/pnas.1308044111

Herrero M, Fawcett RH, Dent JB (1996) Integrating simulation models to optimise nutrition and management for dairy farms: a methodology. In: Dent JB et al (eds) Livestock farming systems: research, development, socio-economics and the land manager. European Association for Animal Production Publication No. 79, Wageningen Pers, pp 322–326

Herrero M, Havlík P, Valin H, Notenbaert A, Rufino MC, Thornton PK, Blümmel M, Weiss F, Grace D, Obersteiner M (2013) Biomass use, production, feed efficiencies, and greenhouse gas emissions from global livestock systems. Proc Natl Acad Sci U S A 110(52):20888–20893. https://doi.org/10.1073/pnas.1308149110

Higgins G, Kassam A, Kowal J, Sarraf S, Arnoldussen H, Frere M, Hrabovszki J, van Velthuizen H (1978) Report on the Agro-ecological zones project, Vol. 1 Methodology and results for Africa. World soil resources report (48). FAO, Rome

Hlavinka P, Trnka M, Kersebaum KC, Čermák P, Pohanková E, Orsá GM, Pokorný E, Fischer M, Brtnický M, Žalud Z (2013) Modelling of yields and soil nitrogen dynamics for crop rotations by HERMES under different climate and soil conditions in the Czech Republic. J Agric Sci 152 (2):188–204. https://doi.org/10.1017/S0021859612001001

Holzworth DP, Huth NI, deVoil PG, Zurcher EJ, Herrmann NI, McLean G, Chenu K, van Oosterom EJ, Snow V, Murphy C, Moore AD, Brown H, Whish JPM, Verrall S, Fainges J, Bell LW, Peake AS, Poulton PL, Hochman Z, Thorburn PJ, Gaydon DS, Dalgliesh NP, Rodriguez D, Cox H, Chapman S, Doherty A, Teixeira E, Sharp J, Cichota R, Vogeler I, Li FY, Wang E, Hammer GL, Robertson MJ, Dimes JP, Whitbread AM, Hunt J, van Rees H, McClelland T, Carberry PS, Hargreaves JNG, MacLeod N, McDonald C, Harsdorf J, Wedgwood S, Keating BA (2014) APSIM – Evolution towards a new generation of agricultural systems simulation. Environ Model Softw 62:327–350. https://doi.org/10.1016/j.envsoft.2014.07.009

Holzworth D, Huth NI, Fainges J, Brown H, Zurcher E, Cichota R, Verrall S, Herrmann NI, Zheng B, Snow V (2018) APSIM Next Generation: overcoming challenges in modernising a farming systems model. Environ Model Softw 103:43–51. https://doi.org/10.1016/j.envsoft.2018.02.002

Hoogenboom G, White JW (2003) Improving physiological assumptions of simulation models by using gene-based approaches. Agron J 95(1):82–89

Hoogenboom G, Porter CH, Shelia V, Boote KJ, Singh U, White JW, Hunt LA, Ogoshi R, Lizaso JI, Koo J, Asseng S, Singels A, Moreno LP, Jones JW (2019) Decision Support System for Agrotechnology Transfer (DSSAT). https://dssat.net

Hunt LA, Jones JW, Hoogenboom G, Godwin DC, Singh U, Pickering N, Thornton PK, Boote KJ, Ritchie JT (1994) General input and output file structures for crop simulation models. Application of modeling in the semi-arid tropics. Published by CO-DATA, International Council of Scientific Unions, Paris, pp 35–72

Hussain J, Khaliq T, Ahmad A, Akhter J, Asseng S (2018) Wheat responses to climate change and its adaptations: a focus on arid and semi-arid environment. Int J Environ Res. https://doi.org/10.1007/s41742-018-0074-2

Huth NI, Bristow KL, Verburg K (2012) SWIM3: model use, calibration, and validation. Trans ASABE 55(4):1303–1313

IADB (1975) HerdSIM simulation model: user manual. Project analysis paper no. 2. Economic and Social Development Department, Inter-American Development Bank, Washington, DC

Ibrahim A, Harrison MT, Meinke H, Zhou M (2019) Examining the yield potential of barley near-isogenic lines using a genotype by environment by management analysis. Eur J Agron 105:41–51. https://doi.org/10.1016/j.eja.2019.02.003

IBSNAT (1984) Experimental design and data collection procedures for IBSNAT. The minimum data set for systems analysis and crop simulation, first ed. IBSNAT Technical Report no 1. http://pdf.usaid.gov/pdf_docs/PNABK919.pdf

Ijaz W, Ahmed M, Asim M, Aslam M (2017) Models to study phosphorous dynamics under changing climate. In: Ahmed M, Stockle CO (eds) Quantification of climate variability, adaptation and mitigation for agricultural sustainability. Springer International Publishing, Cham, pp 371–386. https://doi.org/10.1007/978-3-319-32059-5_15

IPCC (1990) In: Houghton JT, Jenkins GJ, Ephraums JJ (eds) Climate change: the IPCC scientific assessment. Cambridge University Press, Cambridge/New York, p 410

Jabeen M, Gabriel HF, Ahmed M, Mahboob MA, Iqbal J (2017) Studying impact of climate change on wheat yield by using DSSAT and GIS: a case study of Pothwar region. In: Ahmed M, Stockle CO (eds) Quantification of climate variability, adaptation and mitigation for agricultural sustainability. Springer International Publishing, Cham, pp 387–411. https://doi.org/10.1007/978-3-319-32059-5_16

Jahan MAHS, Sen R, Ishtiaque S, Choudhury AK, Akhter S, Ahmed F, Biswas JC, Manirruzaman M, Miah MM, Rahman MM, Kalra N (2018) Optimizing sowing window for wheat cultivation in Bangladesh using CERES-wheat crop simulation model. Agric Ecosyst Environ 258:23–29. https://doi.org/10.1016/j.agee.2018.02.008

Jalota SK, Vashisht BB, Kaur H, Kaur S, Kaur P (2014) Location specific climate change scenario and its impact on rice and wheat in Central Indian Punjab. Agric Syst 131(0):77–86. https://doi.org/10.1016/j.agsy.2014.07.009

Jiang Y, Zhang L, Zhang B, He C, Jin X, Bai X (2016) Modeling irrigation management for water conservation by DSSAT-maize model in arid northwestern China. Agric Water Manag 177:37–45. https://doi.org/10.1016/j.agwat.2016.06.014

Jing Q, Qian B, Bélanger G, VanderZaag A, Jégo G, Smith W, Grant B, Shang J, Liu J, He W, Boote K, Hoogenboom G (2020) Simulating alfalfa regrowth and biomass in eastern Canada using the CSM-CROPGRO-perennial forage model. Eur J Agron 113:125971. https://doi.org/10.1016/j.eja.2019.125971

Johnson IR, Thornley JHM (1983) Vegetative crop growth model incorporating leaf area expansion and senescence, and applied to grass. Plant Cell Environ 6(9):721–729. https://doi.org/10.1111/1365-3040.ep11589349

Jones MR, Singels A (2018) Refining the Canegro model for improved simulation of climate change impacts on sugarcane. Eur J Agron 100:76–86. https://doi.org/10.1016/j.eja.2017.12.009

Jones JW, Hesketh JD, Kamprath EJ, Bowen HD (1974) Development of a nitrogen balance for cotton growth models: a first approximation. Crop Sci 14(4):541–546

Jones J, Brown L, Hasketh J (1980) COTCROP: a computer model for cotton growth and yield, Predicting photosynthesis for ecosystem models, vol I. CRC Press, Boca Raton, pp 209–241

Jones JW, Hoogenboom G, Porter CH, Boote KJ, Batchelor WD, Hunt LA, Wilkens PW, Singh U, Gijsman AJ, Ritchie JT (2003) The DSSAT cropping system model. Eur J Agron 18 (3–4):235–265. https://doi.org/10.1016/S1161-0301(02)00107-7

Jones JW, Antle JM, Basso B, Boote KJ, Conant RT, Foster I, Godfray HCJ, Herrero M, Howitt RE, Janssen S, Keating BA, Munoz-Carpena R, Porter CH, Rosenzweig C, Wheeler TR (2017) Brief history of agricultural systems modeling. Agric Syst 155:240–254. https://doi.org/10.1016/j.agsy.2016.05.014

Kadiyala MDM, Jones JW, Mylavarapu RS, Li YC, Reddy MD (2015) Identifying irrigation and nitrogen best management practices for aerobic rice–maize cropping system for semi-arid tropics using CERES-rice and maize models. Agric Water Manag 149(Supplement C):23–32. https://doi.org/10.1016/j.agwat.2014.10.019

Karimi T, Stöckle CO, Higgins SS, Nelson RL, Huggins D (2017) Projected dryland cropping system shifts in the Pacific northwest in response to climate change. Front Ecol Evol 5(20). https://doi.org/10.3389/fevo.2017.00020

Kassie BT, Van Ittersum MK, Hengsdijk H, Asseng S, Wolf J, Rötter RP (2014) Climate-induced yield variability and yield gaps of maize (Zea mays L.) in the Central Rift Valley of Ethiopia. Field Crop Res 160(0):41–53. https://doi.org/10.1016/j.fcr.2014.02.010

Kassie BT, Asseng S, Porter CH, Royce FS (2016) Performance of DSSAT-Nwheat across a wide range of current and future growing conditions. Eur J Agron 81:27–36. https://doi.org/10.1016/j.eja.2016.08.012

Keating BA, Godwin DC, Watiki JM (1991) Optimising nitrogen inputs in response to climatic risk. Climatic risk in crop production. Proc Int Symp, Brisbane 1990:329–358

Keating BA, Carberry PS, Hammer GL, Probert ME, Robertson MJ, Holzworth D, Huth NI, Hargreaves JNG, Meinke H, Hochman Z, McLean G, Verburg K, Snow V, Dimes JP, Silburn M, Wang E, Brown S, Bristow KL, Asseng S, Chapman S, McCown RL, Freebairn DM, Smith CJ (2003) An overview of APSIM, a model designed for farming systems simulation. Eur J Agron 18(3–4):267–288. https://doi.org/10.1016/S1161-0301(02)00108-9

Keig G, McAlpine JR (1969) WATBAL: a computer system for the estimation and analysis of soil moisture regimes from simple climatic data. Tech. Memo. 69/9 CSIRO Division of Land Use Research, Canberra

Keily J, MacGregor DR, Smith RW, Millar AJ, Halliday KJ, Penfield S (2013) Model selection reveals control of cold signalling by evening-phased components of the plant circadian clock. Plant J 76(2):247–257

Kheir AMS, El Baroudy A, Aiad MA, Zoghdan MG, Abd El-Aziz MA, Ali MGM, Fullen MA (2019) Impacts of rising temperature, carbon dioxide concentration and sea level on wheat production in North Nile delta. Sci Total Environ 651:3161–3173. https://doi.org/10.1016/j.scitotenv.2018.10.209

Kierzkowski D, Nakayama N, Routier-Kierzkowska A-L, Weber A, Bayer E, Schorderet M, Reinhardt D, Kuhlemeier C, Smith RS (2012) Elastic domains regulate growth and organogenesis in the plant shoot apical meristem. Science 335(6072):1096–1099. https://doi.org/10.1126/science.1213100

Konandreas PA, Anderson FM (1982) Cattle herd dynamics: an integer and stochastic model for evaluating production alternatives. ILRI (aka ILCA and ILRAD)

Li ZT, Yang JY, Drury CF, Hoogenboom G (2015) Evaluation of the DSSAT-CSM for simulating yield and soil organic C and N of a long-term maize and wheat rotation experiment in the Loess Plateau of Northwestern China. Agric Syst 135(0):90–104. https://doi.org/10.1016/j.agsy.2014.12.006

Liben FM, Wortmann CS, Tirfessa A (2020) Geospatial modeling of conservation tillage and nitrogen timing effects on yield and soil properties. Agric Syst 177:102720. https://doi.org/10.1016/j.agsy.2019.102720

Liu B, Asseng S, Liu L, Tang L, Cao W, Zhu Y (2016) Testing the responses of four wheat crop models to heat stress at anthesis and grain filling. Glob Chang Biol 22(5):1890–1903. https://doi.org/10.1111/gcb.13212

Liu B, Martre P, Ewert F, Porter JR, Challinor AJ, Müller C, Ruane AC, Waha K, Thorburn PJ, Aggarwal PK, Ahmed M, Balkovič J, Basso B, Biernath C, Bindi M, Cammarano D, De Sanctis G, Dumont B, Espadafor M, Eyshi Rezaei E, Ferrise R, Garcia-Vila M, Gayler S, Gao Y, Horan H, Hoogenboom G, Izaurralde RC, Jones CD, Kassie BT, Kersebaum KC, Klein C, Koehler A-K, Maiorano A, Minoli S, Montesino San Martin M, Naresh Kumar S, Nendel C, O'Leary GJ, Palosuo T, Priesack E, Ripoche D, Rötter RP, Semenov MA, Stöckle C, Streck T, Supit I, Tao F, Van der Velde M, Wallach D, Wang E, Webber H, Wolf J, Xiao L, Zhang Z, Zhao Z, Zhu Y, Asseng S (2019) Global wheat production with 1.5 and 2.0°C above pre-industrial warming. Glob Chang Biol 25(4):1428–1444. https://doi.org/10.1111/gcb.14542

Long SP, Ainsworth EA, Leakey ADB, Nösberger J, Ort DR (2006) Food for thought: lower-than-expected crop yield stimulation with rising CO_2 concentrations. Science 312(5782):1918–1921. https://doi.org/10.1126/science.1114722

Luo Q, Williams MAJ, Bellotti W, Bryan B (2003) Quantitative and visual assessments of climate change impacts on South Australian wheat production. Agric Syst 77(3):173–186. https://doi.org/10.1016/S0308-521X(02)00109-9

Malik W, Dechmi F (2020) Modelling agricultural nitrogen losses to enhance the environmental sustainability under Mediterranean conditions. Agric Water Manag 230:105966. https://doi.org/10.1016/j.agwat.2019.105966

May RM (1976) Simple mathematical models with very complicated dynamics. Nature 261(5560):459–467. https://doi.org/10.1038/261459a0

Mbangiwa NC, Savage MJ, Mabhaudhi T (2019) Modelling and measurement of water productivity and total evaporation in a dryland soybean crop. Agric For Meteorol 266-267:65–72. https://doi.org/10.1016/j.agrformet.2018.12.005

McCown RL (1973) An evaluation of the influence of available soil water storage capacity on growing season length and yield of tropical pastures using simple water balance models. Agric Meteorol 11:53–63. https://doi.org/10.1016/0002-1571(73)90050-2

McCown RL, Keating BA, Probert ME, Jones RK (1992) Strategies for sustainable crop production in semi-arid Africa. Outlook Agric 21(1):21–31. https://doi.org/10.1177/003072709202100105

McCown RL, Hammer GL, Hargreaves JNG, Holzworth DP, Freebairn DM (1996) APSIM: a novel software system for model development, model testing and simulation in agricultural systems research. Agric Syst 50(3):255–271. https://doi.org/10.1016/0308-521X(94)00055-V

McNunn G, Heaton E, Archontoulis S, Licht M, VanLoocke A (2019) Using a crop modeling framework for precision cost-benefit analysis of variable seeding and nitrogen application rates. Front Sustain Food Syst 3(108). https://doi.org/10.3389/fsufs.2019.00108

Mehrabi F, Sepaskhah AR (2019) Winter wheat yield and DSSAT model evaluation in a diverse semi-arid climate and agronomic practices. Int J Plant Prod. https://doi.org/10.1007/s42106-019-00080-6

Meinke H, Rabbinge R, Hammer GL, van Keulen H, Jamieson PD (1998a) Improving wheat simulation capabilities in Australia from a cropping systems perspective II. Testing simulation capabilities of wheat growth. Eur J Agron 8(1):83–99. https://doi.org/10.1016/S1161-0301(97)00016-6

Meinke H, Hammer GL, van Keulen H, Rabbinge R (1998b) Improving wheat simulation capabilities in Australia from a cropping systems perspective III. The integrated wheat model (I_WHEAT). Eur J Agron 8(1):101–116. https://doi.org/10.1016/S1161-0301(97)00015-4

Mesbah M, Pattey E, Jégo G (2017) A model-based methodology to derive optimum nitrogen rates for rainfed crops – a case study for corn using STICS in Canada. Comput Electron Agric 142 (Part B):572–584. https://doi.org/10.1016/j.compag.2017.11.011

Messina CD, Jones JW, Boote KJ, Vallejos CE (2006) A gene-based model to simulate soybean development and yield responses to environment. Crop Sci 46(1):456–466. https://doi.org/10.2135/cropsci2005.04-0372

Mohanty M, Probert ME, Reddy KS, Dalal RC, Mishra AK, Subba Rao A, Singh M, Menzies NW (2012) Simulating soybean–wheat cropping system: APSIM model parameterization and validation. Agric Ecosyst Environ 152(0):68–78. https://doi.org/10.1016/j.agee.2012.02.013

Moreno-Cadena LP, Hoogenboom G, Fisher MJ, Ramirez-Villegas J, Prager SD, Becerra Lopez-Lavalle LA, Pypers P, Mejia de Tafur MS, Wallach D, Muñoz-Carpena R, Asseng S (2020) Importance of genetic parameters and uncertainty of MANIHOT, a new mechanistic cassava simulation model. Eur J Agron 115:126031

Nasrallah A, Belhouchette H, Baghdadi N, Mhawej M, Darwish T, Darwich S, Faour G (2020) Performance of wheat-based cropping systems and economic risk of low relative productivity assessment in a sub-dry Mediterranean environment. Eur J Agron 113:125968. https://doi.org/10.1016/j.eja.2019.125968

Negm LM, Youssef MA, Skaggs RW, Chescheir GM, Jones J (2014) DRAINMOD–DSSAT model for simulating hydrology, soil carbon and nitrogen dynamics, and crop growth for drained crop land. Agric Water Manag 137(0):30–45. https://doi.org/10.1016/j.agwat.2014.02.001

Nendel C, Berg M, Kersebaum KC, Mirschel W, Specka X, Wegehenkel M, Wenkel KO, Wieland R (2011) The MONICA model: testing predictability for crop growth, soil moisture and nitrogen dynamics. Ecol Model 222(9):1614–1625. https://doi.org/10.1016/j.ecolmodel.2011.02.018

Netherlands Scientific Council for Government Policy (1992) Ground for choices. Four perspectives for the rural areas in the European Community. (ISBN 903990367-0; http://www.wrr.nl/fileadmin/en/publicaties/PDF-Rapporten/Ground_for_choices_four_perspectives_for_the_rural_areasin_the_European_Community.pdf)

Ngwira AR, Aune JB, Thierfelder C (2014) DSSAT modelling of conservation agriculture maize response to climate change in Malawi. Soil Tillage Res 143(0):85–94. https://doi.org/10.1016/j.still.2014.05.003

Nissanka SP, Karunaratne AS, Perera R, Weerakoon WMW, Thorburn PJ, Wallach D (2015) Calibration of the phenology sub-model of APSIM-Oryza: going beyond goodness of fit. Environ Model Softw 70(0):128–137. https://doi.org/10.1016/j.envsoft.2015.04.007

Nomoto Y, Kubozono S, Yamashino T, Nakamichi N, Mizuno T (2012) Circadian clock- and PIF4-controlled plant growth: a coincidence mechanism directly integrates a hormone signaling network into the photoperiodic control of plant architectures in Arabidopsis thaliana. Plant Cell Physiol 53(11):1950–1964. https://doi.org/10.1093/pcp/pcs137

NRC (1945) Nutrient requirements of dairy cattle. Committee on Animal Nutrition. National Research Council, Washington, DC

Nyathi MK, van Halsema GE, Annandale JG, Struik PC (2018) Calibration and validation of the AquaCrop model for repeatedly harvested leafy vegetables grown under different irrigation regimes. Agric Water Manag 208:107–119. https://doi.org/10.1016/j.agwat.2018.06.012

O'Leary GJ, Connor DJ (1996) A simulation model of the wheat crop in response to water and nitrogen supply: II. Model validation. Agric Syst 52(1):31–55. https://doi.org/10.1016/0308-521X(96)00002-9

Orskov ER, McDonald I (1979) The estimation of protein degradability in the rumen from incubation measurements weighted according to rate of passage. J Agric Sci 92(2):499–503. https://doi.org/10.1017/S0021859600063048

Osman R, Zhu Y, Ma W, Zhang D, Ding Z, Liu L, Tang L, Liu B, Cao W (2020) Comparison of wheat simulation models for impacts of extreme temperature stress on grain quality. Agric For Meteorol 288–289:107995. https://doi.org/10.1016/j.agrformet.2020.107995

Pala M, Stockle CO, Harris HC (1996) Simulation of durum wheat (*Triticum turgidum* ssp. durum) growth under different water and nitrogen regimes in a Mediterranean environment using CropSyst. Agric Syst 51(2):147–163. https://doi.org/10.1016/0308-521X(95)00043-5

Peng B, Guan K, Tang J, Ainsworth EA, Asseng S, Bernacchi CJ, Cooper M, Delucia EH, Elliott JW, Ewert F, Grant RF, Gustafson DI, Hammer GL, Jin Z, Jones JW, Kimm H, Lawrence DM, Li Y, Lombardozzi DL, Marshall-Colon A, Messina CD, Ort DR, Schnable JC, Vallejos CE, Wu A, Yin X, Zhou W (2020) Towards a multiscale crop modelling framework for climate change adaptation assessment. Nat Plants 6(4):338–348. https://doi.org/10.1038/s41477-020-0625-3

Penning de Vries FWT, van Laar HH, Kropff MJ (eds) (1991) Simulation and systems analysis for rice production (SARP) 1991. PUDOC, Waneningen, p 369

Pinter PJ Jr, Ritchie JC, Hatfield JL, Hart GF (2003) The agricultural research service's remote sensing program: an example of interagency collaboration. Photogramm Eng Remote Sens 69 (6):615–618

Porter JR (1993) AFRCWHEAT2: a model of the growth and development of wheat incorporating responses to water and nitrogen. Eur J Agron 2(2):69–82. https://doi.org/10.1016/S1161-0301(14)80136-6

Probert ME, Dimes JP, Keating BA, Dalal RC, Strong WM (1998) APSIM's water and nitrogen modules and simulation of the dynamics of water and nitrogen in fallow systems. Agric Syst 56 (1):1–28. https://doi.org/10.1016/S0308-521X(97)00028-0

Ran H, Kang S, Li F, Du T, Tong L, Li S, Ding R, Zhang X (2018) Parameterization of the AquaCrop model for full and deficit irrigated maize for seed production in arid Northwest China. Agric Water Manag 203:438–450. https://doi.org/10.1016/j.agwat.2018.01.030

Razzaghi F, Zhou Z, Andersen MN, Plauborg F (2017) Simulation of potato yield in temperate condition by the AquaCrop model. Agric Water Manag 191:113–123. https://doi.org/10.1016/j.agwat.2017.06.008

Ritchie JT (1972) Model for predicting evaporation from a row crop with incomplete cover. Water Resour Res 8(5):1204–1213. https://doi.org/10.1029/WR008i005p01204

Robertson GW (1968) A biometeorological time scale for a cereal crop involving day and night temperatures and photoperiod. Int J Biometeorol 12(3):191–223. https://doi.org/10.1007/bf01553422

Robertson M, Lilley J (2016) Simulation of growth, development and yield of canola (*Brassica napus*) in APSIM. Crop Pasture Sci 67(4):332–344

Roeder AHK, Chickarmane V, Cunha A, Obara B, Manjunath BS, Meyerowitz EM (2010) Variability in the control of cell division underlies sepal epidermal patterning in Arabidopsis thaliana. PLoS Biol 8(5):e1000367. https://doi.org/10.1371/journal.pbio.1000367

Rosenzweig C, Parry ML (1994) Potential impact of climate change on world food supply. Nature 367(6459):133–138. https://doi.org/10.1038/367133a0

Rosenzweig C, Jones JW, Hatfield JL, Ruane AC, Boote KJ, Thorburn P, Antle JM, Nelson GC, Porter C, Janssen S, Asseng S, Basso B, Ewert F, Wallach D, Baigorria G, Winter JM (2013) The Agricultural Model Intercomparison and Improvement Project (AgMIP): protocols and pilot studies. Agric For Meteorol 170(0):166–182. https://doi.org/10.1016/j.agrformet.2012.09.011

Rosenzweig C, Elliott J, Deryng D, Ruane AC, Müller C, Arneth A, Boote KJ, Folberth C, Glotter M, Khabarov N, Neumann K, Piontek F, Pugh TAM, Schmid E, Stehfest E, Yang H, Jones JW (2014) Assessing agricultural risks of climate change in the 21st century in a global gridded crop model intercomparison. Proc Natl Acad Sci 111(9):3268–3273. https://doi.org/10.1073/pnas.1222463110

Rötter RP, Palosuo T, Kersebaum KC, Angulo C, Bindi M, Ewert F, Ferrise R, Hlavinka P, Moriondo M, Nendel C, Olesen JE, Patil RH, Ruget F, Takáč J, Trnka M (2012) Simulation of spring barley yield in different climatic zones of Northern and Central Europe: a comparison of nine crop models. Field Crop Res 133:23–36. https://doi.org/10.1016/j.fcr.2012.03.016

Rötter RP, Tao F, Höhn JG, Palosuo T (2015) Use of crop simulation modelling to aid ideotype design of future cereal cultivars. J Exp Bot. https://doi.org/10.1093/jxb/erv098

Russell JB, O'Connor JD, Fox DG, Van Soest PJ, Sniffen CJ (1992) A net carbohydrate and protein system for evaluating cattle diets: I. Ruminal fermentation. J Anim Sci 70(11):3551–3561. https://doi.org/10.2527/1992.70113551x

Samperio A, Moñino MJ, Marsal J, Prieto MH, Stöckle C (2014) Use of CropSyst as a tool to predict water use and crop coefficient in Japanese plum trees. Agric Water Manag 146(0):57–68. https://doi.org/10.1016/j.agwat.2014.07.019

Schaphoff S, von Bloh W, Rammig A, Thonicke K, Biemans H, Forkel M, Gerten D, Heinke J, Jägermeyr J, Knauer J, Langerwisch F, Lucht W, Müller C, Rolinski S, Waha K (2018a) LPJmL4 – a dynamic global vegetation model with managed land – part 1: model description. Geosci Model Dev 11(4):1343–1375. https://doi.org/10.5194/gmd-11-1343-2018

Schaphoff S, Forkel M, Müller C, Knauer J, von Bloh W, Gerten D, Jägermeyr J, Lucht W, Rammig A, Thonicke K, Waha K (2018b) LPJmL4 – a dynamic global vegetation model with managed land – part 2: model evaluation. Geosci Model Dev 11(4):1377–1403. https://doi.org/10.5194/gmd-11-1377-2018

Schepen A, Everingham Y, Wang QJ (2020) An improved workflow for calibration and downscaling of GCM climate forecasts for agricultural applications – a case study on prediction of sugarcane yield in Australia. Agric For Meteorol 291:107991. https://doi.org/10.1016/j.agrformet.2020.107991

Seligman N, Keulen H (1980) 4.10 PAPRAN: a simulation model of annual pasture production limited by rainfall and nitrogen. In: Simulation of nitrogen behaviour of soil-plant systems. PUDOC, Wageningen, pp 192–221

Shibu ME, Leffelaar PA, van Keulen H, Aggarwal PK (2010) LINTUL3, a simulation model for nitrogen-limited situations: application to rice. Eur J Agron 32(4):255–271. https://doi.org/10.1016/j.eja.2010.01.003

Singh P, Nedumaran S, Ntare BR, Boote KJ, Singh NP, Srinivas K, Bantilan MCS (2014a) Potential benefits of drought and heat tolerance in groundnut for adaptation to climate change in India and West Africa. Mitig Adapt Strat Glob Change 19(5):509–529. https://doi.org/10.1007/s11027-012-9446-7

Singh P, Nedumaran S, Boote KJ, Gaur PM, Srinivas K, Bantilan MCS (2014b) Climate change impacts and potential benefits of drought and heat tolerance in chickpea in South Asia and East Africa. Eur J Agron 52(Part B):123–137. https://doi.org/10.1016/j.eja.2013.09.018

Singh PK, Singh KK, Baxla AK, Rathore LS (2015) Impact of climatic variability on wheat yield predication using DSSAT v 4.5 (CERES-Wheat) model for the different Agroclimatic zones in India. In: Singh AK, Dagar JC, Arunachalam ARG, Shelat KN (eds) Climate change modelling, planning and policy for agriculture. Springer India, pp 45–55. https://doi.org/10.1007/978-81-322-2157-9_6

Sitch S, Smith B, Prentice IC, Arneth A, Bondeau A, Cramer W, Kaplan JO, Levis S, Lucht W, Sykes MT, Thonicke K, Venevsky S (2003) Evaluation of ecosystem dynamics, plant geography and terrestrial carbon cycling in the LPJ dynamic global vegetation model. Glob Chang Biol 9(2):161–185. https://doi.org/10.1046/j.1365-2486.2003.00569.x

Slatyer RO (1960) Agricultural climatology of the Yass Valley, vol 6. Commonwealth Scientific and Industrial Research Organization, Australia

Slatyer R (1964) Climate of the Leichhardt-Gilbert area. Land Res Ser (CSIRO Australia) 11:90

Smith AP, Moore AD (2020) Whole farm implications of lucerne transitions in temperate crop-livestock systems. Agric Syst 177:102686. https://doi.org/10.1016/j.agsy.2019.102686

Soler CMT, Sentelhas PC, Hoogenboom G (2007) Application of the CSM-CERES-Maize model for planting date evaluation and yield forecasting for maize grown off-season in a subtropical environment. Eur J Agron 27(2–4):165–177. https://doi.org/10.1016/j.eja.2007.03.002

Soltani A, Hoogenboom G (2007) Assessing crop management options with crop simulation models based on generated weather data. Field Crop Res 103(3):198–207. https://doi.org/10.1016/j.fcr.2007.06.003

Soltani A, Sinclair TR (2015) A comparison of four wheat models with respect to robustness and transparency: Simulation in a temperate, sub-humid environment. Field Crop Res 175(0):37–46. https://doi.org/10.1016/j.fcr.2014.10.019

Spedding CRW (1976) Editorial. Agric Syst 1(1):1–3. https://doi.org/10.1016/0308-521X(76)90017-2

Stapleton H, Buxton D, Watson F, Noiting D (1974) Cotton: A computer simulation of cotton growth. College of Agriculture, University of Arizona, Tucson

Steinfeld H, Gerber P, Wassenaar T, Castel V, Rosales M, de Haan C (2006) Livestock's long shadow. FAO, Rome

Stockle CO, Martin SA, Campbell GS (1994) CropSyst, a cropping systems simulation model: water/nitrogen budgets and crop yield. Agric Syst 46(3):335–359. https://doi.org/10.1016/0308-521X(94)90006-2

Stöckle CO, Kemanian AR (2020) Can crop models identify critical gaps in genetics, environment, and management interactions. Front Plant Sci 11(737). https://doi.org/10.3389/fpls.2020.00737

Stöckle CO, Donatelli M, Nelson R (2003) CropSyst, a cropping systems simulation model. Eur J Agron 18(3–4):289–307. https://doi.org/10.1016/S1161-0301(02)00109-0

Stöckle C, Nelson R, Higgins S, Brunner J, Grove G, Boydston R, Whiting M, Kruger C (2010) Assessment of climate change impact on Eastern Washington agriculture. Clim Chang 102 (1–2):77–102. https://doi.org/10.1007/s10584-010-9851-4

Stöckle CO, Higgins S, Nelson R, Abatzoglou J, Huggins D, Pan W, Karimi T, Antle J, Eigenbrode SD, Brooks E (2018) Evaluating opportunities for an increased role of winter crops as adaptation to climate change in dryland cropping systems of the U.S. Inland Pacific Northwest. Clim Chang 146(1):247–261. https://doi.org/10.1007/s10584-017-1950-z

Strullu L, Beaudoin N, Thiébeau P, Julier B, Mary B, Ruget F, Ripoche D, Rakotovololona L, Louarn G (2020) Simulation using the STICS model of C&N dynamics in alfalfa from sowing to crop destruction. Eur J Agron 112:125948. https://doi.org/10.1016/j.eja.2019.125948

Subash N, Ram Mohan HS (2012) Evaluation of the impact of climatic trends and variability in rice–wheat system productivity using Cropping System Model DSSAT over the Indo-Gangetic Plains of India. Agric For Meteorol 164(0):71–81. https://doi.org/10.1016/j.agrformet.2012.05.008

Summerfield RJ, Collinson ST, Ellis RH, Roberts EH, Devries FWTP (1992) Photothermal Responses of Flowering in Rice (Oryza sativa). Ann Bot 69(2):101–112. https://doi.org/10.1093/oxfordjournals.aob.a088314

Tan S, Wang Q, Zhang J, Chen Y, Shan Y, Xu D (2018) Performance of AquaCrop model for cotton growth simulation under film-mulched drip irrigation in southern Xinjiang, China. Agric Water Manag 196:99–113. https://doi.org/10.1016/j.agwat.2017.11.001

Tao F, Zhang Z, Liu J, Yokozawa M (2009) Modelling the impacts of weather and climate variability on crop productivity over a large area: a new super-ensemble-based probabilistic projection. Agric For Meteorol 149(8):1266–1278. https://doi.org/10.1016/j.agrformet.2009.02.015

Tao F, Palosuo T, Rötter RP, Díaz-Ambrona CGH, Inés Mínguez M, Semenov MA, Kersebaum KC, Cammarano D, Specka X, Nendel C, Srivastava AK, Ewert F, Padovan G, Ferrise R, Martre P, Rodríguez L, Ruiz-Ramos M, Gaiser T, Höhn JG, Salo T, Dibari C, Schulman AH (2020) Why do crop models diverge substantially in climate impact projections? a comprehensive analysis based on eight barley crop models. Agric For Meteorol 281:107851. https://doi.org/10.1016/j.agrformet.2019.107851

Thorburn PJ, Biggs JS, Collins K, Probert ME (2010) Using the APSIM model to estimate nitrous oxide emissions from diverse Australian sugarcane production systems. Agric Ecosyst Environ 136(3-4):343–350. https://doi.org/10.1016/j.agee.2009.12.014

Thorp KR, DeJonge KC, Kaleita AL, Batchelor WD, Paz JO (2008) Methodology for the use of DSSAT models for precision agriculture decision support. Comput Electron Agric 64 (2):276–285. https://doi.org/10.1016/j.compag.2008.05.022

Uehara G, Tsuji GY (1998) Overview of IBSNAT. In: Tsuji GY, Hoogenboom G, Thornton PK (eds) Understanding options for agricultural production. Springer Netherlands, Dordrecht, pp 1–7. https://doi.org/10.1007/978-94-017-3624-4_1

Van Bavel C (1953) A drought criterion and its application in evaluating drought incidence and hazard. Agron J 45(4):167–172

van Keulen H, Asseng S (2019) Simulation models as tools for crop management. In: Savin R, Slafer GA (eds) Crop science. Springer New York, New York, pp 433–452. https://doi.org/10.1007/978-1-4939-8621-7_1047

Vogeler I, Cichota R, Thomsen IK, Bruun S, Jensen LS, Pullens JWM (2019) Estimating nitrogen release from Brassicacatch crop residues—comparison of different approaches within the APSIM model. Soil Tillage Res 195:104358. https://doi.org/10.1016/j.still.2019.104358

von Bloh W, Schaphoff S, Müller C, Rolinski S, Waha K, Zaehle S (2018) Implementing the nitrogen cycle into the dynamic global vegetation, hydrology, and crop growth model LPJmL (version 5.0). Geosci Model Dev 11(7):2789–2812. https://doi.org/10.5194/gmd-11-2789-2018

Wallach D, Martre P, Liu B, Asseng S, Ewert F, Thorburn PJ, van Ittersum M, Aggarwal PK, Ahmed M, Basso B, Biernath C, Cammarano D, Challinor AJ, De Sanctis G, Dumont B, Eyshi Rezaei E, Fereres E, Fitzgerald GJ, Gao Y, Garcia-Vila M, Gayler S, Girousse C, Hoogenboom G, Horan H, Izaurralde RC, Jones CD, Kassie BT, Kersebaum KC, Klein C, Koehler A-K, Maiorano A, Minoli S, Müller C, Naresh Kumar S, Nendel C, O'Leary GJ, Palosuo T, Priesack E, Ripoche D, Rötter RP, Semenov MA, Stöckle C, Stratonovitch P, Streck T, Supit I, Tao F, Wolf J, Zhang Z (2018) Multimodel ensembles improve predictions of crop–environment–management interactions. Glob Chang Biol 24(11):5072–5083. https://doi.org/10.1111/gcb.14411

Wang B, Liu DL, Asseng S, Macadam I, Yu Q (2015) Impact of climate change on wheat flowering time in eastern Australia. Agric For Meteorol 209–210(0):11–21. https://doi.org/10.1016/j.agrformet.2015.04.028

White JW, Hoogenboom G (1996) Simulating effects of genes for physiological traits in a process-oriented crop model. Agron J 88(3):416–422. https://doi.org/10.2134/agronj1996.00021962008800030009x

White JW, Hunt LA, Boote KJ, Jones JW, Koo J, Kim S, Porter CH, Wilkens PW, Hoogenboom G (2013) Integrated description of agricultural field experiments and production: the ICASA Version 2.0 data standards. Comput Electron Agric 96:1–12. https://doi.org/10.1016/j.compag.2013.04.003

Wilkerson GG, Jones JW, Boote KJ, Ingram KT, Mishoe JW (1983) Modeling soybean growth for crop management. Trans Am Soc Agric Eng 26(1):63–73

Williams JR, Jones CA, Dyke PT (1984) A modeling approach to determining the relationship between erosion and soil productivity. Trans ASAE 27(1):129–144. https://doi.org/10.13031/2013.32748

Woli P, Hoogenboom G (2018) Simulating weather effects on potato yield, nitrate leaching, and profit margin in the US Pacific Northwest. Agric Water Manag 201:177–187. https://doi.org/10.1016/j.agwat.2018.01.023

Xin Y, Tao F (2019) Optimizing genotype-environment-management interactions to enhance productivity and eco-efficiency for wheat-maize rotation in the North China Plain. Sci Total Environ 654:480–492. https://doi.org/10.1016/j.scitotenv.2018.11.126

Yan Z, Zhang X, Rashid MA, Li H, Jing H, Hochman Z (2020) Assessment of the sustainability of different cropping systems under three irrigation strategies in the North China Plain under climate change. Agric Syst 178:102745. https://doi.org/10.1016/j.agsy.2019.102745

Yang X, Chen F, Lin X, Liu Z, Zhang H, Zhao J, Li K, Ye Q, Li Y, Lv S, Yang P, Wu W, Li Z, Lal R, Tang H (2015) Potential benefits of climate change for crop productivity in China. Agric For Meteorol 208(0):76–84. https://doi.org/10.1016/j.agrformet.2015.04.024

Yin X, Kersebaum K-C, Beaudoin N, Constantin J, Chen F, Louarn G, Manevski K, Hoffmann M, Kollas C, Armas-Herrera CM, Baby S, Bindi M, Dibari C, Ferchaud F, Ferrise R, de Cortazar-Atauri IG, Launay M, Mary B, Moriondo M, Öztürk I, Ruget F, Sharif B, Wachter-Ripoche D, Olesen JE (2020) Uncertainties in simulating N uptake, net N mineralization, soil mineral N and N leaching in European crop rotations using process-based models. Field Crop Res:107863. https://doi.org/10.1016/j.fcr.2020.107863

Zeleke KT (2019) AquaCrop calibration and validation for faba bean (Vicia faba L.) under different agronomic managements. Agronomy 9(6):320

Models Calibration and Evaluation

5

Mukhtar Ahmed, Shakeel Ahmad, Muhammad Ali Raza, Uttam Kumar, Muhammad Ansar, Ghulam Abbas Shah, David Parsons, Gerrit Hoogenboom, Taru Palosuo, and Sabine Seidel

Abstract

Calibration of crop model is standard practice, and it involves estimation of crop parameters based upon observed field data. It is the process of estimation of unknown parameters using practical observations. It is generally carried out manually by adjusting the parameters of the model. It consists of choosing the accurate numbers of coefficients that play a significant role in the adjustment of soil nitrogen, soil organic carbon, soil phosphorus, crop growth, phenological development, biomass accumulation, dry-matter partitioning, nutrients uptake,

M. Ahmed (✉)
Department of Agricultural Research for Northern Sweden, Swedish University of Agricultural Sciences, Umeå, Sweden

Department of Agronomy, Pir Mehr Ali Shah Arid Agriculture University, Rawalpindi, Pakistan
e-mail: mukhtar.ahmed@slu.se; ahmadmukhtar@uaar.edu.pk

S. Ahmad
Department of Agronomy, Bahauddin Zakariya University, Multan, Pakistan

M. A. Raza
College of Agronomy, Sichuan Agricultural University, Chengdu, Sichuan, China

U. Kumar · D. Parsons
Department of Agricultural Research for Northern Sweden, Swedish University of Agricultural Sciences, Umeå, Sweden

M. Ansar · G. A. Shah
Department of Agronomy, Pir Mehr Ali Shah Arid Agriculture University, Rawalpindi, Pakistan

G. Hoogenboom
Institute for Sustainable Food Systems, University of Florida, Gainesville, FL, USA

T. Palosuo
Natural Resources Institute Finland (Luke), Helsinki, Finland

S. Seidel
Institute of Crop Science and Resource Conservation, University of Bonn, Bonn, Germany

M. Ahmed (ed.), *Systems Modeling*, https://doi.org/10.1007/978-981-15-4728-7_5

grain dry weight, grain numbers, grain yield, grain nitrogen (N) at maturity and protein content. A minimum data set (MDS) is required for the calibration of the model. A number of different steps could be used to calibrate the crop model. The initial step involves running of the model with default crop parameters and comparison of simulation outcomes with the observed data set. Afterwards, crop parameters are adjusted to have good agreement with observed and simulated data. It starts with phenology, then vegetative growth and biomass, afterwards yield components and finally yield. Optimization tools such as generalized likelihood uncertainty estimation (GLUE) and Markov chain Monte Carlo (MCMC) can be used for the calibration. Finally, evaluation of models needs to be performed with independent data set. The quantification of calibration and evaluation goodness should be evaluated by different skill scores such as root-mean-squared error (RMSE)/root-mean-square deviation (RMSD), relative RMSE (RRMSE) or normalized objective function (NOF), root-mean-square deviation-systematic error ($RMSD_{se}$), root-mean-square deviation-non-systematic error (RMSDnse), mean absolute error (MAE), mean bias error (ME), coefficient of determination (R^2), Nash-Sutcliffe modelling efficiency (EF) test, maximum difference (MD) and *D* index (index of agreement). These skill scores confirm the calibrated model performances under different sets of scenarios.

Keywords

Calibration · Estimation · Minimum data set · Phenology · Optimization tools · Skills scores

5.1 Introduction

Calibration of crop models is the common practice; it involves the estimation of model parameters to get a better fit of the model to the observed data. Wallach (2011) provided a statistical framework to understand crop model calibration in a better way. He considered the asymptotic limit of the parameter estimators firstly under a finite set of data which helped to remove noise and separated the fundamental behaviour of calibration. Secondly, he stated that theory should only be applied to such cases where only a single type of measurement is present. Finally, he concluded that calibration uses lease squares. According to his theoretical result, crop model could be specified, and this misspecification could be helpful for crop model calibration. Furthermore, according to him, calibration involves compensation of errors. Calibration of crop model is the estimation process of unknown parameters using practical observations (Ahmed et al. 2014, 2016, 2017, 2018, 2019; Ahmad et al. 2017, 2019). It is generally done manually by adjusting the model parameters, which test the skill and patience of the modeller, and it also consists of choosing the accurate numbers of crop coefficients that play a significant role in crop growth, phenological development (anthesis and maturity dates), biomass accumulation, dry-matter partitioning, nutrients uptake, grain dry weight, grain numbers, grain

Table 5.1 Minimum data sets (MDS) for crop model calibration and validation

Site information
Geographical coordinates (latitude and longitude), altitude, average annual maximum and minimum temperature, average annual amplitude in temperature, slope
Weather
Daily total solar radiation, daily maximum and minimum temperatures and rainfall
Soils
Soil surface and soil profile
Initial conditions
Previous field conditions
Managements
Cultivar name and type
Planting geometry
Sowing date
Fertilizer application methods and rates
Irrigation and water management
Chemical applications
Tillage
Harvesting
Calibration
All of the above plus crop parameters such as date of emergence, date of flowering and maturity, leaf area index, crop dry matter and yield and N dynamics in plant parts
Validation
Model outcomes (crop phenology, biomass, leaf area and yield) comparison with observed field-based data set

Source: Hunt and Boote (1998)

yield, grain nitrogen (N) at maturity and protein content. The calibration process requires the data set needed to run the model. The data involves climatic variables (solar radiation, temperature, rainfall, humidity, etc.), crop management, soil environment and genotypic parameters of crop. Similarly, previous history of the field is also very important to have accurate calibration of the model. Minimum data set (MDS) required to calibrate and validate crop model is given in Table 5.1. It shows that all crop model requires aerial and soil environment information with proper details for model calibration and validation. This MDS was already well described by the IBSNAT (International Benchmark Sites Network for Agrotechnology Transfer) project (Hunt and Boote 1998). Wallach (2011) defined model calibration as the procedure of estimating unknown model parameters by comparing with observed data. It is also model parameters tuning to increase agreement between observed field data and model outcomes. It decreases model prediction uncertainty, and it involves judicious use of parameters based upon expert opinions or using sensitivity analysis. It is an essential part of modelling which confirms that model is acceptable for its use under different circumstances. For example, in the case of calibration of any crop trait, different crop parameters or coefficients or genetic-specific parameters (GSPs) (e.g. thermal time to a single development stage; vernalisation;

Table 5.2 Cultivar-specific parameters of DSSAT CSM-CERES-wheat in species, ecotype and cultivar files

Crop file
Species
T_{RGFW} = temperature, response grain filling, dry weight (°C)
T_{base} = base temperature below which increase in grain weight is = 0
T_{opt1} = first optimum temperature at which increase in grain weight is most rapid
T_{opt2} = second optimum temperature, highest temperature at which increase in grain weight is still at its maximum
T_{max} = maximum temperature at which increase in grain weight = 0
Ecotype
P_1 = duration of phase end juvenile to terminal spikelet (growing degree days (GDD))
P_2 = duration of phase terminal spikelet to end leaf growth (GDD)
P_3 = duration of phase end leaf growth to end spike growth (GDD)
P_4 = duration of phase end spike growth to end grain fill lag (GDD)
SLAS = specific leaf area ($\mathrm{cm}^2\ \mathrm{g}^{-1}$)
PARUE = PAR conversion to dry matter ratio before the last leaf stage ($\mathrm{g\ MJ}^{-1}$)
PARU2 = PAR conversion to dry matter ratio after the last leaf stage ($\mathrm{g\ MJ}^{-1}$)
Genotype
P1V = days at optimum vernalising temperature required to complete vernalisation
P1D = percentage reduction in development rate in a photoperiod 10 h shorter than the
P5 = grain filling period duration (GDD)
G1 = kernel number per unit canopy weight at anthesis (g^{-1})
G2 = standard kernel size under optimum condition (mg)
G3 = standard non-stressed dry weight (total including grain) of a single tiller at maturity (g)
PHINT = phyllochron interval (GDD)

photoperiod; phyllochron; etc.) could be used. Calibration then allows us to modify the values for the coefficients and minimize the differences between the simulated and observed trait. Crop phenology involves phasic development, and it is an essential element in the crop model calibration. It is vital to predicting crop phenology accurately to have acceptable biomass and yield. A major determinant of crop yield is phenology as it describes the timing of plant development. Since climate change is affecting crop phenology significantly, thus, most of the simulation efforts were on the prediction of penology as a function of the environment (Ahmed 2020). Many previous studies elaborated how phenology responds to weather by using different equations, but calibration was not given so much importance. Thus Wallach et al. (2019) conducted the study with the objectives to evaluate the prediction capability of crop phenology and role of calibration. The study concluded that most of the prediction error was due to using different calibration approaches. They suggested that calibration could be improved using proper calibration tool and appropriate parameters. Thus, the estimation of GSPs is fundamental to have reliable predictions from crop models. However, most of the crop models have a large number of crop parameters (>100), but some are fixed and specific. The example of some of GSPs from DSSAT, APSIM and EPIC crop models have

Table 5.3 Generic coefficients used in DSSAT for potato, sugarcane and sunflower models

Generic coefficients for potato model DSSAT-SUBSTOR	
G2	Leaf area expansion rate in degree days(cm^2/m^2 d)
G3	Potential tuber growth rate(g/m^2 d)
PD	Index that suppresses tuber growth during the period that immediately follows tuber induction
P2	Index that relates photoperiod response to tuber initiation
TC	Upper critical temperature for tuber initiation (°C)
Genetic coefficients for DSSAT-Canegro-sugarcane	
P1	Degree days from emergence to harvest maturity
RATPOT	Maximum # of ratoon crops before reseeding
LFMAX	Maximum # of green leaves on a shoot
G1	General leaf shape to be used to calculate the maximum area, leaf width and total leaf populations. Users can choose either 1.0, 2.0 or 3.0, depending on the cultivar characteristics. G1 = 1.0 corresponds to the NCO376 and N14 leaf type—high population (greater than 13 plants/m^2) and narrow leaf (less than 30 mm in width)
	G1 = 2.0 corresponds to the N12 leaf type—medium population (10–13 plants/m^2) and medium leaf width (30–50 mm in width)
	G1 = 3.0 corresponds to the R570 leaf type—low population (less than 10 plants/m^2) and broad leaf (greater than 50 mm in width)
PI1	Phyllochron interval #1. When 0 < heat units < DDTPI
PI2	Phyllochron interval #2. When heat units > DTTPI
DTTPI	Degree day threshold between phyllochron interval 1 and 2
Genetic coefficients for DSSAT-oilcrop-sunflower	
P1	Duration of juvenile phase (in degree days, with a base temperature of 4 °C)
P2	Amount (in days/hour) that development is slowed when crop is grown in a photoperiod shorter than the optimum (which is considered to be 15 h)
P5	Duration of the first anthesis-physiological maturity stage (in degree days above a base of 4 °C)
G2	Maximum possible number of grains per head (measured in plants grown under optimum conditions and low plant population density)
G3	Potential kernel growth rate during the linear kernel filling phase (in mg/day, measured in plants grown under optimum conditions and low plant population density)
O1	Maximum kernel oil content (%)

been shown in Tables 5.2, 5.3, 5.4 and 5.5. Since there are many crop varieties which have the area-specific characters, and additionally new crop varieties are developed and released regularly, thus obtaining GSPs is a never-ending process. Calibration of model is usually performed by using field-based data. It involves searching for GSPs that have a good fit for the field data. GSPs concepts could be used to characterize genotypes or cultivars as these GSPs define the crop growth and development (Boote et al. 2003). Similarly, they can also be used to describe quantitative response of crop to environmental factors. EasyGrapher (EG) is a graphical and statistical software program designed for the DSSAT to allow users to manipulate hundreds of graphs within minutes and calculates evaluation statistics (Yang et al. 2014). If new

Table 5.4 Generic coefficients in APSIM-wheat

Name	Unit	Range
Cultivars parameters		
photop_sens (photoperiod sensitivity)	–	3–3.5
vern_sens (vernalisation sensitivity)	–	0–1
tt_end_of_juvenile (thermal time needed from sowing to end of juvenile)	°C days	250–650
tt_flowering (thermal time needed in anthesis phase)	°C days	80–180
tt_floral_initiation (thermal time from floral initiation to flowering)	°C days	300–900
tt_start_grain_fill (thermal time from start of grain filling to maturity)	°C days	450–1000
max_grain_size (maximum grain size)	g	0.03–0.065
potential_grain_growth_rate (grain growth rate from flowering to grain filling)	ggrain^{-1} day^{-1}	0.001–0.002
potential_grain_filling rate (potential daily grain filling rate)	ggrain^{-1} day^{-1}	0.002–0.006
grains_per_gram_stem (grain number per stem weight at the start of grain filling)	g	30–60

Table 5.5 EPIC model generic coefficients

Parameters	EPIC model default value
Crop parameters (spring wheat)	
Biomass to energy ratio (WA)	30
Harvest index (HI	0.42
Optimal temperature for plant growth (top)	15.0
Minimum temperature for plant growth (TBS)	0.0
Maximum potential leaf area index (DMLA)	5.0
Fraction of growing season when leaf area declines (DLAI)	0.6
First point on optimal leaf area development curve (DLAP1)	20.1
Second point on optimal leaf area development curve (DLAP2)	49.95
Maximum stomatal conductance (GSI)	0.007
Minimum harvest index (WSFY)	0.21
Heat units required for germination (GMHU)	100.0
Potential heat units (PHU)	2340

breeding lines or local cultivars need to be used in the modelling, firstly, cultivar coefficients were determined and then reconfirmed/evaluated with independent data. Suriharn et al. (2007) reported that well-designed detailed field experiments are ways to derive cultivar coefficients. The procedure involves sampling of growth and development data throughout the plant's life cycle. End-of-season data approach as proposed by Mavromatis et al. (2001, 2002) can be used to derive cultivar coefficients. However, in these yield trial end-of-season studies, optimization procedure is difficult due to the availability of limited data set. Thus, genotype coefficient calculator (GENCALC) technique is needed for the optimization which will be further discussed below.

5.2 Genotype Coefficient Calculator (GENCALC)

The GENCALC software was developed to facilitate the estimation of cultivar coefficients from field data. Hoogenboom et al. (2004) reported that new version of software is in progress to incorporate GENCALC into the DSSAT. Long-term yield trial data of different crops can be used to estimate cultivar coefficients using GENCALC. Anothai et al. (2008) used GENCALC optimization procedures to determine the new peanut line cultivar coefficient feasibility. Field trial data from the studies of Suriharn et al. (2007, 2008) were used to estimate the cultivar coefficients and model evaluation using GENCALC-DSSAT Version 4.5. Buddhaboon et al. (2018) compared two methods, i.e. GENCALC and GLUE, to estimate genetic coefficients of rice. The outcome of studies concluded that GENCALC and GLUE have good potential to calculate genetic coefficients. Li et al. (2015) calibrated maize and wheat varieties in China for DSSAT which have not been used previously. The disadvantage of this technique is that parameters will be available after variety release which could delay time period between model calibration and development of crop variety. Another option is gene-based modelling (GBM) where paraments could be estimated using the allelic composition of the genotype. Crop models can be calibrated before the release of variety through this GBM. White and Hoogenboom (2003) developed first gene-based model by using six levels of genetic detail. Development of this kind of model is a major topic in modelling nowadays (Wallach et al. 2018). Different phenotyping techniques (e.g. high-throughput phenotyping) using standard protocol are also used for the calibration of crop models. Statistical models such as non-dynamic regression as elaborated by Lobell (2013) are an alternative option to show crop responses where process-based models are potentially unable to perform well (Lobell and Asseng 2017). The main issue in statistical models is they do not consider mechanism involved in different biological processes and reactions to be considered during modelling biogeochemical cycling. Thus, these models are not suitable when genetic and other adaptation (e.g. agronomic management, climate change, greenhouse gases (GHG) balance and organic systems modelling) options need to be evaluated. However, model like SIMPLE (generic, simple dynamic model) could be a good option as it has fewer data requirements and parameters (Table 5.6) (Zhao et al. 2019). CERES-Wheat (Ritchie et al. 1985) cumulative temperature approach was used to determine crop phenological development. In this simple model, time to maturity was calculated by considering temperature higher than T_{base} (base temperature) of the crop only without putting OTT (optimum threshold temperature). Cumulative temperature needed for the model calibration from sowing to maturity was calculated by using the following formulae:

Table 5.6 SIMPLE model generic coefficients

Cultivar parameters	
T_{sum}:	Cumulative temperature requirement from sowing to maturity (°C days)
HI:	Potential harvest index
I50A:	Cumulative temperature requirement for leaf area development to intercept 50% of radiation (°C days)
I50B:	Cumulative temperature till maturity to reach 50% radiation interception due to leaf senescence (°C days)
Species parameters	
T_{base}:	Base temperature for phenology development and growth (°C)
T_{opt}:	Optimal temperature for biomass growth (°C)
RUE:	Radiation use efficiency (aboveground only and without respiration) (g MJ^{-1} m^{-2})
I50maxH:	The maximum daily reduction in I50B due to heat stress (°C days)
I50maxW:	The maximum daily reduction in I50B due to drought stress (°C days)
T_{max}:	Threshold temperature to start accelerating senescence from heat stress (°C)
T_{ext}:	The extreme temperature threshold when RUE becomes 0 due to heat stress (°C)
SCO_2:	Relative increase in RUE per ppm elevated CO_2 above 350 ppm
Swater:	Sensitivity of RUE (or harvest index) to drought stress (ARID index)

$$\Delta TT = \begin{cases} T - T_{base} & T > T_{base} \\ 0, & T \leq T_{base} \end{cases}$$

$$TT_{i+1} = TT_i + \Delta TT$$

where TT_i is the cumulative mean temperature of ith day, ΔTT is the mean temperature daily added, T is the daily average temperature and T_{base} is the base temperature for crop growth and phenological development.

Monteith (1965) concept of radiation use efficiency (RUE) was used in which plant canopy intercept daily PAR (photosynthetically active radiation) and converted to crop biomass considered as total biomass. Stress variables (high temperature, drought and atmospheric CO_2 concentration) affect plant daily biomass production. Finally, biomass and harvest index (HI) were used to calculate the final yield.

$$\text{Biomass}_{\text{rate}} = \text{radiation} \times f_{\text{solar}} \times \text{RUE} \times f_{\text{CO}_2} \times f_{\text{temp}} \times \min\left(\left(f_{\text{heat}}\right), \left(f_{\text{water}}\right)\right)$$

$$\text{Biomass\_cum}_{i+1} = \text{biomass\_cum}_i + \text{biomass\_rate}$$

$$\text{Yield} = \text{biomass\_cum}_{\text{maturity}} \times \text{HI}$$

where $\text{biomass}_{\text{rate}}$ is the daily biomass growth rate, biomass_cum is the cumulative biomass until the ith day, f_{solar} is the fraction of the solar radiation intercepted by the crop canopy based on Beer-Lambert's law of light attenuation, f_{CO2} is the CO_2 impact, f_{heat} is the heat stress function and f_{water} is the water stress function.

Calibration of the model is possible by doing a simulation in a number of steps as elaborated in Figs. 5.1 and 5.2. Simulation zero (S0) was conducted with default crop parameters, and results were compared with the observed data set. Next

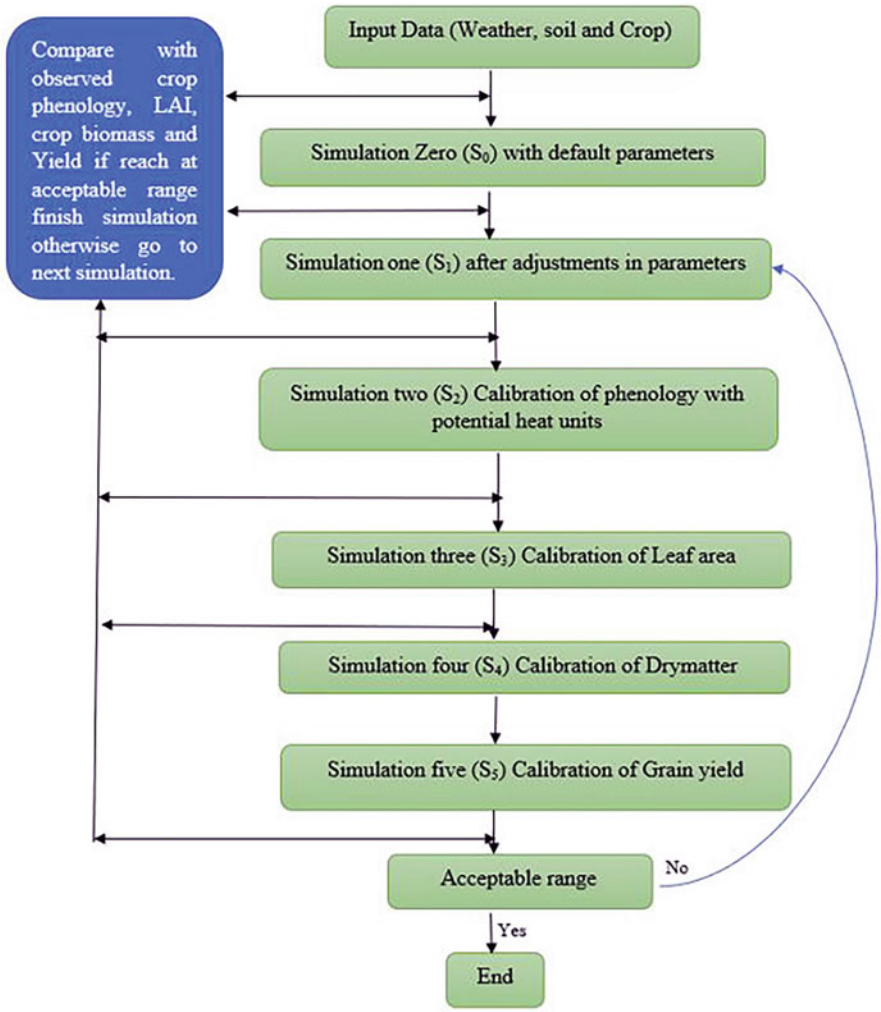

Fig. 5.1 Model calibration steps

simulation (S1) should be performed by adjusting the crop parameters. Afterwards, in simulation 2 (S2), crop phenology needs to be calibrated by adjusting crop parameters. Similarly, step-by-step crop leaf area, biomass and grain yield were calibrated if all comes in the required range; this ends the simulation otherwise needs to go back to simulation 1 (S1).

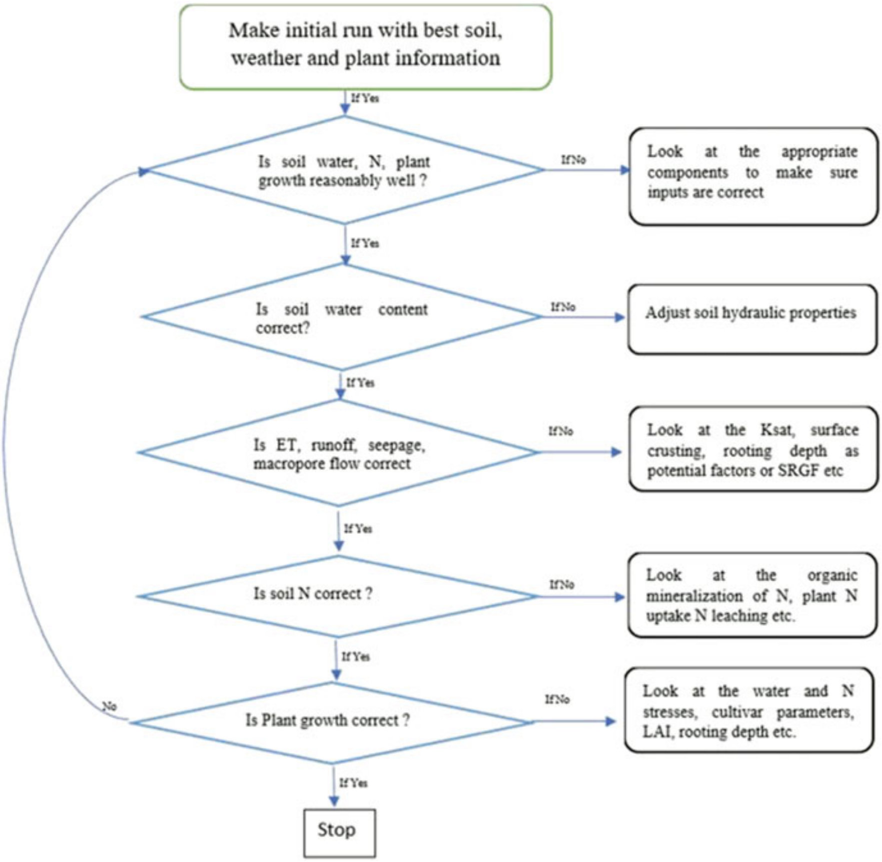

Fig. 5.2 Simple model calibration steps

5.3 Inferential Statistics

The branch of statistics which has been used dominantly for the parameter optimization is called inferential statistics, and it has two important categories, i.e. frequentist inference and Bayesian inference. In frequentist inference (FI) parameters are considered as fixed value, while in Bayesian approach (BsA), it is assumed that a parameter follows a probability distribution. The choice between the use of an FI and BsA would have a reasonable impact on the parameter estimated values and uncertainties related to it. Thus, the reliable approach in the selection of estimation parameters is very important. Beven and Binley (1992) reported that in BsA generally generalized likelihood uncertainty estimation (GLUE) is considered, while Gasparini (1997) and Gilks et al. (1995) reported Markov chain Monte Carlo (MCMC) technique for the estimation of crop model parameters. These two parameter optimization techniques have been commonly used in the assessment of crop models (Tan et al. 2019; Sheng et al. 2019) and environmental models (Rankinen et al. 2006; Jin et al. 2010; Whitehead et al. 2018; Leandro et al. 2019). The Markov chain Monte Carlo can separate the effect of input/output, model structural and parameter error, but interaction among these sources makes statistical inference difficult. Similarly, this method dependence on error model assumption has been criticized. In the case of agricultural systems, it is generally assumed in earlier studies that model residual errors are normally distributed. This assumption can be violated in many studies as model errors coupled with the agricultural production systems are often highly correlated (Beven et al. 2008; Dumont et al. 2014; Sexton et al. 2016). Another popular Bayesian method is DREAM (differential evolution adaptive metropolis) which has been used for the parameter estimation in crop model like Agricultural Production Systems Simulator (APSIM) by Sheng et al. (2019). APSIM-maize parameters were estimated by using DREAM and GLUE, and the study concluded that GLUE is more appropriate and simpler to use than DREAM. These two methods were evaluated theoretically and practically in which maize yield from 2003–2006 was used for model calibration, while validation was performed from 2007–2013 yield data set. The uncertainty bands of DREAM were wider than GLUE. He et al. (2017) investigated how different data impacted on the efficacy of process-based model (APSIM-Canola) calibration. A Bayesian optimisation approach was used to have cultivar parameters. Parameters used for the optimisations includes maximum thermal time required to complete the juvenile process at no vernalisation ($TT_{\mathrm{Juv,max}}$; 1551 °C d^{-1}); maximum thermal time required to complete the photoperiod sensitive stage at photoperiod less than 10.8 h ($TT_{\mathrm{FI,max}}$; 240–300 °C d^{-1}); thermal time for grain filling period (TT_{GF}, 540–610 °C d^{-1}); radiation use efficiency (RUE, 1–2 g MJ^{-1}); potential leaf area per node (Leaf size; node$_1$ = 200–5000 node$_5$ = 1000–12,000, node$_{13}$ = 10,000–30,000, node$_{16}$ = 11,000–35,000 mm^2); number of leaves per node (leaf number, node$_0$ = 1 node$_5$ = 1 node$_8$ = 1–2 node$_{14}$ = 1.5–2.5 leaves node^{-1}); potential node appearance rate (Node Phyllochron, 20–120 °C d node^{-1}) and harvest index (HI = 0.1–0.5). Eight different strategies for the model calibration (Cali$_1$–Cali$_8$) were used, and results showed that the best data for the calibration should be from different environments.

5.4 Quantification of the Goodness of a Calibration

Different skill scores are used to quantify the goodness of a calibration. It includes root-mean -squared error (RMSE)/root-mean-square deviation (RMSD) which aggregate the magnitude of errors in simulation outcomes into a single measure of predictive power. It can be calculated using the following equations:

$$\mathrm{RMSE} = \sqrt{\frac{\sum_{i=1}^{N} (P_i - O_i)^2}{n}} \tag{5.1}$$

where P_i is the predicted values, O_i is the observed values and n is the observed data points.

The RMSE can be used to find normalized objective function (NOF) using the following formulae:

$$\mathrm{NOF} = \frac{\mathrm{RMSE}}{O_{\mathrm{avg}}} \tag{5.2}$$

where O_{avg} is the average observed values, if NOF = 0 (perfect match between observed and simulated values).

Root-mean-square deviation-systematic error ($\mathrm{RMSD_{se}}$) and root-mean-square deviation-non-systematic error ($\mathrm{RMSD_{nse}}$) can be calculated using the following formulae:

$$\mathrm{RMSD_{se}} = \sqrt{\frac{1}{n-1} \sum_{i=1}^{n} \left(\widehat{S}_i - O_i\right)^2} \tag{5.3}$$

$$\mathrm{RMSD_{nse}} = \sqrt{\frac{1}{n-1} \sum_{i=1}^{n} \left(S_i - \widehat{S}_i\right)^2} \tag{5.4}$$

Mean difference between two continuous variables such as × and Y could be calculated by mean absolute error (MAE) using the following formulae:

$$\mathrm{MAE} = \frac{\sum_{i=1}^{N} |O_i - P_i|}{N} \tag{5.5}$$

Similarly, the mean bias error (ME) could also be used to check the performance of models. It can be calculated by using the following formulae:

$$\mathrm{ME} = \frac{\sum_{i=1}^{N} (P_i - O_i)}{N} \tag{5.6}$$

Systematic bias in the prediction could be indicated by ME values; if it is positive, it means overprediction, and if negative values come, it means overall under prediction.

Coefficient of determination (R^2) is another approach to conduct regression evaluation between experimental and predicted data. It can be determined by using the following formulae:

$$R^2 = \frac{\left[\sum_{i=1}^{N} \left(O_i - O_{\text{avg}}\right)\left(P_i - P_{\text{avg}}\right)\right]^2}{\sum_{i=1}^{N} \left(O_i - O_{\text{avg}}\right)^2 \sum_{i=1}^{N} \left(P_i - P_{\text{avg}}\right)^2} \tag{5.7}$$

The R^2 value ranges from 0–1. If $R^2 = 1$, it indicates a perfect correlation between observed (O) and predicted (P) values, and if $R^2 = 0$, it shows no correlation between O and P results. The R^2 approach does not consider systematic bias, so it might be misleading.

Different other indices such as Nash-Sutcliffe modelling efficiency (NSEF) test, maximum difference (MD) and D index (index of agreement) could also be used to check model performance after calibration. They can be calculated using the following formulas:

$$\text{NSEF} = 1.0 - \frac{\sum_{i=1}^{N} (O_i - P_i)^2}{\sum_{i=1}^{N} \left(O_i - O_{\text{avg}}\right)^2} \ \text{EF} = 1 \ (\text{perfect simulation}) \tag{5.8}$$

$$\text{MD} = \max |P_i - O_i|_{i=1}^{N} \tag{5.9}$$

$$D = 1.0 - \frac{\sum_{i=1}^{N} (O_i - P_i)^2}{\sum_{i=1}^{N} \left\langle \left|P_i - O_{\text{avg}}\right| + \left|O_i - O_{\text{avg}}\right| \right\rangle^2} \ D = 0 - 1; 1$$
$$= \text{perfect simulation} \tag{5.10}$$

Coefficient of residual mass (CRM) is another useful indicator which could be used to check the differences among observed and simulated data sets. It can be calculated using the following equation:

$$\text{CRM} = \frac{\left[\sum_{i=1}^{N} O_i - \sum_{i=1}^{N} P_i\right]}{\sum_{i=1}^{N} O_i} \tag{5.11}$$

The indices such as percent bias (PBIAS) and the ratio of RMSE to the SD (standard deviation) of measured data (RSR) have also been utilized to quantify model performance. These can be computed by using the following formulae:

$$\text{PBIAS} = \frac{\sum_{i=1}^{N} \frac{1}{N}(O_i - P_i)100}{\sum_{i=1}^{N} O_i} \tag{5.12}$$

$$\text{RSR} = \frac{\sqrt{\sum_{i=1}^{N} \frac{1}{N}(O_i - P_i)^2}}{\sqrt{\sum_{i=1}^{N} \frac{1}{N}\left(O_i - O_{\text{avg}}\right)^2}} \tag{5.13}$$

5.5 Case Studies of Calibration and Evaluation

The 7-year maize variety trial data (2003–2010) was used by Bao et al. (2017) for the calibration and evaluation of EPIC and CSM-CERES-maize models. Average grain yield (kg ha^{-1}) of seven maize varieties from six sites in Georgia (irrigated and rainfed) were used by considering different years for calibration (2007, 2008, 2009 and 2010) and evaluation (2003, 2005, 2007, 2008 and 2009). Crop cultivar coefficients were adjusted to have the best fit with the observed field data. The cultivar coefficients used for CSM-CERES-maize model includes P1, thermal time from seedling emergence to the end of the juvenile phase (110–458°days); P2, extent to which development is delayed for each hour increase in photoperiod above the longest photoperiod at which development proceeds at a maximum rate (0–-3 day h^{-1}); P5, thermal time from silking to physiological maturity (390–1000°days); G2, maximum possible number of kernels per plant (248–990 kernel plant^{-1}); G3, kernel filling rate during the linear grain filling state and under optimum conditions (4.4–16.5 Mg day^{-1}) and PHINT, the interval in thermal time (degree days) between successive leaf tip appearances (30–75°days). Similarly, SLPF, soil fertility factor (0.70–0.94), was adjusted as it affects the overall growth rate of modelled total biomass by adjusting daily canopy photosynthesis. It is also attributed with soil fertility and soil-based pests (Guerra et al. 2008; Mavromatis et al. 2001). Crop-specific coefficients used for the EPIC includes, PHU, potential heat units (total number of heat units from planting to physiological maturity) (1600–200 °C); WA, biomass energy ratio (40–55); BE, crop parameter, converts energy to biomass (kg ha MJ^{-1} m^{-2}); HI, potential harvest index, ratio of crop yield to aboveground biomass (0.1–0.6); T_o, optimal temperature for a crop; T_b, base temperature for a crop (plant start growing); DMLA, maximum LAI potential for a crop (2–6); DLAI, fraction of growing season when leaf area starts declining (0.5–0.95); HUI_o, heat unit index value when leaf area index starts declining; ah_1 and ah_2, crop parameters that determine the shape of the leaf area index development curve; af_1 and af_2, crop parameters for frost sensitivity; Ad, crop parameters that governs leaf area index decline rate; ALT, aluminium tolerance index number; CAF, critical aeration factor for a crop; HMX, maximum crop height; RDMX, maximum root depth for a crop; WSFY, water stress factor for adjusting harvest index; bn_1, bn_2 and bn_3, crop parameters for plant N concentration equation; and bp_1, bp_2 and bp_3, crop parameters for plant *P* concentration equation. The statistical criteria used for the model calibration and evaluation were the coefficient of determination (R^2), index of agreement (d) and root-mean-square error (RMSE) and mean absolute error (MAE). Model calibration and evaluation results showed that both models were able to predict grain yield. In the case of CSM-CERES-maize model, differences between simulated and observed yield were not more than 3% and 8% for calibration and evaluation, respectively. However, EPIC overestimated grain yield and range of differences between predicted and observed grain yield for calibration and evaluation were 2–23% and 10–20%, respectively. Model calibration under stress conditions need to be given higher importance as reported in the study of Mehrabi and Sepaskhah (2019). Wheat growth and yield under diverse semi-arid climate with different management strategies (e.g. irrigation, plant methods and nitrogen rates) were predicted through DSSAT. Six data sets were used to calibrate and validate the APSIM model by Balboa et al. (2019). Results indicated that APSIM was able to simulate crop biomass, yield and N dynamics with modelling efficiency of 0.75–0.92 and relative RMSE of 18–31% (Fig. 5.3).

Falconnier et al. (2019) calibrated and evaluated the STICS model for faba bean, which is widely grown grain legumes in Europe. The STICS model was calibrated using 38 crop-related parameters based on literature, field measurements and sequential estimation through OptimiSTICS optimisation tool (Fig. 5.4). In total, 35 different plots were used from which 22 experimental plots data were used for the model calibration and 13 plots data were used for the model evaluation. Three steps used for calibration, as shown in Fig. 5.4, involve the determination of existing crop parameters values using literature review, while in the second step, crop parameters were adjusted based upon field data set. Finally, in the third step, the optimisation of parameters was performed to have the best parameters. Furthermore, sensitivity analysis and expert knowledge were used to have parameters which have the strongest impact on model output, and 29 crop parameters were mathematically optimized. Model results after calibration show that it can reproduce crop phenology, leaf area index, aboveground biomass, uptake of N, N_2 fixation and grain yield with good accuracy.

DSSAT-Canegro model was calibrated and validated by Jones and Singels (2018) using a data set from Singels and Bezuidenhout (2002). Aerial dry biomass (ADM, t ha^{-1}), stalk dry mass (SDM, t ha^{-1}) and stalk sucrose mass were used for model calibration and validation. Results were more realistic in this study compared to the old model. In another study, three commonly used calibration methods (generalized likelihood uncertainty estimation (GLUE), ordinary least square (OLS) and Markov chain Monte Carlo (MCMC)) were compared by Gao et al. (2020) for rice phenology calibration using DSSAT-CSM-CERES-rice model. The results showed that the selection of the calibration method has an important impact on parameter estimation and quantification of the uncertainties. If goodness-of-fit is the main criterion, then OLS is the effective and fastest method, while for the quantification of uncertainties,

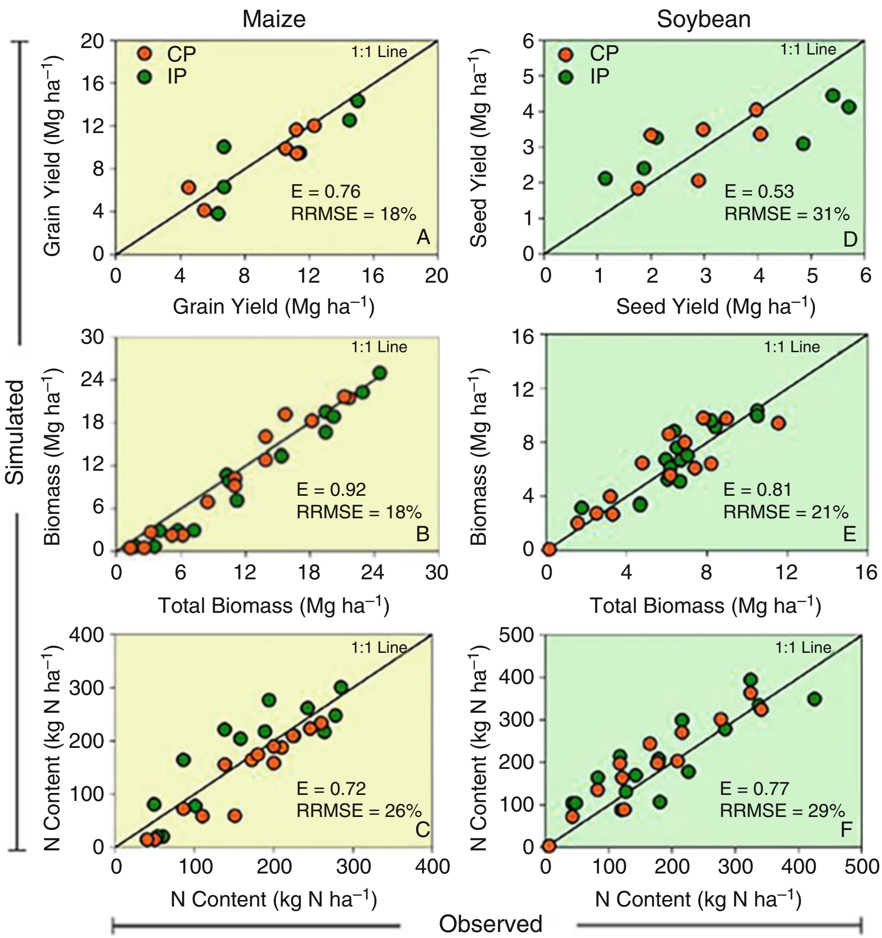

Fig. 5.3 APSIM-simulated and observed grain yield of maize and soybean (**a** and **d**), biomass (**b** and **e**) and N content (**c** and **f**) (orange circles: common practices (CP); green circles: intensified practices (IP); *E* efficiency of the model and RRMSE: relative root mean square error). (Source: Balboa et al. 2019 with permission from Elsevier)

MCMC is a reliable method. Thus, they concluded that MCMC should be incorporated into the crop modelling platforms.

CSM-CROPGRO-perennial forage model (CSM-CROGRO-PFM) was used to predict alfalfa regrowth under Canadian conditions (Jing et al. 2020). The results show that aboveground biomass was simulated with good accuracy at all sites with RMSE of 936 kg dry matter ha^{-1} and a normalized *RMSE* of 24%. Similarly, CSM-CROGRO-PFM was able to show the effect of a rise in temperature on annual herbage yield. Since the model was able to simulate alfalfa physiological processes, more model functions are required to simulate the alfalfa regrowth for the studies related to the climate change. The functions should include a decline in the plant

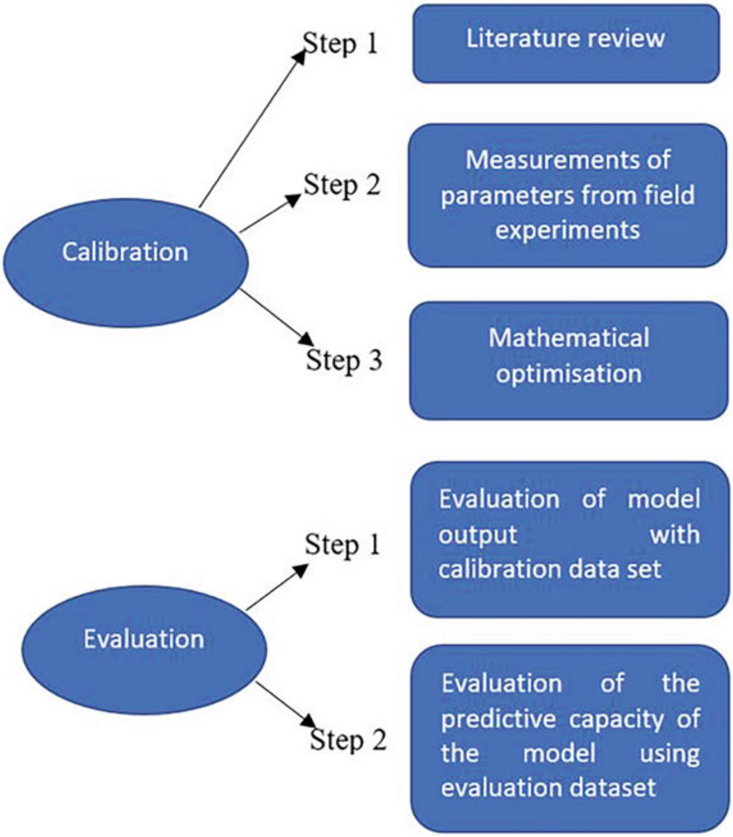

Fig. 5.4 Model calibration steps used by Falconnier et al. (2019) for calibration and evaluation of faba bean with the STICS soil/crop model

density quantification and its relationships with dry matter during post-seeding years, crowns temperature estimation during the overwintering period and nutritive quality of herbage.

Parametrisation of crop phenology is a major challenge for newly released crop varieties. This challenge becomes worse under climate warming. Ahmad et al. (2016) quantified the effect of climate warming and crop management on sugarcane using CSM-CANEGRO-sugarcane model. The calibrated model was able to simulate the impact of rising temperature on sugarcane phenology. The study concluded that adoption in planting date and the use of new cultivars with higher total GDD requirements could be good for the future. Similarly, in another study by Ahmad et al. (2019), CSM-CERES-rice and CSM-CERES-wheat models were calibrated to simulate the impact of climate warming on the rice-wheat cropping system.

The performance of CSM-CERES-rice model was evaluated to determine the impact of nitrogen application and plant densities on rice grain yield in semi-arid conditions (Ahmad et al. 2012) (Table 5.7). The simulation results showed that two seedlings per hill and 200 kg N ha^{-1} produced the highest yield (Figs. 5.5 and 5.6). CSM-CERES-rice model was evaluated by Ahmad et al. (2013) to determine the appropriate combination of plant densities (PD1 = one seedling per hill, PD2 = two seedling per hill and PD3 = three seedling per hill) and irrigation regimes ($Irri_1$ = 625 mm, $Irri_2$ = 775 mm, $Irri_3$ = 925 mm, $Irri_4$ = 1075 mm and $Irri_5$ = 1225 mm) (Table 5.7). Evaluation results showed that the model was able to accurately simulate rice growth and yield under different agronomic managements (Figs. 5.7 and 5.8). Process-based CSM-CROPGRO-canola model was calibrated using field data from different locations of Punjab Pakistan by Ahmad et al. (2017). The results show that climate warming resulted in the earlier phenological development as compared with the observed crop phenological stages. APSIM-wheat and CERES-wheat were calibrated by Ahmed et al. (2016) using manual calibration method under rainfed conditions. Calibration model was evaluated and results show that both models were able to predict the impact of climate variability on wheat crop phenology (days to flowering and maturity), leaf area, biomass and grain yield of wheat crop.

A Web-based survey about crop calibration practices was conducted by Seidel et al. (2018). About 211 responses related to the calibration procedures were used. These involve calibration of crop parameters, the method used for calibration, software for calibration, uncertainty and evaluation of calibration procedures. The results show that most calibration studies used less than ten parameters, and there was huge variability in approaches to crop model calibration. Therefore, proper guidance is needed for accurate crop model calibration. This will help to answer how to decide which parameters to estimate, how many parameters need to be estimated and how to avoid overfitting. Since in this study, actual estimation is done by using GLUE or trial and error search, the least squares approach and a Bayesian approach, thus guidelines are primarily needed to have accurate model calibration techniques with a good estimation of parameter uncertainty.

5.6 Conclusion

Model calibration and evaluation are needed to use the process-based model accurately as decision-making tool under different management options. Availability of good-quality long-term data is needed for model calibration, while observed independent data could be used for the accurate evaluation of crop models. Different statistical criteria such as coefficient of determination (R^2), index of agreement (d), root-mean-square error (RMSE), normalized objective function (NOF), root-mean-square deviation-systematic error ($RMSD_{se}$), root-mean-square deviation-non-systematic error (RMSDnse), mean absolute error (MAE), mean bias error, Nash-Sutcliffe modelling efficiency (NSME), coefficient of residual mass and ratio of RMSE to the SD (standard deviation) of measured data (RSR) are good to be used for comparison between observed and simulated values during the process of calibration and evaluation.

Table 5.7 Rice crop field experiments used for CERES-rice model calibration and evaluation

Treatments and description				
$PD_2 \times N_{100}$	02 seedlings hill^{-1} × 200 kg N ha^{-1}	C∗	02 seedlings hill^{-1} × 16 irrigations	$PD_2 \times I_5$
Nitrogen experiment (2000)		Evaluation	Irrigation experiment (2000)	
$PD_1 \times N_0$	01 seedling hill^{-1} × 0 kg N ha^{-1}		01 seedling hill^{-1} × 8 irrigations	$PD_1 \times I_1$
$PD_1 \times N_{50}$	01 seedling hill^{-1} × 50 kg N ha^{-1}		01 seedling hill^{-1} × 10 irrigations	$PD_1 \times I_2$
$PD_1 \times N_{100}$	01 seedling hill^{-1} × 100 kg N ha^{-1}		01 seedling hill^{-1} × 12 irrigations	$PD_1 \times I_3$
$PD_1 \times N_{150}$	01 seedling hill^{-1} × 150 kg N ha^{-1}		01 seedling hill^{-1} × 14 irrigations	$PD_1 \times I_4$
$PD_1 \times N_{200}$	01 seedling hill^{-1} × 200 kg N ha^{-1}		01 seedling hill^{-1} × 16 irrigations	$PD_1 \times I_5$
$PD_2 \times N_0$	02 seedlings hill^{-1} × 0 kg N ha^{-1}		02 seedling hill^{-1} × 8 irrigations	$PD_2 \times I_1$
$PD_2 \times N_{50}$	02 seedlings hill^{-1} × 50 kg N ha^{-1}		02 seedling hill^{-1} × 10 irrigations	$PD_2 \times I_2$
$PD_2 \times N_{150}$	02 seedlings hill^{-1} × 150 kg N ha^{-1}		02 seedling hill^{-1} × 12 irrigations	$PD_2 \times I_3$
$PD_2 \times N_{200}$	02 seedlings hill^{-1} × 200 kg N ha^{-1}		02 seedling hill^{-1} × 14 irrigations	$PD_2 \times I_4$
$PD_3 \times N_0$	03 seedlings hill^{-1} × 0 kg N ha^{-1}		03 seedling hill^{-1} × 8 irrigations	$PD_3 \times I_1$
$PD_3 \times N_{50}$	03 seedlings hill^{-1} × 50 kg N ha^{-1}		03 seedling hill^{-1} × 10 irrigations	$PD_3 \times I_2$
$PD_3 \times N_{100}$	03 seedlings hill^{-1} × 100 kg N ha^{-1}		03 seedling hill^{-1} × 12 irrigations	$PD_3 \times I_3$
$PD_3 \times N_{150}$	03 seedlings hill^{-1} × 150 kg N ha^{-1}		03 seedling hill^{-1} × 14 irrigations	$PD_3 \times I_4$
$PD_3 \times N_{200}$	03 seedlings hill^{-1} × 200 kg N ha^{-1}		03 seedling hill^{-1} × 16 irrigations	$PD_3 \times I_5$

(continued)

Table 5.7 (continued)

Treatments and description				
$PD_2 \times N_{100}$	02 seedlings hill^{-1} × 200 kg N ha^{-1}	C∗	02 seedlings hill^{-1} × 16 irrigations	$PD_2 \times I_5$
Nitrogen experiment (2001)		Evaluation (independent data set)	Irrigation experiment (2001)	
$PD_1 \times N_0$	01 seedling hill^{-1} × 0 kg N ha^{-1}		01 seedling hill^{-1} × 8 irrigations	$PD_1 \times I_1$
$PD_1 \times N_{50}$	01 seedling hill^{-1} × 50 kg N ha^{-1}		01 seedling hill^{-1} × 10 irrigations	$PD_1 \times I_2$
$PD_1 \times N_{100}$	01 seedling hill^{-1} × 100 kg N ha^{-1}		01 seedling hill^{-1} × 12 irrigations	$PD_1 \times I_3$
$PD_1 \times N_{150}$	01 seedling hill^{-1} × 150 kg N ha^{-1}		01 seedling hill^{-1} × 14 irrigations	$PD_1 \times I_4$
$PD_1 \times N_{200}$	01 seedling hill^{-1} × 200 kg N ha^{-1}		01 seedling hill^{-1} × 16 irrigations	$PD_1 \times I_5$
$PD_2 \times N_0$	02 seedlings hill^{-1} × 0 kg N ha^{-1}		02 seedling hill^{-1} × 8 irrigations	$PD_2 \times I_1$
$PD_2 \times N_{50}$	02 seedlings hill^{-1} × 50 kg N ha^{-1}		02 seedling hill^{-1} × 10 irrigations	$PD_2 \times I_2$
$PD_2 \times N_{100}$	02 seedlings hill^{-1} × 100 kg N ha^{-1}		02 seedling hill^{-1} × 12 irrigations	$PD_2 \times I_3$
$PD_2 \times N_{150}$	02 seedlings hill^{-1} × 150 kg N ha^{-1}		02 seedling hill^{-1} × 14 irrigations	$PD_2 \times I_3$
$PD_2 \times N_{200}$	02 seedlings hill^{-1} × 200 kg N ha^{-1}		02 seedling hill^{-1} × 16 irrigations	$PD_2 \times I_5$
$PD_3 \times N_0$	03 seedlings hill^{-1} × 0 kg N ha^{-1}		03 seedling hill^{-1} × 8 irrigations	$PD_3 \times I_1$
$PD_3 \times N_{50}$	03 seedlings hill^{-1} × 50 kg N ha^{-1}		03 seedling hill^{-1} × 10 irrigations	$PD_3 \times I_2$
$PD_3 \times N_{100}$	03 seedlings hill^{-1} × 100 kg N ha^{-1}		03 seedling hill^{-1} × 12 irrigations	$PD_3 \times I_3$
$PD_3 \times N_{150}$	03 seedlings hill^{-1} × 150 kg N ha^{-1}		03 seedling hill^{-1} × 14 irrigations	$PD_3 \times I_4$
$PD_3 \times N_{200}$	03 seedlings hill^{-1} × 200 kg N ha^{-1}		03 seedling hill^{-1} × 16 irrigations	$PD_3 \times I_5$

Modified and adopted; Ahmad et al. (2012, 2013)
C∗ = $PD_2 \times N_{100}$ and $PD_2 \times I_5$ C = calibrated treatments for nitrogen and irrigation experiments, respectively

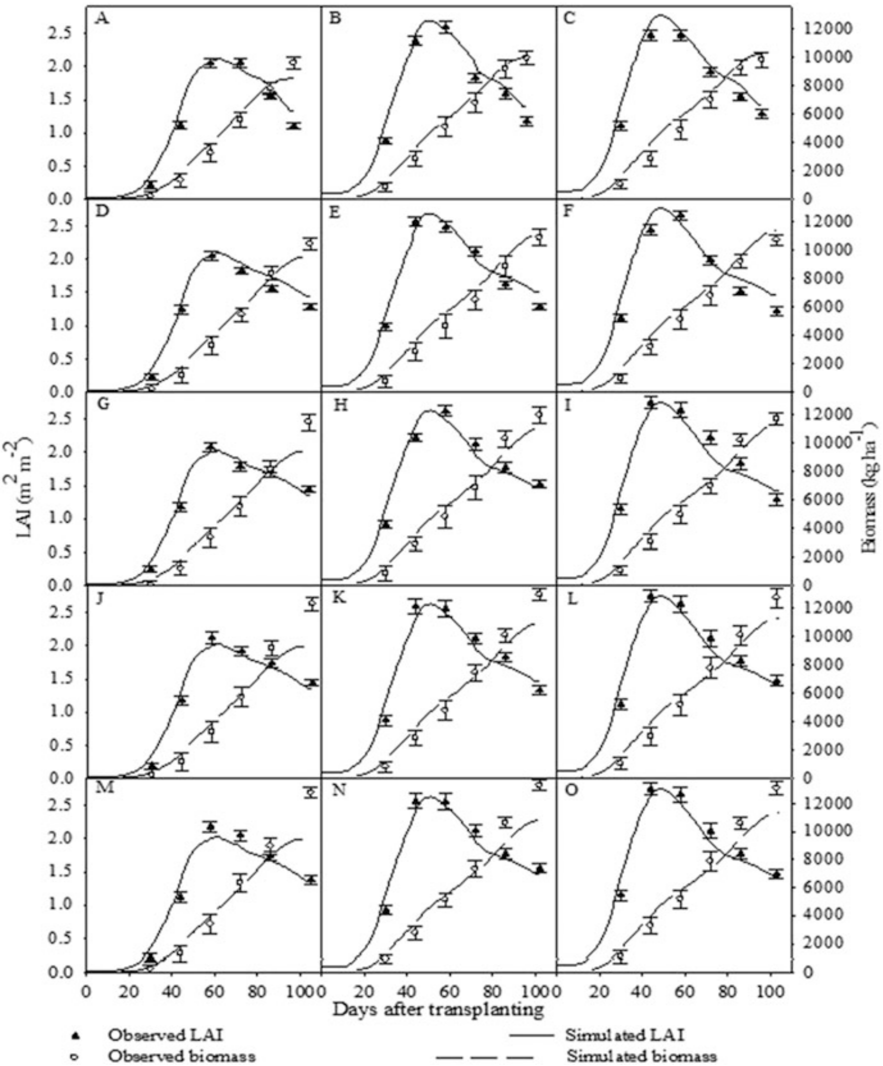

Fig. 5.5 Simulated (continuous line) and observed (triangular symbols) leaf area index and simulated (dotted lines) and observed (round symbols) biomass of rice Basmati-385 at variable plant density and nitrogen application rates under irrigated semi-arid conditions at Faisalabad, Pakistan, during 2000, used for model calibration (N) and all others treatments for model evaluation. (Adopted from Ahmad et al. 2012)

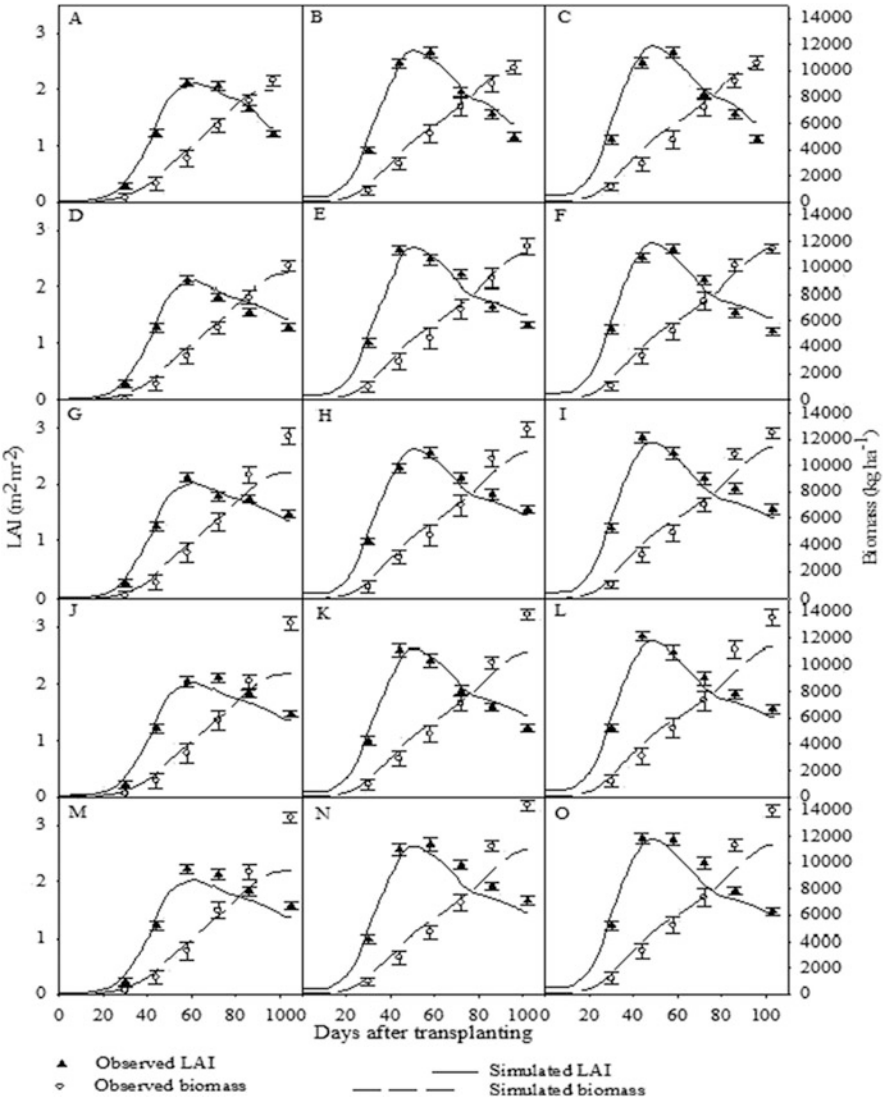

Fig. 5.6 Simulated (continuous line) and observed (triangular symbols) leaf area index and simulated (dotted lines) and observed (round symbols) biomass of rice Basmati-385 at variable plant density and nitrogen application rates under irrigated semiarid conditions at Faisalabad, Pakistan, during 2001 used for model evaluation. (Adopted from Ahmad et al. 2012)

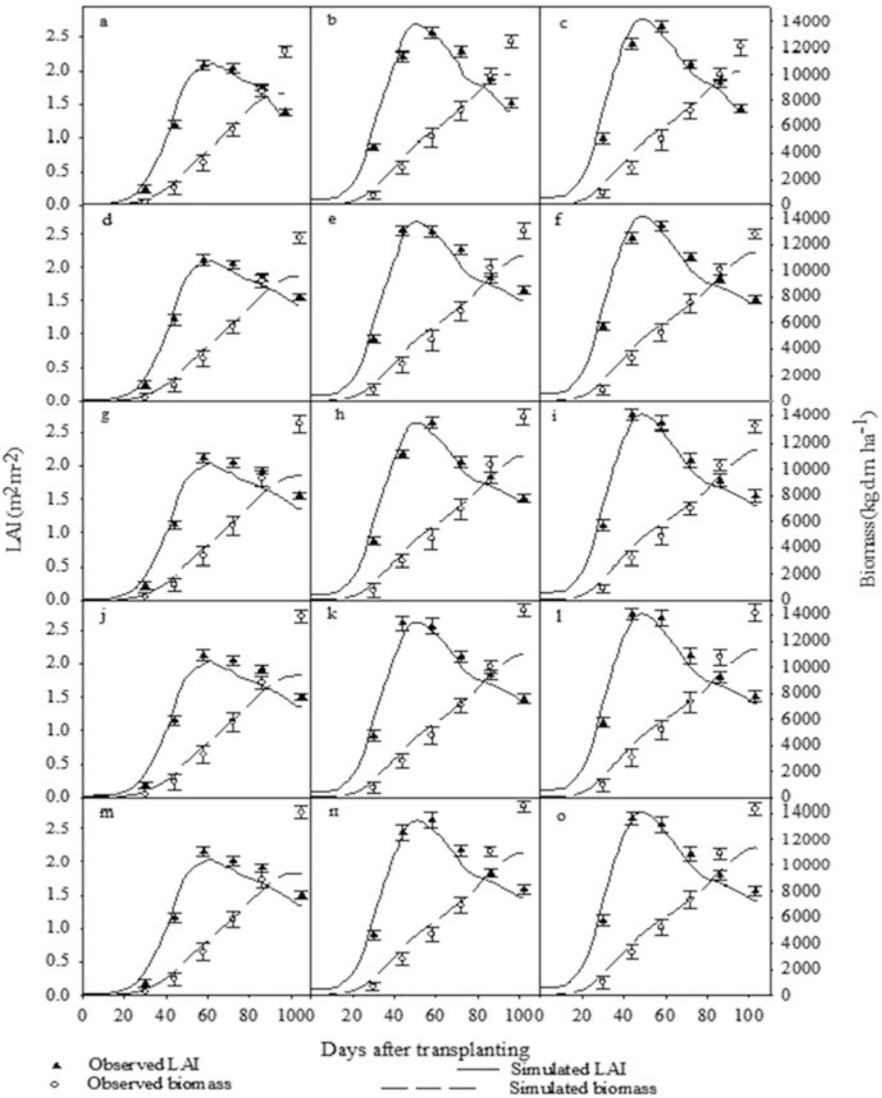

Fig. 5.7 Simulated (continuous line) and observed (triangular symbols) leaf area index and simulated (dotted lines) and observed (round symbols) biomass of rice Basmati-385 at variable plant density and irrigation levels (n part; calibrated treatment) and all other treatments used for model evaluation during 2000 under irrigated semi-arid conditions at Faisalabad, Pakistan. (Adopted from Ahmad et al. 2013)

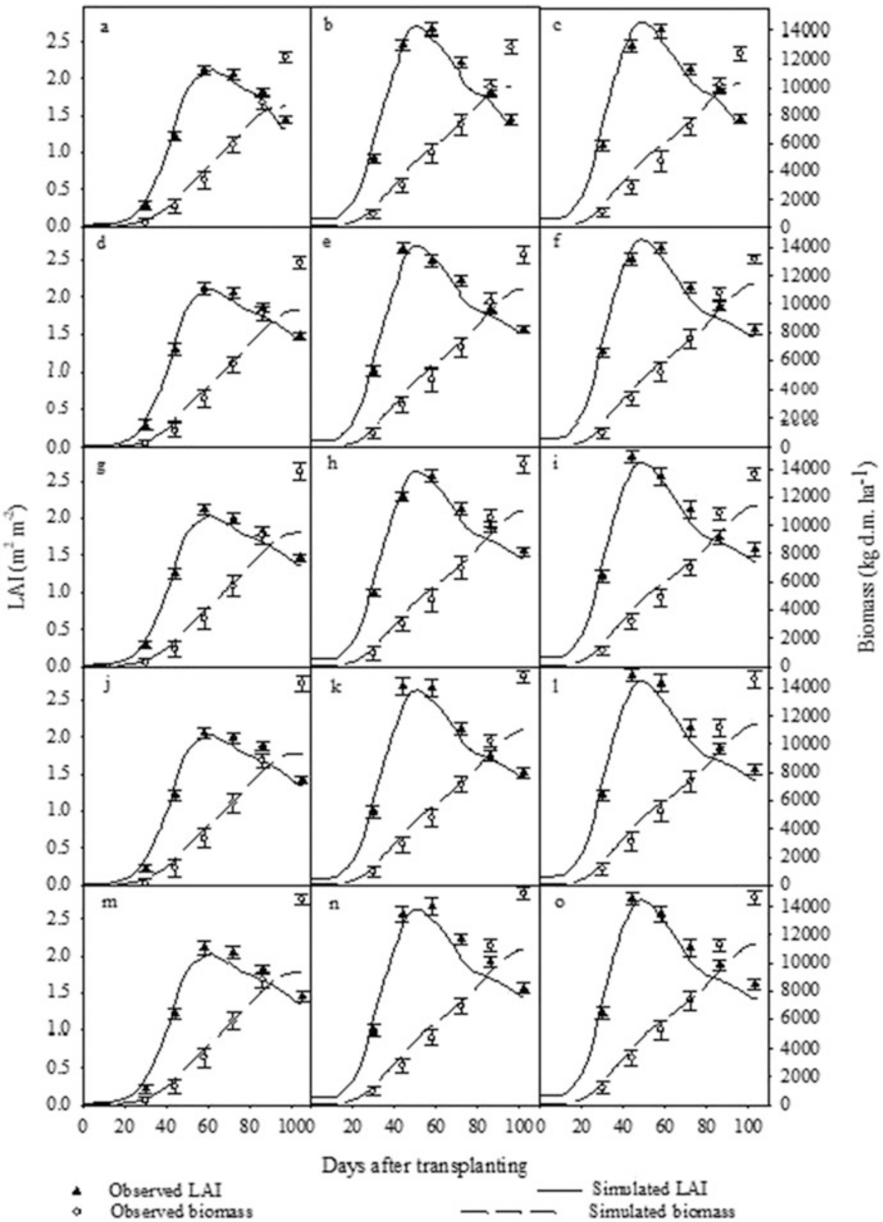

Fig. 5.8 Simulated (continuous line) and observed (triangular symbols) leaf area index and simulated (dotted lines) and observed (round symbols) biomass of rice Basmati-385 at variable plant density and irrigation levels during 2001 under irrigated semi-arid conditions at Faisalabad, Pakistan, used for model evaluations. (Adopted from Ahmad et al. 2013)

References

Ahmad S, Ahmad A, Soler CMT, Ali H, Zia-Ul-Haq M, Anothai J, Hussain A, Hoogenboom G, Hasanuzzaman M (2012) Application of the CSM-CERES-Rice model for evaluation of plant density and nitrogen management of fine transplanted rice for an irrigated semiarid environment. Precis Agric 13(2):200–218. https://doi.org/10.1007/s11119-011-9238-1

Ahmad S, Ahmad A, Ali H, Hussain A, Garcia y Garcia A, Khan MA, Zia-Ul-Haq M, Hasanuzzaman M, Hoogenboom G (2013) Application of the CSM-CERES-Rice model for evaluation of plant density and irrigation management of transplanted rice for an irrigated semiarid environment. Irrig Sci 31(3):491–506. https://doi.org/10.1007/s00271-012-0324-6

Ahmad S, Nadeem M, Abbas G, Fatima Z, Zeb Khan RJ, Ahmed M, Ahmad A, Rasul G, Azam Khan M (2016) Quantification of the effects of climate warming and crop management on sugarcane phenology. Clim Res 71(1):47–61

Ahmad S, Abbas G, Fatima Z, Khan RJ, Anjum MA, Ahmed M, Khan MA, Porter CH, Hoogenboom G (2017) Quantification of the impacts of climate warming and crop management on canola phenology in Punjab, Pakistan. J Agron Crop Sci 203(5):442–452. https://doi.org/10.1111/jac.12206

Ahmad S, Abbas G, Ahmed M, Fatima Z, Anjum MA, Rasul G, Khan MA, Hoogenboom G (2019) Climate warming and management impact on the change of phenology of the rice-wheat cropping system in Punjab, Pakistan. Field Crop Res 230:46–61. https://doi.org/10.1016/j.fcr.2018.10.008

Ahmed M (2020) Introduction to modern climate change. Andrew E. Dessler: Cambridge University Press, 2011, 252 pp, ISBN-10: 0521173159. Sci Total Environ 734:139397. https://doi.org/10.1016/j.scitotenv.2020.139397

Ahmed M, Aslam MA, Hassan FU, Asif M, Hayat R (2014) Use of APSIM to model nitrogen use efficiency of rain-fed wheat. Int J Agric Biol 16:461–470

Ahmed M, Akram MN, Asim M, Aslam M, F-u H, Higgins S, Stöckle CO, Hoogenboom G (2016) Calibration and validation of APSIM-wheat and CERES-wheat for spring wheat under rainfed conditions: models evaluation and application. Comput Electron Agric 123:384–401. https://doi.org/10.1016/j.compag.2016.03.015

Ahmed M, Stöckle CO, Nelson R, Higgins S (2017) Assessment of climate change and atmospheric CO_2 impact on winter wheat in the Pacific Northwest using a multimodel ensemble. Front Ecol Evol 5(51). https://doi.org/10.3389/fevo.2017.00051

Ahmed M, Ijaz W, Ahmad S (2018) Adapting and evaluating APSIM-SoilP-wheat model for response to phosphorus under rainfed conditions of Pakistan. J Plant Nutr 41(16):2069–2084. https://doi.org/10.1080/01904167.2018.1485933

Ahmed M, Stöckle CO, Nelson R, Higgins S, Ahmad S, Raza MA (2019) Novel multimodel ensemble approach to evaluate the sole effect of elevated CO2 on winter wheat productivity. Sci Rep 9(1):7813. https://doi.org/10.1038/s41598-019-44251-x

Anothai J, Patanothai A, Jogloy S, Pannangpetch K, Boote KJ, Hoogenboom G (2008) A sequential approach for determining the cultivar coefficients of peanut lines using end-of-season data of crop performance trials. Field Crop Res 108(2):169–178. https://doi.org/10.1016/j.fcr.2008.04.012

Balboa GR, Archontoulis SV, Salvagiotti F, Garcia FO, Stewart WM, Francisco E, Prasad PVV, Ciampitti IA (2019) A systems-level yield gap assessment of maize-soybean rotation under high- and low-management inputs in the Western US Corn Belt using APSIM. Agric Syst 174:145–154. https://doi.org/10.1016/j.agsy.2019.04.008

Bao Y, Hoogenboom G, McClendon R, Vellidis G (2017) A comparison of the performance of the CSM-CERES-maize and EPIC models using maize variety trial data. Agric Syst 150:109–119. https://doi.org/10.1016/j.agsy.2016.10.006

Beven K, Binley A (1992) The future of distributed models: model calibration and uncertainty prediction. Hydrol Process 6(3):279–298. https://doi.org/10.1002/hyp.3360060305

Beven KJ, Smith PJ, Freer JE (2008) So just why would a modeller choose to be incoherent? J Hydrol 354(1):15–32. https://doi.org/10.1016/j.jhydrol.2008.02.007

Boote KJ, Jones JW, Batchelor WD, Nafziger ED, Myers O (2003) Genetic coefficients in the CROPGRO–soybean model: links to field performance and genomics. Agron J 95(1):32–51. https://doi.org/10.2134/agronj2003.3200

Buddhaboon C, Jintrawet A, Hoogenboom G (2018) Methodology to estimate rice genetic coefficients for the CSM-CERES-rice model using GENCALC and GLUE genetic coefficient estimators. J Agric Sci 156(4):482–492. https://doi.org/10.1017/S0021859618000527

Dumont B, Leemans V, Mansouri M, Bodson B, Destain JP, Destain MF (2014) Parameter identification of the STICS crop model, using an accelerated formal MCMC approach. Environ Model Softw 52:121–135. https://doi.org/10.1016/j.envsoft.2013.10.022

Falconnier GN, Journet E-P, Bedoussac L, Vermue A, Chlébowski F, Beaudoin N, Justes E (2019) Calibration and evaluation of the STICS soil-crop model for faba bean to explain variability in yield and N2 fixation. Eur J Agron 104:63–77. https://doi.org/10.1016/j.eja.2019.01.001

Gao Y, Wallach D, Liu B, Dingkuhn M, Boote KJ, Singh U, Asseng S, Kahveci T, He J, Zhang R, Confalonieri R, Hoogenboom G (2020) Comparison of three calibration methods for modeling rice phenology. Agric For Meteorol 280:107785. https://doi.org/10.1016/j.agrformet.2019.107785

Gasparini M (1997) Markov chain Monte Carlo in practice. Technometrics 39(3):338–338. https://doi.org/10.1080/00401706.1997.10485132

Gilks WR, Richardson S, Spiegelhalter D (1995) Markov chain Monte Carlo in practice. Chapman and Hall/CRC

Guerra LC, Hoogenboom G, Garcia y Garcia A, Banterng P, Beasley JP (2008) Determination of cultivar coefficients for the CSM-CROPGRO-peanut model using variety trial data. Trans ASABE 51(4):1471–1481. https://doi.org/10.13031/2013.25227

He D, Wang E, Wang J, Robertson MJ (2017) Data requirement for effective calibration of process-based crop models. Agric For Meteorol 234-235:136–148. https://doi.org/10.1016/j.agrformet.2016.12.015

Hoogenboom G, Jones JW, Wilkens PW, Porter CH, Batchelor WD, Hunt LA, Boote KJ, Singh U, Uryasev O, Bowen WT, Gijsman AJ, du Toit AS, White JW, Tsuji GY (2004) Decision support system for Agrotechnology transfer version 4.0 [CD-ROM]. University of Hawaii, Honolulu, HI

Hunt LA, Boote KJ (1998) Data for model operation, calibration, and evaluation. In: Tsuji G, Hoogenboom G, Thornton P (eds) Understanding options for agricultural production, vol 7. Systems approaches for sustainable agricultural development. Springer, Dordrecht, pp 9–39. https://doi.org/10.1007/978-94-017-3624-4_2

Jin X, Xu C-Y, Zhang Q, Singh VP (2010) Parameter and modeling uncertainty simulated by GLUE and a formal Bayesian method for a conceptual hydrological model. J Hydrol 383 (3):147–155. https://doi.org/10.1016/j.jhydrol.2009.12.028

Jing Q, Qian B, Bélanger G, VanderZaag A, Jégo G, Smith W, Grant B, Shang J, Liu J, He W, Boote K, Hoogenboom G (2020) Simulating alfalfa regrowth and biomass in eastern Canada using the CSM-CROPGRO-perennial forage model. Eur J Agron 113:125971. https://doi.org/10.1016/j.eja.2019.125971

Jones MR, Singels A (2018) Refining the Canegro model for improved simulation of climate change impacts on sugarcane. Eur J Agron 100:76–86. https://doi.org/10.1016/j.eja.2017.12.009

Leandro J, Gander A, Beg MNA, Bhola P, Konnerth I, Willems W, Carvalho R, Disse M (2019) Forecasting upper and lower uncertainty bands of river flood discharges with high predictive skill. J Hydrol 576:749–763. https://doi.org/10.1016/j.jhydrol.2019.06.052

Li ZT, Yang JY, Drury CF, Hoogenboom G (2015) Evaluation of the DSSAT-CSM for simulating yield and soil organic C and N of a long-term maize and wheat rotation experiment in the Loess Plateau of Northwestern China. Agric Syst 135:90–104. https://doi.org/10.1016/j.agsy.2014.12.006

Lobell DB (2013) Errors in climate datasets and their effects on statistical crop models. Agric For Meteorol 170(0):58–66. https://doi.org/10.1016/j.agrformet.2012.05.013

Lobell DB, Asseng S (2017) Comparing estimates of climate change impacts from process-based and statistical crop models. Environ Res Lett 12(1):015001. https://doi.org/10.1088/1748-9326/aa518a

Mavromatis T, Boote KJ, Jones JW, Irmak A, Shinde D, Hoogenboom G (2001) Developing genetic coefficients for crop simulation models with data from crop performance trials Florida Agric. Exp. Stn., J. Series No R-07163. Crop Sci 41(1):40–51. https://doi.org/10.2135/cropsci2001.41140x

Mavromatis T, Boote KJ, Jones JW, Wilkerson GG, Hoogenboom G (2002) Repeatability of model genetic coefficients derived from soybean performance trials across different states Florida Agricultural Experiment Station, Journal Series No. R-07981. Crop Sci 42(1):76–89. https://doi.org/10.2135/cropsci2002.7600

Mehrabi F, Sepaskhah AR (2019) Winter wheat yield and DSSAT model evaluation in a diverse semi-arid climate and agronomic practices. Int J Plant Prod. https://doi.org/10.1007/s42106-019-00080-6

Monteith JL (1965) Light distribution and photosynthesis in field crops. Ann Bot 29(1):17–37. https://doi.org/10.1093/oxfordjournals.aob.a083934

Rankinen K, Karvonen T, Butterfield D (2006) An application of the GLUE methodology for estimating the parameters of the INCA-N model. Sci Total Environ 365(1):123–139. https://doi.org/10.1016/j.scitotenv.2006.02.034

Ritchie J, Godwin D, Otter-Nacke S (1985) CERES-wheat: a user-oriented wheat yield model. Preliminary documentation. AGRISTARS Publication No. YM-U3-04442-JSC-18892

Seidel SJ, Palosuo T, Thorburn P, Wallach D (2018) Towards improved calibration of crop models – where are we now and where should we go? Eur J Agron 94:25–35. https://doi.org/10.1016/j.eja.2018.01.006

Sexton J, Everingham Y, Inman-Bamber G (2016) A theoretical and real world evaluation of two Bayesian techniques for the calibration of variety parameters in a sugarcane crop model. Environ Model Softw 83:126–142. https://doi.org/10.1016/j.envsoft.2016.05.014

Sheng M, Liu J, Zhu AX, Rossiter DG, Liu H, Liu Z, Zhu L (2019) Comparison of GLUE and DREAM for the estimation of cultivar parameters in the APSIM-maize model. Agric For Meteorol 278:107659. https://doi.org/10.1016/j.agrformet.2019.107659

Singels A, Bezuidenhout CN (2002) A new method of simulating dry matter partitioning in the Canegro sugarcane model. Field Crop Res 78(2):151–164. https://doi.org/10.1016/S0378-4290(02)00118-1

Suriharn B, Patanothai A, Pannangpetch K, Jogloy S, Hoogenboom G (2007) Determination of cultivar coefficients of peanut lines for breeding applications of the CSM-CROPGRO-peanut model. Crop Sci 47(2):607–619. https://doi.org/10.2135/cropsci2006.01.0050

Suriharn B, Patanothai A, Pannangpetch K, Jogloy S, Hoogenboom G (2008) Yield performance and stability evaluation of peanut breeding lines with the CSM-CROPGRO-peanut model. Crop Sci 48(4):1365–1372. https://doi.org/10.2135/cropsci2007.09.0523

Tan J, Cao J, Cui Y, Duan Q, Gong W (2019) Comparison of the generalized likelihood uncertainty estimation and Markov chain Monte Carlo methods for uncertainty analysis of the ORYZA_V3 model. Agron J 111(2):555–564. https://doi.org/10.2134/agronj2018.05.0336

Wallach D (2011) Crop model calibration: a statistical perspective. Agron J 103(4):1144–1151. https://doi.org/10.2134/agronj2010.0432

Wallach D, Hwang C, Correll MJ, Jones JW, Boote K, Hoogenboom G, Gezan S, Bhakta M, Vallejos CE (2018) A dynamic model with QTL covariables for predicting flowering time of common bean (Phaseolus vulgaris) genotypes. Eur J Agron 101:200–209. https://doi.org/10.1016/j.eja.2018.10.003

Wallach D, Palosuo T, Thorburn P, Seidel SJ, Gourdain E, Asseng S, Basso B, Buis S, Crout NMJ, Dibari C, Dumont B, Ferrise R, Gaiser T, Garcia C, Gayler S, Ghahramani A, Hochman Z, Hoek S, Horan H, Hoogenboom G, Huang M, Jabloun M, Jing Q, Justes E, Kersebaum KC, Klosterhalfen A, Launay M, Luo Q, Maestrini B, Mielenz H, Moriondo M, Nariman Zadeh H, Olesen JE, Poyda A, Priesack E, Pullens JWM, Qian B, Schütze N, Shelia V, Souissi A, Specka X, Srivastava AK, Stella T, Streck T, Trombi G, Wallor E, Wang J, Weber TKD, Weihermüller L, de Wit A, Wöhling T, Xiao L, Zhao C, Zhu Y (2019) How well do crop models predict phenology, with emphasis on the effect of calibration? bioRxiv:708578. https://doi.org/10.1101/708578

White JW, Hoogenboom G (2003) Gene-based approaches to crop simulation. Agron J 95 (1):52–64. https://doi.org/10.2134/agronj2003.5200

Whitehead PG, Jin L, Macadam I, Janes T, Sarkar S, Rodda HJE, Sinha R, Nicholls RJ (2018) Modelling impacts of climate change and socio-economic change on the Ganga, Brahmaputra, Meghna, Hooghly and Mahanadi river systems in India and Bangladesh. Sci Total Environ 636:1362–1372. https://doi.org/10.1016/j.scitotenv.2018.04.362

Yang J, Drury C, Yang J, Li Z, Hoogenboom G (2014) EasyGrapher: software for data visualization and statistical evaluation of DSSAT cropping system model and the CANB model. Int J Comp Theory Eng 6(3):210

Zhao C, Liu B, Xiao L, Hoogenboom G, Boote KJ, Kassie BT, Pavan W, Shelia V, Kim KS, Hernandez-Ochoa IM, Wallach D, Porter CH, Stockle CO, Zhu Y, Asseng S (2019) A SIMPLE crop model. Eur J Agron 104:97–106. https://doi.org/10.1016/j.eja.2019.01.009

Wheat Crop Modelling for Higher Production

6

Ahmed Mohammed Saad Kheir, Zheli Ding,
Marwa Gamal Mohamed Ali, Til Feike, Aly Ismail Nagib Abdelaal,
and Abdelrazek Elnashar

Abstract

Due to quick growth of population, climate change and diminished natural resources, food security and nutrition issues face major challenges. Crop models successfully proved crop yield simulation under diverse environments, biotic constraints, gene factors and climate change impacts and adaptation. But, the accuracy of crop models for yield estimates needs to be improved with other limitation factors affecting yield growth and production to ensure global food security. These factors include short-term severe stresses (i.e. cold and heat), pest and diseases, soil dynamic changes due to climate changes, soil nutrient balance, grain quality (i.e. protein, iron and zinc) as well as the potential integration between genotype and phenotype in crop models. Here, we outlined the potential

A. M. S. Kheir (✉)
Haikou Experimental Station, Chinese Academy of Tropical Agricultural Sciences (CATAS), Haikou, China

Agricultural Research Center, Soils, Water and Environment Research Institute, Giza, Egypt

Z. Ding
Haikou Experimental Station, Chinese Academy of Tropical Agricultural Sciences (CATAS), Haikou, China

M. G. M. Ali · A. I. N. Abdelaal
Agricultural Research Center, Soils, Water and Environment Research Institute, Giza, Egypt

T. Feike
Institute for Strategies and Technology Assessment, Julius Kühn-Institut (JKI), Federal Research Centre for Cultivated Plants, Kleinmachnow, Germany

A. Elnashar
State Key Laboratory of Remote Sensing Science, Aerospace Information Research Institute, Chinese Academy of Sciences, Beijing, China

Department of Natural Resources, Faculty of African Postgraduate Studies, Cairo University, Giza, Egypt

M. Ahmed (ed.), *Systems Modeling*, https://doi.org/10.1007/978-981-15-4728-7_6

and limitation of wheat crop models to assist breeders, researchers, agronomists and decision-makers to address the current and future challenges linked with global food security.

Keywords

Wheat production and consumption · Food security · Nutrition · Wheat models · Climate change · Impacts · Adaptation

6.1 Introduction

The global population is growing vastly, causing challenges to agricultural practices to ensure food security (Godfray et al. 2010) and to minimize the projected malnutrition (Godfray et al. 2011). The major calorific intake for human society is mainly derived from the botanical family of grasses (i.e. wheat, rice, maize, barley, sorghum, millet and pasture grasses). The maximum production of these crops requires balance of interactions between the environment, genotype and crop management practices (Chenu et al. 2017). In this connection, these factors influence the efficiencies of captured nutrients, water and solar radiation by crop for calories and nutritional value production. The simple mathematical formulations were initiated and used as models into computers for crop processes during the mid-1960s (de Wit 1995). Following that, many developments in crop models were achieved and arose for wheat crop such as ARC-Wheat (Porter 1984), CERES-Wheat (Ritchie et al. 1985) as well as developed photosynthesis models still used today (Farquhar et al. 1980). Crop modelling is a powerful tool representing the quantitative knowledge of interaction between crop development and the environment through mathematical algorithms (Asseng et al. 2019; Ahmed and Stockle 2016; Asseng et al. 2014; Ahmed 2012; Ahmed et al. 2011, 2013, 2014, 2016, 2017, 2018, 2019; Ahmad et al. 2017, 2019). Crop models could simulate crop production dynamically based on the fundamentals of soil science, agrometeorology and crop physiology (Loomis et al. 1979). The minimum data required for simulating crop development, biomass, water and nutrient use include crop management and cultivar characteristics, soil properties, initial soil conditions, rainfall, daily maximum and minimum temperature as well as daily solar radiation. Climate change impacts were incorporated with crop models during the 1990s, to explore the projected effects of carbon dioxide concentration (CO_2) (Rosenzweig and Parry 1994). At the same time, merging models to crop modelling platforms were initiated and developed. The crop modelling platforms could ensure combining models of many crops with a specific software, facilitating model testing and applications for various purposes (Jones et al. 2003). Crop modelling platforms include but not limited to Agricultural Production Systems Simulator (APSIM) (Keating et al. 2003), Environmental Policy Integrated Climate (EPIC) (Kiniry et al. 1995), Decision Support System for Agrotechnology Transfer (DSSAT) (Jones et al. 2003), CropSyst (Stockle et al. 2003a), Wageningen crop models and Simulator mulTIdisciplinary pour les Cultures Standards (STICS) (Brisson et al. 1998). Over the last

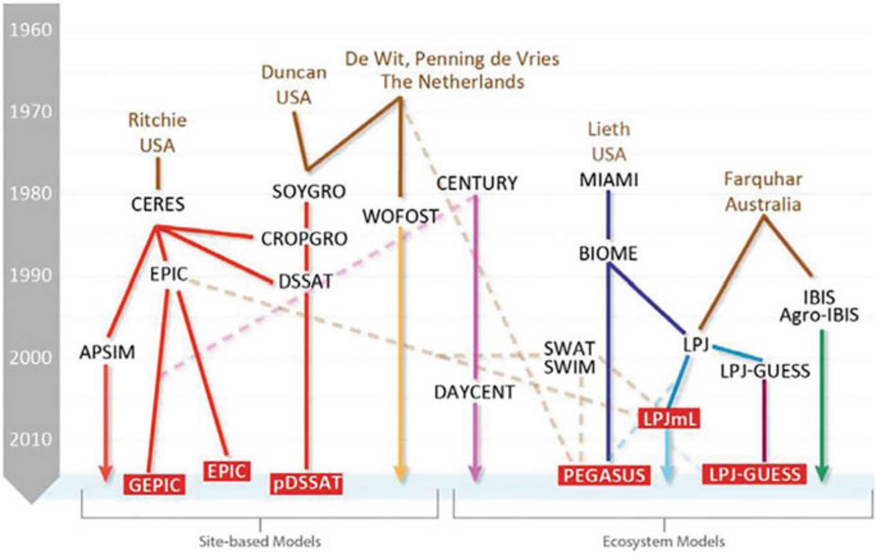

Fig. 6.1 Integration between single crop models and crop modelling platforms including wheat models (Rosenzweig et al. 2014b)

decade, new approaches have been added to both single model and crop modelling platforms creating a consolidated integration between them (Fig. 6.1). The most currently used models for wheat in research and applications are listed in Table 6.1. These models depict in a wide range of details for both plant leaf interception with solar radiation and dynamic action between roots and water and nutrient uptake. In general, crop models could simulate crop growth and development as outputs using different types of inputs such as climatic data, soil characteristics and management practices based on genetic parameters of cultivars and specific equations. Meanwhile, the modern wheat models are developed in complexity and could simulate crop development daily, predicting grain yield at the final step (Chenu et al. 2017).

Therefore, crop models are considered powerful tools to predict crop growth, development and yield by integrating the crop processes with their response to external and internal factors (Jabeen et al. 2017). Furthermore, they allow facilitating the result extrapolation from a small number of experiments to large-scale conditions. Consequently, crop models are valuable tools to explore the effect of external cues (i.e. management and weather) and internal factors (i.e. gene and traits) on crop development and yield. Despite such development in crop models, new challenges have been found and need to be tackled including (1) developing models with climate extreme impacts (i.e. higher temperature, drought, frost, CO_2 and O_3), (2) simulating many complex interactions of climate, (3) including aspects of grain yield quality and nutrition (i.e. protein, Fe and Zn), (4) incorporating environmental aspects (e.g. pesticides and nitrate leaching) and soil restrictions (e.g. salinity, sodicity, acidity and excess water), (5) incorporating biotic factors (e.g. pest and

Table 6.1 The current available wheat crop models

Model (version)	Reference	Documentation
AFRCWHEAT2	Porter (1993)	Send to jrp@plen.ku.dk
APSIM-E	Wang et al. (2002), Keating et al. (2003)	http://www.apsim.info
APSIM-Nwheat (V.1.55)	Asseng et al. (1998), Keating et al. (2003), Asseng et al. (2004)	http://www.apsim.info
APSIM-Wheat (V.7.4)	Keating et al. (2003)	http://www.apsim.info
AquaCrop (V.4.0)	Steduto et al. (2009), Vanuytrecht et al. (2014)	http://www.fao.org/nr/water/aquacrop.html
CropSyst (V.3.04.08)	Stockle et al. (2003b)	http://modeling.bsyse.wsu.edu/CS_Suit_4/CropSyst/index.html
DAISY (V.5.19)	Hansen et al. (1991), Hansen et al. (2012)	https://code.google.com/p/daisy-model/
DSSAT-CERES (V.4.0.1.0)	Ritchie et al. (1985), Hoogenboom and White (2003), Jones et al. (2003)	http://www.dssat.net
DSSAT-CROPSIM (V4.5.1.013)	Hunt and Pararajasingham (1995), Jones et al. (2003)	http://www.dssat.net
DSSAT-Nwheat (V4.7.1)	Holzworth et al. (2014), Kassie et al. (2016)	http://www.dssat.net
EPIC-Wheat (V1102)	Williams et al. (1989), Kiniry et al. (1995)	http://epicapex.brc.tamus.edu/
Expert-N (V3.0.10)-CERES (V2.0)	Ritchie et al. (1987), Stenger et al. (1999), Biernath et al. (2011)	http://www.helmholtz-muenchen.de/en/iboe/expertn/
Expert-N (V3.0.10)-GECROS (V1.0)	Stenger et al. (1999), Biernath et al. (2011)	http://www.helmholtz-muenchen.de/en/iboe/expertn/
Expert-N (V3.0.10)-SPASS (2.0)	Stenger et al. (1999), Biernath et al. (2011)	http://www.helmholtz-muenchen.de/en/iboe/expertn/
Expert-N (V3.0.10)-SUCROS (V2)	Stenger et al. (1999), Biernath et al. (2011)	http://www.helmholtz-muenchen.de/en/iboe/expertn/
FASSET (V.2.0)	Olesen et al. (2002), Berntsen et al. (2003)	http://www.fasset.dk
GLAM (V.2)	Challinor et al. (2004), Li et al. (2010)	http://www.see.leeds.ac.uk/research/icas/climate-impacts-group/research/glam
HERMES (V.4.26)	Kersebaum (2007, 2011)	http://www.zalf.de/en/forschung/institute/lsa/forschung/oekomod/hermes
INFOCROP (V.1)	Aggarwal et al. (2006)	http://www.iari.res.in
LINTUL4 (V.6)	Spitters and Schapendonk (1990), Shibu et al. (2010)	http://models.pps.wur.nl/models
LINTUL5 (V.5)	Spitters and Schapendonk (1990), Shibu et al. (2010)	http://models.pps.wur.nl/models

(continued)

Table 6.1 (continued)

Model (version)	Reference	Documentation
LOBELL	Gourdji et al. (2013)	dlobell@stanford.edu
LPJmL (V3.2)	Gerten et al. (2004), Beringer et al. (2011)	http://www.pik-potsdam.de/research/projects/lpjweb
MCWLA-Wheat (V.2.0)	Tao et al. (2009), Tao and Zhang (2013)	taofl@igsnrr.ac.cn
MONICA (V.1.0)	Nendel et al. (2011)	http://monica.agrosystem-models.com
OLEARY (V.7)	O'Leary et al. (1985), Latta and O'Leary (2003)	gjoleary@yahoo.com
SALUS (V.1.0)	Senthilkumar et al. (2009), Basso et al. (2010)	http://salusmodel.glg.msu.edu
SIMPLACE (V.1)	Angulo et al. (2013)	Frank.ewert@uni-bonn.de
SIRIUS (V2010)	Semenov and Shewry (2011)	http://www.rothamsted.ac.uk/mas-models/sirius.php
SiriusQuality (V.2.0)	He et al. (2010)	http://www1.clermont.inra.fr/siriusquality/
SSM-Wheat	Soltani et al. (2013)	Macro.bindi@unifi.it
STICS (V.1.1)	Brisson et al. (2003)	http://www.avignon.inra.fr/agroclim_stics_eng/
WHEATGROW	Pan et al. (2007)	yanzhu@njau.edu.cn
WOFOST (V.7.1)	Boogaard and Kroes (1998)	http://www.wofost.wur.nl

Source: Modified after Guarin and Asseng (2017)

diseases) and (6) linking genetics and molecular science to crop models (Aslam et al. 2017b). These challenges could be tackled through incorporating these processes into crop models using detailed field experiments with high-quality data over time. This chapter outlines crop model evaluation using global field experiments and extrapolation. In addition, it outlines the potential and limitations and adaptation of current wheat models for higher production.

6.2 Crop Model Extrapolation

One of the most advantages of crop models is their ability to extrapolate data from minimum experimental data. The input methodology and model design are considered the main factors for crop model simulations leading to different spatial and time outputs. Therefore, it is necessary to investigate the projected interactions between modelling the environment and crop.

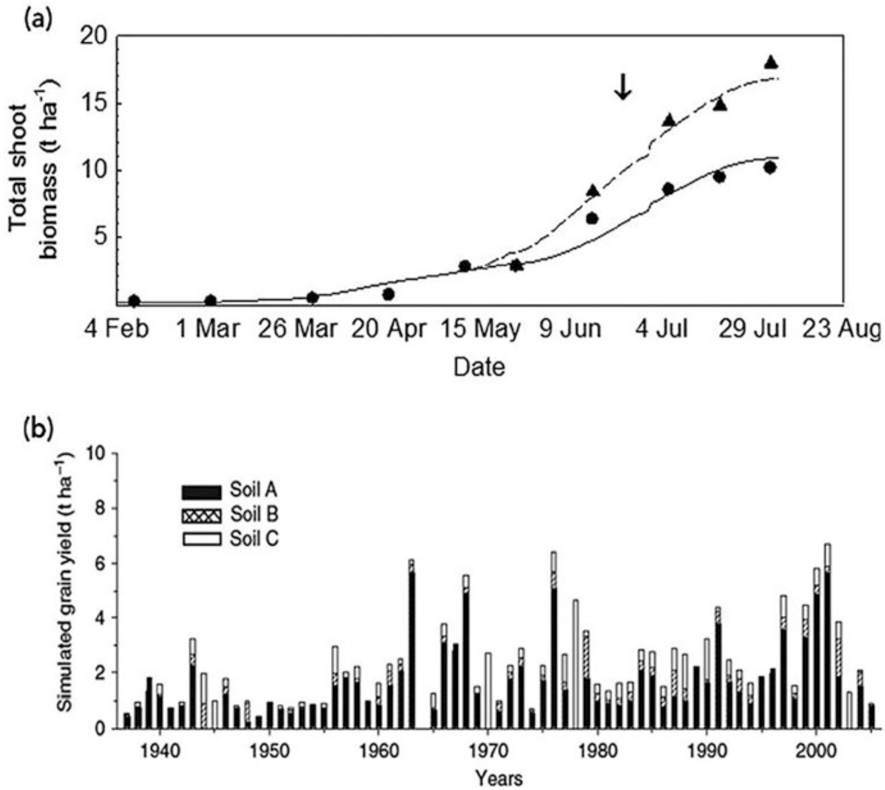

Fig. 6.2 (**a**) Simulated (lines) and observed (symbols) total wheat biomass subjected to different levels of nitrogen fertilizer N1 (circle) and N2 (triangle) in the Netherlands (1993). The arrow refers to date of anthesis. (Source: Asseng et al. 2000) (**b**) Simulated wheat grain yield in Argentina from 1937 to 2005 in three soil types (A, fine sand; B, coarse sand; and C, loam). (Source: Asseng et al. 2013b)

6.3 Treatments and Time

Like treatments in field experiments, crop models could simulate the agronomic treatments very well. These simulations characterize with their complexity allowing a wider range of variables over time than field experiments, making crop models a powerful tool for evaluating treatments in different environments. As clear in Fig. 6.2a, the total wheat biomass was simulated using two different nitrogen fertilizer treatments over the growing season. These simulations could avoid repeating the field experiments, saving time, efforts and energy. Furthermore, crop models could predict yield over a long time (e.g. many decades) in different soil types with difficult achievement in the field (Fig. 6.2b). Therefore, crop models could simulate yield using multiple treatments across many seasons, saving time and efforts in

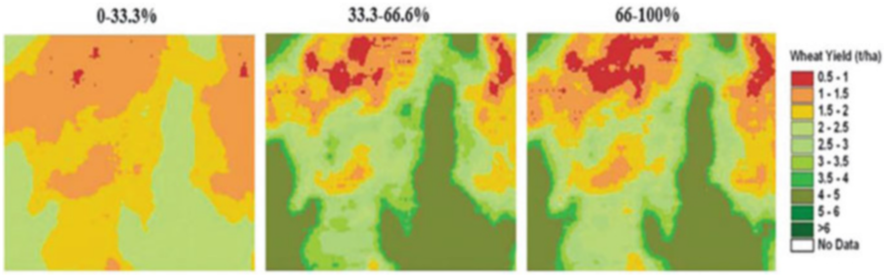

Fig. 6.3 Simulated wheat yields for soil with 60 kg N/ha fertilizer under three rainfall levels 0–33.3% (260 mm), 33.3–66.6% (370 mm) and 66–100% (470 mm). (Source: Wong and Asseng 2006)

understanding cropping systems, and thus can help decision-makers in policy planning.

6.4 Farm or Field

Based on the hierarchy theory (Ewert et al. 2009) and using a conceptual framework, crop models could simulate components in different spatial scales. This theory could divide crop model application into a nested approach with the same time and spatial scale for each level (Ewert et al. 2009). Farm or field represents the smallest level in this approach. Figure 6.3 shows simulating wheat yield on a specific field in the semiarid environment using different records of rainfall and soil properties.

6.5 Region

Larger than field or small-scale area, crop models could simulate and aggregate many points to form a large scale or region. Figure 6.4 shows a simulation of many points in Egypt to predict the gap between wheat production and demand in the region (Asseng et al. 2018). They used three crop models to simulate wheat yield across 100 years (1980–2100) using experimental data and climate change scenarios of 48 locations in Egypt. Also, crop models used to predict wheat production under multilevels of temperature and CO_2 in Nile Delta in Egypt (Fig. 6.5) (Kheir et al. 2019).

6.6 Global

Crop models could simulate the global scale by aggregating multipoints worldwide. Figure 6.6 shows the prediction of global wheat yield and protein using 32 crop models and different climate change scenarios around the mid-century (2050).

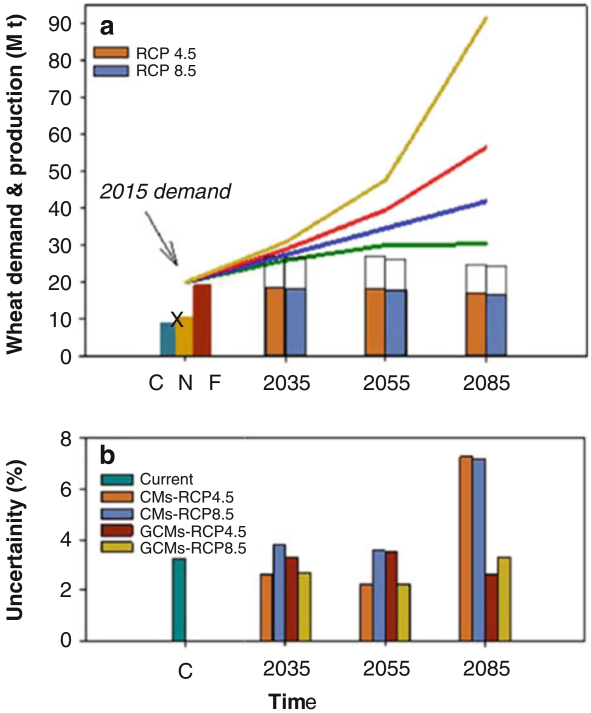

Fig. 6.4 Regional estimation of wheat production and demand in Egypt through the century under different climate change scenarios, population scenarios and proposed adaptation options. (Source: Asseng et al. 2018)

Multi-models and climate change scenarios were used globally to predict wheat yield and protein with and without genotype adaptation using the specific crop management, soils and cultivars of each region (Asseng et al. 2019). These findings would have been impossible to determine globally by field experiments. Upscaling simulation from the field or regional to global scale requires determination of uncertainties (Zhao et al. 2015).

6.7 Experiments for Crop Model Evaluation

To test and evaluate crop models, the outputs should always be compared with field experiments (Ziska and Bunce 2007). Crop models were tested and validated with field experimental data in diverse environments (Asseng et al. 1998; Jamieson et al. 1998; Lv et al. 2013). The required dataset for model's calibration and validation include but not limited to daily weather, soil properties, crop phenology, crop management, yield and yield attributes, nutrient and water balance, energy measurements and CO_2 and water fluxes (Kersebaum et al. 2015). For grain yield validation, comparing the simulated growth dynamics with observed values is required under a wide range of crop management and diverse environments. The quality of validation could be quantified using different statistical parameters

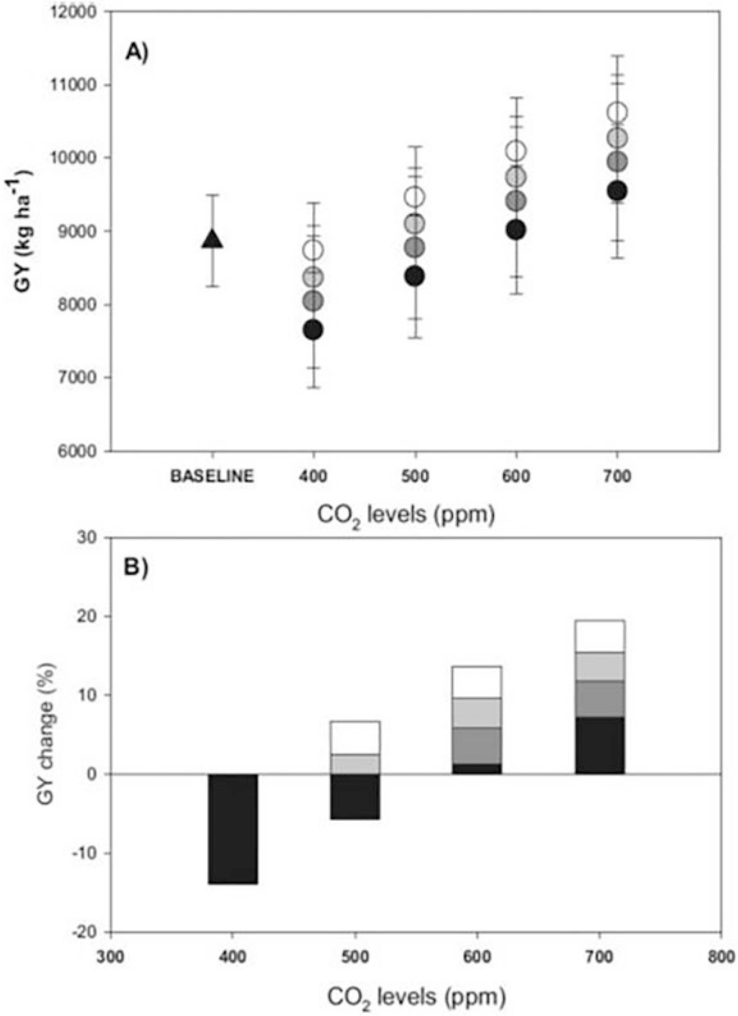

Fig. 6.5 The combined effect of rising temperature and carbon dioxide on wheat yield (**a**) and the relative reduction compared to the baseline (**b**) in Nile Delta

(i.e. determination coefficient, degree of agreement and root mean square deviation). Here are subsections of good-quality experiments used for model evaluation.

6.7.1 Nitrogen Experiment in the Netherlands

Field data of winter wheat from different sites, growing seasons and nitrogen fertilization levels in the temperate climate of the Netherlands were collected by

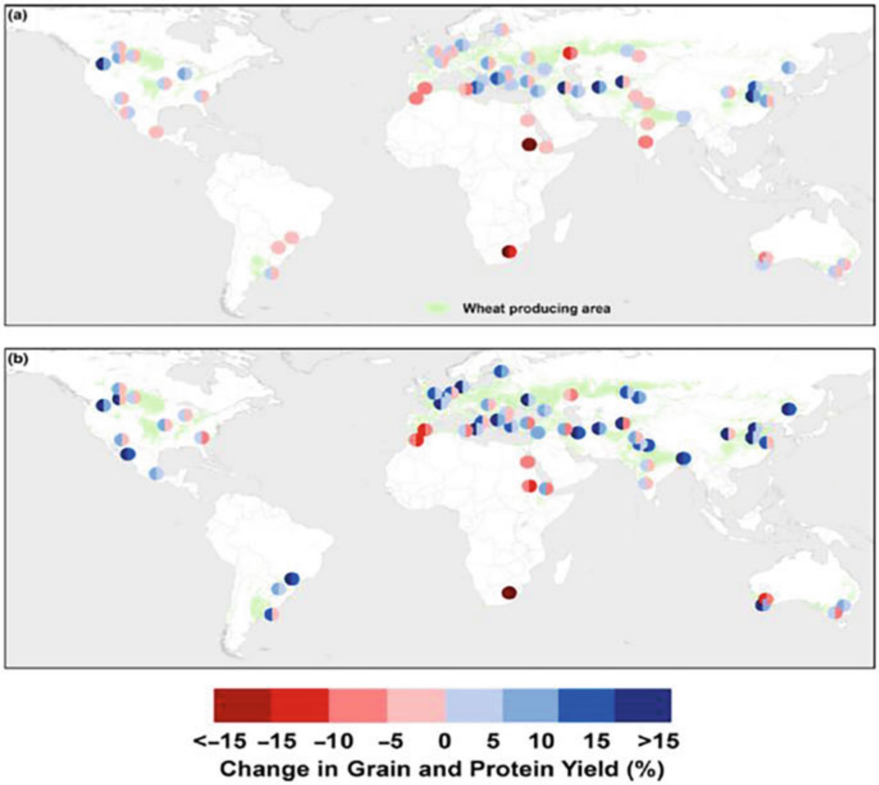

Fig. 6.6 Multi-model ensemble projection to simulate the global wheat yield (left half) and protein (right half) without genotype adaptation (**a**) and with genotype adaptation (**b**)

Groot and Verberne (1991). These experiments are assigned to three levels of N at each site. Many measurements were recorded over the season such as soil moisture, soil N content, production and distribution of dry matter, groundwater contribution, N distribution and uptake and density of root length. Hereafter, these experiments have been widely used in model testing and evaluation for crop production (Asseng et al. 2000; Olesen et al. 2000; Wang and Engel 2002). Crop models were used here to determine different N rate and timing following calibration. Additional field data were used for model validation, proving high accuracy based on the used statistical indicators (coefficient determination, r^2 and root mean square deviation).

6.7.2 Deficit Water Experiment in New Zealand

Experimental study had been conducted in New Zealand to explore the response of wheat to drought when sown in a mobile rain shelter (Jamieson et al. 1995). Eleven treatments of drought were used to change the duration with wheat growth stages and determining yield in each treatment. The findings included that wheat yield reduction was mainly due to reduced grain number under drought stress. The collected data from this experiment has been widely used in simulation modelling to compare the output accuracy of different wheat models and to simulate wheat yield and biomass under different scenarios of water stress (Jamieson et al. 1998; Asseng et al. 2004).

6.7.3 FACE Experiment in Arizona

The free-air carbon dioxide enrichment (FACE) experiment was conducted at Maricopa, Arizona, in several years to explore the combined effects of elevated CO_2 with limited water and N level on spring wheat. Despite increasing wheat yield due to elevated CO_2, limited water and N supply influenced the overall effect of CO_2 concentrations (Kimball et al. 2002). Using this experiment, several crop models have been evaluated to predict wheat grain yield and phenology under projected climate change scenarios, achieving high accuracy (GRANT et al. 1995; Kartschall et al. 1995; Tubiello et al. 1999; Asseng et al. 2004; Ko et al. 2010). This indicates that crop models could successfully simulate crop growth and development using different levels of CO2, water and N in the cropping systems.

6.7.4 FACE Experiment in Australia

Field experiments were conducted for 3 years at the semiarid environment in Australian Grains FACE experiment to measure wheat yield and water use (Mollah et al. 2009). This experiment aimed at exploring the combined effects of elevated CO_2 with different regimes of water and N on wheat yield and water use. Several studies used these data for simulation models to compare models' outputs by experiment measurements (Nuttall et al. 2012; O'Leary et al. 2015). Six models were tested using these data in one study and found that wheat yield, biomass and water use simulated in a good performance by these models in rainfed and low-input systems (O'Leary et al. 2015).

6.7.5 Hot Serial Cereal Experiment in Arizona

Spring wheat cultivar was sown in well-irrigated and fertilized environment and exposed to artificial heating and different sowing dates under field conditions at Maricopa, Arizona (WALL et al. 2011; Ottman et al. 2012). The infrared radiation heaters were used for artificial heat treatments using thermometers to control the canopy temperature through growing season. The main findings concluded that rising temperature reduced wheat growth and yield, particularly in late and earlier planting dates. Using these data, a global modelling study (30 models) predicted wheat yield in response to rising temperature (Asseng et al. 2015). The main findings highlighted that rising temperature by 1 °C reduced global wheat production by 6%.

6.7.6 INRA Temperature Experiment

In containers with total area 2 m^2 for each and depth 0.5 m, wheat was sown in black and peat soil. The experiments included three planting dates 10, 08, and 07 November for years 1999, 2000, and 2006, respectively, in INRA, France (45.8°N, 3.2°E, 329 m elevation) (Majoul-Haddad et al. 2013). After 1–5 days from anthesis date, containers were transferred to crop climate control and gas exchange measurement units. In these units, plants were exposed to different temperature regimes (28, 38, and 38 °C) for three experiments, respectively. Wheat phenology, growth, yield and protein contents in grains were measured in all experiments. This data were used after that in global modelling study to explore the impact of climate change and adaptation on global wheat production and protein using 32 crop models (Asseng et al. 2019).

6.8 Potential and Limitations of Current Crop Models

6.8.1 Agronomy

Wheat crop is the oldest cultivated crop worldwide, while cultivated over 8000 years ago by Ancient Egyptians. The recent technology improved the yield of wheat up to 16.5 t ha^{-1} as achieved recently in the UK. This improvement in yield is a result of using crop models in research for decades. Recently, crop models help researchers, agronomists and decision-makers in the assessment of gains and risks of new agricultural techniques, the possibility of expanding crops into new regions, exploring the adaptation of new varieties and responding to challenges of food security, nutrition and sustainability. The most common use of wheat crop models is to quantify the gap between simulated yield using factors limiting production and farmers' yield (Hochman et al. 2013). Several studies have evaluated the impacts of management practices on simulated crop productivity including but not limited to irrigation (Liu et al. 2007), tillage systems (Basso et al. 2006), planting methods (Andarzian et al. 2015), fertilization (Dumont et al. 2015) and weed control (Hunt and Kirkegaard 2011). All these studies aimed at exploring the best management option ensuring the sustainable productivity and profitability on the long term.

Although crop models were widely used to help farmers, extension specialists, consultants, retailers and decision-makers (Robertson et al. 2015), they were still limited and costly to be used for the individual commercial applications (i.e. individual farm). To tackle this problem, different communication strategies and technology tools have been developed and used (Adam et al. 2010). For example, "Yield Prophet" application has been widely used in Australia to assess the risk during wheat yield simulations and provide farmers and advisors with information in a digested format, enabling them to select the appropriate management system to avoid such risks. As part of these tools, integration between socio-economic and crop modelling could be used to provide the suitable recommendations for both irrigation and fertilization management, ensuring sustainability (Basso et al. 2013).

Due to the growing population and the importance of farming systems, crop models could be used to assist in planning and designing of strategies to increase the crop productivity and profitability while avoiding the environmental footprint (Godfray et al. 2011). Recently, many applications have been assessed by farming system models such as crop residue management, tillage, crop rotation, nitrate balance and leaching (Hasegawa and Denison 2005), emissions of nitrous oxide (Huth et al. 2010), soil carbon sequestration (Huth et al. 2010) and environmental and economic impacts (Basso et al. 2016). However, there are some constraints in using crop models in farming systems such as soil salinity, acidity and toxicity. The base of model applications depends mainly on science and the embedded parameters in models. In case of new conditions like new region and new varieties, models need to be assessed first using experimental data (Asseng et al. 2013a). Crop models are always supposing a homogenous in simulation of soil conditions, and this does not exist in nature, causing some limitations and major uncertainty in model outputs. This issue could be tackled by simulating multiple subregions at the farm level or catchment area (Paydar and Gallant 2007).

6.8.2 Breeding

By the mid-century (2050), the global wheat demand is projected to increase by 70%, requiring improvement in the global production from current lower percent (<1%) (Fischer and Edmeades 2010) to about 1.7% (Tester and Langridge 2010). Due to the climate change, improvements in wheat yield are too modest and going slow (Brisson et al. 2003). The key factors driving the changes in wheat development are abiotic stresses such as drought and heat (Ahmed et al. 2020). Producing new cultivar takes about 8–12 years; thus using crop models to help wheat breeding in producing cultivars adapted with agronomic practices and current and future environments is an urgent need (Brisson et al. 2003; Kirkegaard and Hunt 2010). Consequently, some wheat models were developed for breeding needs as shown in Fig. 6.7. However, wheat models need more improvements with breeding in diverse environments and cultivars worldwide (Stöckle and Kemanian 2020).

6.8.3 The Global Impact

The complex issues of climate change, environmental footprints, overpopulation and food security (Godfray et al. 2011), require global tactics. Consequently, crop models have been widely used from the regional to global scale to predict the sustainable yield across different environments (Wallach et al. 2018; Asseng et al.

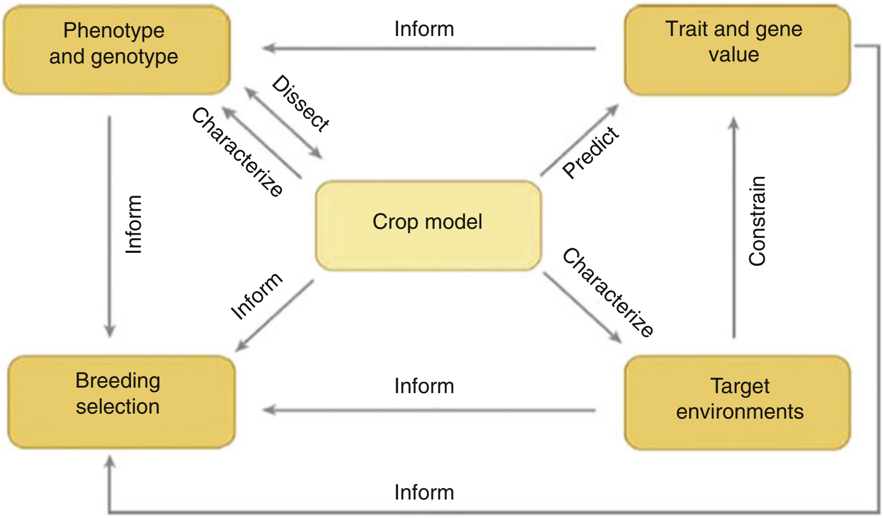

Fig. 6.7 Breeding and using crop modelling. Crop models could be used to (I) convert complex traits to simple traits, (II) characterize the target environment, (III) simulate and predict yield subjected to traits and genetic factors and (IV) inform breeding using the interaction between breeding models and analysis

2015). The range of applications should be done from a unit to a field (Chenu et al. 2011), farm (Rodriguez et al. 2011), region (Basso et al. 2006), continent (Chenu et al. 2013) and upscale (Rosenzweig et al. 2014a). As the essential scale for modelling systems is the homogenous unit or field, any simulations in the global scale induce uncertainty in outputs. This uncertainty may be due to insufficient information about soil, climate, crop management and/or model parameters. Therefore, many recent efforts were exerted to better understand this uncertainty (Zhao et al. 2015). The first studies of uncertainty were conducted in some parts of Europe and found that uncertainty induced by climate manipulation is relatively smaller than that related to soil conditions (van Bussel et al. 2015). However, much less work has been done to explore the upscale effects of crop management and model parameters, particularly in the case of diverse cultivars in a region or a country (van Bussel et al. 2015). Recently, crop models have been widely used to estimate the potential impacts of crop production on food security even under climate change scenarios. Although the application of crop models in a global scale is too new, the specific demands of crop modelling increased and were considered a current hot spot (Asseng et al. 2015). This requires a better understanding of interactions between modelling G × E × M in a large scale and factors affecting yield production such as management and genetic factors. However, the improvement in crop modelling depends mainly on the availability of detailed data of soil, weather, management and cultivar information to cover upscale issue. This is especially important for developing countries and tropics vulnerable to climate change and with limited resources for data, analysis and adaptation resources (Hertel and Lobell 2014; Wing and De Cian 2014).

6.8.4 Climate Change

The better understanding of climate change impacts on crop yield and sustainability could assist developing the best adaptation option in the future. Using the interactions between G × E × M, crop models could quantify the potential impacts of climate change on crop productivity and generate the suitable adaptation option that would offset the climate drawbacks on yield (Martín et al. 2014). Climate change will negatively influence on the distribution and mean of climate factors (IPCC 2014). Despite recent changes in patterns of temperature, CO_2 and rainfall have been recently recorded, the climate models have also projected analogous changes in the future including the heat waves (Ahmed and Ahmad 2019; Ahmed 2020). Therefore, crop models need to be used to simulate yield production under interaction between the climatic factors and processes affecting yield. Eventually, crop models were not developed in climate change studies and restricted to study only the average values of temperature, CO_2 and rainfall. Meanwhile, studies of climate change impacts and adaptation are developed recently using crop models (Liu et al. 2019; Zheng et al. 2016; Challinor et al. 2014), with better understanding to uncertainties.

Wheat crop models simulate the effect of temperature on different processes in crop development such as photosynthesis, phenology (Aslam et al. 2017a), evapotranspiration and respiration. Nevertheless, few models can consider the potential effects of rising temperature on leaf senescence, fertility of floret and grain development (Lobell et al. 2015; ASSENG et al. 2011). Furthermore, model improvements should include simulation of heat stress on wheat grain quality such as glutenin aggregation (Nuttall et al. 2017); grain protein, iron and zinc; as well as the combined effects of abiotic stresses such as drought and heat. In addition to temperature, crop models have widely tested with elevated concentration on CO_2 (O'Leary et al. 2015). There are also additional opportunities to include other climatic factors in wheat models on the future such as ozone (Ewert and Porter 2000), frost (Brisson et al. 2003), snow, hail, excess water and limited oxygen in root zone and wind damage. However, predicting the impacts of higher events remains a big challenge.

6.9 Concluding and Future Perspectives

Overpopulation growth, climate change and diminished natural resources are considered major challenges for food security and nutrition. Due to the considerable challenges, new notions called "sustainable intensification" and "climate smart agriculture" need to be widely applied. Sustainable intensification is aimed at increasing the production and resource use efficiency of nutrient, water and solar radiation, while climate smart agriculture is most related to minimizing the emissions of greenhouse gases in both unit area and harvested yield. Therefore, great efforts are necessary to include simulation of climate smart agriculture and sustainable intensification using crop models. Crop models have been widely used to provide comprehensive appraisals of different agricultural, environmental and climatic scenarios. However, there is lack of sensitivity in most crop models towards the short-term severe stresses (i.e. cold and warm) that can affect crop growth and development. Therefore, extending research and field experiments to explore the effect of heat on crop growth stages is urgently necessary for model simulation improvement.

Due to diminished natural resources (land, nutrient and water), crop models were used to assist decision-makers in related issues. However, most of the crop models consider only N uptake and dynamic, with limited information about other important nutrients (i.e. phosphorus and potassium). Furthermore, climate change will effect on soil nutrient dynamics and alterations, requiring improvement in crop models to consider such factors.

Climate change is likely to influence crop yield quality (i.e. protein), while considered simulations by crop models are still poor. To improve further simulations, integration between crop physiology and yield quality into crop models should be understood. In addition, pests and diseases have negative effects on crop quality. Crop models can simulate the effects of pests and diseases on crop yield through including disease models into crop models. However, simulation of interaction between dynamic of disease and occurrence movement is still a major challenge. Crop models can also be extended to crop genetic factors, but integration between genotype and phenotype into crop models is still unknown.

Crop models are considered powerful tools in agricultural research and can assist decision-makers in policy and strategic planning to offset the negative impacts of climate change on food security and nutrition. However, future applications in breeding, agronomy, NRM and climate change need to be considered for new cropping systems and improving model accuracy.

References

Adam M, Ewert F, Leffelaar PA, Corbeels M, Keulen HV, Wery J (2010) CROSPAL, software that uses agronomic expert knowledge to assist modules selection for crop growth simulation. Environ Model Softw 25(8):946–955

Aggarwal P, Banerjee B, Daryaei M, Bhatia A, Bala A, Rani S, Chander S, Pathak H, Kalra N (2006) InfoCrop: a dynamic simulation model for the assessment of crop yields, losses due to pests, and environmental impact of agro-ecosystems in tropical environments. II. Performance of the model. Agric Syst 89(1):47–67

Ahmad S, Abbas G, Fatima Z, Khan RJ, Anjum MA, Ahmed M, Khan MA, Porter CH, Hoogenboom G (2017) Quantification of the impacts of climate warming and crop management on canola phenology in Punjab, Pakistan. J Agron Crop Sci 203(5):442–452. https://doi.org/10.1111/jac.12206

Ahmad S, Abbas G, Ahmed M, Fatima Z, Anjum MA, Rasul G, Khan MA, Hoogenboom G (2019) Climate warming and management impact on the change of phenology of the rice-wheat cropping system in Punjab, Pakistan. Field Crop Res 230:46–61. https://doi.org/10.1016/j.fcr.2018.10.008

Ahmed M (2012) Improving soil fertility recommendations in Africa using the decision support system for Agrotechnology transfer (DSSAT); a book review. Exp Agric 48(4):602–603

Ahmed M (2020) Introduction to modern climate change. Andrew E. Dessler: Cambridge University Press, 2011, 252 pp, ISBN-10: 0521173159. Sci Total Environ 734:139397. https://doi.org/10.1016/j.scitotenv.2020.139397

Ahmed M, Ahmad S (2019) Carbon dioxide enrichment and crop productivity. In: Hasanuzzaman M (ed) Agronomic crops. Management practices, vol 2. Springer Singapore, Singapore, pp 31–46. https://doi.org/10.1007/978-981-32-9783-8_3

Ahmed M, Stockle CO (2016) Quantification of climate variability, adaptation and mitigation for agricultural sustainability. Springer Nature Singapore Pvt. Ltd., Singapore, 437 pp. https://doi.org/10.1007/978-3-319-32059-5

Ahmed M, Aslam MA, Hassan FU, Asif M, Hayat R (2014) Use of APSIM to model nitrogen use efficiency of rain-fed wheat. Int J Agric Biol 16:461–470

Ahmed M, Hassan FU, Aslam MA, Akram MN, Akmal M (2011) Regression model for the study of sole and cumulative effect of temperature and solar radiation on wheat yield. Afr J Biotechnol 10(45):9114–9121. https://doi.org/10.5897/AJB11.1318

Ahmed M, Asif M, Hirani AH, Akram MN, Goyal A (2013) Modeling for agricultural sustainability: a review. In: Bhullar GS, Bhullar NK (eds) Agricultural sustainability progress and prospects in crop research. Elsevier, London

Ahmed M, Akram MN, Asim M, Aslam M, Hassan F-u, Higgins S, Stöckle CO, Hoogenboom G (2016) Calibration and validation of APSIM-Wheat and CERES-Wheat for spring wheat under rainfed conditions: models evaluation and application. Comput Electron Agric 123:384–401. https://doi.org/10.1016/j.compag.2016.03.015

Ahmed M, Stöckle CO, Nelson R, Higgins S (2017) Assessment of climate change and atmospheric CO_2 impact on winter wheat in the Pacific Northwest using a multimodel ensemble. Front Ecol Evol 5(51). https://doi.org/10.3389/fevo.2017.00051

Ahmed M, Ijaz W, Ahmad S (2018) Adapting and evaluating APSIM-SoilP-Wheat model for response to phosphorus under rainfed conditions of Pakistan. J Plant Nutr 41(16):2069–2084. https://doi.org/10.1080/01904167.2018.1485933

Ahmed M, Stöckle CO, Nelson R, Higgins S, Ahmad S, Raza MA (2019) Novel multimodel ensemble approach to evaluate the sole effect of elevated CO_2 on winter wheat productivity. Sci Rep 9(1):7813. https://doi.org/10.1038/s41598-019-44251-x

Ahmed K, Shabbir G, Ahmed M, Shah KN (2020) Phenotyping for drought resistance in bread wheat using physiological and biochemical traits. Sci Total Environ 729:139082. https://doi.org/10.1016/j.scitotenv.2020.139082

Andarzian B, Hoogenboom G, Bannayan M, Shirali M, Andarzian B (2015) Determining optimum sowing date of wheat using CSM-CERES-Wheat model. J Saudi Soc Agric Sci 14(2):189–199

Angulo C, Rötter R, Lock R, Enders A, Fronzek S, Ewert F (2013) Implication of crop model calibration strategies for assessing regional impacts of climate change in Europe. Agric For Meteorol 170:32–46

Aslam MA, Ahmed M, Stöckle CO, Higgins SS, Hassan FU, Hayat R (2017a) Can growing degree days and photoperiod predict spring wheat phenology? Front Environ Sci 5:57

Aslam MU, Shehzad A, Ahmed M, Iqbal M, Asim M, Aslam M (2017b) QTL modelling: an adaptation option in spring wheat for drought stress. In: Ahmed M, Stockle CO (eds) Quantification of climate variability, adaptation and mitigation for agricultural sustainability. Springer International Publishing, Cham, pp 113–136. https://doi.org/10.1007/978-3-319-32059-5_6

Asseng S, Keating BA, Fillery IRP, Gregory PJ, Bowden JW, Turner NC, Palta JA, Abrecht DG (1998) Performance of the APSIM-wheat in Western Australia. Field Crop Res 57:163–179

Asseng S, van Keulen H, Stol W (2000) Performance and application of the APSIM Nwheat model in the Netherlands. Eur J Agron 12:37–54

Asseng S, Jamieson PD, Kimball B, Pinter P, Sayre K, Bowden JW, Howden SM (2004) Simulated wheat growth affected by rising temperature, increased water deficit and elevated atmospheric CO2. Field Crop Res 85:85–102

Asseng S, Foster I, Turner NC (2011) The impact of temperature variability on wheat yields. Glob Chang Biol 17(2):997–1012

Asseng S, Ewert F, Rosenzweig C, Jones JW, Hatfield JL, Ruane AC, Boote KJ, Thorburn PJ, Rötter RP, Cammarano D, Brisson N, Basso B, Martre P, Aggarwal PK, Angulo C, Bertuzzi P, Biernath C, Challinor AJ, Doltra J, Gayler S, Goldberg R, Grant R, Heng L, Hooker J, Hunt LA, Ingwersen J, Izaurralde RC, Kersebaum KC, Müller C, Naresh Kumar S, Nendel C, O'Leary G, Olesen JE, Osborne TM, Palosuo T, Priesack E, Ripoche D, Semenov MA, Shcherbak I, Steduto P, Stöckle C, Stratonovitch P, Streck T, Supit I, Tao F, Travasso M, Waha K, Wallach D, White JW, Williams JR, Wolf J (2013a) Uncertainty in simulating wheat yields under climate change. Nat Clim Chang 3:827–832

Asseng S, Travasso MI, Ludwig F, Magrin GO (2013b) Has climate change opened new opportunities for wheat cropping in Argentina? Clim Chang 117(1–2):181–196

Asseng S, Zhu Y, Basso B, Wilson T, Cammarano D (2014) Simulation modeling: applications in cropping systems. In: Van Alfen NK (ed) Encyclopedia of agriculture and food systems. Academic, Oxford, pp 102–112

Asseng S, Ewert F, Martre P, Rotter RP, Lobell DB, Cammarano D, Kimball BA, Ottman MJ, Wall GW, White JW, Reynolds MP, Alderman PD, Prasad PVV, Aggarwal PK, Anothai J, Basso B, Biernath C, Challinor AJ, De Sanctis G, Doltra J, Fereres E, GarciaVile M, Gayler S, Hoogenboom G, Hunt LA, Izaurralde RC, Jabloun M, Jones CD, Kersebaum KC, Koehler AK, Muller C, Kumar SN, Nendel C, O'Leary G, Olesen JE, Palosuo T, Priesack E, Rezaei EE, Ruane AC, Semenov MA, Shcherbak I, Stockle C, Stratonovitch P, Streck T, Supit I, Tao F, Thorburn PJ, Waha K, Wang E, Wallach D, Wolf I, Zhao Z, Zhu Y (2015) Rising temperatures reduce global wheat production. Nat Clim Chang 5:143–147

Asseng S, Kheir AMS, Kassie BT, Hoogenboom G, Anbdelaal AIN, Haman DZ, Ruane AC (2018) Can Egypt become self-sufficient in wheat? Environ Res Lett 13:094012

Asseng S, Martre P, Maiorano A, Rötter RP, O'Leary GJ, Fitzgerald GJ, Girousse C, Motzo R, Giunta F, Babar MA, Reynolds MP, Kheir AMS, Thorburn PJ, Waha K, Ruane AC, Aggarwal PK, Ahmed M, Balkovič J, Basso B, Biernath C, Bindi M, Cammarano D, Challinor AJ, De Sanctis G, Dumont B, Rezaei EE, Fereres E, Ferrise R, Garcia-Vila M, Gayler S, Gao Y, Horan H, Hoogenboom G, Izaurralde RC, Jabloun M, Jones CD, Kassie BT, Kersebaum K, Klein C, Koehler A, Liu B, Minoli S, San Martin MM, Müller C, Kumar SN, Nendel C, Olesen JE, Palosuo T, Porter JR, Priesack E, Ripoche D, Semenov MA, Stöckle C, Stratonovitch P, Streck T, Supit I, Tao F, Van der Velde M, Wallach D, Wang E, Webber H, Wolf J, Xiao L, Zhang Z, Zhao Z, Zhu Y, Ewert F (2019) Climate change impact and adaptation for wheat protein. Glob Chang Biol 25:155–173. https://doi.org/10.1111/gcb.14481

Basso B, Ritchie JT, Grace PR, Sartori L (2006) Simulation of tillage systems impact on soil biophysical properties using the SALUS model Italian. J Agron 4:677–688

Basso B, Cammarano D, Troccoli A, Chen D, Ritchie J (2010) Long-term wheat response to nitrogen in a rainfed Mediterranean environment: field data and simulation analysis. Eur J Agron 33:182–188

Basso B, Cammarano D, Fiorentino C, Ritchie JT (2013) Wheat yield response to spatially variable nitrogen fertilizer in Mediterranean environment. Eur J Agron 51:65–70

Basso B, Liu L, Ritchie JT (2016) A comprehensive review of the CERES-Wheat, −maize and -Rice models' performances. Adv Agron 136:27–132

Beringer T, Lucht W, Schaphoff S (2011) Bioenergy production potential of global biomass plantations under environmental and agricultural constraints. Glob Change Biol Bioenergy 3:299–312

Berntsen J, Petersen B, Jacobsen B, Olesen J, Hutchings N (2003) Evaluating nitrogen taxation scenarios using the dynamic whole farm simulation model FASSET. Agric Syst 76:817–839

Biernath C, Gayler S, Bittner S, Klein C, Hogy P, Fangmeier A, Priesack E (2011) Evaluating the ability of four crop models to predict different environmental impacts on spring wheat grown in open-top chambers. Eur J Agron 35:71–82

Boogaard H, Kroes J (1998) Leaching of nitrogen and phosphorus from rural areas to surface waters in the Netherlands. Nutr Cycl Agroecosyst 50:321–324

Brisson N, Mary B, Ripoche D, Jeuffroy MH, Ruget F, Nicoullaud B, Gate P, Devienne-Barret F, Antonioletti R, Durr C, Richard G, Beaudoin N, Recous S, Tayot X, Plenet D, Cellier P, Machet JM, Meynard JM, Delecolle R (1998) STICS: a generic model for the simulation of crops and their water and nitrogen balances. I. theory and parameterization applied to wheat and corn. Agronomie 18:311–346
Brisson N, Gary C, Justes E, Roche R, Mary B, Ripoche D, Zimmer D, Sierra J, Bertuzzi P, Burger P, Bussiere F, Cabidoche YM, Cellier P, Debaeke P, Gaudillere JP, Henault C, Maraux F, Seguin B, Sinoquet H (2003) An overview of the crop model STICS. Eur J Agron 18:309–332
Challinor A, Wheeler T, Craufurd P, Slingo J, Grimes D (2004) Design and optimisation of a large area process based model for annual crops. Agric For Meteorol 124:99–120
Challinor AJ, Watson J, Lobell DB, Howden SM, Smith DR, Chhetri N (2014) A meta-analysis of crop yield under climate change and adaptation. Nat Clim Chang 4:287–291
Chenu K, Cooper M, Hammer GL, Mathews KL, Dreccer MF, Chapman SC (2011) Environment characterization as an aid to wheat improvement: interpreting genotype–environment interactions by modelling water-deficit patterns in North-Eastern Australia. J Exp Bot 62 (6):1743–1755. https://doi.org/10.1093/jxb/erq1459
Chenu K, Deihimfard R, Chapman SC (2013) Large-scale characterization of drought pattern: a continent-wide modelling approach applied to the Australian wheatbelt – spatial and temporal trends. New Phytol 198(3):801–820
Chenu K, Porter JR, Martre P, Basso B, Chapman SC, Ewert F, Bindi M, Asseng S (2017) Contribution of crop models to adaptation in wheat. Trends Plant Sci 22(6). https://doi.org/10.1016/j.tplants
de Wit CT (1995) Photosynthesis of leaf canopies, Agricultural research report 663. Centre for Agricultural Publications and Documentation, Wageningen
Dumont B, Basso B, Bodson B, Destain JP, Destain MF (2015) Climatic risk assessment to improve nitrogen fertilisation recommendations: a strategic crop model-based approach. Eur J Agron 65:10–17
Ewert F, Porter JR (2000) Ozone effects on wheat in relation to CO2: modeling short-term and long-term responses of leaf photosynthesis and leaf duration. Glob Chang Biol 6:735–750
Ewert F, van Ittersum MK, Bezlepkina I, Therond O, Andersen E, Belhouchette H, Bockstaller C, Brouwer F, Heckelei T, Janssen S, Knapen R, Kuiper M, Louhichi K, Olsson JA, Turpin N, Wery J, Wien JE, Wolf J (2009) A methodology for enhanced flexibility of integrated assessment in agriculture. Environ Sci Pol 12:546–561
Farquhar GD, Caemmerer SV, Berry JA (1980) A biochemical model of photosynthetic CO2 assimilation in leaves of C3 species. Planta 149:78–90
Fischer RA, Edmeades GO (2010) Breeding and cereal yield progress. Crop Sci 50:85–98
Gerten D, Schaphoff S, Haberlandt U, Lucht W, Sitch S (2004) Terrestrial vegetation and water balance – hydrological evaluation of a dynamic global vegetation model. J Hydrol 286:249–270
Godfray HCJ, Beddington JR, Crute IR, Haddad L, Lawrence D, Muir JF, Pretty J, Robinson S, Thomas SM, Toulmin C (2010) Food security: the challenges of feeding 9 billion people. Science 327:812–818
Godfray HCJ, Pretty J, Thomas SM, Warham JR, Beddington JR (2011) Linking policy on climate and food. Science 331:1013–1014
Gourdji SM, Mathews KL, Reynolds M, Crossa J, Lobell DB (2013) An assessment of wheat yield sensitivity and breeding gains in hot environments. Proc R Soc B Biol Sci 280:1–8
Grant RF, Garcia RL, Pinter JPJ, Hunsaker D, Wall GW, Kimball BA, Lamorte RL (1995) Interaction between atmospheric CO2 concentration and water deficit on gas exchange and crop growth: testing of ecosys with data from the Free Air CO2 Enrichment (FACE) experiment. Glob Chang Biol 1(6):443–454
Groot JJR, Verberne ELJ (1991) Response of wheat to nitrogen fertilization, a data set to validate simulation models for nitrogen dynamics in crop and soil. Fertil Res 27:349–383

Guarin JR, Asseng S (2017) Wheat crop modelling to improve yields. https://doi.org/10.19103/AS.2016.0004.27

Hansen S, Jensen H, Nielsen N, Svendsen H (1991) Simulation of nitrogen dynamics and biomass production in winter-wheat using the Danish simulation model DAISY. Fertil Res 27:245–259

Hansen S, Abrahamsen P, Petersen CT, Styczen M (2012) DAISY: model use, calibration, and validation. Trans ASABE 55:1317–1335

Hasegawa H, Denison RF (2005) Model predictions of winter rainfall effects on N dynamics of winter wheat rotation following legume cover crop or fallow. Field Crop Res 91(2–3):251–261

He J, Stratonovitch P, Allard V, Semenov MA, Martre P (2010) Global sensitivity analysis of the process-based wheat simulation model siriusquality1 identifies key genotypic parameters and unravels parameters interactions. Procedia Soc Behav Sci 2:7676–7677

Hertel TW, Lobell DB (2014) Agricultural adaptation to climate change in rich and poor countries: current modeling practice and potential for empirical contributions. Energy Econ 46:562–575

Hochman Z, Gobbett D, Holzworth D, Mcclelland T, Van Rees H, Marinoni O, Garcia JN, Horan H (2013) Quantifying yield gaps in rainfed cropping systems: a case study of wheat in Australia. Field Crop Res 143:65–75

Holzworth DP, Huth NI, Devoil PG, Zurcher EJ, Herrmann NI, McLean G, Chenu K, van Oosterom EJ, Snow V, Murphy C, Moore AD, Brown H, Whish JPM, Verrall S, Fainges J, Bell LW, Peake AS, Poulton PL, Hochman Z, Thorburn PJ, Gaydon DS, Dalgliesh NP, Rodriguez D, Cox H, Chapman S, Doherty A, Teixeira E, Sharp J, Cichota R, Vogeler I, Li FY, Wang EL, Hammer GL, Robertson MJ, Dimes JP, Whitbread AM, Hunt J, van Rees H, McClelland T, Carberry PS, Hargreaves JNG, MacLeod N, McDonald C, Harsdorf J, Wedgwood S, Keating BA (2014) APSIM –evolution towards a new generation of agricultural systems simulation. Environ Model Softw 62:327–350

Hoogenboom G, White JW (2003) Improving physiological assumptions of simulation models by using gene-based approaches. Agron J 95:92–90

Hunt JR, Kirkegaard JA (2011) Re-evaluating the contribution of summer fallow rain to wheat yield in Southern Australia. Crop Pasture Sci 62:915–929

Hunt LA, Pararajasingham S (1995) CROPSIM-wheat- a model describing the growth and development of wheat. Can J Plant Sci 75:619–632

Huth NI, Thorburn PJ, Radford BJ, Thornton CM (2010) Impacts of fertilisers and legumes on N2O and CO2 emissions from soils in subtropical agricultural systems: a simulation study. Agric Ecosyst Environ 136(3–4):351–357

IPCC (2014) Climate change. 2014 synthesis report. IPCC, Geneva

Jabeen M, Gabriel HF, Ahmed M, Mahboob MA, Iqbal J (2017) Studying impact of climate change on wheat yield by using DSSAT and GIS: a case study of Pothwar region. In: Ahmed M, Stockle CO (eds) Quantification of climate variability, adaptation and mitigation for agricultural sustainability. Springer International Publishing, Cham, pp 387–411. https://doi.org/10.1007/978-3-319-32059-5_16

Jamieson PD, Martin RJ, Francis GS (1995) Drought influences on grain yield of barley, wheat, and maize. N Z J Crop Hortic Sci 23(1):55–66

Jamieson PD, Porter JR, Goudriaan J, Ritchie JT, Keulen HV, Stol W (1998) A comparison of the models AFRCWHEAT2, CERES-Wheat, Sirius, SUCROS2 and SWHEAT with measurements from wheat grown under drought. Field Crop Res 55(1–2):23–44

Jones JW, Hoogenboom G, Porter CH, Boote KJ, Batchelor WD, Hunt LA, Wilkens PW, Singh U, Gijsman AJ, Ritchie JT (2003) The DSSAT cropping system model. Eur J Agron 18:235–265

Kartschall T, Grossman S, Pinter PJ, Garcia RL, Kimball BA, Wall GW, Hunsaker DJ, LaMORT RL (1995) A simulation of phenology, growth, carbon dioxide exchange and yields under ambient atmosphere and Free-Air Carbon Dioxide Enrichment (FACE) Maricopa, Arizona, for wheat. J Biogeogr 22(4/5):611–622

Kassie BT, Asseng S, Porter CH, Royce FS (2016) Performance of DSSAT-Nwheat across a wide range of current and future growing conditions. Eur J Agron 81:27–36

Keating BA, Carberry PS, Hammer GL, Probert ME, Robertson MJ, Holzworth D, Huth NI, Silburn M, Wang E, Brown S, Bristow KL, Asseng S, Chapman S, McCown RL, Freebairn DM, Smith CJ (2003) An overview of APSIM, a model designed for farming systems simulation. Eur J Agron 18:267–288

Kersebaum K (2007) Modelling nitrogen dynamics in soil-crop systems with HERMES. Nutr Cycl Agroecosyst 77:39–52

Kersebaum K (2011) Special features of the HERMES model and additional procedures for parameterization, calibration, validation, and applications. In: Ahuja LR, Ma L (eds) Methods of introducing system models into agricultural research, Advances in agricultural systems modeling series 2. ASA-CSSA-SSSA, Madison, pp 65–94

Kersebaum KC, Boote KJ, Jorgenson JS, Nendel C, Bindi M, Fruhauf C, Gaiser T, Hoogenboom G, Kollas C, Olesen JE, Rotter RP, Ruget F, Thorburn PJ, Trnka M, Wegehenkel M (2015) Analysis and classification of data sets for calibration and validation of agro-ecosystem models. Environ Model Softw 72:402–417

Kheir AMS, El Baroudy A, Aiad MA, Zoghdan MG, Abd El-Aziz MA, Ali MGM, Fullen MA (2019) Impacts of rising temperature, carbon dioxide concentration and sea level on wheat production in North Nile delta. Sci Total Environ 651:3161–3173

Kimball B, Kobayashi B, Bindi M (2002) Responses of agricultural crops to free-air CO2 enrichment. Adv Agron 77:293–368

Kiniry JR, Major DJ, Izaurralde RC, Williams JR, Gassman PW, Morrison M, Bergentine R, Zentner RP (1995) EPIC model parameters for cereal, oilseed, and forage crops in the northern great plains region. Can J Plant Sci 75:679–688

Kirkegaard JA, Hunt JR (2010) Increasing productivity by matching farming system management and genotype in water-limited environments. J Exp Bot 61(15):4129–4143

Ko J, Ahuja L, KIMBALL BA, Anapalli S, Ma L, Green TR, Ruane AC, WALL GW, PINTER JPJ, Bader DA (2010) Simulation of free air CO2 enriched wheat growth and interactions with water, nitrogen, and temperature. Agric For Meteorol 150(10):1331–1346

Latta J, O'Leary G (2003) Long-term comparison of rotation and fallow tillage systems of wheat in Australia. Field Crop Res 83:173–190

Li S, Wheeler T, Challinor A, Lin E, Xu Y, Ju H (2010) Simulating the impacts of global warming on wheat in China using a large area crop model. Acta Meteor Sin 24:123–135

Liu J, Wiberg D, Zehnder AJB, Yang H (2007) Modeling the role of irrigation in winter wheat yield, crop water productivity, and production in China. Irrig Sci 26(1):21–33

Liu B, Martre P, Ewert F, Porter JR, Challinor AJ, Müller C, Ruane AC, Waha K, Thorburn PJ, Aggarwal PK, Ahmed M, Balkovič J, Basso B, Biernath C, Bindi M, Cammarano D, De Sanctis G, Dumont B, Espadafor M, Eyshi Rezaei E, Ferrise R, Garcia-Vila M, Gayler S, Gao Y, Horan H, Hoogenboom G, Izaurralde RC, Jones CD, Kassie BT, Kersebaum KC, Klein C, Koehler A-K, Maiorano A, Minoli S, Montesino San Martin M, Naresh Kumar S, Nendel C, O'Leary GJ, Palosuo T, Priesack E, Ripoche D, Rötter RP, Semenov MA, Stöckle C, Streck T, Supit I, Tao F, Van der Velde M, Wallach D, Wang E, Webber H, Wolf J, Xiao L, Zhang Z, Zhao Z, Zhu Y, Asseng S (2019) Global wheat production with 1.5 and 2.0°C above pre-industrial warming. Glob Chang Biol 25(4):1428–1444. https://doi.org/10.1111/gcb.14542

Lobell DB, Hammer GL, Chenu K, Zheng B, McLean G, Chapman SC (2015) The shifting influence of drought and heat stress for crops in Northeast Australia. Glob Chang Biol 21 (11):4115–4127

Loomis RS, Rabbinge R, Ng E (1979) Explanatory models in crop physiology. Annu Rev Plant Physiol Plant Mol Biol 30:339–367

Lv ZF, Liu XJ, Cao WX, Zhu Y (2013) Climate change impacts on regional winter wheat production in main wheat production regions of China. Agric For Meteorol 171:234–248

Majoul-Haddad T, Bancel E, Triboi E, Branlard G, Martre P (2013) Effect of short heat shocks applied during grain development on wheat (Triticum aestivum L.) grain proteome. J Cereal Sci 57(3):486–495

Martín MM, Olesen JE, Porter JR (2014) A genotype, environment and management (GxExM) analysis of adaptation in winter wheat to climate change in Denmark. Agric For Meteorol 187:1–13
Mollah M, Norton R, Huzzey J (2009) Australian grains free-air carbon dioxide enrichment (AGFACE) facility: design and performance. Crop Pasture Sci 60(8):697–707. https://doi.org/10.1071/CP08354
Nendel C, Berg M, Kersebaum K, Mirschel W, Specka X, Wegehenkel M, Wenkel K, Wieland R (2011) The MONICA model: testing predictability for crop growth, soil moisture and nitrogen dynamics. Ecol Model 222:1614–1625
Nuttall JG, O'Leary GJ, Khimashia N, Asseng S, Fitzgerald G, Norton R (2012) 'Haying-off' in wheat is predicted to increase under a future climate in South-Eastern Australia. Crop Pasture Sci 63(7):593–605. https://doi.org/10.1071/CP12062
Nuttall JG, O'Leary GJ, Panozzo JF, Walker CK, Barlow KM, Fitzgerad GJ (2017) Models of grain quality in wheat—a review. Field Crop Res 202:136–145
O'Leary GJ, Connor DJ, White DH (1985) A simulation-model of the development, growth and yield of the wheat crop. Agric Syst 17:1–26
O'Leary GJ, Christy B, Nuttall J, Huth N, Cammarano D, Stöckle C, Basso B, Shcherbak L, Fitzgerald G, Luo Q, Farre-Codina I, Palta J, Asseng S (2015) Response of wheat growth, grain yield and water use to elevated CO2 under a Free-Air CO2 enrichment (FACE) experiment and modelling in a semi-arid environment. Glob Chang Biol 21:2670–2686
Olesen JE, Jensen T, Petersen J (2000) Sensitivity of field-scale winter wheat production in Denmark to climate variability and climate change. Clim Res 15:221–238
Olesen J, Petersen B, Berntsen J, Hansen S, Jamieson P, Thomsen A (2002) Comparison of methods for simulating effects of nitrogen on green area index and dry matter growth in winter wheat. Field Crop Res 74:131–149
Ottman MJ, Kimball BA, White JW, Wall GW (2012) Wheat growth response to increased temperature from varied planting dates and supplemental infrared heating. Agron J 104:7–16
Pan J, Zhu Y, Cao W (2007) Modeling plant carbon flow and grain starch accumulation in wheat. Field Crop Res 101:276–284
Paydar Z, Gallant J (2007) A catchment framework for one-dimensional models: introducing FLUSH and its application. Hydrol Process 22(13):2094–2104
Porter JR (1984) A model of canopy development in winter wheat. J Agric Sci 102:383–392
Porter JR (1993) AFRCWHEAT2: a model of the growth and development of wheat incorporating responses to water and nitrogen. Eur J Agron 2:69–82
Ritchie JT, Godwin DC, Otter-Nacke S (1985) CERES-wheat. A simulation model of wheat growth and development. Texas A&M University Press, College Station
Ritchie S, Nguyen H, Holaday A (1987) Genetic diversity in photosynthesis and water use efficiency of wheat and wheat relatives. J Cell Biochem 11 (Supplement B):43–43
Robertson MJ, Rebetzke GJ, Norton RM (2015) Assessing the place and role of crop simulation modelling in Australia. Crop Pasture Sci 66(9):877–893
Rodriguez D, deVoil P, Power B, Cox H, Crimp S, Meinke H (2011) The intrinsic plasticity of farm businesses and their resilience to change. An Australian example. Field Crop Res 124 (2):157–170
Rosenzweig C, Parry ML (1994) Potential impact of climate change on world food supply. Nature 367:133–138
Rosenzweig C, Elliott J, Deryng D, Ruane AC, Müller C, Arneth A, Boote KJ, Folberth C, Glotter M, Khabarov N, Neumann K, Piontek F, Pugh TAM, Schmid E, Stehfest E, Yang H, Jones JW (2014a) Assessing agricultural risks of climate change in the 21st century in a global gridded crop model intercomparison. PNAS 111(9):3268–3273
Rosenzweig C, Elliott J, Deryng D, Ruane AC, Muller C, Arneth A, Boote KJ, Folberth C, Yang H, Jones J, W. (2014b) Assessing agricultural risks of climate change in the 21st century in a global gridded crop model intercomparison. PNAS 111:3268–3273

Semenov MA, Shewry PR (2011) Modelling predicts that heat stress, not drought, will increase vulnerability of wheat in Europe. Sci Rep 1:5

Senthilkumar S, Basso B, Kravchenko AN, Robertson GP (2009) Contemporary evidence of soil carbon loss in the US corn belt. Soil Sci Soc Am J 73:2078–2086

Shibu M, Leffelaar P, van Keulen H, Aggarwal P (2010) LINTUL3, a simulation model for nitrogen-limited situations: application to rice. Eur J Agron 32:255–271

Soltani A, Maddah V, Sinclair R (2013) SSM-Wheat: a simulation model for wheat development, growth and yield. Int J Plant Prod 7:711–740

Spitters CJT, Schapendonk AHCM (1990) Evaluation of breeding strategies for drought tolerance in potato by means of crop growth simulation. Plant Soil 123:193–203

Steduto P, Hsiao T, Raes D, Fereres E (2009) Aquacrop-the FAO crop model to simulate yield response to water: I. concepts and underlying principles. Agron J 101:426–437

Stenger R, Priesack E, Barkle G, Sperr C (1999) Espert-N A tool for simulating nitrogen and carbon dynamics in the soil-plant-atmosphere system. In: Tomer M, Robinson M, Gieleng G (eds) NZ land treatment collective proceedings technical session 20: modeling of land treatment systems. New Plymouth, New Zealand, pp 19–28

Stockle C, Donatelli M, Nelso R (2003a) CropSyst, a cropping systems simulation model. Eur J Agron 18:289–307

Stockle C, Donatelli M, Nelson R (2003b) CropSyst, a cropping systems simulation model. Eur J Agron 18:289–307

Stöckle CO, Kemanian AR (2020) Can crop models identify critical gaps in genetics, environment, and management interactions? Front Plant Sci 11:737. https://doi.org/10.3389/fpls.2020.00737

Tao F, Zhang Z (2013) Climate change, wheat productivity and water use in the North China plain: a new super-ensemble-based probabilistic projection. Agric For Meteorol 170:146–165

Tao F, Zhang Z, Liu J, Yokozawa M (2009) Modelling the impacts of weather and climate variability on crop productivity over a large area: a new super-ensemble-based probabilistic projection. Agric For Meteorol 149:1266–1278

Tester M, Langridge P (2010) Breeding technologies to increase crop production in a changing world. Science 327(5967):818–822

Tubiello FN, Rosenzweig C, Kimball BA, Pinter PJ, Wall GW, Hunsaker DJ, LaMorte RL, Garcia RL (1999) Testing CERES-wheat with Free-Air Carbon Dioxide Enrichment (FACE) experiment data: CO2 and water interactions. Agron J 91:247–255

van Bussel LGJ, Stehfest E, Siebert S, Müller C, Ewert F (2015) Simulation of the phenological development of wheat and maize at the global scale. Glob Ecol Biogeogr 24(9):1018–1029

Vanuytrecht E, Raes D, Stedduto P, Hsiao T, Heng LK, Vila MG, Moreno PM (2014) AquaCrop: FAO's crop water productivity and yield response model. Environ Model Softw 62:351–360

Wall GW, Kimball BA, White J, Ottman MJ (2011) Gas exchange and water relations of spring wheat under full-season infrared warming. Glob Chang Biol 17:2113–2133

Wallach D, Martre P, Liu B, Asseng S, Ewert F, Thorburn PJ, van Ittersum M, Aggarwal PK, Ahmed M, Basso B, Biernath C, Cammarano D, Challinor AJ, De Sanctis G, Dumont B, Eyshi Rezaei E, Fereres E, Fitzgerald GJ, Gao Y, Garcia-Vila M, Gayler S, Girousse C, Hoogenboom G, Horan H, Izaurralde RC, Jones CD, Kassie BT, Kersebaum KC, Klein C, Koehler A-K, Maiorano A, Minoli S, Müller C, Naresh Kumar S, Nendel C, O'Leary GJ, Palosuo T, Priesack E, Ripoche D, Rötter RP, Semenov MA, Stöckle C, Stratonovitch P, Streck T, Supit I, Tao F, Wolf J, Zhang Z (2018) Multimodel ensembles improve predictions of crop–environment–management interactions. Glob Chang Biol 24(11):5072–5083. https://doi.org/10.1111/gcb.14411

Wang E, Engel T (2002) Simulation of growth, water and nitrogen uptake of a wheat crop using the SPASS model. Environ Model Softw 17(4):387–402

Wang E, Robertson MJ, Hammer GL, Carberry PS, Holzworth D, Meinke H, Chapman SC, Hargreaves JNG, Huth NI, McLean G (2002) Development of a generic crop model template in the cropping system model APSIM. Eur J Agron 18:121–140

Williams JR, Jones CA, Kiniry JR, Spanel DA (1989) The EPIC crop growth-model. Trans ASABE 32:497–511

Wing IS, De Cian E (2014) Modelling agricultural adaptation. Nat Clim Chang 4:535–536

Wong MTF, Asseng S (2006) Determining the causes of spatial and temporal variability of wheat yields at sub-field scale using a new method of upscaling a crop model. Plant Soil 283 (1–2):203–215

Zhao G, Hoffmann H, van Bussel LGJ, Enders A, Specka X, Sosa C, Yeluripati J, Tao F, Constantin J, Raynal H, Teixeira E, Grosz B, Doro L, Zhao Z, Nendel C, Kiese R, Eckersten H, Haas E, Vanuytrecht E, Wang E, Kuhnert M, Trombi G, Moriondo M, Bindi M, Lewan E, Bach M, Kersebaum K, Rötter R, Roggero PP, Wallach D, Cammarano D, Asseng S, Krauss G, Siebert S, Gaiser T, Ewert F (2015) Effect of weather data aggregation on regional crop simulation for different crops, production conditions, and response variables. Clim Res 65:141–157. https://doi.org/10.3354/cr01301

Zheng B, Chenu K, Chapman SC (2016) Velocity of temperature and flowering time in wheat – assisting breeders to keep pace with climate change. Glob Chang Biol 22(2):921–933

Ziska LH, Bunce JA (2007) Predicting the impact of changing CO2 on crop yields: some thoughts on food. New Phytol 175:607–618

Genetic Analysis

7

Munir Ahmad and Rashid Mehmood Rana

Abstract

Analysis of complex relationships between genotype and phenotype is imperative for crop improvement and better production. Genetic analysis started when humans practiced selective breeding for crop improvement and reorganized with the advent of the Mendelian genetic principles. Genetic analysis requires phenotyping and genotyping followed by application of statistical principles. Advances in the field of automation and informatics lead to high-throughput phenotyping and genotyping which eventually revolutionized the field of genetic analysis. Massive parallel sequencing (MPS) based on genotyping by sequencing (GBS) is one of the best high-throughput genotyping techniques utilized for discovering single-nucleotide polymorphism (SNP) in crop genomes and provides the insight into the genome, epigenome, and transcriptome on an extraordinary scale. Estimation of the type and extent of gene action controlling the inheritance of quantitative traits is made possible through genetic analysis. Genotype by genotype by environment (GGE) interaction is useful for evaluation of genotypes in mega-environment. Mapping of quantitative trait loci (QTL) is made through association between genotypic and phenotypic data and reveals the genetic basis of variation of multifactor traits in crop plants. The identified QTLs could be utilized as marker-assisted selection tool to enhance the efficiency of a breeding program dealing with the improvement of quantitative traits in a crop breeding program.

M. Ahmad (✉) · R. M. Rana
Department of Plant Breeding and Genetics, PMAS-Arid Agriculture University, Rawalpindi, Pakistan
e-mail: muneer.ahmad@uaar.edu.pk

M. Ahmed (ed.), *Systems Modeling*, https://doi.org/10.1007/978-981-15-4728-7_7

Keywords

Genotype environment interaction · Heritability · Association mapping · Sequencing · Molecular markers

Abbreviation

AFLP	Amplified fragment length polymorphism
AMMI	Additive main effects and multiplicative interaction
ANOVA	Analysis of variance
BC	Backcross
CIMMYT	International Maize and Wheat Improvement Center
COI	Crossover interaction
CSSLs	Chromosome segment substitution lines
DH	Double haploid
DNA	Deoxyribonucleic acid
EDTA	Ethylenediaminetetraacetic acid
GBS	Genotyping by sequencing
GEI	Genotype by environment interaction
GGE	Genotype by genotype by environment
IL	Introgressive lines
MPS	Massive parallel sequencing
NGS	Next-generation sequencing
NILs	Near-isogenic lines
PCA	Principal component analysis
QEI	QTL-by-environment interactions
QTL	Quantitative trait analysis
RAPD	Random amplified polymorphic DNA
RFLP	Restriction fragment length polymorphism
RHLs	Residual heterozygous lines
RIL	Recombinant inbred line
SNP	Single-nucleotide polymorphism
SSLs	Single-segment lines
SSR	Simple sequence repeats
SVD	Singular value decomposition

7.1 Introduction

Genetic analyses are related to understand the complex relationships between genotype and phenotype. Fundamental research work which laid down the foundation of genetic analysis started in ancient time when human practiced selective breeding for crop improvement. Modern genetic analysis started with the advent of the Mendelian genetic works and principles. Gregor Mendel was the first who studied the transmission genetics and genetic analysis. His major findings included that traits were transferred from parents to offspring and traits can differ among offspring. Later on it was confirmed that these traits are controlled by genes. The study of biologically inherited traits, including traits that are influenced in part by the environment, is referred as genetics (Wilstermann 2019), whereas the overall process of studying and researching in fields of science that involve genetics and molecular biology is called as genetic analysis. Numerous techniques and processes have been developed to study the genetic analysis including conventional and modern approaches.

Genetic analysis involves a set of genetic populations. A genetic population is derived from F_1 obtained after a cross between two genetically distinct parents. There are two main types of populations used for genetic analysis. (1) Primary population includes F_2 and its derivatives (e.g., F_3, F_4 lines), BC_1, BC_2, DH, RIL, and IF_2 (immortalized F_2). (2) Secondary populations included NILs, residual heterozygous lines (RHLs), QTL isogenic recombinant lines (QIRs), introgressive lines (ILs), single-segment lines (SSLs), and chromosome segment substitution lines (CSSLs) (Tian et al. 2015a).

7.2 Prerequisite of Genetic Analysis

7.2.1 Plant Phenomics

Plant phenomics is the study of plant growth, performance and composition. It is derived from the word phenome which means expression of a gene in an environment. The term forward phenomics is used to screen large population for important traits. Screening of germplasm could be high-throughput higher-resolution or lower-throughput measurements (Furbank and Tester 2011). The process of collecting the information of phenotype or characterizing a phenotype is called phenotyping. An essential principle of genetics is the phenotype-genotype relationship. Phenotype is the combination of all the morphological, physiological, biochemical, and developmental characteristics (Ahmed et al. 2020). Genotype is the hereditary information contained in the individual. In plant breeding, agronomy, ecology, and physiology, phenotyping is frequently practiced (Pieruschka and Poorter 2012).

Crop improvement programs for biotic or abiotic stress tolerance through conventional or nonconventional techniques depend on high-quality measurements of field experiment. Field experiments conducted for abiotic stress tolerance require special attention. Understanding the ecology of target population, site selection of experiment, maintenance of suitable large plant population, plant border rows to minimize the border effects, application of recommended dose of fertilizers, effective control of weed and insect pests, and drought treatment imposition and resumption are important considerations for accurate phenotyping (Zaidi 2019).

Phenotypes can be characterized in different ways.

(i) Manual or conventional phenotyping: Traits visible to the naked eyes are in general measured manually. Various plant traits are measured manually, e.g., plant height, spike length, spikelets and grain number, fruit or pod number, etc. In some cases destructive sampling is required for the measurement of trait, e.g., fresh shoot and root weight, dry shoot and root weight, fruit fresh weight, etc. Manual phenotyping is laborious, low-throughput, and time-consuming, and it is difficult to evaluate large number of sample. Due to variation between the observers, there are more chances of experimental error.

(ii) High-throughput or automated phenotyping: Automated phenotyping provides precise, accurate, large-scale, and fast trait measurements; nevertheless, its adoption in crop improvement is limited due to high cost of equipments. A high-throughput phenotyping system mechanically observes and grows many plant samples for analysis. Advancement in automated imaging has made possible the use of digital imaging for high-throughput phenotyping of plants. The use of whole shoot imaging is nondestructive, and plant growth and development can be studied throughout their life cycle.

7.2.2 High-Throughput Phenotyping in Plants

High-throughput phenotyping of important plant traits is getting significant consideration to characterize gene function and circadian rhythms. Digital imaging is not a recent technique; it has been in use for a long time. Automated digital imaging made plant shoot phenotyping high-throughput. Digital imaging is nondestructive; therefore, the same plant can be used for sampling throughout its life cycle. Digital images can be saved and reanalyzed through improved image processing techniques.

Plant root monitoring system has made possible the high-throughput phenotyping of seedlings. The extraordinary accuracy of automated image processing software made it much suitable for exploration of root elongation rate and detection of circadian and diurnal rhythms in root elongation. Chlorophyll content is an important indicator of plant growth under stress conditions. Conventional methods used for the determination of chlorophyll content are time-consuming and not suitable for evaluating large numbers of samples. High-throughput chlorophyll determination analysis of fluorescence images presents better choice. Additionally, these methods also permit evaluation of the same leaf repetitively at different growth stages.

Prediction of effects of climate change and efficient ecosystem management needs better models to know how plants and climate interact from individual to ecosystem levels. Monitoring of phenological plant stages over large spatial and temporal scales through conventional methods is time-consuming, laborious, and intricate. Conventional sampling and satellite imaging have no sufficient spatial and temporal resolution for the collection of plant data. Therefore, there is a dire need of high-throughput technology for large-scale data collection. This type of data collection has been recently termed “near-surface” remote sensing. Development of economical, high-resolution imaging systems, dynamic computers, and wireless and solar technology offers break through to revolutionize the quality of phenological data that can be collected in the field. A latest developed camera system called Gigavision has the ability to record hourly, gigapixel resolution panoramic image set in the field (Normanly 2012).

7.3 Mendelian and Non-Mendelian Genetics

Mendelian genetics is a type of inheritance which follows the Mendel's laws of dominance, segregation, and independent assortment. A trait controlled by a single locus of qualitative nature is called Mendelian trait, e.g., pod shape, seed color, and flower position in pea plant. Any mutation in Mendelian trait follows the typical Mendelian inheritance, e.g., sickle cell anemia. Genetic analyses of Mendelian traits are carried out following monohybrid, dihybrid, trihybrid, test cross ratios, chi-square test, etc.

On the other hand, non-Mendelian genetics do not follow the Mendel's laws of inheritance. There are numerous exceptions where traits do not follow the Mendelian inheritance, e.g., cytoplasmic inheritance, incomplete dominance, codominance, epistasis, pleiotropy, multiple alleles, polygenic and sex influenced traits, linkage, epigenetics, bar bodies, domestication, reduced penetrance, variable expressivity, etc.

7.4 Forward and Reverse Genetic Analysis

Forward genetics studies the genetic basis of an inherited variation. "Forward genetic analysis starts with a genetic screen that identifies specific phenotypic abnormalities in a population of organisms that have been mutagenized." Reverse genetic analysis starts with a gene sequence and looks for the identification of subsequent mutant phenotype. In this technique loss-of-function alleles of particular genes are created by various methods, and consequential phenotypes are studied to know how they vary from the wild type.

Forward genetic approach is used to recognize genes concerned with a biological process through screening of mutated population having random variation throughout the genome that can alter the gene function. In forward genetic analysis first of all, heritable mutations are generated in a population that are screened for a particular phenotypic effect. Large numbers of individuals (inbred lines) are mutated through a mutagenic approach called saturation mutagenesis followed by screening of mutant individuals. These mutations are variable and only individual with useful mutations are selected. The heritable mutated variation is then used to study the inheritance pattern and the normal functions of associated gene. Eventually, the gene sequence responsible for the anomaly is determined and may propose the function of resultant gene product. Dominance/recessiveness of the mutated allele is evaluated following the Mendelian inheritance. Homozygous mutant individuals are crossed with wild type, and resulting F_1will help us to designate the allele as recessive or dominant (Sanders and Bowman 2014).

7.5 Qualitative and Quantitative Genetics

Traits regulated by single or a few genes with major effects are known as qualitative traits, and their inheritance is called qualitative inheritance. Qualitative traits can be easily distinguished, least affected by environment, and have discrete classes, e.g., seven Mendelian traits, two-row or six-row barley, and hooded or awned wheat spike. Mendel used monohybrid, dihybrid, trihybrid, and test crosses to analyze the qualitative traits in *Pisum sativum*. Traits regulated by polygene with additive effects are known as quantitative traits, and their inheritance is called quantitative inheritance. Quantitative traits are much influenced by environment, continuous in their expression, and cannot be classified into discrete classes, e.g., grain yield and plant height in wheat. The effect of individual gene in controlling a particular trait is so small to be calculated; instead the effect of all the genes controlling a trait is measured. Johannsen and Nilssen-Ehle measured the seed size and weight in princess bean and seed color in wheat and concluded that inheritance of these traits is not as simple as of monogenic traits (Poehlman 2013).

7.5.1 Genetic Analysis of Quantitative Traits

There is simplest relationship between genotype and phenotype when a genetic variation is controlled by a single gene. In the absence of gene interaction, segregation of alleles of a single gene determines if a pea plant will be tall or short. Many traits are regulated by interaction among the genes at different loci. Additionally various traits are polygenic in nature which are also influenced by environment; these are called multifactorial traits, e.g., weight and height in plants and animals (Sanders and Bowman 2014).

Quantitative traits can be controlled by oligogenes with major effect or by a numerous genes with minor effect. The genetic effect of every minor gene can be of diverse nature. Gene action can be of additive, dominant, or epistatic type; in addition to this, there may be interaction between genes and environment (Tian et al. 2015b). Abiotic stress (drought, heat, salinity) tolerance is a multifactorial trait controlled by 16 genes (Yu et al. 2018).

Sir Ronald Fisher utilized statistical approaches for genetic analysis of quantitative traits in 1918. He used statistical techniques and concluded that quantitative traits arise due to segregation of alleles of polygenes having additive effects. Frequency distribution is the first step in the quantification of phenotypic variation of quantitative traits. Sample size and number of classes are very important for the reliability of frequency distribution of data set. Identification of mode and median is also significant for the study of quantitative trait distribution.

Variance is the “numerical measurement of the spread of distribution around the mean.” Variance analysis is useful when data is normally distributed and not skewed. The value of the variance will be small when most of the observations are present around the mean. Large variance value indicates the wide spread of the data around the mean and shows greater genetic variation for that trait (Sanders and Bowman 2014). Variance is calculated following the formula given below:

$$S^2 = \frac{\sum x^2 - \frac{\left(\sum x\right)^2}{n}}{n - 1}$$

Total variance or phenotypic variance is further divided as

$$V_{\mathrm{p}} = V_{\mathrm{G}} + V_{\mathrm{E}}$$

$$V_{\mathrm{G}} = V_{\mathrm{A}} + V_{\mathrm{D}} + V_{\mathrm{I}} + V_{\mathrm{E}}$$

V_{P} = phenotypic variance (variance due to variation in quantitative trait).
V_{G} = genotypic variance (proportion of phenotypic variance that is due to variation in genotypes).
V_{A} = additive variance (variance due to genes having additive effect).
V_{D} = dominance variance (variance due to genes having dominant effect).
V_{I} = interaction variance (variance due to interaction between genotype and environment).
V_{E} = environmental variance (proportion of phenotypic variance that is due to variation in the environment of the individual's habitat).

7.5.2 Heritability and Its Role in Selection

"The degree to which the variability of a quantitative character is transmitted to the progeny is referred to as its heritability." When genetic differences in a progeny are greater than environmental differences, then heritability will be high and vice versa. When genetic variation is higher than environmental variation, then selection is more efficient.

Broad-sense heritability (H^2) is the proportion of phenotypic variance that is due to genetic variance. It is called broad sense because it estimates heritability from all types of genetic variances.

$$H^2 = {}^{V_{\mathrm{G}}}\!/_{V_{\mathrm{P}}}$$

or

$$H^2 = {}^{V_{\mathrm{G}}}\!/_{V_{\mathrm{P}}} \times 100$$

The narrow-sense heritability (h^2) is the proportion of phenotypic variance that is only due to additive variance. It is more useful and usually less than the broad-sense heritability.

Polygenic traits are greatly influenced by the environment; that is why they differ in heritability estimates. Yield of the plant is a quantitative trait, greatly influenced by the environment, and has low heritability. On the other hand, qualitative trait has high heritability as they are least affected by the environment. Selection procedure depends on the genetics and heritability of the trait. Traits having low heritability (e.g., yield) cannot be selected efficiently in the early segregating generation (F_2). For such traits selection in the lateral generation will be successful. Traits having high heritability can be selected efficiently in the early segregating generation (Poehlman 2013).

7.6 Genotype by Environment Interaction (GEI)

Genotype by environment interaction (GEI) can be explained by the combined effect of genotype and environmental factors that alter the gene frequency in a population. Changing environment can change the gene frequency in population, or the genotype is not independent of change in environment. It is a major factor that can alter a phenotype and hence shows a range of variation, hence shows the statistical concept of "heteroscedasticity," where a single variance is insufficient to explain the variability of different genotypes (Shah et al. 2009).

GEI may be unsystematic or directional (if the mean of subgroup increases so does the variance). Experimental analysis on *Drosophila* have revealed that GEI commonly occurs in many systems, but rarely accounts for more than 20% of the total phenotypic variation (Saltz et al. 2018).

7.6.1 Genotypic Performance Stability

The performance of genotypes is explained and grouped into static and dynamic stability. Static stability is explained by stable performance of genotypes in different environments, and no environmental variations occur. It is also referred as biological stability, and increase in inputs does not affect the genotypic performance. With regard to dynamic performance (also known as agronomic stability), the genotypic performance varies among different environments (Kaya and Turkoz 2016).

7.6.2 Linear-Bilinear Model

Linear-bilinear models determine the subgroups of genotype and environment with neglecting the COI (crossover interaction). It is classified into many models, among which two-way ANOVA is the basic one and used widely to determine the GEI.

The environment and genotype stability is estimated by AMMI (additive main effects and multiplicative interaction) model and describes the least square of parameter with their mean values (Das et al. 2018). So by substituting the genotypic and environment means on x-axis and PCA score on y-axis forms a bi-plot model. Based on the PCA values, by supposing the first PCA as the most important pattern of the GEI, specific interaction single genotype and environment are determined. It also estimates the identification of pattern of GEI. It may also help to estimate the eigenvalues for genotype and environment and also for PCA1 means. If the PCA1 value is closed to zero, it represents the common adaptation to tested environment. Poor genotype shows PCA1 value zero. If it is a large value, then performance is also high. The positive values show linear relation with the environment and genotype, while negative PCA1 values show the relation is inverse (Mohammed 2009).

7.6.3 Analysis Based on GGE Bi-plot

Genotype by genotype by environment (GGE) interaction bi-plot was first described by Gabriel (1971) and modified by Yan et al. (2000), Yan and Kang (2002), and Yan and Tinker (2006). It is useful for detecting the GEI in many fields including agriculture for evaluation of mega-environment (Ahmed et al. 2020). These provide the two sources of variation related to cultivar evaluation of both G and GE with singular value decomposition (SVD) of the environment focused.

$$\bar{y}ij - \mu j = \sum_{k=1}^{t} \aleph \mathrm{k}\ \alpha ik\ \gamma j + \bar{\varepsilon} ij$$

7.7 Molecular Events

Looking at molecular events, at population level, polymorphism is highly demanding because through the combination of many alleles in population, many recombinant-tolerant genotypes may be obtained. Haploids are more polymorphic and require no maintenance of genetic variation in population for diploids and sexual reproduction. GEI is very laborious for alleles favored by the environment if selection is done in it. So no surety of protection of polymorphism is ensured while changes in ranking occur. Experiment made on natural and laboratory lactose operon mutant of *E. coli* determines environment and genetic variation. This reveals the growth rate was limited by nutrient galactosides in varying environment. This result shows the significant differences in fitness among operon strain in varying environment which was estimated by one-way ANOVA. Also estimation made by linear additive model shows this differences is due to GEI. Molecular investigation also proves this by using the strain DD320, which has no ability to metabolize any galactosides (Dean 1995).

Molecular markers are now widely used for finding region on chromosome responsible for variation, and approaches are also developed to quantify these traits in different environments. Molecular techniques can also investigate the environmental portioning of various environmental components and genetic control of various environmental traits such as phototropism, male sterility, and temperature sensitivity. For instance, taking the example of rice recombinant inbred lines (RILs), CO39 exposed to different photo-regimes and individual lines were evaluated for 10-h and 14-h day length for days to flowering. Associated loci have been identified on the basis of delay in flowering less than the 14 h. For this 15 QTLs were distinguish, out of which four were also identified as associated to photoperiod and present on chromosome 7. Marker-based investigation provides better understanding about quantitative traits evaluation of QEI and GEI (Rodrigues 2018).

7.7.1 Molecular Marker-Based Linkage Maps

Quantitative trait loci (QTL) mapping requires phenotypic as well as genotypic data. Genotypic data is obtained through molecular marker. Molecular marker is a trackable and quantifiable segment of DNA having association with a particular trait of interest (Hayward et al. 2015). There have been several molecular marker techniques evolved since the discovery of molecular markers. These techniques include RFLP (restriction fragment length polymorphism), AFLP (amplified fragment length polymorphism), RAPD (random amplified polymorphic DNA), microsatellite/SSR (simple sequence repeats), SNP (single-nucleotide polymorphism), etc. Among these techniques, SNPs are latest and considered as best markers as these markers could be discovered on whole-genome basis. The SNPs are best discovered by sequencing, hence called as genotyping by sequencing (GBS) (He et al. 2014). There are different types of platforms used for sequencing. Massive parallel sequencing (MPS) and Illumina dye sequencing are the most famous methods used for SNP discovery through GBS. A short detail of MPS is given as under.

7.7.2 Massive Parallel Sequencing (MSP)

Massive parallel sequencing is a next-generation sequencing (NGS) approach using massive parallel sequencing (He et al. 2014). The MPS starts with the sequencing of in vitro synthesized DNA sequencing libraries followed by sequencing by synthesis. Finally, simultaneous sequencing of spatially segregated, amplified DNA templates is carried out in a massively parallel fashion without the requirement for a physical separation step (He et al. 2014).

7.7.3 DNA Extraction and Quality Assessment

There are several methods available for DNA extraction (Table 7.1). However, the most utilized, easy, and cost-effective method is CTAB (cetyltrimethylammonium bromide) DNA extraction method (Yu et al. 2019). Plant samples are ground in liquid nitrogen to make fine powder. The powder is then homogenized with CTAB buffer (2% cetyltrimethylammonium bromide, 1% polyvinylpyrrolidone, 100 mM Tris-HCl, 1.4 M NaCl, 20 mM EDTA). The homogenate is mixed by vortexing and incubated at 65° C for 30 min. After incubation, the homogenate is centrifuged

Table 7.1 DNA extraction methods commonly used for plants

Methods	Plant source	Solution
DNeasy Plant Mini Kit	Plant cells, plant tissues and fungi	Buffers DNeasy Plant Mini Kit EtOH 100%
Sorbitol DNA extraction	Endocarp, hard leaves, woody bark	Liquid nitrogen Extraction buffer (0.1 M Tris-HCl 0.005 M EDTA 0.35 M sorbitol 10 nM 2-mercaptoethanol) lysis buffer (0.2 M Tris-HCl 0.05 M EDTA 2 M NaCl 2% CTAB) Chloroform-isoamyl alcohol (24:1) Isopropanol 80% EtOH TE
CTAB extraction	Leaves root endocarp, stem, or embryo	CTAB isolation buffer chloroform-isoamyl alcohol (24:1) isopropanol EtOH TE
Genome DNA purification GenElute™ plant genomic DNA purification kit	Leaves root endocarp, stem, or embryo and fungi	Liquid nitrogen Lysis solution (part A + part B) Precipitation solution Binding solution Wash solution EtOH 100%

(14,000×g) for 5 min. The resultant supernatant is treated with RNase at 32° C for 20 min to digest any RNA present in the solution. An equal volume of chloroform/ isoamyl alcohol (24:1) is added to the samples followed by centrifugation (14,000×g) for 1 min. Supernatant is separated into a new tube, and 0.7 volume isopropanol (chilled) is added to the samples and mixed by inversion. The samples are incubated on ice for 10 min and centrifuged (14,000×g) for 10 min. Supernatant is discarded to recover pellet containing DNA. The DNA pallet is washed twice with 70% ethanol. After drying the ethanol residues, DNA pallet is resuspended in TE buffer (10 mM Tris, pH 8, 1 mM EDTA).

The extracted DNA is evaluated for quality through gel electrophoresis as well as spectrophotometer. A good-quality DNA shows intact band while runs on 1% agarose gel. DNA purity is evaluated by measuring absorbance of sample at 260 and 280 nm. A ratio of A260/A280 is calculated, and samples having the ratio of 1.7–2.0 are ranked as good for their DNA quality (Canforaa and Rosb 2018).

7.8 QTL Mapping Across Environments

Environmental factors act as the regulator of gene expression for quantitative traits. Great phenotypic variation occurs in these traits due to varying external conditions. Soil moisture, temperature, and humidity are the key factors responsible for change in phenotypic expression of that traits. Many QTLs were identified for varying environmental conditions (Aslam et al. 2017). Some of them are shows that QTL detection depends on special environment, and these were called as "environmental-dependent" QTLs. Results obtained from multiple environment from QTL detection tells the strong estimation of QEI (QTL + GEI) and GEI and explains the trait dependence on the environment (Courtois et al. 2009).

7.9 Breeding for GEI

For efficient use of GEI in breeding, three strategies must adopted by utilization of genotypic mean in the environment even when GEI exists. These three ways are ignoring them, avoiding them, and exploiting them. If interaction is significant and of crossover type, then interaction should not be ignored. If interaction is less significant, then avoid them. For this, make cluster of similar environments. In this type of environment, genotype may show the same performance and COIs would not be expected, and useful data may be lost. Different research areas working on wheat and rice, such as CIMMYT, propose the broad-range adaptation of these crops (Kang 2002). Broad adaptation of these crops can be done by using few environmental sites and optimizing the environment to eliminate factors that are the same to each other. Stability of genotype in any environment can be explained by using the third approach, exploitation. This can help in estimating the GEI and give an approach to correct them. Genotype can only be improved if problem is known, and utilization of genetic means and proper environment can be provided to increase the productivity (Eisemann 1981).

7.10 Conclusion

All the traits of an organism are controlled either by single or multiple genes. The traits controlled by multiple genes are known as quantitative traits harboring continuous variation. Quantitative traits are affected by the environment; hence understanding genotype by the environment interaction is a prerequisite to study such traits. Molecular markers are used to detect genomic regions responsible for controlling quantitative traits. These regions are called quantitative trait loci (QTL). These QTLs are greatly helpful in identifying genes controlling a trait. Moreover, markers associated to a QTL could be employed in marker-assisted breeding for improving a quantitative trait.

References

Ahmed K, Shabbir G, Ahmed M, Shah KN (2020) Phenotyping for drought resistance in bread wheat using physiological and biochemical traits. Sci Total Environ 729:139082. https://doi.org/10.1016/j.scitotenv.2020.139082

Aslam MU, Shehzad A, Ahmed M, Iqbal M, Asim M, Aslam M (2017) QTL Modelling: an adaptation option in spring wheat for drought stress. In: Ahmed M, Stockle CO (eds) Quantification of climate variability, adaptation and mitigation for agricultural sustainability. Springer International Publishing, Cham, pp 113–136. https://doi.org/10.1007/978-3-319-32059-5_6

Canforaa L, Rosb M (2018) 2. Deoxyribonucleic acid (DNA) extraction. In: Crop diversification and low-input farming across Europe: from practitioners' engagement and ecosystems services to increased revenues and value chain organisation: 22–25

Courtois B, Ahmadi N, Khowaja F, Price AH, Rami J-F, Frouin J, Hamelin C, Ruiz M (2009) Rice root genetic architecture: meta-analysis from a drought QTL database. Rice 2(2):115

Das CK, Bastia D, Naik B, Kabat B, Mohanty M, Mahapatra S (2018) GGEBiplot and AMMI analysis of grain yield stability & adaptability behaviour of paddy (Oryza sativa L.) genotypes under different agro-ecological zones of Odisha. Oryza 55(4):528–542

Dean AM (1995) A molecular investigation of genotype by environment interactions. Genetics 139 (1):19–33

Eisemann R (1981) Two methods of ordination and their application in analysing genotype environment interactions. In: Byth DE, Mungomery VE (eds) Interpretation of plant response and adaptation to agricultural environments. Australian Institute of agricultural Sciences, Brisbane, pp 293–307

Furbank RT, Tester M (2011) Phenomics–technologies to relieve the phenotyping bottleneck. Trends Plant Sci 16(12):635–644

Gabriel KR (1971) The biplot graphic display of matrices with application to principal component analysis. Biometrika 58(3):453–467

Hayward AC, Tollenaere R, Dalton-Morgan J, Batley J (2015) Molecular marker applications in plants. In: Plant genotyping. Springer, New York, pp 13–27

He J, Zhao X, Laroche A, Lu Z-X, Liu H, Li Z (2014) Genotyping-by-sequencing (GBS), an ultimate marker-assisted selection (MAS) tool to accelerate plant breeding. Front Plant Sci 5:484

Kang MS (2002) Chapter 15: Genotype–environment interaction: progress and prospects. In: Quantitative genetics, genomics, and plant breeding. CAB International, Wallingford, p 219

Kaya Y, Turkoz M (2016) Evaluation of genotype by environment interaction for grain yield in durum wheat using non-parametric stability statistics. Turk J Field Crops 21(1):51–59

Mohammed MI (2009) Genotype × environment interaction in bread wheat in northern Sudan using AMMI analysis. Am Eurasian J Agric Environ Sci 6:427–433

Normanly J (2012) High-throughput phenotyping in plants: methods and protocols. Springer, Totowa

Pieruschka R, Poorter H (2012) Phenotyping plants: genes, phenes and machines. Funct Plant Biol 39(11):813–820

Poehlman JM (2013) Breeding field crops. Springer, New York

Rodrigues PC (2018) An overview of statistical methods to detect and understand genotype-by-environment interaction and QTL-by-environment interaction. Biometr Lett 55(2):123–138

Saltz JB, Bell AM, Flint J, Gomulkiewicz R, Hughes KA, Keagy J (2018) Why does the magnitude of genotype-by-environment interaction vary? Ecol Evol 8(12):6342–6353

Sanders MF, Bowman JL (2014) Genetic analysis: an integrated approach. Pearson Education, New York

Shah SH, Shah SM, Khan MI, Ahmed M, Hussain I, Eskridge KM (2009) Nonparametric methods in combined heteroscedastic experiments for assessing stability of wheat genotypes in Pakistan. Pak J Bot 41(2):711–730

Tian J, Deng Z, Zhang K, Yu H, Jiang X, Li C (2015a) Genetic analysis methods of quantitative traits in wheat. In: Genetic analyses of wheat and molecular marker-assisted breeding, vol 1. Springer, Dordrecht, pp 13–40

Tian J, Zhiying D, Zhang K, Yu H, Jiang X, Li C (2015b) Genetic analyses of wheat and molecular marker-assisted breeding, volume 1: genetics map and QTL mapping. Springer, Dordrecht

Wilstermann AM (2019) THE GENE: from genetics to postgenomics. Perspect Sci Christ Faith 71 (3):184–187

Yan W, Hunt LA, Sheng Q, Szlavnics Z (2000) Cultivar evaluation and mega-environment investigation based on the GGE biplot. Crop Sci 40(3):597–605

Yan W, Kang MS (2002) GGE biplot analysis: a graphical tool for breeders, geneticists, and agronomists. CRC press, Boca Raton, FL

Yan W, Tinker NA (2006) Biplot analysis of multi-environment trial data: principles and applications. Can J Plant Sci 86(3):623–645

Yu Z, Wang X, Zhang L (2018) Structural and functional dynamics of dehydrins: a plant protector protein under abiotic stress. Int J Mol Sci 19(11):3420

Yu D, Zhang J, Tan G, Yu N, Wang Q, Duan Q, Qi X, Cheng M, Yan C, Wei Z (2019) An easily-performed high-throughput method for plant genomic DNA extraction. Anal Biochem 569:28–30

Zaidi PH (2019) Management of drought stress in field phenotyping. CIMMYT, Mexico

8 Sugarcane: Contribution of Process-Based Models for Understanding and Mitigating Impacts of Climate Variability and Change on Production

Henrique Boriolo Dias and Geoff Inman-Bamber

Abstract

Sugarcane is cultivated on about 26 M ha across tropics and subtropics worldwide as a source of many industrial products, especially sugar and also bioenergy purposes (biofuel as ethanol and electricity). As the crop is grown in a wide range of climates, soils, and countries, different cropping systems are adopted across producing areas, resulting in large genotype × environment × management interactions, consequently large variations in yield levels are found. Climate and its variability and change play an important role in plant processes. In this chapter, a climate characterization of the main producing countries is presented along with the influence of main weather variables on sugarcane growth, development, and yields. The key variables of climate change are also explored. The effect of weather conditions on key sugarcane yield-building processes are well captured by process-based models. Two are embedded in the well-known and readily available agricultural systems modeling platforms; DSSAT/CANEGRO and APSIM-Sugar. These two models and a third (WaterSense) are described briefly with highlights of recent improvements and weaknesses. Finally, this chapter lists a series of application papers found so far in literature that included, at least to some extent, the intrinsic effect of climate and its variability mostly based on long-term weather data series. Special focus is then given to irrigation and nitrogen management, yield analysis (gaps, benchmarking, and forecasting), climate change issues, drought adaptation, and breeding studies. Even though

H. B. Dias (✉)
Biosystems Engineering Department, "Luiz de Queiroz" College of Agriculture, University of São Paulo, Piracicaba, SP, Brazil
e-mail: henrique.boriolo.dias@usp.br

G. Inman-Bamber
College of Science, Technology and Engineering, James Cook University, Townsville, QLD, Australia
e-mail: geoff.inmanbamber@jcu.edu.au

M. Ahmed (ed.), *Systems Modeling*, https://doi.org/10.1007/978-981-15-4728-7_8

sugarcane models have some weaknesses, they are considered as powerful tools for understanding and proposing management and adaptive actions to mitigate or increase yields in risky climates, in the present or future.

Keywords

Saccharum spp. · Crop modeling · Sustainability · Review

8.1 Introduction

Sugarcane (*Saccharum* spp.) is grown in the tropics and subtropics around the world as a source of food (mainly as sugar, and also as molasses), bioenergy (biofuel as ethanol and electricity), and others (for instance, alcoholic beverages and chemicals). Sugarcane products (especially sugar) are important components of the economy of many countries worldwide, many of which are developing countries. Sugarcane is produced by nearly 100 countries and occupies roughly 26 M ha of land (Table 8.1;

Table 8.1 Sugarcane production, area, and yield of the 20 largest producing countries worldwide in 2017 (FAO 2019)

Country	Production (M t)[a]	% Total	Area (M ha)[b]	% Total	Yield (t/ha)
Brazil (BRA)	758.5	41.19	10.18	39.2	74.5
India (IND)	306.1	16.62	4.39	16.9	69.7
China (CHN)	104.8	5.69	1.38	5.3	76.1
Thailand (THA)	102.9	5.59	1.37	5.3	75.2
Pakistan (PAK)	73.4	3.99	1.22	4.7	60.3
Mexico (MEX)	57.0	3.09	0.77	3.0	73.8
Australia (AUS)	36.6	1.99	0.45	1.7	80.6
Colombia (COL)	34.6	1.88	0.40	1.5	87.2
Guatemala (GTM)	33.8	1.83	0.28	1.1	121.0
United States (USA)	30.2	1.64	0.37	1.4	82.4
Philippines (PHL)	29.3	1.59	0.44	1.7	66.9
Indonesia (IDN)	21.2	1.15	0.43	1.7	49.3
Argentina (ARG)	19.2	1.04	0.38	1.5	50.6
Viet Nam (VNM)	18.4	1.00	0.28	1.1	65.3
South Africa (ZAF)	17.4	0.94	0.26	1.0	65.7
Cuba (CUB)	16.1	0.87	0.39	1.5	41.5
Egypt (EGY)	15.3	0.83	0.14	0.5	112.7
Myanmar (MMR)	10.4	0.56	0.16	0.6	63.5
Peru (PER)	9.4	0.51	0.08	0.3	121.2
Ecuador (ECU)	9.0	0.49	0.11	0.4	81.6
Others	138.2	7.50	2.51	9.7	55.1
Overall	1841.5	100.00	25.98	100.00	70.9

[a]M t, mega tonnes (metric tons $\times 10^6$)
[b]M ha, mega hectare (ha $\times 10^6$)

FAO 2019). The largest producer is Brazil, followed by India, China, and Thailand, which together produce more than two-thirds (~ 69%) of the entire world's sugarcane (Table 8.1).

A spatial view of sugarcane production by each country can be found in Fig. 8.1. The crop is grown between roughly 35° north and south of the equator, where a wide range of climates is found. A comparison between producing regions in terms of climate in some countries is presented in Sect. 8.2. In addition to the variability faced year by year, climate is changing arguably due to anthropic greenhouse gases emissions, and further changes are predicted by climate scientists of the Intergovernmental Panel on Climate Change (IPCC 2014). Increments in global temperatures and weather extremes such as heat and cold waves, drought, and flooding are likely to be more severe and more often, which will affect agriculture, livestock, location and production from forestry, and many others sectors of society and environment (IPCC 2014). Hence, it is important to develop an overall understanding of sugarcane production systems worldwide to assess its vulnerability to climate change and adaptation strategies. The sugarcane industry has a considerable potential to offset greenhouse gases emissions (Börjesson 2009) considering its capability to produce renewable energy (bioelectricity and ethanol). Thus it is likely that the cultivated area with this crop will increase in regions where land is available for expansion, like under degraded pastures in Brazil (Goldemberg et al. 2014; Alkimim and Clarke 2018).

A wide variety of production systems have evolved across the world in response to local climates and soils as well as the availability of resources and genetic material. Traditional and evolving arrangements between growers and millers and scales of production also influence the way the crop is grown and delivered for processing. The range of genotypes (varieties), planting dates and crop ages, row spacings, irrigation methods, harvest methods, residue management, crop nutrition (especially nitrogen), and pest, weed and disease control methods is large. Thus, there are large genotype × environment × management (G × E × M) interactions that affect crop growth, development, yield, and quality. Differences in yield levels between producing countries can be found in Table 8.1. A basic understanding of

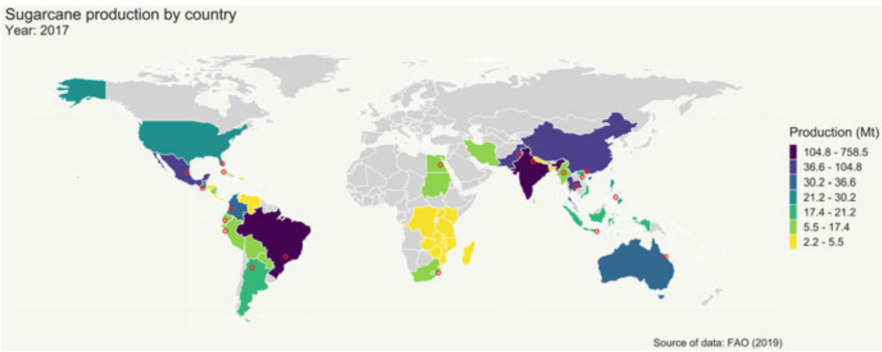

Fig. 8.1 Schematic representation of production quantities of sugarcane by country in 2017. Red circles represent the 20 largest producing countries

sugarcane yield-building processes responsive to climatic factors, including elevated CO_2 and high temperature, is described in Sect. 8.3.

Mechanistic or process-based crop models are useful tools that integrate crop/genotype, weather/climate, and soil and management practices and can be used to help with the understanding of G × E × M interactions, thus serving as powerful tools for several sectors, such as consulting, farmers, agro-industry, government, and policy makers (Boote et al. 1996; Lisson et al. 2005; Singels 2014; Wallach 2006). In Sect. 8.4 we briefly describe crop models dedicated to sugarcane and summarize the history of the two most important ones, with details of their most recent improvements. Applications of sugarcane models for sustainability of the cropping systems regarding irrigation, nitrogen fertilization, yield gap analysis, yield forecasting, impacts of climate change, drought adaptation and breeding are also shown and discussed in Sect. 8.5.

This chapter therefore aims to present the main sugarcane models and their role in understanding and mitigating the impacts of climate variability and change on sugarcane systems toward sustainable crop production.

8.2 Climate of Sugarcane Growing Regions Around the World

Climate is the average condition of weather variables at a given spatial scale (for instance farm, site, region, or country) in a given time scale (for example, month and year), thus, has a static pattern. The climate is influenced by basically two types of factors: fixed and changeable. Latitude, altitude, distance of water bodies and main oceans, and air and snow currents can be categorized as fixed factors. On the other hand, changeable factors drive the variability within the same area and are influenced by global, regional and local circulation of atmosphere. An important phenomenon that affects climate variability worldwide, and thus crop yields, is the El Niño–Southern Oscillation (ENSO), and also others like the Indian Ocean Dipole (IOD), the North Atlantic Oscillation (NAO) and Tropical Atlantic Variability (TAV) (Heino et al. 2018; Anderson et al. 2019).

Regarding climate variables for sugarcane growing regions, the monthly maximum air temperatures across sites range from 19 °C (January at Nanning, CHN) to 45 °C (June at Faisalabad, PAK), whereas minimum temperatures range from 6 °C (July at Tucumán, ARG) to 31 °C (July at Faisalabad, PAK). Annual solar radiation ranges from around 5000 MJ/m^2/year (at Nanning, CHN) to more than 7000 MJ/m^2/year (at sites in EGY, PER, AUS, IDN, and GTM). Radiation and temperature are the main drivers of sugarcane biomass accumulation under non-limiting (potential) conditions (Muchow et al. 1997b; Inman-Bamber 2014; Sage et al. 2014). Rainfall, evaporation from the soil and plant transpiration (evapotranspiration), air humidity, and wind speed also affect yields and demand for irrigation (Thornthwaite 1948; Allen et al. 1998; Inman-Bamber and McGlinchey 2003).

Rainfall varies through the year in all sugarcane countries and some monsoonal countries have extremes with excessive rain in some months and very little in others (Fig. 8.2). Sugarcane is grown in desert areas, such as in EGY, PER, and MMR,

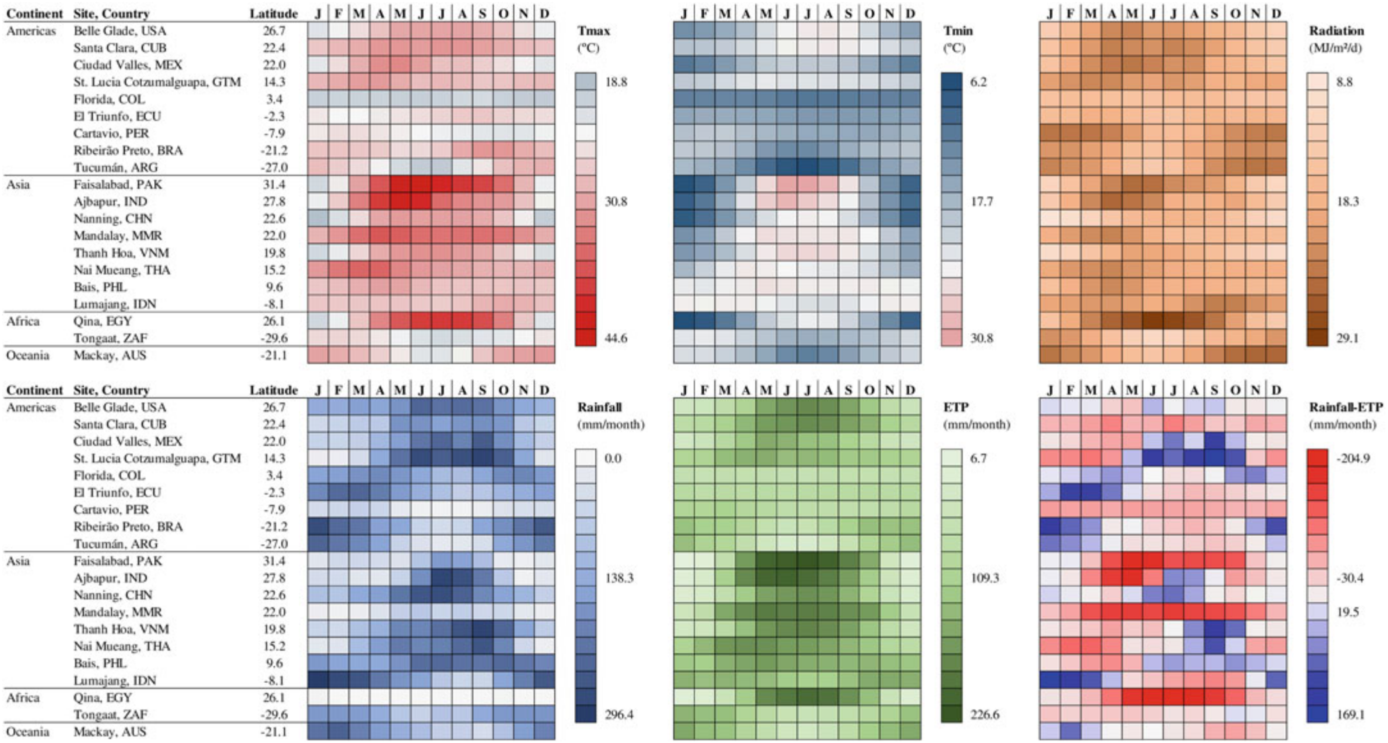

Fig. 8.2 Comparison of main monthly average climate variables driving sugarcane yield at important sites in the 20 largest producing countries highlighted in Fig. 8.1

Source of data: NASA/POWER Agroclimatology database (https://power.larc.nasa.gov/data-access-viewer/)

Where Tmax and Tmin are maximum and minimum air temperatures, respectively, and ET is the potential evapotranspiration estimated by Thornthwaite (1948)'s method where average annual rainfall is less than 200 mm, and also in regions where rain is more than 1500 mm, such as in GTM, PHL, and IND. Annual potential evapotranspiration ranges from 719 mm (at Florida, COL, highest place in terms of altitude) to more than 1600 mm (at Mandalay, MMR). An integrative index called annual water deficit, represented by the difference between rainfall and potential evapotranspiration, can also be employed to compare the climate across sugarcane growing regions. This index varies between −36 mm (at Florida, COL) to less than −1311 mm at sites in MMR, EGY, and PAK. On the other hand, there are areas with excess of water, especially in the monsoon months, such as those in the tropics where annual rainfall surpasses potential evapotranspiration by more than 500 mm (GTM and IND).

Even in the same country, many types of climate and degrees of variability are found, therefore, the better the understanding of the climate where the crop is grown, the lower the risk of failure for new decisions and business plans. Climate zones (CZ) may be distinguished within a production region based on homogeneity in weather variables that have the greatest influence on crop growth and yield (van Wart et al. 2013). CZs already exist for the South African sugar industry (Bezuidenhout and Singels 2007a) and are used as a basis for providing forecasts of sugarcane yield using a model-based system (presented in Sect. 8.5.4).

A recent spatial analysis framework called "technology extrapolation domain" or TED (Edreira et al. 2018) couples soil with climatic factors and aims to facilitate the assessment of cropping system performance across producing regions, including continents, which in turn could facilitate the sharing of better management practices toward improved yields. A simulation study with wheat in Argentina and Australia was done to show the potential of the TED approach. The study revealed that an annual rainfed double-crop (as adopted in Argentina) of wheat-mungbean would be a superior alternative to the crop-fallow system that currently predominates in the analog TED in Australia. While the use of CZs or TED approaches in the sugarcane industry could be highly beneficial, the only country to adopt this approach to date is South Africa. These types of approaches would also be useful for understanding and adapting the current sugarcane production systems worldwide to changing climates.

8.3 Climate Influence on Sugarcane Performance

The performance of a particular crop, ultimately yields, can be categorized in terms of the following levels (Rabbinge 1993; van Ittersum and Rabbinge 1997; Evans and Fischer 1999; Lobell et al. 2009; van Ittersum et al. 2013; Fischer 2015):

- Potential yield (Yp): yield of a given cultivar grown in an environment to which it is adapted that is not significantly affected by water, nutrients, lodging, and biotic factors; being determined by solar radiation, air temperature, photoperiod, CO_2 concentration, and other air constituents (determining factors).

- Water-limited yield (Yw): similar to Yp, but influenced by water stress (limiting factor) as determined by rainfall amount and distribution along the crop cycle, evapotranspiration, soil water holding capacity, and topography.
- Water- and nutrient-limited yield: Yw plus nutrient deficiency (ies) and other limiting factors.
- Attainable, exploitable, or economic yield: yield attained by farmers or a particular agro-industry with average natural resources when economically optimal practices and levels of inputs have been adopted while facing all the vagaries of weather in rainfed, supplementary- and full-irrigated cropping systems.
- Actual or average yield (Ya): yield actually obtained by farmers or a particular agro-industry, considering the determining, limiting, and also reducing factors associated with pests, diseases, weeds, and mechanical (harvester) damage.

Apart from its role in determining, limiting, and reducing factors that affect sugarcane yield, climate also indirectly limits industry performance by affecting field operations, and the transport, processing, and marketing of sugar (Muchow et al. 1997b), and other products such as ethanol. While climate is important for these processes, only yield determining and limiting processes are considered in this chapter.

Before moving into climate interactions with the crop, a brief elucidation of sugarcane plant is needed. Sugarcane species (*Saccharum* spp.) are generally large, perennial, tropical, or subtropical grasses that evolved in environments with high radiation incidence, high air temperatures, and large quantities of water (Moore et al. 2014). Commercial sugarcane genotypes are complex interspecific hybrids primarily between *Saccharum officinarum* L. (also known as noble canes) and other species (Moore et al. 2014). According to (Bonnett 2014), sugarcane phenology can be divided into the following stages: (1) germination from true seed or sprouting of buds (from culm pieces or ratoons), (2) leaf development, (3) tillering, (4) stalk elongation, (5) development of harvestable stalks, (6) maturation (sucrose accumulation), and (7) flowering.

For commercial purposes, mainly for sugar production, the ideal climate for sugarcane according to (Mangelsdorf 1950) is "a long, warm growing season and a fairly dry, cool, but frost-free, ripening and harvest season, free from hurricanes and typhoons". As previously shown, however, sugarcane is grown in a wide range of environments and many of these would never experience such ideal conditions over a given crop. Furthermore, inter- and intra-seasonal meteorological conditions during crop growth and development influence the yield-building and yield-limiting processes of sugarcane, culminating in different levels of yields (Muchow et al. 1997b; Inman-Bamber 2014).

As sugarcane is planted with culm pieces in most industries worldwide, the following description is based on this type of planting strategy. After planting or harvesting, sprouting strongly depends on temperature and on soil water to some extent (Yang and Chen 1980; Donaldson 2009; Smit 2010). Compared to other C_4 plants, such as maize, sorghum, and napier grass, sugarcane grows slowly during the early part of its growth period, characterized by rates of leaf and tiller production

(Allison et al. 2007). Leaf and tiller production are both dependent on temperature, soil water (Inman-Bamber 2004), and management (Bell and Garside 2005; Singels and Smit 2009), all of which affect light interception by the canopy. The characteristic initial slow growth of sugarcane is responsible for "wasting" radiation in the first few months (Inman-Bamber 2014). Generally, the warmer the climate, the faster is the canopy development and the greater is the proportion of incident radiation captured by the crop (Inman-Bamber 1994; Donaldson 2009; Dias et al. 2019).

As the sugarcane canopy develops, the ratio of leaf to ground area (leaf area index or LAI) increases as does solar radiation interception and biomass production. Solar radiation (approximately 300–3000 nm) is an important component of the energy and water balances affecting crop growth and development, but photosynthetically active radiation (PAR, 400–700 nm) is the component of radiation that is important for the carbon balance and, hence, biomass accumulation. Canopy closure occurs when 70% of PAR is intercepted by leaves, which depends on climate and variety, as well crop management (Inman-Bamber 1994, 2014; Singels and Smit 2009). Leaf and stalk initiation, elongation, and senescence are to a large extent influenced by temperature and water stress (Inman-Bamber and Jager 1988; Inman-Bamber 1995, 2004; Robertson et al. 1996, 1998; Sinclair et al. 2004; Inman-Bamber and Smith 2005; Grof et al. 2010). However, Robertson et al. (1999a, b) found that water deficits imposed during the tillering phase ($LAI < 2$), while having large impacts on leaf area, tillering, and biomass accumulation, had little impact on final yield. Many other factors in the $G \times E \times M$ interaction during the long growth cycle of sugarcane influence its biomass yield at harvest.

Biomass accumulation can be expressed in terms of radiation use efficiency (RUE). RUE can be defined as the mass of aboveground biomass accumulated by a crop per MJ of solar radiation or of PAR intercepted or absorbed by the green leaf canopy (Monteith 1972; Sinclair and Muchow 1999; Bonhomme 2000). Sugarcane is one of the most efficient crops in terms of RUE (Sinclair and Muchow 1999), associated with high C_4 rates of photosynthesis (Sage et al. 2014), a long growing season (Inman-Bamber 2014), and low metabolic cost of plant organs (de Vries et al. 1989). RUE ranging between 1.38 g MJ^{-1} and 2.09 g MJ^{-1} are found in literature (Robertson et al. 1996; Muchow et al. 1997a; da Silva 2009; Singels and Smit 2009; De Silva and De Costa 2012; Ferreira Junior et al. 2015), which appears to be strongly controlled by temperature during sugarcane growth (Donaldson 2009). However, a recent study suggest that this trait is quite conservative between elite varieties across production countries (Dias et al. 2019).

An important constraint in sugarcane yield, mainly in high input conditions, is known as reduced growth phenomenon or RGP (Park et al. 2005; van Heerden et al. 2010). RGP was recognized in an indirect way in the past by authors such as Rostron (1974), Lonsdale and Gosnell (1976), Thompson (1978), Inman-Bamber and Thompson (1989), and Muchow et al. (1994). Factors such as lodging, reduced nitrogen leaf content, stalk loss, negative feedback of sucrose accumulation on photosynthesis, and increasing maintenance respiration during development and maturation (sucrose) have been associated with RGP, but none of these causes have been clearly defined. Those factors for which meteorological conditions play an important role are discussed next.

Lodging disrupts the canopy, damages stalks, and reduces yield through reducing RUE in high-yielding areas where roots may be poorly supported in wet soil and a wet canopy raises the crop's center of gravity and in windy conditions (> 200 km d^{-1}) (Singh et al. 2002; van Heerden et al. 2010). Field experiments in Australia (Singh et al. 2002) and South Africa (van Heerden et al. 2010) showed that lodging reduces cane yields by 7.3–15% and sucrose yields by 8.8–35%, depending on the variety and weather conditions.

The larger the biomass, the higher the maintenance respiration, which is also increased with temperature up to a certain point (de Vries et al. 1989; Liu and Bull 2001; Jones and Singels 2019). It is likely therefore that global warming will exacerbate the maintenance respiration rates of sugarcane. In high-yielding areas where temperatures are consistently high, this process could be important for biomass accumulation during the late stages of the growth cycle, thus contributing to RGP (van Heerden et al. 2010). Maintenance respiration also depends of the type of tissue (de Vries et al. 1989; Jones and Singels 2019) being maintained. A finding in the van Heerden et al. (2010) study, based on data from well-watered and well-managed crops in South Africa (Donaldson et al. 2008), was that crops which started in summer (December) gave lower yields than those starting in winter (July). In summer crops, the slowdown commenced in the next spring due to low temperatures, but then persisted after temperatures rose again. Maintenance respiration of high biomass yields in summer was thought to be a limiting factor for sugarcane yield of summer crops.

Flowering, an undesired stage for commercial purposes (Moore and Berding 2014), is highly dependent on climate. After an initial juvenile stage of 2–3 months, a decline of photoperiod (or day-length) from 12.5 to 12.0 h per day can lead to flower induction in an unstressed crop and, in most cases, the emergence of the inflorescence (Bonnett 2014; Moore and Berding 2014). As the photoperiod is entirely latitude-dependent, the window for flower induction is easily found through astronomical equations. Temperature also plays an important role in sugarcane flowering which is favored by values higher than 18.3 °C (Coleman 1963) and lower than 32 °C (Berding and Moore 2001), but other factors such as water and nutrient status, genotype, and crop age also have their influence (Gosnell 1973; Moore and Berding 2014). Thus, flower induction and emergence are highly dependent on climate and its variability.

8.3.1 Climate Change-Related Environmental Variables

The global concentration of atmospheric CO_2 is currently around 411 ppm (NOOA 2019), about 147% higher than pre-Industrial Revolution levels in the nineteenth century (~ 280 ppm). Elevation of CO_2 and other greenhouse gases with current and future emission scenarios will lead to changes in climate patterns worldwide (IPCC 2014). Therefore, it is crucial to understand how sugarcane plants and cropping systems will be influenced by changing climates in order to predict impacts and to design adaptive and mitigation actions.

The effect of CO_2 on agricultural crops has been extensively studied, but for sugarcane there are only a few studies that assess the impact of this gas on crop performance. Photosynthesis and biomass yields increased and transpiration decreased when CO_2 was increased to 720 ppm for 70–350 days in pot studies under near-optimum conditions (Vu et al. 2006; de Souza et al. 2008; Vu and Allen 2009a, b). The reported increments in photosynthesis might be influenced by reduced transpiration and better water relations and also by short-term measurements using small segments of leaves, not representing the whole-canopy (Stokes et al. 2016). Stokes et al. (2016) found no difference in photosynthesis or biomass yield at elevated CO_2 when plants were watered on demand, suggesting that the reported increments in biomass were due to water-related processes. Even under water stress, elevated CO_2 does not directly enhance C_4 species photosynthesis (Ghannoum et al. 2003). Sorghum and maize (C_4 crops) grown in free-air CO_2 enrichment field experiments (FACE) showed higher shoot biomass and yields only when water stress was imposed (Kimball 2016). It is known that crop responses to CO_2 in FACE experiments are lower than open-top chambers or glasshouses (Ainsworth et al. 2008). Although FACE experiments with sugarcane have not been reported so far, Stokes et al. (2016) presented model simulations to show how open canopy (FACE) conditions would dampen the response to CO_2 measured on single leaves or plants. Summing up, the CO_2 responses in sugarcane might be predominantly restricted to reductions in water use rather than an augmented photosynthesis rate, which is quite well represented with model simulations (Stokes et al. 2016; Jones and Singels 2019). It does not necessarily minimize the need for new experiments, particularly under field conditions, which will confirm or bring new evidence to this important matter.

Climate change is likely to increase the frequency and intensity of weather extreme events, such as droughts, floods, and heat and cold waves (IPCC 2014). Drought is a common concern and some countries have already started programs to improve varietal resistance to drought (Basnayake et al. 2012). Heat stress physiology is a topic that has received little attention in sugarcane research (Inman-Bamber et al. 2011; Lakshmanan and Robinson 2014). According to Lakshmanan and Robinson (2014), heat stress is an abiotic stress that refers to a condition in which plants experience irreversible physical or metabolic injury following exposure to a threshold temperature for a period of time that varies from species to species. Despite being adapted to warm climates, air temperatures beyond 40 °C affect sugarcane germination and shoot emergence, leaf phenology, and increase plant respiration (Bonnett et al. 2006; Lakshmanan and Robinson 2014; Jones and Singels 2019), thus affecting yields.

8.4 Process-Based Models Dedicated to Sugarcane

According to Wallach (2006) "crop models are mathematical models which describe the growth and development of a crop interacting with soil" that "consist of a set of dynamic equations that are integrated to get predictions of responses *versus* inputs". The dynamic nature of crop models is essential for simulating G $\times$ E $\times$ M interactions when climate variability and change are involved. Thereby, crop models can be used for many application studies (Boote et al. 1996; Wallach 2006), including some for the sugarcane industry (Lisson et al. 2005; Singels 2014).

This section presents the current crop models dedicated to sugarcane and summarizes the history and recent improvements for three of them after Singels (2014), highlighting their strengths and weaknesses. Simple statistical or empirical models (i.e. Thompson 1976; Kingston 2002; Cardozo et al. 2015) and those based on data mining techniques (i.e. Everingham et al. 2016; de Oliveira et al. 2017; Peloia et al. 2019) are not addressed here despite their usefulness in the conditions where they were developed and tested (see Chap. 4).

Process-based crop models found in literature that are dedicated to, or adapted for, sugarcane are listed in Table 8.2. Further details about some of them can be

Table 8.2 List of process-based sugarcane models

Model	Main references
Developed specifically for sugarcane crop	
CANEGRO	Inman-Bamber (1991), Singels and Bezuidenhout (2002), Singels et al. (2008), Jones and Singels (2019)
CANESIM	Bezuidenhout and Singels (2007a, b)
AUSCANE	Jones et al. (1989)
APSIM-Sugar	Keating et al. (1999), Thorburn et al. (2005), Inman-Bamber et al. (2016)
QCANE	Liu and Kingston (1994), Liu and Bull (2001)
WaterSense	Inman-Bamber et al. (2005, 2007), Armour et al. (2013), Stokes et al. (2016)
Singels & Inman-Bamber	Singels and Inman-Bamber (2011)
MOSICAS	Martiné (2003)
CASUPRO	Villegas et al. (2005)
SimCana	Machado (1981)
SAMUCA	Marin and Jones (2014)
Included in, or adapted from, other crop model platforms	
AquaCrop	Steduto et al. (2009), Bello (2013)
CropSyst	Stöckle et al. (2003), Tatsch et al. (2009), Scarpare et al. (2018)
SWAP-WOFOST	Qureshi et al. (2002), van Dam et al. (2008), Scarpare (2011), Boogaard et al. (2014)
ALMANAC	Kiniry et al. (1992), Meki et al. (2015), Baez-Gonzalez et al. (2018)
BioCro	Miguez et al. (2009), Jaiswal et al. (2017)
PS123	Driessen and Konijn (1992), van den Berg et al. (2000)
Agro-IBIS	Kucharik and Brye (2003), Cuadra et al. (2012)
STICS	Brisson et al. (1998), Valade et al. (2014)

found in Singels (2014) and the papers listed in Table 8.2. The majority of these sugarcane models are not available publicly and this limits model evaluation, intercomparison, identification of shortcomings for improvements and application.

Sugarcane models usually employ the concepts of yield levels as in Sect. 8.3 and are able to predict Yp and Yw at least, and some of them simulate the interaction with nitrogen and residues (such as APSIM-Sugar and QCANE). The time step of calculations is usually 1 day, but some sub-models operate hourly. Phenology or developmental stages are commonly driven by thermal time (or growing degree-days), using one or more cardinal temperatures. Light interception by the canopy is mostly simulated using Beer's Law (Monsi and Saeki et al. 1953, cited by Saeki 1963), where the exponent is the product of LAI and a light extinction coefficient. The amount of solar radiation or PAR intercepted is then converted via RUE to generate crop biomass. Some sophisticated photosynthesis and respiration sub-models are employed such as in BioCro, or a more simplified RUE-transpiration use efficiency (TUE) approach such as in APSIM-Sugar. The biomass produced, limited or not by environmental stresses, is then partitioned to several plant components or just to stalks or sucrose, via allometric fractions or a simple harvest index. A common limitation in many of the sugarcane models, including those with continuous improvements, is the lack of traits or parameters for varieties that are currently grown commercially. Efforts to improve a model's ability and applicability to simulate variety differences are rare in sugarcane modeling with a few exceptions (Cheeroo-Nayamuth et al. 2000; Singels and Bezuidenhout 2002; Suguitani 2006; Singels et al. 2010a; Singels and Inman-Bamber 2011; Sexton et al. 2014; Thorburn et al. 2014; Leal 2016; Hoffman et al. 2018; Dias et al. 2020).

The two models widely used and currently available, APSIM-Sugar and CANEGRO, are explored in Sects. 8.4.1 and 8.4.2, with a focus on recent improvements after the comprehensive review by Singels (2014). WaterSense is another important sugarcane model that was not explored in Singels' review, thus we review this model concerning its concepts and performance in Sect. 8.4.3. Lastly, strengths and weaknesses of the models are briefly explored in Sect. 8.4.4 and gaps for advancing the knowledge on sugarcane modeling are highlighted as well.

8.4.1 CANEGRO

The development of the CANEGRO model started in the 1980s after questions posed by South African sugar industry to their local sugarcane scientists. One of the key questions was in regard to the optimum crop age at harvest because of a problem with an important sugarcane pest (Eldana borer) particularly for crops older than 12 months (Inman-Bamber and Thompson 1989). South African Sugarcane Research Institute (SASRI, former SASEX) is the institution involved with past and present CANEGRO activities. CANEGRO modeling group is also involved with other initiatives such as the International Consortium for Sugarcane Modelling

(ICSM, https://sasri.sasa.org.za/agronomy/icsm/index.php) and The Agricultural Model Intercomparison and Improvement Project (AgMIP, http://www.agmip.org/).

A timeline of main events of CANEGRO development, reviews, and improvements is presented in Fig. 8.3, in which many of these events were described and detailed by Inman-Bamber (2000), O'Leary (2000), Lisson et al. (2005), Singels et al. (2008) and Singels (2014). Currently, the model is readily available in the Decision Support System for Agrotechnology Transfer (DSSAT, latest version 4.7.5, Hoogenboom et al. 2019) software.

Jones and Singels (2019) recently proposed improvements to CANEGRO regarding deficiencies found in the model, and in key plant processes influenced by changing climate variables (temperature and CO_2). Thermal time calculations, a main driver of canopy development and growth in the model, is now limited by high as well as low temperature. A simpler, more dynamic tiller sub-model that accounts for water and temperature stresses, bud population, and the shading effect of the developing canopy was implemented. Maintenance respiration for total biomass was replaced by respiration required for living tissue and the cycling of stored sucrose in the stalk. The CERES water stress approach (Jones and Kiniry 1986) was replaced with the simpler AquaCrop model (Steduto et al. 2009), which according to the authors, enables a more gradual and realistic transition from well-watered to water-stressed states. CO_2 effects are simulated by modifying the stomatal resistance term in the calculation of canopy resistance (Allen et al. 1985), which together with canopy radiation interception and sugarcane reference evaporation is used to calculate potential transpiration, following Singels et al. (2008) and Boote et al. (2010). The direct effect of CO_2 on sugarcane photosynthesis is accommodated in a new algorithm but will have no influence on photosynthesis with current or higher CO_2 levels unless new evidence from physiological studies shows otherwise (topic discussed in Sect. 8.3).

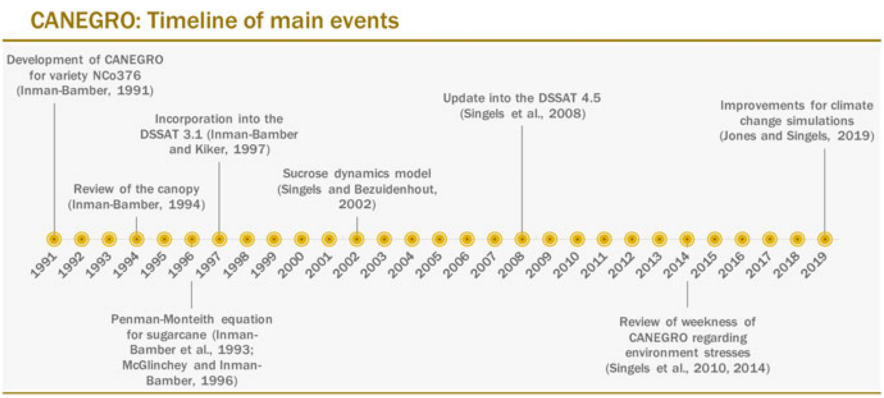

Fig. 8.3 Timeline of main events of the CANEGRO model currently embodied in the DSSAT cropping system

Although CANEGRO was built to benefit the South African sugar industry rather than other growing regions worldwide (Inman-Bamber 2000), many versions of the model have been successfully adapted for other varieties/cropping systems worldwide, including Brazil (Marin et al. 2011, 2015; Dias and Sentelhas 2017), Mauritius (Cheeroo-Nayamuth et al. 2003), and India (Bhengra et al. 2016). Recent improvements by Jones and Singels (2019) could well replace the various versions around the world given that the modifications have been introduced to make the model more representative of a wide range of varieties and cropping systems. This would help to concentrate testing and improvement on just one version for the model.

8.4.2 APSIM-Sugar

The Agricultural Production Systems SIMulator (APSIM) is a modular modeling framework that allows for farming system simulations according to a "plugged in/out" approach of desired modules, such as crop, soil and management practices (McCown et al. 1996; Keating et al. 2003; Holzworth et al. 2014). APSIM was first designed and developed in the early 1990s by a group called the Agricultural Production Systems Research Unit (APSRU) formed by a collaboration between regional Australian government agencies (Queensland State) and the Commonwealth Scientific and Industrial Research Organisation (CSIRO). A module for sugarcane was built by Keating et al. (1999) as one of APSIM's many crop modules to overcome the weakness of key biological aspects of a previous widely distributed cane model in Australia called AUSCANE (O'Leary 2000). Currently, APSIM is an initiative headed by Australian and New Zealand organizations, in which the CSIRO is an important leader. Version control is a key aspect of their approach, so there is only one version of the "Sugar" module available for any one release of the APSIM platform.

A timeline of main events of APSIM-Sugar development, reviews, and improvements is presented in Fig. 8.4. Unlike CANEGRO, APSIM-Sugar's first version was evaluated across a diverse range of varieties and environments from Australia, South Africa, Swaziland, and USA (Hawaii) with considerable success (Keating et al. 1999; O'Leary 2000). The nitrogen and carbon cycles were important to the Australia sugar industry due to off-site impacts on the Great Barrier Reef and the impact of residues on water conservation, soil health, and mechanization. The nitrogen and residue modules were reviewed and improved in the early 2000s (Thorburn et al. 2005). Greenhouse gases emissions in sugarcane fields were also a target for model improvement in 2000s (Thorburn et al. 2010).

The sugarcane crop module itself has received little attention in terms of improvements since its development. The user is allowed a large degree of control through various parameter files and the model has been quite successfully adapted for other varieties/cropping systems worldwide, including Brazil (Marin et al. 2015; de Oliveira et al. 2016; Costa 2017; Dias and Sentelhas 2017), Mauritius (Cheeroo-Nayamuth et al. 2000) and USA for bioenergy grasses species (Ojeda et al. 2017). A

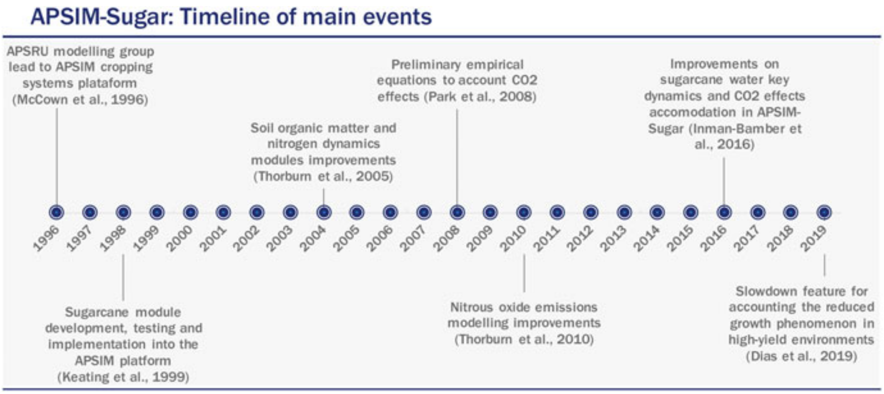

Fig. 8.4 Timeline of main events of the APSIM-Sugar model

preliminary assessment raised the question of whether APSIM-Sugar was able to predict yield differences between varieties after the inclusion of their specific phenology traits (Thorburn et al. 2014). The study suggested that vital phenology data for varieties may be deficient or the APSIM-Sugar model (and real sugarcane crops) are not overly sensitive to these traits when it comes to yield comparisons. Some of the model's shortcomings were recently raised and reasonably addressed by Inman-Bamber et al. (2012, 2016) and Dias et al. (2019), and are briefly described next.

Inman-Bamber et al. (2012) performed a theoretical study assessing traits for water-limited environments and found that transpiration efficiency and rooting depth were the ones with potentially important commercial impacts. Nevertheless, APSIM-Sugar lacked the capability for determining the trade-offs and interactions between traits. The shortcomings were later addressed by Inman-Bamber et al. (2016) resulting in the enhanced capability of APSIM-Sugar to simulate water-related physiological processes aiming to support crop improvement in breeding programs and to better distinguish between varieties in the model. The following four features were included and tested against the original dataset used for the model's development as well additional data from other field experiments: (1) the response of transpiration efficiency to water stress, (2) the midday flattening of hourly transpiration when plants are stressed, (3) conductance limits to hourly transpiration, which can apply even without stress, and (4) the separation of soil hydraulic conductivity (*k*) and root length density (*l*) rather than the use of a combined *kl* for determining root water supply. The new features allowed APSIM-Sugar to account well for observed yields and thus to accommodate genetic differences in stomatal conductance, responses to vapor pressure deficit, and differences in shoot:root ratio. The response of transpiration efficiency to CO_2 was also incorporated, in line with the CO_2 responses found in the literature for C_4 crops. No field data is yet available to validate the CO_2 response, however.

Dias et al. (2019) tested APSIM-Sugar in a new, hot environment where sugarcane is expected to expand in Brazil. Outstanding yields under high input conditions (water and nutrients) were achieved by six Brazilian varieties grown in six planting dates and harvested at about 8, 11.5 and 15 months. High yields were explained by high but not excessive temperatures allowing the canopy to close after 73 days on average. Fresh cane yield accumulated on average at about 23 t/ha per month up to 8 months and then at about 10 t/ha per month thereafter. A new modeling feature was proposed to deal with the observed growth slowdown when the crop was about 8 months old and stalk dry mass yields were about 40 t/ha. This slowdown was attributed to a reduced growth phenomenon (RGP) discussed above (Sect 8.3). While a number of factors are thought to contribute to the RGP (Sect. 8.3) the new version of APSIM allows for RUE to be modified by leaf stage as a catchall for all RGP factors. Canopy parameters and slowdown factors linked to leaf stage were validated with independent experiments as well as with the original dataset used for developing the model. APSIM-Sugar now allows for reliable simulations in environments where high yields are expected. Despite the advances with these empirical slowdown coefficients, a mechanistic way to deal with RGP is still needed.

8.4.3 WaterSense

WaterSense was developed as a web-based irrigation scheduling system from concepts embodied in APSIM-Sugar and CANEGRO. The CANEGRO model was considered to be more reliable for representing the energy balance and APSIM the carbon balance (Inman-Bamber et al. 2005, 2006, 2007). WaterSense is no longer available as web service but the concepts are worth discussing here because of the benefits that were, and still can be obtained from combining concepts used in the two most widely applied modeling platforms for sugarcane. The concepts in WaterSense can also be easily adapted for use in other crops. Armour et al. (2013) showed how well drainage was simulated for both banana and sugarcane using WaterSense. Stokes et al. (2016) showed how WaterSense could be used to scale up from leaf to canopy in regard to CO_2 effects on stomatal resistance. Everingham et al. (2015) used this capability to for assessing climate change impacts on sugarcane in Australia.

In WaterSense, the development of the canopy, radiation interception, biomass accumulation and root water extraction are all based on concepts embodied in APSIM-Sugar. Potential transpiration is derived from reference evapotranspiration from FAO56 Penman-Monteith equation (Allen et al. 1998) and a crop factor (Kc) approach, similar to the recent version of the CANEGRO model. Evaporation from the soil surface is obtained from the amount of radiation reaching the soil surface and the water content of the top layer of soil (Armour et al. 2013).

The development of WaterSense in conjunction with farmers is an example of how research tools can be appropriated for end-users, provided the "technological frames" of developers and users overlap sufficiently after a "mutual" or "participatory action" learning process (Inman-Bamber et al. 2006; Webb et al. 2006; Jakku and Thorburn 2010). The outcome of the successful merging of technological frames for irrigation management during the development of WaterSense are now embodied in an active web service for sugarcane farmers in Australia provided by consultants (Wang et al. 2018a).

8.4.4 Model's Weaknesses

Historically, sugarcane models were developed on existing knowledge of crop physiology. It soon became evident that the knowledge available to account for available observations of crop growth, development, and yield was incomplete, and this led to an iterative process between field research and model building. For example, Lisson et al. (2005) acknowledged that crop aging processes, sucrose accumulation, water stress physiology, and the physiology of water retention in stalks, were important gaps for sugarcane at that time. Inman-Bamber et al. (2012) identified weaknesses in modeling the interaction between various drought resistance mechanisms. Some of these gaps have been filled at least to some extent; for example, Inman-Bamber et al. (2016) on drought resistance mechanisms and Dias et al. (2019) on aging. Knowledge gaps in water stress physiology have received more attention than other gaps in physiological knowledge because of the large influence of the water balance on crop production (Inman-Bamber and Jager 1988; Robertson et al. 1999a; Inman-Bamber and Smith 2005; Smit and Singels 2006; Singels et al. 2010b; Basnayake et al. 2012, 2015; Jackson et al. 2016; Marchiori et al. 2017; Zhao et al. 2017a). Generally, sugarcane models have been predicting Yw (rainfed conditions) quite well worldwide (see validations of Keating et al. 1999; Cheeroo-Nayamuth et al. 2000; Liu and Bull 2001, Inman-Bamber et al. 2001, 2016; Singels et al. 2008, 2010a; Sexton et al. 2014; Marin et al. 2015; Dias and Sentelhas 2017; Jones and Singels 2019).

O'Leary (2000) tested and reviewed three sugarcane models (APSIM-Sugar, CANEGRO and QCANE) regarding sucrose dynamics. This author proposed a (conceptual) process-based model that takes into account the dynamics between sucrose and reducing sugars and factors such as water, nitrogen, and temperatures stresses. Singels and Bezuidenhout (2002) improved the dry matter partitioning of CANEGRO regarding water stress and temperature, and suggested an interesting option to accommodate effects of nitrogen, variety differences, and ripener as well. Singels and Inman-Bamber (2011) proposed a process-based model that helped to understand genetic differences in sucrose accumulation and responses to water and temperature, by accounting for the differences in plant development and partitioning to structural components such as leaf and stalk fiber. Aging processes and lodging have received some attention in the literature (Park et al. 2005) and in improvements to some models such as CANEGRO (van Heerden et al. 2015) and APSIM-Sugar (Dias et al. 2019). Water retention in stalks remains as a weakness in current models and is an important issue because of its impact on costs of cane harvesting and transportation (Lisson et al. 2005).

Other important topics on sugarcane physiology for advancing our understanding and improving existing models are root dynamics and its role in crop yield-building processes, nutrients, flowering, and heat stress effects. Theoretical studies by Inman-Bamber et al. (2012) and Singels et al. (2016) with APSIM-Sugar and CANEGRO, respectively, indicated that roots are an important component for drought adaptation and that knowledge is limiting for modeling and understating adaptation to water stress. Studies by Chopart et al. (2008, 2010), Laclau and Laclau (2009) and Otto et al. (2011) provided valuable information for improved simulation of root profiles, penetration rate, and specific root length. This knowledge has not yet been used in models as far as we know.

While some models include a comprehensive nitrogen balance, the high nitrogen use efficiency found in Brazilian cropping systems (Robinson et al. 2011; Otto et al. 2016), particularly for plant cane (Franco et al. 2011), has not been well clarified. This is a topic that deserves attention because it could bring important insights for nitrogen management worldwide.

Sugarcane models do not currently simulate flowering even though flowering in favorable environments causes large losses in yield and quality worldwide. Simulation of this process would help in many applications such as determining yield potential, harvest management, varietal planning, and decision-making for chemical control.

Lastly, but not least, heat stress is expected to be an important crop constraint in tropical areas under changing climates where temperatures and heat waves are predicted to increase considerably. Temperature response functions in wheat and maize process-based models have been recently revised and improved for predicting yields in changing climates (Wang et al. 2017, 2018b). Jones and Singels (2019) made improvements in CANEGRO regarding temperature effects, but in other models this topic has received little attention.

The future of sugarcane models will also depend on advances and cooperation with genetics research, which has indeed already started for annual crops (Singels 2014). Simulations could indicate the desirability of traits (or QTL or genes) in target environments and thus help for ideotyping and breeding by design (Singels 2014; Hoffman et al. 2018).

Targeted experimentation and perhaps revisitation of existing experimental data to gain insight into sugarcane processes that still are poorly understood, such as crop slowdown with age, lodging, and roots-related and heat stress, will be needed.

8.5 Toward Sustainable Sugarcane Production: Usefulness of Process-Based Models Applications

Applications of sugarcane process-based models started in the beginning of 1990s with the development of CANEGRO (Fig. 8.3), ramping up considerably after CANEGRO's inclusion in the DSSAT platform in 1997 and 2008 (Figs. 8.5 and 8.6). During the end of 1900s and beginning of 2000s, APSIM-Sugar applications increased substantially with a peak of papers published in 2001 (Figs. 8.5 and 8.6).

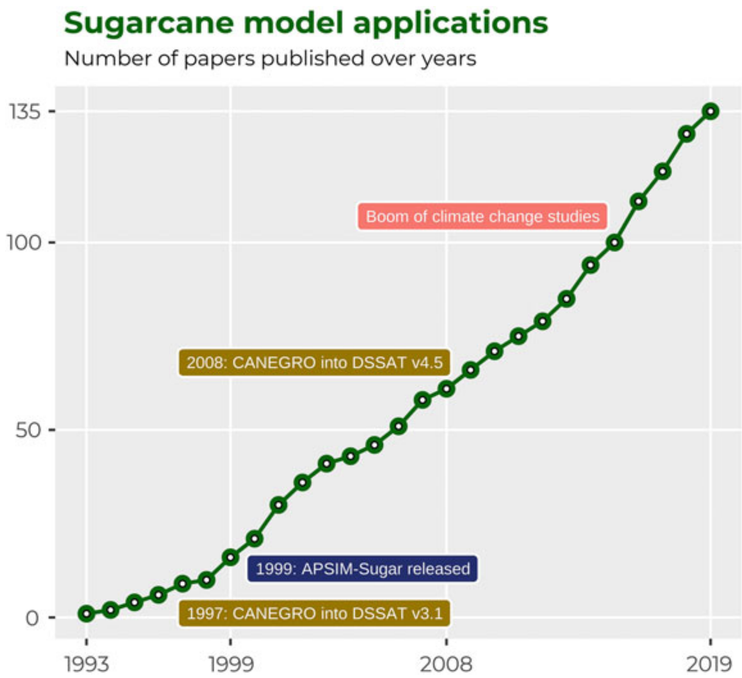

Fig. 8.5 Sugarcane process-based model application papers published over years

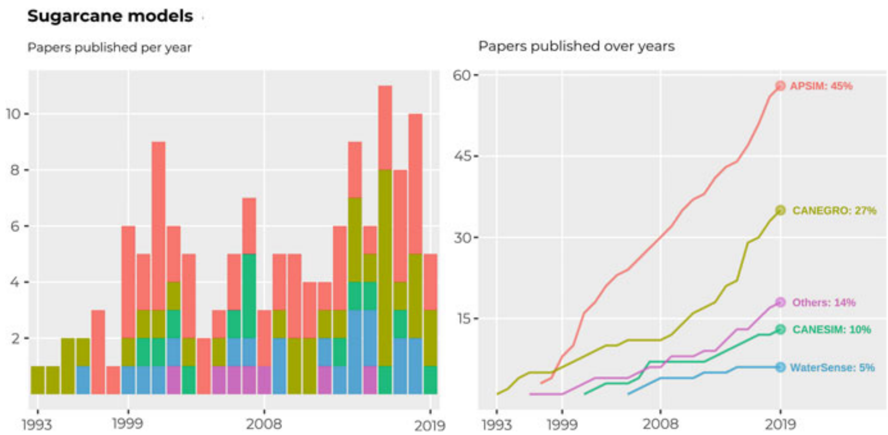

Fig. 8.6 Papers published per and over years categorized according to the main models

The second boom of the use of sugarcane models happened around 2007 and since then, modeling publications increased year by year, reaching other peaks in 2016 and 2018 (Fig. 8.5). Table 8.3 lists many of the referenced studies that employed sugarcane models we have found so far, categorized by the type of application. The

Table 8.3 List of various types of applications of the sugarcane models and example references that describe these applications in detail, organized by continent on which the studies were conducted. Participations, as a percentage of total number of papers, of each continent are shown in brackets

Continent	Application	References
Americas	Breeding support & variety comparison	Suguitani (2006), Leal (2016)
(22%)	Climate variability & change	da Silva (2012), Bello (2013), Singels et al. (2014), dos Vianna and Sentelhas (2014), de Carvalho et al. (2015), Marin et al. (2015), Jaiswal et al. (2017), Baez-Gonzalez et al. (2018), Sentelhas and Pereira (2019)
	Crop/Farm management	Galdos et al. (2009a, b) Brandani et al. (2015), de Oliveira et al. (2016)
	Fertilizer management	Costa et al. (2014), Marin et al. (2014), de Oliveira et al. (2016), de Barros et al. (2018)
	Water management & efficiency	dos Vianna and Sentelhas (2016), Costa (2017), Dias and Sentelhas (2018a)
	Yield benchmarking & gap	van den Berg et al. (2000), Marin et al. (2016), Dias and Sentelhas (2018b
	Yield forecasting	Pagani et al. (2017)
Asia	Breeding support & variety comparison	Bhengra et al. (2016)
(7%)	Climate variability & change	Jintrawet and Prammaneem (2005), Ahmad et al. (2016), Mishra et al. (2017), Ruan et al. (2018), Gunarathna et al. (2019)
	Water management & efficiency	Qureshi et al. (2002)
	Yield benchmarking & gap	Zu et al. (2018)
	Yield forecasting	Promburom et al. (2001), Piewthongngam et al. (2009),
Africa	Breeding support & variety comparison	Cheeroo-Nayamuth et al. (2003, 2011), Hoffman et al. (2018)
(32%)	Climate variability & change	Inman-Bamber (1994), Martiné et al. (1999), Cheeroo-Nayamuth and Nayamuth (2001), Walker and Schulze (2010), Knox et al. (2010), Black et al. (2012), Singels et al. (2018), Jones et al. (2014, 2015), Singels et al. (2014), Hoffman et al. (2017), Jones and Singels (2019)
	Crop/Farm management	Bezuidenhout et al. (2002), McGlinchey and Dell (2010), Paraskevopoulos et al. (2016)
	Drought adaptation	Singels et al. (2016)
	Fertilizer management	Thorburn et al. (2001b), Van Antwerpen et al. (2002), van der Laan et al. (2011)
	Water management & efficiency	Inman-Bamber et al. (1993), McGlinchey et al. (1995), Donaldson and Bezuidenhout (2000), Olivier and Singels (2001), Singels and Smith (2006), Kunz et al. (2014), Paraskevopoulos and Singels (2014), Singels et al. (2019)
	Yield benchmarking & gap	Inman-Bamber (1995), Cheeroo-Nayamuth et al. (2000, 2011), Singels (2007), van den Berg and Singels (2013), Jones and Singels (2015), Christina et al. (2019)

(continued)

Table 8.3 (continued)

Continent	Application	References
	Yield forecasting	Lumsden et al. (1998), McGlinchey (1999), de Lange and Singels (2003), Bezuidenhout and Singels (2007a, b), Martiné (2007), Morel et al. (2014a, b)
Oceania	Breeding support & variety comparison	Sexton et al. (2014)
(40%)	Climate variability & change	Lisson et al. (2000), Park et al. (2007), Park (2008), Webster et al. (2009), Biggs et al. (2013), Singels et al. (2014), Everingham et al. (2015)
	Crop/Farm management	McDonald and Lisson (2001)
	Drought adaptation	Inman-Bamber et al. (2012, 2016)
	Environmental pollution	Thorburn et al. (2001a, 2010, 2011), Webster et al. (2009), Armour et al. (2013), Biggs et al. (2013)
	Fertilizer management	(Keating et al. (1997), Thorburn et al. (1999, 2001b, 2003, 2004, 2017, 2018), Stewart et al. (2006), Park et al. (2010), Skocaj et al. (2013), Meier and Thorburn (2016), Zhao et al. (2017b), Kandulu et al. (2018)
	Land management	Mallawaarachchi and Quiggin (2001)
	Pest management	Liu and Allsop (1996)
	Water management & efficiency	Robertson et al. (1997, 1999b), Muchow and Keating (1998), Inman-Bamber et al. (1999, 2001, 2004, 2005, 2006), Attard et al. (2003), Everingham et al. (2002, 2008), Stoeckl and Inman-Bamber (2003), Lisson et al. (2003), Webb et al. (2006), Inman-Bamber and Attard (2008), An-Vo et al. (2019)
	Yield benchmarking & gap	Muchow et al. (1997b), Liu and Bull (2001)
	Yield forecasting	Everingham et al. (2002, 2005, 2007, 2009, 2016)

majority of model applications found employed APSIM-Sugar (45%) mostly in Australia, and CANEGRO plus CANESIM (a simpler version of CANEGRO) (37%) mostly in South Africa (Fig. 8.5). Use and applications of APSIM-Sugar and CANEGRO have increased in Americas in this decade, especially in Brazil (Table 8.3).

Water management and efficiency, nitrogen management, yield benchmarking, gap, and forecasting, and most recently climate change impact studies predominate in sugarcane model applications (Table 8.3 and Fig. 8.7). A common aspect in applications of models is the intrinsic effect of climate and its variability on production. Long-term climate series were employed in the majority of these studies. The following subsections provide some examples of model applications aimed at informing sustainable planning and decision-making processes in the sugarcane sector (Fig. 8.7).

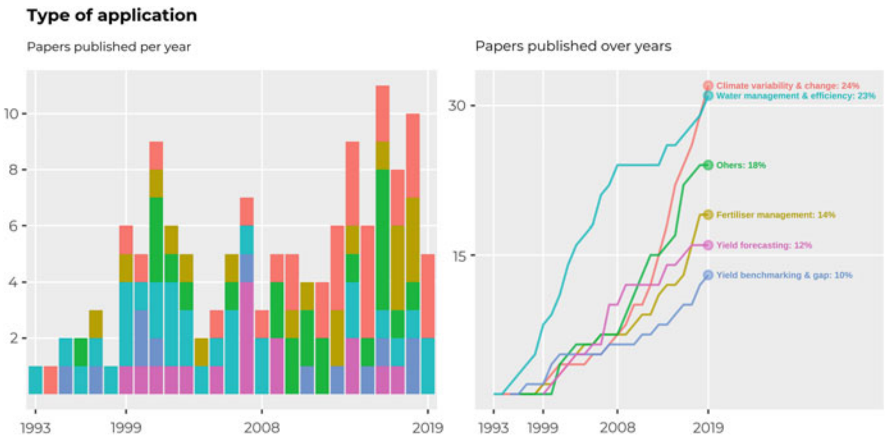

Fig. 8.7 Papers published per year and over years categorized according to the main types of application

8.5.1 Irrigation Management

Irrigation and its associated topics (for example, water allocation and water use efficiency assessment) are some of the most common areas of sugarcane model applications (Table 8.3). Examples are:

- Helping farmers with irrigation planning and management with web-based tools (McGlinchey et al. 1995; Inman-Bamber et al. 2005, 2007; Singels and Smith 2006; Inman-Bamber and Attard 2008), by coupling with seasonal climate forecasts (Everingham et al. 2002, 2008; An-Vo et al. 2019), or for new environments where little is known (Muchow and Keating 1998; Lisson et al. 2000; Inman-Bamber et al. 2006);
- Optimizing yields and making the best use of limited irrigation water (Inman-Bamber et al. 1999, 2007; Singels et al. 1999, 2019);
- Estimating drying-off days before harvest to optimize sucrose yields (Robertson et al. 1999b; Donaldson and Bezuidenhout 2000; Dias and Sentelhas 2018a);
- Dimensioning dam building for water storage (Lisson et al. 2003);
- Assessing risks of crop lodging considering irrigation strategies across varieties, environments, and growing months (Inman-Bamber et al. 2004; Paraskevopoulos et al. 2016).

Consultants are now using models to provide some of these irrigation applications as well as other services for sugarcane production (https://www.sqrsoftware.com/; http://agritechsolutions.com.au/).

8.5.2 Nitrogen Management and Its Implications to Environment

Nitrogen management is a particular topic that has been evaluated using sugarcane models (Table 8.3), mostly with APSIM-Sugar. Mechanization in sugarcane fields has increased in many areas worldwide, especially at harvesting, requiring adjustments in the cropping systems due to the residues left in the soil. Impacts of the green cane trash blanket on cane yield, soil components, and nitrogen fertilizer requirements have been assessed in Australia (Thorburn et al. 1999, 2001b, 2004; Meier and Thorburn 2016), South Africa (Thorburn et al. 2001b; Van Antwerpen et al. 2002) and Brazil (Costa et al. 2014; Marin et al. 2014; de Oliveira et al. 2016; de Barros et al. 2018) by using APSIM-Sugar.

Crop rotation with legumes to provide nitrogen through biological fixation is a practice that is recommended in many sugarcane cropping systems worldwide. Park et al. (2010) employed APSIM-Sugar to assess the impact of soybean rotation on nitrogen requirements in six sites (four of them in the Burdekin region) across Australia. Long-term simulations showed that nitrogen fertilizer could be reduced around 60–100%, 40–100%, 20–60%, 5–30% and $< 10\%$ for plant crops and the subsequent four ratoons, respectively, when compared to bare fallow systems. Their findings suggest a potential economic and environmental win–win outcome from refining and adopting sugarcane–legume rotation cropping systems in Australia and perhaps other countries.

Thorburn et al. (2017) simulated nitrogen management practices such as fertilizer rate, timing, and splitting, fallow management and tillage intensity with APSIM-Sugar across several sites in Australia and concluded that optimizing the application rate and fallow management should be prioritized for improving the nutrient efficiency. Thorburn et al. (2018) recently showed that rather than trying to improve nitrogen recommendations by changing concepts around target yields, the direct prediction of optimum nitrogen rates through the application APSIM-Sugar would be more beneficial for Australian environments, since the model captures soil and crop physiological processes, and their interactions with climate and management.

Environment implications of nitrogen fertilization can be also assessed through sugarcane models. Reducing impacts into the World Heritage listed Great Barrier Reef Marine Park from sugarcane farming is a particular concern in Australia. Sugarcane models (mainly APSIM-Sugar) have been applied to estimate nitrogen losses through runoff and leaching at several sites in the Australia Northeast region (Thorburn et al. 2003, 2011, 2017; Stewart et al. 2006; Armour et al. 2013; Biggs et al. 2013) and at Pongola, South Africa (van der Laan et al. 2011). Kandulu et al. (2018) integrated the APSIM-Sugar model with other techniques (probability theory, Monte Carlo simulation, and financial risk analysis) in a framework that allowed an assessment of economic and environmental trade-offs for nitrogen management strategies considering variable climatic and economic conditions. The framework was applied to a high rainfall production area close to the Great Barrier Reef in Australia. On average, net economic returns and nitrogen fertilizer rates were lowered when environmental costs were taken into account (Kandulu et al. 2018). This framework is interesting because it incorporates farmer risk behavior and environmental impacts, which in turn enhances the sustainability of a particular cropping system.

8.5.3 Yield Gap and Benchmarking

There are at least four approaches to estimate Yp and Yw and then to perform yield gap and benchmarking analysis; however, crop simulation models are recommended as a preference for such analyses, once they take into account the biological, biochemical, and biophysical aspects related to crop yield (van Ittersum et al. 2013).

Inman-Bamber (1995) first used CANEGRO to assess Yp and Yw (stalk and sucrose fresh mass yields) for 32 sites in South Africa considering two types of soils (a shallow loamy-sand and a deep structured one). These estimates were validated with variety trials, where variety NCo376 was common at 17 sites. Differences between Yp and Yw varied greatly depending on rainfall. In South Africa, irrigation is essential where Yw is less than 75% Yp. Years later van den Berg and Singels (2013) compared Yw estimates of CANESIM with Ya from small- and large-scale farmers using a CZ approach. Considering the period from 1988 to 2010, on average, Ya of large-scale farmers reached 77% of Yw, while for small-scale growers Ya stayed below 50% Yw. Factors such as damaging effects of a new pest (sugarcane thrips), inadequate nutrition and inadequate replanting, apparently linked to unfavorable socioeconomic conditions, were hypothesized to be the causes of the suboptimal production, revealing important points to be tackled by South African sugar industry.

Muchow et al. (1997b) demonstrated the remarkable variation in commercial sugar yields (Ya) across 14 sites along the Australian east coast and compared these to Yp using long-term APSIM-Sugar simulations. Maximum yields at four of these sites in some growing seasons were equivalent to Yp in less than 5% of the area harvested. District mean yields were 53–69% of Yp showing considerable room for improvement in the Australian sugar industry.

CANEGRO was used to develop norms for yield decline over successive ratoons in Swaziland (McGlinchey and Dell 2010). Yields tended to decline by about 1% for each successive ratoon in good soils but as much as 2.8% in poor soils. Ya/Yp for plant crops ranged from 0.81 to 0.90 depending on soil type.

Similar studies were performed using CANEGRO, APSIM-Sugar and other crop models in Mauritius (Cheeroo-Nayamuth et al. 2000, 2011), Brazil (Marin et al. 2016; Dias and Sentelhas 2018b), China (Zu et al. 2018) and Réunion (Christina et al. 2019). In Brazil, despite water being the factor that contributes most to cane yield gaps (Dias and Sentelhas 2018b), the gap attributed to general deficiencies in crop management, ranged from as low as 6 t/ha to as much as 79 t/ha depending on the region (Marin et al. 2016; Dias and Sentelhas 2018b).

Such analyses can help to quantify, identify the causes of, and mitigate yield gaps, in order to increase efficiency and consequently the production and sustainability of sugarcane industries worldwide. For instance, by increasing the national yield of Brazil on average by 10 t/ha (8.9 mi ha of crop area), an increment of 89 mi t would approach the total production of China (105 mi t) and Thailand (103 mi t) (Table 8.1). Such a vertical increase in production could meet future demands for sugarcane products (Marin et al. 2016) and relieve land use (Dias and Sentelhas 2018b) for other activities such as growing other crops or forest restoration in Brazil.

8.5.4 Yield Forecasting

Sugarcane and sugar yield forecasts are, or can be, useful for many agents involved in the sugarcane industries. Everingham et al. (2002), Higgins et al. (2007) and Bocca et al. (2015) provided examples of how forecasts can benefit planning and decision-making processes in the sugarcane industry. Sugarcane models can be used to generate the forecasts and two systems that are currently operating based on two models are briefly described below.

The CANESIM model is employed in an operational way in the South African sugar industry since 2000 and provides monthly yield forecasts for 48 CZs covering 14 mill supply areas. Further details can be found in Everingham et al. (2002) and Bezuidenhout and Singels (2007a, b). Basically, the system uses daily data from several automatic weather stations and completes the time-series with likely future weather conditions, to forecast yields for the pending harvest season, through model simulations at district, mill, and industry scales. Ten analog daily weather sequences are selected from past climate records, which best represent future weather conditions expected from ENSO indices provided by the South African Weather Service. Yields are represented as a percentage of those for the previous season. Forecasts are released monthly from November, 4 months before the start of the milling season (April to December), to September. Harvesting schedules and milling decisions are based on CANESIM forecasts, which are also used by South African Sugar Association as a support for planning and decision-making regarding sugar marketing.

TempoCampo is a recent yield forecasting system that is being developed for the Brazilian sugarcane industry and intended to extend the forecasts to other agro-industries (Marin 2017). The systems firstly used CANEGRO, but now is using the recently built SAMUCA model (Marin and Jones 2014), which relies on modeling approaches similar to those of CANEGRO and APSIM-Sugar. The system operates in a similar way to the South African one for supporting some mills in Southern Brazil.

Apart from the two systems presented previously, sugarcane models have been employed in studies worldwide together with other techniques, such as remote sensing (Morel et al. 2014a, b), statistics (Martiné 2007; Pagani et al. 2017) and data mining (Everingham et al. 2009, 2016). These all deserve attention for further development of integrated and operational yield forecasting systems for sugarcane industries worldwide.

Irrigation management, yield benchmarking, and yield forecasting are services based on the CANEGRO model that are offered by a commercial software developer (https://www.sqrsoftware.com/) providing many options for managing large and small sugarcane production systems in Africa, the Americas, and Australia (pers. com. Mark McGlinchey 2019).

8.5.5 Climate Change

Climate change is a huge concern of many societies globally, and this phenomenon will certainly influence sugarcane industries. Process-based crop models such as those previously discussed are preferred because they tend to include the effects of CO_2 increases that accompany warming, whereas statistical models typically do not (Lobell and Asseng 2017). Therefore, despite many approaches being used to assess climate change effects on the sugarcane crop/industry (Linnenluecke et al. 2018), only those with process-based sugarcane models are considered here. Studies involving this topic have increased substantially in the past few years (Tables 8.3 and 8.4).

The majority of climate change studies using crop models for sugarcane worldwide can be classified as impact studies (Table 8.4; Linnenluecke et al. 2018). The methodology varies considerably in regard to timeframe, future climate scenarios, type of global circulation models, downscaling, and other methods (Table 8.4; Linnenluecke et al. 2018), which makes comparisons difficult. Overall, the impact of climate change is predicted to be positive for sugarcane yields; however, it is also variable (Table 8.4). A recent assessment by Linnenluecke et al. (2019) has shown that sugarcane production in Australia of 1964–1995 compared to 1996–2012 has already been negatively affected by changes in climate variables, which reinforces the need for attention from policymakers and future research.

Sensitivity analyses, considering ranges for the main weather variables under changing climates (CO_2, air temperature, and rainfall), were performed for several sites worldwide mainly by using CANEGRO (Jones et al. 2014; Marin et al. 2015; Jones and Singels 2019). The simulations showed that sugarcane yields would, in general, be enhanced by changes in CO_2 and air temperature within the expected ranges predicted by IPCC (2014). Decreases in yields were predicted when rainfall was decreased within the expected ranges. Jones and Singels (2019) refined CANEGRO with regard to some plant processes, including CO_2 interactions and high temperature effects (see Sect. 8.4.1), and confirmed previous findings, except that the increments in yields were lower due to the inclusion of a more rational representation of the effect of temperature on sugarcane physiological processes.

Climate change adaptation studies using sugarcane models are scarce (Linnenluecke et al. 2018), but some can be found in literature. Cheeroo-Nayamuth and Nayamuth (2001) explored climate change adaptation strategies for sugar yields in Mauritius by using APSIM-Sugar, which included irrigation, cultivar and changes in harvest date. They concluded that irrigation was the best adaptive option depending on water availability, water storage, and cost. Park et al. (2007) used APSIM-Sugar to assess the adaptive strategy of changing planting dates in the most important growing regions in Australia. The simulations suggested that yield

Table 8.4 Climate change impacts studies on sugarcane crop using process-based crop models

Reference	Country (ies)	Model (version)	Climate baseline	Time frame	Emission scenarios	GCM or RCM	General impact
Cheeroo-Nayamuth and Nayamuth (2001)	Mauritius	APSIM-Sugar	MWD (1954–1996)	NA	Effect of CO_2 not considered	4 GCMs	–
Jintrawet and Prammaneem (2005)	Thailand	CANEGRO (3.5)	MWD (1986–1999)	2006–2024	720 ppm	CCAM model	+
Park et al. (2007)	Australia	APSIM-Sugar	NA	2030	Effect of CO_2 not considered	Ensemble of 12 GCMs and RCMs combined	+ or -
Webster et al. (2009)	Australia	APSIM-Sugar	NA	2030, 2070	425–449 ppm in 2030, 518–702 ppm in 2070	NA	+
Knox et al. (2010)	Swaziland	CANEGRO (4.0)	MWD (1980–2007)	2050	A2 and B2	HadCM3	+
Walker and Schulze (2010)	South Africa	APSIM-Sugar	–	2055	CO_2 effect on C_3 crop	NA	+
Black et al. (2012)	Ghana, Brazil	JULES	NCEP (1984–2008)	NA	345 ppm, 690 ppm	NA	+
Marin et al. (2013)	Brazil	CANEGRO (4.5)	MWD (at least 8 years between 1992–2007)	2050	A2 and B2	PRECIS, CSIRO	+
Biggs et al. (2013)	Australia	APSIM-Sugar	MWD (1957–2007)	2030	B1, A1B, A1FI	3 GCMs	+ or -
Bello (2013)	Colombia	AquaCrop	MWD (1994–2010)	2021–2030, 2041–2050	A1 and B2	3 GCMs	+
Jones et al. (2014)	7 countries	CANEGRO (4.5)	MWD (NA)	Sensitivity analysis			+

(continued)

Table 8.4 (continued)

Reference	Country (ies)	Model (version)	Climate baseline	Time frame	Emission scenarios	GCM or RCM	General impact
Singels et al. (2014)	South Africa, Australia, Brazil	CANEGRO (4.5)	MWD (1980–2010)	NA	734 ppm (A2)	3 GCMs from CMIP3	+
Marin et al. (2014)	Brazil	CANEGRO (4.5), APSIM-Sugar	MWD (1992–2007)	Sensitivity analysis			+
Marin et al. (2015)	Brazil	CANEGRO (4.5), APSIM-Sugar	MWD (NA)	Sensitivity analysis			+
Jones et al. (2015)	South Africa	CANEGRO (4.5)	MWD (1980–2010)	2040–2070	571 ppm	5 GCMs from CMIP5	+
de Carvalho et al. (2015)	Brazil	Century (v.5)	MWD (1950–2012)	3 future periods	A1B	Eta/CPTEC, HadCM3	–
Everingham et al. (2016)	Australia	WaterSense	AWAP (1970–2000)	2046–2065	B1 and A2 scenarios, with and without elevated CO_2	Ensemble of 11 GCMs from CMIP3	= or +
Jaiswal et al. (2017)	Brazil	BioCro	NCEP (1980–2010)	2040, 2050	494 ppm (2040), 540 ppm (2050)	5 GCMs	- or +
Ruan et al. (2018)	China	APSIM-Sugar	MWD (1961–2010)	3 future periods	RCPs 4.5 and RCP8.5	Ensemble of 28 GCMs from CMIP5	+
Singels et al. (2018)	South Africa	CANEGRO (4.7)	MWD (1971–1990)	2046–2065	NA	4 GCMs	+
Baez-Gonzalez et al. (2018)	Mexico	ALMANAC	MWD (1961–2010)	2021–2050	A2	10 GCMs	+
Jones and Singels (2019)	5 countries	CANEGRO (4.7)	MWD (1980/84–2008/10)	Sensitivity analysis			+

Based on Linnenluecke et al. (2018)
NA not available, found, or specified, *MWD* measured weather data from ground weather stations, *GCM* global circulation models, *RCM* regional circulation models

potential will increase marginally by the year 2030 if planting the date occurs earlier than is presently practiced in the south of the industry and later in the north.

8.5.6 Drought Adaptation and Breeding

Water deficit, caused by lack of or irregular distribution of rainfall throughout the sugarcane cycle, is one of the main causes of yield losses in sugarcane regions around the world (Inman-Bamber and Smith 2005; Basnayake et al. 2012; Dias and Sentelhas 2018b). Even for irrigated cropping systems, there is an increasing concern about the amount and efficiency of water use, owing to the rising costs of applying water, limited availability of water for irrigation, and environmental issues (Jackson et al. 2016) (see Sect. 8.5.2).

There is an increasing interest in breeding for crops grown in water-limited environments (Inman-Bamber et al. 2012). Inman-Bamber et al. (2012) employed APSIM-Sugar for a theoretical assessment aiming to find traits that could reduce the loss of sugarcane yield under rainfed conditions. Simulations showed that reduced root conductance or stomatal conductance would increase biomass yield in only about 5% in the driest climates on well-structured soils. Transpiration efficiency, a genotype-dependent trait (Saliendra and Meinzer 1992; Jackson et al. 2016), was also tested and an improvement in this trait arising from increased intrinsic water use efficiency would usually improve biomass under water deficit. Leaf and culm senescence were generally unsuccessful in conferring adaptation to water deficit.

In South Africa crop modelers are working together with breeders for sugarcane yield improvement. Ngobese et al. (2018) assessed traits for several varieties described in CANEGRO, to explore G × E interactions across environments and crop classes to assist in breeding efforts, according to the authors. Hoffman et al. (2018) predicted stalk dry mass yields reasonably well by estimating the RUE-related trait parameter in CANEGRO using leaf level photosynthesis and stomatal conductance measurements for several varieties, thus, showing that it is possible to apply crop models for helping sugarcane breeding.

8.6 Final Considerations

Sugarcane production is highly dependent on climate and its variability, and therefore also to climate change. Modeling groups and process-based models have been helping industries across the sugarcane producing regions worldwide, of which we can highlight irrigation management and yield forecasting as the most common applications. Possible climate change impacts are now quite well elucidated for some environments through model simulations, but studies focusing on adaptation strategies that minimize or even take further advantage of these impacts are necessary. Usefulness of sugarcane models in breeding started being demonstrated for South African and Australian programs. Nevertheless, there is room for improvements that were also discussed, many of which were previously acknowledged in the past. Continuous physiology experimentation and modeling efforts are needed to fill the knowledge gaps in these sugarcane research areas. Collaboration between research groups worldwide might speed up this process. Despite their weaknesses, sugarcane models are a powerful tool to understand and propose management and adaptive actions to mitigate losses or increase yields under current and future climates.

Acknowledgments This contribution was not funded by any institution. However, the first author (HBD) is truly grateful to the São Paulo Research Foundation (FAPESP), which facilitated his studies in sugarcane agrometeorology, physiology, and modeling in the past few years through the grants #2014/05173-3, #2016/11170-2, and #2017/24424-5.

Climate data used in Fig. 8.2 were obtained from the NASA Langley Research Center (LaRC) POWER Project funded through the NASA Earth Science/Applied Science Program.

References

Ahmad S, Nadeem M, Abbas G et al (2016) Quantification of the effects of climate warming and crop management on sugarcane phenology. Clim Res 71:47–61. https://doi.org/10.3354/cr01419

Ainsworth EA, Leakey ADB, Ort DR, Long SP (2008) FACE-ing the facts: inconsistencies and interdependence among field, chamber and modeling studies of elevated [CO_2] impacts on crop yield and food supply. New Phytol 179:5–9. https://doi.org/10.1111/j.1469-8137.2008.02500.x

Alkimim A, Clarke KC (2018) Land use change and the carbon debt for sugarcane ethanol production in Brazil. Land Use Policy 72:65–73. https://doi.org/10.1016/j.landusepol.2017.12.039

Allen LH, Jones P, Jones JW (1985) Rising atmospheric CO_2 and evapotranspiration. In: Proceedings of the national conference on advances in evapotranspiration. ASAE, St Joseph/Chicago, pp 13–27

Allen RG, Pereira LS, Raes D, Smith M (1998) Crop evapotranspiration: guidelines for computing crop water requirements. FAO, Rome

Allison JCS, Pammenter NW, Haslam RJ (2007) Why does sugarcane (*Saccharum* sp. hybrid) grow slowly? S Afr J Bot 73:546–551. https://doi.org/10.1016/j.sajb.2007.04.065

Anderson WB, Seager R, Baethgen W et al (2019) Synchronous crop failures and climate-forced production variability. Sci Adv 5:eaaw1976. https://doi.org/10.1126/sciadv.aaw1976

An-Vo DA, Mushtaq S, Reardon-Smith K et al (2019) Value of seasonal forecasting for sugarcane farm irrigation planning. Eur J Agron 104:37–48. https://doi.org/10.1016/j.eja.2019.01.005

Armour JD, Nelson PN, Daniells JW et al (2013) Nitrogen leaching from the root zone of sugarcane and bananas in the humid tropics of Australia. Agric Ecosyst Environ 180:68–78. https://doi.org/10.1016/j.agee.2012.05.007

Attard SJ, Inman-Bamber NG, Engelke J (2003) Irrigation scheduling in sugarcane based on atmospheric evaporative demand. Proc Aust Soc Sugar Cane Technol 25 (CD-ROM)

Baez-Gonzalez AD, Kiniry JR, Meki MN et al (2018) Potential impact of future climate change on sugarcane under dryland conditions in Mexico. J Agron Crop Sci:1–14. https://doi.org/10.1111/jac.12278

Basnayake J, Jackson PA, Inman-Bamber NG, Lakshmanan P (2012) Sugarcane for water-limited environments. Genetic variation in cane yield and sugar content in response to water stress. J Exp Bot 63:6023–6033. https://doi.org/10.1093/jxb/ers251

Basnayake J, Jackson PA, Inman-Bamber NG, Lakshmanan P (2015) Sugarcane for water-limited environments. Variation in stomatal conductance and its genetic correlation with crop productivity. J Exp Bot 66:3945–3958. https://doi.org/10.1093/jxb/erv194

Bell MJ, Garside AL (2005) Shoot and stalk dynamics and the yield of sugarcane crops in tropical and subtropical Queensland, Australia. Field Crop Res 92:231–248. https://doi.org/10.1016/j.fcr.2005.01.032

Bello CAC (2013) Uso del modelo Aquacrop para estimar rendimientos para el cultivo de caña de azúcar en el departamento del Valle del Cauca

Berding N, Moore PH (2001) Advancing from opportunistic sexual recombination in sugarcane. Lessons from tropical photoperiodic research. Proc Int Soc Sugar Cane Technol 24:482–487

Bezuidenhout CN, Singels A (2007a) Operational forecasting of South African sugarcane production: part 1 – system description. Agric Syst 92:23–38. https://doi.org/10.1016/j.agsy.2006.02.001

Bezuidenhout CN, Singels A (2007b) Operational forecasting of South African sugarcane production: part 2 – system evaluation. Agric Syst 92:39–51. https://doi.org/10.1016/j.agsy.2006.02.001

Bezuidenhout CN, Singels A, Hellmann D (2002) Whole farm harvesting strategy optimisation using the CANEGRO model: a case study for irrigated and rainfed sugarcane. Proc S Afr Sugar Technol Assoc 76:250–259

Bhengra AH, Yadav MK, Patel C et al (2016) Calibration and validation study of sugarcane (DSSAT-CANEGRO V4.6.1) model over North Indian region. J Agrometeorol 18:234–239

Biggs JS, Thorburn PJ, Crimp S et al (2013) Interactions between climate change and sugarcane management systems for improving water quality leaving farms in the Mackay Whitsunday region, Australia. Agric Ecosyst Environ 180:79–89. https://doi.org/10.1016/j.agee.2011.11.005

Black E, Vidale PL, Verhoef A et al (2012) Cultivating C4 crops in a changing climate: sugarcane in Ghana. Environ Res Lett 7:044027. https://doi.org/10.1088/1748-9326/7/4/044027

Bocca FF, Rodrigues LHA, Arraes NAM (2015) When do I want to know and why? Different demands on sugarcane yield predictions. Agric Syst 135:48–56. https://doi.org/10.1016/j.agsy.2014.11.008

Bonhomme R (2000) Beware of comparing RUE values calculated from PAR vs solar radiation or absorbed vs intercepted radiation. Field Crop Res 68:247–252. https://doi.org/10.1016/S0378-4290(00)00120-9

Bonnett GD (2014) Developmental stages (phenology). In: Moore PH, Botha FC (eds) Sugarcane: physiology, biochemistry, and functional biology. Wiley, Chichester, pp 35–53

Bonnett GD, Hewitt ML, Glassop D (2006) Effects of high temperature on the growth and composition of sugarcane internodes. Aust J Agric Res 57:1087–1095. https://doi.org/10.1071/AR06042

Boogaard HL, Van Diepen CA, Rötter RP et al (2014) WOFOST Control Centre 2.1 and WOFOST 7.1.7. 133

Boote KJ, Jones JW, Pickering NB (1996) Potential uses and limitations of crops models. Agron J 88:704–716. https://doi.org/10.2134/agronj1996.00021962008800050005x

Boote KJ, Allen LH, Prasad PVV, Jones JW (2010) Testing effects of climate change in crop models. In: Hillel D, Rosenzweig C (eds) Handbook of climate change and agroecosystems – impacts, adaptation and mitigation. Imperial College Press, London, pp 109–129

Börjesson P (2009) Good or bad bioethanol from a greenhouse gas perspective – what determines this? Appl Energy 86:589–594. https://doi.org/10.1016/j.apenergy.2008.11.025

Brandani CB, Abbruzzini TF, Williams S et al (2015) Simulation of management and soil interactions impacting SOC dynamics in sugarcane using the CENTURY Model. GCB Bioenergy 7:646–657. https://doi.org/10.1111/gcbb.12175

Brisson N, Mary B, Ripoche D, Jeuffroy MH, Ruget F, Nicoullaud B, Gate P, Devienne-Barret F, Antonioletti R, Durr C, Richard G, Beaudoin N, Recous S, Tayot X, Plenet D, Cellier P, Machet JM, Meynard J-M, Delécolle R (1998) STICS: a generic model for the simulation of crops and their water and nitrogen balances, I. Theory and parameterization applied to wheat and corn. Agronomie 18:311–346

Cardozo NP, Sentelhas PC, Panosso AR et al (2015) Modeling sugarcane ripening as a function of accumulated rainfall in Southern Brazil. Int J Biometeorol 59:1913–1925. https://doi.org/10.1007/s00484-015-0998-6

Cheeroo-Nayamuth FB, Nayamuth RAH (2001) Climate change and sucrose production in Mauritius. Proc Int Soc Sugar Cane Technol 24:107–112

Cheeroo-Nayamuth F, Robertson M, Wegener M, Nayamuth AR (2000) Using a simulation model to assess potential and attainable sugar cane yield in Mauritius. Field Crop Res 66:225–243. https://doi.org/10.1016/S0378-4290(00)00069-1

Cheeroo-Nayamuth BF, Bezuidenhout CN, Kiker GA, Nayhamuth AR (2003) Validation of CANEGRO-DSSAT V3.5 for contrasting sugarcane varieties in Mauritius. Proc S Afr Sugar Technol Assoc 7:601–604

Cheeroo-Nayamuth B, Nayamuth A, Koonjah S (2011) Yield analysis in the west sector of the Mauritian sugarcane industry. Proc S Afr Sugar Technol Assoc 84:106–115

Chopart J-L, Rodrigues SR, Carvalho de Azevedo M, de Conti Medina C (2008) Estimating sugarcane root length density through root mapping and orientation modelling. Plant Soil 313:101–112. https://doi.org/10.1007/s11104-008-9683-4

Chopart JL, Azevedo MCB, Le Mézo L, Marion D (2010) Functional relationship between sugarcane root biomass and length for cropping system applications. Sugar Tech 12:317–321. https://doi.org/10.1007/s12355-010-0044-2

Christina M, Le Mezo L, Mezino M et al (2019) Modelling the annual yield variability in sugarcane in Réunion. Proc Int Soc Sugar Cane Technol 30:393–401

Coleman RE (1963) Effect of temperature on flowering in sugarcane. Int Sugar J 6:351–353

Costa LG (2017) Crescimento, desenvolvimento e consumo hídrico de cana-de-açúcar sob dois sistemas de manejo da palha. Universidade de São Paulo, Escola Superior de Agricultura “Luiz de Queiroz”. Piracicaba, Brasil [in Portuguese]

Costa LG, Marin FR, Nassif DSP et al (2014) Simulação do efeito do manejo da palha e do nitrogênio na produtividade da cana-de-açúcar. Rev Bras Eng Agrícola e Ambient 18:469–474. https://doi.org/10.1590/S1415-43662014000500001

Cuadra SV, Costa MH, Kucharik CJ et al (2012) A biophysical model of sugarcane growth. GCB Bioenergy 4:36–48. https://doi.org/10.1111/j.1757-1707.2011.01105.x

da Silva TGF (2009) Análise de crescimento, interação biosfera-atmosfera e eficiência do uso de água da cana-de-açúcar irrigada no submédio do Vale do São Francisco. Universidade Federal de Viçosa, Viçosa, Brasil [In Portuguese]

da Silva RF (2012) Calibração do modelo DSSAT/Canegro para a cana-de-açúcar e seu uso para a avaliação do impacto das mudanças climáticas. Universidade Federal de Viçosa, Viçosa, Brasil [In Portuguese]

de Barros I, Thorburn PJ, Biggs JS, et al (2018) Simulações de Práticas de Manejo na Produção de Cana-de-Açúcar nos Tabuleiros Costeiros de Alagoas. Aracaju, SE, Brazil

de Carvalho AL, Menezes RSC, Nóbrega RS et al (2015) Impact of climate changes on potential sugarcane yield in Pernambuco, northeastern region of Brazil. Renew Energy 78:26–34. https://doi.org/10.1016/j.renene.2014.12.023

de Lange JDE, Singels A (2003) Using the internet-based Canesim model for crop estimation in the Umfolozi mill supply area. Proc S Afr Sugar Technol Assoc 77:592–595

de Oliveira APP, Thorburn PJ, Biggs JS et al (2016) The response of sugarcane to trash retention and nitrogen in the Brazilian coastal tablelands: a simulation study. Exp Agric 52:69–86. https://doi.org/10.1017/S0014479714000568

de Oliveira MPG, Bocca FF, Rodrigues LHA (2017) From spreadsheets to sugar content modeling: a data mining approach. Comput Electron Agric 132:14–20. https://doi.org/10.1016/J.COMPAG.2016.11.012

De Silva ALC, De Costa WAJM (2012) Growth and radiation use efficiency of sugarcane under irrigated and rain-fed conditions in Sri Lanka. Sugar Tech 14:247–254. https://doi.org/10.1007/s12355-012-0148-y de Souza AP, Gaspar M, Da Silva EA et al (2008) Elevated CO2 increases photosynthesis, biomass and productivity, and modifies gene expression in sugarcane. Plant Cell Environ 31:1116–1127. https://doi.org/10.1111/j.1365-3040.2008.01822.x

de Vries FWTP, Jansen DM, ten Berge HFM, Bakema A (1989) Simulation of ecophysiological process of growth in several annual crops. Pudoc/IRRI, Wageningen

Dias HB, Sentelhas PC (2017) Evaluation of three sugarcane simulation models and their ensemble for yield estimation in commercially managed fields. Field Crop Res 213:174–185. https://doi.org/10.1016/j.fcr.2017.07.022

Dias HB, Sentelhas PC (2018a) Drying-off periods for irrigated sugarcane to maximize sucrose yields under Brazilian conditions. Irrig Drain 67:527–537. https://doi.org/10.1002/ird.2263

Dias HB, Sentelhas PC (2018b) Sugarcane yield gap analysis in Brazil – a multi-model approach for determining magnitudes and causes. Sci Total Environ 637–638:1127–1136. https://doi.org/10.1016/j.scitotenv.2018.05.017

Dias HB, Inman-Bamber G, Bermejo R, Sentelhas PC, Christodoulou D (2019) New APSIM-Sugar features and parameters required to account for high sugarcane yields in tropical environments. Field Crop Res 235:38–53. https://doi.org/10.1016/j.fcr.2019.02.002

Dias HB, Inman-Bamber G, Everingham Y, Sentelhas PC, Bermejo R, Christodoulou D (2020) Traits for canopy development and light interception by twenty-seven Brazilian sugarcane varieties. Field Crop Res 249:107716. https://doi.org/10.1016/j.fcr.2020.107716

Donaldson RA (2009) Seasonal effects on the potential biomass and sucrose accumulation of some commercial cultivars of sugarcane. University of KwaZulu-Natal, Faculty of Science and Agriculture

Donaldson RA, Bezuidenhout CN (2000) Determining the maximum drying-off periods for sugarcane grown in different regions of the South African Industry. Proc S Afr Sugar Technol Assoc 74:162–166

Donaldson RA, Redshaw KA, Rhodes R, van Antwerpen R (2008) Season effects on productivity of some commercial south African sugarcane cultivars, I: biomass and radiation use efficiency. Proc S Afr Sugar Technol Assoc 81:517–527

dos Vianna MS, Sentelhas PC (2014) Simulação do risco de deficit hídrico em regiões de expansão do cultivo de cana-de-açúcar no Brasil. Pesqui Agropecuária Bras 49:237–246. https://doi.org/10.1590/S0100-204X2014000400001

dos Vianna MS, Sentelhas PC (2016) Performance of DSSAT CSM-CANEGRO under operational conditions and its use in determining the 'saving irrigation' impact on sugarcane crop. Sugar Tech 18:75–86. https://doi.org/10.1007/s12355-015-0367-0

Driessen PM, Konijn NT (1992) Land-use system analysis. Wageningen Agricultural University, Wageningen

Edreira JIR, Cassman KG, Hochman Z et al (2018) Beyond the plot: technology extrapolation domains for scaling out agronomic science. Environ Res Lett 13:054027. https://doi.org/10.1088/1748-9326/aac092

Evans LT, Fischer RA (1999) Yield potential: its definition, measurement, and significance. Crop Sci 39:1544–1551. https://doi.org/10.2135/cropsci1999.3961544x

Everingham YL, Muchow RC, Stone RC et al (2002) Enhanced risk management and decision-making capability across the sugarcane industry value chain based on seasonal climate forecasts. Agric Syst 74:459–477. https://doi.org/10.1016/S0308-521X(02)00050-1

Everingham Y, Ticehurst C, Barrett D et al (2005) Yield forecasting for marketers. Proc Aust Soc Sugar Cane Technol 27:51–60

Everingham YL, Inman-Bamber NG, Thorburn PJ, McNeill TJ (2007) A Bayesian modelling approach for long lead sugarcane yield forecasts. Aust J Agric Res 58:87–94

Everingham Y, Baillie C, Inman-Bamber G, Baillie J (2008) Forecasting water allocations for Bundaberg sugarcane farmers. Clim Res 36:231–239. https://doi.org/10.3354/cr00743

Everingham YL, Smyth CW, Inman-Bamber NG (2009) Ensemble data mining approaches to forecast regional sugarcane crop production. Agric For Meteorol 149:689–696. https://doi.org/10.1016/j.agrformet.2008.10.018

Everingham YL, Inman-Bamber NG, Sexton J, Stokes C (2015) A dual ensemble agroclimate modelling procedure to assess climate change impacts on sugarcane production in Australia. Agric Sci 6:870–888. https://doi.org/10.4236/as.2015.68084

Everingham YL, Sexton J, Skocaj D, Inman-Bamber NG (2016) Accurate prediction of sugarcane yield using a random forest algorithm. Agron Sustain Dev 36. https://doi.org/10.1007/s13593-016-0364-z

FAO (2019) FAOSTAT. Food and Agriculture Organization of the United Nations. http://www.fao.org/faostat/en/#home. Accessed 8 May 2019

Ferreira Junior RA, de Souza JL, Lyra GB et al (2015) Energy conversion efficiency in sugarcane under two row spacings in northeast of Brazil. Rev Bras Eng Agrícola e Ambient 19:741–747. https://doi.org/10.1590/1807-1929/agriambi.v19n8p741-747

Fischer RA (2015) Definitions and determination of crop yield, yield gaps, and of rates of change. Field Crop Res 182:9–18. https://doi.org/10.1016/j.fcr.2014.12.006

Franco HCJ, Otto R, Faroni CE et al (2011) Nitrogen in sugarcane derived from fertilizer under Brazilian field conditions. Field Crop Res 121:29–41. https://doi.org/10.1016/j.fcr.2010.11.011

Galdos MV, Cerri CC, Cerri CEP et al (2009a) Simulation of soil carbon dynamics under sugarcane with the CENTURY model. Soil Sci Soc Am J 73:802. https://doi.org/10.2136/sssaj2007.0285

Galdos MV, Cerri CC, Cerri CEP (2009b) Soil carbon stocks under burned and unburned sugarcane in Brazil. Geoderma 153:347–352. https://doi.org/10.1016/j.geoderma.2009.08.025

Ghannoum O, Conroy JP, Driscoll SP et al (2003) Nonstomatal limitations are responsible for drought-induced photosynthetic inhibition in four C_4 grasses. New Phytol 159:599–608. https://doi.org/10.1046/j.1469-8137.2003.00835.x

Goldemberg J, Mello FFC, Cerri CEP et al (2014) Meeting the global demand for biofuels in 2021 through sustainable land use change policy. Energy Policy 69:14–18. https://doi.org/10.1016/j.enpol.2014.02.008

Gosnell JM (1973) Some factors affecting flowering in sugarcane. Proc S Afr Sugar Technol Assoc 47:144–147

Grof CPL, Campbell JA, Kravchuk O et al (2010) Temperature effect on carbon partitioning in two commercial cultivars of sugarcane. Funct Plant Biol 37:334. https://doi.org/10.1071/fp09216

Gunarathna MHJP, Sakai K, Nakandakari T et al (2019) Sensitivity analysis of plant- and cultivar-specific parameters of APSIM-Sugar model: variation between climates and management conditions. Agronomy 9:242. https://doi.org/10.3390/agronomy9050242

Heino M, Puma MJ, Ward PJ et al (2018) Two-thirds of global cropland area impacted by climate oscillations. Nat Commun 9:1257. https://doi.org/10.1038/s41467-017-02071-5

Higgins A, Thorburn P, Archer A, Jakku E (2007) Opportunities for value chain research in sugar industries. Agric Syst 94:611–621. https://doi.org/10.1016/J.AGSY.2007.02.011

Hoffman N, Patton A, Malan C et al (2017) An experimental and crop modelling assessment of elevated atmospheric CO_2 effects on sugarcane productivity. Proc S Afr Sugar Technol Assoc 90:131–134

Hoffman N, Singels A, Patton A, Ramburan S (2018) Predicting genotypic differences in irrigated sugarcane yield using the Canegro model and independent trait parameter estimates. Eur J Agron 96:13–21. https://doi.org/10.1016/j.eja.2018.01.005

Holzworth DP, Huth NI, deVoil PG et al (2014) APSIM – evolution towards a new generation of agricultural systems simulation. Environ Model Softw 62:327–350. https://doi.org/10.1016/j.envsoft.2014.07.009

Hoogenboom G, Porter CH, Shelia V et al (2019) Decision Support System for Agrotechnology Transfer (DSSAT) Version 4.7.5

Inman-Bamber NG (1991) A growth model for sugar-cane based on a simple carbon balance and the CERES-Maize water balance. S Afr J Plant Soil 9:37–41. https://doi.org/10.1080/02571862.1991.10634587

Inman-Bamber NG (1994) Temperature and seasonal effects on canopy development and light interception of sugarcane. Field Crop Res 36:41–51. https://doi.org/10.1016/0378-4290(94)90051-5

Inman-Bamber NG (1995) Climate and water constraints to production in the south African sugar industry. Proc S Afr Sugar Technol Assoc 69:55–59

Inman-Bamber NG (2000) History of the Canegro model. In: Proceedings of international CANEGRO work. South African Sugarcane Research Institute, Mount Edgecombe, South Africa, pp 5–8

Inman-Bamber NG (2004) Sugarcane water stress criteria for irrigation and drying off. Field Crop Res 89:107–122. https://doi.org/10.1016/j.fcr.2004.01.018

Inman-Bamber NG (2014) Sugarcane yields and yield-limiting processes. In: Moore PH, Botha FC (eds) Sugarcane: physiology, biochemistry, and functional biology. Wiley, Chichester, pp 579–600

Inman-Bamber NG, Attard SJ (2008) Water savings and water accounting in irrigated sugarcane. Proc Aust Soc Sugar Cane Technol 30:251–259

Inman-Bamber NG, Jager MDE (1988) Effect of water stress on sugarcane stalk growth and quality. Proc S Afr Sugar Technol Assoc 52:140–144

Inman-Bamber NG, Kiker GA (1998) DSSAT/CANEGRO 3.10: DSSAT version 3.1. University of Hawaii, Honolulu

Inman-Bamber NG, McGlinchey MG (2003) Crop coefficients and water-use estimates for sugarcane based on long-term Bowen ratio energy balance measurements. Field Crop Res 83:125–138. https://doi.org/10.1016/S0378-4290(03)00069-8

Inman-Bamber NG, Smith DM (2005) Water relations in sugarcane and response to water deficits. Field Crop Res 92:185–202. https://doi.org/10.1016/j.fcr.2005.01.023

Inman-Bamber NG, Thompson GD (1989) Models of dry matter accumulation by sugarcane. Proc S Afr Sugar Technol Assoc 63:212–216

Inman-Bamber NG, Culverwell TL, McGlinchey MG (1993) Predicting yield responses to irrigation of sugarcane from a growth model and field records. Proc S Afr Sugar Technol Assoc 67:66–72

Inman-Bamber NG, Robertson MJ, Muchow RC et al (1999) Boosting yields with limited irrigation water. Proc Aust Soc Sugar Cane Technol 21:203–211

Inman-Bamber NG, Everingham YL, Muchow RC (2001) Modelling water stress response in sugarcane: validation and application of the APSIM-Sugarcane model. In: Proceedings of the 10th Australian agronomy conference, Hobart, Australia

Inman-Bamber NG, Attard SJ, Spillman MF (2004) Can lodging be controlled through irrigation? Proc Aust Soc Sugar Cane Technol 26:1–11

Inman-Bamber NG, Attard SA, Baillie C et al (2005) A web-based system for planning use of limited irrigation water in sugarcane. Proc Aust Soc Sugar Cane Technol 27:170–181

Inman-Bamber NG, Webb WA, Verrall SA (2006) Participatory irrigation research and scheduling in the Ord: R&D. Proc Aust Soc Sugar Cane Technol 28:155–163

Inman-Bamber NG, Attard SJ, Verrall SA et al (2007) A web-based system for scheduling irrigation in sugarcane. Proc Aust Soc Sugar Cane Technol 26:459–464

Inman-Bamber NG, Jackson P, Bourgault M (2011) Genetic adjustment to changing climates: sugarcane. In: Yadav SS, Redden R, Hatfield JL et al (eds) Crop adaptation to climate change. Wiley, Chichester, pp 439–447

Inman-Bamber NG, Lakshmanan P, Park S (2012) Sugarcane for water-limited environments: theoretical assessment of suitable traits. Field Crop Res 134:95–104. https://doi.org/10.1016/j.fcr.2012.05.004

Inman-Bamber NG, Jackson PA, Stokes CJ et al (2016) Sugarcane for water-limited environments: enhanced capability of the APSIM sugarcane model for assessing traits for transpiration efficiency and root water supply. Field Crop Res 196:112–123. https://doi.org/10.1016/j.fcr.2016.06.013

IPCC (2014) Climate change 2014: synthesis report. Contribution of working groups I, II and III to the fifth assessment report of the intergovernmental panel on climate change. IPCC, Geneva

Jackson P, Basnayake J, Inman-Bamber G et al (2016) Genetic variation in transpiration efficiency and relationships between whole plant and leaf gas exchange measurements in Saccharum spp. and related germplasm. J Exp Bot 67:861–871. https://doi.org/10.1093/jxb/erv505

Jaiswal D, De Souza AP, Larsen S et al (2017) Brazilian sugarcane ethanol as an expandable green alternative to crude oil use. Nat Clim Chang 7:788–792. https://doi.org/10.1038/nclimate3410

Jakku E, Thorburn PJ (2010) A conceptual framework for guiding the participatory development of agricultural decision support systems. Agric Syst 103:675–682. https://doi.org/10.1016/J.AGSY.2010.08.007

Jintrawet A, Prammaneem P (2005) Simulating the impact of climate change scenarios on sugarcane production systems in Thailand. Proc Int Soc Sugar Cane Technol 25:64–68

Jones CA, Kiniry JR (1986) CERES-maize: a simulation model of maize growth and development. Texas A&M University Press, College Station

Jones MR, Singels A (2015) Analysing yield trends in the South African sugar industry. Agric Syst 141:24–35. https://doi.org/10.1016/j.agsy.2015.09.004

Jones MR, Singels A (2019) Refining the Canegro model for improved simulation of climate change impacts on sugarcane. Eur J Agron 100:76–86. https://doi.org/10.1016/j.eja.2017.12.009

Jones CA, Wegener MK, Russel JS (1989) AUSCANE – simulation of Australian sugarcane with EPIC, Tropical agronomy technical paper no. 29. CSIRO Division of Tropical Crops and Pastures, Brisbane

Jones MR, Singels A, Thornburn P et al (2014) Evaluation of the DSSAT-Canegro model for simulating climate change impacts at sites in seven countries. Proc S Afr Sugar Technol Assoc 87:323–329. https://doi.org/10.1007/BF02722738

Jones MR, Singels A, Ruane AC (2015) Simulated impacts of climate change on water use and yield of irrigated sugarcane in South Africa. Agric Syst 139:260–270. https://doi.org/10.1016/j.agsy.2015.07.007

Kandulu J, Thorburn P, Biggs J, Verburg K (2018) Estimating economic and environmental trade-offs of managing nitrogen in Australian sugarcane systems taking agronomic risk into account. J Environ Manag 223:264–274. https://doi.org/10.1016/j.jenvman.2018.06.023

Keating BA, Verburg K, Huth NI, Robertson MJ (1997) Nitrogen management in intensive agriculture: sugarcane in Australia. In: Keating BA, Wilson JR (eds) Intensive sugarcane production: meeting the challenges beyond 2000. CAB International, Wallingford, pp 20–23

Keating BA, Robertson MJ, Muchow RC, Huth NI (1999) Modelling sugarcane production systems I. Development and performance of the sugarcane module. Field Crop Res 61:253–271. https://doi.org/10.1016/S0378-4290(98)00167-1

Keating BA, Carberry PS, Hammer GL et al (2003) An overview of APSIM, a model designed for farming systems simulation. Eur J Agron 18:267–288. https://doi.org/10.1016/S1161-0301(02)00108-9

Kimball BA (2016) Crop responses to elevated CO_2 and interactions with H_2O, N, and temperature. Curr Opin Plant Biol 31:36–43. https://doi.org/10.1016/J.PBI.2016.03.006

Kingston G (2002) Recognising the impact of climate on CCS of sugarcane across tropical and sub-tropical regions of the Australian sugar industry. Proc Aust Soc Sugar Cane Technol 24 (CD-ROM)

Kiniry JR, Williams JR, Gassman PW, Debaeke P (1992) A general, process-oriented model for two competing plant species. Trans ASAE 35:801–810. https://doi.org/10.13031/2013.28665

Knox JW, Rodríguez Díaz JA, Nixon DJ, Mkhwanazi M (2010) A preliminary assessment of climate change impacts on sugarcane in Swaziland. Agric Syst 103:63–72. https://doi.org/10.1016/j.agsy.2009.09.002

Kucharik CJ, Brye KR (2003) Integrated BIosphere Simulator (IBIS) yield and nitrate loss predictions for Wisconsin maize receiving varied amounts of nitrogen fertilizer. J Environ Qual 32:247–268. https://doi.org/10.2134/jeq2003.2470

Kunz R, Schulze R, Mabhaudhi T, Mokonoto O (2014) Modelling the potential impacts of climate change on yield and water use of sugarcane and sugar beet: preliminary results based on the AquaCrop model. Proc S Afr Sugar Technol Assoc 87:285–289

Laclau PB, Laclau JP (2009) Growth of the whole root system for a plant crop of sugarcane under rainfed and irrigated environments in Brazil. Field Crop Res 114:351–360. https://doi.org/10.1016/j.fcr.2009.09.004

Lakshmanan P, Robinson N (2014) Stress physiology: abiotic stresses. In: Moore PH, Botha FC (eds) Sugarcane: physiology, biochemistry, and functional biology. Wiley, Chichester, pp 411–434

Leal DPV (2016) Parametrização do modelo CANEGRO (DSSAT) e caracterização biométrica de oito variedades de cana-de-açúcar irrigadas por gotejamento. Universidade de São Paulo, Escola Superior de Agricultura “Luiz de Queiroz”. Piracicaba, Brasil [In Portuguese]

Linnenluecke MK, Nucifora N, Thompson N (2018) Implications of climate change for the sugarcane industry. Wiley Interdiscip Rev Clim Chang 9:1–34. https://doi.org/10.1002/wcc.498

Linnenluecke MK, Zhou C, Smith T et al (2019) The impact of climate change on the Australian sugarcane industry. J Clean Prod. https://doi.org/10.1016/j.jclepro.2019.118974

Lisson SN, Robertson MJ, Keating BA, Muchow RC (2000) Modelling sugarcane production systems II: analysis of system performance and methodology issues. Field Crop Res 68:31–48

Lisson S, Brennan L, Bristow K et al (2003) DAM EA$Y—software for assessing the costs and benefits of on-farm water storage based production systems. Agric Syst 76:19–38. https://doi.org/10.1016/S0308-521X(02)00112-9

Lisson SN, Inman-Bamber NG, Robertson MJ, Keating BA (2005) The historical and future contribution of crop physiology and modelling research to sugarcane production systems. Field Crop Res 92:321–335. https://doi.org/10.1016/j.fcr.2005.01.010

Liu DL, Allsop PG (1996) QCANE and armyworms: to spray or no to spray, that is the question. Proc Aust Soc Sugar Cane Technol 18:106–112

Liu DL, Bull TA (2001) Simulation of biomass and sugar accumulation in sugarcane using a process-based model. Ecol Model 144:181–211. https://doi.org/10.1016/S0304-3800(01)00372-6

Liu DL, Kingston G (1994) QCANE: a simulation model of sugarcane growth and sugar accumulation. In: Robertson MJ (ed) Research and modeling approaches to assess sugarcane production opportunities and constraints. Workshop Proceedings University of Queensland, St. Lucia, p 144

Lobell DB, Asseng S (2017) Comparing estimates of climate change impacts from process-based and statistical crop models. Environ Res Lett 12:1–12. https://doi.org/10.1088/1748-9326/015001

Lobell DB, Cassman KG, Field CB (2009) Crop yield gaps: their importance, magnitudes, and causes. Annu Rev Environ Resour 34:179–204. https://doi.org/10.1146/annurev.environ.041008.093740

Lonsdale JE, Gosnell JM (1976) Growth and quality of four sugarcane varieties as influenced by age and season. Proc S Afr Sugar Technol Assoc 50:82–86

Lumsden TG, Lecler NL, Schulze RE, S African Sugar Technologists Assoc SASTA (1998) Simulation of sugarcane yield at the scale of a mill supply area. Proc S Afr Sugar Technol Assoc 72:12–17

Machado EC (1981) Um modelo matemático-fisiológico para simular o acúmulo de matéria seca na cultura de cana-de-açúcar (Saccharum spp.). Universidade de Campinas, Campinas, Brasil [in Portuguese]

Mallawaarachchi T, Quiggin J (2001) Modelling socially optimal land allocations for sugar cane growing in North Queensland: a linked mathematical programming and choice modelling study. Aust J Agric Resour Econ 45:383–409. https://doi.org/10.1111/1467-8489.00149

Mangelsdorf AJ (1950) Sugar-cane—as seen from Hawaii. Econ Bot 4:150–176. https://doi.org/10.1007/bf02873319

Marchiori PER, Machado EC, Sales CRG et al (2017) Physiological plasticity is important for maintaining sugarcane growth under water deficit. Front Plant Sci 8:1–12. https://doi.org/10.3389/fpls.2017.02148
Marin FR (2017) Tempocampo: a system for operational forecasting of Brazilian sugarcane and soybean yield. In: ASA, CSSA and SSSA international annual meeting. ACS Societies, Tampa, FL, USA
Marin FR, Jones JW (2014) Process-based simple model for simulating sugarcane growth and production. Sci Agric 71:1–16
Marin FR, Jones JW, Royce F et al (2011) Parameterization and evaluation of predictions of DSSAT/CANEGRO for Brazilian sugarcane. Agron J 103:304–315. https://doi.org/10.2134/agronj2010.0302
Marin FR, Jones JW, Singels A, Royce F, Assad ED, Pellegrino GQ, Justino J (2013) Climate change impacts on sugarcane attainable yield in southern Brazil. Clim Chang 117:227–239. https://doi.org/10.1007/s10584-012-0561-y
Marin FR, Thorburn PJ, Costa LG, Otto R (2014) Simulating Long-term effects of trash management on sugarcane yield for Brazilian cropping systems. Sugar Tech 16:164–173. https://doi.org/10.1007/s12355-013-0265-2
Marin FR, Thorburn PJ, Nassif DSP, Costa LG (2015) Sugarcane model intercomparison: structural differences and uncertainties under current and potential future climates. Environ Model Softw 72:372–386. https://doi.org/10.1016/j.envsoft.2015.02.019
Marin FR, Martha GB, Cassman KG, Grassini P (2016) Prospects for increasing sugarcane and bioethanol production on existing crop area in Brazil. Bioscience 66:307–316. https://doi.org/10.1093/biosci/biw009
Martiné J-F (2003) Modélisation de la production potentielle de la Canne à Sucre en zone tropicale, sous conditions hydriques et thermiques contrastées. Applications du Modèle. Thése de Docteur de l'Institut National Agronomique Paris-Grignon [in French]
Martiné J-F (2007) Analysis and forecasting of the sucrose content of sugarcane crops during the harvest period in Reunion Island. Proc Int Soc Sugar Cane Technol 26:607–612
Martiné J-F, Siband P, Bonhomme R (1999) Simulation of the maximum yield of sugar cane at different altitudes: effect of temperature on the conversion of radiation into biomass. Agronomie 19:3–12. https://doi.org/10.1051/agro:19990101
McCown RL, Hammer GL, Hargreaves JNG et al (1996) APSIM: a novel software system for model development, model testing and simulation in agricultural systems research. Agric Syst 50:255–271. https://doi.org/10.1016/0308-521X(94)00055-V
McDonald L, Lisson SN (2001) The effect of planting and harvest time on sugarcane productivity. In: Proceedings of the 10th Australian agronomy conference. Hobart, Australia
McGlinchey MG (1999) Computer crop model applications: developments in Swaziland. Proc S Afr Sugar Technol Assoc 73:35–44
McGlinchey MG, Dell MP (2010) Using computer simulation models to aid replant planning and harvest decisions in irrigated sugarcane. Proc Int Soc Sugar Cane Technol 27:1–10
McGlinchey MG, Inman-Bamber NG, Culverwell TL (1995) An irrigation scheduling method based on a crop model and an automatic weather station. Proc S Afr Sugar Technol Assoc 69:69–73
Meier EA, Thorburn PJ (2016) Long term sugarcane crop residue retention offers limited potential to reduce nitrogen fertilizer rates in Australian wet tropical environments. Front Plant Sci 7:1–14. https://doi.org/10.3389/fpls.2016.01017
Meki MN, Kiniry JR, Youkhana AH et al (2015) Two-year growth cycle sugarcane crop parameter attributes and their application in modeling. Agron J 107:1310–1320. https://doi.org/10.2134/agronj14.0588
Miguez FE, Zhu X, Humphries S et al (2009) A semimechanistic model predicting the growth and production of the bioenergy crop Miscanthus × giganteus: description, parameterization and validation. GCB Bioenergy 1:282–296. https://doi.org/10.1111/j.1757-1707.2009.01019.x

Mishra SK, Singh G, Singh K (2017) Sugarcane growth and yield simulation under varying planting dates in sub tropical India. J Agrometeorol 19:200–204
Monteith JL (1972) Solar radiation and productivity in tropical ecosystems. J Appl Ecol 9:747–766. https://doi.org/10.2307/2401901
Moore PH, Berding N (2014) Flowering. In: Moore PH, Botha FC (eds) Sugarcane: physiology, biochemistry, and functional biology. Wiley, Chichester, pp 379–410
Moore PH, Paterson AH, Tew T (2014) Sugarcane: the crop, the plant, and domestication. In: Moore PH, Botha FC (eds) Sugarcane: physiology, biochemistry, and functional biology. Wiley, Chichester, pp 1–17
Morel J, Bégué A, Todoroff P et al (2014a) Coupling a sugarcane crop model with the remotely sensed time series of fIPAR to optimise the yield estimation. Eur J Agron 61:60–68. https://doi.org/10.1016/j.eja.2014.08.004
Morel J, Todoroff P, Bégué A et al (2014b) Toward a satellite-based system of sugarcane yield estimation and forecasting in smallholder farming conditions: a case study on reunion island. Remote Sens 6:6620–6635. https://doi.org/10.3390/rs6076620
Muchow RC, Keating BA (1998) Assessing irrigation requirements in the Ord Sugar Industry using a simulation modelling approach. Aust J Exp Agric 38:345–354. https://doi.org/10.1071/EA98023
Muchow RC, Spillman MF, Wood AW, Thomas MR (1994) Radiation interception and biomass accumulation in a sugarcane crop grown under irrigated tropical conditions. Aust J Agric Res 45:37–49. https://doi.org/10.1071/AR9940037
Muchow RC, Evensen CI, Osgood RV, Robertson MJ (1997a) Yield accumulation in irrigated sugarcane: II. Utilization of intercepted radiation. Agron J 89:646–652. https://doi.org/10.2134/agronj1997.00021962008900040017x
Muchow RC, Robertson MJ, Keating BA (1997b) Limits to Autralian sugar industry: climate and biological factors. In: Keating BA, Wilson J (eds) Intensive sugarcane production: meeting the challenges beyond 2000. CAB International, Wallingford, pp 37–54
Ngobese I, Ramburan S, Labuschagne M (2018) Quantifying sugarcane cultivar differences in tiller and stalk phenology: identifying traits suited to crop model-assisted breeding. J Crop Improv 32:847–860. https://doi.org/10.1080/15427528.2018.1534762
NOOA (2019) Trends in atmospheric carbon dioxide – global greenhouse gas reference network. https://www.esrl.noaa.gov/gmd/ccgg/trends/global.html. Accessed 26 Jun 2019
O'Leary GJ (2000) A review of three sugarcane simulation models with respect to their prediction of sucrose yield. Field Crop Res 68:97–111. https://doi.org/10.1016/S0378-4290(00)00112-X
Ojeda JJ, Volenec JJ, Brouder SM et al (2017) Evaluation of Agricultural Production Systems Simulator as yield predictor of *Panicum virgatum* and *Miscanthus x giganteus* in several US environments. GCB Bioenergy 9:796–816. https://doi.org/10.1111/gcbb.12384
Olivier FC, Singels A (2001) A database of crop water use coefficients for irrigation scheduling of sugarcane. Proc S Afr Sugar Technol Assoc 75:81–83
Otto R, Silva AP, Franco HCJ et al (2011) High soil penetration resistance reduces sugarcane root system development. Soil Tillage Res 117:201–210. https://doi.org/10.1016/j.still.2011.10.005
Otto R, Castro SAQ, Mariano E et al (2016) Nitrogen use efficiency for sugarcane-biofuel production: what is next? Bioenergy Res 9:1272–1289. https://doi.org/10.1007/s12155-016-9763-x
Pagani V, Stella T, Guarneri T et al (2017) Forecasting sugarcane yields using agro-climatic indicators and Canegro model: a case study in the main production region in Brazil. Agric Syst 154:45–52. https://doi.org/10.1016/j.agsy.2017.03.002
Paraskevopoulos AL, Singels A (2014) Integrating soil water monitoring technology and weather based crop modelling to provide improved decision support for sugarcane irrigation management. Comput Electron Agric 105:44–53. https://doi.org/10.1016/j.compag.2014.04.007
Paraskevopoulos AL, Singels A, Tweeddle PB, van Heerden PDR (2016) Quantifying the negative impact of lodging on irrigated sugarcane productivity: a crop modelling assessment. Proc S Afr Sugar Technol Assoc 89:154–158

Park SE (2008) A review of climate change impact and adaptation assessments on the Australian sugarcane industry. Proc Aust Soc Sugar Cane Technol 30:1–9

Park SE, Robertson M, Inman-Bamber NG (2005) Decline in the growth of a sugarcane crop with age under high input conditions. Field Crop Res 92:305–320. https://doi.org/10.1016/j.fcr.2005.01.025

Park SE, Howden M, Horan HL (2007) Evaluating the impact of and capacity for adaptation to climate change on sectors in the sugar industry value chain in Australia. Proc Int Soc Sugar Cane Technol 26:312–326

Park SE, Webster TJ, Horan HL et al (2010) A legume rotation crop lessens the need for nitrogen fertiliser throughout the sugarcane cropping cycle. Field Crop Res 119:331–341. https://doi.org/10.1016/j.fcr.2010.08.001

Peloia PR, Bocca FF, Rodrigues LHA et al (2019) Identification of patterns for increasing production with decision trees in sugarcane mill data. Sci Agric 76:281–289. https://doi.org/10.1590/1678-992x-2017-0239

Piewthongngam K, Pathumnakul S, Setthanan K (2009) Application of crop growth simulation and mathematical modeling to supply chain management in the Thai sugar industry. Agric Syst 102:58–66. https://doi.org/10.1016/j.agsy.2009.07.002

Promburom P, Jintrawet A, Ekasingh M (2001) Estimating sugarcane yields with Oy-Thai interface. Proc Int Soc Sugar Cane Technol 24:81–86

Qureshi SA, Madramootoo CA, Dodds GT (2002) Evaluation of irrigation schemes for sugarcane in Sindh, Pakistan, using SWAP93. Agric Water Manag 54:37–48. https://doi.org/10.1016/S0378-3774(01)00142-1

Rabbinge R (1993) The ecological background of food production. In: Chadwick D, Marsh J (eds) Crop protection and sustainable agriculture, Ciba found. Wiley, Chichester, pp 2–29

Robertson MJ, Wood AW, Muchow RC (1996) Growth of sugarcane under high input conditions in tropical Australia, I. Radiation use, biomass accumulation and partitioning. Field Crop Res 48:11–25. https://doi.org/10.1016/S0378-4290(96)00043-3

Robertson MJ, Inman-Bamber NG, Muchow RC (1997) Opportunities for improving the use of limited water by the sugarcane crop. In: Keating BA, Wilson J (eds) Intensive sugarcane production: meeting the challenges beyond 2000. CAB International, Wallingford, pp 287–304

Robertson MJ, Bonnett GD, Highes RM et al (1998) Temperature and leaf area expansion of sugarcane: integration of controlled-environment, field and model studies. Aust J Plant Physiol 25:819–828

Robertson MJ, Inman-Bamber NG, Muchow RC, Wood AW (1999a) Physiology and productivity of sugarcane with early and mid-season water deficit. Field Crop Res 64:211–227. https://doi.org/10.1016/S0378-4290(99)00042-8

Robertson MJ, Muchow RC, Donaldson RA et al (1999b) Estimating the risk associated with drying-off strategies for irrigated sugarcane before harvest. Aust J Agric Res 50:65–77

Robinson N, Brackin R, Vinall K et al (2011) Nitrate paradigm does not hold up for sugarcane. PLoS One 6:e19045. https://doi.org/10.1371/journal.pone.0019045

Rostron H (1974) Some effects of environment, age and growth regulating compounds on the growth, yield and quality of sugarcane in Southern Africa. University of Natal, Pietermaritzburg

Ruan H, Feng P, Wang B et al (2018) Future climate change projects positive impacts on sugarcane productivity in southern China. Eur J Agron 96:108–119. https://doi.org/10.1016/j.eja.2018.03.007

Saeki T (1963) Light relations in plant communities. In: Evans LT (ed) Environmental control of plant growth. Academic Press, New York, pp 79–84

Sage RF, Peixoto MM, Sage TL (2014) Photosynthesis in sugarcane. In: Moore PH, Botha FC (eds) Sugarcane: physiology, biochemistry, and functional biology. Wiley, Chichester, pp 121–154

Saliendra NZ, Meinzer FC (1992) Genotypic, developmental and drought-induced differences in root hydraulic conductance of contrasting sugarcane cultivars. J Exp Bot 43:1209–1217. https://doi.org/10.1093/jxb/43.9.1209

Scarpare FV (2011) Simulação do crescimento da cana-de-açúcar pelo modelo agrohidrológico SWAP/WOFOST. Universidade de São Paulo, Escola Superior de Agricultura “Luiz de Queiroz”. Piracicaba, Brasil [In Portuguese]

Scarpare FV, Stockle CO, Nelson RL et al (2018) Sugarcane CropSyst assessment under Brazilian environmental conditions. In: AGU fall meeting abstracts. American Geophysical Union, Washington

Sentelhas PC, Pereira AB (2019) El Niño–Southern oscillation and its impacts on local climate and sugarcane yield in Brazil. Sugar Tech 21:976–985. https://doi.org/10.1007/s12355-019-00725-w

Sexton J, Inman-Bamber NG, Everingham Y et al (2014) Detailed trait characterisation is needed for simulation of cultivar responses to water stress. Proc Aust Soc Sugar Cane Technol 36:82–92

Sinclair TR, Muchow RC (1999) Radiation use efficiency. In: Sparks DL (ed) Advances in agronomy, 65th edn. Academic, San Diego, pp 215–265

Sinclair TR, Gilbert RA, Perdomo RE et al (2004) Sugarcane leaf area development under field conditions in Florida, USA. Field Crop Res 88:171–178. https://doi.org/10.1016/j.fcr.2003.12.005

Singels A (2007) A new approach to implementing computer-based decision support for sugarcane farmers and extension staff: the case of My CANESIM. Proc Int Soc Sugar Cane Technol 26:211–219

Singels A (2014) Crop models. In: Moore PH, Botha FC (eds) Sugarcane: physiology, biochemistry, and functional biology. Wiley, Chichester, pp 541–577

Singels A, Bezuidenhout CN (2002) A new method of simulating dry matter partitioning in the Canegro sugarcane model. Field Crop Res 78:151–164. https://doi.org/10.1016/S0378-4290(02)00118-1

Singels A, Inman-Bamber NG (2011) Modelling genetic and environmental control of biomass partitioning at plant and phytomer level of sugarcane grown in controlled environments. Crop Pasture Sci 62:66–81. https://doi.org/10.1071/CP10182

Singels A, Smit MA (2009) Sugarcane response to row spacing-induced competition for light. Field Crop Res 113:149–155. https://doi.org/10.1016/j.fcr.2009.04.015

Singels A, Smith MT (2006) Provision of irrigation scheduling advice to small scale sugarcane farmers using a web-based crop model and cellular technology: a south African case study. Irrig Drain 55:363–372. https://doi.org/10.1002/ird.231

Singels A, Bezuidenhout CN, Smith EJ (1999) Evaluation strategies for scheduling supplementary irrigation of sugarcane in South Africa. Proc Aust Soc Sugar Cane Technol 21:219–226

Singels A, Jones M, van den Berg M (2008) DSSAT v4.5 Canegro sugarcane plant module: scientific documentation. S Afr Sugarcane Res Inst (Mount Edgecombe) 34

Singels A, Jones MR, Porter CH (2010a) The DSSAT4.5 Canegro model: a useful decision support tool for research and management of sugarcane production. Proc Int Soc Sugar Cane Technol 27:1–5

Singels A, van den Berg M, Smit MA et al (2010b) Modelling water uptake, growth and sucrose accumulation of sugarcane subjected to water stress. Field Crop Res 117:59–69. https://doi.org/10.1016/j.fcr.2010.02.003

Singels A, Jones M, Marin FR et al (2014) Predicting climate change impacts on sugarcane production at sites in Australia, Brazil and South Africa using the Canegro model. Sugar Tech 16:347–355. https://doi.org/10.1007/s12355-013-0274-1

Singels A, Jones MR, van der Laan M (2016) Modelling impacts of stomatal drought sensitivity and root growth rate on sugarcane yield. In: International crop modelling symposium. MACSUR & AgMIP, Berlin, pp 392–393

Singels A, Jones MR, Lumsden TG (2018) Sugarcane productivity and water use in South Africa under a future climate: what can we expect? Proc S Afr Sugar Technol Assoc 91:57–61

Singels A, Paraskevopoulos AL, Mashabela ML (2019) Farm level decision support for sugarcane irrigation management during drought. Agric Water Manag 222:274–285. https://doi.org/10.1016/j.agwat.2019.05.048

Singh G, Chapman LS, Jackson PA, Lawn R (2002) Lodging reduces sucrose accumulation of sugarcane in the wet and dry tropics. Aust J Agric Res 53:1183–1195

Skocaj DM, Everingham YL, Schroeder BL (2013) Nitrogen management guidelines for sugarcane production in Australia: can these be modified for wet tropical conditions using seasonal climate forecasting? Springer Sci Rev 1:51–71. https://doi.org/10.1007/s40362-013-0004-9

Smit MA (2010) Characterising the factors that affect germination and emergence in sugarcane. Proc S Afr Sugar Technol Assoc 83:230–234

Smit MA, Singels A (2006) The response of sugarcane canopy development to water stress. Field Crop Res 98:91–97. https://doi.org/10.1016/j.fcr.2005.12.009

Steduto P, Hsiao TC, Raes D, Fereres E (2009) Aquacrop-the FAO crop model to simulate yield response to water: I. concepts and underlying principles. Agron J 101:426–437. https://doi.org/10.2134/agronj2008.0139s

Stewart LK, Charlesworth PB, Bristow KL, Thorburn PJ (2006) Estimating deep drainage and nitrate leaching from the root zone under sugarcane using APSIM-SWIM. Agric Water Manag 81:315–334. https://doi.org/10.1016/j.agwat.2005.05.002

Stöckle CO, Donatelli M, Nelson R (2003) CropSyst, a cropping systems simulation model. Eur J Agron 18:289–307. https://doi.org/10.1016/S1161-0301(02)00109-0

Stoeckl N, Inman-Bamber NG (2003) Value of irrigation water with uncertain future rain: a simulation case study of sugarcane irrigation in northern Australia. Water Resour Res 39:1–7. https://doi.org/10.1029/2003WR002054

Stokes CJ, Inman-Bamber NG, Everingham YL, Sexton J (2016) Measuring and modelling CO_2 effects on sugarcane. Environ Model Softw 78:68–78. https://doi.org/10.1016/j.envsoft.2015.11.022

Suguitani C (2006) Entendendo o crescimento e produção da cana de açúcar: avaliação do modelo Mosicas. Universidade de São Paulo, Escola Superior de Agricultura "Luiz de Queiroz". Piracicaba, Brasil [In Portuguese]

Tatsch JD, Bindi M, Moriondo M (2009) A preliminary evaluation of the Cropsyst model for sugarcane in the southeast of Brazil. In: Bind M, Brandani G, Dibari C et al (eds) Impact of climate change on agricultural and natural ecosystems. Firenze University, Firenze, pp 75–84

Thompson GD (1976) Water use by sugarcane. S Afr Sugar J 60:593–600. and 627–635

Thompson GD (1978) The production of biomass by sugarcane. Proc S Afr Sugar Technol Assoc 52:180–187

Thorburn PJ, Probert M, Lisson S et al (1999) Impacts of trash retention on soil nitrogen and water: an example from the Australian sugarcane industry. Proc S Afr Sugar Technol Assoc 73:75–79

Thorburn PJ, Biggs JS, Keating BA et al (2001a) Nitrate in groundwaters in the Australian sugar industry. Proc Int Soc Sugar Cane Technol 24:131–134

Thorburn PJ, Van Antwerpen R, Meyer JH et al (2001b) Impact of trash blanketing on soil nitrogen fertility: Australian and South African experience. Proc Int Soc Sugar Cane Technol 24:33–39

Thorburn PJ, Park SE, Biggs IM (2003) Nitrogen fertiliser management in the Australia sugar industry: strategic opportunities for improved efficiency. Proc Aust Soc Sugar Cane Technol 25:1–12

Thorburn PJ, Horan HL, Biggs JS (2004) The impact of trash management on sugarcane production and nitrogen management: a simulation study. Proc Aust Soc Sugar Cane Technol 26:1–12

Thorburn PJ, Meier EA, Probert ME (2005) Modelling nitrogen dynamics in sugarcane systems: recent advances and applications. Field Crop Res 92:337–351. https://doi.org/10.1016/j.fcr.2005.01.016

Thorburn PJ, Biggs JS, Collins K, Probert ME (2010) Using the APSIM model to estimate nitrous oxide emissions from diverse Australian sugarcane production systems. Agric Ecosyst Environ 136:343–350. https://doi.org/10.1016/j.agee.2009.12.014

Thorburn PJ, Biggs JS, Attard SJ, Kemei J (2011) Environmental impacts of irrigated sugarcane production: nitrogen lost through runoff and leaching. Agric Ecosyst Environ 144:1–12. https://doi.org/10.1016/j.agee.2011.08.003

Thorburn PJ, Biggs J, Jones MR et al (2014) Evaluation of the APSIM-Sugar model for simulation sugarcane yield at sites in seven countries: initial results. Proc S Afr Sugar Technol Assoc 87:318–322

Thorburn PJ, Biggs JS, Palmer J et al (2017) Prioritizing crop management to increase nitrogen use efficiency in Australian sugarcane crops. Front Plant Sci 8:1–16. https://doi.org/10.3389/fpls.2017.01504

Thorburn PJ, Biggs JS, Skocaj D et al (2018) Crop size and sugarcane nitrogen fertiliser requirements: is there a link? Proc Aust Soc Sugar Cane Technol 40:210–218

Thornthwaite CW (1948) An approach toward a rational classification of climate. Geogr Rev 38:55. https://doi.org/10.2307/210739

Valade A, Vuichard N, Ciais P, Ruget F, Viovy N, Gabrielle B, Huth N, Martiné J-F (2014) ORCHIDEE-STICS, a process-based model of sugarcane biomass production: calibration of model parameters governing phenology. GCB Bioenergy 6:606–620. https://doi.org/10.1111/gcbb.12074

Van Antwerpen R, Thorburn PJ, Horan HL et al (2002) The impact of trashing on soil carbon and nitrogen: II: implications for sugarcane production in South Africa. Proc S Afr Sugar Technol Assoc 76:269–280

van Dam JC, Groenendijk P, Hendriks RFA, Kroes JG (2008) Advances of modeling water flow in variably saturated soils with SWAP. Vadose Zone J 7:640–653. https://doi.org/10.2136/vzj2007.0060

van den Berg M, Singels A (2013) Modelling and monitoring for strategic yield gap diagnosis in the south African sugar belt. Field Crop Res 143:143–150. https://doi.org/10.1016/j.fcr.2012.10.009

van den Berg M, Burrough PA, Driessen PM (2000) Uncertainties in the appraisal of water availability and consequences for simulated sugarcane yield potentials in Sao Paulo state, Brazil. Agric Ecosyst Environ 81:43–55. https://doi.org/10.1016/S0167-8809(00)00167-5

van der Laan M, Miles N, Annandale JG, du Preez CC (2011) Identification of opportunities for improved nitrogen management in sugarcane cropping systems using the newly developed Canegro-N model. Nutr Cycl Agroecosyst 90:391–404. https://doi.org/10.1007/s10705-011-9440-6

van Heerden PDR, Donaldson RA, Watt DA, Singels A (2010) Biomass accumulation in sugarcane: unravelling the factors underpinning reduced growth phenomena. J Exp Bot 61:2877–2887. https://doi.org/10.1093/jxb/erq144

van Heerden PDR, Singels A, Paraskevopoulos A, Rossler R (2015) Negative effects of lodging on irrigated sugarcane productivity – an experimental and crop modelling assessment. Field Crop Res 180:135–142. https://doi.org/10.1016/j.fcr.2015.05.019

van Ittersum MK, Rabbinge R (1997) Concepts in production ecology for analysis and quantification of agricultural input-output combinations. Field Crop Res 52:197–208

van Ittersum MK, Cassman KG, Grassini P et al (2013) Yield gap analysis with local to global relevance—a review. Field Crop Res 143:4–17. https://doi.org/10.1016/j.fcr.2012.09.009

van Wart J, van Bussel LGJ, Wolf J et al (2013) Use of agro-climatic zones to upscale simulated crop yield potential. Field Crop Res 143:44–55. https://doi.org/10.1016/j.fcr.2012.11.023

Villegas FD, Daza OH, Jones JW, Royce FS (2005) CASUPRO: an industry-driven sugarcane model. In: ASAE annual international meeting. Presented at the Transactions of American Society of Agricultural and Biological Engineer, Tampa

Vu JCV, Allen LH (2009a) Stem juice production of the C4 sugarcane (*Saccharum officinarium*) is enhanced by growth at double-ambient CO2 and high temperature. J Plant Physiol 166:1141–1151. https://doi.org/10.1016/J.JPLPH.2009.01.003

Vu JCV, Allen LH (2009b) Growth at elevated CO_2 delays the adverse effects of drought stress on leaf photosynthesis of the C4 sugarcane. J Plant Physiol 166:107–116. https://doi.org/10.1016/J.JPLPH.2008.02.009

Vu JCV, Allen LH, Gesch RW (2006) Up-regulation of photosynthesis and sucrose metabolism enzymes in young expanding leaves of sugarcane under elevated growth CO_2. Plant Sci 171:123–131. https://doi.org/10.1016/J.PLANTSCI.2006.03.003

Walker NJ, Schulze RE (2010) Simulations of rainfed and irrigated sugarcane yields at the scale of mill supply areas in South Africa with the APSIM Model: a verification analysis and study of sensitivities of yields to scenarios of climate change. In: Schulze RE (ed) Climate change and the South African sugarcane sector: a 2010 perspective. University of KwaZulu-Natal, School of Bioresources Engineering and Environmental Hydrology, Pietermaritzburg, pp 83–104

Wallach D (2006) The two forms of crop models. In: Wallach D, Makowski D, Jones JW (eds) Working with dynamic crop models, 1st edn. Elsevier, Amsterdam, pp 3–10

Wang E, Martre P, Zhao Z et al (2017) The uncertainty of crop yield projections is reduced by improved temperature response functions. Nat Plants 3:1–11. https://doi.org/10.1038/nplants.2017.102

Wang E, Attard SJ, Everingham YL et al (2018a) Smarter irrigation management in the sugarcane farming system using internet of things. Proc Aust Soc Sugar Cane Technol 40:14

Wang N, Wang E, Wang J et al (2018b) Modelling maize phenology, biomass growth and yield under contrasting temperature conditions. Agric For Meteorol 250–251:319–329. https://doi.org/10.1016/J.AGRFORMET.2018.01.005

Webb WA, Inman-Bamber NG, Mock O (2006) Participatory irrigation research and scheduling in the Ord: extension. Proc Aust Soc Sugar Cane Technol 28:155–163

Webster AJA, Thorburn PJB, Roebeling PCC et al (2009) The expected impact of climate change on nitrogen losses from wet tropical sugarcane production in the Great Barrier Reef region. Mar Freshw Res 60:1159–1164

Yang S, Chen J (1980) Germination response of sugarcane cultivars. Proc Int Soc Sugar Cane Technol 17:30–37

Zhao P, Jackson PA, Basnayake J et al (2017a) Genetic variation in sugarcane for leaf functional traits and relationships with cane yield, in environments with varying water stress. Field Crop Res 213:143–153. https://doi.org/10.1016/j.fcr.2017.08.004

Zhao Z, Verburg K, Huth N (2017b) Modelling sugarcane nitrogen uptake patterns to inform design of controlled release fertiliser for synchrony of N supply and demand. Field Crop Res 213:51–64. https://doi.org/10.1016/j.fcr.2017.08.001

Zu Q, Mi C, Liu DL et al (2018) Spatio-temporal distribution of sugarcane potential yields and yield gaps in Southern China. Eur J Agron 92:72–83. https://doi.org/10.1016/j.eja.2017.10.005

Forecasting of Rainfed Wheat Yield in Pothwar Using Landsat 8 Satellite Imagery and DSSAT

9

Sana Younas, Mukhtar Ahmed, and Naeem Abbas Malik

Abstract

Drought leads to serious reduction in the yield of wheat in rainfed regions, which is a growing environmental phenomenon faced by wheat crop. The effect of drought stress during grain filling on yield and some physiological traits of wheat confirms that post-anthesis drought significantly reduces photosynthesis rate and grain yield. We tested the DSSAT (Decision Support System for Agrotechnology Transfer) CERES-Wheat model with details of field experimental data having different sowing dates, and their effect on yield and result were compared with the maps obtained by the Landsat 8 satellite imagery using ERDAS. ERDAS IMAGINE is an easy-to-use, raster-based software designed specifically to extract information from images. The field trial was carried out at Islamabad and the University Research Farm (URF)-Koont, Chakwal Road. Field survey was also carried out in rainfed region to collect field data from farmers, and Landsat imagery was downloaded from the EarthExplorer USGS website. Yield simulated from DSSAT (Decision Support System for Agrotechnology Transfer) was compared with the maps obtained from Landsat 8 satellite imagery using ERDAS. Simulated grain yields during 2017–2018 have close association with observed data for different sowing date experiments. At Islamabad maximum grain yield (3263 kg/ha) was observed for Sd2 (sowing date two), while

S. Younas
Department of Agronomy, Pir Mehr Ali Shah Arid Agriculture University, Rawalpindi, Pakistan

M. Ahmed (✉)
Department of Agricultural Research for Northern Sweden, Swedish University of Agricultural Sciences, Umeå, Sweden

Department of Agronomy, Pir Mehr Ali Shah Arid Agriculture University, Rawalpindi, Pakistan
e-mail: ahmadmukhtar@uaar.edu.pk

N. A. Malik
Department of Remote Sensing and GIS, PMAS Arid Agriculture University, Rawalpindi, Pakistan

M. Ahmed (ed.), *Systems Modeling*, https://doi.org/10.1007/978-981-15-4728-7_9

minimum (1126.66 kg/ha) was recorded for Sd5 (sowing date five). At URF-Koont, maximum grain yield (3024 kg/ha) was observed for Sd2 (sowing date two), whereas minimum (1058.33 kg/ha) was recorded for Sd5 (sowing date five). Simulated harvest index showed close association with observed data for different treatments during 2017–2018. Higher harvest index (35%) was observed for Sd2 (sowing date two, 15 November), while minimum (28%) was recorded for Sd5 (sowing date five, 30 December). At URF-Koont, maximum grain yield (35%) was observed for Sd2 (15 November), whereas minimum (28%) was recorded for Sd5 (30 December).

Keywords

Landsat 8 satellite · Wheat · DSSAT · Modeling · Phenology · Yield

9.1 Introduction

The change that occurs for a long period of time due to natural and anthropogenic activities is known as climate change. Increasing concentration of carbon dioxide, rising temperature, and severity of extreme events are involved in climate change (Rosenzweig and Tubiello 2007). Anthropogenic activities resulted in the emissions of greenhouse gases (carbon dioxide, methane, nitrous oxide, and water vapors) (Motha and Baier 2005). Due to these activities, the concentration of greenhouse gases is increasing at the rate of 23 ppm/decade, which is a maximum increase since the past 6.5 million years. Sectors such as agriculture (13%), energy (53%), forestry (18%), and other wastes (13%) are contributing in the emission of greenhouse gases (Rosegrant et al. 2008). Similarly, during combustion of fossil fuels, wood, and wastes, carbon dioxide is produced. From the past years, concentration of carbon dioxide is high and increasing rapidly (Siegenthaler et al. 2005). Deforestation and massive uses of fossil fuels are the main causes of increased concentration of carbon dioxide. In the future greenhouse gases may increase from 500 to 700 ppm if there will be no policy to control the emission of these gases which would result in the increased temperature from 3 to 6 °C. Crop growth, development, and yield have been affected by climate change directly or indirectly from few decades (Ahmed and Stockle 2016; Ahmed 2020; Liu et al. 2019). The increasing concentration of carbon dioxide results in the increase in photosynthesis and water use efficiency, and it falls in direct effect (Ahmed and Ahmad 2019; Challinor and Wheeler 2008). The net revenue of crop yield and productivity has been directly affected by temperature and rainfall (Amassaib et al. 2015).

Wheat is an important food grain cereal which contributes about 21% to world food supply. According to the FAO, Pakistan is one of the ten major producers of wheat in the world. In Pakistan, 14% of value added in agriculture is contributed by wheat and provides 3% of the country's GDP. The total cultivable area is 34.54 M/ha, in Pakistan of which 22 M/ha is under cultivation. Wheat is cultivated over the largest area about 9.18 M/ha. Of this total 9.18 M/ha area, about 6 M/ha is irrigated and the rest is under rainfed (Kazmi and Rasul 2012). Wheat is a major food crop in Pakistan grown in irrigated and rainfed regions during winter. Rainfed area contributes only about 12% of wheat production to the country. In rainfed regions drought leads to serious reduction in the yield of wheat which is one of the most vital cereal crops of the rainfed regions. The severe reduction in wheat yield occurs due to the long duration of drought stress which is a growing environmental phenomenon faced by wheat crop. The average wheat yield reduction is up to 50% due to inadequate rainfall in arid and semiarid regions limiting crop production. In dry land areas, grain filling in wheat crop depends upon the stem reserves as compared to current photosynthesis (Ehdaie et al. 2006). The effect of drought stress during grain filling on yield and some physiological traits of wheat cultivars confirms that post-anthesis drought significantly reduced photosynthesis rate and grain yield (Ahmed et al. 2020; Saeidi and Abdoli 2015). In rainfed regions crops are grown in Rabi season which are susceptible to change in minimum temperature and tolerate high temperature (Venkateswarlu and Rao 2010).

Crop yield forecasting refers to the prediction of crop yield and production prior to harvesting. Reliable timely and accurate crop yield forecasts can provide information for food security planning, particularly in the context of climate variability, change, and extremes. Crop yield forecasting uses meteorological data, cultivar-specific genotype, soil properties, and various management practice data to stimulate plant-weather-soil interactions in quantitative terms and predict the crop yield over a given area, prior to the harvest. Models like DSSAT (Decision Support System for Agrotechnology Transfer) and APSIM (Agriculture Production Systems Simulator) try to mimic fundamental mechanisms of plant growth and related processes in the soil-plant-atmospheric continuum to stimulate specific outcomes. For any soil, cultivar, and management conditions, weather is a prime driver of interannual variations in the crop yield. To determine wheat production on the basis of the cultivated area in the long run, there is a need to use model which can estimate wheat production forecasting in cultivated areas. Many studies have been conducted to forecast and determine constraints in the production of major crops such as wheat, cotton, rice, and canola in Pakistan (Ahmed et al. 2017).

Modeling concept was used to find the easiest way of evaluating the interactions of genotype, environment, and management (G $\times$ E $\times$ M) (Wallach et al. 2018; Cooper and Hammer 1996). Crop models are powerful tools used broadly for the analysis of crop growth, quality and cropping systems (Matthews et al. 2013; Ahmed et al. 2013; Asseng et al. 2019; White et al. 2011). Previous studies revealed that simulation models can successfully simulate all growth and development stages of the crop (Asseng et al. 2001; Ahmed et al. 2014, 2016, 2017, 2018, 2019; Ahmad et al. 2017, 2019). International network of scientists developed DSSAT (Decision Support System for Agrotechnology Transfer) which facilitates the crop researcher. The Decision Support System for Agrotechnology Transfer is a software application program that comprises crop simulation models for over 42 crops. To simulate crop growth, development, and yield on a uniform area of land and change in soil water, nitrogen, and carbon that take place in the cropping system, the model DSSAT (Decision Support System for Agrotechnology Transfer) is designed which is most widely used. To select improved agricultural practices, DSSAT has been proven to be a useful tool. Further modification of DSSAT was made like soil organic matter model was incorporated into DSSAT to improve tillage, soil carbon and nitrogen dynamics, soil water, and crop residues (Ahmed 2012). Under various environmental and management conditions and a wide range of growing conditions, crop models are used to predict yield (White et al. 2011). DSSAT is also used to measure the performance of conservation agriculture systems and compare the yield of crop grown in conservation agriculture (CA) system with conservation tillage-based practices under different climatic conditions.

Landsat imagery allows yield predictions at a higher resolution, and the pattern of measurements highlights yield performance difference due to soil type and topographic location, and large variations in yield are evident. Precision agriculture and more specifically yield mapping provide an alternative method to collect yield measurements at a matching scale. Yield and spatial position are collected via a combined harvester every 1 to 3 seconds, allowing maps of yield to be produced at a high spatial resolution that is similar to the resolution of the spectral indices produced by the Landsat sensor. Previous studies have reported a strong relationship between yield and Landsat imagery, but most studies are from individual fields and rarely have these relationships been used to predict yields elsewhere. The observatory through which Landsat 8 developed was NASA (National Aeronautics and Space Administration) and USGS (US Geological Survey), Landsat 8 was launched on 11 February 2013 from Vandenberg Air Force Base, California (Irons and Loveland 2013). The OLI (Operational Land Imager) and TIRS (Thermal Infrared Sensor) are two sensors which are carried by the Landsat 8 satellite (Irons et al. 2012). These two sensors OLI and TIRS provide improved radiometric resolution, geometric fidelity, and signal-to-noise characteristics compared to the earlier Landsat sensors (Lee et al. 2004). In a year maximum 22 or 23 Worldwide Reference System (WRS)-2/row is overpassed which is a 16-day repeat cycle, and Landsat 8 has completed its one cycle in 16 days. By using Landsat data and information, we can understand the Earth system and its response to natural and human-induced changes enabling prediction of weather, climate, and natural hazards (Irons et al. 2012). Landsat 8 imagery predicts wheat yield by using Normalized Difference Vegetation Index (NDVI) and using wheat yield prediction model for the comparison of two high resolutions over different growing seasons, and the result helps the agriculture decision-making (Jabeen et al. 2017; Lyle et al. 2013). Maps are obtained by the Landsat 8 satellite imagery using ERDAS. ERDAS IMAGINE is an easy-to-use, raster-based software designed specifically to extract information from the images. A geographic imaging toolset extends the capabilities of IMAGINE Essentials by adding more precise mapping and image processing functions. ERDAS IMAGINE includes a complete set of tools to analyze data from imagery via mosaicking, surface interpolation, preprocessing like radiometric correction and environmental correction advanced image interpretation and ortho-rectification. QGIS was launched by Gary Sherman in July 2002 and was also known as Quantum GIS till 2012. By using raster (satellite images) and vector data, it helped in making maps, and analysis of spatial data imagery preprocessing can be done by using QGIS and extraction of NDVI values. ArcMap can be used for supervised classification and mapping of Landsat 8 satellite imagery. Normalized Difference Vegetation Index (NDVI) can be used for analyzing Landsat 8 imagery and is a graphical indicator of green vegetation; it can be measured by using band 5 which is near infrared (NIR) and bad four red of LANDSAT 8 imagery.

Various indices such as Normalized Difference Wheat Index, Normalized Difference Vegetation Index (NDVI), Vegetation Condition Index (VCI), and Temperature Condition Index (TCI) are used for mapping and monitoring of drought and assessment of vegetation health and productivity. NDVI, soil moisture, surface temperature, and rainfall are valuable sources of information for the estimation and prediction of crop conditions (Prasad et al. 2006). MODIS (Moderate Resolution Imaging Spectroradiometer), a two-band Enhanced Vegetation Index (EVI2), provides a better basis for predicting yields relative to the widely used Normalized Difference Vegetation Index (NDVI) (Bolton and Friedl 2013).

9.2 Methodology

The experiment was conducted to study "Yield forecasting of wheat in rainfed region." The field experiment was carried out at Islamabad (38.78° N, 73.57° E) having altitude of (1722 ft) and (1770 ft), with an elevation of (1634 ft) and (1663 ft) above sea level, respectively, and in the URF-Koont, Chakwal Road (33.40° N, 72.51° E) with elevation range from 500 to 1200 m. While wheat yield data will be collected from different sites of Pothwar region through field survey of farmers, e.g., Jhelum, Landsat imagery was collected from EarthExplorer USGS website. The experiment was laid out in Randomized Complete Block Design (RCBD); each treatment was replicated thrice during the growing season of 2017 and 2018. Wheat genotype Pak-13 will be used as planting material. The treatments include study sites (SS1 = Islamabad and SS2 = URF-Koont) and sowing dates (ST1 = October 21–30 (2017–18), ST2 = November 11–20 (2017–18), ST3 = December 1–10 (2017–18), and ST4 = December 21–30 (2017–18)). Crop phenological and agronomic parameters were recorded using standard protocol.

9.2.1 Landsat 8 Methodology for Crop Map

Landsat 8 imagery was collected from the EarthExplorer USGS website (https://earthexplorer.usgs.gov/). We used the Landsat 8 images for the yield forecasting of wheat. Landsat 8 has 11 bands. Landsat 8 consists of Operational Land Imager, and Thermal Infrared Sensor images consist of nine spectral bands with a spatial resolution of 30 m band 1 to 7 of different wavelengths where red, green, and blue sensors were combined to produce true color image. New band 9 is useful for cloud detection. The band 8 has 15 m resolution. Bands 10 and 11 are thermal bands which are useful in providing more accurate surface temperature with resolution of 100 meters (Table 9.1).

Table 9.1 Landsat 8 bands and resolutions

Band	Wavelength (micro, m)	Resolution (m)
Band 1 – Coastal aerosol	0.43–0.45	30
Band 2 – Blue	0.45–0.51	30
Band 3 – Green	0.53–0.59	30
Band 4 – Red	0.64–0.67	30
Band 5 – Near infrared (NIR)	0.85–0.88	30
Band 6 – SWIR 1	1.57–1.65	30
Band 7 – SWIR 2	2.11–2.29	30
Band 8 – Panchromatic	0.50–0.68	15
Band 9 – Cirrus	1.36–1.38	30
Band 10 – Thermal Infrared Sensor (TIRS) 1	10.60–11.19	100
Band 11 – Thermal Infrared Sensor (TIRS) 2	11.50–12.51	100

9.2.2 ERDAS

ERDAS IMAGINE is an easy-to-use, raster-based software designed specifically to extract information from the images. ERDAS IMAGINE includes a complete set of tools to analyze data from imagery via.

- Mosaicking
- Surface interpolation
- Advanced image interpretation
- Ortho-rectification
- Radiometric correction
- Mapping

9.2.3 QGIS

QGIS was initiated by Gary Sherman in July 2002 and also known as Quantum GIS till 2012. By using raster (satellite images) and vector data, it helped in making maps and analysis of spatial data. QGIS was used for preprocessing (radiometric correction and environmental correction) of Landsat 8 satellite imagery and extraction of Normalized Difference Vegetation Index (NDVI) values.

QGIS comprised the following menu bars:

1. Project
2. Edit
3. View
4. Layer
5. Setting
6. Plug-ins
7. Vector

Fig. 9.1 Download Landsat 8 images (EarthExplorer USGS website)

8. Raster
9. Database
10. Web
11. Processing
12. Help

9.2.4 ArcGIS

Image processing is done by using ArcGIS 10.8. It is used for supervised classification and creating maps, compiling geographic data, and analyzing mapped information. For forecasting of wheat yield using Landsat imagery, we extracted maps and geographic information using ArcGIS as shown below (Figs. 9.1, 9.2, 9.3, and 9.4).

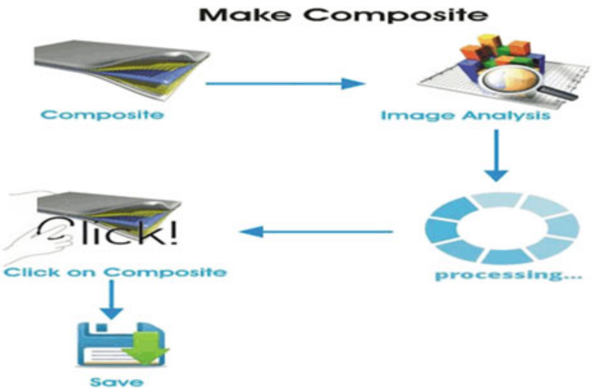

Fig. 9.2 Composite

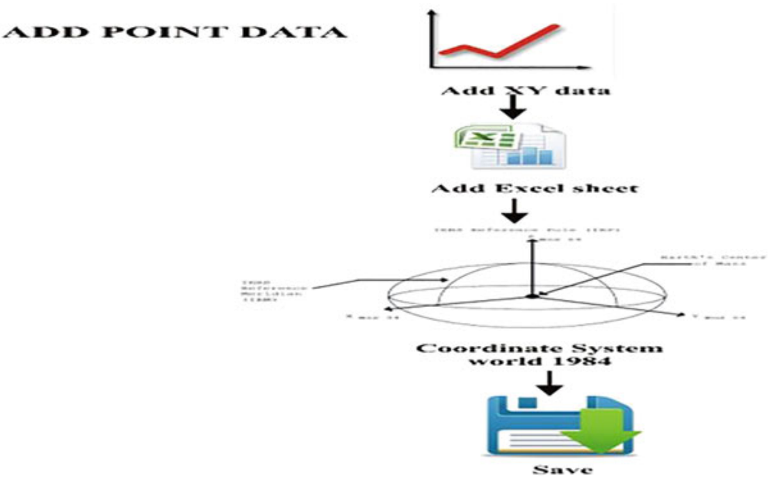

Fig. 9.3 Add point data

9.2.5 Image Processing

Image processing involves making of composite first and addition of point data and finally classification of image (Figs. 9.2, 9.3, and 9.4). Landsat 8 bands and resolutions have been presented in Table 9.1.

9.2.5.1 Normalized Difference Vegetation Index (NDVI)

NDVI was used in this study, and its index is sensitive to the presence of green vegetation. NDVI can be defined by following equation:

$$\mathrm{NDVI} = \mathrm{NIR} - \mathrm{R}/\mathrm{NIR} + \mathrm{R}$$

where NIR and R are the reflectance in the near infrared and red region, respectively.

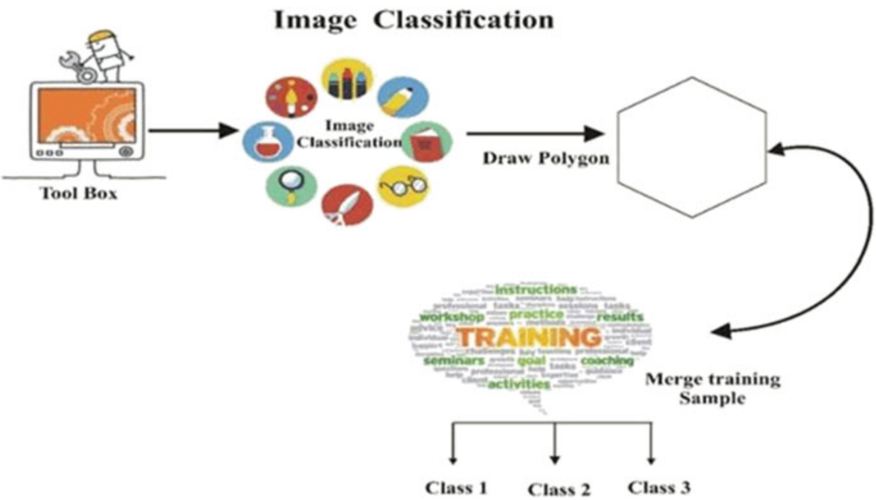

Fig. 9.4 Image classification

9.2.5.2 Enhanced Vegetation Index (EVI)

Enhanced Vegetation Index can be defined by the formula:

$$\mathrm{EVI} = 2.5\ \mathrm{NIR} - \mathrm{RED}/\mathrm{NIR} + 2.4\ \mathrm{RED} + 1$$

9.3 Results

9.3.1 Land Cover Classification

Accessing and mapping the Islamabad and URF-Koont, Chakwal Road, by using Landsat 8 satellite imagery for the classification. QGIS software was used for the preprocessing of imagery and extraction of NDVI values, while ArcMap was applied for the supervised classification of Landsat 8 satellite imagery. Supervised classification was performed which created different classes of land cover of Islamabad and URF-Koont, Chakwal Road. Five main surface classes including water, built-up area, Baran land, other vegetation, and wheat were produced. Land classification of Islamabad is shown in Fig. 9.5, whereas land classification of URF-Koont, Chakwal Road, is shown in Fig. 9.6.

9.3.2 Remote Sensing-Based Yield Forecasting

Landsat 8 imageries cover growth of wheat from its sowing to harvesting stage. Different five wheat sowing dates are 31 October, 15 November, 30 November,

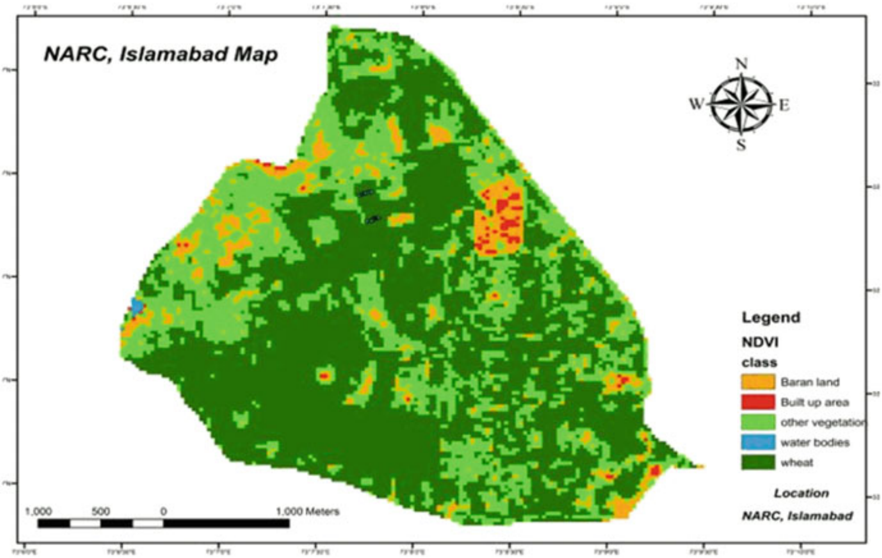

Fig. 9.5 Land cover classification map of NARC Islamabad 2017–2018

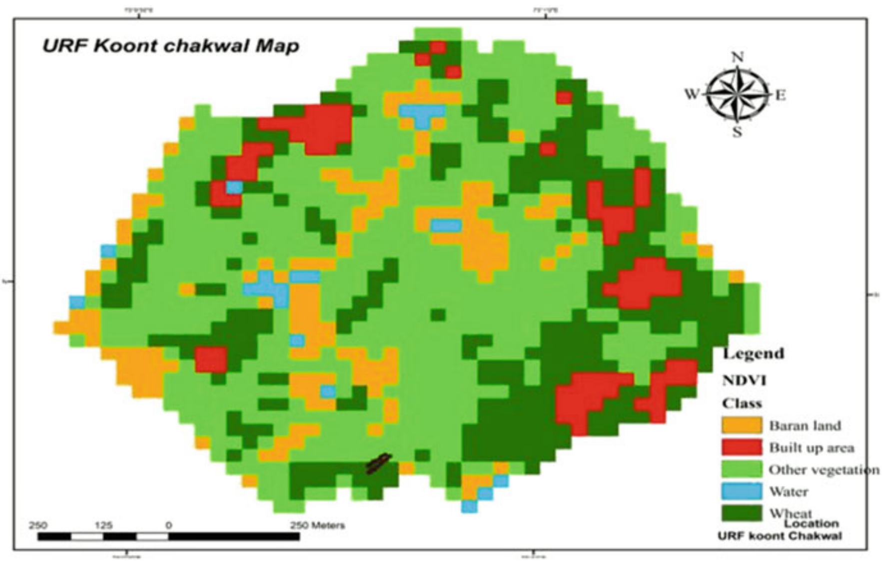

Fig. 9.6 Land cover classification map of URF-Koont, Chakwal Road, 2017–2018

15 December, and 30 December. We have different sowing date experiments, so we collected imagery throughout the season from November to April. The imageries of November, December, January, February, March, and April were used for the analysis. Full processing of the Landsat imagery for NDVI was done, and NDVI

is calculated using the mean values of the reflectance in green, red, and NIR portion of the electromagnetic spectrum. NDVI proposed a band ratio demonstrating the feasibility of forecasting the wheat yield throughout the growing season of 2017–2018. NDVI for each month were used for the simple regression analysis which was performed on the field yield data to calculate equations for predicting wheat yield.

9.3.2.1 Yield Forecasting by NDVI

By using Normalized Difference Vegetation Index (NDVI), we calculated the photosynthetically absorbed radiation. NDVI map showed the wheat yield of Islamabad in Figs. 9.7, 9.8, and 9.9 and wheat yield of URF-Koont, Chakwal Road, in Figs. 9.10, 9.11, and 9.12. NDVI value ranges between −1 and +1. Water bodies and built-up area showed negative value, while rainfed area has zero value. Maps of NDVI were made with the help of GIS software like QGIS, ArcMap, and ERDAS using Landsat 8 imagery band 5 near infrared (NIR) and band 4 red. NDVI values of NARC Islamabad observed on 28 November ($R^2 = 0.1655$) and 12 December ($R^2 = 0.0154$) were very low (Table 9.2). Similarly, NDVI values of URF-Koont, Chakwal Road, observed on 12 December $R^2 = 0.1952$ and 15 January $R^2 = 0.2375$ were very low (Table 9.3). That was attributing to the continuity of early vegetation growth stages. The factors that contributed to lower NDVI values of those images were lesser crop leaf area and background reflection of soil in the red band. The highest NDVI values were observed on the imagery of 16 February of both Islamabad and URF-Koont, Chakwal Road, when the chlorophyll content and biomass were maximum. In March the NDVI values of NARC Islamabad as well as URF-Koont, Chakwal Road, started decreasing due to low chlorophyll content and leaf senescence, which caused increased reflectance in the red band.

9.3.2.2 Linear Regression Model Development

The linear regression model was developed between the observed yield and mean NDVI values of the points of NARC Islamabad (Figs. 9.13, 9.14, and 9.15) and URF-Koont, Chakwal Road, field (Figs. 9.16, 9.17, and 9.18). After observing the linear relationship between field yields and the six imagery mean NDVI values, the 16 February imagery showed the highest fit between NDVI and yield of NARC Islamabad and URF-Koont, Chakwal Road. The correlation between the wheat grain yield and corresponding NDVI values of NARC Islamabad during early vegetation growth period in December was very low $R^2 = 0.0514$ because of reflectance from mixed pixel of wheat, other vegetation and soil background. While the correlation between the wheat grain yield and NDVI values of URF-Koont, Chakwal Road, was very low in the months of December $R^2 = 0.1952$ and January $R^2 = 0.2375$. Subsequently the relationship between NDVI and wheat grain yield of NARC Islamabad started increasing up-to the month of February $R^2 = 0.7075$ because of increase in chlorophyll content and biomass as well. However, it declined in March $R^2 = 0.2246$ and April $R^2 = 0.002$ because crop is at harvest stage and chlorophyll content is very low in the leaves. While the relationship between NDVI and wheat grain yield of URF-Koont started increasing up-to March $R^2 = 0.5462$ and highest in

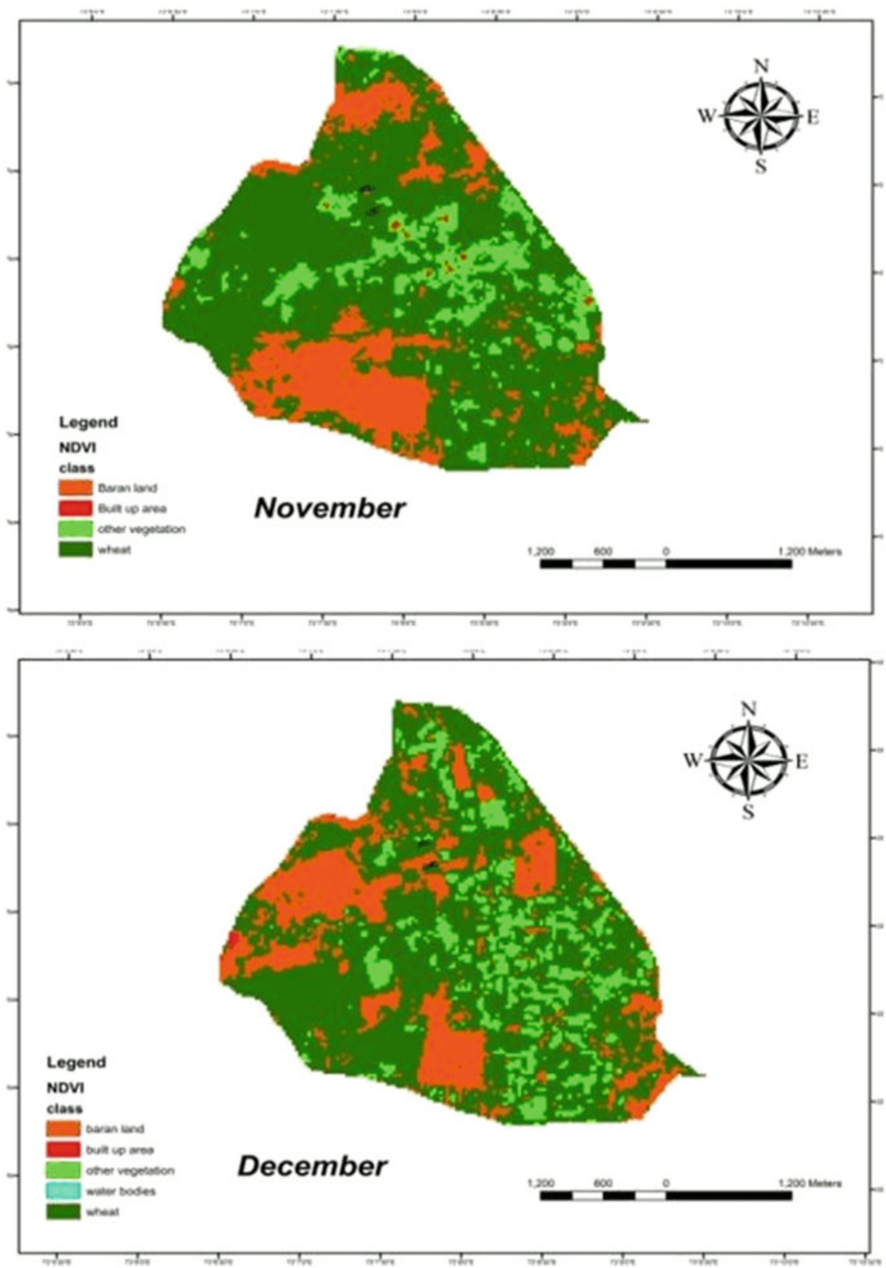

Fig. 9.7 NDVI map of Islamabad during the wheat growing season of 2017–2018

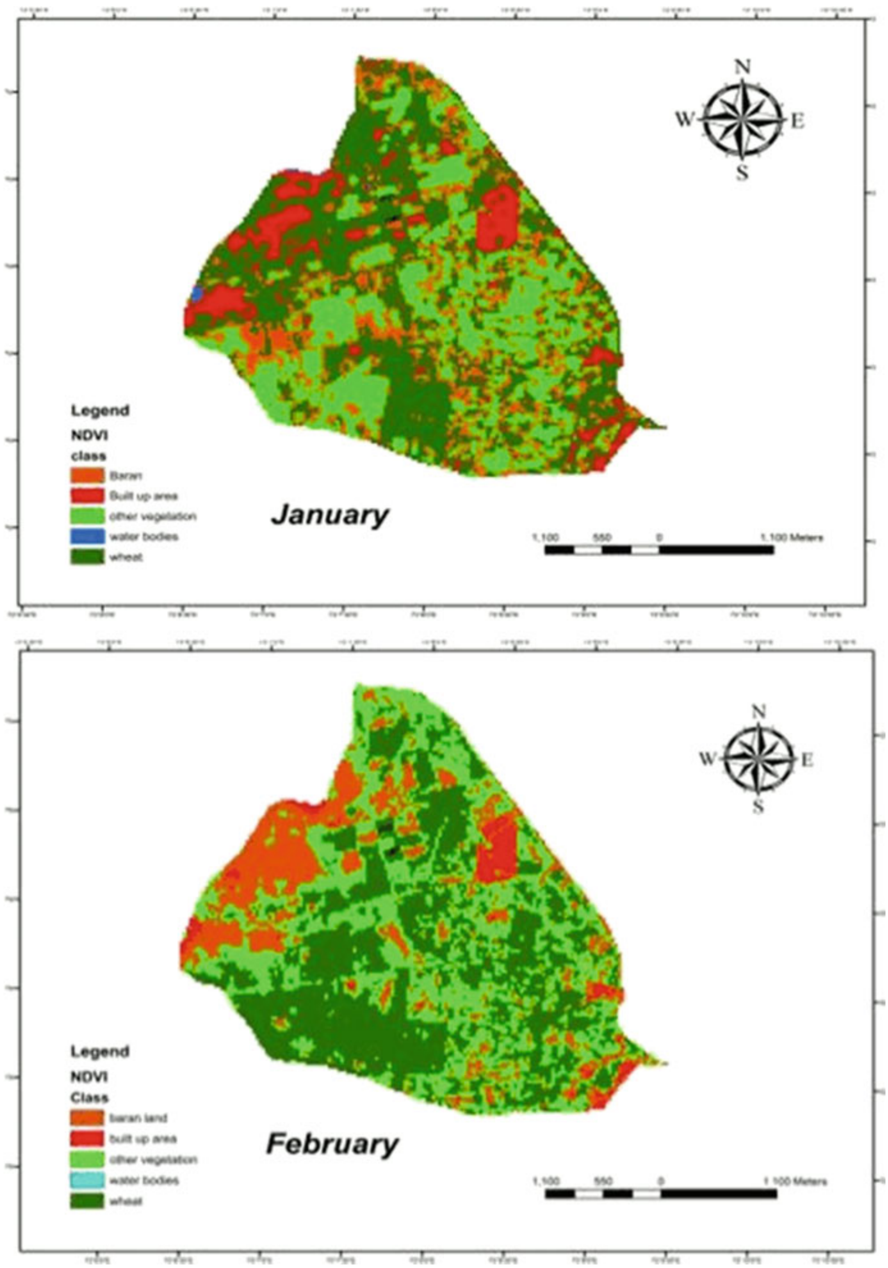

Fig. 9.8 NDVI map of Islamabad during the wheat growing season of 2017–2018

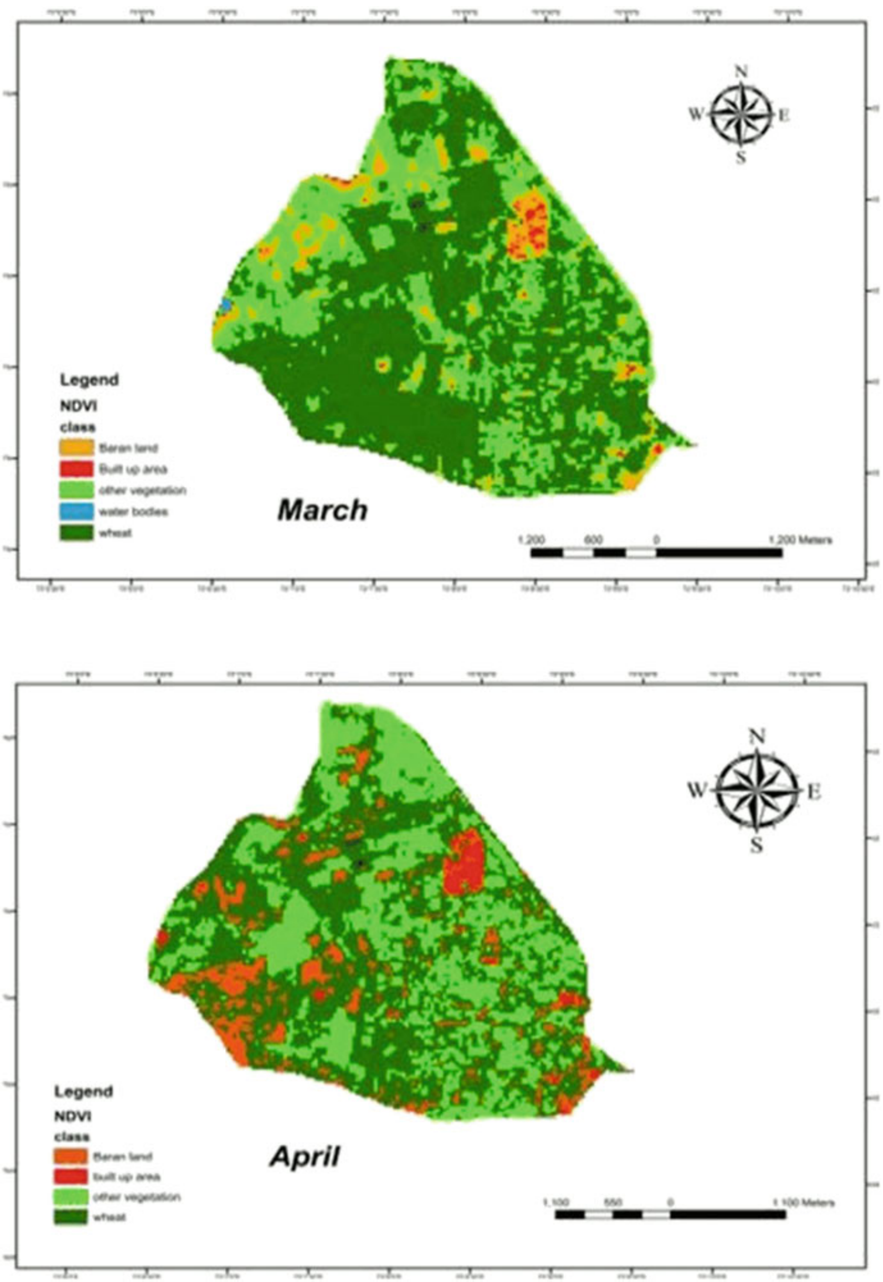

Fig. 9.9 NDVI map of Islamabad during the wheat growing season of 2017–2018

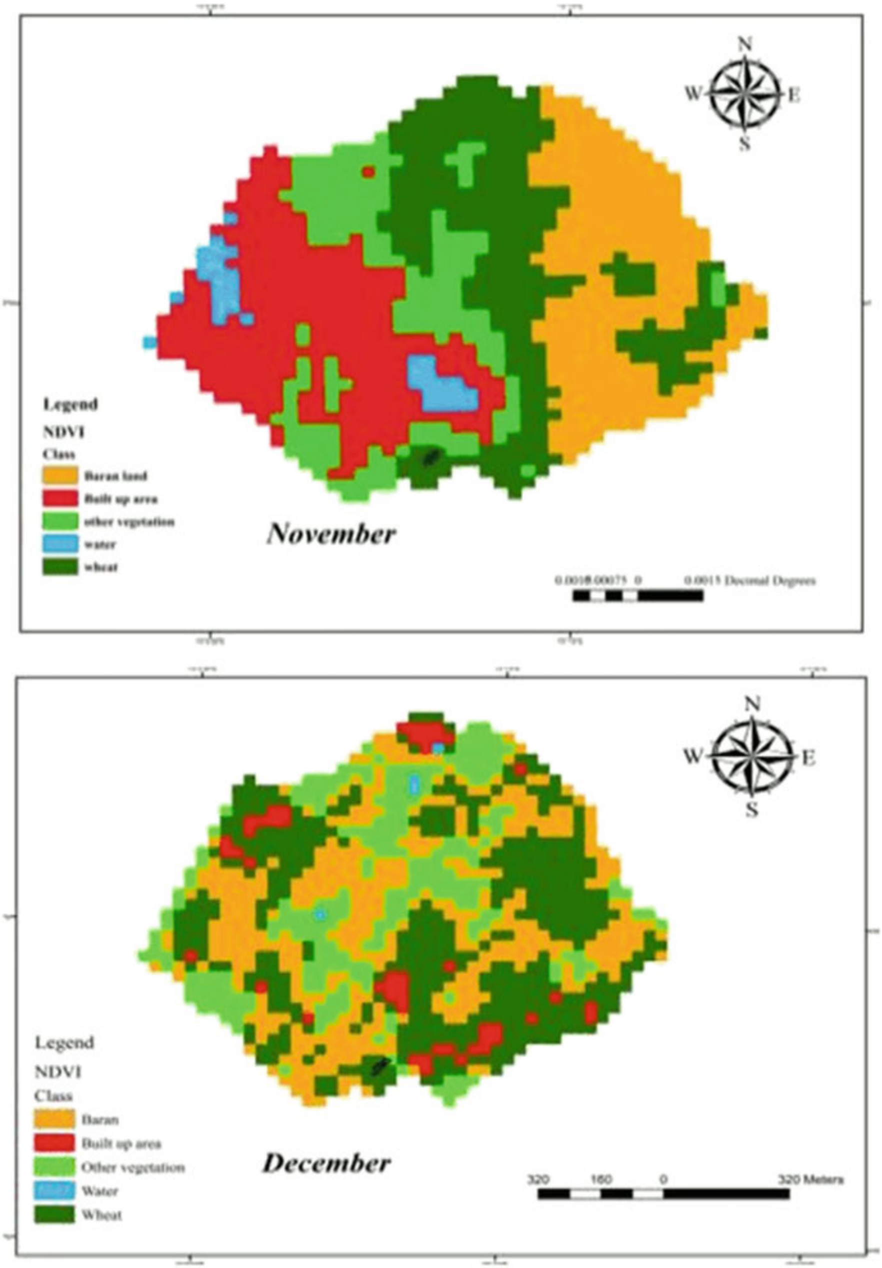

Fig. 9.10 NDVI map of URF-Koont, Chakwal Road, during the wheat growing season of 2017–2018

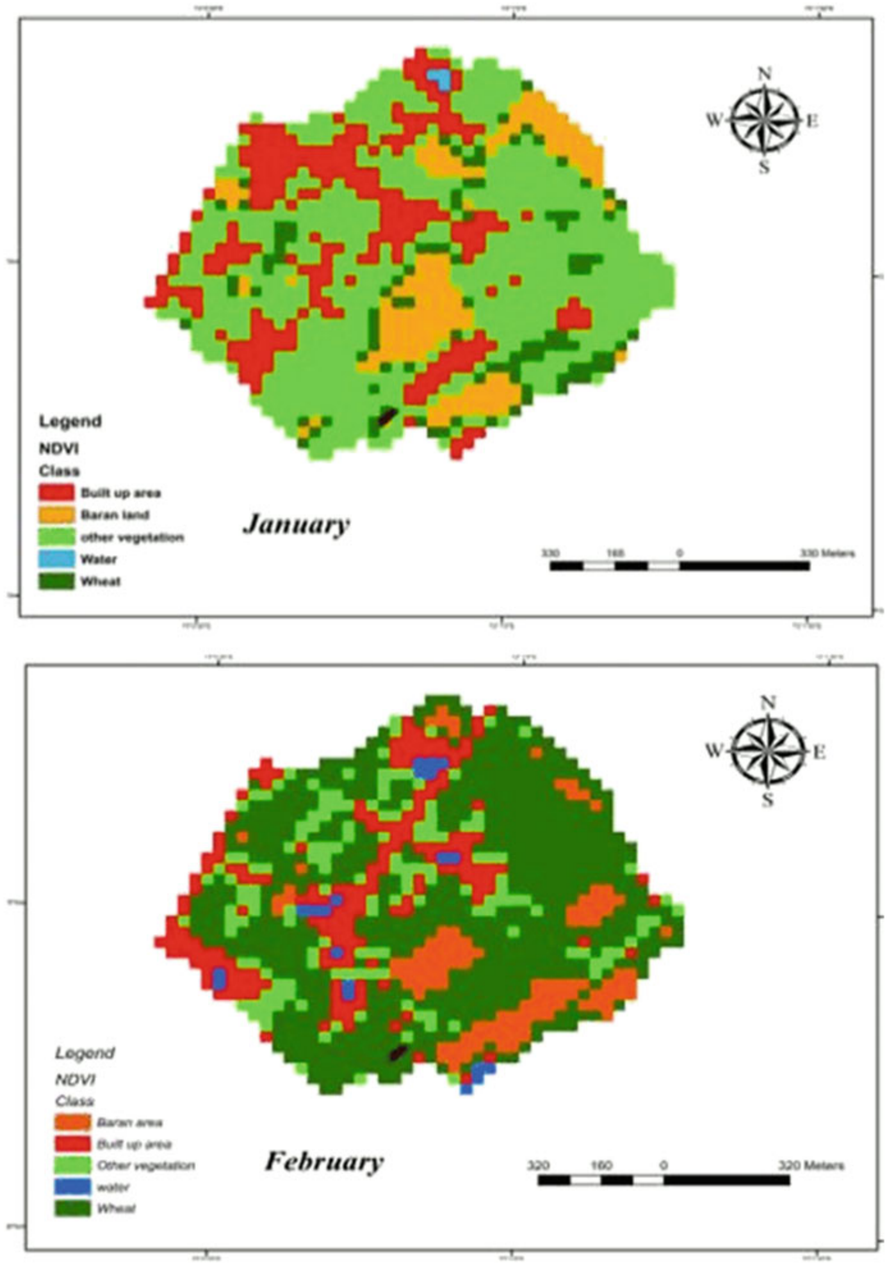

Fig. 9.11 NDVI map of URF-Koont, Chakwal Road, during the wheat growing season of 2017–2018

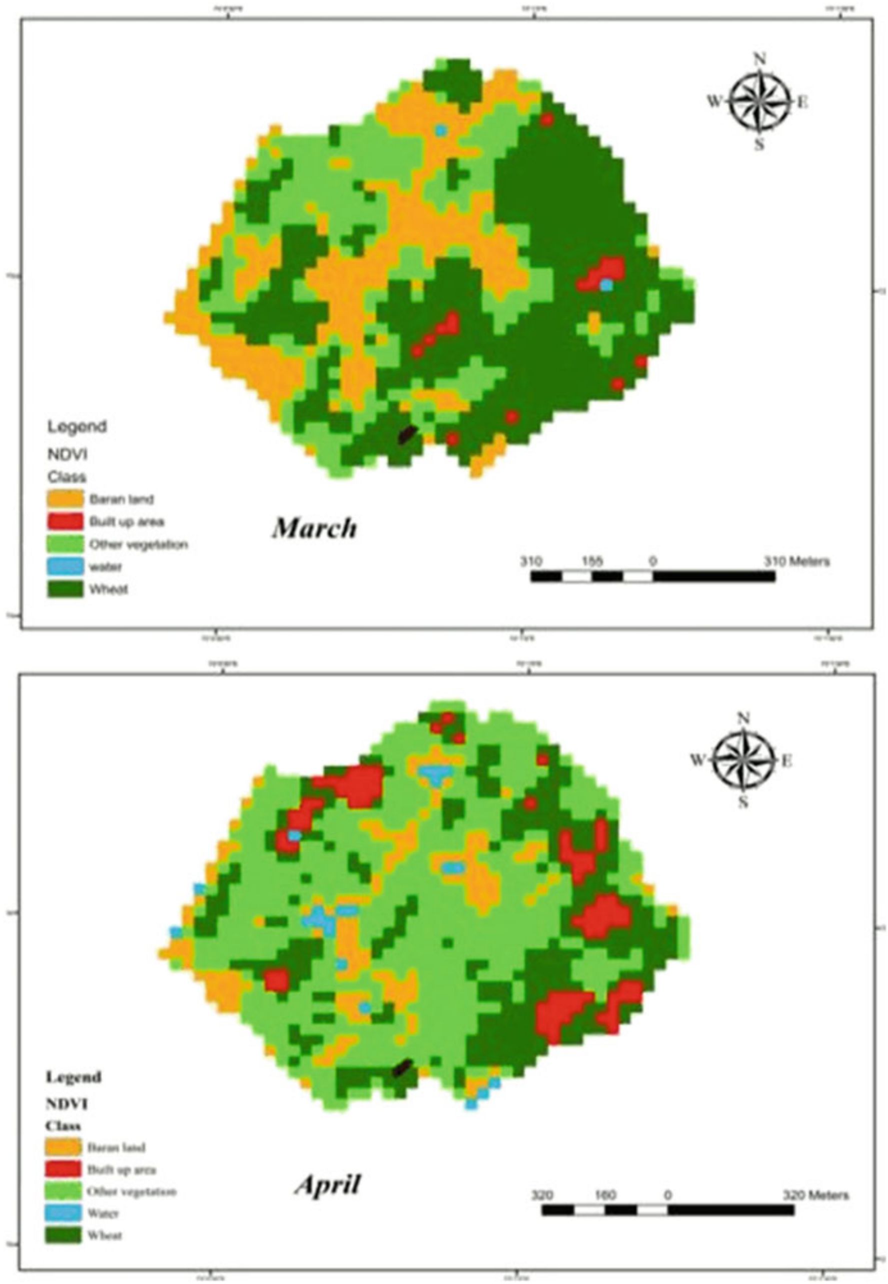

Fig. 9.12 NDVI map of URF-Koont, Chakwal Road, during the wheat growing season of 2017–2018

Table 9.2 Mean NDVI of Islamabad and the R^2 values for 15 points of field

S. no.	Date of acquisition	Mean NDVI of NARC Islamabad	R^2 of mean NDVI and observed yield
1	28 Nov. 2017	0.10746807	0.1655
2	12 Dec. 2017	0.5479084	0.0154
3	15 Jan. 2018	0.332320	0.4498
4	16 Feb. 2018	0.322173	0.7075
5	4 March 2018	0.697954	0.2246
6	21 April 2018	0.464193	0.002

Table 9.3 Mean NDVI of URF-Koont, Chakwal Road, and the R^2 values for 15 points of field

S. no.	Date of acquisition	Mean NDVI of URF-Koont	R^2 of mean NDVI and observed yield
1	28 Nov. 2017	0.242683	0.3923
2	12 Dec. 2017	0.065125	0.1952
3	15 Jan. 2018	0.043119	0.2375
4	16 Feb. 2018	0.433295	0.6312
5	4 March 2018	0.042297	0.5462
6	21 April 2018	0.041880	0.33

the February $R^2 = 0.6312$ due to high chlorophyll content and biomass. It declined in the April $R^2 = 0.33$ due to deceasing chlorophyll content. The relation between the observed yield and NDVI values was used in forecasting the wheat yield using the following equation:

$$\mathbf{y = -9837.5x + 5497.7}$$

9.3.3 Simulation Outcomes

9.3.3.1 Days to Anthesis

Simulated days to anthesis during 2017–2018 have close association with observed data for different sowing date experiments (Fig. 9.19). At NARC maximum (123) days to anthesis were observed for sowing date one (Sd1), while minimum (82) were counted for sowing date five (Sd5). Meanwhile, maximum (120) and minimum (90) simulated days to anthesis were recorded for sowing date one (Sd1) and sowing date five (Sd5), respectively. The comparison of model performance was measured by using validation skills scores R^2 RMSE which was (0.92). At URF-Koont highest (135) number of days to anthesis was counted for Sd1 (sowing date one), whereas minimum (90) was recorded for Sd5 (sowing date five). DSSAT model was able to reproduce the effect of different sowing dates on wheat phenology. The model predicted maximum (120) number of days to anthesis Sd1 followed by Sd5, whereas

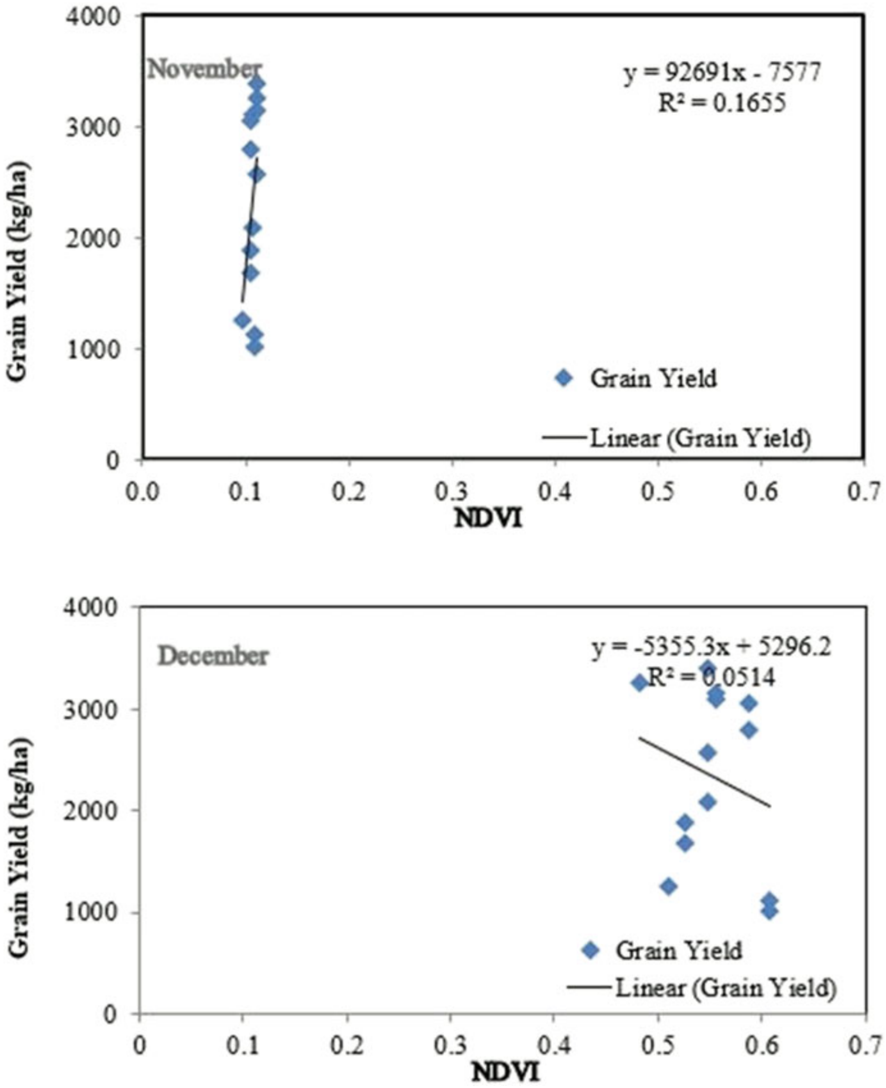

Fig. 9.13 Linear regression curve showing the relationship between NDVI values and observed wheat yield of Islamabad

minimum (90) were predicted for Sd5. The comparison of model performance was measured by using validation skills scores R^2 RMSE which was (0.96).

9.3.3.2 Days to Maturity

Predicted days to maturity have close association with observed data for different sowing date experiments during the wheat growing season of 2017–2018 (Fig. 9.20). At NARC higher (181) days to maturity were observed for Sd1 (sowing date one),

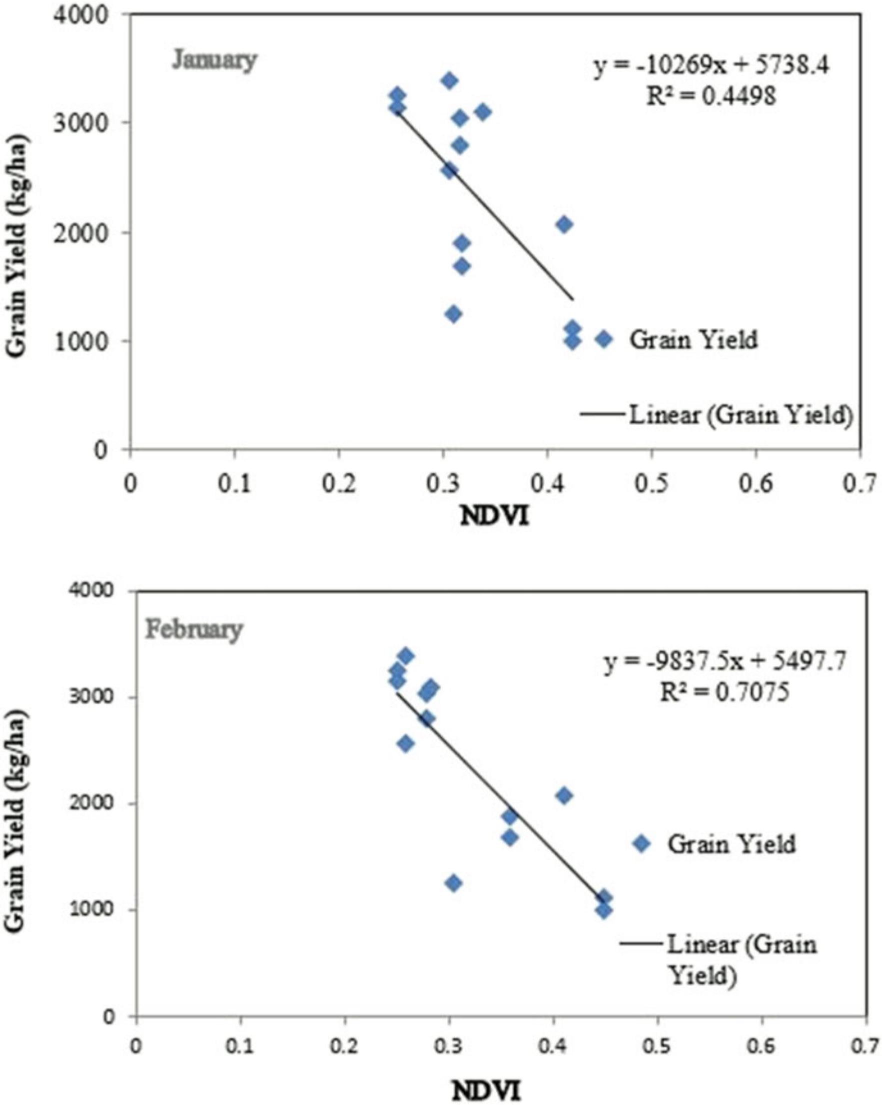

Fig. 9.14 Linear regression curve showing the relationship between NDVI values and observed wheat yield of Islamabad

while minimum (119) were counted for Sd5 (sowing date five). DSSAT model was able to reproduce the effect of different sowing dates on wheat phenology. The model predicted maximum (151) number of days to anthesis Sd1 followed by Sd5, whereas minimum (114) were predicted for Sd5. Validation skills scores (R^2 RMSE) were used for the comparison of model performance which was (0.99). At URF-Koont the highest (181) number of days to maturity was counted for Sd1

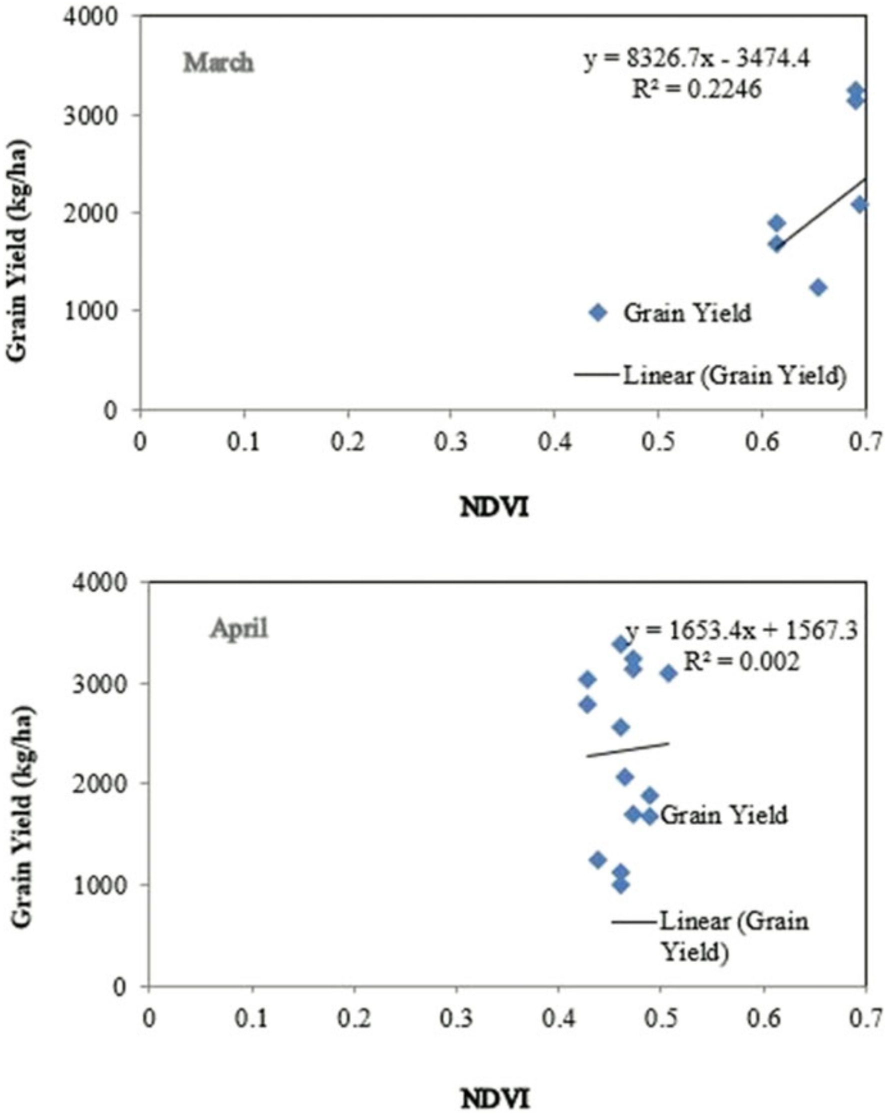

Fig. 9.15 Linear regression curve showing the relationship between NDVI values and observed wheat yield of Islamabad

(sowing date one), whereas minimum (119) was recorded for Sd5 (sowing date five). DSSAT model significantly reproduced the effect of different sowing date experiments on wheat phenology. The model predicted maximum (151) number of days to anthesis Sd1 followed by Sd5, whereas minimum (114) were predicted for Sd5. Validation skills scores (R^2 RMSE) were used for the comparison of model performance which was (0.99).

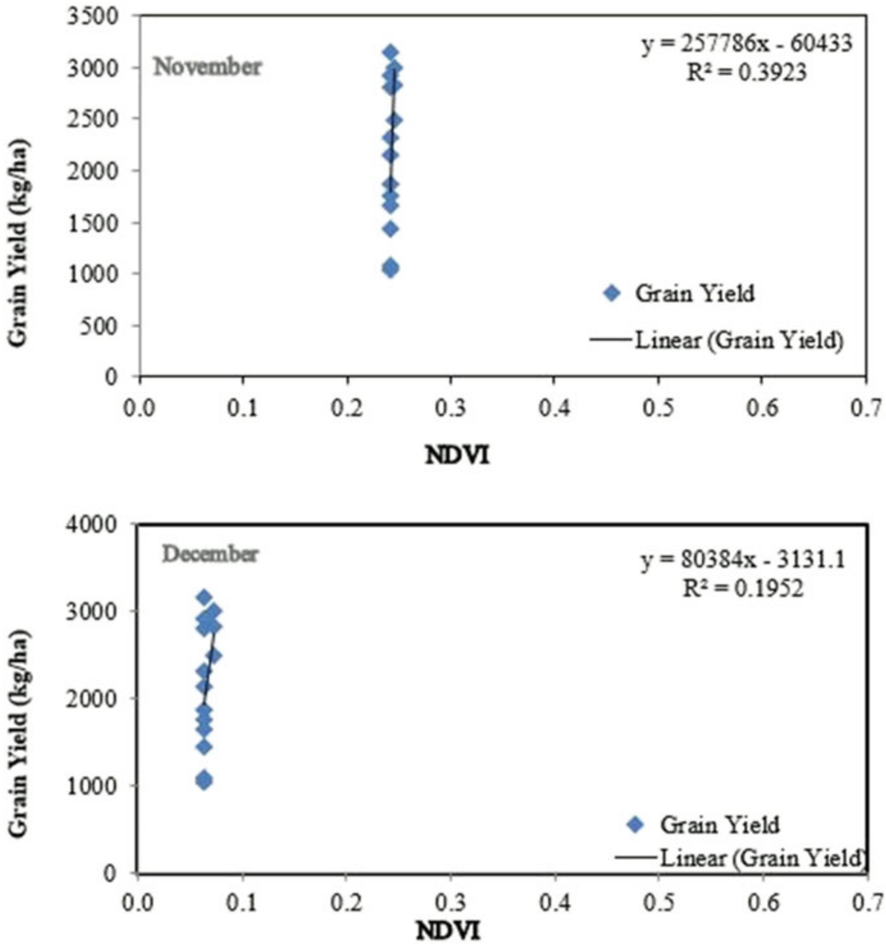

Fig. 9.16 Linear regression curve showing the relationship between NDVI values and observed wheat yield of URF-Koont, Chakwal Road

9.3.3.3 Leaf Area Index

Simulated leaf area index during 2017–2018 has close association with observed data for different sowing date experiments (Fig. 9.21). At Islamabad maximum (5) leaf area index was observed for Sd1 and Sd2 (sowing dates one and two), while minimum (4.5) were calculated for Sd5 (sowing date five). Meanwhile, the model's predicted maximum (5.1) and minimum (4.7) leaf area indices were recorded for Sd2 (sowing date two) and Sd5 (sowing date five) experiment of different sowing dates. The comparison of model performance was measured by using validation skills scores R^2 RMSE which was (0.89). At URF-Koont highest (5.1) leaf area index was counted for Sd2 (sowing date two), whereas minimum (4.4) was recorded for Sd5 (sowing date five). DSSAT model efficiently reproduced the

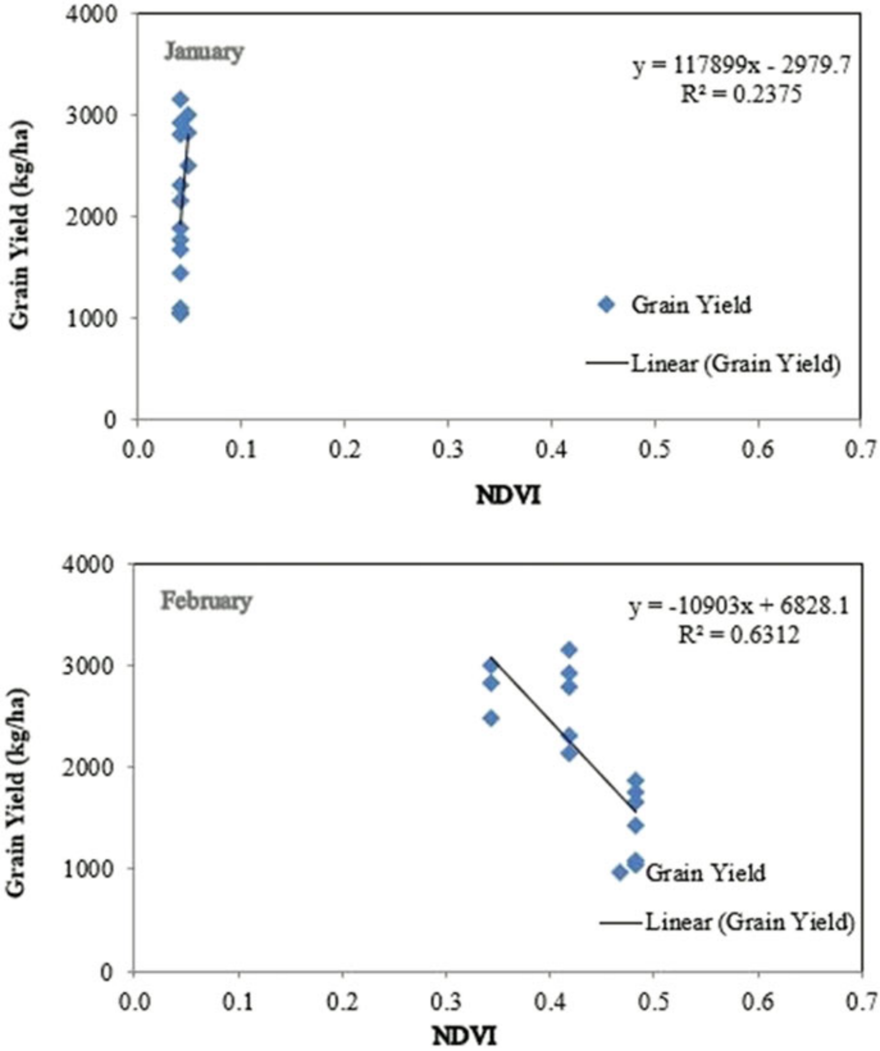

Fig. 9.17 Linear regression curve showing the relationship between NDVI values and observed wheat yield of URF-Koont, Chakwal Road

effect of different sowing dates on wheat phenology. The model predicted maximum (5.1) leaf area index for Sd2, whereas minimum (4.7) was predicted for Sd5. The comparison of model performance was measured by using validation skills scores R^2 RMSE which was (0.7).

9.3.3.4 Grain Yield (kg/ha)

Simulated grain yield during 2017–2018 has close association with observed data for different sowing date experiments (Fig. 9.22). At Islamabad maximum grain yield

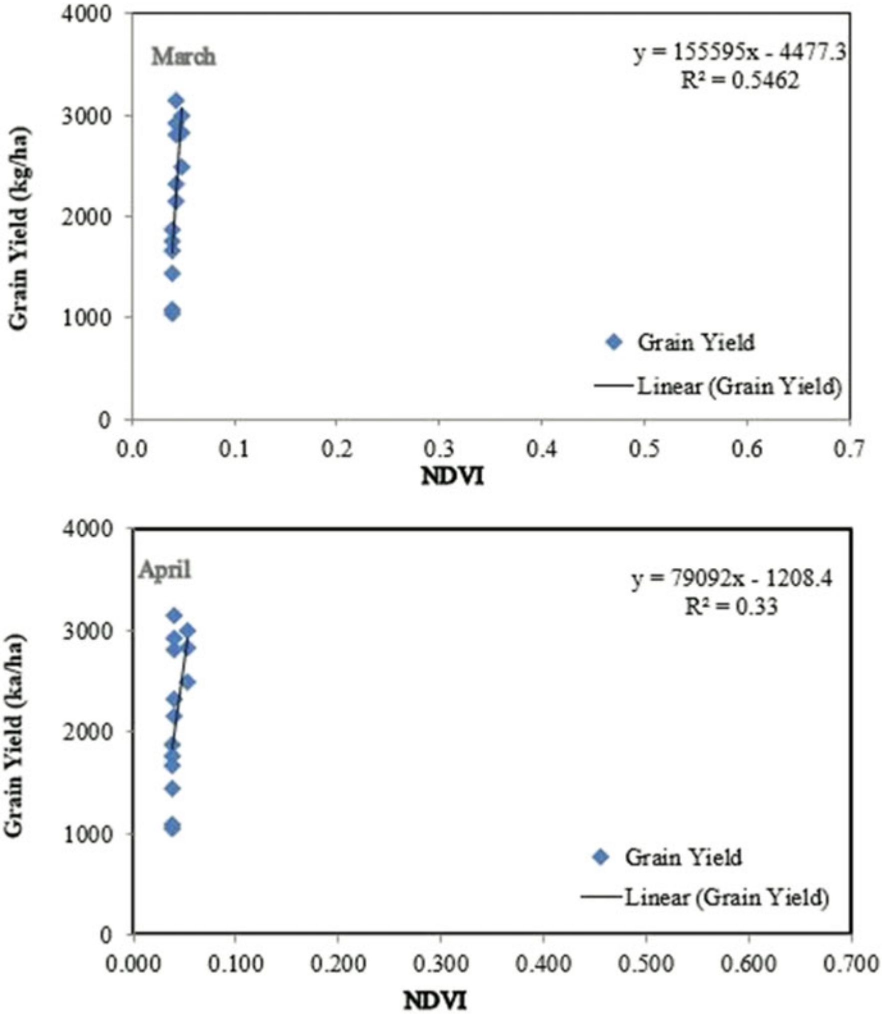

Fig. 9.18 Linear regression curve showing the relationship between NDVI values and observed wheat yield of URF-Koont, Chakwal Road

(3263 kg/ha) was observed for Sd2 (sowing date two), while minimum (1126.66 kg/ha) was recorded for Sd5 (sowing date five). Meanwhile, the model predicted maximum (3802 kg/ha) for Sd2 (sowing date two), and minimum (1098 kg/ha) grain yield was recorded for Sd5 (sowing date five) treatment experiment of different sowing dates. Delay in sowing dates reduces grain yield effectively. The comparison of model performance was measured by using validation skills scores R^2 RMSE which was (0.88). At URF-Koont maximum grain yield (3024 kg/ha) was observed for Sd2 (sowing date two), whereas minimum (1058.33 kg/ha) was recorded for Sd5 (sowing date five).The model reproduced the effect of different sowing date

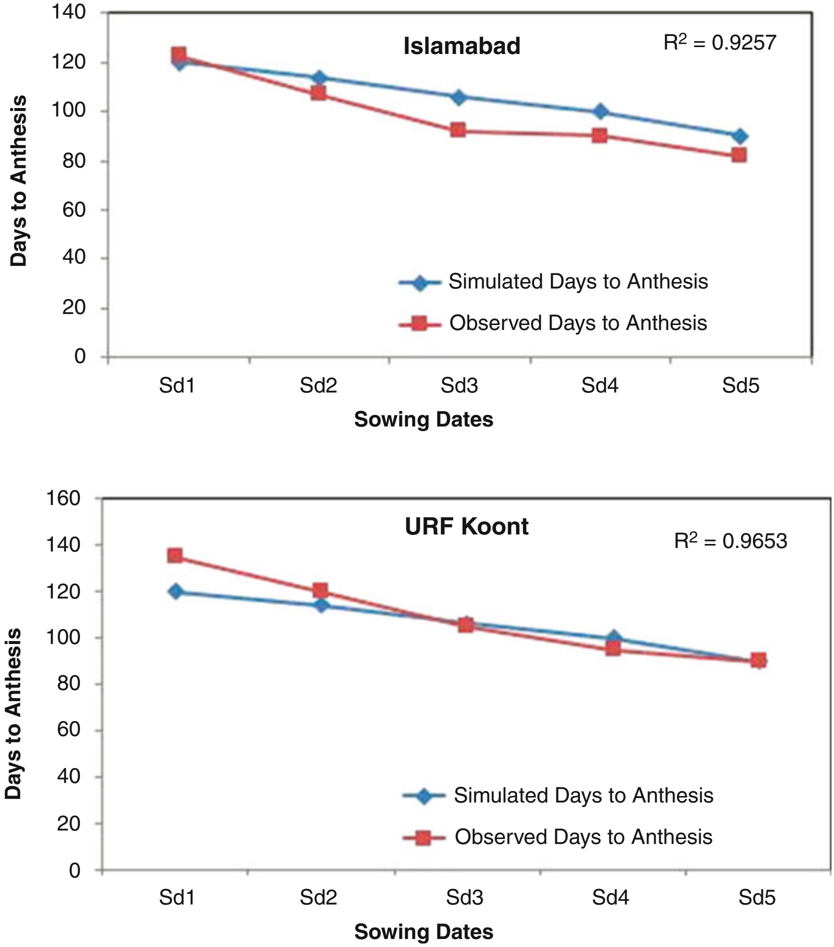

Fig. 9.19 Observed and simulated days to anthesis at Islamabad and URF-Koont under different climatic conditions and different sowing date experiments

experiments on wheat phenology. Maximum simulated grain yield (2802 kg/ha) was recorded for Sd2, whereas minimum (1098 kg/ha) was predicted for Sd5. The comparison of model performance was measured by using validation skills scores R^2 RMSE which was (0.86).

9.3.3.5 Biomass Yield (kg/ha)

Wheat biomass has close association with observed data for different sowing date experiments during the wheat growing season of 2017–2018 (Fig. 9.23). The highest value of biomass accumulation (8410 kg/ha) was recorded for Sd2 (sowing date two) at Islamabad, while the lowest (4040 kg/ha) was observed for Sd5 (sowing date five).

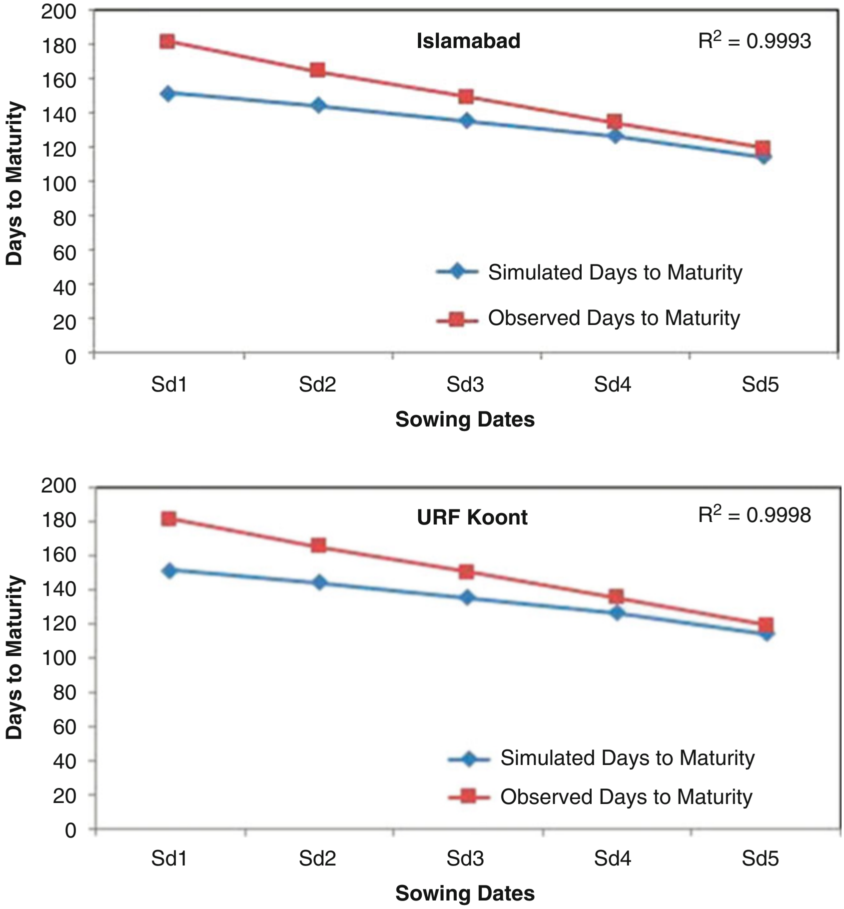

Fig. 9.20 Observed and simulated days to maturity under different climatic conditions and different sowing date experiments

However, the model estimated maximum (9432 kg/ha) and minimum (4289 kg/ha) of biomass for Sd2 and Sd5. However, statistic index values for evaluation of CERES-Wheat were R^2 RMSE which was (0.93). The highest observed biomass (8700 kg/ha) was observed for Sd1 (sowing date one), while lower (3635.13 kg/ha) was recorded for Sd5 (sowing date five) at URF-Koont. However, the model efficiently estimated maximum (9432 kg/ha) and minimum (4289 kg/ha) of biomass for Sd2 and Sd5. Statistic index values for evaluation of CERES-Wheat were R^2 RMSE which was (0.95).

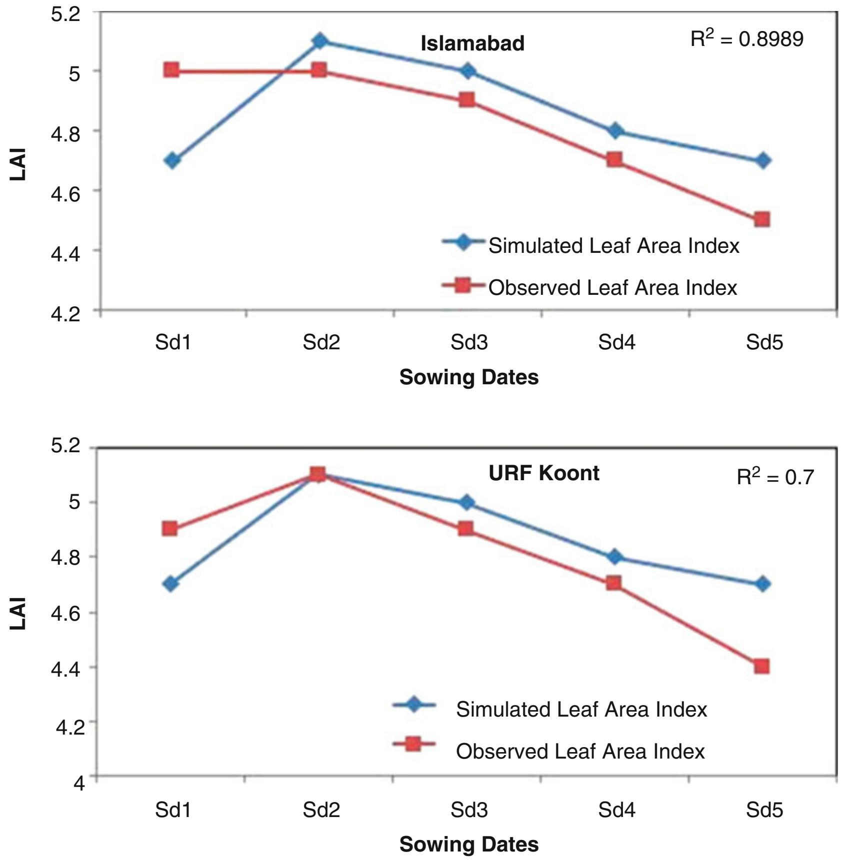

Fig. 9.21 Observed and simulated leaf area index under different climatic conditions and different sowing date experiments

9.3.3.6 Harvest Index

Simulated harvest index has close association with observed data for different source sink partitioning and varying nitrogen regimes during 2017–2018 (Fig. 9.24). Higher harvest index (35%) was observed for Sd2 (sowing date two, 15 November), while minimum (28%) was recorded for Sd5 (sowing date five, 30 December). Meanwhile, the model predicted maximum (30%) for Sd2 (sowing date two, 15 November), and minimum (24%) harvest index was recorded for Sd1 (sowing date one, 31 October). At URF-Koont maximum grain yield (35%) was observed for Sd2 (15 November), whereas minimum (28%) was recorded for Sd5 (30 December). The model reproduced the effect of different sowing dates on wheat phenology. Maximum simulated harvest index (30%) was recorded for S_2, whereas minimum (24%) was predicted for Sd5.

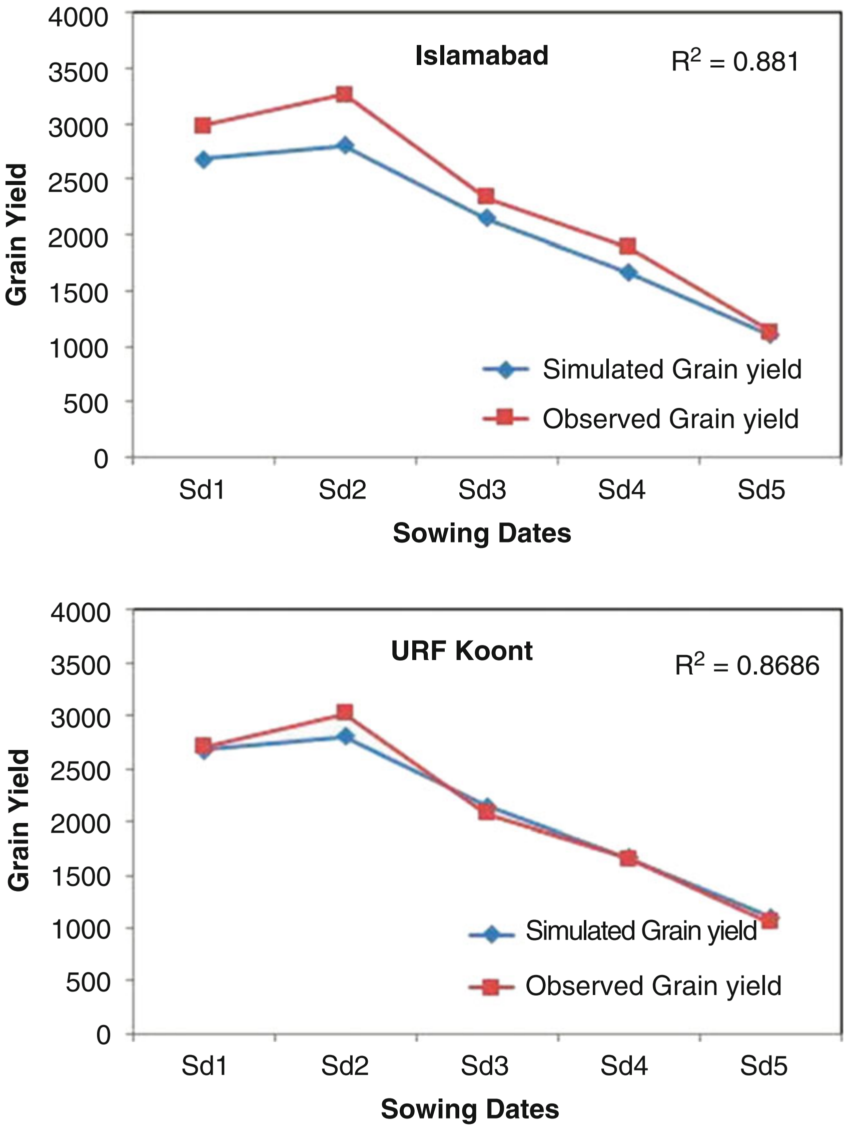

Fig. 9.22 Observed and simulated grain yield (kg/ha) under different climatic conditions and sowing date experiments

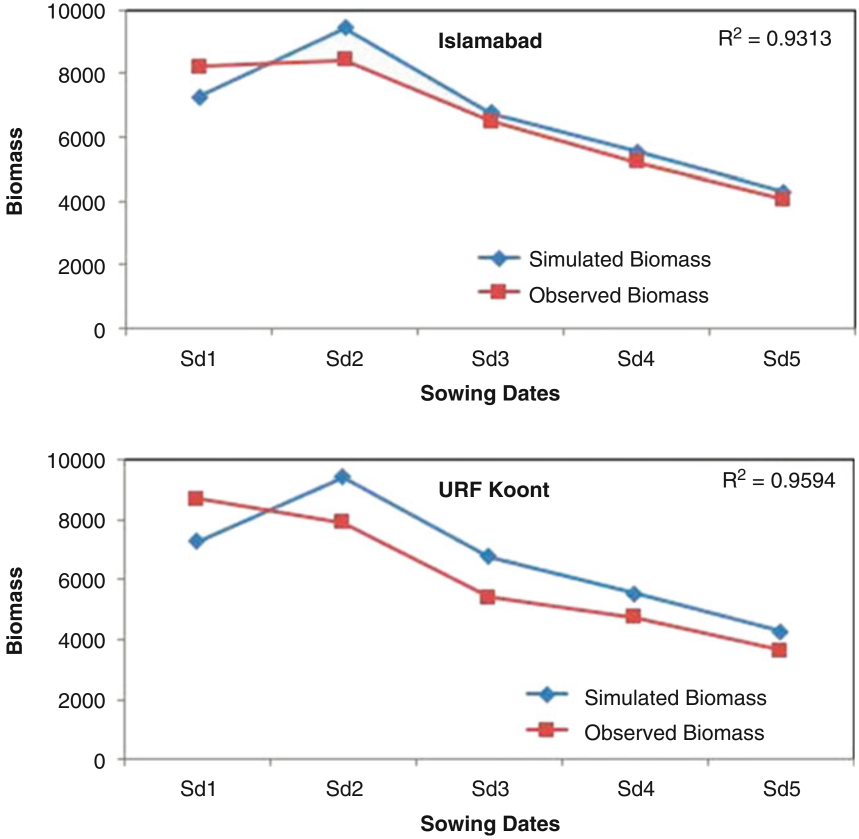

Fig. 9.23 Observed and simulated biomass (kg/ha) under different climatic conditions and sowing date experiments

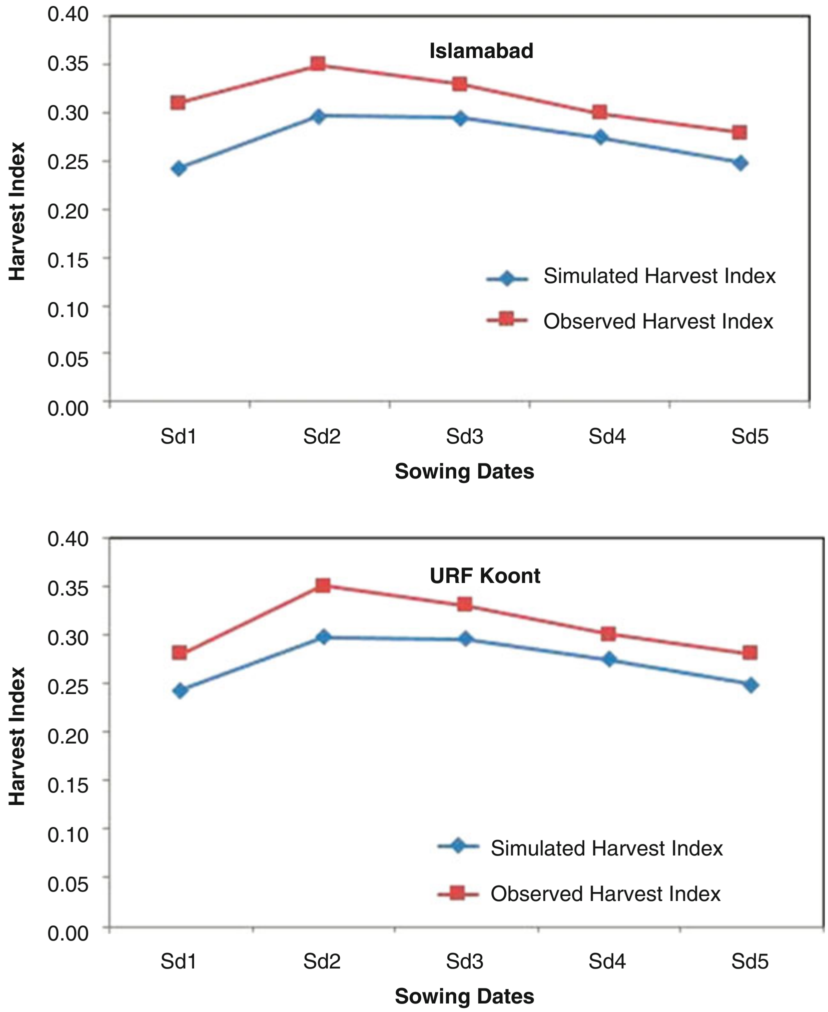

Fig. 9.24 Observed and simulated harvest index under different climatic conditions and sowing date experiments

References

Ahmad S, Abbas G, Fatima Z, Khan RJ, Anjum MA, Ahmed M, Khan MA, Porter CH, Hoogenboom G (2017) Quantification of the impacts of climate warming and crop management on canola phenology in Punjab, Pakistan. J Agron Crop Sci 203(5):442–452. https://doi.org/10.1111/jac.12206

Ahmad S, Abbas G, Ahmed M, Fatima Z, Anjum MA, Rasul G, Khan MA, Hoogenboom G (2019) Climate warming and management impact on the change of phenology of the rice-wheat cropping system in Punjab, Pakistan. Field Crop Res 230:46–61. https://doi.org/10.1016/j.fcr.2018.10.008

Ahmed M (2012) Improving soil fertility recommendations in Africa using the decision support system for Agrotechnology transfer (DSSAT); a book review. Exp Agric 48(4):602–603

Ahmed M (2020) Introduction to modern climate change. Andrew E. Dessler: Cambridge University Press, 2011, 252 pp, ISBN-10: 0521173159. Sci Total Environ 734:139397. https://doi.org/10.1016/j.scitotenv.2020.139397

Ahmed M, Ahmad S (2019) Carbon dioxide enrichment and crop productivity. In: Hasanuzzaman M (ed) Agronomic crops. Management practices, vol 2. Springer Singapore, Singapore, pp 31–46. https://doi.org/10.1007/978-981-32-9783-8_3

Ahmed M, Stockle CO (2016) Quantification of climate variability, adaptation and mitigation for agricultural sustainability. Springer Nature Singapore Pvt. Ltd., Singapore, 437 pp. https://doi.org/10.1007/978-3-319-32059-5

Ahmed M, Asif M, Hirani AH, Akram MN, Goyal A (2013) Modeling for agricultural sustainability: a review. In: Bhullar GS, Bhullar NK (eds) Agricultural sustainability progress and prospects in crop research. Elsevier, London

Ahmed M, Aslam MA, Hassan FU, Asif M, Hayat R (2014) Use of APSIM to model nitrogen use efficiency of rain-fed wheat. Int J Agric Biol 16:461–470

Ahmed M, Akram MN, Asim M, Aslam M, F-u H, Higgins S, Stöckle CO, Hoogenboom G (2016) Calibration and validation of APSIM-wheat and CERES-wheat for spring wheat under rainfed conditions: models evaluation and application. Comput Electron Agric 123:384–401. https://doi.org/10.1016/j.compag.2016.03.015

Ahmed M, Stöckle CO, Nelson R, Higgins S (2017) Assessment of climate change and atmospheric CO_2 impact on winter wheat in the Pacific Northwest using a multimodel ensemble. Front Ecol Evol 5(51). https://doi.org/10.3389/fevo.2017.00051

Ahmed M, Ijaz W, Ahmad S (2018) Adapting and evaluating APSIM-SoilP-wheat model for response to phosphorus under rainfed conditions of Pakistan. J Plant Nutr 41(16):2069–2084. https://doi.org/10.1080/01904167.2018.1485933

Ahmed M, Stöckle CO, Nelson R, Higgins S, Ahmad S, Raza MA (2019) Novel multimodel ensemble approach to evaluate the sole effect of elevated CO_2 on winter wheat productivity. Sci Rep 9(1):7813. https://doi.org/10.1038/s41598-019-44251-x

Ahmed K, Shabbir G, Ahmed M, Shah KN (2020) Phenotyping for drought resistance in bread wheat using physiological and biochemical traits. Sci Total Environ 729:139082. https://doi.org/10.1016/j.scitotenv.2020.139082

Amassaib MA, El Naim AM, Adam MN (2015) Climate change impacts on net revenues of Sorghum and millet in North Kordofan environment. World J Agric Res 3(2):52–56

Asseng S, Turner N, Keating BA (2001) Analysis of water-and nitrogen-use efficiency of wheat in a Mediterranean climate. Plant Soil 233(1):127–143

Asseng S, Martre P, Maiorano A, Rötter RP, O'Leary GJ, Fitzgerald GJ, Girousse C, Motzo R, Giunta F, Babar MA, Reynolds MP, Kheir AMS, Thorburn PJ, Waha K, Ruane AC, Aggarwal PK, Ahmed M, Balkovič J, Basso B, Biernath C, Bindi M, Cammarano D, Challinor AJ, De Sanctis G, Dumont B, Eyshi Rezaei E, Fereres E, Ferrise R, Garcia-Vila M, Gayler S, Gao Y, Horan H, Hoogenboom G, Izaurralde RC, Jabloun M, Jones CD, Kassie BT, Kersebaum K-C, Klein C, Koehler A-K, Liu B, Minoli S, Montesino San Martin M, Müller C, Naresh Kumar S, Nendel C, Olesen JE, Palosuo T, Porter JR, Priesack E, Ripoche D, Semenov MA, Stöckle C, Stratonovitch P, Streck T, Supit I, Tao F, Van der Velde M, Wallach D, Wang E, Webber H, Wolf J, Xiao L, Zhang Z, Zhao Z, Zhu Y, Ewert F (2019) Climate change impact and adaptation for wheat protein. Glob Chang Biol 25(1):155–173. https://doi.org/10.1111/gcb.14481

Bolton DK, Friedl MA (2013) Forecasting crop yield using remotely sensed vegetation indices and crop phenology metrics. Agric For Meteorol 173:74–84. https://doi.org/10.1016/j.agrformet.2013.01.007

Challinor A, Wheeler T (2008) Use of a crop model ensemble to quantify CO 2 stimulation of water-stressed and well-watered crops. Agric For Meteorol 148(6):1062–1077

Cooper M, Hammer GL (1996) Plant adaptation and crop improvement. IRRI, Wallingford
Ehdaie B, Alloush G, Madore M, Waines J (2006) Genotypic variation for stem reserves and mobilization in wheat. Crop Sci 46(5):2093–2103
Irons JR, Loveland TR (2013) Eighth Landsat satellite becomes operational. Photogramm Eng Remote Sens 79(5):398–401
Irons JR, Dwyer JL, Barsi JA (2012) The next Landsat satellite: the Landsat data continuity mission. Remote Sens Environ 122:11–21
Jabeen M, Gabriel HF, Ahmed M, Mahboob MA, Iqbal J (2017) Studying impact of climate change on wheat yield by using DSSAT and GIS: a case study of Pothwar region. In: Ahmed M, Stockle CO (eds) Quantification of climate variability, adaptation and mitigation for agricultural sustainability. Springer International Publishing, Cham, pp 387–411. https://doi.org/10.1007/978-3-319-32059-5_16
Kazmi DH, Rasul G (2012) Agrometeorological wheat yield prediction in rainfed Potohar region of Pakistan. Agric Sci 3(02):170
Lee DS, Storey JC, Choate MJ, Hayes RW (2004) Four years of Landsat-7 on-orbit geometric calibration and performance. IEEE Trans Geosci Remote Sens 42(12):2786–2795
Liu B, Martre P, Ewert F, Porter JR, Challinor AJ, Müller C, Ruane AC, Waha K, Thorburn PJ, Aggarwal PK, Ahmed M, Balkovič J, Basso B, Biernath C, Bindi M, Cammarano D, De Sanctis G, Dumont B, Espadafor M, Eyshi Rezaei E, Ferrise R, Garcia-Vila M, Gayler S, Gao Y, Horan H, Hoogenboom G, Izaurralde RC, Jones CD, Kassie BT, Kersebaum KC, Klein C, Koehler A-K, Maiorano A, Minoli S, Montesino San Martin M, Naresh Kumar S, Nendel C, O'Leary GJ, Palosuo T, Priesack E, Ripoche D, Rötter RP, Semenov MA, Stöckle C, Streck T, Supit I, Tao F, Van der Velde M, Wallach D, Wang E, Webber H, Wolf J, Xiao L, Zhang Z, Zhao Z, Zhu Y, Asseng S (2019) Global wheat production with 1.5 and 2.0°C above pre-industrial warming. Glob Chang Biol 25(4):1428–1444. https://doi.org/10.1111/gcb.14542
Lyle G, Lewis M, Ostendorf B (2013) Testing the temporal ability of Landsat imagery and precision agriculture technology to provide high resolution historical estimates of wheat yield at the farm scale. Remote Sens 5(4):1549–1567
Matthews RB, Rivington M, Muhammed S, Newton AC, Hallett PD (2013) Adapting crops and cropping systems to future climates to ensure food security: the role of crop modelling. Glob Food Sec 2(1):24–28
Motha RP, Baier W (2005) Impacts of present and future climate change and climate variability on agriculture in the temperate regions: North America. Clim Chang 70(1):137–164
Prasad AK, Chai L, Singh RP, Kafatos M (2006) Crop yield estimation model for Iowa using remote sensing and surface parameters. Int J Appl Earth Observ Geoinf 8(1):26–33. https://doi.org/10.1016/j.jag.2005.06.002
Rosegrant MW, Msangi S, Ringler C, Sulser TB, Zhu T, Cline SA (2008) International model for policy analysis of agricultural commodities and trade (IMPACT): model description. International Food Policy Research Institute, Washington, DC
Rosenzweig C, Tubiello FN (2007) Adaptation and mitigation strategies in agriculture: an analysis of potential synergies. Mitig Adapt Strateg Glob Chang 12(5):855–873
Saeidi M, Abdoli M (2015) Effect of drought stress during grain filling on yield and its components, gas exchange variables, and some physiological traits of wheat cultivars. J Agric Sci Technol 17 (4):885–898
Siegenthaler U, Stocker TF, Monnin E, Lüthi D, Schwander J, Stauffer B, Raynaud D, Barnola J-M, Fischer H, Masson-Delmotte V (2005) Stable carbon cycle–climate relationship during the late Pleistocene. Science 310(5752):1313–1317
Venkateswarlu B, Rao CR (2010) Rainfed agriculture: challenges of climate change. Agriculture Today Year Book:43–45
Wallach D, Martre P, Liu B, Asseng S, Ewert F, Thorburn PJ, van Ittersum M, Aggarwal PK, Ahmed M, Basso B, Biernath C, Cammarano D, Challinor AJ, De Sanctis G, Dumont B, Eyshi

Rezaei E, Fereres E, Fitzgerald GJ, Gao Y, Garcia-Vila M, Gayler S, Girousse C, Hoogenboom G, Horan H, Izaurralde RC, Jones CD, Kassie BT, Kersebaum KC, Klein C, Koehler A-K, Maiorano A, Minoli S, Müller C, Naresh Kumar S, Nendel C, O'Leary GJ, Palosuo T, Priesack E, Ripoche D, Rötter RP, Semenov MA, Stöckle C, Stratonovitch P, Streck T, Supit I, Tao F, Wolf J, Zhang Z (2018) Multimodel ensembles improve predictions of crop–environment–management interactions. Glob Chang Biol 24(11):5072–5083. https://doi.org/10.1111/gcb.14411

White JW, Hoogenboom G, Kimball BA, Wall GW (2011) Methodologies for simulating impacts of climate change on crop production. Field Crop Res 124(3):357–368

Methane Production in Dairy Cows, Inhibition, Measurement, and Predicting Models

10

Mohammad Ramin, Juana C. Chagas, and Sophie J. Krizsan

Abstract

Methane is a potent greenhouse gas that is produced in many sectors. Agriculture and, more specifically, livestock contribute to this phenomenon. Methane is produced as a result of fermentation in the rumen of dairy cows with a significant amount of gas being released in the atmosphere via the mouth of ruminants. The total intake is the main factor influencing methane production followed by digestibility, fat, and the amount of fibre in the diet. Many strategies exist to reduce methane emissions such as chemicals, essential oils, and the red macroalgae in the diet of dairy cows. The majority of these strategies are either expensive or not feasible to use in a long-term period of time since the microbes in the rumen will adapt to this change. There is a wide range of methods and tools to measure methane emissions both in vitro and in vivo. The respiration chamber is the golden method to measure and quantify the fluxes (methane emissions) in dairy cows. In some cases where measurements of methane are impossible, vitro techniques together with modelling approaches could be used to predict methane emissions. Empirical and mechanistic modelling is a technique widely used to predict methane emissions. In this case by knowing some feed and animal characteristics methane could be reliably estimated.

Keywords

Methane · Livestock · Fermentation · Rumen · In vitro and In vivo · Respiration chamber · Empirical and mechanistic modelling

M. Ramin (✉) · J. C. Chagas · S. J. Krizsan
Swedish University of Agricultural Sciences (SLU), Umeå, Sweden
e-mail: mohammad.ramin@slu.se

M. Ahmed (ed.), *Systems Modeling*, https://doi.org/10.1007/978-981-15-4728-7_10

10.1 Methane Gas

Water vapour is the number one contributor to greenhouse gas (GHG) effect followed by carbon dioxide (CO_2) and methane (CH_4) (Kiehl and Trenberth 1997). Methane is a compound with relatively high energy combustion of 55.5 MJ/kg (Crutzen 1995) that contributes to about 20% of total anthropogenic GHG emissions as shown by Lassey (2007). Methane has a very short turn-over time of about 10 years in the atmosphere as compared to CO_2, but it can trap the heat 20 times greater than CO_2, playing a key part in global climate change. The concentration of CH_4 gas has been rising rapidly in the atmosphere over the past decade compared to three centuries ago; it has raised over 2.5-fold (Lassey 2007). Emissions of CH_4 lead to increased ground-level ozone, with significant damage to public health and agriculture (Howarth 2019), giving an estimated social cost of 2700 USD per ton of CH_4 (Shindell 2015).

10.2 Sources of Methane Emissions

There are many sources that CH_4 originates from; it can be from wetlands, rice paddies, termites, agriculture, and burning biomass (Immig 1996). The rice paddies have been shown to be an important contributor with annual emissions reported to be around 115 teragrams (Tg) per year (Thorpe 2009). The agriculture sector contributes to about 10–12% of the total global anthropogenic GHG emissions (McAllister et al. 2011) with livestock sector (enteric fermentation) contributing the most within the agricultural sector of around 37% of total anthropogenic CH_4 emissions. Other reports claim that CH_4 emissions from the livestock sector is about 51% of the total agricultural CH_4 emissions and that the contribution of rice paddies and livestock is rather similar, 100 and 110 Tg/year, respectively (Moss et al. 2000).

There is a high demand by the Intergovernmental Panel on Climate Change (IPCC) to evaluate the number of gases produced and to develop methods and strategies to reduce the emissions of GHG within a time frame (Ahmed 2017; Moss et al. 2000). Within the European countries, livestock, mainly the enteric fermentation, has been reported to be the leading CH_4 producer within the agriculture sector (Moss et al. 2000).

Within the European Union (EU-27) and based on data that was obtained in 2003, Lesschen et al. (2011) reported that dairy cow and beef cattle contributed to the most GHG emissions (Fig. 10.1).

As shown in Fig. 10.1, the enteric fermentation from dairy cow and beef cattle contributes the most to the GHG emissions followed by the N_2O soil emission and manure management.

Recently published data based on radioactive carbon (C^{14}) content in CH_4 indicates that anthropogenic emissions of CH_4 in recent decades have been higher than previously estimated (Petrenko et al. 2017). Satellite data (Howarth 2019) suggest that the increased global CH_4 emissions in the period 2005–2015 were

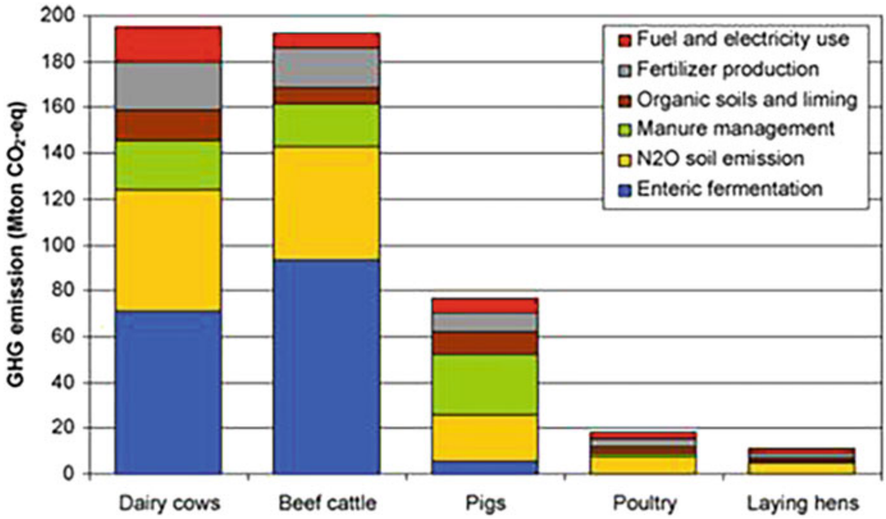

Fig. 10.1 Greenhouse gas emissions from the livestock production in the EU-27. (Source: Lesschen et al. 2011)

mostly due to increased extraction of shale gas and that the natural gas and oil industry contributes twice as much CH_4 emissions as animal agriculture.

10.3 Methane in Ruminants

Methane is produced in the rumen of ruminants with a minor contribution from the hindgut as a result of food digestion and fermentation. The majority (95%) of CH_4 gas is produced during the enteric fermentation and is lost to the atmosphere via belching, whereas the remaining 5% is emitted through the rectal (Fig. 10.2).

The food eaten by dairy cows (mainly silage and concentrates) is then fermented in the rumen by the help of microorganisms. A result of this fermentation is hydrogen (H_2) gas which then needs to be absorbed in order to make this fermentation pathway happening all time. There are specific microorganisms in the rumen belonging to the domain of Archaea (*Methanobrevibacter* spp.) which uses the H_2 to produce CH_4 gas. One of the dominant species of methanogenic bacteria living in the rumen is *Methanobacterium ruminantium* (Miller et al. 1986). The phenomenon of CH_4 emission starts around 4 weeks after birth in dairy cows when the rumen is almost shaped, and solid particles are kept in the rumen (Johnson and Johnson 1995). Methanogenic bacteria are mainly in both the liquid and solid phases in the rumen (Morgavi et al. 2010). The food entering the rumen (stomach) of a cow is first digested by microorganisms that contain mainly bacteria, protozoa, and fungi. The simple monomers produced by primary microorganisms are then used by both primary and secondary fermenters to produce end products such as volatile fatty acids (VFA), CO_2, and H_2 (McAllister et al. 1996). In the final step of fermentation,

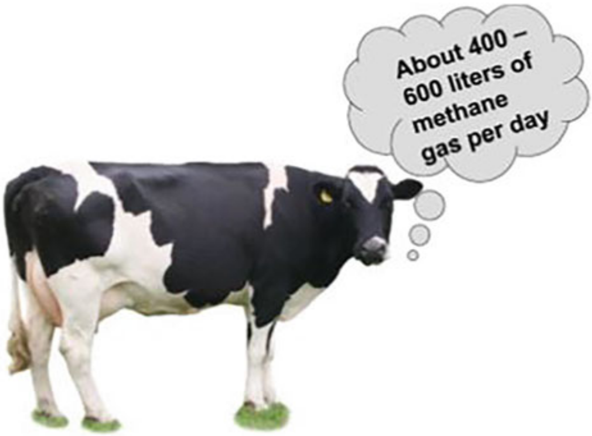

Fig. 10.2 Picture showing that the majority of CH_4 is eructated from the mouth of dairy cows

the H_2 that is produced in previous steps is then used together with CO_2 to produce CH_4 gas by methanogens in the rumen (Eq. 10.1).

$$CO_2 + 4H_2 \rightarrow CH_4 + 2H_2O \tag{10.1}$$

Methane emission from dairy cows depends on many factors, such as type of feed, the amount of feed intake, quality of the feed, and digestibility. Grass contains energy; this energy is called gross energy (GE) and once eaten by dairy cows a part of this energy is lost as CH_4 gas. Depending on the factors mentioned above, CH_4 emission as a proportion of GE varies between 2% and 12% of GE intake (Johnson and Johnson 1995).

10.4 Factors Affecting Methane Emission

There are many factors influencing CH_4 emission in dairy cows. The main element is dry matter intake. In addition to intake, diet digestibility, amount of fat and fibre in the diet has effects on CH_4 emission in dairy cows (Ramin and Huhtanen 2013).

There are some feed characteristics influencing CH_4 emission in dairy cows as there is a close relationship between rumen-fermented organic matter and CH_4 emission (Ramin and Huhtanen 2013). Diets that contain high amounts of digestible fibre will increase the digestibility in the diet resulting in higher emissions of CH_4. The forage to concentrate ratio in the diet also affects CH_4 emission, for example, feeding high concentrate proportions (above 90%) in the diet of feedlot beef cattle can reduce CH_4 significantly (Johnson and Johnson 1995). Moss et al. (1995) showed that CH_4 as a proportion of GE increased more when the concentrate was increased in the diet of sheep fed on a low level of intake. The effect of fat in the diet is another factor influencing CH_4 emission (Grainger and Beauchemin 2011). There are some theories behind the effect of fat on CH_4 emissions: (1) unsaturated fatty acids are bio-hydrogenated in the rumen, a process that utilizes H_2, (2) inclusion of fat in the diet simply reduces the supply of carbohydrates resulting in less fermentable substrates, and (3) inclusion of fat in the diet favours the pathway of propionic acid production (H_2 sink) in the rumen (Ramin and Huhtanen 2013).

10.5 Factors Inhibiting CH_4 Emissions

To date, there are many strategies to reduce CH_4 emission in dairy cows, ranging from chemicals to algae. Some show direct effects on methanogenic bacteria and some act by interrupting the last step in the biochemical process of producing CH_4 in the rumen. For the chemicals, the efficient methane inhibitor identified is 3-nitrooxypropanol (3NOP). The 3NOP has proven to be the most effective inhibitor without showing any adverse effect on milk production (Hristov et al. 2015). The amount of 3NOP needed to reduce enteric methane from cows is very small, 80 mg per kg of DM intake showed reductions up to 30% of methane production from high producing dairy cows (Hristov et al. 2015). In addition, other chemicals have been reported in the literature decreasing CH_4 emissions, such as 2-nitroethanol and bromoform (Chagas et al. 2019; Zhang and Yang 2011).

Regarding dietary strategies with the potential to mitigate CH_4 emission, the rapeseed oil added to a grass silage-based diet reduced ruminal CH_4 emissions from lactating cows as reported by Bayat et al. (2018), where the decrease in CH_4 was explained by reductions in DM intake and the dilution effect on fermentable organic matter. Franco et al. (2017) in an in vitro study replaced soybean meal by dried distiller's grain in grass silage-based diet, and the authors reported a decrease in predicted in vivo CH_4 production, which was related to a shift in the ruminal fermentation pattern to decreased acetate and butyrate production and increased propionate production. Further, the use of oats in the diet has also been shown as a potential strategy to reduce CH_4 emission, and a recent study conducted by Fant et al. (2020) showed that predicted in vivo CH_4 emission was 8.5% lower for a diet that used oats compared to barley.

Several studies have recently reported the potential of essential oils to reduce enteric CH_4 production, primarily in vitro and short-term trials. The most common essential oils reported in the literature as methane mitigate strategies are derived from thyme, oregano, horseradish, rhubarb, frangula, and highlighting garlic, cinnamon, and its derivatives (Benchaar and Greathead 2011). However, the authors draw attention to the need for in vivo investigation to propose whether these ingredients/additives can be used successfully to inhibit rumen methanogenesis, without depressing feed intake, digestibility, and animal productivity.

Recently, the red macroalgae *Asparagopsis taxiformis* (AT) has shown promising effects on reducing CH_4 emission from dairy cows. In vivo (Stefenoni et al. 2019) and in vitro (Chagas et al. 2019) studies showed a decrease of 80% on CH_4 emission by adding 0.5% of AT on a dry matter basis and inhibition of CH_4 by adding 0.5% of AT on organic matter basis, respectively. Previous in vitro studies also had reported the potential to mitigate methane emission to adding AT in ruminants diets (Machado et al. 2014, 2016).

Fig. 10.3 This cartoon shows the side effects of dietary CH_4 inhibitors. (Reprinted from: An Introduction to Rumen Studies by J.W. Czerkawski, page 172. Copyright © (1986))

One major problem with additives used in the diet is the excess of H_2 gas in the rumen if there is no other sink to uptake the H_2 production (Fig. 10.3).

10.6 Methods and Models for Measuring or Predicting CH_4 Emission

There are many tools and models in the literature to predict CH_4 emission. Respiration chamber is the most accurate method of measuring CH_4 emission in dairy cows (Johnson and Johnson 1995). The animal is basically allocated in a chamber for 2–3 days in which all exhaled breath is measured including CH_4. The technique is laborious with high construction costs. The alternative to in vivo techniques measuring CH_4 emissions, in vitro methods, is also used. In the in vitro method, a small sample size (1 g) is incubated in fermentation units in which buffered rumen fluid is added. The fermentation takes place in an anaerobic condition at the same temperature of the rumen (39 °C). The unit is then gently shacked for about 48 h.

The in vitro gas production system's main advantage is that it provides a large number of data points, which allow accurate estimates of CH_4 emissions. In another hand, this system has some limitations compared with in vivo studies (e.g. no absorption of VFA over time and the intake dynamics).

Recently, Ramin and Huhtanen (2012) developed the application of an in vitro method so CH_4 emission could be predicted in vivo by applying the data obtained from the in vitro in a rumen model. The method allows estimation of CH_4 emissions every 20 min of incubating a sample up to 48 h. Figure 10.4 shows the curve of CH_4

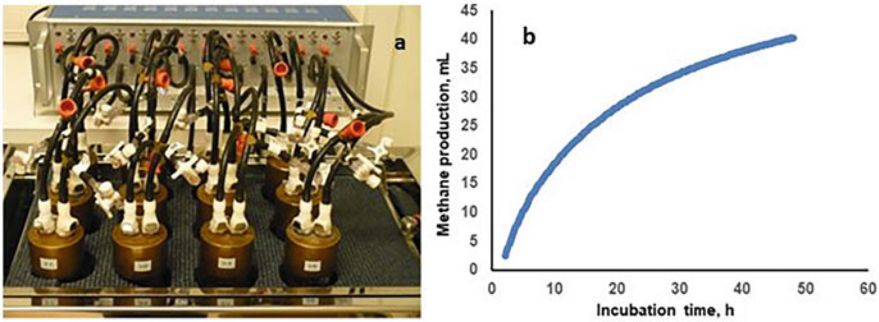

Fig. 10.4 In vitro method (**a**) and methane emission (**b**) over a 48 h incubation period from a silage-based diet using the model as described by Ramin and Huhtanen (2012)

emission over a 48 h incubation time for a diet consisting of silage. One main advantage of in vitro systems is that it allows digestion kinetics to be evaluated from feeds and that the method could be used as a screening tool for assessing different CH_4 inhibitors.

Danielsson et al. (2017) evaluated the in vitro system developed by Ramin and Huhtanen (2012) by formulating 49 diets used in 13 in vivo studies in which CH_4 emission was measured by the respiration chamber. The results indicated that the in vitro system predicted in vivo CH_4 emissions very well with a high $R^2 = 0.96$. However, the values obtained (mean 399 L/d) also showed a slight underestimation compared to the observed (mean 418 L/d) in vivo CH_4 emissions (Fig. 10.5).

Models are developed from data sets that consist of animal and dietary characteristics. The most widely used models to predict CH_4 emissions are the empirical models. However, models can be categorized into two main groups: empirical models (e.g. Ellis et al. 2007; Ramin and Huhtanen 2013; Niu et al. 2018) or dynamic mechanistic models (Huhtanen et al. 2015).

Empirical models relate CH_4 emissions to the total amount of intake and dietary composition (Ramin and Huhtanen 2013). The empirical models developed by Ramin and Huhtanen (2013) use a data set in which no additive study is used. It is also advisable to use a mixed model regression analysis so that random study effect will be taken into account (St-Pierre 2001) when developing models predicting CH_4 emission. The model predicting CH_4 as a proportion of GE developed by Ramin and Huhtanen (2013) takes into account total dry matter intake per kg of body weight (DMIBW), organic matter digestibility estimated at the maintenance level of feeding (OMDm), and dietary concentrations of neutral detergent fibre (NDF), non-fibre carbohydrates (NFC), and ether extract (EE).

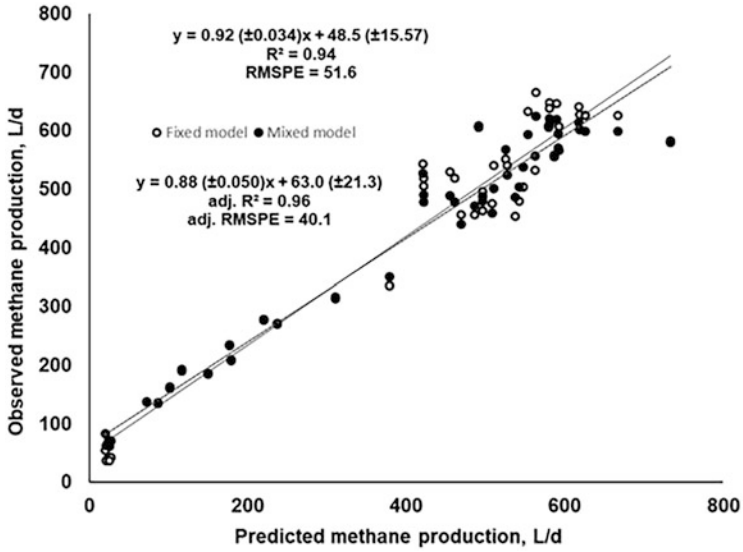

Fig. 10.5 Relationship between predicted in vivo CH_4 emission by the in vitro technique and observed CH_4 emission in vivo (L/d; $n = 49$), with fixed and mixed model regression analysis. (Source: Danielsson et al. 2017)

$$\begin{aligned}CH_4 - E/GE\ (\mathrm{kJ/MJ}) = & -0.6\ (\pm 12.76) - 0.70\ (\pm 0.072)\\ & \times \mathrm{DMIBW}\ (\mathrm{g/kg}) + 0.076\ (\pm 0.0118)\\ & \times \mathrm{OMDm}\ (\mathrm{g/kg}) - 0.13\ (\pm 0.020)\\ & \times \mathrm{EE}\ (\mathrm{g/kg\ DM}) + 0.046\ (\pm 0.0097)\\ & \times \mathrm{NDF}\ (\mathrm{g/kg\ DM}) + 0.044\ (\pm 0.0094)\\ & \times \mathrm{NFC}\ (\mathrm{g/kg\ DM})\end{aligned} \tag{10.2}$$

And the equation predicting total CH_4 emission (litres per day) developed by Ramin and Huhtanen (2013) was closely related to total DMI, and further adding other variables improved the model:

$$\begin{aligned}CH_4(\mathrm{L/d}) = & -64.0\ (\pm 35.0) + 26.0\ (\pm 1.02) \times \mathrm{DMI}\ (\mathrm{kg/d})\\ & - 0.61\ (\pm 0.132) \times \mathrm{DMI2}\ (\mathrm{centered}) + 0.25\ (\pm 0.051)\\ & \times \mathrm{OMDm}\ (\mathrm{g/kg}) - 66.4\ (\pm 8.22) \times \mathrm{EE\ intake}(\mathrm{kg\ DM/d})\\ & - 45.0\ (\pm 23.50) \times \mathrm{NFC}/(\mathrm{NDF} + \mathrm{NFC})\end{aligned} \tag{10.3}$$

Mechanistic models are a little bit more complicated as compared to empirical models. Mechanistic models simulate CH_4 emissions using mathematical formulas and descriptions of ruminal fermentation biochemistry, making it a great tool for understanding the mechanisms and factors influencing CH_4 emissions in the rumen. Karoline is a dynamic, deterministic, and mechanistic simulation model of a lactating dairy cow developed by Danfær et al. (2006). The sub-model predicting CH_4 emission was further developed by Huhtanen et al. (2015). A recent evaluation of the

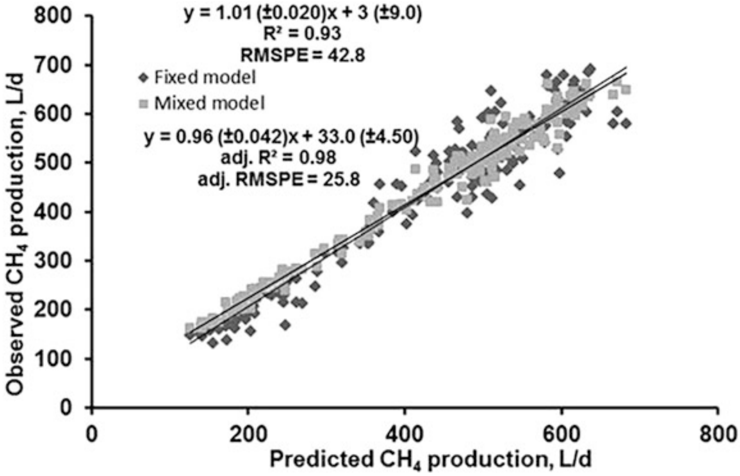

Fig. 10.6 Relationship between predicted (using the Karoline model) and observed CH_4 emissions (L/d) ($n = 184$) with fixed and mixed model regression analysis. (Source: Ramin and Huhtanen 2015)

Table 10.1 The comparison of empirical and mechanistic models in predicting CH_4 emission

Reference	Observation	R^2	RMSE
Empirical models			
Axelsson (1949)	175	0.75	0.131
Ellis et al. (2007)	172	0.71	0.296
Ramin and Huhtanen (2013)	184	0.93	0.104
Mechanistic models			
Mills et al. (2001)	32	0.76	0.154
Ramin and Huhtanen (2015)	184	0.93	0.101

Karoline model using a data set developed from studies that respiration chamber was used to measure CH_4 emission suggested that the model has a potential to predict CH_4 emissions accurately and precisely as shown in Fig. 10.6 (Ramin and Huhtanen 2015). Furthermore, evalution of CH_4 at whole farm scale is need of time (Ahmed et al. 2020).

Table 10.1 summarizes some empirical and mechanistic models developed in the literature. The empirical model developed by Ramin and Huhtanen (2013) predicted CH_4 emission better than other models as observed by a smaller root mean square error (RMSE). The mechanistic model Karoline also showed better predictions of CH_4 emission (Table 10.1) compared to the mechanistic model evaluated by Mills et al. (2001).

There are many equations developed in the literature predicting CH_4 production. Equations are basically developed from larger data sets in which intake and dietary factors are gathered. Since dry matter intake is the driving force in predicting CH_4

Table 10.2 Equations predicting CH_4 production

Source	Equation
Ellis et al. (2007)	CH_4 [MJ/d] = 3.41 + 0.520 × DMI[a] [kg/d]−0.996 × ADF[b] [kg/d] + 1.15 × NDF[c] [kg/d]
Jentsch et al. (2007)	CH_4 [kJ] = 1802–21.1 × DMI [g/kg BW]
Bell et al. (2016)	CH_4 (g/kg DM intake) = 0.046 (±0.001) × DOMD[d]–0.113 (±0.023) × EE[e]–2.47 (±0.29) × (feeding level – 1)
Ramin and Huhtanen (2013)	CH_4 (L/d) = −64.0 (±35.0) + 26.0 (±1.02) × DMI (kg/d)−0.61 (±0.132) × $DMI^2{}_{(centred)}$ + 0.25 (±0.051) × $OMD^f{}_m$ (g/kg)−66.4 (±8.22) × EE (kg DM/d)−45.0 (±23.50) × NFC[g]/(NDF + NFC)

[a]*DMI* dry matter intake, [b]*ADF* acid detergent fibre, [c]*NDF* neutral detergent fibre, [d]*DOMD* digestible organic matter, [e]*EE* ether extract, [f]OMD_m organic matter digestibility at maintenance level of feeding, [g]*NFC* non-fibrous carbohydrate

production, often all equations require this parameter for predicting CH_4 production. Table 10.2 summarizes some equations predicting CH_4 production in dairy cattle.

10.7 Conclusion

Methane is emitted from ruminants as a result of fermentation in rumen. There are many strategies to inhibit CH_4 emissions from ruminants. Most strategies reducing CH_4 emission require adaptation of the inhibitor used in the rumen and that the rechannelling of H_2 remains unclear in the rumen upon using any inhibitor. There are both in vitro and in vivo methods to measure CH_4 emission from dairy cows. Empirical and mechanistic models such as the Karoline model usually predicts CH_4 emission reliably in which they could be used by national inventories and advisory services for predicting CH_4 emission.

References

Ahmed M (2017) Greenhouse gas emissions and climate variability: an overview. In: Ahmed M, Stockle CO (eds) Quantification of climate variability, adaptation and mitigation for agricultural sustainability. Springer International Publishing, Cham, pp 1–26. https://doi.org/10.1007/978-3-319-32059-5_1

Ahmed M, Ahmad S, Waldrip HM, Ramin M, Raza MA (2020) Whole farm modeling: a systems approach to understanding and managing livestock for greenhouse gas mitigation, economic viability and environmental quality. In: Waldrip H, Pagliari P, He Z (eds) Animal manure. https://doi.org/10.2134/asaspecpub67.c25

Axelsson J (1949) The amount of produced methane energy in the European metabolic experiments with adult cattle. Ann R Agric Coll Sweden 16:404–418

Bayat AR, Tapio I, Vilkki J et al (2018) Plant oil supplements reduce methane emissions and improve milk fatty acid composition in dairy cows fed grass silage-based diets without affecting milk yield. J Dairy Sci 101:1136–1151

Bell M, Eckard R, Moate PJ, Yan T (2016) Modelling the effect of diet composition on enteric methane emissions across sheep, beef cattle and dairy cows. Animals 54:1–16

Benchaar C, Greathead H (2011) Essential oils and opportunities to mitigate enteric methane emissions from ruminants. Anim Feed Sci Technol 166:338–355

Chagas et al (2019) In vitro evaluation of different dietary methane mitigation strategies. In: Udén P, Eriksson T, Spörndly R et al (eds) 10th Nordic feed science conference, Uppsala July 2019. SLU Repro, Uppsala, p 62

Crutzen PJ (1995) Ruminant physiology: digestion, metabolism, growth and reproduction. In: Engelhardt WV et al (eds) The role of Methane in atmospheric chemistry and climate. Ventura, pp 291–313

Czerkawski JW (1986) An introduction to rumen studies. Robert Maxwell MC, Oxford

Danfaer A, Huhtanen P, Udén P (2006) The Nordic dairy cow model, Karoline-description. In: Kebreab E, Dijkstra J, Bannink A et al (eds) Nutrient digestion and utilization in farm animals. Modeling approaches. CABI publishing, Wallingford, p 383

Danielsson R, Ramin M, Bertilsson J et al (2017) Evaluation of an in vitro system for predicting methane production in vivo. J Dairy Sci 100:8881–8894

Ellis JL, Kebreab E, Odongo NE et al (2007) Prediction of methane production from dairy and beef cattle. J Dairy Sci 90:3456–3466

Fant P, Ramin M, Jaakkola S et al (2020) Effects of different barley and oat varieties on methane production, digestibility and fermentation pattern in vitro. J Dairy Sci In press

Franco MO et al (2017) *In vitro* evaluation of agro-industrial by-products replacing soybean meal in two different basal diets for ruminants. In: Udén P, Eriksson T, Spörndly R et al (eds) 8th Nordic feed science conference, Uppsala July 2017. SLU Repro, Uppsala, p 170613

Grainger C, Beauchemin KA (2011) Can enteric methane emissions from ruminants be lowered without lowering their production? Anim Feed Sci Technol 166-167:308–320

Howarth RW (2019) Ideas and perspectives: is shale gas a major driver of recent increase in global atmospheric methane? Biogeosciences 16:3033–3046

Hristov AN, Oh J, Giallongo F et al (2015) An inhibitor persistently decreased enteric methane emission from dairy cows with no negative effect on milk production. Proc Natl Acad Sci U S A 112:10663–10668

Huhtanen P, Ramin M, Udén P (2015) Nordic dairy cow model Karoline in predicting methane emissions: 1. Model description and sensitivity analysis. Livest Sci 178:71–80

Immig I (1996) The rumen and hindgut as source of ruminant methanogenesis. Environ Monit Assess 42:57–72

Jentsch W, Schweigel M, Weissbach F, Scholze H, Pitroff W, Derno M (2007) Methane production in cattle calculated by the nutrient composition of the diet. Arch Anim Nutr 61:10–19

Johnson KA, Johnson DE (1995) Methane emissions from cattle. J Anim Sci 73:2483–2492

Kiehl JT, Trenberth KE (1997) Earth's annual global mean energy budget. Bull Am Meteorol 78:197–208

Lassey KR (2007) Livestock methane emission: from the individual grazing animal through national inventories to the global methane cycle. Agric For Meteorol 142:120–132

Lesschen JP, van den Berg M, Westhoek HJ et al (2011) Greenhouse gas emission profiles of European livestock sectors. Anim Feed Sci Technol 166-167:16–28

Machado L, Magnusson M, Paul NA et al (2014) Effects of marine and freshwater macroalgae on in vitro total gas and methane production. PLoS One. https://doi.org/10.1371/journal.pone.0085289

Machado L, Magnusson M, Paul NA et al (2016) Identification of bioactives from the red seaweed Asparagopsis taxiformis that promote antimethanogenic activity in vitro. J Appl Phycol 28:3117–3126

McAllister TA, Okine EK, Mathison GW et al (1996) Dietary, environmental and microbiological aspects of methane production in ruminants. Can J Anim Sci 76:31–243

McAllister TA, Beauchemin KA, McGinn SM et al (2011) Greenhouse gases in animal agriculture. Finding a balance between food production and emissions. Anim Feed Sci Technol 166-167:1–6

Miller TL, Wolin MJ, Zhao H et al (1986) Characteristics of methanogens isolated from bovine rumen. Appl Environ Microbiol 51:201–202
Mills JAN, Dijkstra J, Bannink A et al (2001) A mechanistic model of whole-tract digestion and methanogenesis in the lactating dairy cow: model development, evaluation, and application. J Anim Sci 79:1584–1597
Morgavi DP, Forano E, Martin C et al (2010) Microbial ecosystem and methanogenesis in ruminants. Animal 4:1024–1036
Moss AR, Givens DI, Garnsworthy PC (1995) The effect of supplementing grass silage with barley on digestibility, in sacco degradability, rumen fermentation and methane production in sheep at two levels of intake. Anim Feed Sci Technol 55:9–33
Moss AR, Jouany JP, Newbold J (2000) Methane production by ruminants: its contribution to global warming. Ann Zootech 49:231–253
Niu M, Kebreab E, Hristov AN et al (2018) Enteric methane production, yield and intensity prediction models of various complexity levels using a global database. Glob Chang Biol 24:3368–3389
Petrenko VV, Smith AM, Schaefer H et al (2017) Minimal geological methane emissions during the Younger Dryas–Preboreal abrupt warming event. Nature 548:443–446
Ramin M, Huhtanen P (2012) Development of an in vitro method for determination of methane production kinetics using a fully automated in vitro gas system – a modelling approach. Anim Feed Sci Technol 174:190–200
Ramin M, Huhtanen P (2013) Development of equations for predicting methane emissions from ruminants. J Dairy Sci 96:2476–2493
Ramin M, Huhtanen P (2015) Nordic dairy cow model Karoline in predicting methane emissions: 2. Model evaluation. Livest Sci 178:81–93
Shindell D (2015) The social cost of atmospheric release. Clim Chang 130:313–326
Stefenoni H, Räisänen S, Melgar A et al (2019) Dose-response effect of the macroalga *Asparagopsis taxiformis* on enteric methane emission in lactating dairy cows. Paper presented at the American Dairy Science Association, Ohio, 23–26 June 2019
St-Pierre NR (2001) Integrating quantitative findings from multiple studies using mixed model methodology. J Dairy Sci 84:741–755
Thorpe A (2009) Enteric fermentation and ruminant eructation: the role (and control?) of methane in the climate change debate. Clim Chang 93:407–431
Zhang DF, Yang HJ (2011) *In vitro* ruminal methanogenesis of a hay-rich substrate in response to different combination supplements of nitrocompounds; pyromellitic diimide and 2-bromoethanesulphonate. Anim Feed Sci Technol 163:20–23

Sunflower Modelling: A Review

11

Adnan Arshad, Muhammad Usman Ghani, Mahmood ul Hassan,
Huma Qamar, and Muhammad Zubair

Abstract

Vegetable oils are a key component of human dietary need and health worldwide. Oil quality of sunflower is better than all others because of the higher percentage of the linoleic acid that is the most appropriate character missing in all other oilseed crops. Changing climate and extreme weather events are making crop highly vulnerable and threatening global food security. Application of different crop models was evaluated to quantify the sunflower genotypes selection, assessment of phenotypic plasticity, physiology, and estimation of seed yield and oil concentration in response to the climate variability. The present study evaluated the worldwide sunflower modelling performance, and a case study of SUNFLO hybrid modelling technique was assessed for crop model adaptation to new genotypes under contrasting environment. Extended field experiment was conducted at 52 locations (28 genotypes) at the 75% of the total sunflower cultivated region in France. Compared to initial models the experiential correlation decreased mean square error (MSE) on an average of 54% for seed yield production, and 26% for oil content concentration. The study also identified smart management practices and evaluated the performance of different models and concluded with the utilization of hybrid modelling skills. Further research expresses the thrust to use system modelling for screening the existing hybrids on grounds of their responses to several growth parameters and adaptation

A. Arshad (✉) · M. u. Hassan
College of Resources and Environmental Sciences, China Agricultural University, Beijing, China
e-mail: ad@cau.edu.cn

M. U. Ghani
State Key Laboratory of Grassland Agro-ecosystems, College of Pastoral Agriculture Science and Technology, Lanzhou University, Lanzhou, Gansu, China

H. Qamar · M. Zubair
Oilseeds Research Institute, Ayub Agricultural Research Institute, Faisalabad, Pakistan

M. Ahmed (ed.), *Systems Modeling*, https://doi.org/10.1007/978-981-15-4728-7_11

capacity to rapidly changing climatic conditions. This will eventually minimize the yield losses and help in increasing the crop yield even in limited resources. The present study is also proposing a clear optimization framework for genetic diversity of sunflower hybrids and management practices under changing climatic scenario.

Keywords

Climate variability · Crop adaptation · Smart management · Modelling sunflower

11.1 Introduction

Sunflower belongs to the Asteraceae family, formerly denoted as the Compositae. The wild sunflower (diploid annual *Helianthus annuus*) has history back to 0.5 to 1 million years for producing seeds (Rieseberg et al. 1991; Harter et al. 2004), and widely dispersed across many states of the United States, i.e. temperate North America. Currently, wild annual *Helianthus annuus* nurture throughout the United States but habitats are more confined to north of the Trans-Mexican Volcanic Belt (Heiser et al. 1969; Lentz et al. 2008a). Domesticated *Helianthus annuus* are planted throughout Northern America (Lentz et al. 2008a, 2008b). Sunflower (*Helianthus annuus* L.), a famous ornamental plant due to its sun like artistic flower shape (Badouin et al. 2017; Ma et al. 2019), is one of the major oil seed crops in the world (Salunkhe et al. 1992; Putt 1997; Stefansson et al. 2007). Globally, it is planted on 24.77 million hectares with an average yield of 44.31 million metric tons and covers 8% of the world oil seed market (USDA 2016). Pakistan being deficient in edible oil production invests almost 2.71 billion US dollars to import edible oil (Govt. of Pakistan 2017). Sunflower shares 9.19% in local edible oil production followed by cotton and rapeseed/mustard (Govt. of Pakistan 2017; Amin et al. 2017; Nasim et al. 2018).

Edible oils, especially vegetable oils, are a key component of human dietary need and also health (Gholamhoseini et al. 2013; Manivannan et al. 2015). Oil quality of sunflower is better than all others because of the higher percentage of the linoleic acid that is the most appropriate character missing in all other oilseed crops (Nasim et al. 2011). The sunflower oil is also rich in the A, D, E and K vitamins. Sunflower oil is also free from the toxic compounds (Abbas et al. 2017). Sunflower seed comprises of 40–50% oil and 17–20% proteins (Abbas et al. 2017; Amin et al. 2018). This high percentage of edible oil highlighted its potential to minimize the feed gap between production and consumption and ensure food security for future population of the world. Sunflower belongs to tropical and subtropical lands, where semi-arid to arid climate persists. It can be grown in different environmental conditions ranging from humid to dry lands accompanying irrigation. However, like other agri-crops, sunflower productivity is affected by different biotic (pests) and abiotic factors (drought, heat and salinity) (Pekcan et al. 2015; Robert et al. 2016). The optimum growth and development temperature for sunflower plant ranges from 26 to 29 °C (Rondanini et al. 2006; Awais et al. 2017; Hammad et al.

2017). Climate change is a threat to sustainable crop production (Kalyar et al. 2013) and agricultural land is shrinking day by day due to urbanization (Farooq et al. 2012) leading to the competition for water between different users, and plants will suffer from drought (Elliott et al. 2014).

In the past few decades, different areas of the world (Asia and Africa) faced hilarious drought stresses (Miyan 2015; Farooq et al. 2014) which raised the value of climate study. Drought stress mostly affects the crops at early stages of growth (Debaeke et al. 2017) depending on the plant species, like in sunflower; it suppresses the seed germination, stem elongation and leaf expansion (Fulda et al. 2011; Fatemi 2014). Even though domesticated sunflower has potential to adapt climate variations due to its drought escape nature and likely to maintain yield under drought and heat stress conditions, but aforementioned stresses can affect early flowering and achene filling stages due to imbalance in leaf growth and evapotranspiration under deficient soil water (García-López et al. 2014). Leaf wilting under water deficit is the major challenge in semiarid areas due to limited rainfall because ample water at early stage improves vegetative growth (Aboudrare et al. 2006). It is widely reported that drought and heat stresses caused substantial decreases in achene and oil yield as well as affected the oil quality (Soleimanzadeh et al. 2010; Ibrahim et al. 2016). Drought stress is more prune in sunflower at flowering and achene development stage and caused almost 50% yield loss (Kalarani et al. 2004; Hussain et al. 2008) due to pollen infertility resulting empty achene (Lyakh and Totsky 2014; Totsky and Lyakh 2015).

Climate change drives the productivity shift in agriculture, for instance abrupt changes in day and night temperatures severely affect crops production (Ahmed 2020; Farooq et al. 2014). Modern approaches are compulsory to achieve sustainable crop production of current crops to cope the food security challenge (Reddy et al. 2003; Nasim et al. 2016b). According to the Intergovernmental Panel on Climate Change (IPCC), temperature will raise almost 1.4 to 5.8 °C in this century (IPCC et al. 2014; Arshad et al. 2020; Nasim et al. 2016b). Use of modern technologies along with exiting germplasm of sunflower is dire need under limited water supply in the future agriculture. Many researchers tried to observe the impacts of drought and heat stress on oil yield and quality (Gholamhoseini et al. 2013; Manivannan et al. 2015), defined mitigation strategies about drought stress and discovered physiological and molecular responses of crops to stress (Ahmed et al. 2020; Baloğlu et al. 2012; Ghobadi et al. 2013; Bowsher et al. 2016), but no roadmap was developed for sustainable productivity of the sunflower crop.

Use of genetic material from wild and domesticated sunflower is technically possible to improve production of drought-efficient hybrids (Burke et al. 2002). Different population of the sunflower from the world can be used to get valuable genetic resource for further breeding of the sunflower (Van et al. 1997; Burke et al. 2002; Lentz et al. 2008a). Because crop management and genetic improvements (Wang et al. 2016a, b; Awais et al. 2017; Jabran et al. 2017; Nasim et al. 2016a), along with variable phenology of genotypes, are major attributes to cope climate change (Visser and Both 2005; Miller-Rushing et al. 2007; Gordo and Sanz 2010; Szabó et al. 2016). Further research expresses the thrust to use system modelling for screening the existing hybrids on grounds of their responses to several growth parameters and adaptation capacity to rapidly changing climatic conditions (Lentz et al. 2008a). This will eventually minimize the yield losses and help in increasing the crop yield even in limited resources. This review chapter summarizes the potential role of sunflower underutilized crop modelling systems to enhance the efficacy of hybrids system modelling to oilseed security under the changing climate. The present study is also proposing a clear optimization framework for genetic diversity of sunflower hybrids and management practices under future climate scenarios. The objective of the study is to analyse multiple sunflower crop models' skills to simulate the phenotypic variability of composite plant characteristics under ambient climatic conditions, along with observation of several possible modelling approaches to reach high yields.

11.2 Crop Modelling as Agriculture Decision Support Tools

Agriculture science provokes knowledge that allow the researcher to estimate future problems. The world has become complex with several factors threatening the integrity of life from recent years, including increasing pressure of population, scarcity of food, contamination of water, unavailability of land for cultivation of crop and reduction of natural resources. All these factors further effected by climatic condition will lead to changes in the world as we have known it (Wheeler and von Braun 2013). System models component and their interactions are well understood by the scientific studies in the sustainable agroecosystem. Models are considered necessary for understanding agricultural problems. Thus, the overall performance of agroecosystem predicted with the help of models. Agricultural system models play increasingly important roles in the development of sustainable land management across diverse agroecological and socioeconomic conditions because field and farm experiments require large amounts of resources and may still not provide sufficient information in space and time to identify appropriate and effective management practices (Teng and Penning de Vries 1992; Jones et al. 2017).

Models prove helpful for land managers and policy-makers to recognize management option which enhance sustainability of agro-ecosystem (Ahmed and Stockle 2016; Aslam et al. 2017; Ijaz et al. 2017; Jabeen et al. 2017; Wallach et al. 2018; Liu et al. 2019; Asseng et al. 2019; Gyldengren et al. 2020; Schepen et al. 2020; Peng et al. 2020; Stöckle and Kemanian 2020). The soil management and socio-economical and metrological information get across space and time by using these models (Jones et al. 2017). The field study may be carried at potential risk areas. Thus, potential risk area was screened with the help of models. The computer software programmes such as Decision Support Systems (DSSs) make use of other information and model to make site-specific recommendations. These recommendations are helpful in farm financial planning, pest and livestock enterprises management and general crop and land management (Plant 1989; Basso et al. 2013). The evidence-based decision-making is helpful in agriculture to manage environment output. Decision support tools that are software-based may be important to searching for evidence-based decision-making in agriculture. These decisions may be helpful to improve productivity and environmental outputs. The evidence-based decision was improved by using information based upon these tools, and these tools can lead users through clear steps and suggest optimal decision paths. Users design efficient decisions with the help of decision support tools (DSTs). The recommendation of these dynamics' tools was varied according to the inputs from users. These tools may recommend an optimal decision path. Such softer tools facilitate the adviser of farmer for management of farm by recording data and its analysis. Several management techniques and recommendations may be decided based on of the evidence (Ahmed 2011; Ahmed et al. 2012, 2013, 2014, 2016, 2017, 2018, 2019; Ahmad et al. 2017, 2019; Rossi et al. 2014).

Several models are used in agroecosystems such as Environmental Policy Integrated Climate (EPIC) which are considered as cropping model. From a long time, EPIC has been used in a wide range of applications such as irrigation, environmental change, erosion of soil, quality of water and in the crop productivity (Rosenzweig et al. 2014; Wriedt et al. 2009; Elliott et al. 2015). As a combined meteorology and air quality modelling system, WRF/CMAQ is an important decision support tool that is widely used for increasing our understanding of the chemical and physical processes contributing to air quality impairment and for facilitating the development of policies to mitigate harmful effects of air pollution on human health and the environment (Cohan et al. 2007; Compton et al. 2011; Wang et al. 2016a). N deposition to FEST_C EPIC and WRF/CMAQ model provides daily weather inputs, which stimulates growth of plant along with fertilization, planting, harvesting, hydrology and complete biogeochemical properties, under several management practices and soil conditions. In return, information on daily nitrogen fertilization, properties of soil along with the soil moisture, pH or NH_3 conditions stimulated by FEST-C extracts EPIC need input for CMAQ bidirectional NH_3 modelling. The Soil and Water Assessment Tool (SWAT) is important tool that has been used to assess the impact of management of land, soil and weather/climate upon sediments, water and agro-chemical at water shed scale (Abbaspour et al. 2015; Saleh et al. 2000; White et al. 2014).

11.3 Climatic Variability and Smart Practices

Climate Smart Agriculture (CSA) is an approach to help people who manage agricultural systems respond effectively to climate change. The CSA approach pursues the objectives of sustainably increasing productivity and income, adapting to climate change and reducing greenhouse gas emissions whenever possible. CSA is an approach to help smallholder owners implement a variety of smart climate agriculture practices and technologies in order to minimize the negative effects of climate change and variability, but their adoption depends on much of the economic benefits associated with the practices. The goal of CSA practices is to improve the ability of agricultural systems to support food security, sustainably increasing productivity and income, adapting to climate change by incorporating the need for adaptation and mitigation potential into development strategies. However, production Climate Intelligent Farming is a sustainable agricultural production system that addresses climate change. Sustainable agricultural systems offer opportunities for adaptation and mitigation of climate change by contributing to the delivery and maintenance of a wide range of public goods, such as clean water, carbon sequestration, flood protection, recharging groundwater and the value of landscape services. By definition, sustainable agricultural systems are less vulnerable to shocks and stresses. In terms of technologies, productive and sustainable agricultural systems take full advantage of crop varieties and animal breeds and their agroecological and agronomic management (Beddington et al. 2012).

At the field level, there are a wide range of agricultural practices and approaches that are currently available and can contribute to increased production while still focusing on environmental sustainability. Climate change causes some serious challenges to the agricultural sector like temperature increase, heat stress or increased disease which could reduce yields, leading to increased production costs. Appropriate CSA practices are heat tolerant varieties, mulching, water management, shade house, boundary trees. Weeds, Pests and Disease: It is also possible that increases in temperature, moisture and carbon dioxide could result in higher populations of destructive pests so appropriate CSA practices such as intercropping, crop diversity, mulching, container gardening and encased beds should be applied. Irrigation and Rainfall: Changes in climate may also impact the water availability and water needs for agriculture. Rain shortage leads to extended dry spells, and excessive rains lead to erosion and loss of soil fertility, so follow appropriate rainwater harvesting, efficient irrigation, mulching, composting, treated manure and nitrogen fixing trees.

11.4 Uncertainties and Phenotype Optimization: A Case Study

Present global accounting for the annual climatic variability is a recognized issue for projection-based studies of environmental models. Worldwide sunflower is considered as a major oilseed crop. Mainly sunflower seed production considered regions, Europe produces 62% of the total world sunflower production, 19% by the United States and 15% by Asian region (FAO). Improvements in yield with changing environmental conditions depend on the genotype's adaptability to the local climate and cropping systems. It frequently involves intensive field sampling and averaging the simulation outputs over many series of replications. Therefore, researchers need to develop and evaluate the performance of promising sunflower genotypes of every potential variety. Crop modelling can help scientists and breeders in assessment of genotypes, by their capacity to simulate the phenotypic plasticity in response to the climate variability (Fig.11.1). For sunflower, crop physiology has been combined with complementary and different methods in few crop models (Casadebaig et al.

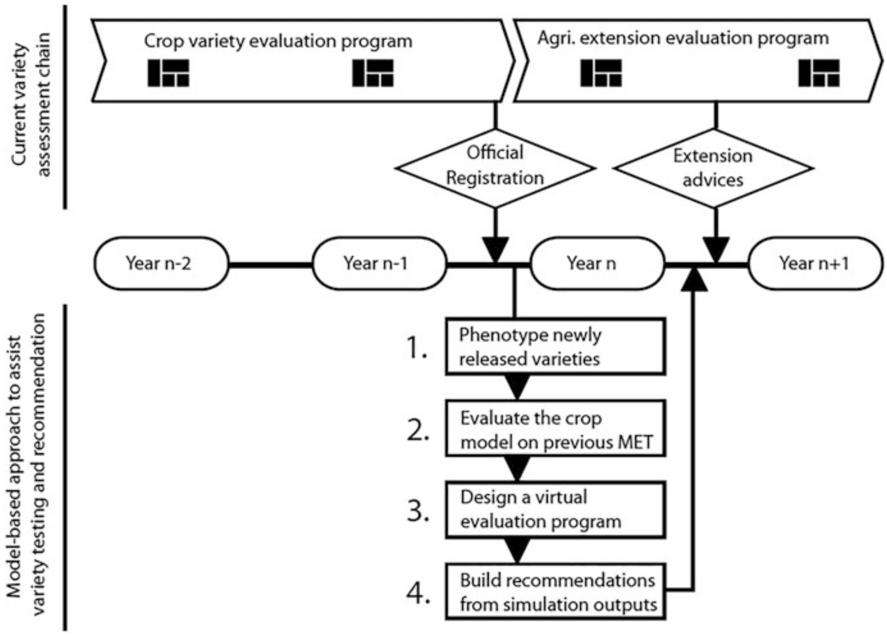

Fig. 11.1 Variety of evaluation processes in crop modelling. (Source: Casadebaig et al. 2016, with permission from Elsevier)

2011). The SUNFLO is a process-based simulation model for sunflower crop that was developed to estimate the grain yield and oil concentration (%) as a function of time, environment (soil and climate), management practices and genetic diversity.

The crop SUNFLO model can simulate variation in promising genotype's performance among different environmental conditions. Model SUNFLO simulates the above-ground biomass production of a sunflower crop from incident solar radiation and mean air temperature. The model works in daily period steps and designates the phenology of plant, leaf area expansion, the biomass production and canopy allocation (Lecoeur et al. 2015). SUNFLO crop model takes into account the behaviour of several genotypes at the same time by the mode of some parameters that are genotype dependent. SUNFLO crop model has the ability to rank the sunflower genotypes with relative performance from its predictive quality. SUNFLO might be helpful to evaluate the capacity ranking of different genotypes due to an appropriate phenotypic variability description. These interactions play important role in yield variability between simulated and actual networks. The originality of the model is that it is SUNFLO tested for estimate differences between genotypes on different criteria (penology, architecture, abiotic stresses). The model also allows forecasting the performance of the oil content of sunflower on the scale and dimensions of a plot and calculates indicators of experienced stresses. Cadic et al. (2012) used the

Table 11.1 Classification characteristic of sunflower crop models to different parameters

Models	Region	Remarks	References
SUNFLO	America Europe Asia	Assessment of genotypes performance Phenotypic plasticity to different environment conditions Simulate grain yield and oil concentration Management practices and field budgeting Abiotic stresses, light interception, fertilizers and water demand	Lecoeur et al. (2015) Cadic et al. (2012) Casadebaig et al. (2011) Lecoeur et al. (2011)
APSIM (APSIM-Sunflower)	Asia Australia	Simulate crop phenology in the intercropping system Under different saline soil conditions to water-extraction coefficient (KL) Root growth pattern in soil profile (XF) N-levels to leaf area (LAI), dry matter (DM) and seed yield (SY) Different sowing (SD) dates and irrigation	Holzworth et al. (2014)
WOFOST (WOFOST-ES)	Asia	Simulate and calibrate environmental stresses factors to estimate best management practices	Zhu et al. (2018)
DSSAT (OILCROP-SUN)	Asia South America	Simulate different hybrids crop growth and development Water and nitrogen limited demands to yield variability Different sowing dates, fertilizer levels and yield potential	Ahmad et al. (2017) Awais et al. (2017) Leite et al. (2014)
SWB	Africa	Simulate the soil water balance and crop growth and development Irrigation scheduling and WUE	
EPIC and ALMANAC	America	Crop phenology, growth, and yield Growth degree days (GDD) and radiation use efficiency (RUE) Combine high yield potential with great adaptability by different management schemes	Kiniry et al. (1992)

SUNFLO crop model for estimation of drought stress index in each environment condition through the response of previously characterized probe genotypes. Furthermore, approach by Picheny et al. (2015) achieves good performances even with limited computational budgets, outclassing significantly more simple practices. In another study, SUNFLO model was developed to simulate the oil concentration and achene yield of sunflower crop with a distinct attention paid to the report of varietal range. The results of Lecoeur et al.'s (2015) SUNFLO biophysical model account for 80 to 90% accuracy of observed variability in different genotype's yield potential. The model is also an interesting tool for investigating the phenotypic variability of complex plant characteristics, i.e. drought, water demand and light interception efficiency. SUNFLO model showed multiple approaches that in several ways are possible to reach high yields (Table 11.1).

The SUNFLO model has 10 genotype-dependent parameters: 2 parameters for growth degree days (GDD) to important development stages, 4 for shoot architecture, 2 for response to water deficit and 2 for biomass allocation in plant. A case study of SUNFLO hybrid modelling technique was evaluated for crop model adaptation to new genotypes. To train the liner model applied in calibration method an extended field experiment was conducted at 52 locations (28 genotypes) at the 75% of the total sunflower cultivated region in France in 2009/10. A total 82 number of trials were conducted and observed over the complete model calibration. The data set of Casadebaig et al. (2016) was reused to validate the model performance. The two major output variables (grain yield, oil concentration) of the simulation were calibrated. Compared to initial models the experiential correlation decreased mean square error (MSE) on an average of 54% for yield production and 26% for oil content. This modelling approach combines the recompenses of phenotyping (genotype-specific) parameters that have a clear meaning and are equal between different genotypes. The benefit of fitting model to the observation data from field, specifically that the modified model, is adapted to a changing environmental condition.

Models often cover a maximum number of crop parameters, perhaps more than one hundred. Some parameters are presumed to apply very commonly and so are not meant to be changed for different applications. For example, in the SUNFLO model (Casadebaig et al. 2011; Lecoeur et al. 2011), there are parameters representing the effect of soil moisture and temperature on rate of nitrogen (N) mineralization. Additional set of parameters is specific to a particular species, which applies to generic models like DSSAT (Jones et al. 2003; Hoogenboom et al. 2012), Agricultural Production System Simulator (APSIM; Holzworth et al. 2014) or (STICS; Jones and Kiniry 1986; Jones 1993; Ritchie and Otter 1984) which can simulate for various species. The SUNFLO model has 10 genotype-dependent parameters (two for degree days to key development stages, four for shoot architecture, two for response to water deficit and two for biomass allocation).

11.5 Sunflower Modelling Way Forward

Development and applications of crop growth models is an effective tool for sustainable agricultural planning and decision-making process. Outdated experimental approaches are overpriced, time-consuming and not resourceful to adopt with changing climatic condition. Modelling of sunflower (*Helianthus annuus* L.) is stimulating because the crop species combines high harvest potential with excessive adaptability. Crop modelling might be an advantageous tool for identifying appropriate and economical management practices for sunflower, particularly climate change vulnerable regions worldwide. The key sunflower crop models are reviewed

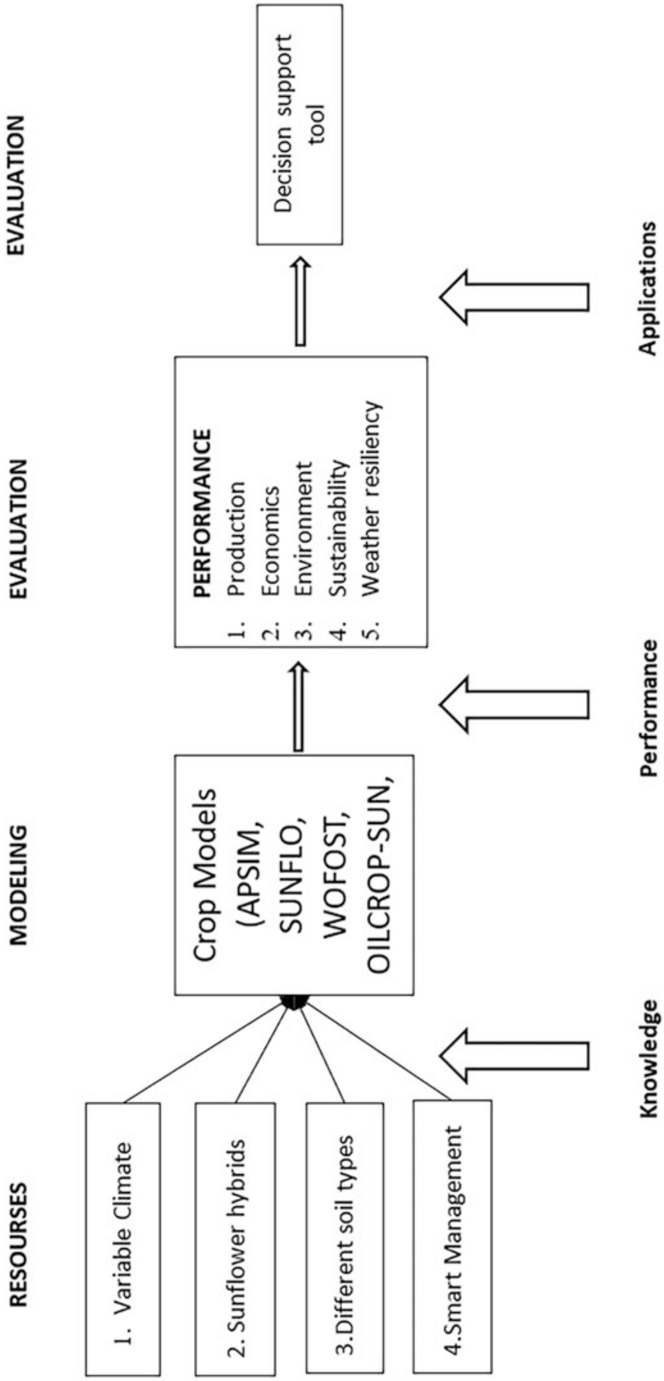

Fig. 11.2 Application of different sunflower models

in this section, with an emphasis on their capability to contribute to smart sunflower crop management (Fig. 11.2).

Numerous research experimentations proved that the modelling skills are effective to evaluate the applicability of the sunflower model within the APSIM to observe the climatic adaptation and resilience by shifting the sowing windows or other parameters (Table 11.1). Zheng et al. tested the APSIM sunflower model on different salinity levels and nitrogen application rates and studied the characteristics including the seed yield (SY), dry matter (DM), and leaf area index (LAI) by modifying the crop lower limit (CLL), the water-extraction coefficient (KL) and the pattern of root exploration in the soil profile (XF). APSIM-SUNFLO modelling tool help researchers to precisely simulate the crop phenology in the intercropping system to signify for the valuation and optimization of intercropping production systems. Based on APSIM-Sunflower model, interaction analysis of irrigation, sowing date and nitrogen application on oil yield of sunflower was simulated, calibrated and validated.

Agricultural monitoring and evaluation of crop plants to environmental stress is vital for the sustainable development of agriculture and food security. Zhu et al. (2018) tested World Food Studies (WOFOST) crop model, WOFOST-ES, which was developed by the addition of a general environmental stress factor (ES) for sunflower simulation to calibrate and validate with observational data to estimate the best managing practices for future (Table 11.1). In another study Leite et al. (2014) evaluated the performance of the crop model OILCROP-SUN to simulate growth and development of sunflower under Brazilian conditions and to discover sunflower water nitrogen-limited, water-limited and potential yield and yield variability over an arrangement of sowing dates. The Soil Water Balance (SWB) was used by Jovanovic and Annandale to simulate the soil water balance and growth of sunflower crop. The detailed meteorological, soil and irrigation data were analysed to calibrate and validate the subroutines of the model. SWB simulations of crop growth and soil water deficit presented the field capacity were inside, or marginally outside the reliability criteria imposed during the modelling.

Meanwhile, other studies showed that the combination of EPIC and ALMANAC models gave realistic yield simulations over changing environment and management possibilities (Kiniry et al. 1992). The application of sunflower models should be valuable both for evaluating the impacts of extreme climate to different management systems and for identifying focus zones where additional basic research is needed. Besides, the drought and limited supplies of water in many countries of the world have increased attention to favourable system modelling approaches in farm management such as efficient irrigation and climate resilient planting system. Furthermore, AquaCrop model has also been successfully applied to estimate the sunflower crop productivity under irrigated and rainfed agricultural conditions to enhance the water use efficiency of the crop plants.

For evaluation of adaptive sunflower hybrids, the SUNFLO model might be supportive to advance genotypic estimation. It will also assist scientists in identification, quantification and modelling of phenotypic changeability of sunflower performance in response to field stresses (abiotic) conditions (Fig. 11.3)

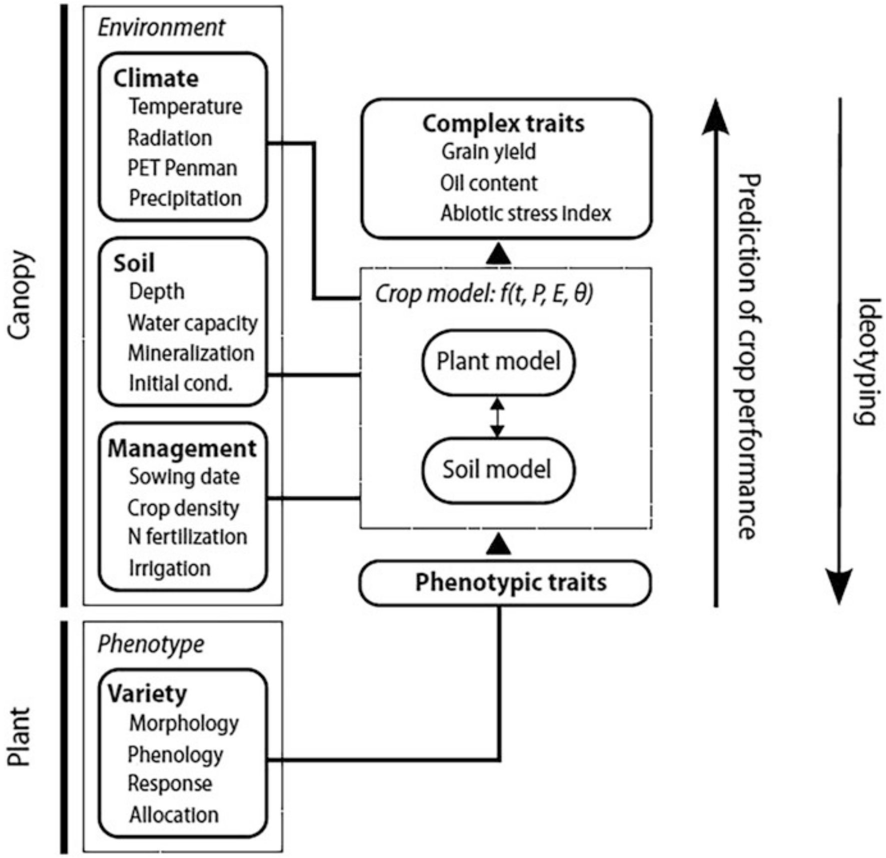

Fig. 11.3 SUNFLO crop model. (Source: Casadebaig et al. 2016, with permission from Elsevier)

(Casadebaig et al. 2016). Furthermore, SUNFLO crop model appears adequately more robust in evaluation of breeding traits which influence on yield to discover innovative practices while diagnosing environmental challenges, respectively (Fig.11.4).

11.6 Summary

In a situation of global climatic change, improving yield under different environmental uncertainties is a major challenge for crop production and food security. The present study proposes various hybrid approaches from adapting a crop model to promising genotypes. This will also combine phenotyping estimation of genotype-dependent parameters with calibration using field data. Review research also suggested that the genotype-dependent constraints of the crop model could be obtained by phenotype or gene-based modelling. Then field data, especially variety trials, could be used to provide a simple empirical correction to the model. The

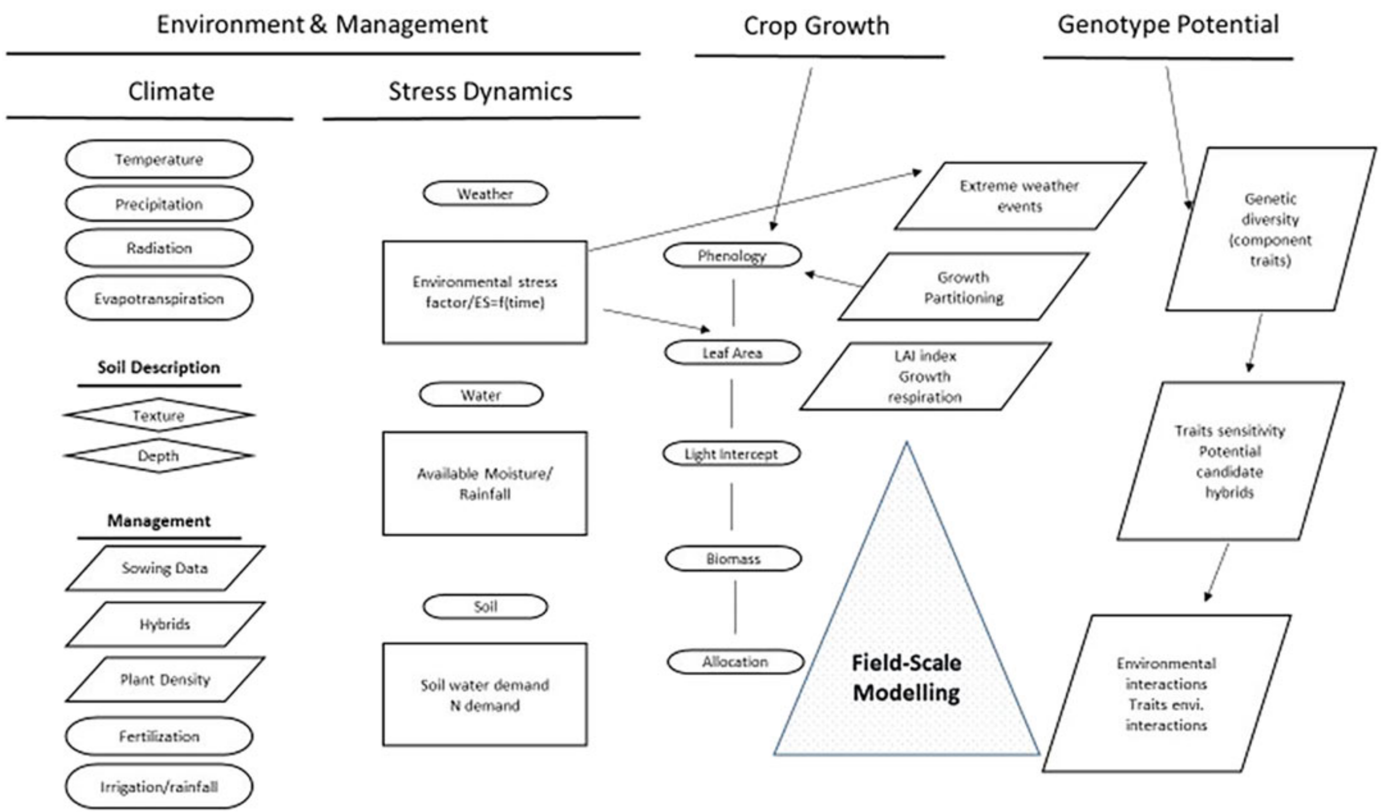

Fig. 11.4 Flow diagram of sunflower crop model

combination the different modelling approach achieves might provide good performances even for limited research budgets, outperforming suggestively more simple strategies. The present study is also proposing a clear optimization framework for genetic diversity of sunflower hybrids and management practices under changing climatic scenario.

References

Abbas G, Ahmad S, Ahmad A, Nasim W, Fatima Z, Hussain S, Habib-ur-Rehman M, Khan MA, Hasanuzzaman M, Fahad S, Boote KJ, Hoogenboom G (2017) Quantification the impacts of climate change and crop management on phenology of maize-based cropping system in Punjab, Pakistan. Agric For Meteorol 247:42–55

Abbaspour KC, Rouholahnejad E, Vaghefi S, Srinivasan R, Yang H, Kløve B (2015) Aontinental-scale hydrology and water quality model for Europe: calibration and uncertainty of a high-resolution large-scale SWAT model. J Hydrol 524:733–752. https://doi.org/10.1016/j.jhydrol.2015.03.027

Aboudrare A, Debaeke P, Bouaziz A, Chekli H (2006) Effects of soil tillage and fallow management on soil water storage and sunflower production in a semiarid Mediterranean climate. Agric Water Manag 83:183–196

Ahmad S, Abbas G, Fatima Z, Khan RJ, Anjum MA, Ahmed M, Khan MA, Porter CH, Hoogenboom G (2017) Quantification of the impacts of climate warming and crop management on canola phenology in Punjab, Pakistan. J Agron Crop Sci 203(5):442–452. https://doi.org/10.1111/jac.12206

Ahmad S, Abbas G, Ahmed M, Fatima Z, Anjum MA, Rasul G, Khan MA, Hoogenboom G (2019) Climate warming and management impact on the change of phenology of the rice-wheat cropping system in Punjab, Pakistan. Field Crop Res 230:46–61. https://doi.org/10.1016/j.fcr.2018.10.008

Ahmed M (2011) Climatic resilience of wheat using simulation modeling in Pothwar. PhD thesis. Arid Agriculture University, Rawalpindi

Ahmed M (2020) Introduction to modern climate change. Andrew E. Dessler: Cambridge University Press, 2011, 252 pp, ISBN-10: 0521173159. Sci Total Environ 734:139397. https://doi.org/10.1016/j.scitotenv.2020.139397

Ahmed M, Stockle CO (2016) Quantification of climate variability, adaptation and mitigation for agricultural sustainability. Springer Nature Singapore Pvt. Ltd., Singapore, 437 pp. https://doi.org/10.1007/978-3-319-32059-5

Ahmed M, Hassan FU, Aslam M, Aslam MA (2012) Physiological attributes based resilience of wheat to climate change. Int J Agric Biol 14:407–412

Ahmed M, Asif M, Hirani AH, Akram MN, Goyal A (2013) Modeling for agricultural sustainability: a review. In: Bhullar GS, Bhullar NK (eds) Agricultural sustainability progress and prospects in crop research. Elsevier, London

Ahmed M, Aslam MA, Hassan FU, Asif M, Hayat R (2014) Use of APSIM to model nitrogen use efficiency of rain-fed wheat. Int J Agric Biol 16:461–470

Ahmed M, Akram MN, Asim M, Aslam M, F-u H, Higgins S, Stöckle CO, Hoogenboom G (2016) Calibration and validation of APSIM-wheat and CERES-wheat for spring wheat under rainfed conditions: models evaluation and application. Comput Electron Agric 123:384–401. https://doi.org/10.1016/j.compag.2016.03.015

Ahmed M, Stöckle CO, Nelson R, Higgins S (2017) Assessment of climate change and atmospheric CO_2 impact on winter wheat in the Pacific northwest using a multimodel ensemble. Front Ecol Evol 5(51). https://doi.org/10.3389/fevo.2017.00051

Ahmed M, Ijaz W, Ahmad S (2018) Adapting and evaluating APSIM-SoilP-wheat model for response to phosphorus under rainfed conditions of Pakistan. J Plant Nutr 41(16):2069–2084. https://doi.org/10.1080/01904167.2018.1485933

Ahmed M, Stöckle CO, Nelson R, Higgins S, Ahmad S, Raza MA (2019) Novel multimodel ensemble approach to evaluate the sole effect of elevated CO_2 on winter wheat productivity. Sci Rep 9(1):7813. https://doi.org/10.1038/s41598-019-44251-x

Ahmed K, Shabbir G, Ahmed M, Shah KN (2020) Phenotyping for drought resistance in bread wheat using physiological and biochemical traits. Sci Total Environ 729:139082. https://doi.org/10.1016/j.scitotenv.2020.139082

Amin A, Nasim W, Mubeen M, Kazmi DH, Lin Z, Wahid A, Sultana SR, Gibbs J, Fahad S (2017) Comparaison of future and base précipitation anomalies by SimCLIM statistical projection through ensemble approach in Pakistan. Atmos Res 194:214–225

Amin A, Nasim W, Mubeen M, Ahmad A, Nadeem M, Urich P, Fahad S, Ahmad S, Wajid A, Tabassum F, Hammad HM, Sultana SR, Anwar S, Baloch SK, Wahid A, Wilkerson CJ, Hoogenboom G (2018). Simulated CSM-CROPGRO-cotton yield under projected future climate by SimCLIM for southern Punjab, Pakistan Agric Syst. https://doi.org/10.1016/j.agsy.2017.05.010

Arshad A, Ashraf M, Sundari RS, Wajid M, Qamar H, Hasan M (2020) Vulnerability assessment of urban expansion and modelling green spaces to build heat waves risk resiliency in Karachi. Int J Disaster Risk Reduct 46:101468

Aslam MA, Ahmed M, Stöckle CO, Higgins SS, Hassan FU, Hayat R (2017) Can growing degree days and photoperiod predict spring wheat phenology? Front Environ Sci 5:57

Asseng S, Martre P, Maiorano A, Rötter RP, O'Leary GJ, Fitzgerald GJ, Girousse C, Motzo R, Giunta F, Babar MA, Reynolds MP, Kheir AMS, Thorburn PJ, Waha K, Ruane AC, Aggarwal PK, Ahmed M, Balkovič J, Basso B, Biernath C, Bindi M, Cammarano D, Challinor AJ, De Sanctis G, Dumont B, Eyshi Rezaei E, Fereres E, Ferrise R, Garcia-Vila M, Gayler S, Gao Y, Horan H, Hoogenboom G, Izaurralde RC, Jabloun M, Jones CD, Kassie BT, Kersebaum K-C, Klein C, Koehler A-K, Liu B, Minoli S, Montesino San Martin M, Müller C, Naresh Kumar S, Nendel C, Olesen JE, Palosuo T, Porter JR, Priesack E, Ripoche D, Semenov MA, Stöckle C, Stratonovitch P, Streck T, Supit I, Tao F, Van der Velde M, Wallach D, Wang E, Webber H, Wolf J, Xiao L, Zhang Z, Zhao Z, Zhu Y, Ewert F (2019) Climate change impact and adaptation for wheat protein. Glob Chang Biol 25(1):155–173. https://doi.org/10.1111/gcb.14481

Awais M, Wajid A, Bashir MU, Habib-ur-Rahman M, Raza MAS, Ahmad A, Saleem MF, Hammad HM, Mubeen M, Saeed U, Arshad MN, Fahad S, Nasim W (2017) Nitrogen and plant population change radiation capture and utilization capacity of sunflower in semi-arid environment. Environ Sci Pollut Res 24(21):17511–17525

Badouin H, Gouzy J, Grassa C et al (2017) The sunflower genome provides insights into oil metabolism, flowering and Asterid evolution. Nature 546:148–152. https://doi.org/10.1038/nature22380

Baloğlu MC, Kavas M, Aydin G, Öktem HA, Yücel AM (2012) Antioxidative and physiological responses of two sunflower (Helianthus annuus) cultivars under PEG-mediated drought stress. Turk J Bot 36(6):707–714

Basso B, Cammarano D, Fiorentino D, Ritchie JT (2013) Wheat yield response to spatially variable nitrogen fertilizer in Mediterranean environment. Eur J Agron 51:65–70

Beddington J, Asaduzzaman M, Clark M, Fernandez A, Guillou M, Jahn M, Erda L, Mamo T, Van Bo N, Nobre CA, Scholes R, Sharma R, Wakhungu J (2012) Achieving food security in the face of climate change. Final report from the Commission on Sustainable Agriculture and Climate Change. Copenhagen, CGIAR Research Program on Climate Change, Agriculture and Food Security (CCAFS). Available at www.ccafs.cgiar.org/commission

Bowsher AW, Ali R, Harding SA, Tsai CJ, Donovan LA (2016) Evolutionary di vergences in root exudate composition among ecologically-contrasting Helianthus species. PLoS One 11(1): e0148280

Burke JM, Tang S, Knapp SJ, Rieseberg L (2002) Genetic analysis of sunflower domestication. Genetics 161:1257–1267

Cadic E, Debaeke P, Langlade N (2012) Phenotyping the response of sunflower (Helianthus annuus L.) to drought scenarios in multi-environmental trials for the purpose of association genetics. International Plant and Animal Genome Conference XX 2012

Casadebaig P, Mestries E, Debaeke P (2016) A model-based approach to assist variety evaluation in sunflower crop. Eur J Agron 81:92–105. https://doi.org/10.1016/j.eja.2016.09.001

Casadebaiga P et al (2011) SUNFLO, a model to simulate genotype-specific performance of the sunflower crop in contrasting environments. Agric For Meteorol 151(2):163–178. https://doi.org/10.1016/j.agrformet.2010.09.012

Cohan DS, Boylan JW, Marmur A, Khan MN (2007) An integrated framework for multipollutant air quality management and its application in Georgia. Environ Manag 40(4):545–554. https://doi.org/10.1007/s00267-006-0228-4

Compton JE, Harrison JA, Dennis RL, Greaver TL, Hill BH, Jordan et al (2011) Ecosystem services altered by human changes in the nitrogen cycle: a new perspective for US decision making. Ecol Lett 14(8):804–815. https://doi.org/10.1111/j.1461-0248.2011.01631.x

Debaeke P, Bedoussac L, Bonnet C, Bret-Mestries E, Seassau C, Gavaland A, Raffaillac D, Tribouillois H, Véricel G, Justes E (2017) Sunflower crop: environmental-friendly and agro-ecological. OCL 23:1–12

Elliott J, Deryng D, Müller C, Frieler K, Konzmann M, Gerten D, Glotter M, Flörke M, Tang Q, Eisner S (2014) Constraints and potentials of future irriga-ion water availability on agricultural production under climate change. Proc Natl Acad Sci 111(9):3239–3244

Elliott J, Müller C, Deryng D, Chryssanthacopoulos J, Boote KJ, Büchner M et al (2015) The global gridded crop model intercomparison: data and modeling protocols for phase 1 (v1. 0). Geosci Model Dev 8(2):261–277. https://doi.org/10.5194/gmd-8-261-2015

Farooq M, Hussain M, Wahid A, Siddique KHM (2012) Drought stress in plants: an overview. In: Aroca R (ed) Plant responses to drought stress: from morphological to molecular features. Springer-Verlag, Germany, pp 1–36

Farooq M, Hussain M, Siddique KHM (2014) Drought stress in wheat during flowering and grain-filling periods. Crit Rev Plant Sci 33:331–349

Fatemi SN (2014) Germination and seedling growth in primed seeds of sunflower under water stress. Ann Res Rev Biol 4(23):3459

Fulda S, Mikkat S, Stegmann H, Horn R (2011) Physiology and proteomics of drought stress acclimation in sunflower (Helianthus annuus L.). Plant Biol 13(4):632–642

García-López J, Lorite IJ, García-Ruiz R, Domínguez J (2014) Evaluation of three simulation approaches for assessing yield of rainfed sunflower in a Mediterranean environment for climate change impact modelling. Clim Chang 124(1–2):147–162

Ghobadi M, Taherabadi S, Ghobadi ME, Mohammadi GR, Jalali-Honarmand S (2013) Antioxidant capacity: photosynthetic characteristics and water relations of sunflower (Helianthus annuus L.) cultivars in response to drought stress. Ind Crop Prod 50:29–38

Gholamhoseini M, Ghalavand A, Dolatabadian A, Jamshidi E, Khodaei-Joghan A (2013) Effects of Arbuscular mycorrhizal inoculation on growth, yield, nutrient uptake and irrigation water productivity of sunflowers grown under drought stress. Agric Water Manag 117:106–114

Gordo O, Sanz JJ (2010) Impact of climate change on plant phenology in Mediterranean ecosystems. Glob Change Biol 16:1082–1106

Government of Pakistan (2017) Agricultural statistics of Pakistan 2017–18. http://www.mnfsr.gov.pk/frmDetails.aspx

Gyldengren JG, Abrahamsen P, Olesen JE, Styczen M, Hansen S, Gislum R (2020) Effects of winter wheat N status on assimilate and N partitioning in the mechanistic agroecosystem model DAISY. J Agro Crop Sci 1–22. https://doi.org/10.1111/jac.12412

Hammad HM, Farhad W, Abbas F, Fahad S, Saeed S, Nasim W, Bakhat HF (2017) Maize plant nitrogen uptake dynamics at limited irrigation water and nitrogen. Environ Sci Pollut Res 24 (3):2549–2557

Harter AV et al (2004) Origin of extant domesticated sunflowers in eastern North America. Nature 430:201–205

Heiser CB Jr, Smith DM, Clevenger SB, Martin WC (1969) The North American sun-flowers. Mem Torrey Bot Club 22:1–218

Holzworth D et al (2014) APSIM – Evolution towards a new generation of agricultural systems simulation. Environ Model Softw 62:327–350. https://doi.org/10.1016/j.envsoft.2014.07.009

Hoogenboom G, Jones JW, Wilkens PW, Porter CH, Boote KJ, Hunt LA, Singh U, Lizaso JL, White JW, Uryasev O, Royce FS, Ogoshi R, Gijsman AJ, Tsuji GY, Koo J (2012) Decision Support System for Agrotechnology Transfer (DSSAT) Version 4.5 [CD-ROM]. University of Hawaii, Honolulu, Hawaii

Hussain M, Malik MA, Farooq M, Ashraf MY, Cheema MA (2008) Improving drought tolerance by exogenous application of glycine betaine and salicylic acid in sunflower. J Agron Crop Sci 194:193–199

Ibrahim MFM, Faisal A, Shehata SA (2016) Calcium chloride alleviates water stress in sunflower plants through modifying some physio-biochemical parameters. American-Eurasian J Agric Environ Sci 16(4):677–693

Ijaz W, Ahmed M, Asim M, Aslam M (2017) Models to study phosphorous dynamics under changing climate. In: Ahmed M, Stockle CO (eds) Quantification of climate variability, adaptation and mitigation for agricultural Sustainabilit. Springer International Publishing, Cham, pp 371–386. https://doi.org/10.1007/978-3-319-32059-5_15

IPCC (2014) Climate change 2014. In: Field CB, Barros VR, Dokken DJ, Mach KJ, Mastrandrea MD, Bilir TE, Chatterjee M, Ebi KL, Estrada YO, Genova RC, Girma B, Kissel ES, Levy AN, MacCracken S, Mastrandrea PR, White LL (eds) Impacts, adaptation and vulnerability. Contribution of working group II to the fifth assessment report of the intergovernmental panel on climate change. Cambridge University Press, Cambridge

Jabeen M, Gabriel HF, Ahmed M, Mahboob MA, Iqbal J (2017) Studying impact of climate change on wheat yield by using DSSAT and GIS: a case study of Pothwar region. In: Ahmed M, Stockle CO (eds) Quantification of climate variability, adaptation and mitigation for agricultural sustainability. Springer International Publishing, Cham, pp 387–411. https://doi.org/10.1007/978-3-319-32059-5_16

Jabran KE, Akbar N, Yasin M, Zaman U, Nasim W, Riaz M, Arjumend T, Azhar MF, Hussai M (2017) Growth and physiology of basmati rice under conventional and water-saving production systems. Arch Agron Soil Sci 63(10):1465–1476

Jones JW (1993) Decision support systems for agricultural development. In: Penning de Vries F, Teng P, Metselaar K (eds) Systems approaches for agricultural development. Kluwer Academic Press, Boston, pp 459–471

Jones CA, Kiniry JR (eds) (1986) CERES-Maize: a simulation model of maize growth and development. Texas A&M University Press, College Station, p 208

Jones JWG, Hoogenboom CH, Porter KJ, Boote WD, Batchelor LA, Hunt PWW, Singh U, Gijsman AJ, Ritchie JT (2003) The DSSAT cropping system model. Eur J Agron 18(3–4):235–265

Jones JW, Antle JM, Basso B, Boote KJ, Conant RT, Foster I, Godfray HCJ, Herrero M, Howitt RE, Janssen S, Keating BA (2017) Brief history of agricultural systems modeling. Agric Syst 155:240–254

Kalarani MK, Senthil A, Thangaraj M (2004) Effect of water stress on morpho-phy-siological traits of sunflower (Helianthus annus L.) genotypes. Madras Agric J 91(4–6):239–224

Kalyar T, Rauf S, Da Silva JAT, Shahzad M (2013) Handling sunflower (Helianthus annuus L.) populations under heat stress. Arch Agron Soil Sci 60(5):655–672

Kiniry JR, Blanchet R, Williams JR, Texier V, Jones CA, Cabelguenne M (1992) Sunflower simulation using the EPIC and ALMANAC models. Field Crop Res 30(3–4):403–423

Lecoeur J, Richard AF, Poiré-Lassus A, Christophe B, Pallas P, Casadebaig P, Debaeke F, Vear LG (2011) SUNFLO: a model-based analysis. Funct Plant Biol 38:246–259

Lecoeur J, Poiré-Lassus R, Christophe A, Guilioni L (2015) SUNFLO: a joint phenotyping and modelling approach to analyse and predict the differences in yield potential of sunflower genotypes. 17th International Sunflower Conference at: Cordoba, Spain, pp 429–434

Leite JGDL, Silva JVS, Justino FB, Martin K (2014) A crop model-based approach for sunflower yields. Sci Agric 71(5):345–355. https://doi.org/10.1590/0103-9016-2013-0356

Lentz DL, Pohl MDL, Alvarado JL, Tarighat S, Bye R (2008a) Sunflower (Helianthus annuus L.) as a pre-Columbian domesticate in Mexico. Proc Natl Acad Sci 105(17):6232–6237. https://doi.org/10.1073/pnas.0711760105

Lentz DL, Bye R, Sánchez-Cordero V (2008b) Ecological niche modeling and distribution of wild sunflower (Helianthus annuusL.) in Mexico. Int J Plant Sci 169(4):542–549

Liu B, Martre P, Ewert F, Porter JR, Challinor AJ, Müller C, Ruane AC, Waha K, Thorburn PJ, Aggarwal PK, Ahmed M, Balkovič J, Basso B, Biernath C, Bindi M, Cammarano D, De Sanctis G, Dumont B, Espadafor M, Eyshi Rezaei E, Ferrise R, Garcia-Vila M, Gayler S, Gao Y, Horan H, Hoogenboom G, Izaurralde RC, Jones CD, Kassie BT, Kersebaum KC, Klein C, Koehler A-K, Maiorano A, Minoli S, Montesino San Martin M, Naresh Kumar S, Nendel C, O'Leary GJ, Palosuo T, Priesack E, Ripoche D, Rötter RP, Semenov MA, Stöckle C, Streck T, Supit I, Tao F, Van der Velde M, Wallach D, Wang E, Webber H, Wolf J, Xiao L, Zhang Z, Zhao Z, Zhu Y, Asseng S (2019) Global wheat production with 1.5 and 2.0°C above pre-industrial warming. Glob Chang Biol 25(4):1428–1444. https://doi.org/10.1111/gcb.14542

Lyakh VA, Totsky IV (2014) Selective elimination of gametes during pollen storage at low temperature as a way to improve the genetic structure of sporophytic population for cold tolerance. Helia 37(61):227–235

Ma G, Song Q, Underwood WR et al (2019) Molecular dissection of resistance gene cluster and candidate gene identification of Pl_{17} andPl_{19} in sunflower by whole-genome resequencing. Sci Rep 9:14974. https://doi.org/10.1038/s41598-019-50394-8

Manivannan P, Rabert GA, Rajasekar M, Somasundaram R (2015) Drought stress induced modification on growth and Pigments composition in different genotypes of Helianthus annuus L. Curr Bot 5:7–13

Miller-Rushing AJ, Katsuki T, Primack RB, Ishii Y, Lee SD, Higuchi H (2007) Impact of global warming on a group of related species and their hybrids: cherry tree (rosaceae) flowering at Mt. Takao, Japan. Am J Bot 94(9):1470–1478

Miyan MA (2015) Droughts in Asian least developed countries: vulnerability and sus-tainability. Weather Clim Extrem 7:8–23

Nasim W, Ahmad A, Wajid A, Akhtar J, Muhammad D (2011) Nitrogen effects on growth and development of sunflower hybrids under agro-climatic conditions of Multan. Pak J Bot 43 (4):2083–2092

Nasim W, Ahmad A, Belhouchette H, Fahad S, Hoogenboom G (2016a). Evaluation of the OILCROP-SUN model for sunflower hybrids under different agro-meteorological conditions of Punjab-Pakistan. F Crop Res. https://doi.org/10.1016/j.fcr.2016.01.011

Nasim W, Ahmad A, Habib-ur-Rahman M, Jabran K, Ullah K, Fahad S, Shakeel M, Hoogenboom G (2016b). Modelling climate change impacts and adaptation strategies for sunflower in Pakistan. Outlook Agric. https://doi.org/10.5367/oa.2015.0226

Nasim W, Ahmad A, Amin A, Tariq M, Awais M, Saqib M, Jabran K, Shah GM, Sultana SR, Hammad HM, Rehmani MIA, Hashmi MZ, Rahman MHU, Turan V, Fahad S, Suad S, Khan A, Ali S (2018) Radiation efficiency and nitrogen fertilizer impacts on sunflower crop in contrasting environments of Punjab-Pakistan. Environ Sci Pollut Res 25(2):1822–1836

Pekcan V, Evci G, Yilmaz MI, Nalcaiyi ASB, Erdal ŞÇ, Cicek N, Ekmekci Y, Kaya Y (2015) Drought effects on yield traits of some sunflower inbred lines. Agric For 61(4):101–107

Peng B, Guan K, Tang J, Ainsworth EA, Asseng S, Bernacchi CJ, Cooper M, Delucia EH, Elliott JW, Ewert F, Grant RF, Gustafson DI, Hammer GL, Jin Z, Jones JW, Kimm H, Lawrence DM, Li Y, Lombardozzi DL, Marshall-Colon A, Messina CD, Ort DR, Schnable JC, Vallejos CE, Wu A, Yin X, Zhou W (2020) Towards a multiscale crop modelling framework for climate change adaptation assessment. Nat Plants 6(4):338–348. https://doi.org/10.1038/s41477-020-0625-3

Picheny V, Trépos R, Poublan B, Casadebaig P (2015) Sunflower phenotype optimization under climatic uncertainties using crop models. arXiv: INRA, UR875 Math́ ematiques et Informatique Appliqú ees Toulouse
Plant RE (1989) An integrated expert decision support system for agricultural management. Agric Syst 29:49–66
Putt ED (1997) Early history of sunflower. In: Schneiter AA (ed) Sunflower technology and production. American Society of Agronomy, Madison, WI, pp 1–19
Reddy GKM, Dangi KS, Kumar SS, Reddy AV (2003) Effect of moisture stress on seed yield and quality in sunflower (Helianthus annuus L.). J Oilseeds Res 20(2):282–283
Rieseberg LH, Beckstrom-Sternberg SM, Liston A, Arias DM (1991) Phylogenetic and systematic inferences from Chloroplast DNA and isozyme variation in Helianthus sect. Helianthus (Asteraceae). Syst Bot 16:50–76
Ritchie JT, Otter S (1984) Description and performance of CERES-wheat: a user-oriented wheat yield model. In: Wheat Yield Project, A.R.S (ed) ARS-38. National technical information service, Springfield, pp 159–175
Robert GA, Rajasekar M, Manivannan P (2016) Triazole-induced drought stress amelioration on growth yield, and pigments composition of Helianthus annuus L. (sunflower). Int Multidiscip Res J 5:6–15
Rondanini D, Mantese A, Savin R, Hall AJ (2006) Responses of sunflower yield and grain quality to alternating day/night high temperature regimes during grainfilling: effects of timing, duration and intensity of exposure to stress. Field Crop Res 96:48–62
Rosenzweig C, Elliott J, Deryng D, Ruane AC, Müller C, Arneth A et al (2014) Assessing agricultural risks of climate change in the 21st century in a global gridded crop model intercomparison. Proc Natl Acad Sci 111(9):3268–3273. https://doi.org/10.1073/pnas.1222463110
Rossi V, Salinari F, Poni S, Caffi T, Bettati T (2014) Addressing the implementation problem in agricultural decision support systems: the example of vite.net. Comput Electron Agric 100:88–99. https://doi.org/10.1016/j.compag.2013.10.011
Saleh A, Arnold JG, Gassman PWA, Hauck LM, Rosenthal WD, Williams JR, McFarland AMS (2000) Application of SWAT for the upper North Bosque River watershed. Trans ASAE 43 (5):1077–1087. https://doi.org/10.13031/2013.3000
Salunkhe DK, Chavan JK, Adsule RN, Kadam SS (1992) World oilseeds: chemistry, technology, and utilization. Van Nostrand, New York
Schepen A, Everingham Y, Wang QJ (2020) An improved workflow for calibration and downscaling of GCM climate forecasts for agricultural applications – A case study on prediction of sugarcane yield in Australia. Agric For Meteorol 291:107991. https://doi.org/10.1016/j.agrformet.2020.107991
Soleimanzadeh H, Habibi D, Ardakani MR, Paknejad F, Rejali F (2010) Effect of potassium levels on antioxidant enzymes and malondialdehyde content under drought stress in sunflower (Helianthus annuus L.). Am J Agric Biol Sci 5(1):56–61
Stefansson BR (2007) Oilseed crops. The Canadian Encyclopedia (Historica Foundation Toronto). Available http://www.thecanadianencyclopedia.com. Accessed 10 April 2008
Stöckle CO, Kemanian AR (2020) Can crop models identify critical gaps in genetics, environment, and management interactions? Front Plant Sci 11(737). https://doi.org/10.3389/fpls.2020.00737
Szabó B, Vincze E, Czúcz B (2016) Flowering phenological changes in relation to climate change in Hungary. Int J Biometeorol 60:1347–1356
Teng PS, Penning de Vries FWT (eds) (1992) Systems approaches for agricultural development applied science. Elsevier. (ISBN: 1851668918. 309 pp.)
Totsky IV, Lyakh VA (2015) Pollen selection for drought tolerance in sunflower. Helia 38 (63):211–220
United State Department of Agriculture (USDA) (2016) National Agricultural Statistics Service. USDA-NASS 1400 Independence Ave., SW Washington, DC 20250

Van Rossum F, Vekemans X, Meerts P, Gratia E, Lefébvre C (1997) Allozyme variation in relation to ecotypic differentiation and population size in marginal populations of Silene nutans. Heredity 78:552–560

Visser ME, Both C (2005) Shifts in phenology due to global climate change: the need for a yardstick. Proc R Soc B 272:2561–2569

Wallach D, Martre P, Liu B, Asseng S, Ewert F, Thorburn PJ, van Ittersum M, Aggarwal PK, Ahmed M, Basso B, Biernath C, Cammarano D, Challinor AJ, De Sanctis G, Dumont B, Eyshi Rezaei E, Fereres E, Fitzgerald GJ, Gao Y, Garcia-Vila M, Gayler S, Girousse C, Hoogenboom G, Horan H, Izaurralde RC, Jones CD, Kassie BT, Kersebaum KC, Klein C, Koehler A-K, Maiorano A, Minoli S, Müller C, Naresh Kumar S, Nendel C, O'Leary GJ, Palosuo T, Priesack E, Ripoche D, Rötter RP, Semenov MA, Stöckle C, Stratonovitch P, Streck T, Supit I, Tao F, Wolf J, Zhang Z (2018) Multimodel ensembles improve predictions of crop–environment–management interactions. Glob Chang Biol 24(11):5072–5083. https://doi.org/10.1111/gcb.14411

Wang J, Xing J, Mathur R, Pleim JE, Wang S, Hogrefe C et al (2016a) Historical trends in PM2.5-related premature mortality during 1990–2010 across the northern hemisphere. Environ Health Perspect 125(3):400–408. https://doi.org/10.1289/EHP298

Wang Z, Chen J, Li Y, Li C, Zhang L, Chen F (2016b) Effects of climate change and cultivar on summer maize phenology. Int J Plant Prod 10(4):509–525

Wheeler T, von Braun J (2013) Climate change impacts on global food security. Science 341 (6145):508–513

White MJ, Santhi C, Kannan N, Arnold JG, Harmel D, Norfleet L et al (2014) Nutrient delivery from the Mississippi River to the Gulf of Mexico and effects of cropland conservation. J Soil Water Conserv 69(1):26–40. https://doi.org/10.2489/jswc.69.1.26

Wriedt G, Van der Velde M, Aloe A, Bouraoui F (2009) Estimating irrigation water requirements in Europe. J Hydrol 373(3–4):527–544. https://doi.org/10.1016/j.jhydrol.2009.05.018

Zhu J, Zeng W, Ma M, Lei G, Zha Y, Fang Y (2018) Testing and improving the WOFOST model for sunflower simulation on saline soils of Inner Mongolia, China. Agronomy 8(9):172. https://doi.org/10.3390/agronomy8090172

Disease Modeling as a Tool to Assess the Impacts of Climate Variability on Plant Diseases and Health

12

Muhammad Zeeshan Mehmood, Obaid Afzal, Muhammad Aqeel Aslam, Hasan Riaz, Muhammad Ali Raza, Shakeel Ahmed, Ghulam Qadir, Mukhtar Ahmad, Farid Asif Shaheen, Fayyaz-ul-Hassan, and Zahid Hussain Shah

Abstract

Biotic stress is one of the major environmental factors that affect the plant's growth and life cycle. Plant pathogens are major constraints and severe threats to agricultural production in changing climate scenarios. The effects of climate variability on plant diseases and pathogens have been examined in various plant pathosystems. Climate change is predicted to affect the development of pathogens, their survival, vigor, sporulation, multiplicity, and host susceptibility that ultimately cause changes in the crop diseases. It also affects the inoculum dispersion and pathogenicity. These effects vary depending on pathosystems and geographic locations. Climate change not only affects optimal conditions of infection but also host specificity and infection mechanism in plants.

M. Z. Mehmood (✉) · O. Afzal · M. A. Aslam · G. Qadir · Fayyaz-ul-Hassan
Department of Agronomy, Pir Mehr Ali Shah Arid Agriculture University, Rawalpindi, Pakistan

H. Riaz
Institute of Plant Protection, MNS University of Agriculture, Multan, Pakistan

M. A. Raza
College of Agronomy, Sichuan Agricultural University, Chengdu, Sichuan, China

S. Ahmed
Department of Agronomy, Bahauddin Zakariya University, Multan, Pakistan

M. Ahmad
Department of Agronomy, Pir Mehr Ali Shah Arid Agriculture University, Rawalpindi, Pakistan

Department of Agricultural Research for Northern Sweden, Swedish University of Agricultural Sciences, Umeå, Sweden

F. A. Shaheen
Department of Entomology, PMAS Arid Agriculture University, Rawalpindi, Pakistan

Z. H. Shah
Department of Plant Breeding & Genetics, Pir Mehr Ali Shah Arid Agriculture University, Rawalpindi, Pakistan

M. Ahmed (ed.), *Systems Modeling*, https://doi.org/10.1007/978-981-15-4728-7_12

Temperature, light, and humidity are the major factors that control the development and growth of diseases. So, climate change is an emerging challenge that is impacting and driving the plants and pathogens growth, disease development in a pathosystem. This overview is aimed to summarize the previous research, reviews, opinions, and recent trends in studying the effects of climate variability on pathogens and plants health. However, managing and predicting climate change impacts are complicated because of the interaction between the indirect effects and global climate change drivers. Similarly, uncertainty in plant disease development models in changing climate needs the diversification in management strategies. Protection of plants against diseases and pathogens is an essential direction for researchers to make the plants more resistant to pests and diseases. There is a need for further research in different areas under multiple climate-changing factors and scenarios using the disease modeling frameworks such as BIOMA and APSIM-DYMEX.

Keywords

Pathosystems Climate change Biotic stress Disease modeling

12.1 Introduction

Change in the statistical distribution of weather for an extended period of time is called climate change. The end of the twentieth century and the start of the twenty-first century were the warmest periods globally. The availability of information on the effects of climate variability upon plant diseases is very limited. It was documented that plant diseases will be affected by the changing climate like other global change components (Regniere 2011; Bradley et al. 2012). The influence of the environment on plant disease is considered by plant pathologists disease studies, and the disease triangle illustrates the interaction among host plants, environment, and pathogen for disease development (Grulke 2011). Climate variability is one of the ways in which the environment can be suppressive or conducive for disease (Ahmed 2020; Ahmed and Stockle 2016; Perkins et al. 2011; Fuhrer 2003). Therefore plant diseases are indicators of climate variability (Garrett et al. 2015). Since the last decade plant virus distribution and the population is increasing swiftly as well as many new infectious diseases are also identified. Plant diseases are not only accelerated by increased activity of pathogens but also due to declined tolerance in plants as a result of adverse environmental conditions (Huseynova et al. 2014). Anthropogenic activities are the important causes of plant diseases spread; sudden oak death is an example of these activities (Prospero et al. 2009). Climate variability is impacting the plants in agriculture ecosystems globally (Stern 2008). Little work has been carried out on modeling the impacts of climate variability on disease epidemics in plants. However, several tree diseases are emerging because of climate change (Garrett et al. 2006; Garrett et al. 2015). This change is affecting the crops directly as well as indirectly by interacting with microbial pests and resulting in several disease epidemics in plants (Bosch et al. 2007; Chakraborty 2005). A variety of mechanisms can affect the health of plants in changing climates such as acceleration in pathogen evolution, fewer incubation periods, and extreme climatic events (Sutherst et al. 2011). Climate change is impacting the hosts and pathogens directly and indirectly by altering their physiology (Desprez-Loustau et al. 2006; Garbelotto et al. 2010).

12.2 Recently Occurred Changes

Climate variability has been measured, and these changes have been associated with plant pathosystems. Environment and climatic conditions strongly affect the plant diseases in the forests. Pathogens, moisture, temperature, and stress interaction influence the severity of infections and diseases. Climate changes result in the evolvement of more invasive species and increase stress on plants leading to the condition that is favorable for diseases in plants. Changes in temperature, moisture, and precipitation in North America were associated with tree death events (Van Mantgem et al. 2009; Sturrock et al. 2011). In central Europe rise in winter temperature and fluctuations in the rain favored the root rot diseases in forests by supporting infection through *Phytophthora* spp. (Jung 2009). At Oregon coast climatic changes resulted in the Swiss needle epidemic, and a further increase of 0.4 °C in temperature is predicted by 2050 in Pacific Northwest forests that will further increase the severity of the epidemic and increase the outbreak (Stone et al. 2008; Sturrock et al. 2011). In Oregon and California sudden death of Oak trees caused by *Phytophthora ramorum* abruptly increased due to extreme climatic events. Heavy rains and extension of moist weather in warm season favor the infection in plants and lead to the death (Swiecki and Bernhardt 2016; Frankel 2007). In Europe study was carried out for *Phytophthora cinnamomi* in Oak. Results demonstrated that an increase in temperature worsens the root disease (Brasier 1996; Brasier and Scott 1994). A similar study was carried out for eucalyptus (Booth et al. 2000). In Alaska yellow cedar tree’s mortality rate is also increasing due to changing climatic conditions. As earlier, melting of snow exposed roots to the cold conditions that result in freezing and cause injury (Thompson 2007).

Several studies were carried out to assess the climate change impacts on plant diseases. Most studies investigated the head blight, leaf rust and blotch in wheat, downy mildew in grapes, and phoma stem canker in oilseed rapes. These studies are mostly carried out in European countries and Brazil (Juroszek and von Tiedemann 2015). However, rice is a major crop in Asian countries, and rice blast is an important disease that results in major losses in rice production. Luo et al. (1995) conducted an analysis of the blast epidemic produced by *Magaporthe grisea*. Results showed that change in rainfall has no impacts, while in subtropical regions, disease severity is increased because of high temperatures. However, the opposite trend was observed in humid areas. An experiment was conducted to study the impacts on soil-borne pathogens. Results showed an increase in damping-off in cotton plants under elevated CO_2 (Ahmad and Hasanuzzaman 2020; Runion et al. 1994). In barley an increase in growth was observed at high CO_2 concentrations but after the infection of powdery mildew, the growth was retarded (Hibberd et al. 1996). The incidence of leaf rust was studied in spring wheat under elevated CO_2 and ozone. The infection rate was inhibited by the ozone; however, ozone damage on leaves was altered by infection and CO_2 (Tiedemann and Firsching 2000). Temperature evaluation can increase the yellow dwarf symptoms in wheat and barley (Mikkelsen et al. 2015). In maize crop, increased CO_2 makes it more prone to *Fusarium* (Vaughan et al. 2014). Fusarium Crown rot diseases in wheat increased with more CO_2 (Melloy et al. 2014) while reduced in elevated temperature (Vary et al. 2015). Increased CO_2 effects were studied on a C_3 *Scirpus olneyi*, and the C_4 grass *Spartina patens*. However, shoot N and water content were also determined. Plants with increased CO_2 levels showed an increase of 37% in resistance while in reduced N and increased water content the disease severity was also enhanced (Thompson and Drake 1994). Similarly, in Finland, climate variability will affect potato production. The risk of potato blight resulted from *Phytophthora infestans* will be increased and a nematode called *Globodera rostochiensis* will also be distributed all over the country because it has the ability to support many generations in a single year (Carter et al. 1996). In tomato plants, climate change will not affect diseases like white mold, late blight, verticillium wilt, septoria leaf spot, and tomato mosaic. But the importance of powdery mildew, early blight, bacterial wilt, and leaf curl will increase (Gioria et al. 2008).

12.3 Climate Change Impacts on Pathogens

The rise in temperature may initiate the growth and development of inactive pathogens (Fig. 12.1). Temperature and rainfall changes may cause alteration in growth, rate of progress, physiology, and resistivity of the host (Chakraborty and Datta 2003). Temperature affects the diseases caused by bacteria like *Acidovorax avenae*, *Ralstonia solanacearum*, and *Burkholderia glumae*. Bacteria can move to the areas where temperature depending diseases are not previously noticed (Kudela 2009). As the rise in temperature reduce winter length, whereas growth and reproduction of pathogens get modified (Ladanyi and Horvath 2010). Researches indicated that wheat and oats are becoming more susceptible to the rust disease due to the increase in temperature and humidity, while resistant has been shown by few forage species to alleviated temperatures (Coakley et al. 1999). In the cold duration of the year, warming can release cold stress but in the hot period of the year, it increases heat stress. Various models have been used for forecasting the epidemics based on the rise in pathogen growth and infection in a specific range of temperatures. Fungi that are causing the disease to plant at cold temperatures experience longer suitable temperature periods for reproduction and growth in a warmer climate. Late blight epidemic became more severe and required more fungicide to control diseases if warm temperature onset earlier. These effects of increased temperature vary throughout the year as increase in temperature in colder parts may reduce plant stress while in hotter parts it results in increase of alleviated

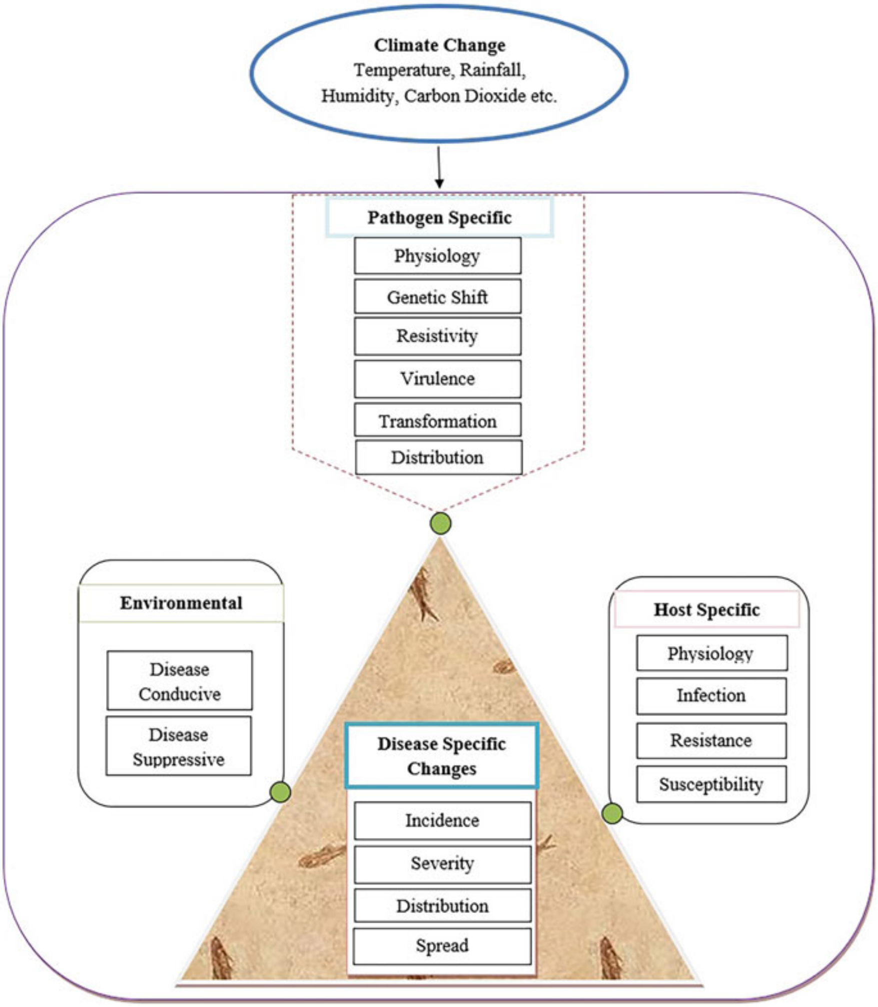

Fig. 12.1 Impacts of climate variability on plant diseases

temperature stress. Lower rainfall decreases the incidence of downy mildew infections in grape plants. Temperature and moisture are corelated and affect the pathogens reproduction (Caffarra et al. 2012) and also affect the populations of pathogens (Legler et al. 2012). When the temperature is higher, the moisture will be reduced and result in reduced risk of disease (Desprez-Loustau et al. 2006). Dense canopies result in more moisture and increase leaf wetness that will favor the growth and development of pathogens.

Alleviated CO_2 impacts both pathogen and host in multiple manners. Under alleviated CO_2 and temperature, new races are evolving very rapidly, and the population of pathogens is boosted as well as infectious cycles are also increasing due to favorable climate in the large canopy (Chakraborty 2013). Higher concentrations of CO_2 lead to the increased production of biomass depending on the availability of nutrients and water, weeds, diseases, and pests damage. However, the increased carbohydrates amount in plant tissues favors the biotrophic fungi, that is, rust (Chakraborty and Datta 2003). Therefore, biomass increase can alter the microclimate of plants and also the chances of infection. More CO_2 will result in slow decomposition of residues that will favor in overwintering of harmful organisms and more fugal spore production will occur. Increased CO_2 can affect the growth of pathogens by leading to higher production of fungal spores but it can also cause some physiological alterations in host plants that enhance the resistance against pathogens (Coakley et al. 1999). At higher concentrations of CO_2 growth of germ tube and germination rate were slower in conidium of *C. gleosprioides* fungi but after infection fungi develop quickly and attain sporulation (Chakraborty et al. 2002). Similarly, higher ozone concentration can increase rust infection on the tree of poplar but it is minimized by increased CO_2 (Karnosky et al. 2002).

12.4 Climate Change Impacts on Plants

Plants show alteration in their gene expression in response to the climatic changes, while transcriptome enables plants to respond to these changes (Garrett et al. 2006). Climate variability directly impacts the plant's biology, physiology, biochemical process, and morphology (Fig. 12.1). These changes affect the pathogens colonization, symptoms expression, colonization infection, etc.

Drought can reduce stomatal activity as well as photosynthesis and affect leaf growth and morphology of root and shoot (Ahmed et al. 2020). Temperature and moisture stress affects the plants by changes in abscisic acid, salicylic acid, jasmonic acid, and adversely affect the plant resistance to stresses (Asselbergh et al. 2008). It may also reduce the plant's ability to produce growth and defense substances, making the plant susceptible to pathogens.

Increased CO_2 affect photosynthesis and change the structure of plants as well as affect the functioning of ecosystems. Under increased CO_2 conditions, plant organ size also increases, such as leaves and branches (Pritchard et al. 1999), and water use efficiency of plants also increases (Ahmed and Ahmad 2019; Wong et al. 2002). It results in the humid climate, and plant pathogen infection rate may rise. Similarly, elevated ozone can increase the attack of necrotrophic fungi (Sandermann 2000) because leaf composition and structure are affected by the ozone (Karnosky et al. 2002).

12.5 Climate Change Impacts on Host Resistance

The assessment of plant resistance in the context of climate change is complicated. Under drought conditions, infection rate and success tend to decrease (Huber and Gillespie 1992). Fewer symptoms were observed under drought conditions when alfalfa plants were exposed to *verticillium albo-atrum* (Pennypacker et al. 1991). However, in some cases, plant resistance is reduced under drought stress (Christiansen 1982). Resistance genes are also affected by temperature, but it is complicated to assess the effect of temperature on resistance genes and pathogen aggressiveness. Effects of temperature on wheat and barley were studied, and the response of resistance was different to different ranges of temperature (Browder and Eversmeyer 1986; Newton and Young 1996). A higher level of ozone and CO_2 also affects the host resistance (Plazek et al. 2001; Plessl et al. 2005). Reduction in host resistance was observed under elevated CO_2 (Chakraborty and Datta 2003). An increase or decrease in the conduciveness of the disease environment due to climate change can cause shifts in the presence and diversity of resistance genes (Fig. 12.1).

12.6 Climate Change Impacts on Microbial Interaction

Climate change is impacting the microbial communities in the soil and causing various shifts in different interactions. Temperature, CO_2, nitrogen, etc. are the main factors influencing interactions in soils. Increased CO_2 results in a reduction of soil nitrates in grasslands (Barnard et al. 2005) and enhances the nitrogen uptake of plants because of increased growth in plants (Hu et al. 2001). In tallgrass prairies, increased temperature favors plant growth that facilitates fungi dominance in the community and uptake of nitrogen. Lesser availability of nitrogen is experienced by microbial communities, while the type of soil and composition of plants have effects on these observed responses (Hungate et al. 1996). In both agricultural and natural ecosystems prediction of climate change impacts on the disease; suppression is complicated due to variations in the interaction between the microbial species (Davelos et al. 2004). Recent advancements in technology like metagenomic analysis will enhance knowledge about the dynamics of microbes in soil and various environments (Riesenfeld et al. 2004).

Host response to climate change may be affected by symbiosis, as fungal endophytes had shown tolerance to heat, nutrient availability, and water stress (Kannadan and Rudgers 2008; Rodriguez et al. 2008). Brosi et al. (2011) studied the effects of climate change on endophytes, and results concluded that higher infection rates in tall fescue are led by elevated CO_2 levels than the precipitation and temperature.

12.7 Simulation Modeling for Disease Prediction

There are several approaches that can be used in modeling the impacts of climate variability on pathogens and diseases. Different empirical or regressions models can be used to predict the pathogens' success and development of epidemics (Booth et al. 2000). Models can be used for predicting the success of the pathogen in changing environments in the context of a reference climate where pathogens are successful. Climate variability occurs gradually that causes difficulty in studying its effects directly, and hence simulation models can become helpful in outcomes prediction over broader range scenarios. However, problems have been identified in models application for disease forecasting in climate change scenarios (Scherm 2004; Seherm and Coakley 2003). Major issues involve difficulty in acquiring data regarding climate and epidemiological responses (Otten et al. 2004), disease geographic distribution that may lead to higher uncertainties (Katz 2002; Scherm 2000), and ignorance of adaptation potential of plants in simulation models.

12.7.1 History of Disease Modeling

Since the 1960s, models for disease prediction are available, and the first mathematical model was published by Van der Plank (Van der Plank 2013). At the start, the models were empirical. Later on, mechanistic and analytical models were developed. The early model's focus was only based on the units of pathogen and diseased tissue, while the growth of plants was neglected. With the passage of time models for disease prediction became more sophisticated as they included host, environment, and management effects as well. GIS-based models may also be used for disease predictions (Aurambout et al. 2009). At present, a wide range of simple and complex models is in practice for the forecasting and management of disease (Pavan et al. 2011; Rakotonindraina et al. 2012).

Climate change affects the various stages of crops and pathogens, both directly and indirectly. Pathosystems are generally affected by the response of organisms to climate change. However, it is not well understood whether the effects are either positive or negative. To predict the plant diseases in response to climate change, various models had been used in the past (Table 12.1).

12.7.2 Recent Goals and Challenges in Disease Modeling

Integration of crop disease modeling in decision support systems development is mainly dominated by short-term strategic planning to support the scheduling of pesticide application, pest scouting activities, adaptation, and mitigation measures to prevent the diseases (Isard et al. 2015; Magarey et al. 2002). Disease modeling activities are frequently based on the development of relationships using multi-seasonal crop and environmental variables in a specific pest-crop system (Madden et al. 2007). The development of effective decision support systems involves the knowledge of key aspects and dynamics of a system based on the reliable multiple seasonal and specific crop-pest environment data (Madden et al. 2007). Representation of biotic stress and host interaction has been simplified by focusing on the specific environment and pathogens in a system. Moreover, the controlled experiment data can be used to parameterize the model to identify the responses of targeted host and pathogen under a variety of environmental changes. Infection models and Susceptible-Exposed-Infectious-removed (SEIR) models are well-known examples of such disease models (Magarey et al. 2005; Zadoks 1971). For instance, such

Table 12.1 Models used in different regions of the world to study various crop diseases

Region	Crop	Predicted diseases/Pests	References
Australia	Wheat	Yellow dwarf virus	Nancarrow et al. (2014)
Australia	Wheat	Fusarium crown rot	Vary et al. (2015)
Europe	Wheat	Karnal bunt	Baker et al. (2000)
Europe	Rice	Fungal diseases	Bregaglio et al. (2013)
Brazil	Corn	Rust	Moraes et al. (2011)
Denmark	Barley	Powdery mildew	Mikkelsen et al. (2015)
France	Barley	Net blotch	Launay et al. (2014)
United Kingdom	Oilseed rape	Phoma stem canker	Barnes et al. (2010)
Brazil	Soybean	Rust	Alves et al. (2011)
Europe	Sugar beet	Soil borne pathogens	Manici et al. (2014)
Germany	Sugar beet	Leaf spot	Richerzhagen et al. (2011)
Australia	Pea	Ascochyta blight	Salam et al. (2011)
Globally	Potato	Late blight	Sparks et al. (2014)
Brazil	Cocoa	Moniliasis	Moraes et al. (2012b)
Brazil	Coffee	Rust	Ghini et al. (2011)
Brazil	Coffee	Leaf miner	Hamada et al. (2006)
Brazil	Coffee	Nematodes and leaf miner	Ghini et al. (2008)
Brazil	Coffee	Leaf spot	Moraes et al. (2012a)
Globally	Date palm	Fusarium wilt	Shabani and Kumar (2013)
Northern Italy	Grapevines	Powdery mildew	Caffarra et al. (2012)
Italy	Grapevines	Downy mildew	Francesca et al. (2006)
Globally	Grapevines	Downy mildew	Salinari et al. (2007)
France	Grapevines	Botrytis	Gouache et al. (2011)
Brazil	Banana	Black sigtoka	Ghini et al. (2007)
Globally	Banana	Black sigtoka	Junior et al. (2008)
Switzerland	Apple	Fire blight	Hirschi et al. (2012)

disease prediction models can be used to predict the host alterations, disease severity, and yield losses in changing climate (Dillehay et al. 2005).

Priorities for disease modeling are rerouting due to the newly arising challenges and more specific goals. The major challenge for disease modeling is climate change, as it is resulting in the variable average temperature, more erratic rainfall, and humidity. These climate irregularities indicate that previously observed datasets are losing their importance in reliable disease prediction modeling. Moreover, due to these variabilities, several pathogens that were previously unharmful are now becoming detrimental for crops (Gramaje et al. 2016; Berger et al. 2007). Presently, there are increasing concerns about the goal to estimate and predict global food security risks. But it requires the addition of production systems and geographical areas to develop the baseline data for local and robust empirical relationships. However, climate variability makes this goal impossible to achieve due to the nonlinearity of the process involved in statistical models (Garrett et al. 2006). Similarly, climate change impacts the goal of seeking effective estimation and prediction of disease dynamics in future scenarios and impedes the trend analysis based on the several observed weather patterns. To address these challenges, the most efficient and appealing way involves the use of process-based modeling with efficiently designed scenarios and shared modeling approaches among the scientist related to a variety of field. Additionally, the utilization of disease modeling increased its important manifolds, ranging from the strategic decisions making (Duveiller et al. 2007), risk analysis (Venette et al. 2010), research priority and policy making (Willocquet et al. 2004), and resource allocation (Beddow et al. 2015). A new generation of technologically advanced tools is needed to understand the system processes and their dynamics to allow system analysis.

12.7.3 Modeling Approaches in Disease Modeling

Crop growth, performance, and disease dynamics are linked with discrete sets of developmental processes. Efficient understanding and knowledge of these processes can be mobilized to address the problems related to crop pests and diseases. Recently, the concept of integrating pest and disease models with crop models has made easier and effective to study pest and disease dynamics. However, complex disease and crop models are hard to link with each other.

12.7.3.1 Existing Trends in Disease Modeling

Several recent advances have been documented in the domain of designing and integrating the generic disease simulation models to predict the reliable disease and pest damage to crops (Esker et al. 2012; Savary et al. 2006). Process-based disease modeling has emerged as a key approach to quantitatively understand the behavior and address the problems related to the complex crop-pest systems. A typical process-based disease modeling encompasses four basic steps: (1) Infection chain in a disease cycle is considered as the prime focus for analysis (Kranz 1974). (2) Then the functional traits of a pathogen corresponding to infection chain are studied (Pariaud et al. 2009). (3) The efficiency and performance of these traits based on the environment are studied in a pathosystem, as these functional traits are involved in quantitative processes (Zadoks and Schein 1979). (4) Finally, the observed and measured information from these processes is used for the development of process-based models (Savary and Willocquet 2014; Bregaglio and Donatelli 2015). There is a number of disease modeling structures that have been developed with an emphasis on inoculum mobility, spread, efficiency, and production (Rossi et al. 2009). Moreover, a wider range of concepts and development of mechanistic simulation models made it possible to study the interaction between crops, pests, and diseases within a given pathosystem.

The development of generic simulators enables the illustration of several species in a pathosystem. The application of these generic simulators can be extended by adding several specialized biological mechanisms of species. Generic simulators make the disease modeling approach simpler due to the possibility of developing the species-specific disease model. Moreover, these simulators provide a framework to collect adequate data for disease modeling regarding insect phenology, physiology (Welch et al. 1978), populations (Yonow et al. 2004), development, and reproduction (Hong et al. 2015; Sutherst et al. 2007).

Knowledge sharing and modification among the wider scientific communities can enhance the impacts and progress of disease modeling (Stein et al. 2002; Tatusov et al. 2000). For instance, AgMIP (Agricultural Model Inter-comparison and Improvement Project) is a recent knowledge sharing example of international collaboration to assess the impacts of climate change on global agriculture based on global agricultural modeling (Rosenzweig et al. 2013). These approaches can mobilize the generic disease modeling platform by combining all fragmented theories and concepts existing in disease modeling globally. APSnet (American Phytopathology Society) plant health instructor is a well-known illustration of such approaches (Bregaglio and Donatelli 2015; Savary and Willocquet 2014). Simulated disease epidemics can be used as input in crop models accounting for the physiological impacts of disease on crops and damage mechanisms (Rouse 1988). Over the past few decades, crop growth models involving damage mechanisms have been developed with the concept of integration of disease and crop models to simulate the crop yield losses due to disease epidemics (Boote et al. 1983; Bastiaans et al. 1994).

12.7.3.2 Data Requirements for Disease Modeling

Most common data inputs for disease modeling are based on variables such as temperature, precipitation, relative humidity, and leaf wetness with hourly or daily resolutions (Magarey et al. 2001). However, the soil variables and wind are considered in more complex models focusing on soil pathogens. Mostly the daily data is sufficient for disease models, but some models need hourly data to improve the accuracy and reliability of disease simulations and scenarios development (Bregaglio et al. 2010). However, the gridded current and forecasted data with fine resolution can be obtained by numerical weather models such as AGRI4CAST in Europe, RTMA (Real Time Mesoscale Analysis System) in the United States (De Pondeca et al. 2011), and CFSR (Climate Forecast System Reanalysis) globally (Saha et al. 2014). Data regarding leaf wetness is a limitation due to the unavailability of such data, but simulations models are now being used as alternatives to target the climate change scenarios (Magarey et al. 2006; Bregaglio et al. 2012).

12.7.3.3 Calibration and Evaluation of Disease Models

Models calibration is the fine-tuning of models with real-time data to improve the model accuracy and application in a desired environment or pathosystem. Most of the disease and pest models are calibrated with experimental data obtained from controlled conditions. Data regarding variables such as pest virulence, development, fecundity, longevity, mortality, and environment of pathosystem is needed to parameterize and calibrate the models (Régnière et al. 2012). Similarly, data from the experiments with controlled temperature and leaf wetness can be used to calibrate the infection models (Magarey et al. 2005; Madden and Ellis 1988). Moreover, when the data is unavailable to calibrate the model, then closely related species can be used to identify parameter, and then field studies are enabled to see if the estimated parameters are in line with observed data or not.

Model evaluation is necessary to estimate the accuracy of simulations in comparison with real-time data. Several ways and methods can be used to evaluate the pest and disease models (Rabbinge 1993). The most common approach to evaluate the models involves the comparison of observed and simulated data in terms of disease severity, incidence, and damage. However, evaluation of disease models is usually done by the developing party or by the end-user according to their pathosystems. Overfitting is a serious concern in the model evaluation and to perform simulation in different pathosystems. Overfitting occurs when the output of model adjusted parameters closely matches the data used for calibration but leads to compromised accuracy when simulations are performed over an independent dataset.

12.7.4 Frameworks for Disease Modeling

In the past various types of models were being used by scientists to model plant pathogens and disease. Matrix models have been used widely over several decades in the past for determining the population densities of pests and insects in a certain region (Lewis 1977). Several equations were used in competitive models to determine the effects of competition between crops and pathogen species (Kaplan and Denno 2007).

12.7.5 Recent Development and Addition in Modeling Frameworks

Recently, disease modeling gained importance and various developments occurred. Different modeling frameworks are developed for pests and disease modeling in the last few years.

12.7.5.1 APSnet

It is an (American Phytopathology Society) website that provides a module to help in modeling epidemiology and crop loss analysis. It has various models such as GENEPEST for simulations (Donatelli et al. 2017) and provides guidance for running the simulation models. Savary et al. (2006) summarized an overall disease modeling framework to simulate the disease impacts on agriculture systems using such models. The development of this platform involved several steps. Multilocational farmer's field survey was conducted for several years to observe the production systems and associated injuries. Similarly, the field experiments performed to assess disease damage and crop losses. Mechanistic models were developed by using this collected data based on the damage mechanisms. This approach was used to simulate pest and disease systems in Asian rice-growing regions (Willocquet et al. 2004; Willocquet et al. 2002) and European and UK wheat-growing regions (Willocquet et al. 2008; Foster et al. 2004).

12.7.5.2 APSIM-DYMEX

APSIM (Agriculture Production Systems Simulator) is a modeling framework developed over the last two decades (Holzworth et al. 2015). APSIM does not have the ability to consider pests and diseases. But recently, it has been linked with DYMEX (Whish et al. 2015). DYMEX is a mechanistic model for simulation of pests, diseases, and weeds life cycles. Models involved in DYMEX are enabled to run in the DYMAX simulator (Whish et al. 2015). The coupling of these modules enabled the multi-point APSIM features with simplified communication within both models. Both these frameworks can simultaneously model the crop growth and disease dynamics.

12.7.5.3 BioMA-Diseases

For fungal plant disease modeling, this framework was developed, having four extendable software (Bregaglio and Donatelli 2015). This framework is used for modeling the impacts of fungal epidemics on plant growth. It simulates and quantifies the polycyclic fungal epidemics and impacts of epidemics on crops. BioMA is a public-domain framework to parameterize and run the biophysical models in the agriculture field (Fig.12.2). This module was applied to study major diseases such as brown rust (wheat) and leaf blast (Carlsson et al. 2008) in Europe, China, and Italy and assess the model behavior under diverse environments (Bregaglio et al. 2016).

12.7.5.4 NAPPFAST

NAPPFAST (North Carolina State University/Animal and Plant Health Inspection Service Plant Pest Forecasting System) module was developed during a project from 2002 to 2013 (Magarey et al. 2007; Magarey et al. 2015) with having an Internet-based GUI (graphical user interface). This module was interlinked with the weather datasets. It has three simulation modeling templates: phenology models (with degree-day approach), infection models (with pathogens and diseases approach), and generic models (with a simple empirical model approach). All these templates were generic to meet the diverse needs of users. NAPPFAST has the ability of pest risk mapping with several resolutions (Magarey et al. 2011).

12.7.6 Case Study

Climate variability has significant impact on interactions among plants, pests, and diseases. However, limited research has been conducted on disease severity, incidence, and distribution in response to the changing climate. Few studies simulated the future potential changes in disease epidemics and plant health (Sparks et al. 2014; Bregaglio et al. 2013). Application of disease models can dissect the role of climate change in disease spread, severity, and plant health.

Black Sigatoka is a major disease of tropical crops especially banana. The causal agent of this disease *Pseudocercospora fijiensis* is dependent on microclimate and weather variables. It requires the high relative humidity and leaf wet surface to

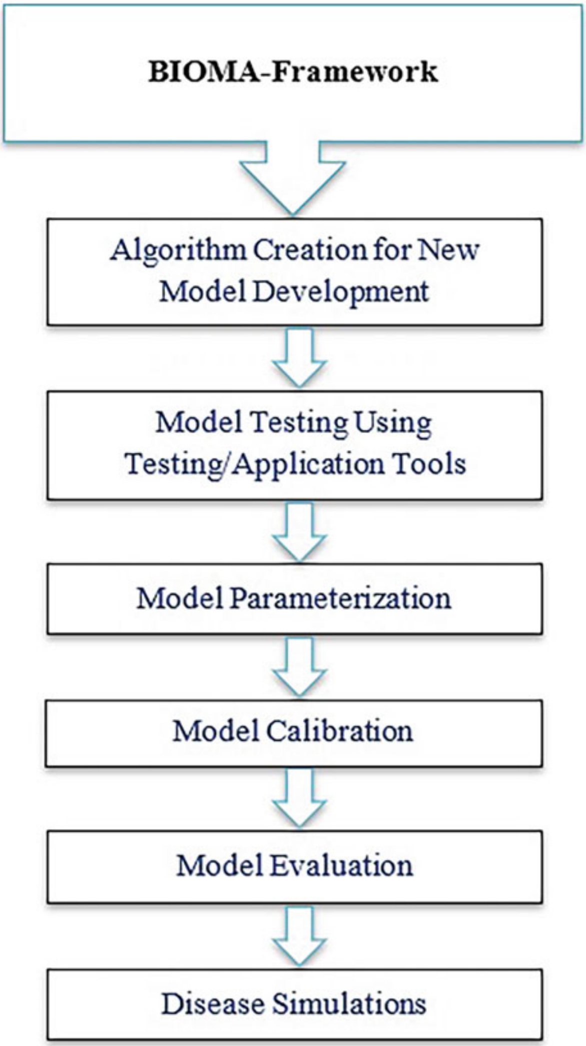

Fig. 12.2 BIOMA modeling framework

germinate and cause infections in banana plant (Uchôa et al. 2012). A disease model for simulating the Black Sigatoka in future climate change scenarios was developed by using the climate data of banana growing areas in Caribbean and Latin America (Bebber 2019). During the process of model development past 60 years observed and reported climate data was used to parameterize the model. The temperature (T_{min}, T_{max}, and T_{opt}) and leaf wetness data were used to develop and parameterize the model. The data regarding these variables was observed at 3-h intervals in studied regions.

The model simulated the fraction of spore's cohort development F (t) over the time (t) during the wet intervals and had a Weibull hazard (H) function based on prevailing temperature (T). The temperature-dependent cohort development rate (r) was simulated on the basis of cardinal temperatures such as $T_{\min}$, $T_{\max}$, and T_{opt}. Model was parameterized using observations and simulations based on $T_{\min}$, $T_{\max}$, T_{opt}, the scale factor (α) and shape parameter (ɤ) for hazard function.

$$F\ (t, T) = 1 - \bar{e}^{H(t,T)}$$

$$H\ (t, T) = r(T)\ [t/\alpha]^{\gamma}$$

$$r(T) = \left[T_{\max} - T/T_{\max} - T_{\text{opt}}\right] * \left[T - T_{\min}/T_{\text{opt}} - T_{\min}\right]^{T_{\text{opt}} - T_{\min}/T_{\max} - T_{\text{opt}}}$$

Disease simulations using this model defined the Black Sigatoka infection risks on the basis of total number of simulated spore's cohorts per hour over a specific time duration. Disease simulations predicted the 44% increase in infection rate of Black Sigatoka across Caribbean and Latin America since 1960. This simulated increase was due to the increased temperature and leaf surface wetness that favored the pathogen infection ability. Conclusively, the changing climate and global trading of banana resulted in the establishment of more conducive environment in banana growing regions for Black Sigatoka infection.

12.7.7 Strategies for Effective Disease Modeling

There are some effective strategies that can be used to enhance the reliability of simulation in agricultural disease and crop modeling. These strategies comprise the actions to enhance the availability of quality data for disease model input and model evaluation, coupling with crop models, and develop the modeler's community to share the knowledge.

Process-based disease modeling is aimed to reproduce the dynamics of biophysical processes depending on the input variables. Pathogen growth and development are highly dependent on weather variables; hence the model should modulate the responses according to the fluctuations in model input variables (Pfender et al. 2012; Magarey et al. 2005). Therefore, the availability of high resolution and quality data is essential to calibrate the model, especially for the moisture- and temperature-mediated responses. Low-quality data reduces the reliability of model empirical coefficients and impede the model fitness and application. Hence, the quality input dataset is a key in crop disease modeling and the high-resolution real-time data regarding temperature, humidity, and leaf wetness are required to minimize the uncertainties during model calibration and evaluation.

Field measurements and data about the impacts of diseases on crops have been collected in previous years, but these observation methods had no standards and usually are not coupled with crop and weather data to be used as disease modeling data input (Esker et al. 2012; Nutter Jr 1989). Consequently, the disease model validation was limited across diversified environments (Willocquet et al. 2004; Willocquet et al. 2002). Hence, the development of designs, guides, templates, and protocols is needed to collect the adequate and required standard data to validate the disease models effectively (Willocquet et al. 2000). Detailed observations should include the disease or pest data (Disease severity, incidence, injury level), weather data (temperature, humidity, and leaf wetness), and crop data (physiological processes such as respiration, photosynthesis, senescence, etc.) (Esker et al. 2012; Savary et al. 2006).

The disease and host crop dynamics are the coupling points among disease and crop models. Quantification of disease damage and injuries can be assessed by performing experiments in different pathosystems (Robert et al. 2005; Bassanezi et al. 2001). Mathematical representation of these injuries may enable the integration into crop models for simulation of biophysical processes (Pavan and Fernandes 2009). Disease simulation modeling can be done in conjunction with crop growth models to assess the impacts of disease on crop growth. However, the integration of disease and crop models may lead to issues such as complexity in model structures, binary incompatibilities, and sharing difficulties. There are some critical points to be considered for integrating the disease and crop models. Identification and adequate knowledge about damage mechanisms are necessary to simulate the disease impacted outputs by crop models. The disease model's output must be compatible directly or indirectly with the crop model variables. Moreover, the communication compatibilities of both types of models must also be considered for the efficient integration of disease and crop models. Crop model selection to integrate with the disease model must consider the presence of variables affected by the disease in both kinds of models.

Lack of modeling community and cohesive research hampered the development of improved and advanced disease models. Such modelers community development efforts may help in the efficient understanding of biophysical processes, system behaviors, and bridge the communication gaps. However, there are several limitations in such efforts like limited availability of generic disease model frameworks that allow the shift between pathogens and pests. Similarly, modeling cooperation efforts are limited due to the inadequate availability of standard data. In 2015, PeDiMiP (Pest and Disease Modeling Inter-comparison Project) was launched as part of the AgMIP (Agricultural Modeling Inter-comparison Project) to improve disease and pest modeling and to assess the impacts of climate change on crop losses. This project is mainly focused on modeling of crop health, wheat rust, and potato late blight diseases.

12.8 Plant Disease Management

Climate change increases the plant protection complexity. It also causes changes in the chemical market due to the changes in pathogen distribution. Similarly, climate change results in the resistance development in pathogens which ultimately leads to the increased cost for crop production due to high application rates and treatments (Juroszek and Von Tiedemann 2011). Some production systems show more flexibility than others to adopt better practices and strategies to reduce certain diseases.

However, adaptation strategies depend on cost-benefit analyses. One of the great strategies in changing climate involves the efficiency evaluation of current biological, physical, and chemical practices. We can prevent the increased risk of diseases under predicted climate change by using various agronomic practices (irrigation, crop rotation, etc.) that can minimize the overwintering amount of inoculum (Juroszek and Von Tiedemann 2011). There is a need for adjustment in management strategies under changing climate. In biological control, the populations vary with changes in environmental conditions. Under the extreme condition of the environment, the populations of biological agents may become smaller and do not recover even in favorable conditions. Disease management may be affected by climate change and results in uncertainties in decision making when climate variability is greater. But, El Nino-based climate predictions were useful in decision making for farmers of Zimbabwe (Patt et al. 2005).

12.9 Knowledge Gaps and Future Directions

Over the past decade, climate change studies have improved the understanding of how environmental factors impact plant disease epidemics. Climate change is not occurring in isolation, and it may intensify in the coming years. While only a few studies were carried out to evaluate the combined impact of multiple factors, evaluation of the combined effect of various factors on hosts, pathogens, and diseases is needed. Simulation modeling provides an opportunity to simulate several factors simultaneously. While climatic models used to study the impacts of climate change on plant diseases focused on a few variables like precipitation and rainfall, models based on multiple factors should be used to study climate changes and plant disease relationships. Molecular analysis and mechanistic studies can help to consider the change in plant diseases as a result of climate change. Over the past few years, foliar diseases are mainly focused while little work has been done on soilborne diseases. Therefore, studies should be conducted to evaluate the climate change impacts on soilborne diseases.

Plant disease management and severity will probably be increased due to climate change. Prediction of diseases and their management is of great interest to farmers and agro-industries. The following plant protection strategies can help in disease management to a certain extent:

1. Use of models to forecast disease epidemics
2. Crop rotation
3. Diversity in crop species
4. Use cultivars with superior disease resistance
5. Adjustment in sowing time
6. Effective quarantine measures
7. Use of Integrated Pest Management strategy

12.10 Conclusion

Climate change is impacting the crops, trees, and agricultural productivity and, at the same time, influencing the pathogens and disease development in plants. It is a major challenge to understand and realize the impacts of climate change in terms of plant diseases, pathogens, and health of plants because of the limitation in the knowledge that how various changes in the atmosphere are affecting the physiology of host and pathogens development, spread and resistance in host and pathogen. Achievements in plant protection are limited due to the lack of knowledge about changes in the environment, pathogen, and host interaction globally. For effective plant protection and disease management, detailed study and research are needed to understand the relationship among the changing environment, pathogens, and hosts under the climate change scenario. Modeling of diseases can become more effective if we combine the developed tools in our studies.

References

Ahmad S, Hasanuzzaman M (2020) Cotton production and uses. Springer Nature Singapore Pvt. Ltd., Singapore, 641 pp. https://doi.org/10.1007/978-981-15-1472-2

Ahmed M (2020) Introduction to modern climate change. Andrew E. Dessler: Cambridge University Press, 2011, 252 pp, ISBN-10: 0521173159. Sci Total Environ 734:139397. https://doi.org/10.1016/j.scitotenv.2020.139397

Ahmed M, Ahmad S (2019) Carbon dioxide enrichment and crop productivity. In: Hasanuzzaman M (ed) Agronomic crops, Management practices, vol 2. Springer Singapore, Singapore, pp 31–46. https://doi.org/10.1007/978-981-32-9783-8_3

Ahmed M, Stockle CO (2016) Quantification of climate variability, adaptation and mitigation for agricultural sustainability. Springer Nature Singapore Pvt. Ltd., Singapore, 437 pp. https://doi.org/10.1007/978-3-319-32059-5

Ahmed K, Shabbir G, Ahmed M, Shah KN (2020) Phenotyping for drought resistance in bread wheat using physiological and biochemical traits. Sci Total Environ 729:139082. https://doi.org/10.1016/j.scitotenv.2020.139082

Alves MC, de Carvalho L, Pozza E, Sanches L, Maia JS (2011) Ecological zoning of soybean rust, coffee rust and banana black sigatoka based on Brazilian climate changes. Procedia Environ Sci 6:35–49

Asselbergh B, De Vleesschauwer D, Hofte M (2008) Global switches and fine-tuning—ABA modulates plant pathogen defense. Mol Plant-Microbe Interact 21(6):709–719

Aurambout J, Finlay KJ, Luck J, Beattie G (2009) A concept model to estimate the potential distribution of the Asiatic citrus psyllid (Diaphorina citri Kuwayama) in Australia under climate change—a means for assessing biosecurity risk. Ecol Model 220(19):2512–2524

Baker R, Sansford C, Jarvis C, Cannon R, MacLeod A, Walters K (2000) The role of climatic mapping in predicting the potential geographical distribution of non-indigenous pests under current and future climates. Agric Ecosyst Environ 82(1–3):57–71

Barnard R, Leadley PW, Lensi R, Barthes L (2005) Plant, soil microbial and soil inorganic nitrogen responses to elevated CO2: a study in microcosms of Holcus lanatus. Acta Oecol 27(3):171–178

Barnes AP, Wreford A, Butterworth MH, Semenov MA, Moran D, Evans N, Fitt BD (2010) Adaptation to increasing severity of phoma stem canker on winter oilseed rape in the UK under climate change. J Agric Sci 148(6):683–694

Bassanezi R, Amorim L, Filho AB, Hau B, Berger R (2001) Accounting for photosynthetic efficiency of bean leaves with rust, angular leaf spot and anthracnose to assess crop damage. Plant Pathol 50(4):443–452

Bastiaans L, Rabbinge R, Zadoks J (1994) Understanding and modeling leaf blast effects on crop physiology and yield. In: Rice blast disease. IRRI, Los Baños, pp 357–380

Bebber DP (2019) Climate change effects on black Sigatoka disease of banana. Philos Trans R Soc B 374(1775):20180269

Beddow JM, Pardey PG, Chai Y, Hurley TM, Kriticos DJ, Braun H-J, Park RF, Cuddy WS, Yonow T (2015) Research investment implications of shifts in the global geography of wheat stripe rust. Nat Plants 1(10):15132

Berger S, Sinha AK, Roitsch T (2007) Plant physiology meets phytopathology: plant primary metabolism and plant–pathogen interactions. J Exp Bot 58(15–16):4019–4026

Boote K, Jones J, Mishoe J, Berger R (1983) Coupling pests to crop growth simulators to predict yield reductions [Mathematical models]. Phytopathology (USA) 73:1581

Booth T, Jovanovic T, Old K, Dudzinski M (2000) Climatic mapping to identify high-risk areas for Cylindrocladium quinqueseptatum leaf blight on eucalypts in mainland South East Asia and around the world. Environ Pollut 108(3):365–372

Bosch J, Carrascal LM, Duran L, Walker S, Fisher MC (2007) Climate change and outbreaks of amphibian chytridiomycosis in a montane area of Central Spain; is there a link? Proc R Soc Lond B Biol Sci 274(1607):253–260

Bradley BA, Blumenthal DM, Early R, Grosholz ED, Lawler JJ, Miller LP, Sorte CJ, D'Antonio CM, Diez JM, Dukes JS (2012) Global change, global trade, and the next wave of plant invasions. Front Ecol Environ 10(1):20–28

Brasier CM (1996) Phytophthora cinnamomi and oak decline in southern Europe. Environmental constraints including climate change. In: Annales des Sciences Forestieres. EDP Sciences (Édition Diffusion Presse Sciences), Ray Ulysse, vol 2–3, pp 347–358

Brasier CM, Scott JK (1994) European oak declines and global warming: a theoretical assessment with special reference to the activity of Phytophthora cinnamomi. EPPO Bull 24(1):221–232

Bregaglio S, Donatelli M (2015) A set of software components for the simulation of plant airborne diseases. Environ Model Softw 72:426–444

Bregaglio S, Donatelli M, Confalonieri R, Acutis M, Orlandini S (2010) An integrated evaluation of thirteen modelling solutions for the generation of hourly values of air relative humidity. Theor Appl Climatol 102(3–4):429–438

Bregaglio S, Cappelli G, Donatelli M (2012) Evaluating the suitability of a generic fungal infection model for pest risk assessment studies. Ecol Model 247:58–63

Bregaglio S, Donatelli M, Confalonieri R (2013) Fungal infections of rice, wheat, and grape in Europe in 2030–2050. Agron Sustain Dev 33(4):767–776

Bregaglio S, Titone P, Cappelli G, Tamborini L, Mongiano G, Confalonieri R (2016) Coupling a generic disease model to the WARM rice simulator to assess leaf and panicle blast impacts in a temperate climate. Eur J Agron 76:107–117

Brosi GB, McCulley RL, Bush LP, Nelson JA, Classen AT, Norby RJ (2011) Effects of multiple climate change factors on the tall fescue–fungal endophyte symbiosis: infection frequency and tissue chemistry. New Phytol 189(3):797–805

Browder L, Eversmeyer M (1986) Interactions of temperature and time with some Puccinia recondita: triticum corresponding gene pairs. Phytopathology (USA) 76:1286

Caffarra A, Rinaldi M, Eccel E, Rossi V, Pertot I (2012) Modelling the impact of climate change on the interaction between grapevine and its pests and pathogens: european grapevine moth and powdery mildew. Agric Ecosyst Environ 148:89–101

Carlsson AS, Chanana NP, Gudu S, Suh MC, Were BAI (2008) Sesame. compendium of transgenic crop plants

Carter TR, Saarikko RA, Niemi KJ (1996) Assessing the risks and uncertainties of regional crop potential under a changing climate in Finland. Agric Food Sci 5(3):329–350

Chakraborty S (2005) Potential impact of climate change on plant-pathogen interactions. Australas Plant Pathol 34(4):443–448
Chakraborty S (2013) Migrate or evolve: options for plant pathogens under climate change. Glob Chang Biol 19(7):1985–2000
Chakraborty S, Datta S (2003) How will plant pathogens adapt to host plant resistance at elevated CO2 under a changing climate? New Phytol 159(3):733–742
Chakraborty S, Murray G, White N (2002) Impact of climate change on important plant diseases in Australia: a report for the Rural Industries Research and Development Corporation
Christiansen MN (1982) Breeding plants for less favorable environments
Coakley SM, Scherm H, Chakraborty S (1999) Climate change and plant disease management. Annu Rev Phytopathol 37(1):399–426
Davelos AL, Kinkel LL, Samac DA (2004) Spatial variation in frequency and intensity of antibiotic interactions among Streptomycetes from prairie soil. Appl Environ Microbiol 70(2):1051–1058
De Pondeca MS, Manikin GS, DiMego G, Benjamin SG, Parrish DF, Purser RJ, Wu W-S, Horel JD, Myrick DT, Lin Y (2011) The real-time mesoscale analysis at NOAA's National Centers for Environmental Prediction: current status and development. Weather Forecast 26(5):593–612
Desprez-Loustau M-L, Marcais B, Nageleisen L-M, Piou D, Vannini A (2006) Interactive effects of drought and pathogens in forest trees. Ann For Sci 63(6):597–612
Dillehay B, Calvin DD, Roth GW, Hyde J, Kuldau GA, Kratochvil R, Russo J, Voight D (2005) Verification of a European corn borer (Lepidoptera: Crambidae) loss equation in the major corn production region of the northeastern United States. J Econ Entomol 98(1):103–112
Donatelli M, Magarey RD, Bregaglio S, Willocquet L, Whish JP, Savary S (2017) Modelling the impacts of pests and diseases on agricultural systems. Agric Syst 155:213–224
Duveiller E, Singh RP, Nicol JM (2007) The challenges of maintaining wheat productivity: pests, diseases, and potential epidemics. Euphytica 157(3):417–430
Esker PD, Savary S, McRoberts N (2012) Crop loss analysis and global food supply: focusing now on required harvests. CAB Rev 7(052):1–14
Foster GN, Blake S, Tones SJ, Barker I, Harrington R (2004) Occurrence of barley yellow dwarf virus in autumn-sown cereal crops in the United Kingdom in relation to field characteristics. Pest Manag Sci Formerly Pestic Sci 60(2):113–125
Francesca S, Simona G, Francesco Nicola T, Andrea R, Vittorio R, Federico S, Cynthia R, Maria Lodovica G (2006) Downy mildew (Plasmopara viticola) epidemics on grapevine under climate change. Glob Chang Biol 12(7):1299–1307
Frankel S (2007) Climate change's influence on sudden oak death, PACLIM 2007, Monterey, CA, 13–15 May 2007
Fuhrer J (2003) Agroecosystem responses to combinations of elevated CO2, ozone, and global climate change. Agric Ecosyst Environ 97(1–3):1–20
Garbelotto M, Linzer R, Nicolotti G, Gonthier P (2010) Comparing the influences of ecological and evolutionary factors on the successful invasion of a fungal forest pathogen. Biol Invasions 12 (4):943–957
Garrett KA, Dendy SP, Frank EE, Rouse MN, Travers SE (2006) Climate change effects on plant disease: genomes to ecosystems. Annu Rev Phytopathol 44:489–509
Garrett KA, Nita M, De Wolf E, Esker PD, Gomez-Montano L, Sparks AH (2015) Plant pathogens as indicators of climate change. In: Climate change, Second edn. Elsevier, Dordrecht, pp 325–338
Ghini R, Hamada E, Goncalves RR, Gasparotto L, Pereira JCR (2007) Risk analysis of climatic change on black Sigatoka on banana in Brazil. Fitopatol Bras 32(3):197–204
Ghini R, Hamada E, Júnior P, José M, Marengo JA, Gonçalves RRDV (2008) Risk analysis of climate change on coffee nematodes and leaf miner in Brazil. Pesq Agrop Brasileira 43 (2):187–194
Ghini R, Hamada E, Junior P, Jose M, Goncalves RRDV (2011) Incubation period of Hemileia vastatrix in coffee plants in Brazil simulated under climate change. Summa Phytopathol 37 (2):85–93

Gioria R, Brunelli K, Kobori R (2008) Impacto potencial das mudanças climáticas sobre as doenças de hortaliças: tomate, um estudo de caso. Summa Phytopathologica 34(supl):187–194
Gouache D, Roche R, Pieri P, Bancal M-O (2011) Evolution of some pathosystems on wheat and vines. Climate change, agriculture and forests in France: simulations of the impacts on the main species The Green Book of the CLIMATOR project (2007–2010), part C (The crops), section B5 Health:113–126
Gramaje D, Baumgartner K, Halleen F, Mostert L, Sosnowski M, Úrbez-Torres J, Armengol J (2016) Fungal trunk diseases: a problem beyond grapevines. Plant Pathol 65(3):355–356
Grulke NE (2011) The nexus of host and pathogen phenology: understanding the disease triangle with climate change. New Phytol 189(1):8–11
Hamada E, Ghini R, GONÇALVES RdV (2006) Efeito da mudança climática sobre problemas fitossanitários de plantas: metodologia de elaboração de mapas. Embrapa Meio Ambiente-Artigo em periódico indexado (ALICE)
Hibberd J, Whitbread R, Farrar J (1996) Effect of 700 μmol mol− $1CO_2$ and infection with powdery mildew on the growth and carbon partitioning of barley. New Phytol 134(2):309–315
Hirschi M, Stoeckli S, Dubrovsky M, Spirig C, Calanca P, Rotach M, Fischer A, Duffy B, Samietz J (2012) Downscaling climate change scenarios for apple pest and disease modeling in Switzerland. Earth Syst Dynam 3(1):33–47
Holzworth DP, Snow V, Janssen S, Athanasiadis IN, Donatelli M, Hoogenboom G, White JW, Thorburn P (2015) Agricultural production systems modelling and software: current status and future prospects. Environ Model Softw 72:276–286
Hong SC, Magarey R, Borchert DM, Vargas RI, Souder S (2015) Site-specific temporal and spatial validation of a generic plant pest forecast system with observations of Bactrocera dorsalis (oriental fruit fly). NeoBiota 27:37
Hu S, Chapin F III, Firestone M, Field C, Chiariello N (2001) Nitrogen limitation of microbial decomposition in a grassland under elevated CO 2. Nature 409(6817):188
Huber L, Gillespie T (1992) Modeling leaf wetness in relation to plant disease epidemiology. Annu Rev Phytopathol 30(1):553–577
Hungate BA, Canadell J, Chapin FS (1996) Plant species mediate changes in soil microbial N in response to elevated CO2. Ecology 77(8):2505–2515
Huseynova I, Sultanova N, Mammadov A, Suleymanov S, Aliyev JA (2014) Biotic stress and crop improvement. In: Improvement of crops in the era of climatic changes. Springer, New York, pp 91–120
Isard SA, Russo JM, Magarey RD, Golod J, VanKirk JR (2015) Integrated pest information platform for extension and education (iPiPE): progress through sharing. J Integr Pest Manag 6 (1):15
Jung T (2009) Beech decline in Central Europe driven by the interaction between Phytophthora infections and climatic extremes. For Pathol 39(2):73–94
Junior J, Valadares Júnior R, Cecílio RA, Moraes WB, FXRD V, Alves FR, Paul PA (2008) Worldwide geographical distribution of Black Sigatoka for banana: predictions based on climate change models. Scientia Agricola 65(SPE):40–53
Juroszek P, Von Tiedemann A (2011) Potential strategies and future requirements for plant disease management under a changing climate. Plant Pathol 60(1):100–112
Juroszek P, von Tiedemann A (2015) Linking plant disease models to climate change scenarios to project future risks of crop diseases: a review. J Plant Dis Prot 122(1):3–15
Kannadan S, Rudgers J (2008) Endophyte symbiosis benefits a rare grass under low water availability. Funct Ecol 22(4):706–713
Kaplan I, Denno RF (2007) Interspecific interactions in phytophagous insects revisited: a quantitative assessment of competition theory. Ecol Lett 10(10):977–994
Karnosky D, Percy KE, Xiang B, Callan B, Noormets A, Mankovska B, Hopkin A, Sober J, Jones W, Dickson R (2002) Interacting elevated CO2 and tropospheric O3 predisposes aspen (Populus tremuloides Michx.) to infection by rust (Melampsora medusae f. sp. tremuloidae). Glob Chang Biol 8(4):329–338

Katz RW (2002) Techniques for estimating uncertainty in climate change scenarios and impact studies. Clim Res 20(2):167–185

Kranz J (1974) The role and scope of mathematical analysis and modeling in epidemiology. In: Epidemics of plant diseases. Springer, Berlin, pp 7–54

Kudela V (2009) Potential impact of climate change on geographic distribution of plant pathogenic bacteria in Central Europe. Plant Prot Sci 45(Special Issue):S27–S32

Ladanyi M, Horvath L (2010) A review of the potential climate change impact on insect populations- general and agricultural aspects. Appl Ecol Environ Res 8(2):143–152

Launay M, Caubel J, Bourgeois G, Huard F, de Cortazar-Atauri IG, Bancal M-O, Brisson N (2014) Climatic indicators for crop infection risk: application to climate change impacts on five major foliar fungal diseases in Northern France. Agric Ecosyst Environ 197:147–158

Legler SE, Caffi T, Rossi V (2012) A nonlinear model for temperature-dependent development of Erysiphe necator chasmothecia on grapevine leaves. Plant Pathol 61(1):96–105

Lewis E (1977) On the generation and growth of a population. In: Mathematical demography. Springer, Berlin, pp 221–225

Luo Y, Tebeest D, Teng P, Fabellar N (1995) Simulation studies on risk analysis of rice leaf blast epidemics associated with global climate change in several Asian countries. J Biogeography 22:673–678

Madden L, Ellis M (1988) How to develop plant disease forecasters. In: Experimental techniques in plant disease epidemiology. Springer, Berlin, pp 191–208

Madden LV, Hughes G, Van Den Bosch F (2007) The study of plant disease epidemics

Magarey R, Seem R, Russo J, Zack J, Waight K, Travis J, Oudemans P (2001) Site-specific weather information without on-site sensors. Plant Dis 85(12):1216–1226

Magarey R, Travis J, Russo J, Seem R, Magarey P (2002) Decision support systems: quenching the thirst. Plant Dis 86(1):4–14

Magarey R, Sutton T, Thayer C (2005) A simple generic infection model for foliar fungal plant pathogens. Phytopathology 95(1):92–100

Magarey R, Russo J, Seem R (2006) Simulation of surface wetness with a water budget and energy balance approach. Agric For Meteorol 139(3–4):373–381

Magarey R, Fowler G, Borchert D, Sutton T, Colunga-Garcia M, Simpson J (2007) NAPPFAST: an internet system for the weather-based mapping of plant pathogens. Plant Dis 91(4):336–345

Magarey RD, Borchert D, Engle J, Colunga-Garcia M, Koch FH, Yemshanov D (2011) Risk maps for targeting exotic plant pest detection programs in the United States. EPPO Bull 41(1):46–56

Magarey RD, Borchert DM, Fowler GA, Hong SC, Venette R (2015) The NCSU/APHIS plant pest forecasting system (NAPPFAST). Pest risk modelling and mapping for invasive alien species. CABI, Wallingford, pp 82–96

Manici L, Bregaglio S, Fumagalli D, Donatelli M (2014) Modelling soil borne fungal pathogens of arable crops under climate change. Int J Biometeorol 58(10):2071–2083

Melloy P, Aitken E, Luck J, Chakraborty S, Obanor F (2014) The influence of increasing temperature and CO2 on Fusarium crown rot susceptibility of wheat genotypes at key growth stages. Eur J Plant Pathol 140(1):19–37

Mikkelsen BL, Jørgensen RB, Lyngkjær MF (2015) Complex interplay of future climate levels of CO 2, ozone and temperature on susceptibility to fungal diseases in barley. Plant Pathol 64 (2):319–327

Moraes WB, Peixoto L, Jesus Junior W, Moraes W, Cecilio R (2011) Impacts of climate change on the risk on occurrence of the southern corn rust of the maize in Brasil. Enciclopedia Biosfera 7:1–12

Moraes BW, de Jesus Junior CW, de Azevedo Peixoto L, Moraes WB, Coser SM, Cecílio RA (2012a) Impact of climate change on the phoma leaf spot of coffee in Brazil. Interciencia 37:272–278

Moraes BW, Júnior J, Peixoto LA, Moraes WB, Furtado EL, LGD S, Cecílio RA, Alves FR (2012b) An analysis of the risk of cocoa moniliasis occurrence in Brazil as the result of climate change. Summa Phytopathol 38(1):30–35

Nancarrow N, Constable FE, Finlay KJ, Freeman AJ, Rodoni BC, Trebicki P, Vassiliadis S, Yen AL, Luck JE (2014) The effect of elevated temperature on barley yellow dwarf virus-PAV in wheat. Virus Res 186:97–103

Newton A, Young I (1996) Temporary partial breakdown of Mlo-resistance in spring barley by the sudden relief of soil water stress. Plant Pathol 45(5):973–977

Nutter FW Jr (1989) Detection and measurement of plant disease gradients in peanut with a multispectral radiometer. Phytopathology 79(9):958–963

Otten W, Bailey DJ, Gilligan CA (2004) Empirical evidence of spatial thresholds to control invasion of fungal parasites and saprotrophs. New Phytol 163(1):125–132

Pariaud B, Ravigné V, Halkett F, Goyeau H, Carlier J, Lannou C (2009) Aggressiveness and its role in the adaptation of plant pathogens. Plant Pathol 58(3):409–424

Patt A, Suarez P, Gwata C (2005) Effects of seasonal climate forecasts and participatory workshops among subsistence farmers in Zimbabwe. Proc Natl Acad Sci 102(35):12623–12628

Pavan W, Fernandes JMC (2009) Uso de orientação a objetos no desenvolvimento de modelos de simulação de doenças de plantas genéricos. Revista Brasileira de Agroinformática 9(1):12–27

Pavan W, Fraisse C, Peres N (2011) Development of a web-based disease forecasting system for strawberries. Comput Electron Agric 75(1):169–175

Pennypacker B, Leath K, Hill R Jr (1991) Impact of drought stress on the expression of resistance to Verticillium albo-atrum in alfalfa. Phytopathology (USA) 81(9):1014

Perkins LB, Leger EA, Nowak RS (2011) Invasion triangle: an organizational framework for species invasion. Ecol Evol 1(4):610–625

Pfender W, Gent D, Mahaffee W (2012) Sensitivity of disease management decision aids to temperature input errors associated with sampling interval and out-of-canopy sensor placement. Plant Dis 96(5):726–736

Plazek A, Hura K, Rapacz M, Zur I (2001) The influence of ozone fumigation on metabolic efficiency and plant resistance to fungal pathogens. J Appl Bot Food Qual 75:8–13

Plessl M, Heller W, Payer HD, Elstner E, Habermeyer J, Heiser I (2005) Growth parameters and resistance against Drechslera teres of spring barley (Hordeum vulgare L. cv. Scarlett) grown at elevated ozone and carbon dioxide concentrations. Plant Biol 7(6):694–705

Pritchard S, Rogers H, Prior SA, Peterson C (1999) Elevated CO2 and plant structure: a review. Glob Chang Biol 5(7):807–837

Prospero S, Grünwald N, Winton L, Hansen E (2009) Migration patterns of the emerging plant pathogen Phytophthora ramorum on the west coast of the United States of America. Phytopathology 99(6):739–749

Rabbinge R (1993) The ecological background of food production. In: Ciba foundation symposium. Wiley Online Library, pp 2–2

Rakotonindraina T, Chauvin J-E, Pellé R, Faivre R, Chatot C, Savary S, Aubertot J-N (2012) Modeling of yield losses caused by potato late blight on eight cultivars with different levels of resistance to Phytophthora infestans. Plant Dis 96(7):935–942

Regniere J (2011) Invasive species, climate change and forest health. In: Forests in development: a vital balance. Springer, Dordrecht, pp 27–37

Régnière J, Powell J, Bentz B, Nealis V (2012) Effects of temperature on development, survival and reproduction of insects: experimental design, data analysis and modeling. J Insect Physiol 58 (5):634–647

Richerzhagen D, Racca P, Zeuner T, Kuhn C, Falke K, Kleinhenz B, Hau B (2011) Impact of climate change on the temporal and regional occurrence of Cercospora leaf spot in Lower Saxony. J Plant Dis Prot 118(5):168–177

Riesenfeld CS, Schloss PD, Handelsman J (2004) Metagenomics: genomic analysis of microbial communities. Annu Rev Genet 38:525–552

Robert C, Bancal M-O, Lannou C, Ney B (2005) Quantification of the effects of Septoria tritici blotch on wheat leaf gas exchange with respect to lesion age, leaf number, and leaf nitrogen status. J Exp Bot 57(1):225–234

Rodriguez RJ, Henson J, Van Volkenburgh E, Hoy M, Wright L, Beckwith F, Kim Y-O, Redman RS (2008) Stress tolerance in plants via habitat-adapted symbiosis. ISME J 2(4):404
Rosenzweig C, Jones JW, Hatfield JL, Ruane AC, Boote KJ, Thorburn P, Antle JM, Nelson GC, Porter C, Janssen S (2013) The agricultural model intercomparison and improvement project (AgMIP): protocols and pilot studies. Agric For Meteorol 170:166–182
Rossi V, Giosuè S, Caffi T (2009) Modelling the dynamics of infections caused by sexual and asexual spores during Plasmopara viticola epidemics. J Plant Pathol 91:615–627
Rouse D (1988) Use of crop growth-models to predict the effects of disease. Annu Rev Phytopathol 26(1):183–201
Runion G, Curl E, Rogers H, Backman P, Rodriguez-Kabana R, Helms B (1994) Effects of free-air CO2 enrichment on microbial populations in the rhizosphere and phyllosphere of cotton. Agric For Meteorol 70(1–4):117–130
Saha S, Moorthi S, Wu X, Wang J, Nadiga S, Tripp P, Behringer D, Hou Y-T, H-y C, Iredell M (2014) The NCEP climate forecast system version 2. J Clim 27(6):2185–2208
Salam MU, MacLeod WJ, Salam KP, Maling T, Barbetti MJ (2011) Impact of climate change in relation to ascochyta blight on field pea in Western Australia. Australas Plant Pathol 40(4):397
Salinari F, Giosuè S, Rossi V, Tubiello FN, Rosenzweig C, Gullino ML (2007) Downy mildew outbreaks on grapevine under climate change: elaboration and application of an empirical-statistical model. EPPO Bull 37(2):317–326
Sandermann JH (2000) Ozone/biotic disease interactions: molecular biomarkers as a new experimental tool. Environ Pollut 108(3):327–332
Savary S, Willocquet L (2014) Simulation modeling in botanical epidemiology and crop loss analysis. Plant Health Instruct. https://doi.org/10.1094/PHI-A-2014-0314-01
Savary S, Teng PS, Willocquet L, Nutter FW Jr (2006) Quantification and modeling of crop losses: a review of purposes. Annu Rev Phytopathol 44:89–112
Scherm H (2000) Simulating uncertainty in climate–pest models with fuzzy numbers. Environ Pollut 108(3):373–379
Scherm H (2004) Climate change: can we predict the impacts on plant pathology and pest management? Can J Plant Pathol 26(3):267–273
Seherm H, Coakley SM (2003) Plant pathogens in a changing world. Australas Plant Pathol 32 (2):157–165
Shabani F, Kumar L (2013) Risk levels of invasive Fusarium oxysporum f. sp. in areas suitable for date palm (Phoenix dactylifera) cultivation under various climate change projections. PLoS One 8(12):e83404
Sparks AH, Forbes GA, Hijmans RJ, Garrett KA (2014) Climate change may have limited effect on global risk of potato late blight. Glob Chang Biol 20(12):3621–3631
Stein LD, Mungall C, Shu S, Caudy M, Mangone M, Day A, Nickerson E, Stajich JE, Harris TW, Arva A (2002) The generic genome browser: a building block for a model organism system database. Genome Res 12(10):1599–1610
Stern N (2008) The economics of climate change. Am Econ Rev 98(2):1–37
Stone JK, Coop LB, Manter DK (2008) Predicting effects of climate change on Swiss needle cast disease severity in Pacific Northwest forests. Can J Plant Pathol 30(2):169–176
Sturrock R, Frankel S, Brown A, Hennon P, Kliejunas J, Lewis K, Worrall J, Woods A (2011) Climate change and forest diseases. Plant Pathol 60(1):133–149
Sutherst R, Maywald G, Kriticos D (2007) CLIMEX version 3: user's guide
Sutherst RW, Constable F, Finlay KJ, Harrington R, Luck J, Zalucki MP (2011) Adapting to crop pest and pathogen risks under a changing climate. Wiley Interdiscip Rev Clim Chang 2 (2):220–237
Swiecki TJ, Bernhardt EA (2016) Sudden oak death in California. In: Insects and diseases of mediterranean forest systems. Springer, Cham, pp 731–756
Tatusov RL, Galperin MY, Natale DA, Koonin EV (2000) The COG database: a tool for genome-scale analysis of protein functions and evolution. Nucleic Acids Res 28(1):33–36

Thompson J (2007) The mysterious demise of an ice-age relic: exposing the cause of yellow-cedar decline. Science findings 93 Portland, OR: US Department of Agriculture, Forest Service, Pacific Northwest Research Station 5, p 93

Thompson BG, Drake BG (1994) Insects and fungi on a C3 sedge and a C4 grass exposed to elevated atmospheric CO2 concentrations in open-top chambers in the field. Plant Cell Environ 17(10):1161–1167

Tiedemann A, Firsching K (2000) Interactive effects of elevated ozone and carbon dioxide on growth and yield of leaf rust-infected versus non-infected wheat. Environ Pollut 108 (3):357–363

Uchôa CN, Pozza EA, Albuquerque KS, Moraes WS (2012) Relationship between temperature and leaf wetness in Black Sigatoka monocycle. Summa Phytopathol 38(2):144–147

Van der Plank JE (2013) Plant diseases: epidemics and control. Elsevier, New York

Van Mantgem PJ, Stephenson NL, Byrne JC, Daniels LD, Franklin JF, Fulé PZ, Harmon ME, Larson AJ, Smith JM, Taylor AH (2009) Widespread increase of tree mortality rates in the western United States. Science 323(5913):521–524

Vary ZM, Ewen McElwain CJ, Doohan MF (2015) The severity of wheat diseases increases when plants and pathogens are acclimatized to elevated carbon dioxide. Glob Chang Biol 21 (7):2661–2669

Vaughan MM, Huffaker A, Schmelz EA, Dafoe NJ, Christensen S, Sims J, Martins VF, Swerbilow J, Romero M, Alborn HT (2014) Effects of elevated [CO2] on maize defence against mycotoxigenic F usarium verticillioides. Plant Cell Environ 37(12):2691–2706

Venette RC, Kriticos DJ, Magarey RD, Koch FH, Baker RH, Worner SP, Gómez Raboteaux NN, McKenney DW, Dobesberger EJ, Yemshanov D (2010) Pest risk maps for invasive alien species: a roadmap for improvement. Bioscience 60(5):349–362

Welch S, Croft B, Brunner J, Michels M (1978) PETE: an extension phenology modeling system for management of multi-species pest complex. Environ Entomol 7(4):487–494

Whish JP, Herrmann NI, White NA, Moore AD, Kriticos DJ (2015) Integrating pest population models with biophysical crop models to better represent the farming system. Environ Model Softw 72:418–425

Willocquet L, Savary S, Fernandez L, Elazegui F, Teng P (2000) Development and evaluation of a multiple-pest, production situation specific model to simulate yield losses of rice in tropical Asia. Ecol Model 131(2–3):133–159

Willocquet L, Savary S, Fernandez L, Elazegui F, Castilla N, Zhu D, Tang Q, Huang S, Lin X, Singh H (2002) Structure and validation of RICEPEST, a production situation-driven, crop growth model simulating rice yield response to multiple pest injuries for tropical Asia. Ecol Model 153(3):247–268

Willocquet L, Elazegui FA, Castilla N, Fernandez L, Fischer KS, Peng S, Teng PS, Srivastava R, Singh H, Zhu D (2004) Research priorities for rice pest management in tropical Asia: a simulation analysis of yield losses and management efficiencies. Phytopathology 94 (7):672–682

Willocquet L, Aubertot J, Lebard S, Robert C, Lannou C, Savary S (2008) Simulating multiple pest damage in varying winter wheat production situations. Field Crop Res 107(1):12–28

Wong P, Mead J, Croff M (2002) Effect of temperature, moisture, soil type and Trichoderma species on the. Australas Plant Pathol 31(3):253–257

Yonow T, Zalucki M, Sutherst R, Dominiak B, Maywald G, Maelzer D, Kriticos D (2004) Modelling the population dynamics of the Queensland fruit fly, Bactrocera (Dacus) tryoni: a cohort-based approach incorporating the effects of weather. Ecol Model 173(1):9–30

Zadoks J (1971) Systems analysis and the dynamics of epidemics. Phytopathology

Zadoks JC, Schein RD (1979) Epidemiology and plant disease management. Epidemiology and plant disease management

Chickpea Modeling Under Rainfed Conditions

13

Afifa Javaid, Mukhtar Ahmed, Fayyaz-ul-Hassan, Mahmood-ul-Hassan, Munir Ahmad, and Rifat Hayat

Abstract

Climate variability and extreme weather might increase in frequency due to climate change, which could have significant effect on chickpea production. Recently, a study was conducted, aided with simulation modeling approach, in different rainfed regions of Pakistan to check the potential impacts of climate variability on chickpea. Initially, varieties were screened on the basis of germination percentage. Two varieties, Balkasar and Thal 2006, performed best in the germination test and thus grown at two locations, i.e., University Research Farm (URF), Koont, Chakwal Road, Rawalpindi (medium), and Bijwal Farm, Fateh Jang (low), rainfall zones of Pothwar, for field evaluation of best-performing varieties of chickpea. During the course of study, different phenological and yield component parameters have been recorded. Collected data was analyzed statistically to see the performance of varieties under different climatic conditions of these two sites. DSSAT_CROPGRO_Chickpea model was used to simulate crop phenology and yield, i.e., above-ground mass and grain yield of chickpea under

A. Javaid · Fayyaz-ul-Hassan
Department of Agronomy, Pir Mehr Ali Shah Arid Agriculture University, Rawalpindi, Pakistan

M. Ahmed (✉)
Department of Agricultural Research for Northern Sweden, Swedish University of Agricultural Sciences, Umeå, Sweden

Department of Agronomy, Pir Mehr Ali Shah Arid Agriculture University, Rawalpindi, Pakistan
e-mail: ahmadmukhtar@uaar.edu.pk

Mahmood-ul-Hassan · M. Ahmad
Department of Plant Breeding and Genetics, Pir Mehr Ali Shah Arid Agriculture University, Rawalpindi, Pakistan

R. Hayat
Department of Soil Science and Soil Water Conservation, Pir Mehr Ali Shah Arid Agriculture University, Rawalpindi, Pakistan

M. Ahmed (ed.), *Systems Modeling*, https://doi.org/10.1007/978-981-15-4728-7_13

rainfed conditions. The model was calibrated and validated on the basis of experimental data. Values obtained from model runs were compared with observed values by using validation scores. Simulation outcomes from days to anthesis, days to maturity, and above-ground mass, i.e., biological yield and grain yield, showed that the location URF-Koont proved better for chickpea crop. Observed and simulated data were compared for model efficiency. At both locations, Thal 2006 performed best under water-limited conditions of Pothwar. Based upon these values, further yield was predicted for varying environmental scenarios in order to recommend best-performing varieties in this particular climate.

Keywords

Chickpea · Phenology · DSSAT_CROPGRO_Chickpea model · Climate change

13.1 Introduction

Pakistan's rainfed region accounts for 20% of total area under cultivation, which comprises of 1.82 million hectares, and Pothwar accounts for 90% of that region. In Pothwar plateau, amount of rainfall varies from 375 to 1750 mm in different parts from South to North. This variation in rainfall results in inadequate availability of moisture throughout the growing period. Pakistan's rainfed region is regularly facing dry spells during Rabi season (Ahmad et al. 2013). Moisture stress is chiefly dependent on timing, length, and amount of shortages (Pandey et al. 2013).

Climate change in present scenario is due to devastating human activities such as increased greenhouse emissions, higher electricity generation and changes in land use pattern (Stern 2008), refers to global warming, increased levels of atmospheric carbon dioxide generated by the use of fossil fuels. The increasing levels of carbon dioxide and other gases trap heat in the atmosphere and can warm up the Earth, causing global warming, melting of ice, and rising of sea levels, which may result into storms, floods, and tsunamis.

Climate variability is now accepted as a universal phenomenon with far-reaching effects (Ali and Erenstein 2017). The rate at which energy from the Sun is absorbed and dissipated in space regulates the temperature and climate of the Earth. The dispersion of this solar energy around the globe by wind, ocean, and other means affects the climate of different regions. The climate change and warming over the twenty-first century will not be uniform, it will change slowly and gradually but diversely in different countries, some of them will face drought while some may experience higher rainfall leading to floods and disasters (IPCC 2014).

Climate change is assumed to be distressing in deprived agricultural societies and growers have to spend large amounts of money to maintain quality yield (Ali et al. 2017). The rise in global warming gases can damage the low-cost agricultural system and highly degrade its production superiority. According to the Global Climate Risk Index (2020), Pakistan ranks seventh among the most adversely affected countries by climate change. The survey mentions that in the face of having high susceptibility to future climate change, Pakistan is a low Green House Gases (GHG) emitter; however, the susceptibility is due to geographic, demographic, and diverse climate condition, mostly the environmental changes–related threat to food, energy, and water security due to inherent arid climate coupled with the high level of reliance on water from melting glacier. Developing countries are more vulnerable to the adverse effect of climate change because they are key determinants of agricultural productivity in the global geography (Apata, 2011), and yet these countries are most vulnerable to climate change though they only contribute 10% to the annual global carbon dioxide emissions.

Higher temperatures and increasing climate variability projected in different world regions, both mean temperature and climate variability, contribute to the frequency of extreme temperature events. Observed evidence has increasingly shown that short-term high temperatures around flowering may have a greater negative impact on yield production, especially in grain-producing crops, a phenomenon that is increasingly known as heat stress (Rezaei et al. 2015).

Climate change is the mean variability in the precipitation and temperature for longer period of time. Large spatio-temporal variation (magnitude and rate of change) exists in precipitation and temperature among various regions (Ahmed 2020; Ahmed and Ahmad 2019; Aslam et al. 2017; Jabeen et al. 2017; Ijaz et al. 2017; Zhang et al. 2013). Climate variability is most probably considered due to global warming (Ahmed 2017; Ahmed and Stockle 2016; Fisher et al. 2006; Oppenheimer and Alley 2004). Warming trend during the last 50 years has been 0.18 °C per decade due to rise in global average surface temperature (Wang et al. 2015). As per projections by the Intergovernmental Panel on Climate Change (IPCC) fifth assessment, the increase of mean temperature from 2018 to 2100 will likely be 1.8 ± 0.5 °C for RCP4.5 and 3.7 ± 0.7 °C for RCP8.5, relative to 1986 to 2005 globally. It is considered that global warming will influence more evaporation resulting in the increase in intensity and frequency of extreme rainfall events (Meehl et al. 2007). While the average precipitation intensity is generally increasing, the frequency of wet days is decreasing in many parts of the world, leading to drought. Northern China faced a severe drought in the 1920s due to reduced rainfall (Liang et al. 2006).

Chickpea is a cool season legume crop and ranks third among pulses in global production. It serves as a key component of cropping systems in many parts of Asia and Africa, providing families of resource-poor farmers with a valuable source of dietary protein (Knights and Hobson 2016). Major producing countries include India, Pakistan, and Iran. It is broad in adaptation and widely distributed, though its production being limited by several biotic and abiotic stresses.

Chickpea is a valued crop and a nutritious food for an expanding world population and will become increasingly important with climate change. Its production ranks third after beans, a mean annual production of over 10 million tons with most of the production centered in India. Land area devoted to chickpea has increased in recent years and now stands at an estimated 13.5 million hectares. Production per unit area has slowly but steadily increased since 1961 at about 6 kg/ha per annum. Over 1.3 million tons of chickpea enter into the world markets annually to supplement the needs of countries unable to meet demand through domestic production. India, Australia, and Mexico are leading exporters.

Chickpea is comprised of Desi and Kabuli types. The Desi type is characterized by relatively small angular seeds with various coloring and sometimes spotted. The Kabuli type is characterized by larger seed sizes that are smoother and generally light colored. Dal is a major use for chickpea in South Asia while hummus is widely popular in many parts of the world. Research efforts at ICRISAT, ICARDA, and national programs have slowly but steadily increased yield potential of chickpea germplasm (Khan and Abourashed 2011). Overall, global production of chickpea is predominated by the Desi type that accounts for 80% of production with the remaining 20% devoted to Kabuli types. Worldwide, chickpea ranks third among the pulse crops and accounts for 10.1 million tons annually. This ranking places chickpea behind beans (21.5 million tons) and peas (10.4 million tons) with mean annual production of 10.1 million tons from 2004 to 2013. Taken together, annual combined production of peas and chickpea is nearly equal to that of beans, an indication of their overall importance. These three pulses (beans, peas, and chickpeas) account for about 70% of global pulse production, with chickpea accounting for approximately 17% of the total annually (Muehlbauer and Sarker 2017).

Chickpea is more susceptible to high temperature stress at flowering stage as compared to that of podding (Angadi et al. 2000). There are negative impacts of high temperatures and low precipitation, as high temperature (>30 °C) and low precipitation at flowering time results in significant yield losses (Kutcher et al. 2010). This crop requires more moisture to achieve a satisfactory grain size and yield. Low rainfall during the growth cycle and water stress may accelerate the negative impact of high temperature and produce low yield of chickpea crop (Gan et al. 2004; Takashima et al. 2013). Waterlogging at flowering or podding can kill the crop or significantly reduce yield, especially at higher temperatures (Ruchika and Sandhu 2009). Average yield of chickpea is low in Pakistan as compared to other countries. Major factors responsible for poor yield are: (i) continuously changing climatic conditions and inability to cope with their adverse effects; (ii) management factors under climate change, i.e., inadequate seedbed preparation, unavailability of certified seed of improved varieties, low plant population, improper nutrients management, and growing on marginal lands; and (iii) cultivar inherit potential, i.e., low yield potential, reduced breeding, and lack of knowledge about particular cultivars to be grown in specific conditions of the area, etc.

Frost is another significant abiotic stress, one of the main constraining variables for farming around the world, including Australia. Legumes, including field pea, lentil, and chickpea, are exceptionally susceptible to chilling and critically minimum temperatures, especially at the stage of anthesis, early pod development, and seed filling stages (Stoddard et al. 2006). In legumes, the most susceptible levels for frost are the flowering, early pod formation, and seed filling stages (Nayyar et al. 2005). One of the early research findings on chilling damage in chickpea was led under field conditions at different areas in India, and the findings showed difference in flower abscission rates at various temperatures (Nayyar et al. 2005).

Crop simulation models have been developed for evaluation of agronomic management strategies procedures and to help analysts in understanding the bridge linked amid ecosystem, production variation, and management (Ahmed et al. 2013, 2014, 2016, 2017, 2018, 2019; Ahmad et al. 2017, 2019; Berger et al. 2011. Crop phenological modeling is useful in simulation of plant growth processes that in field conditions might acquire years to calculate (Fourcaud et al. 2008). These models have been used by various research groups for decision making in agriculture systems (Bannayan et al. 2003; Hoogenboom et al. 2015). For assessment of daily growth and development of the crops, extreme and minimal temperature, average rainfall data, and daily solar radiations are used as input in such crop models. To assess and to determine the elucidations of problems observed in management of crops, particularly in developing countries where changing climatic conditions prevails, crop model, i.e., decision support system for agro-technology transfer (DSSAT) model, is a best applied tool in such situation (Hoogenboom et al. 2015; Jabeen et al. 2017).

In Pakistan there is little study to evaluate the climate change impacts and adaptation for chickpea crop, whereas this is an issue of prime importance throughout the world. With the passage of time, climate change is becoming a great threat to food security, and that is why there is a need to focus on the subject and carry out necessary research work according to a country's climatic conditions. The present study was carried out for modeling the potential impacts of climate variability on chickpea under contrasting environment, keeping in view the importance of chickpea in Pakistan and the objectives: (i) evaluation of chickpea varieties on the basis of germination percentage, (ii) assessment of the potential impacts of climate variability on chickpea growth and yield, and (iii) application of DSSAT model for evaluation of chickpea.

13.2 Chickpea and Climate Variability

Climate change refers to a statistically significant variation in either the mean state of the climate or in its variability, persisting for an extended period, typically decades or longer (USEPA 2011). Thornton et al. (2014) quoted in a review that the majority of researches and studies related to impacts of climate variability mainly focus on changes in mean climate state. According to a report by Intergovernmental Panel on Climate Change (IPCC 2013) mean climate state is shifting with the passage of time due to global warming and greenhouse gas emissions, and the distribution trend is likely to be more hot weather in summer and less cold weather in winters. This induced global warming climate variability also results in change in precipitation distribution pattern including intensity, frequency, and time of rainfall (Huntingford et al. 2003). Due to changing precipitation distribution pattern, some regions are getting heavy and frequent rains causing floods whereas others are deprived of necessary precipitation resulting in aridity (Christensen and Christensen 2004). However, Greve et al. (2014) reported that only 10.8% of the land area indicates "dry gets drier, wet gets wetter" pattern while 9.5% land area shows the opposite trend, i.e., dry gets wetter, and wet gets drier, globally. Dry areas have increased due to these trends from about 17% in the 1950s to 27% in the 2000s throughout the world (Dai 2011).

Crop production is vulnerable to climate variability related with increments in temperature, increases in CO_2, and changing patterns of rainfall, which may lead to extensive decrease in crop productivity. Additionally, extreme weather occasions, e.g., droughts, extreme heat waves, and substantial rainfall prompting floods, have expanded since the past decades. Enhancing crop production to meet rising demands owing to the increasing population, against the background of the threats of climate change, is a challenging task (Mall et al. 2017).

Growth and development of field crops may accelerate with rise in temperature but extreme changes in temperature either hot or cold effect crop productivity adversely. According to Machado and Paulsen (2001), high temperature combined with one or more factors like water stress may contribute to heat stress. It was documented by various researchers that crop phenology, growth and development rate, and yield are mainly determined by responses that are genetically prescribed to temperature (Slafer 2003; McMaster et al. 2008; Luedeling et al. 2009). As per report of Chmielewski et al. (2004), increasing mean temperature and decreasing photoperiod results into shortening of crop developmental stages and life cycle which ultimately effects crop yield. Similarly, Craufurd and Wheeler (2009) documented that higher temperature causes earlier flowering and maturity of legumes resulting in shortening of growth period in recent decades. This shortening in crop growing seasons causes less absorption of intercepted radiations throughout the period thus resulting less biomass accumulation and crop yield. It is evident from the findings of Siebert and Ewert (2012) that the overall reduction in the length of growing season of oats by 2 weeks has been observed in Germany during the period from 1959 to 2009 as a result of earlier occasion of phonological events. In flowering plant, reproductive phase is highly sensitive to extreme temperature stresses, i.e., cold or hot, within a single day or night being fatal to reproductive process (Zinn et al. 2010). It was investigated by Lobell et al. (2011) that beyond 30 °C, a rise of one degree per day can reduce yield up to 1.7% in maize crop under drought conditions. It was observed that not only the increased temperatures at daytime have detrimental effects on crop growth and development but also impacts of higher temperature at nighttime is worth noticeable. Mohammed and Tarpley (2009) found that rice yield was reduced by 90% with night temperatures of 32 °C as compared to 27 °C.

Moisture availability, temperature, and photoperiod suitability determines the sowing time of this crop for the best yield (Siddique and Krishnamurthy 2016). The time available for chickpea crops to produce adequate vegetative structures and then grain yield is often limited by hot or cold temperatures, rainfall distribution, or competition for use of land by other crops in rotation.

High temperature during the reproductive period can limit grain yield. High temperature (>30 °C) regulates floral initiation and grain yield in chickpea. At present, chickpea is generally produced in warm environments (Devasirvatham et al. 2012).

A pot experiment was conducted at controlled room temperature (21 ± 1 °C) utilizing five sowing depths (2.5–14 cm). Results demonstrated that the response of chickpea emergence to temperature was best pronounced at temperatures of 4.5 °C for base, 20.2 °C for lower optimum, 29.3 °C for upper optimum and, 40 °C for ceiling temperature (Soltani et al. 2006). Extreme temperatures in combination with other factors like water shortage may enhance the impact of heat stress (Kutcher et al. 2010). Stress due to water deficit causes detrimental effects on many physiological processes in plants including reduction in photosynthesis, stomatal exchanges, accumulation of dry matter, and protein synthesis, which have an effect on their growth stages (Ohashi et al. 2006).

Research was conducted for two varieties of chickpea, i.e., drought-tolerant Bivaniej and ILC482, to study the effect of water shortage and moisture stress on biochemical processes such as chlorophyll contents, photosynthesis, and respiration rate along with yield and its parameters. The experimental design was RCBD with four water systems and three replications. Outcomes demonstrated that flowering stage of this crop is more susceptible to moisture shortage and eventually lowers the grain production as compared to vegetative phase (Mafakheri et al. 2010).

Simulation models are widely used to simulate the potential impacts of environmental factors on agricultural and natural ecosystems (Asseng et al. 2019; Liu et al. 2019; Wallach et al. 2018; Ahmed 2012). A particularly active region of application is inquiring about the potential impacts of climate change, and simulations have been a noteworthy information resource for Intergovernmental Panel on Climate Change (IPCC) assessments for agriculture (White et al. 2011).

A study was conducted by using 4 crop models with 20 users arranged in RCBD with 4 replications. Parameters were calibrated. Parameters for maize (well studied by modelers) and rapeseed (almost ignored) were calibrated. While all models which were accurate for maize (RMSE from 16.5% to 25.9%), they were, to some extent, unsuitable for rapeseed. Although differences between biomass simulated by the models were generally significant for rapeseed, they were significant only in 30% of the cases for maize. This could suggest that in case of models well suited to a crop, user subjectivity can hide differences in model algorithms, consequently, the uncertainty due to parameters should be better investigated (Confalonieri et al. 2016).

APSIM model was evaluated for the simulation of different cropping schemes in Asia from many aspects like crop production, its phenology, water use, soil with changing features, and CO_2 response for crops. This simulation was conducted for variable crops, environments, and management strategies and performance of the model was assessed. After appropriate parameterization, model simulation was better for the range of cropping schemes with some recommendations for further improvement of model to be used as a valuable tool for Asian cropping schemes (Gaydon et al. 2017).

For proper testing and validation of crop model, field experimentations under varying climatic scenarios are needed to compare observed and simulated output and to verify their limitations (Andarzian et al. 2011).

Crop simulation modeling approach can help to quantify performance of field crops under diverse climatic scenarios. Adoption of Decision Support System for Agro-technology Transfer (DSSAT) for chickpea is important to check an opportunity for cultivation under varied climatic conditions. Satisfactory simulated results for crop growth parameters were observed when compared with observed values.

Further, it was concluded that CROPGRO model is a valuable tool to predict and simulate phenology, growth, and yield of crop under semi-arid conditions (Raja et al. 2018).

13.3 Materials and Methods

The experiment was carried out to study the potential impacts of climate variability, i.e., variant temperature and precipitation on chickpea (*Cicer arietinum* L.) at different agro-ecological sites. Different varieties of chickpea were first evaluated on the basis of germination test in lab and then the two best-performing varieties, i.e., Balkasar and Thal 2006, were planted on 31st Oct at URF, Koont, Chakwal, and on 1st Nov at Bijwal Farm, Fateh Jang, simultaneously during the year 2017–2018. All the operations were kept uniform for the varieties. The experiment was laid out by Randomized Complete Block Design (RCBD) with three replications at field area. The size of individual plot at both locations was 2.7 m $\times$ 4 m. Total number of sowing lines in individual plot was 6 with the path of 1 m. Sowing was done through hand drill in the field areas. Before sowing, land preparation in all plots was done by using disc followed by cultivator and then surface was planked for good seedbed preparation. Row to row spacing was kept at 35 cm and plant to plant distance was maintained at 10 cm. Data was collected on following the agronomic aspects for chickpea crop. As study was conducted in Pothwar region, which is a rainfed area of Pakistan, thus no irrigation was given throughout the lifecycle of crop. Basal dose of fertilizer was given at the rate of 20–30 kgN/ha and 40–60 kg P/ha through broadcast method. Three varieties of chickpea were taken primarily for the purpose of germination percentage, i.e., Balkasar, Thal 2006, and Vanhar. All these varieties are preferably grown in rainfed areas of the country. Five seeds of individual variety were taken in each petri dish. Seeds were presoaked in water for 1 hour in order to boost imbibition. These varieties were screened on the basis of germination percentage; Thal 2006 and Balkasar showed 100% germination whereas Vanhar variety was screened due to seeds that failed to germinate. Selected varieties were taken to the both locations, i.e., Fateh Jang and URF, Koont, Chakwal. For weather data, previous long-term data was collected from Pakistan Meteorological Department, Islamabad. Daily rainfall and minimum and maximum temperature data was collected for both study sites during the chickpea growing season 2017–2018. Standard method proposed by Hoogenboom et al. (1995; 2019a, b) was used to determine the physiochemical properties of soil. The gravimetric soil moisture content was determined by using the formula:

$$\%\ \text{soil moisture (dw)} = 100 * ((\text{Fresh weight} - \text{dry weight})/\text{dry weight})$$

Other variables like soil organic carbon %, soil pH, Nitrogen %, silt sand and clay %, soil lower limit, and soil upper limit were calculated according to the method proposed by IBSNAT.

Crop phenological data such as days to anthesis were calculated as days when 50% of crop plants-initiated flowering in the respective plot from the date of sowing.

For sample purpose, five plants were taken at random from individual plot. Leaf area index (LAI) was calculated from destructive plant samples at harvest stage by using the following formula given by Pearce et al. 1985:

$$\mathrm{LAI} = \mathrm{LA}/\mathrm{GA}$$

where

LA = Leaf Area.
GA = Ground Area.

Crop Growth Rate (CGR) was calculated at harvest stage by using the formula given by Pearce et al. 1985:

$$\mathrm{CGR} = 1/\mathrm{GA}\,(\mathrm{W}_2 - \mathrm{W}_1/\mathrm{t}_2 - \mathrm{t}_1)$$

where

W_2 and W_1 are the dry weights; t_2 and t_1 times or interval.
1/GA = Ground area.

Numbers of branches of five randomly selected plants from each plot were counted and then average was recorded. Weight of 100 grains was recorded by weighing a sample of 100 grains from every plot on an electric balance. Plant height was obtained by measuring height of five plants at random from each plot at the time of maturity. Biological yield was recorded by harvesting one m^2 area per plot and it was converted to get final yield in kg ha^{-1}. Grain yield was recorded by harvesting a one m^2 area per plot and it was converted to get final yield in kg ha^{-1}. Harvest index was calculated using the formula given by Donald (1962; 1968).

$$\mathrm{HI} = \mathrm{Grain\ \ yield}/\mathrm{Biological\ \ yield}$$

13.3.1 DSSAT Model

Among the inputs required for DSSAT simulation, the detailed physical and hydraulic properties of soil are needed. The model is not programmed with auto validation and calibration. To validate the model for local conditions of any locality, changes are made in its parameters. Various new files are generated for different management zones to precise agriculture using DSSAT. Comparison of simulations with observed results evaluates the model's worth and appropriateness for precise predictions and area (Porter et al. 2010). Diverse packages are easy to incorporate due to their defined and documented modular interface. Independent programs operated together with DSSAT model. Required inputs for model application under different situations are soil, genotypes, weather, and experimental conditions. Improvement of model accuracy and efficiency, comparison of simulated and observed values, and database preparation are aided with software application. Proper crop management for risks assessment can be simulated with DSSAT crop model.

13.3.2 DSSAT Model Parameterization and Evaluation

The model was evaluated on the basis of data collected during chickpea growing season of 2017–2018. Field experiments (Otter-Nacke et al. 1986) were of opinion that calibration and validation are approaches to evaluate model efficiency. Adjustment of genotypic coefficient was performed till the simulation results differ at 10% of actual data for major development stages of chickpea. Comparison between observed and simulated values was developed for parameters regarding growth and development of chickpea to improve cultivar coefficient and for sensitivity analysis of model. Small increase or decrease in genotypic coefficient was done (when needed). Among the inputs required for DSSAT simulation, the detailed physical and hydraulic properties of soil are needed. This model is not programmed with auto validation and calibration. To validate the model for local conditions of any locality, changes are made in its parameters. Various new files are generated for different management zones to precise agriculture using DSSAT. Newly generated modules include weather module, crop module, soil module, and soil–plant atmosphere module to get simulation results from DSSAT. Similarly, a number of genetic coefficients are also incorporated to parameterize DSSAT including vernalization sensitivity coefficient (PIV), thermal time from the onset of linear fill to maturity (P5), photoperiod sensitivity coefficient (PID). Subsequently, comparison of simulations with observed results evaluates model's worth and appropriateness for precise prediction and area (Huntingford et al. 2003).

13.3.3 Statistical Analysis

Analysis of variance (ANOVA) was performed to test the significant differences between means of various parameters for two varieties at two locations for the 2017–2018 growing seasons using Statistics 8.1. The ANOVA was performed to find all the possible interactions of variety and locations. Collected data was statistically analyzed and used to parameterize DSSAT model to run simulating long-term daily climatic data (1985–2018) of above said locations.

Fig. 13.1 Germination test comparison of three varieties Balkasar, Vanhar, and Thal 2006

13.4 Results and Discussion

13.4.1 Germination Test

Three varieties of chickpea (Balkasar, Thal 2006, and Vanhar) were taken for this purpose. All these varieties are preferably grown in rainfed areas of the country. Five seeds of individual variety were taken in each petri dish. Seeds were presoaked in water for 1 hour in order to boost imbibitions. These varieties were screened on the basis of germination percentage; Thal 2006 and Balkasar showed 100% germination whereas Vanhar variety was screened due to its seeds failing to germinate, as shown in Fig. 13.1. Selected varieties were thereafter sown at the both locations, i.e,. Fateh Jang and URF Koont, Chakwal Road, Rawalpindi.

13.4.2 Crop Data

13.4.2.1 Days to Anthesis

Days to anthesis were calculated as days from sowing when 50% of crop plants initiated flowering in the respective plots. For sample purpose, 5 plants were taken at random from individual plot..

Results showed that variety V1 Thal 2006 reached the stage of 50% flowering with the mean of 88 days at University Research Farm, Koont, Rawalpindi, with the standard error of 1.0. The same variety shifted to anthesis with the mean of 91.67 days at Bijwal Farm, Fateh Jang, with standard error of 1.442, as presented in Table 13.1.

Whereas the variety Balkasar switched to flowering stage with the mean of 94 days from sowing at URF, Koont, Rawalpindi, with the standard error of 1.414. This variety showed the anthesis stage with the mean of 104.33 days and standard error of 1.442, as shown in Fig. 13.2. Results also proved the significant

Table 13.1 Days taken to anthesis for chickpea varieties Thal 2006 and Balkasar at Koont and Fateh Jang

Locations	Cultivars	Days to anthesis
Koont	V1	88 a
	V2	94 ab
Fateh Jang	V1	91.7 b
	V2	104.3 a

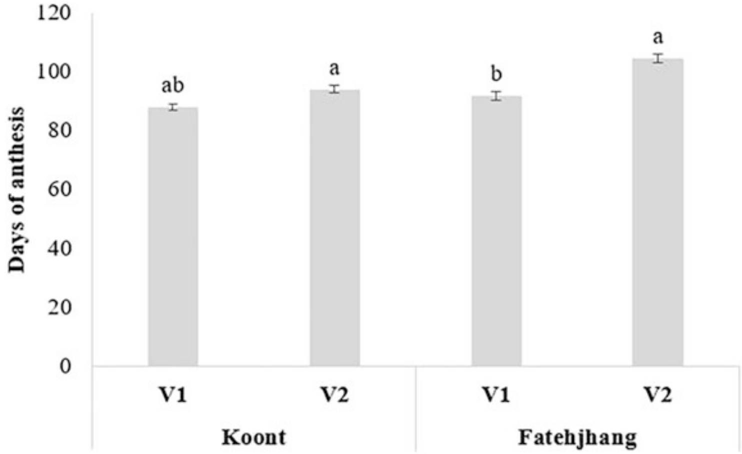

Fig. 13.2 Days taken to anthesis for chickpea varieties Thal 2006 and Balkasar at Koont and Fateh Jang with means followed by the same letters do not differ significantly at 5% level of significance

relationship for varieties at both locations. However, this result was in accordance with (Roberts et al. 1985) who also reported that flowering stage is dependent on photoperiod time of chickpea rather than location of growing area.

13.4.2.2 Days to Maturity

Days to maturity were calculated as days when 50% of the plants started pod development from sowing. For representation of variation, 5 plants were taken at random from each plot. Observation showed that once flowering is induced, then plant is self-capable for pod development and seed setting in respective pods. Crops that belonged to legume family showed numerous flowers but only a little percentage was able to become pod and finally the seed setting. Due to its indeterminate nature, chickpea has some extent of simultaneous development for pod and seed. Results confirmed that Thal 2006 at Koont, Rawalpindi, showed an average of 175.67 for days to maturity with the standard error of 2.53 whereas the same variety at Fateh Jang showed the average of 181.67 for days to maturity with the standard error of 2.34 (Table 13.2). On the other hand, chickpea variety Balkasar showed an average of 178.33 days for days to maturity with the standard error of 2.714 at URF Koont, Rawalpindi (Fig. 13.3). The same variety showed an average of 184 days for days to maturity at Fateh Jang with standard error of 2.645. Results showed significant

Table 13.2 Days taken to maturity for chickpea varieties Thal 2006 and Balkasar at Koont and Fateh Jang

Locations	Cultivars	Days to maturity
Koont	V1	175.7 b
	V2	178.3 a
Fateh Jang	V1	181.7 b
	V2	184 a

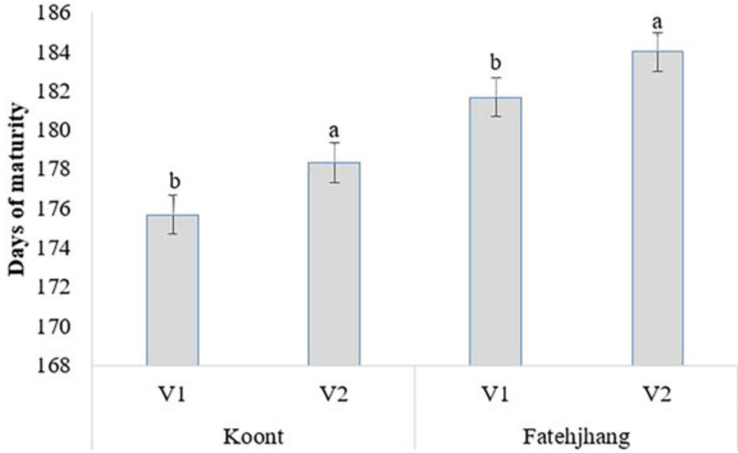

Fig. 13.3 Days taken to maturity for chickpea varieties Thal 2006 and Balkasar at Koont and Fateh Jang with means followed by the same letters do not differ significantly at 5% level of significance

relationship of varieties at both locations for days to maturity and (Monpara and Kalariya 2009) also reported the similar results.

13.5 Yield and Yield Parameters

13.5.1 Leaf Area Index

Leaf area index (LAI) was calculated from destructive plant samples during harvesting by computing leaf area of respective sample plant and its ground area. LAI shows the growth pattern of the crop throughout its life cycle and is considered as an important parameter in agronomic crops. As crop grows and shifts its physiological stages, it tends to increase because of increase in all growth parameters as well as leaf area of the plant. As number of leaves increases as well as leaf growth, LAI increases. However, its decreasing trend has been observed for the harvest stage. It may occur due to falling off leaves as a result of physiological maturity. Results showed that Thal variety at Koont and Fateh Jang showed an average LAI of 1.17 and 1.11 with the standard error of 0.217 and 0.194, respectively, as shown in Table 13.3. Balkasar variety of chickpea showed an average LAI of 1.14 and 1.08 at Koont and Fateh Jang with the standard error of 0.179 and 0.158 as presented in

Table 13.3 Leaf area index of both chickpea varieties Thal 2006 and Balkasar at Koont and Fateh Jang at harvest

Locations	Cultivars	Leaf area index
Koont	V1	1.2 a
	V2	1.1 ab
Fateh Jang	V1	1.1 a
	V2	1.0 ab

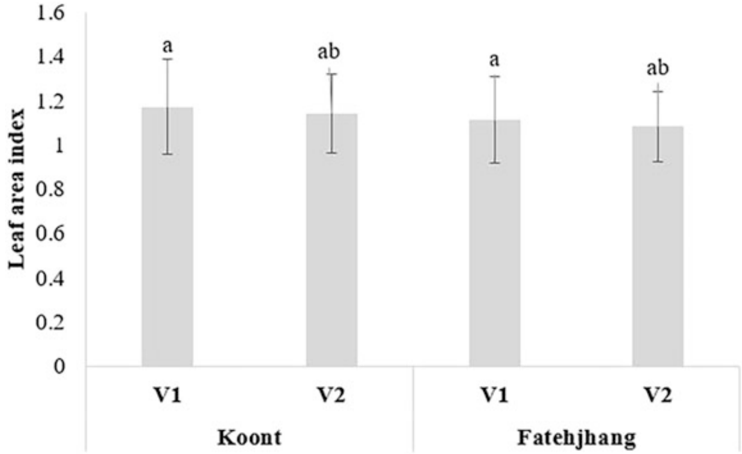

Fig. 13.4 Leaf area index of both chickpea varieties Thal 2006 and Balkasar at Koont and Fateh Jang at harvest with means followed by the same letters do not differ significantly at 5% level of significance

Fig. 13.4. Results showed significant relationship of leaf area index for both varieties at Koont and Fateh Jang and are in confirmation with the findings of Singh (2005) which has reported similar result for leaf area index of chickpea.

13.5.2 Crop Growth Rate (CGR) (gm^{-2} day^{-1})

CGR was calculated by taking the fresh and oven-dry weight of sample plants at respective time interval per unit ground. Crop growth rate is affected by several climatic factors that play the crucial role for determining its value. It also represents the agronomic parameters, i.e., dry matter yield for per unit area. It initiated its lower value and reached at its maximum at certain level and then decreased at later stages of the crop (Azimi et al. 2015). It is an important parameter in this regard that it shows the net activity of photosynthesis, canopy cover, and respiration as a whole (Alam and Haider 2006). Results showed an average value of CGR, for Thal 2006 variety at Koont and Fateh Jang, 0.133 and 0.1 with the standard error of 0.1945 and 0.1626, respectively, as given in Table 13.4. And as given in Fig. 13.5, Balkasar showed an average value of CGR, at Koont and Fateh Jang, 0.103 and 0.07 with the standard error of 0.201 and 0.179, respectively. The decline in the value CGR at the

Table 13.4 Crop growth rate of both chickpea varieties Thal 2006 and Balkasar at Koont and Fateh Jang at harvest

Locations	Cultivars	CGR
Koont	V1	0.133333 a
	V2	0.103333 ab
Fateh Jang	V1	0.1 a
	V2	0.073333 b

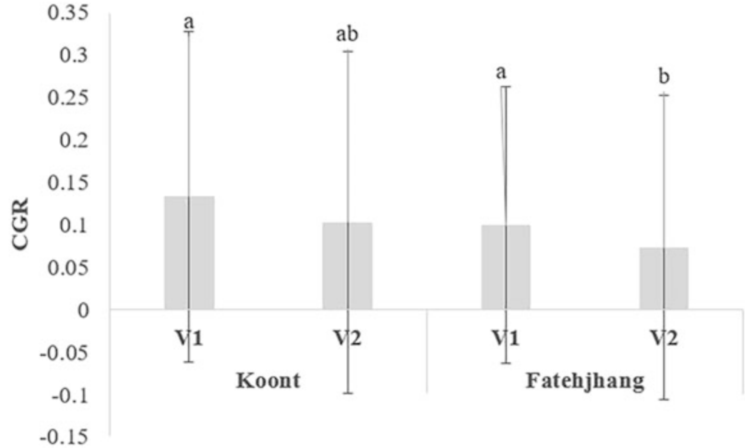

Fig. 13.5 Crop growth rate of both chickpea varieties Thal 2006 and Balkasar at Koont and Fateh Jang at harvest with means followed by the same letters do not differ significantly at 5% level of significance

Table 13.5 Number of branches per plant of both chickpea varieties Thal 2006 and Balkasar at Koont and Fateh Jang

Locations	Cultivars	No. of branches/plant
Koont	V1	5 a
	V2	4.7 ab
Fateh Jang	V1	3.3 a
	V2	3 ab

time of harvest is due to decrease in LAI as well as falling off leaves. Results were significant and in accordance with the research findings of Kibe et al. (2006).

13.5.3 Number of Branches Per Plant Start

Numbers of branches from five randomly selected plants from each plot were counted and then average was recorded (Table 13.5). Branching is an essential parameter in legumes as it is responsible for yield due to pod and grain setting eventually. The sum of branching number also determines the total number of leaves which in return gives an estimation of photosynthetic area in total. Results showed an average value of number of branches per plant for Thal 2006 as 5 and 3.33 with the standard error of 01 and 0.75 at Koont and Fateh Jang. Whereas, the average

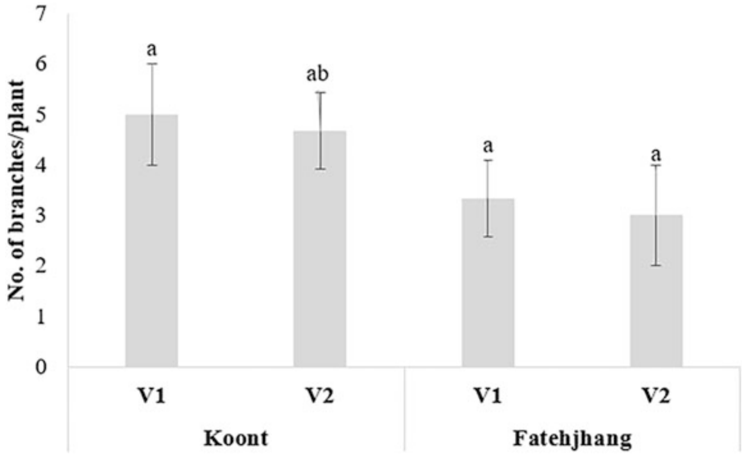

Fig. 13.6 Number of branches per plant of both chickpea varieties Thal 2006 and Balkasar at Koont and Fateh Jang with means followed by the same letters do not differ significantly at 5% level of significance

Table 13.6 Number of pods per plant for both chickpea varieties Thal 2006 and Balkasar at Koont and Fateh Jang

Locations	Cultivars	No. of pods/plant
Koont	V1	28.7 a
	V2	27.3 ab
Fateh Jang	V1	19 a
	V2	16.3 ab

value of number of branches per plant for chickpea variety Balkasar at Koont, Rawalpindi, and Fateh Jang is 4.66 and 3 with standard error of 0.7 and 01 (Fig. 13.6). Results are significant because branching is affected by plant population and planting density, similar results have been reported by Shamsi (2009).

13.5.4 Number of Pods Per Plant

At the time of crop harvest, the pods of five plants selected at random from each plot are counted and average value is taken per plant (Table 13.6). In family of legumes, number of pods per plant has a vital role in determining the yield of seed. It is then dependent on non-aborted sand fertile seeds per pod. Damaged and shriveled seeds are of no use when it comes to economic purpose and number of pods per plant also decreases due to increase in seeding density. Results depicted that variety Thal 2006 showed an average of 30.66 and 19.33 with the standard error of 2.265and 1.442 at Koont and Fateh Jang. However, variety Balkasar showed average number of pods per plant as 28.33 and 19.33 with the standard error of 2.346 and 1.519 at field areas of Koont, Rawalpindi, and Fateh Jang (Fig. 13.7). Results showed significant

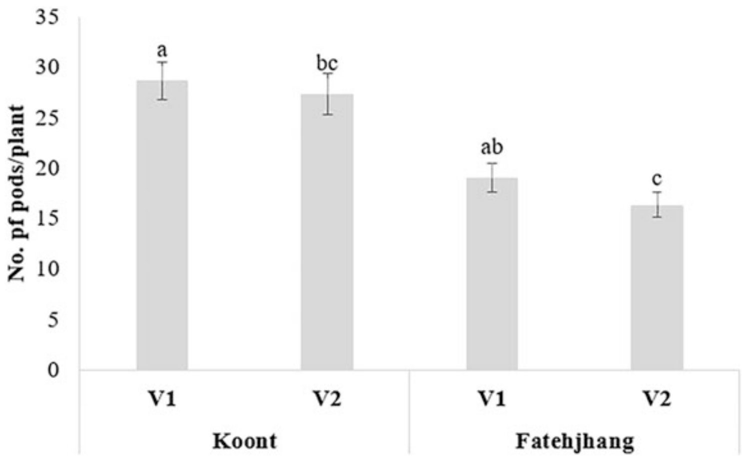

Fig. 13.7 Number of pods per plant for both chickpea varieties at Koont and Fateh Jang with means followed by the same letters does not differ significantly at 5% level of significance

Table 13.7 Number of grains per pod for both chickpea varieties at Koont and Fateh Jang

Locations	Cultivars	No. of grains/pod
Koont	V1	1.7 a
	V2	1.3 ab
Fateh Jang	V1	1.3 a
	V2	1 ab

difference for both varieties at respective locations and this may be due to varietal differences which is coined in research finding of Frade and Valenciano (2005).

13.5.5 Number of Grains Per Pod

The pods of five plants selected at random from each plot were threshed manually, grains were counted, and average value was recorded (Table 13.7). However, in legumes there is lot of variation in pod development per plant and seeds or grains per pod in legume family. Variation is also observed for the number of grains per pod as many of them fail to develop. From experiment it is observed that in desi type, like Thal 2006 and Balkasar, only one seed per pod is present at most, two seeds are also present, however, three seeds per pod are also there under optimum conditions for crop growth and development. Results for Thal 2006 showed an average value of 02 and 1.33 with standard error of 01 and 0.75 at Koont and Fateh Jang. Balkasar showed an average value of 02 and 1.33 with the standard error of 0.1 and 0.76 at Koont and Fateh Jang (Fig. 13.8). Results are significant because seed rate is an important influencing factor which was merely same at both locations and due to more genetic factor for regulating this plant trait rather than ecological or managerial factors. However, similar results have been reported by Togay et al. (2008).

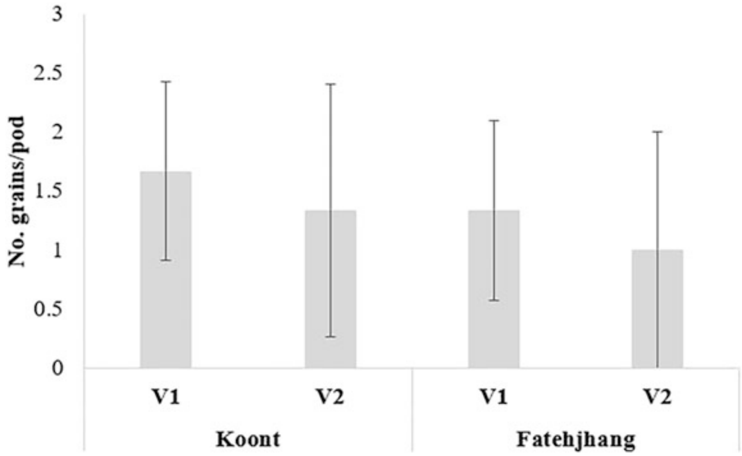

Fig. 13.8 Number of grains per pod for both chickpea varieties at Koont and Fateh Jang with means followed by the same letters do not differ significantly at 5% level of significance

Table 13.8 100-grain weight (g) of Thal 2006 and Balkasar at Koont and Fateh Jang

Locations	Cultivars	100 grain weight (g)
Koont	V1	26.5 a
	V2	23.1 ab
Fateh Jang	V1	20.3 b
	V2	18.0 ab

13.5.6 100-Grain Weight (g)

Weight of 100 grains was recorded by weighing a sample of 100 grains from each plot on an electric balance. Along with several other factors, 100-grain weight is of the prime importance. At Koont, both Thal 2006 and Balkasar showed maximum 100-grain weight, i.e., on average of 26.46 and 23.14 with the standard error of 1.365 and 0.805 at Koont (Table 13.8). However, it is relatively low for Balkasar and Thal 2006 with an average of 23.14 and 18.01 with the standard error of 1.963 and 2.364 at Fateh Jang (Fig. 13.9). Results are significant for both varieties and the location and in accordance with Walley et al. (2005).

13.5.7 Plant Height at Maturity (cm)

Plant height was obtained by measuring height of five plants at random from each plot at the time of maturity. According to results, Thal 2006 showed an average plant height of 50.33 with standard error of 2.04 at Koont, Rawalpindi, whereas the same variety at Fateh Jang showed an average of 51.33 with the standard error of 1.58 as presented in Table 13.9. Whereas, Balkasar variety showed an average plant height of 50.3 with the standard error of 1.58 at Koont and an average of 49.66 with the

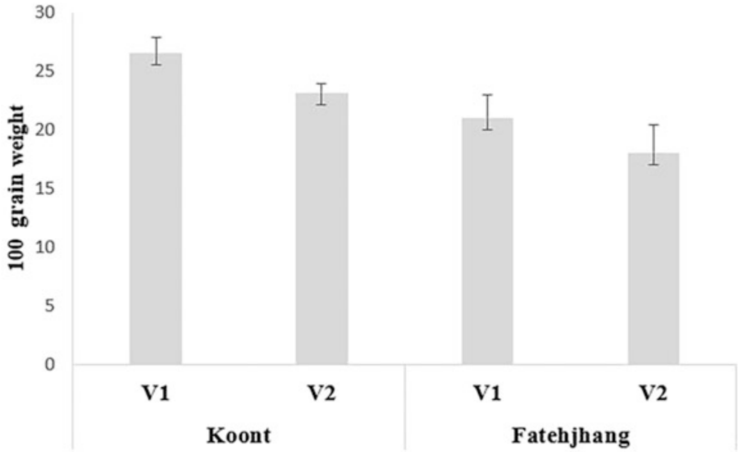

Fig. 13.9 Hundred grain weight of Thal 2006 and Balkasar at Koont and Fateh Jang with means followed by the same letters do not differ significantly at 5% level of significance

Table 13.9 Plant height (cm) of Thal 2006 and Balkasar at Koont and Fateh Jang

Locations	Cultivars	Plant height (cm)
Koont	V1	50.1 a
	V2	50.3 ab
Fateh Jang	V1	51.3 a
	V2	49.7 ab

standard error of 2.65 at Fateh Jang as shown in Fig. 13.10. Results obtained were significant and shows different trend due to genetic factor are in accordance with Rasul et al. (2012).

13.5.8 Biological Yield (kg ha^{-1})

Biological yield was recorded by harvesting one m^2 area per plot and it was converted to get final yield in kg ha^{-1}. It is the yield which is in totality for all dry matter produced as a result of different biochemical and physiological processes. The biological yield obtained for Thal 2006 variety at Koont, Rawalpindi, and Fateh Jang with an average of 5926.66 and 6901.66 kg ha^{-1} with the standard error of 35.26 and 22.22 is given in Table 13.10.Whereas, results showed that Balkasar variety produced an average biological yield of 6183.33 and 6552.33 kg ha^{-1}with the standard error of 28.76 and 31.58 at Koont and Fateh Jang, respectively, as shown in Fig. 13.11. Results obtained were significant for both varieties at both locations and variation in biological yield may be due to the varietal potential at both sites, thus results are in accordance with Khan et al. (2010).

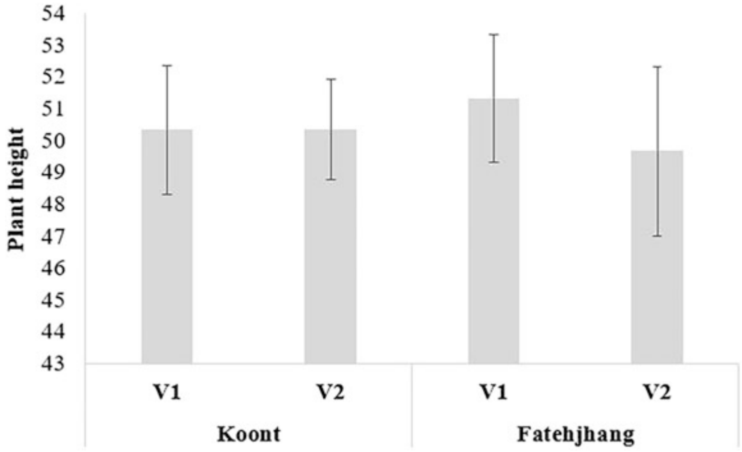

Fig. 13.10 Plant height of Thal 2006 and Balkasar at Koont and Fateh Jang with means followed by the same letters does not differ significantly at 5% level of significance

Table 13.10 Biological yield kg ha^{-1} of Thal 2006 and Balkasar at Koont and Fateh Jang

Locations	Cultivars	Biological yield
Koont	V1	5926.7 a
	V2	6183.3 a
Fateh Jang	V1	6901.7 a
	V2	6552.3 a

13.5.9 Grain Yield (kg ha^{-1})

Grain yield was recorded by harvesting a one m^2 area per plot, converted to get final yield in kg ha^{-1}. It is a consequence of several physiological and phenological developments in the plant throughout its lifecycle. Results showed an average grain yield of Thal 2006 at Koont, Rawalpindi, and Fateh Jang as 1573.33 and 1449.66 kg ha^{-1}with the standard error of 11.76 and 17.37 as given in Table 13.11. Chickpea variety Balkasar showed an average grain yield of 1483.33 at Koont, Rawalpindi, with the standard error of 7.53. However, the same variety showed an average grain yield of 1294.66 with standard error of 20.44 at Fateh Jang. Higher grain yield at Koont, Rawalpindi, for both varieties may be due to the suitable dry conditions at the grain filling stage of the crop (Fig. 13.12). Results were significant for both varieties at Koont, Rawalpindi and Fateh Jang and are in accordance with Valimohamadi et al. (2009).

13.5.10 Harvest Index

Harvest index (HI) is an extent of the physiological potential of the crop under suitable climatic conditions. HI is the capability of a crop plant to convert its

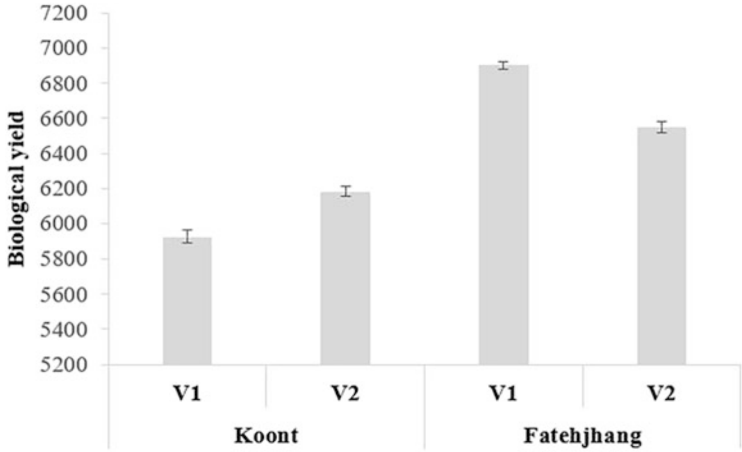

Fig. 13.11 Biological yield of Thal 2006 and Balkasar at Koont and Fateh Jang with means followed by the same letters does not differ significantly at 5% level of significance

Table 13.11 Grain yield kg ha^{-1} of Thal 2006 and Balkasar at Koont and Fateh Jang

Locations	Cultivars	Grain yield
Koont	V1	1573.3 a
	V2	1483.3 ab
Fateh Jang	V1	1449.7 a
	V2	1294.7 ab

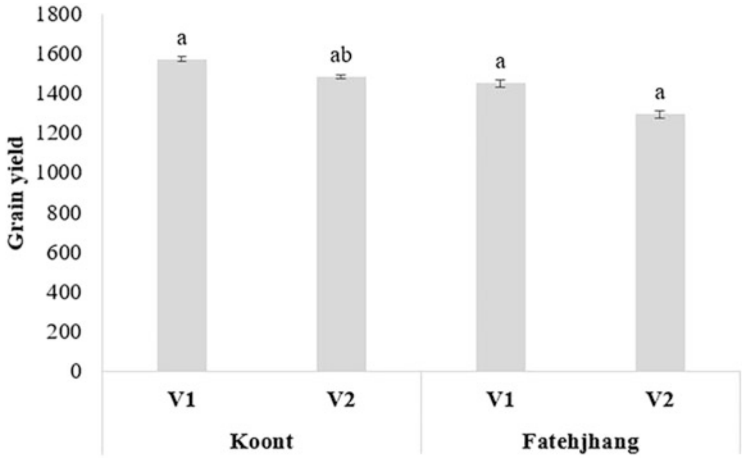

Fig. 13.12 Grain yield kg ha^{-1} of Thal 2006 and Balkasar at Koont and Fateh Jang with means followed by the same letter does not differ significantly at 5% level of significance

Table 13.12 Harvest index of Thal 2006 and Balkasar at Koont and Fateh Jang

Locations	Cultivars	Harvest index
Koont	V1	0.23a
	V2	0.2ab
Fateh Jang	V1	0.21a
	V2	0.19ab

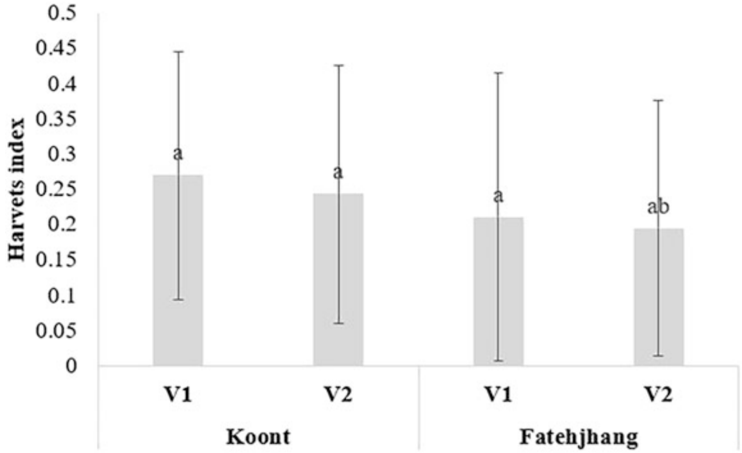

Fig. 13.13 Harvest index of Thal 2006 and Balkasar at Koont and Fateh Jang with means followed by the same letter do not differ significantly at 5% level of significance

produce, i.e., in the form of dry matter preferably into the economic yield. Results showed average values of HI of Thal 2006 variety at Koont, Rawalpindi, and Fateh Jang, i.e., 0.269 and 0.210 with the standard error of 0.175 and 0.204 as mentioned in Table 13.12. The average values of harvest index for Balkasar variety at Koont, Rawalpindi, and Fateh Jang are 0.242 and 0.194 with the standard error of 0.182 and 0.180 as given in Fig. 13.13. The relatively high value of HI for both varieties at Koont was due to more number of grains at this site. Results were significant for Thal 2006 and Balkasar at Koont, Rawalpindi, and Fateh Jang and thus in accordance with Qureshi et al. (2004).

13.6 Simulation Outcomes

13.6.1 Days to Anthesis

Simulated days to anthesis at both locations were closely associated with observed data for different locations and climatic conditions during chickpea growing season of 2017–2018, as presented in Table 13.13. At Koont, Rawalpindi, higher observed value of 94 days for variety Balkasar while minimum of 88 days for Thal 2006 were

Table 13.13 Observed and simulated days to anthesis under varying locations and varieties

Locations	Cultivars	Observed	Simulated	RMSE	d-index
Koont	Thal 2006	88	87	2.3	0.97
	Balkasar	94	93	3.0	0.96
Fateh Jang	Thal 2006	91.7	91	2.0	0.98
	Balkasar	104.3	104	2.1	0.97

Table 13.14 Observed and simulated days to maturity under varying locations and varieties

Locations	Cultivars	Observed	Simulated	RMSE	d-index
Koont	Thal 2006	175.7	174	4.8	0.97
	Balkasar	178.3	177	4.0	0.98
Fateh Jang	Thal 2006	181.7	180	3.5	0.97
	Balkasar	184	183	3.3	0.96

recorded. While at Fateh Jang the higher observed value of 104.3 days of Balkasar variety while minimum of 91.67 days for Thal 2006 were calculated.

In a same way, the predicted days were recorded at both locations, i.e., Fateh Jang and Koont, Rawalpindi, and varieties Thal 2006 and Balkasar. Maximum of 93 days were reported for Balkasar variety and minimum of 87 days for Thal 2006 at Koont, Rawalpindi. Whereas, maximum of104 days for Balkasar and minimum of 91 days were reported at Fateh Jang. Validation skill scores (RMSE and d-index) were used for comparison of model performance which were (0.96), (0.97), and (0.98), respectively.

13.6.2 Days to Maturity

Predicted days to maturity at both locations were closely associated with observed data for different locations and climatic conditions during chickpea growing season of 2017–2018 as presented in Table 13.14. At Koont, Rawalpindi, higher observed value of 178.3 days for variety Balkasar while minimum of 175.7 days for Thal 2006 were recorded. While at Fateh Jang the higher observed value of 184 days of Balkasar variety while minimum of 181.7 days for Thal 2006 were calculated.

In a same way the predicted days were recorded at both locations, i.e., Fateh Jang and Koont, Rawalpindi, and varieties Thal 2006 and Balkasar. Maximum of 177 days were reported for Balkasar variety and minimum of 174 days for Thal 2006 at Koont, Rawalpindi. Whereas, maximum of 183 days for Balkasar variety and minimum of 180 days were reported at Fateh Jang location. Validation skill scores (RMSE and d-index) were used for comparison of model performance which were (0.96), (0.97), and (0.98), respectively.

Table 13.15 Observed and simulated above-ground mass (kg ha^{-1}) under varying locations and varieties

Locations	Cultivars	Observed	Simulated	RMSE	d-index
Koont	Thal 2006	5926.7	5900	5.27	0.98
	Balkasar	6183.3	6100	6.1	0.97
Fateh Jang	Thal 2006	6901.7	6900	6.9183	0.97
	Balkasar	6552.3	6550	5.4	0.98

Table 13.16 Observed and simulated above grain yield (kg ha^{-1}) under varying locations and varieties

Locations	Cultivars	Observed	Simulated	RMSE	d-index
Koont	Thal 2006	1573.3	1500	5.27	0.98
	Balkasar	1483.3	1486	4.6	0.95
Fateh Jang	Thal 2006	1449.7	1400	4.9	0.97
	Balkasar	1294.7	1296	3.8	0.97

13.6.3 Above-Ground Biomass (kg ha^{-1})

Simulated and observed value of above-ground mass has close association for different locations and varieties during growing season of chickpea of 2017–2018 and is given in Table 13.15. The maximum observed value for biological yield is 6183.3 kg ha^{-1}for Balkasar variety of chickpea and minimum value recorded for Thal 2006 is 5926.7 kg ha^{-1} at location Koont, Rawalpindi. Whereas at location Fateh Jang, the highest value for biological yield of 6901.7 kg ha^{-1} is observed for Thal 2006 variety and minimum of 6552.3 kg ha^{-1} for Balkasar variety at Koont, Rawalpindi.

Meanwhile, model simulation showed lowest simulated value of 5900 kg ha^{-1} for Thal 2006 and highest simulated value of 6100 kg ha^{-1} at Koont. Whereas, the highest simulated value of 6900 kg ha^{-1}) for Thal 2006 and minimum value of 6550 kg ha^{-1}) at Fateh Jang were recorded. Statistic indices values for evaluation of CROP-GRO chickpea RMSE and d-index which were (0.97) and (0.98), respectively. Our modeling approach thus consists of a simple quantitative description of climatic effect on chickpea growth and its different developmental stages. The model efficiently simulated above-ground biomass with respect to different varieties and locations.

13.6.4 Grain Yield (kg ha^{-1})

Simulated and observed data for grain yield of chickpea growing season 2017–18 have close association for different locations and varieties and are presented in Table 13.16. The maximum observed value for grain yield is 1573.3 kg ha^{-1}) for Thal 2006 variety of chickpea and minimum value recorded for Balkasar is

1483.3 kg ha^{-1} at location Koont, Rawalpindi. Whereas at location Fateh Jang, the highest value for grain yields of 1449.7 kg ha^{-1}) is observed for Thal 2006 variety and minimum of 1294.7 kg ha^{-1}) for Balkasar variety at Koont, Rawalpindi.

Meanwhile, model simulation showed lowest simulated value (1486) for Balkasar variety and highest simulated value of 1500 kg ha^{-1} at Koont. Whereas, the highest simulated value of 1400 kg ha^{-1}) for Thal 2006 and minimum value of 1296 kg ha^{-1} at Fateh Jang were recorded for variety Balkasar. The comparison of model performance was measured by using validation skill scores, RMSE, and d-index which were (0.95), (0.97), and (0.98), respectively.

References

Ahmad A, Ali A, Khaliq T, Wajid SA, Iqbal Z, Ibrahim M, Javeed HMR, Hoogenboom G (2013) OILCROP-SUN model relevance for evaluation of nitrogen management of sunflower hybrids in Sargodha, Punjab. Am J Plant Sci 4(9):1731

Ahmad S, Abbas G, Fatima Z, Khan RJ, Anjum MA, Ahmed M, Khan MA, Porter CH, Hoogenboom G (2017) Quantification of the impacts of climate warming and crop management on canola phenology in Punjab, Pakistan. J Agron Crop Sci 203(5):442–452. https://doi.org/10.1111/jac.12206

Ahmad S, Abbas G, Ahmed M, Fatima Z, Anjum MA, Rasul G, Khan MA, Hoogenboom G (2019) Climate warming and management impact on the change of phenology of the rice-wheat cropping system in Punjab, Pakistan. Field Crop Res 230:46–61. https://doi.org/10.1016/j.fcr.2018.10.008

Ahmed M (2012) Improving soil fertility recommendations in Africa using the decision support system for Agrotechnology transfer (DSSAT); a book review. Exp Agric 48(4):602–603

Ahmed M (2017) Greenhouse gas emissions and climate variability: an overview. In: Ahmed M, Stockle CO (eds) Quantification of climate variability, adaptation and mitigation for agricultural sustainability. Springer International Publishing, Cham, pp 1–26. https://doi.org/10.1007/978-3-319-32059-5_1

Ahmed M (2020) Introduction to modern climate change. Andrew E. Dessler: Cambridge University Press, 2011, 252 pp, ISBN-10: 0521173159. Sci Total Environ 734:139397. https://doi.org/10.1016/j.scitotenv.2020.139397

Ahmed M, Ahmad S (2019) Carbon dioxide enrichment and crop productivity. In: Hasanuzzaman M (ed) Agronomic crops, Management practices, vol 2. Springer Singapore, Singapore, pp 31–46. https://doi.org/10.1007/978-981-32-9783-8_3

Ahmed M, Stockle CO (2016) Quantification of climate variability, adaptation and mitigation for agricultural sustainability. Springer Nature Singapore Pvt. Ltd, Singapore, 437 pp. https://doi.org/10.1007/978-3-319-32059-5

Ahmed M, Asif M, Hirani AH, Akram MN, Goyal A (2013) Modeling for agricultural sustainability: a review. In: Bhullar GS, Bhullar NK (eds) Agricultural sustainability progress and prospects in crop research. Elsevier, London

Ahmed M, Aslam MA, Hassan FU, Asif M, Hayat R (2014) Use of APSIM to model nitrogen use efficiency of rain-fed wheat. Int J Agric Biol 16:461–470

Ahmed M, Akram MN, Asim M, Aslam M, Hassan F-u, Higgins S, Stöckle CO, Hoogenboom G (2016) Calibration and validation of APSIM-wheat and CERES-wheat for spring wheat under rainfed conditions: models evaluation and application. Comput Electron Agric 123:384–401. https://doi.org/10.1016/j.compag.2016.03.015

Ahmed M, Stöckle CO, Nelson R, Higgins S (2017) Assessment of climate change and atmospheric CO_2 impact on winter wheat in the pacific northwest using a multimodel ensemble. Front Ecol Evol 5(51). https://doi.org/10.3389/fevo.2017.00051

Ahmed M, Ijaz W, Ahmad S (2018) Adapting and evaluating APSIM-SoilP-wheat model for response to phosphorus under rainfed conditions of Pakistan. J Plant Nutr 41(16):2069–2084. https://doi.org/10.1080/01904167.2018.1485933

Ahmed M, Stöckle CO, Nelson R, Higgins S, Ahmad S, Raza MA (2019) Novel multimodel ensemble approach to evaluate the sole effect of elevated CO_2 on winter wheat productivity. Sci Rep 9(1):7813. https://doi.org/10.1038/s41598-019-44251-x

Alam M, Haider S (2006) Growth attributes of barley (Hordeum vulgare L.) cultivars in relation to different doses of nitrogen fertilizer. J Life Earth Sci 1(2):77–82

Ali A, Erenstein O (2017) Assessing farmer use of climate change adaptation practices and impacts on food security and poverty in Pakistan. Clim Risk Manag 16:183–194. https://doi.org/10.1016/j.crm.2016.12.001

Ali S, Liu Y, Ishaq M, Shah T, Ilyas A, Din IU (2017) Climate change and its impact on the yield of major food crops: evidence from Pakistan. Foods 6(6):39

Andarzian B, Bannayan M, Steduto P, Mazraeh H, Barati M, Barati M, Rahnama A (2011) Validation and testing of the AquaCrop model under full and deficit irrigated wheat production in Iran. Agric Water Manag 100(1):1–8

Angadi S, Cutforth H, Miller P, McConkey B, Entz M, Brandt S, Volkmar K (2000) Response of three Brassica species to high temperature stress during reproductive growth. Can J Plant Sci 80 (4):693–701

Apata TG (2011) Effects of global climate change on Nigerian agriculture: an empirical analysis. CBN J Appl Stat 2(1):31–50

Aslam MA, Ahmed M, Hayat R (2017) Modeling nitrogen use efficiency under changing climate. In: Ahmed M, Stockle CO (eds) Quantification of climate variability, adaptation and mitigation for agricultural sustainability. Springer International Publishing, Cham, pp 71–90. https://doi.org/10.1007/978-3-319-32059-5_4

Asseng S, Martre P, Maiorano A, Rötter RP, O'Leary GJ, Fitzgerald GJ, Girousse C, Motzo R, Giunta F, Babar MA, Reynolds MP, Kheir AMS, Thorburn PJ, Waha K, Ruane AC, Aggarwal PK, Ahmed M, Balkovič J, Basso B, Biernath C, Bindi M, Cammarano D, Challinor AJ, De Sanctis G, Dumont B, Eyshi Rezaei E, Fereres E, Ferrise R, Garcia-Vila M, Gayler S, Gao Y, Horan H, Hoogenboom G, Izaurralde RC, Jabloun M, Jones CD, Kassie BT, Kersebaum K-C, Klein C, Koehler A-K, Liu B, Minoli S, Montesino San Martin M, Müller C, Naresh Kumar S, Nendel C, Olesen JE, Palosuo T, Porter JR, Priesack E, Ripoche D, Semenov MA, Stöckle C, Stratonovitch P, Streck T, Supit I, Tao F, Van der Velde M, Wallach D, Wang E, Webber H, Wolf J, Xiao L, Zhang Z, Zhao Z, Zhu Y, Ewert F (2019) Climate change impact and adaptation for wheat protein. Glob Chang Biol 25(1):155–173. https://doi.org/10.1111/gcb.14481

Azimi SM, Kor NM, Ahmadi M, Shaaban M, Motlagh ZR, Shamsizadeh M (2015) Investigation of growth analysis in chickpea (Cicer arietinum L.) cultivars under drought stress. Int J Life Sci 9 (5):91–94

Bannayan M, Crout N, Hoogenboom G (2003) Application of the CERES-wheat model for within-season prediction of winter wheat yield in the United Kingdom. Agron J 95(1):114–125

Berger J, Milroy S, Turner N, Siddique K, Imtiaz M, Malhotra R (2011) Chickpea evolution has selected for contrasting phenological mechanisms among different habitats. Euphytica 180 (1):1–15

Chmielewski F-M, Müller A, Bruns E (2004) Climate changes and trends in phenology of fruit trees and field crops in Germany, 1961–2000. Agric For Meteorol 121(1):69–78

Christensen O, Christensen J (2004) Intensification of extreme European summer precipitation in a warmer climate. Glob Planet Chang 44(1):107–117

Climate Risk Index (2020) World map 1999–2018. www.germanwatch.org/en/cri2

Confalonieri R, Orlando F, Paleari L, Stella T, Gilardelli C, Movedi E, Pagani V, Cappelli G, Vertemara A, Alberti L (2016) Uncertainty in crop model predictions: what is the role of users? Environ Model Softw 81:165–173

Craufurd PQ, Wheeler T (2009) Climate change and the flowering time of annual crops. J Exp Bot 60(9):2529–2539

Dai A (2011) Drought under global warming: a review. Wiley Interdiscip Rev Clim Chang 2 (1):45–65
Devasirvatham V, Gaur PM, Mallikarjuna N, Tokachichu RN, Trethowan RM, Tan DK (2012) Effect of high temperature on the reproductive development of chickpea genotypes under controlled environments. Funct Plant Biol 39(12):1009–1018
Donald C (1962) In search of yield. J. Aust. Inst. Agric. Sci. 28:171–178
Donald CM (1968) The breeding of crop ideotypes. Euphytica 17(3):385–403. https://doi.org/10.1007/BF00056241
Fisher D, Dyke A, Koerner R, Bourgeois J, Kinnard C, Zdanowicz C, De Vernal A, Hillaire-Marcel C, Savelle J, Rochon A (2006) Natural variability of Arctic Sea ice over the Holocene. Eos 87(28):273–280
Fourcaud T, Zhang X, Stokes A, Lambers H, Körner C (2008) Plant growth modelling and applications: the increasing importance of plant architecture in growth models. Ann Bot 101 (8):1053–1063
Frade MM, Valenciano J (2005) Effect of sowing density on the yield and yield components of spring-sown irrigated chickpea (Cicer arietinum) grown in Spain. N Z J Crop Hortic Sci 33 (4):367–371
Gan Y, Angadi S, Cutforth H, Potts D, Angadi V, McDonald C (2004) Canola and mustard response to short periods of temperature and water stress at different developmental stages. Can J Plant Sci 84(3):697–704
Gaydon D, Wang E, Poulton P, Ahmad B, Ahmed F, Akhter S, Ali I, Amarasingha R, Chaki A, Chen C (2017) Evaluation of the APSIM model in cropping systems of Asia. Field Crop Res 204:52–75
Greve P, Orlowsky B, Mueller B, Sheffield J, Reichstein M, Seneviratne SI (2014) Global assessment of trends in wetting and drying over land. Nat Geosci 7(10):716–721
Hoogenboom G, Tsuji GY, Pickering NB, Curry RB, Jones JW, Singh U, Godwin DC (1995) Decision support system to study climate change impacts on crop production. In: Rosenzweig C (ed) Climate change and agriculture: Analysis of potential international impacts, ASA Special Publication, vol 59. Madison, WI, American Society of Agronomy, pp 51–75. https://doi.org/10.2134/asaspecpub59.c3
Hoogenboom G, Jones J, Wilkens P, Porter C, Boote K, Hunt L, Singh U, Lizaso J, White J, Uryasev O (2015) Decision support system for Agrotechnology transfer (DSSAT) version 4.6 (www.DSSAT.net). DSSAT Foundation, Prosser, Washington
Hoogenboom G, Porter CH, Boote KJ, Shelia V, Wilkens PW, Singh U, White JW, Asseng S, Lizaso JI, Moreno LP, Pavan W, Ogoshi R, Hunt LA, Tsuji GY, Jones JW (2019a) The DSSAT crop modeling ecosystem. In: Boote KJ (ed) Advances in crop modeling for a sustainable agriculture. Burleigh Dodds Science Publishing, Cambridge, United Kingdom, pp 173–216. https://doi.org/10.19103/AS.2019.0061.10
Hoogenboom G, Porter CH, Shelia V, Boote KJ, Singh U, White JW, Hunt LA, Ogoshi R, Lizaso JI, Koo J, Asseng S, Singels A, Moreno LP, Jones JW (2019b) Deecision support system for agrotechnology transfer (DSSAT) Version 4.7.5. DSSAT Foundation, Gainesville, Floridea, USA. www.dssat.net.
Huntingford C, Jones R, Prudhomme C, Lamb R, Gash JH, Jones DA (2003) Regional climate-model predictions of extreme rainfall for a changing climate. Q J R Meteorol Soc 129 (590):1607–1621
Ijaz W, Ahmed M, Asim M, Aslam M (2017) Models to study phosphorous dynamics under changing climate. In: Ahmed M, Stockle CO (eds) Quantification of climate variability, adaptation and mitigation for agricultural sustainability. Springer International Publishing, Cham, pp 371–386. https://doi.org/10.1007/978-3-319-32059-5_15
IPCC (2013) Climate change 2013: the physical science basis. Contribution of working group i to the fifth assessment report of the intergovernmental panel on climate change. Cambridge University Press, Cambridge

IPCC (2014) Climate change 2014: Impacts, adaptation, and vulnerability. Part A: Global and sectoral aspects. In: Field CB, Barros VR, Dokken DJ, Mach KJ, Mastrandrea MD, Bilir TE, Chatterjee M, Ebi KL, Estrada YO, Genova RC, Girma B, Kissel ES, Levy AN, MacCracken S, Mastrandrea PR, White LL (eds) Contribution of working group ii to the fifth assessment report of the intergovernmental panel on climate change. Cambridge University Press, Cambridge, United Kingdom, New York, NY, USA

Jabeen M, Gabriel HF, Ahmed M, Mahboob MA, Iqbal J (2017) Studying impact of climate change on wheat yield by using DSSAT and GIS: a case study of Pothwar region. In: Ahmed M, Stockle CO (eds) Quantification of climate variability, adaptation and mitigation for agricultural sustainability. Springer International Publishing, Cham, pp 387–411. https://doi.org/10.1007/978-3-319-32059-5_16

Khan IA, Abourashed EA (2011) Leung's encyclopedia of common natural ingredients: used in food, drugs and cosmetics. John Wiley & Sons, New York

Khan E, Aslam M, Ahmad H, Himayatullah KM, Hussain A (2010) Effect of row spacing and seeding rates on growth, yield and yield components of chickpea. Sarhad J Agric 26(2):201–211

Kibe A, Singh S, Kalra N (2006) Water–nitrogen relationships for wheat growth and productivity in late sown conditions. Agric Water Manag 84(3):221–228

Knights EJ, Hobson KB (2016) Chickpea: overview. In: Encyclopedia of food grains, 2nd edn. Academic Press, Oxford, pp 316–323. https://doi.org/10.1016/B978-0-12-394437-5.00035-8

Kutcher HR, Warland JS, Brandt SA (2010) Temperature and precipitation effects on canola yields in Saskatchewan, Canada. Agric For Meteorol 150(2):161–165. https://doi.org/10.1016/j.agrformet.2009.09.011

Liang E, Liu X, Yuan Y, Qin N, Fang X, Huang L, Zhu H, Wang L, Shao X (2006) The 1920s drought recorded by tree rings and historical documents in the semi-arid and arid areas of northern China. Clim Chang 79(3–4):403–432

Liu B, Martre P, Ewert F, Porter JR, Challinor AJ, Müller C, Ruane AC, Waha K, Thorburn PJ, Aggarwal PK, Ahmed M, Balkovič J, Basso B, Biernath C, Bindi M, Cammarano D, De Sanctis G, Dumont B, Espadafor M, Eyshi Rezaei E, Ferrise R, Garcia-Vila M, Gayler S, Gao Y, Horan H, Hoogenboom G, Izaurralde RC, Jones CD, Kassie BT, Kersebaum KC, Klein C, Koehler A-K, Maiorano A, Minoli S, Montesino San Martin M, Naresh Kumar S, Nendel C, O'Leary GJ, Palosuo T, Priesack E, Ripoche D, Rötter RP, Semenov MA, Stöckle C, Streck T, Supit I, Tao F, Van der Velde M, Wallach D, Wang E, Webber H, Wolf J, Xiao L, Zhang Z, Zhao Z, Zhu Y, Asseng S (2019) Global wheat production with 1.5 and 2.0°C above pre-industrial warming. Glob Chang Biol 25(4):1428–1444. https://doi.org/10.1111/gcb.14542

Lobell DB, Bänziger M, Magorokosho C, Vivek B (2011) Nonlinear heat effects on African maize as evidenced by historical yield trials. Nat Clim Chang 1(1):42–45

Luedeling E, Zhang M, Girvetz EH (2009) Climatic changes lead to declining winter chill for fruit and nut trees in California during 1950–2099. PLoS One 4(7):e6166

Machado S, Paulsen GM (2001) Combined effects of drought and high temperature on water relations of wheat and sorghum. Plant Soil 233(2):179–187

Mafakheri A, Siosemardeh A, Bahramnejad B, Struik P, Sohrabi Y (2010) Effect of drought stress on yield, proline and chlorophyll contents in three chickpea cultivars. Aust J Crop Sci 4(8):580

Mall RK, Gupta A, Sonkar G (2017) 2 – effect of climate change on agricultural crops. In: Current developments in biotechnology and bioengineering. Elsevier, pp 23–46. https://doi.org/10.1016/B978-0-444-63661-4.00002-5

McMaster GS, White JW, Hunt L, Jamieson P, Dhillon S, Ortiz-Monasterio J (2008) Simulating the influence of vernalization, photoperiod and optimum temperature on wheat developmental rates. Ann Bot 102(4):561–569

Meehl GA, Stocker TF, Collins WD, Friedlingstein P, Gaye AT, Gregory JM, Kitoh A, Knutti R, Murphy JM, Noda A (2007) Global climate projections. Clim Change 3495:747–845

Mohammed A, Tarpley L (2009) High nighttime temperatures affect rice productivity through altered pollen germination and spikelet fertility. Agric For Meteorol 149(6):999–1008

Monpara B, Kalariya R (2009) Changes in certain yield traits as influenced by differences in maturity time in bread wheat. Plant Arch 9(1):335–339
Muehlbauer FJ, Sarker A (2017) Economic importance of chickpea: production, value, and world trade. In: The chickpea genome. Springer, New York, pp 5–12
Nayyar H, Bains T, Kumar S (2005) Low temperature induced floral abortion in chickpea: relationship to abscisic acid and cryoprotectants in reproductive organs. Environ Exp Bot 53 (1):39–47
Ohashi Y, Nakayama N, Saneoka H, Fujita K (2006) Effects of drought stress on photosynthetic gas exchange, chlorophyll fluorescence and stem diameter of soybean plants. Biol Plant 50 (1):138–141
Oppenheimer M, Alley RB (2004) The West Antarctic ice sheet and long term climate policy. Clim Chang 64(1):1–10
Otter-Nacke S, Godwin D, Richie J (1986) Testing and validating the CERES-wheat model in diverse environments. Rational Aeronautics and Space Administration, Houston
Pandey S, Kabdal M, Tripathi M (2013) Study of inheritance of erucic acid in Indian mustard (Brassica juncea L. Czern & Coss). Octa J Biosci 1(1):77–84
Pearce RB, Mitchell RL, Gardner FP (1985) Physiology of crop plants. Iowa State University Press, Ames, IA
Porter CH, Jones JW, Adiku S, Gijsman AJ, Gargiulo O, Naab J (2010) Modeling organic carbon and carbon-mediated soil processes in DSSAT v4. 5. Oper Res 10(3):247–278
Qureshi AS, Shaukat A, Bakhsh A, Arshad M, Ghafoor A (2004) An assessment of variability for economically important traits in chickpea (Cicer arietinum L.). Pak J Bot 36(4):779–785
Raja W, Kanth RH, Singh P (2018) Validating the AquaCrop model for maize under different sowing dates. Water Policy 20(4):wp2018123
Rasul F, Cheema M, Sattar A, Saleem M, Wahid M (2012) Evaluating the performance of three mungbean varieties grown under varying inter-row spacing. J Anim Plant Sci 22(4):2012
Rezaei EE, Webber H, Gaiser T, Naab J, Ewert F (2015) Heat stress in cereals: mechanisms and modelling. Eur J Agron 64:98–113
Roberts E, Hadley P, Summerfield R (1985) Effects of temperature and photoperiod on flowering in chickpeas (Cicer arietinum L.). Ann Bot 55(6):881–892
Ruchika B, Sandhu J (2009) Pollen viability and pod formation in chickpea (Cicer arietinum) as a criteria for screening and genetic studies of cold tolerance. Indian J Agric Sci 79(2):152–154
Shamsi K (2009) The effects of planting density on grain filling, yield and yield components of three chick pea (Cicer arietinum L.) varieties in Kermanshah, Iran. Iran J Animal Plant Sci 2 (3):99–103
Siddique KHM, Krishnamurthy L (2016) Chickpea, agronomy. In: Reference module in food science. Elsevier. https://doi.org/10.1016/B978-0-08-100596-5.00192-X
Siebert S, Ewert F (2012) Spatio-temporal patterns of phenological development in Germany in relation to temperature and day length. Agric For Meteorol 152:44–57
Singh T (2005) Influence of moisture conservation practices and fertility levels on mustard and lentil intercropping system under rainfed conditions. Indian Agricultural Research Institute, New Delhi
Slafer G (2003) Genetic basis of yield as viewed from a crop physiologist's perspective. Ann Appl Biol 142(2):117–128
Soltani A, Robertson M, Torabi B, Yousefi-Daz M, Sarparast R (2006) Modelling seedling emergence in chickpea as influenced by temperature and sowing depth. Agric For Meteorol 138(1):156–167
Stern N (2008) The economics of climate change. Am Econ Rev 98(2):1–37
Stoddard F, Balko C, Erskine W, Khan H, Link W, Sarker A (2006) Screening techniques and sources of resistance to abiotic stresses in cool-season food legumes. Euphytica 147 (1–2):167–186

Takashima NE, Rondanini DP, Puhl LE, Miralles DJ (2013) Environmental factors affecting yield variability in spring and winter rapeseed genotypes cultivated in the southeastern argentine pampas. Eur J Agron 48:88–100

Thornton PK, Ericksen PJ, Herrero M, Challinor AJ (2014) Climate variability and vulnerability to climate change: A review. Glob Chan Biol: n/a-n/a. https://doi.org/10.1111/gcb.12581

Togay N, Togay Y, Cimrin KM, Turan M (2008) Effects of rhizobium inoculation, sulfur and phosphorus applications on yield, yield components and nutrient uptakes in chickpea (Cicer arietinum L.). Afr J Biotechnol 7(6):776–782

USEPA UEPA (2011) Office of solid waste and emergency response, U.S. Environmental Protection Agency. Washington, DC, EPA530-R-99-009

Valimohamadi F, Tajbakhsh M, Saeed A (2009) Effect of planting date and plant density on grain yield, yield components and some quality and morphological traits of chickpea (Cicer arietinum L.). JWSS-Isfahan Univ Technol 12(46):31–40

Wallach D, Martre P, Liu B, Asseng S, Ewert F, Thorburn PJ, van Ittersum M, Aggarwal PK, Ahmed M, Basso B, Biernath C, Cammarano D, Challinor AJ, De Sanctis G, Dumont B, Eyshi Rezaei E, Fereres E, Fitzgerald GJ, Gao Y, Garcia-Vila M, Gayler S, Girousse C, Hoogenboom G, Horan H, Izaurralde RC, Jones CD, Kassie BT, Kersebaum KC, Klein C, Koehler A-K, Maiorano A, Minoli S, Müller C, Naresh Kumar S, Nendel C, O'Leary GJ, Palosuo T, Priesack E, Ripoche D, Rötter RP, Semenov MA, Stöckle C, Stratonovitch P, Streck T, Supit I, Tao F, Wolf J, Zhang Z (2018) Multimodel ensembles improve predictions of crop–environment–management interactions. Glob Chang Biol 24(11):5072–5083. https://doi.org/10.1111/gcb.14411

Walley FL, Kyei-Boahen S, Hnatowich G, Stevenson C (2005) Nitrogen and phosphorus fertility management for desi and kabuli chickpea. Can J Plant Sci 85(1):73–79

Wang B, Liu DL, Asseng S, Macadam I, Yu Q (2015) Impact of climate change on wheat flowering time in eastern Australia. Agric For Meteorol 209–210:11–21. https://doi.org/10.1016/j.agrformet.2015.04.028

White JW, Hoogenboom G, Kimball BA, Wall GW (2011) Methodologies for simulating impacts of climate change on crop production. Field Crop Res 124(3):357–368. https://doi.org/10.1016/j.fcr.2011.07.001

Zhang Q, Li J, Singh VP, Xiao M (2013) Spatio-temporal relations between temperature and precipitation regimes: implications for temperature-induced changes in the hydrological cycle. Glob Planet Chang 111:57–76

Zinn KE, Tunc-Ozdemir M, Harper JF (2010) Temperature stress and plant sexual reproduction: uncovering the weakest links. J Exp Bot 61(7):erq053

Potato Modeling

14

Mukhtar Ahmed, Zartash Fatima, Pakeeza Iqbal, Thaira Kalsoom, Kashif Sarfraz Abbasi, Farid Asif Shaheen, and Shakeel Ahmad

Abstract

Potato (*Solanum tuberosum*) is the most significant food crop next to rice and wheat. Climate change could exert critical influences on supply of food; consequently, key challenge for modern agriculture is to develop approaches to handle its harmful impacts for confirming food security by 2050 as well as afterward. Climate variability in the form of higher temperature, rainfall variability, and increased frequency of drought have shown significant impact on potato production. Thus, it is essential to design adaptation strategies that can mitigate influence of climate change for long-term basis. Different process-based models such as Decision Support System for Agrotechnology Transfer (DSSAT), Agricultural Production Systems Simulator (APSIM), CropSyst (CropSyst VB–Simpotato), and STICS (Simulateur mulTIdisciplinaire pour les Cultures Standard) have

M. Ahmed (✉)
Department of Agricultural Research for Northern Sweden, Swedish University of Agricultural Sciences, Umeå, Sweden

Department of Agronomy, Pir Mehr Ali Shah Arid Agriculture University, Rawalpindi, Pakistan
e-mail: mukhtar.ahmed@slu.se; ahmadmukhtar@uaar.edu.pk

Z. Fatima · S. Ahmad
Department of Agronomy, Bahauddin Zakariya University, Multan, Pakistan

P. Iqbal
Department of Botany, University of Agriculture, Faisalabad, Pakistan

T. Kalsoom
Department of Horticulture, Pir Mehr Ali Shah Arid Agriculture University, Rawalpindi, Pakistan

K. S. Abbasi
Institute of Food & Nutritional Sciences, PMAS-Arid Agriculture University, Rawalpindi, Pakistan

F. A. Shaheen
Department of Entomology, PMAS Arid Agriculture University, Rawalpindi, Pakistan

M. Ahmed (ed.), *Systems Modeling*, https://doi.org/10.1007/978-981-15-4728-7_14

shown great potential to develop sustainable agronomic practices as well as virtual potato cultivars to have good potato crop for future.

Keywords

Potato · Climate change · Higher temperature · Rainfall variability and increased frequency of drought · Process-based models

14.1 Introduction

Potato is an important crop in the world after rice and wheat with an annual production of 330 MT (FAO 2017). Major changes are going on in the world potato sector, and until early 1990s, most of the world potato was produced and consumed in Europe, North America, and former Russia. However, after 2005, most of the world potato is produced by developing countries with China at the first place and India at the third place. Almost a third of all potatoes are harvested in these two places (Fig. 14.1). Average share of potatoes production (1994–2018) by regions has been shown in Fig. 14.2. This crop is the source of income besides food security for developing countries (Lutaladio and Castaidi 2009), while burgeoning population is

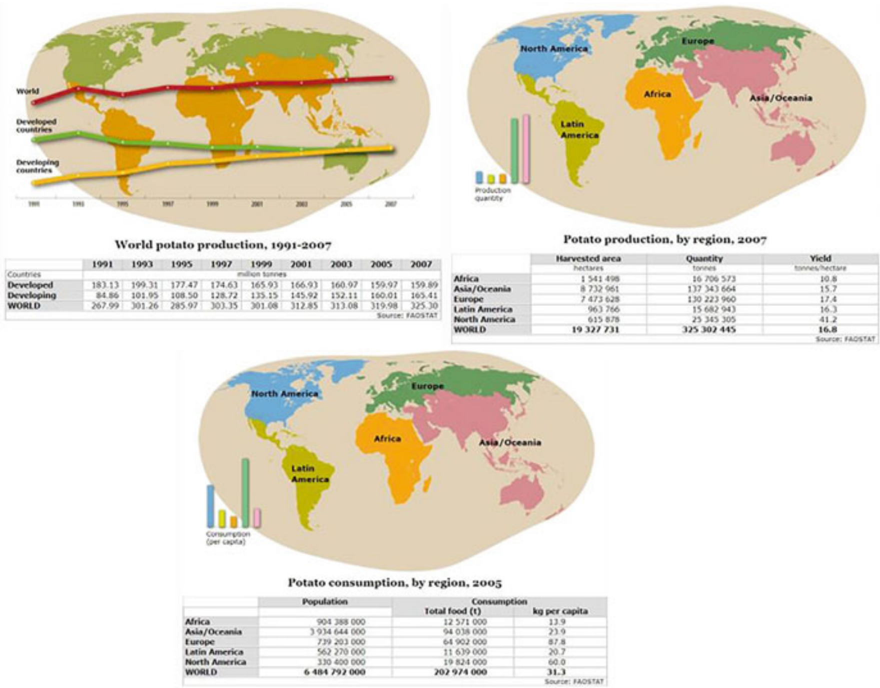

World potato production, 1991-2007

	1991	1993	1995	1997	1999	2001	2003	2005	2007
Countries	million tonnes								
Developed	183.13	199.31	177.47	174.63	165.93	166.93	160.97	159.97	159.89
Developing	84.86	101.95	108.50	128.72	135.15	145.92	152.11	160.01	165.41
WORLD	267.99	301.26	285.97	303.35	301.08	312.85	313.08	319.98	325.30

Source: FAOSTAT

Potato production, by region, 2007

	Harvested area	Quantity	Yield
	hectares	tonnes	tonnes/hectare
Africa	1 541 498	16 706 573	10.8
Asia/Oceania	8 732 961	137 343 664	15.7
Europe	7 473 628	130 223 960	17.4
Latin America	963 766	15 682 943	16.3
North America	615 878	25 345 305	41.2
WORLD	**19 327 731**	**325 302 445**	**16.8**

Source: FAOSTAT

Potato consumption, by region, 2005

	Population	Consumption	
		Total food (t)	kg per capita
Africa	904 388 000	12 571 000	13.9
Asia/Oceania	3 934 644 000	94 038 000	23.9
Europe	739 203 000	64 902 000	87.8
Latin America	562 270 000	11 639 000	20.7
North America	330 400 000	19 824 000	60.0
WORLD	**6 484 792 000**	**202 974 000**	**31.3**

Source: FAOSTAT

Fig. 14.1 Global scenarios of potato production and consumption. (Source: FAO; http://www.fao.org/potato-2008/en/world/)

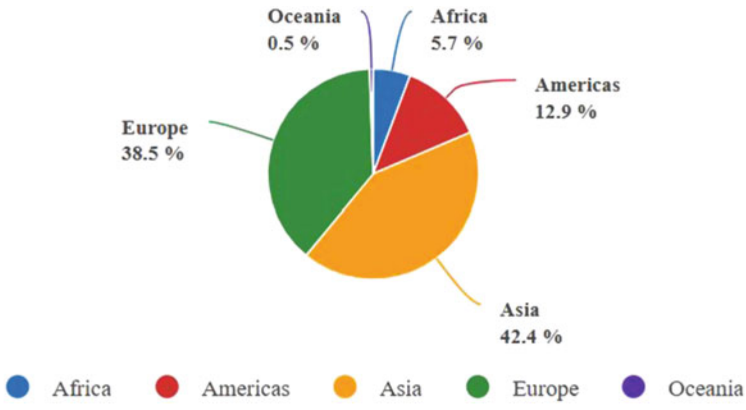

Fig. 14.2 Production share of potatoes by region (average 1994–2018)

increasing at alarming rates compared to other regions across the world (Lutz and Samir 2010). This crop is consumed as vegetable and used for food purposes. Its productivity is dependent on cultivar, management practice, and environmental condition (Dalla Costa et al. 1997; Miglietta et al. 1998; Kooman et al. 1996a, b). High temperature diminishes potato tuberization while injuries due to frost have also been reported for this crop (Hijmans 2003). Increased yield was predicted for England and Wales (Davies et al. 1996), Scotland (Peiris et al. 1996), and Finland due to higher temperature and longer growing season while an overall decreased yield was predicted for USA (Rosenzweig et al. 1996). Increased frequency of drought is another issue, which affects potato yield significantly. Costa et al. (1997) reported greatest reductions in photosynthesis, total biomass and yield when drought was imposed during tuber initiation. Similarly, they concluded that earliest stress resulted in the lowest water use effeciency and nitrogen uptake. Increasing atmospheric CO_2 concentration, increased daily mean temperature, and increased seasonal variability in rainfall are projected by IPCC (2007) worldwide during the twenty-first century. Variability in rainfall is a major concern for rain-fed potato where management practices are already major concern due to limited water availability. Seasonal solar radiation levels can also affect potato growth by potentially inducing drought. Hence, it is vital to understand the effect of short-term "cyclic" water-stress on potato growth besides elevated CO_2.

14.2 Phenological Development of Potato

The description of potato plant is shown in Fig. 14.3. Phenological development of potato is controlled by temperature (Kooman and Haverkort 1995), which will ultimately change the crop growth, development, yield, and quality (van Oort et al. 2012). It grows best at about 20 °C. It is fundamentally a "cool weather crop," as temperature being the key limiting factor for productivity; tuber growth is inhibited at temperatures lower than 10 °C (50 °F) and exceeding 30 °C (86 °F),

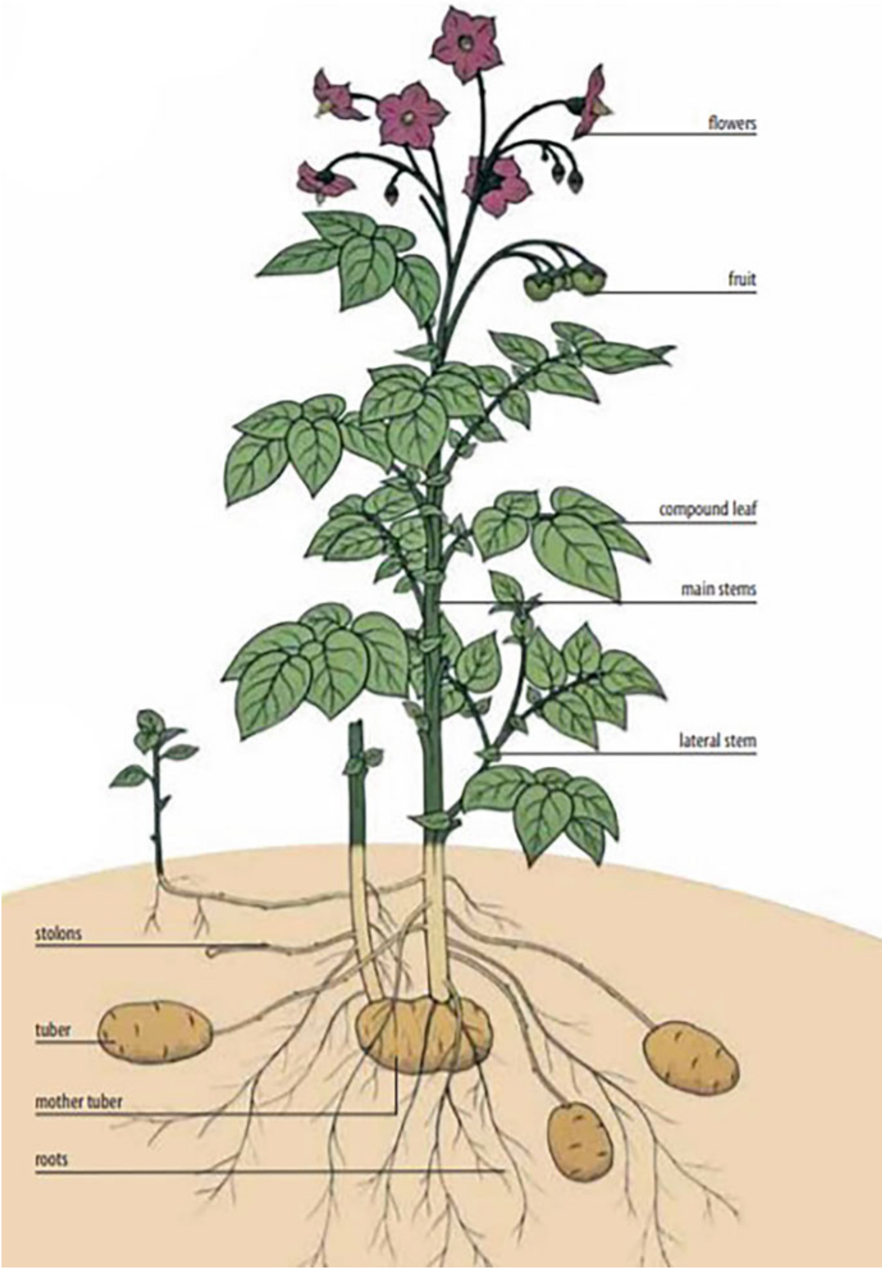

Fig. 14.3 Description of the potato plant

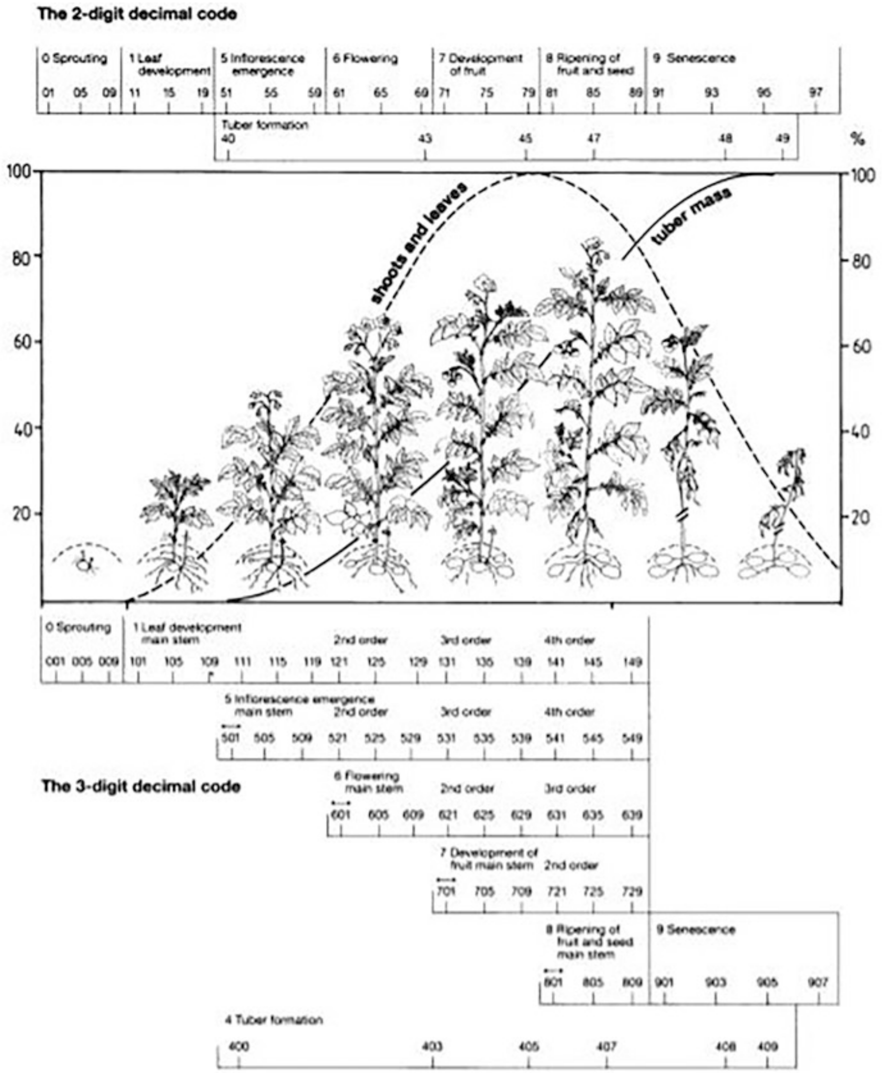

Fig. 14.4 Phenological stages of potato. (Source: Hack et al. 2001)

whereas optimal productivity is attained when daily mean temperature is in the range of 18–20 °C (64–68 °F). Due to this reason, it is planted in early spring in temperate regions while late winter in warmer areas and sown in cooler months in hot-tropical-climate. In some subtropical highlands, mild temperature and higher solar radiation permit growers to produce potatoes all over the year and produce tubers within 90 days of planting. High temperature during growing season causes changes in potatoes resulting in severe decrease in productivity (Rykaczewska 2015). Earlier work reported that the development of haulm is high at 20–25 °C while optimum array for tuberization and tuber development is 15–20 °C. The phenological stages of potato have been presented in Fig. 14.4.

Inhibition in tuberization and reduction in photoassimilate partitioning of tuber were studied by Lafta and Lorenzen (1995). Wahid et al. (2007) concluded that transitory or constant high temperature causes an array of morpho-anatomical, physiological, and biochemical changes in plants which affect plant growth, development, and yield reduction. A rising temperature leads to higher transpiration in plants which in turn increase their water demand. In several areas, drier potato sowing causes water stress, resulting in reduced yield. This effect will be further intensified by variations in rainfall distribution. In numerous countries, mainly in tropics and subtropics, productivity declines up to 20–30%. Night-time temperature has critical effect on deposition of starch in potato tubers. Ideal temperature range is 15–18 °C, and the temperature above 22 °C harshly hampers tuber growth. By contrast, climate change influence on potato productivity is predictable to be favorable in farming zones at high altitudes. In several zones, climatic situations for potato sowing are improving because of increasing temperature. In certain regions, it will be possible to produce potatoes as winter crop. Moreover, increase in potato sowing at high altitudes is also risky. Higher-altitude croplands are often located on steepy slopes, where sowing of potatoes could aggravate degradation of soil because of high tillage intensity. Adverse effect of heat stress can be mitigated by developing thermotolerant-potato varieties which is possible by understanding crop response to high temperature. Therefore, the main objective of this chapter is to quantify the influence of climatic factors like temperature, water stress on potato phenology, growth, yield, and quality on spatiotemporal scale. Hitherto, there is no such study available in which quantitative impact of heat, drought stress at diverse phenological stages and phases of growth, yield, and quality was conducted using remote sensing and modeling approaches.

14.3 Nutritive Values of Potato

Owing to its nutrition values, potato is a balanced food and is an important food crop in Pakistan as well as around the globe. Potato being cultivated across globe belongs to one species *Solanum tuberosum*, whereas it has four documented species besides 200 wild relatives. Around 5000 potato cultivars are sown in Andes. Potatoes chemical composition is effected by several elements, such as area of production, cultivar, climate and soil, husbandry practices, preparation, and cooking. Even though fundamental importance of potato being staple diet, limited is known regarding the nutrient composition of several potato cultivars. Depending on the cultivar, potato can be a valued source of minerals, such as potassium, magnesium, and phosphorus, and dietary antioxidants. Details of nutritional level of potato post boiling and peeling of the skin prior consumption are presented in Fig. 14.5.

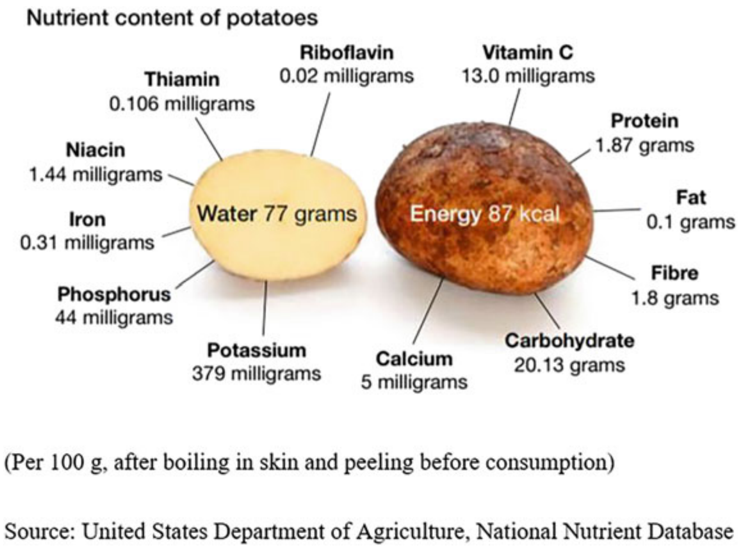

Fig. 14.5 Nutritional value of potato

14.4 Potato Production and Climate Change

Potato production can generate more economic return. This plays a significant part in food security as it can end hunger. In Pakistan, 97% increase in area under potato cultivation reported since its independence, showing how many growers are interested to sow this crop. Similarly, mean yield ha^{-1} has also been improved from 9 to 24 tonnes, and now Pakistan ranks at 20th place in the world (FAOSTAT 2017). Pakistan is self-sufficient in potato production, but due to climate change events more losses have been observed in recent years (Ahmed 2020). Climate change is now reality, and agriculture sector is one which is most vulnerable to it. Pakistan economy and its food security are largely linked with agriculture sector which is under heavy pressure due to high population, urbanization, and poor infrastructure (sowing to marketing). The climate change provides additional pressure which is difficult to sustain (Peins et al. 1996). According to the *Climate Risk Index*, Pakistan is the seventh most vulnerable country to climate change. Disease and pest pressure on potato productivity will increase because of climate change. Late blight is expected to spread to zones that have before been safe from disease. Similarly, in certain areas aphids will increase in number due to diverse seasons as it provide favorable climatic conditions. Since aphids acts as virus vectors thus causes risks in the production of seed. Currently, seed crop is grown at higher altitudes prior to seasonal occurrence of aphids for keeping it virus free. Higher production of potato in Pakistan is due to use of modern technologies and utilization of new seed varieties. However, to have sustainable yield in the context of climate change, it is necessary to have adaptation measures such as impact study analysis of climate variables on potato crop productivity and use of cultivars which can bear abiotic (high temperature and drought) and biotic stresses (late blight by *Phytophthora infestans*). The option can also be for early-maturing potatoes during short rainy seasons. Furthermore, it also requires modification in existing management practices (e.g., use of mulching, sustainable water use (drip irrigation), mixing varieties and intercropping, fertilizer rate, sowing time, access to microcredits, microinsurance, and climate information). In recent years, delay in harvesting of potato crop in Punjab was due to climate change resulting in increase in price. Similarly, cultivation in autumn beginning in September was delayed due to high temperature and rainfall variability. White and red potatoes are grown mainly in Pakistan. In Punjab, potato is mainly grown in Sahiwal, Okara, Dibalpur, Burewala, Arifwala, Kasur, Sialkot, Sheikhupura, Lahore, and Gujranwala. These areas contribute to 83% of potato production, but today these areas are under the negative impact of another climatic event called smog. Dir, Nowshera, and Mansehra from the KPK contribute to 10% production. Killa Saifullah, Kalat, and Pishin from Balochistan contribute 6%, and Hyderabad and Karachi from Sindh contribute 1% in total production of potato. In Pakistan, potatoes are grown in three seasons:. Spring (January–February (Sowing) and April–May (Harvesting)); Summer (March–May (Sowing) and August–October (Harvesting)); and Autumn (September–October (Sowing) and January–February (Harvesting)). The share of potato crop in annual production by spring, summer and autumn is 10%, 15%, and 75% respectively. Biggest shortage of potato has been seen in the start of March due to less production from spring season and poor post-harvest handling such as storage and transportation, which affects the quality of produce. Also, in spring, produce is reduced due to rapid multiplication of virus vector besides other bacterial and fungal diseases. Therefore, we need to control pests and diseases by adopting proper management practices and developing resistant varieties through modeling approaches.

Climate variability has also shown impacts on potato quality which is also affected by various factors such as maturity level of crop, preharvest conditions of crop, handling and harvest conditions, health status of crop such as biochemical changes, pests and disease incidence, and preparation and management of storage environment. Good storage practices cannot enhance the quality of crop if health is compromised during preharvest conditions. Quality of tubers is affected when immature tubers are harvested, soil conditions are very wet or dry, and weather is very warm (Pinhero et al. 2009). Certain glycol-alkaloids and secondary metabolites, i.e., α-chaconine and α-solanine, found in potato are reported to be dangerous for human health (Romanucci et al. 2018). The most common potato disease worldwide is late blight caused by a water mould, *Phytophthora infestans*, that destroys leaves, stems, and tubers. Bacterial wilt is caused by the bacterial pathogen, which leads to severe losses in tropical, subtropical, and temperate regions, while potato blackleg is also a bacterial infection, which causes tubers to rot in the ground and during storage. Viruses can cut yields by 50%, and they are disseminated in tubers. Early blight caused by bacteria results in 20–50% yield losses (Van Der Waals et al. 2001; Leiminger and Hausladen 2011). Low-water supply decreases the fresh and dry tuber yield (El-Abedin et al. 2017). Dry rot is economically affecting the potato produce under storage conditions from 6% to 25% up to 60% in some cases (Stevenson et al. 2001). Similarly, certain species of Aphids are affecting the production of potatoes (Pelletier and Michaud 1995; FAO 2016). Aphids are the main source of transfer of virus-related disease. It transfers virus from one place to another and spreads diseases on large scale. Meanwhile, long-term availability of potatoes depends upon its storage, but it is limited by sprouting of potatoes. Sprouting is the major cause of potato losses during storage. So, it is necessary to maintain endodormancy within potatoes so that sprouting will be low (Eshel and Tepel-Bamnolker 2012). High temperature has remarkable negative impact on the tuber yield, i.e., tuber fresh weighs less than 80 g. Less tuber weight is associated with reduction in total tuber yield and size. Rate of tuber bulking determines total tuber yield of potato (Mihovilovich et al. 2014). Increased temperature is favorable for temperate regions but can cause problems for tropical growing potatoes (Lizana et al. 2017). Excess fertilizer causes the rapid growth of potatoes resulting in hollow tuber formation with empty cavities. Potato psyllid is a serious pest for Solanaceae crops (Jackson et al. 2009). Due to its eating habit, this pest causes significant decrease in crop yield and quality (Munyaneza and Henne 2013). It causes spreading of bacteria which causes zebra chip in potato crop (Crosslin et al. 2010). There are several diseases which are caused by pests such as Colorado potato beetle (*Leptinotarsa decemlineata*), Potato tuber moth (*Phthorimaea operculella*), Leafminer fly (*Liriomyza huidobrensis*), and Cyst nematodes (*Globodera pallida* and *G. rostochiensis*). Therefore, modeling concepts should be applied to study impacts of abiotic (temperature and water) and biotic stresses (diseases and pest) on potato crop production.

14.5 Potato Modeling Across Globe Under Different Scenarios

The APSIM potato model was developed using plant modeling framework (PMF) (Brown et al. 2011, 2014) (Figs. 14.6 and 14.7). APSIM model, as presented in Table 14.1, simulates the development of crop through different developmental stages and uses thermal time approach. Thermal time target and the progression toward peeping can be calculated by using following equations:

$$\text{Progression} = [\text{Phenology}].\text{Thermal Time}$$

Peeping to emergence (sprouting phase)**:**

$$\text{Target} = \text{Sowing depth} \times \text{Shoot rate} + \text{Shoot Lag}$$

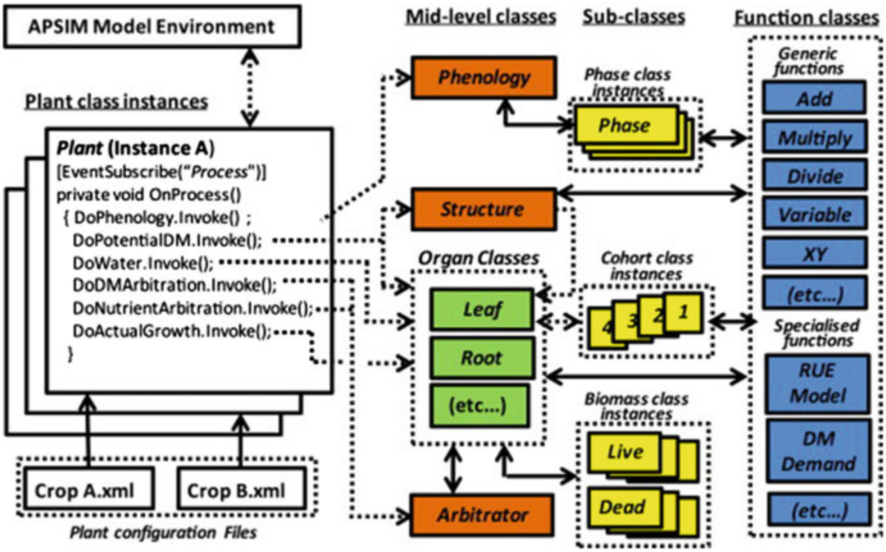

Fig. 14.6 APSIM plant basic structure (e.g., oat (left) and lucerne (right) configuration files). (Source: Brown et al. 2014 with permission from Elsevier)

$$\text{Shoot rate} = 1.35\left(\frac{\text{Degree day}}{\text{mm}}\right)$$

$$\text{Shoot lag} = 72\ (\text{Degree day})$$

$$\text{Sowing depth} = \text{in mm from manager}$$

Further detail about the growth and development of potato used by APSIM is available in the work of Brown et al. (2018).

The SUBSTOR-potato model is a cropping system model of decision support systems for agrotechnology transfer (Jones et al. 2003; Hoogenboom et al. 2019). Ritchie et al. (1995) provide a detailed description of SUBSTOR-potato model. This model can be requested from DSSAT portal (www. DSSAT.net). Relative temperature function for tuber initiation (RTFFTI) in SUBSTOR-potato model uses following equations:

$$\text{RTFFTI} = 0; (\text{Tempearture} \leq 4)$$

$$\text{RTFFTI} = 1 - \left(\frac{1}{36}\right)(10 - \text{Temperature})^2; (\text{Temperature} > 4 \text{ and Temperature} \leq 10)$$

$$\text{RTFFTI} = 1; (\text{Temperature} > 10 \text{ and Temperature} \leq 10)$$

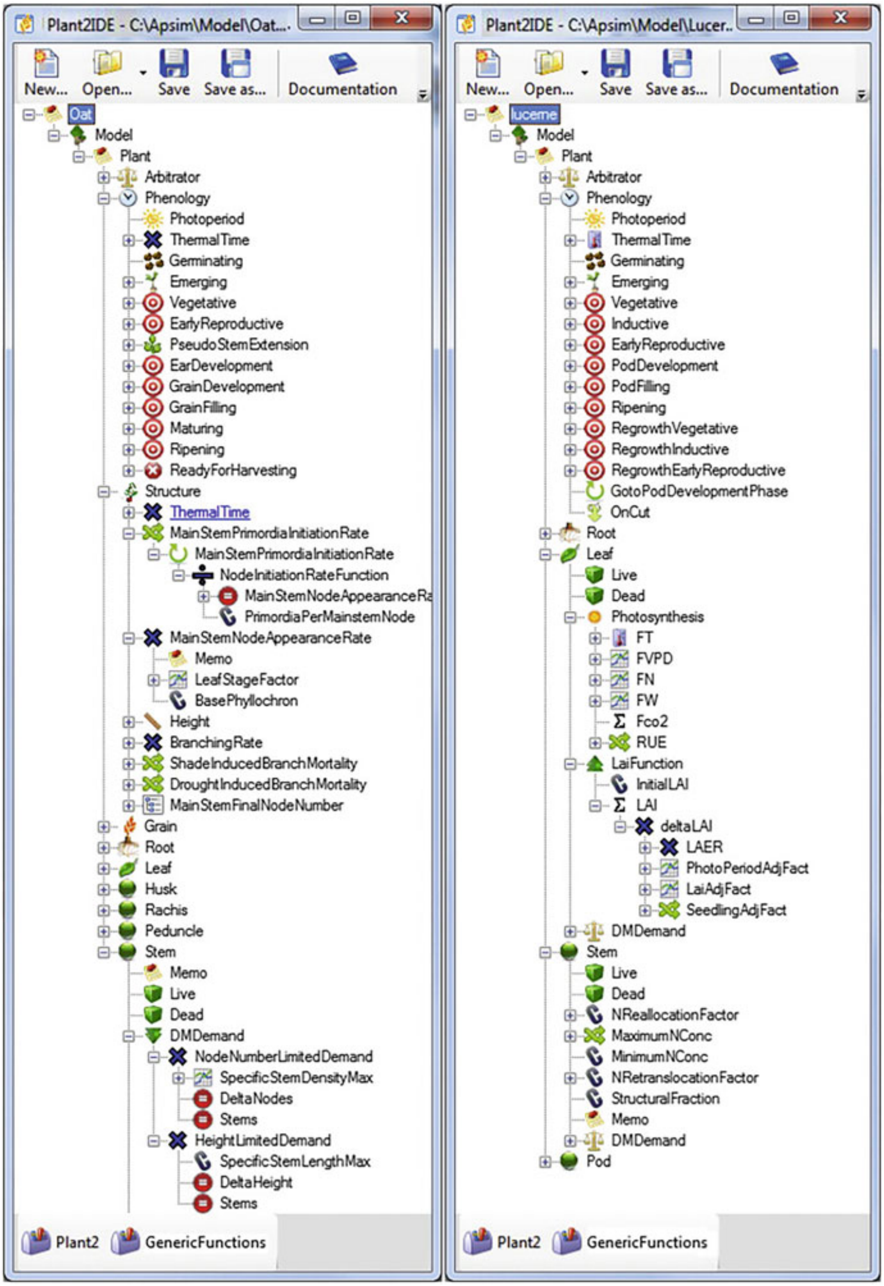

Fig. 14.7 Plant modeling framework of APSIM. (Source: Brown et al. 2014 with permission from Elsevier)

Table 14.1 List of stages and phases used in the simulation of crop phenological development

Phase number	Phase name	Initial stage	Initial stage
1	Dormant	Planting	Peeping
2	Sprouting	Peeping	Emergence
3	Vegetative	Emergence	Tuber initiation
4	Early tuber	Tuber initiation	Final leaf
5	Late tuber	Final leaf	Full senescence
6	Senesced	Full senescence	Maturity
7	Maturity	Maturity	Eternity

Source: APSRU, APSIM; Brown et al. (2018)

$$\mathrm{RTFFTI} = 1; (\mathrm{Temperature} > 10 \text{ and } \mathrm{Temperature} \leq \text{Critical temperature})$$

$$\mathrm{RTFFTI} = 1 - \left(\frac{1}{64}\right)(\mathrm{Temperature} - \text{Critical Temperature})^2;$$
$$(\mathrm{Temperature} > \text{Critical Temperature and Temperature} \leq \text{Critical Temperature} + 8)$$

Relative day length function for tuber initiation (RDLFFTI) can be modeled by using following equation:

$$\mathrm{RDLFFTI} = (1 - \mathrm{P2}) + 0.00694 \times \mathrm{P2} \times (24 - \mathrm{PHPER})^2$$

RDLFFTI is function of day length in hours (PHPER) and sensitivity to day length (P2). RDLFFTI = 1 when photoperiod is less than 12 h.

Biomass accumulation after tuber initiation and partitioning could be calculated by using following equations:

$$\mathrm{PCARB} = \mathrm{RUE} \times \frac{\mathrm{PAR}}{\mathrm{Plants}} (1 - \mathrm{Exp}(-0.55 \times \mathrm{LAI})) \times \mathrm{PCO_2}$$

Here

PCARB = function of RUE (g MJ^{-1})
PAR = photosynthetically active radiation (PAR, MJ m^{-2})
LAI = leaf area index (dimensionless)

Maximum tuber growth (TIND), sink strength (DTII), and carbon demand of tubers after tuber initiation (DEVEFF) are calculated by following equations:

$$\text{Maximum tuber growth (TIND)} = \mathrm{DTII}_{\mathrm{average}}\left(\frac{1}{\mathrm{NFAC}}\right)\mathrm{DEVEFF}; \mathrm{NFAC} > 1$$

$$\text{Maximum tuber growth (TIND)} = \mathrm{DTII}_{\mathrm{average}} \times \mathrm{DEVEFF}; \mathrm{NFAC} > 1$$

$$\text{Maximum tuber growth (TIND)} = \mathrm{RTFFTI}; \text{if no stress}$$

$$\text{Maximum tuber growth (TIND)} = \text{RTFFTI} + 0.5 \times (1 - \min(\text{SWFAC}, \text{NSTRES}, 1))$$

$$\text{DEVEFF} = \min((\text{XSTAGE} - 2) \times 10 \times \text{PD}, 1)$$

$$\text{XSTAGE} = 2.0 + (\text{CUMRTFVINE})/100$$

Here

DTIIavg = three-day moving average of daily values of sink strength (DTII)
DEVEFF = carbon demand of tubers after tuber initiation
XSTAGE = Progression through each phenological stage as a function of the cumulative leaf thermal time (CUMRTFVINE)
PD = index that suppresses tuber growth (PD = 0 or 1)
NFAC = nitrogen deficiency factor (NFAC)

SUBSTOR model simulates potential tuber growth (PTUBGR, g plant^{-1} day^{-1}) as a function of potential tuber growth rate (G3), relative temperature factor for root growth (RTFSOIL), and plant density.

$$\text{PTUBGR} = \text{G3} \times \text{PCO}_2 \times \frac{\text{RTFSOIL}}{\text{Plants}}$$

$$\text{GROTUB (Actual tuber growth)} = \text{PTUBGR} \times \min(\text{TURFAC}, \text{AGEFAC}, 1) \times \text{TIND}$$

$$\text{PLAG (Actual leaf expansion)} = \text{G2} \times \frac{\text{RTFVINE}}{\text{Plants}} \times \min(\text{TURFAC}, \text{AGEFAC}, 1)$$

$$\text{Leaf growth (GROLF)} = \frac{\text{Actual leaf expansion (PLAG)}}{\text{Leaf weight ratio (LALWR)}}$$

$$\text{Stem growth (GROSTM)} = \text{GROLF} \times 0.75$$

$$\text{Root growth (GRORT)} = (\text{GROLF} + \text{GROSTM}) \times 0.2$$

SUBSTOR-potato model converts tuber dry weight to tuber fresh weight assuming dry matter contents of 20%. Performance of the SUBSTOR-potato model across contrasting growing conditions was conducted by Raymundo et al. (2017). CropSyst VB–Simpotato model was used for the evaluation of potato production system in Pacific Northwest of the USA by Alva et al. (2004). This model is used to predict fate and transport of N under different nitrogen and water management options. The Simpotato model was presented by Hodges et al. (1992) using standards of IBSNAT (International Benchmarks Sites Network for Agrotechnology Transfer) project. LINTUL-POTATO-DSS is another important robust model (Haverkort et al. 2015).

STICS model was calibrated and evaluated by Morissette et al. (2016) to determine the cultivar-specific critical N concentration dilution curves and to quantify gain in model performance with cultivar-specific N concentration curves rather than a generic curve. Nitrate leaching was evaluated by Jégo et al. (2008) using STICS crop models in the field of potato and sugar beet crop. This model firstly evaluated using field data and then analyzed the impacts of different practices on nitrate leaching. Results showed that excessive irrigation in potato field resulted in higher nitrate leaching compared to sugarbeet as it has high N uptake capacity. Virtual experiments further suggested that N fertilization should be adjusted based on (1) season (2) crop in field (3) irrigation water, and (4) other factors precisely needed for potato crops.

Precision agriculture technologies, soil maps, and meteorological stations provide minimum data set, but optimal nutrients requirements are possible by the use of multilevel modeling as proposed by Parent et al. (2017). Mitscherlich equation was used to elaborate a multilevel N fertilizer response model for potato. According to Mitscherlich equation, rate of yield response reduces as soil nutrient level along with nutrient addition increases. Following equation is proposed by Rajsic and Weersink (2008):

$$\text{Yield} = \text{Asymptote} \times \left(1 - e^{-\text{Rate} \times (\text{Environment} + \text{Dose})}\right)$$

Here yield = crop production per unit area and dose = fertilizer amount per unit area.

Mitscherlich parameters have been shown in Fig. 14.8. Application of different models and strategies on the potato crop improvements have been presented in Table 14.2.

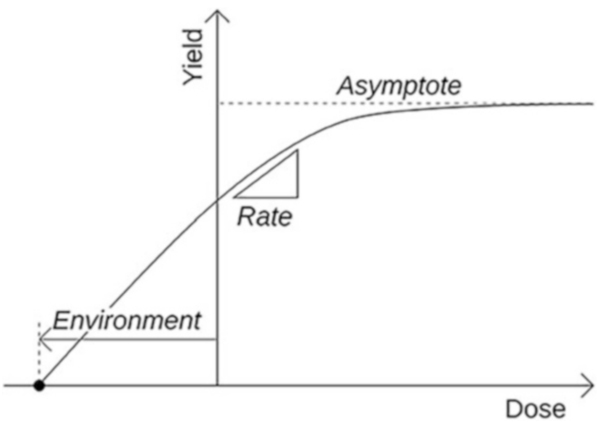

Fig. 14.8 Mitscherlich parameters. (Source: Parent et al. 2017)

Table 14.2 Model applications in tube research

S. No	Model applications	References
1.	Application of APSIM-potato model	Tang et al. (2020)
2.	DSSAT model to manage nitrogen in potato rotations with cover crops	Geisseler and Wilson (2020)
3.	Soil and climate data aggregation on potato yield and irrigation water requirement using APSIM	Ojeda et al. (2020)
4.	SUBSTOR-potato model to design deficit irrigation strategies	Montoya et al. (2020)
5.	Quantification of the canopy cover dynamics in potato	Khan et al. (2019)
6.	Agronomic options for better potato production	Tang et al. (2019)
7.	Mulching-induced variations in tuber productivity and NUE in potato in China	Wang et al. (2019)
8.	Deficit irrigation strategies using MOPECO model	Martínez-Romero et al. (2019)
9.	Protection of potatoes from adverse weather conditions through appropriate mitigation strategies and by the use of cropping system model (CSM)-SUBSTOR-potato	Woli and Hoogenboom (2018)
10.	Optimizing N fertilizer levels besides time of application in potatoes under seepage irrigation	Rens et al. (2018)
11.	FAO dual Kc approach to assess potato transpiration	Paredes et al. (2018)
12.	Application of CropSyst model to simulate potato crop	Montoya et al. (2018)
13.	Change in potato phenology	Tryjanowski et al. (2017)
14.	AquaCrop to simulate potato yield	Razzaghi et al. (2017)
15.	AquaCrop model application for irrigation management in potato	Montoya et al. (2016)
16.	Irrigation scheduling using AquaCrop	Linker et al. (2016)
17.	Root system architecture and abiotic stress tolerance	Khan et al. (2016)
18.	Breeding strategies of table potato	Eriksson et al. (2016)
19.	Effect of high temperature on potato	Rykaczewska (2015)
20.	Benefits of controlled release urea on potato	Gao et al. (2015)
21.	Multivariate analysis between potato and treatments	Šrek et al. (2010)
22.	Yield response of potato to nitrogen	Shillito et al. (2009)
23.	Modeling tuber crops	Singh et al. (1998)
24.	Climate change and potato production	Rosenzweig et al. (1996)
25.	Temperature effect on potato growth and carbohydrate metabolism	Lafta and Lorenzen (1995)
26.	Virtual potato crop modeling	Raymundo et al. (2014)

References

Ahmed M (2020) Introduction to modern climate change. Andrew E. Dessler: Cambridge University Press, 2011, 252 pp, ISBN-10: 0521173159. Sci Total Environ 734:139397. https://doi.org/10.1016/j.scitotenv.2020.139397

Alva A, Marcos J, Stockle C, Reddy V, Timlin D (2004) CropSyst VB–Simpotato, a crop simulation model for potato-based cropping systems: II. Evaluation of nitrogen dynamics. In: Proceedings of the 4th International Crop Science Congress, Brisbane, Australia, 2004

Brown HE, Huth N, Holzworth D (2011) A potato model build using the APSIM Plant. NET framework, pp 961–967

Brown HE, Huth NI, Holzworth DP, Teixeira EI, Zyskowski RF, Hargreaves JNG, Moot DJ (2014) Plant modelling framework: software for building and running crop models on the APSIM platform. Environ Model Softw 62:385–398. https://doi.org/10.1016/j.envsoft.2014.09.005

Brown H, Huth N, Holzworth D (2018) 1 The APSIM Potato Model. http://apsimdev.apsim.info/ApsimxFiles/Potato4403.pdf

Costa LD, Vedove GD, Gianquinto G, Giovanardi R, Peressotti A (1997) Yield, water use efficiency and nitrogen uptake in potato: influence of drought stress. Potato Res 40:19–34

Crosslin JM, Munyaneza JE, Brown JK, Liefting LW (2010) A history in the making: Potato Zebra chip disease associated with a new Psyllid-borne Bacterium – a tale of striped potatoes. APSnet Features. https://doi.org/10.1094/APSnet-Feature-2010-0110

Dalla Costa L, Delle Vedove G, Gianquinto G, Giovanardi R, Peressotti A (1997) Yield, water use efficiency and nitrogen uptake in potato: influence of drought stress. Potato Res 40:19–34

Davies A, Jenkins T, Pike A, Shaq J, Carson I, Pollock CJ, Parry MI (1996) Modelling the predicted geographic and economic response of UK cropping systems to climate change scenarios: the case of potatoes. Asp Appl Biol 45:63–69

El-Abedin TKZ, Mattar MA, Alazba AA, Al-Ghobari HM (2017) Comparative effects of two water-saving irrigation techniques on soil water status, yield, and water use efficiency in potato. Sci Hortic 225:525–532

Eriksson D, Carlson-Nilsson U, Ortíz R, Andreasson E (2016) Overview and breeding strategies of table potato production in Sweden and the Fennoscandian region. Potato Res 59(3):279–294. https://doi.org/10.1007/s11540-016-9328-6

Eshel D, Tepel-Bamnolker P (2012) Can loss of apical dominance in potato tuber serve as a marker of physiological age? Plant Signal Behav 7:1158–1162

FAO (2017). http://faostat.fao.org/. Accessed in Jan 2017

Food and Agriculture Organization of the United Nations (FAO), World crop production statistics (2016). http://www.faostat.fao.org. Accessed 10th Sept 2016

Gao X, Li C, Zhang M, Wang R, Chen B (2015) Controlled release urea improved the nitrogen use efficiency, yield and quality of potato (Solanum tuberosum L.) on silt loamy soil. Field Crop Res 181:60–68. https://doi.org/10.1016/j.fcr.2015.07.009

Geisseler D, Wilson R (2020) Nitrogen in potato rotations with cover crops: field trial and simulations using DSSAT. Agron JAccepted Author Manuscript. https://doi.org/10.1002/agj2.20177

Hack H, Gall H, Klemke Th., Klose R, Meier U, Stauss R, Witzenberger A (2001) The BBCH scale for phonological growth stages of potato (*Solanum tuberosum* L.). In: Meier U (ed) Growth stages of mono and dicotyledonous Plants, BBCH Monograph, Federal Biological Research Centre for Agriculture and Forestry

Haverkort AJ, Franke AC, Steyn JM, Pronk AA, Caldiz DO, Kooman PL (2015) A robust potato model: LINTUL-POTATO-DSS. Potato Res 58(4):313–327. https://doi.org/10.1007/s11540-015-9303-7

Hijmans RJ (2003) The effect of climate change on global potato production. Am J Pot Res 80:271–279. https://doi.org/10.1007/BF02855363

Hodges T, Johnson S, Johnson B (1992) SIMPOTATO: a highly modular program structure for an IBSNAT style crop simulation. Agron J 84:911–915

Hoogenboom G, Porter CH, Shelia V, Boote KJ, Singh U, White JW, Hunt LA, Ogoshi R, Lizaso JI, Koo J, Asseng S, Singels A, Moreno LP, Jones JW (2019) Decision support system for agrotechnology transfer (DSSAT) version 4.7.5 (www.dssat.net). DSSAT Foundation, Gainesville, FL

Jackson BC, Goolsby J, Wyzykowski A, Vitovsky N, Bextine B (2009) Analysis of genetic relationships between potato psyllid (Bactericera cockerelli) populations in the United States, Mexico and Guatemala using ITS2 and Inter Simple Sequence Repeat (ISSR) data. Subtrop Plant Sci 61:1–5

Jégo G, Martínez M, Antigüedad I, Launay M, Sanchez-Pérez JM, Justes E (2008) Evaluation of the impact of various agricultural practices on nitrate leaching under the root zone of potato and sugar beet using the STICS soil–crop model. Sci Total Environ 394(2):207–221. https://doi.org/10.1016/j.scitotenv.2008.01.021

Jones JW, Hoogenboom G, Porter CH, Boote KJ, Batchelor WD, Hunt LA, Wilkens PW, Singh U, Gijsman AJ, Ritchie JT (2003) The DSSAT cropping system model. Eur J Agron 18 (3–4):235–265. https://doi.org/10.1016/S1161-0301(02)00107-7

Khan MA, Gemenet DC, Villordon A (2016) Root system architecture and abiotic stress tolerance: current knowledge in root and tuber crops. Front Plant Sci 7(1584). https://doi.org/10.3389/fpls.2016.01584

Khan MS, Struik PC, van der Putten PEL, Jansen HJ, van Eck HJ, van Eeuwijk FA, Yin X (2019) A model-based approach to analyse genetic variation in potato using standard cultivars and a segregating population. I. Canopy cover dynamics. Field Crop Res 242:107581. https://doi.org/10.1016/j.fcr.2019.107581

Kooman PL, Haverkort AJ (1995) Modelling development and growth of the potato crop influenced by temperature and daylength: LINTUL-POTATO. In: Haverkort AJ, MacKerron DKL (eds) Potato ecology and modelling of crops under conditions limiting growth: proceedings of the second international potato modeling conference, held in Wageningen 17–19 May, 1994. Springer Netherlands, Dordrecht, pp 41–59. https://doi.org/10.1007/978-94-011-0051-9_3

Kooman PL, Fahem M, Tegera P, Haverkort AJ (1996a) Effects of climate on different potato genotypes 2. Dry matter allocation and duration of the growth cycle. Eur J Agron 5:207–217

Kooman PL, Fahem M, Tegera P, Haverkort AJ (1996b) Effects of climate on different potato genotypes 1. Radiation interception, total and tuber dry matter production. Eur J Agron 5:193–205

Lafta AM, Lorenzen JH (1995) Effect of high temperature on plant growth and carbohydrate metabolism in potato. Plant Physiol 109(2):637–643. https://doi.org/10.1104/pp.109.2.637

Leiminger JH, Hausladen H (2011) Early blight control in potato using diseaseorientated threshold values. Plant Dis 96:124–130

Linker R, Ioslovich I, Sylaios G, Plauborg F, Battilani A (2016) Optimal model-based deficit irrigation scheduling using AquaCrop: a simulation study with cotton, potato and tomato. Agric Water Manag 163:236–243. https://doi.org/10.1016/j.agwat.2015.09.011

Lizana XC, Avila A, Tolaba A, Martinez JP (2017) Field responses of potato to increased temperature during tuber bulking: projection for climate change scenarios, at high-yield environments of Southern Chile. Agric For Meteorol 239:192–201

Lutaladio N, Castaidi L (2009) Potato: the hidden treasure. J Food Compos Anal 22(6)

Lutz W, Samir KC (2010) Dimensions of global population projections: what do we know about future population trends and structures? Philos Trans R Soc Lond B-Biol Sci 365 (1554):2779–2791

Martínez-Romero A, Domínguez A, Landeras G (2019) Regulated deficit irrigation strategies for different potato cultivars under continental Mediterranean-Atlantic conditions. Agric Water Manag 216:164–176. https://doi.org/10.1016/j.agwat.2019.01.030

Miglietta F, Magliulo V, Bindi M, Cerio L, Vaccari FP, Loduca V, Peressotti A (1998) Free air CO_2 enrichment of potato (Solanum tuberosum L.): development, growth and yield. Glob Chang Biol 4:163–172

Mihovilovich E, Carli C, De Mendiburu F, Hualla V, Bonierbale M (2014) Protocol for tuber bulking maturity assessment of elite and advanced potato clones. Int. Potato Center, Lima, Peru. 18–19

Montoya F, Camargo D, Ortega JF, Córcoles JI, Domínguez A (2016) Evaluation of Aquacrop model for a potato crop under different irrigation conditions. Agric Water Manag 164:267–280. https://doi.org/10.1016/j.agwat.2015.10.019

Montoya F, Camargo D, Domínguez A, Ortega JF, Córcoles JI (2018) Parametrization of Cropsyst model for the simulation of a potato crop in a Mediterranean environment. Agric Water Manag 203:297–310. https://doi.org/10.1016/j.agwat.2018.03.029

Montoya F, Camargo D, Córcoles JI, Domínguez A, Ortega JF (2020) Analysis of deficit irrigation strategies by using SUBSTOR-potato model in a semi-arid area. J Agric Sci:1–14. https://doi.org/10.1017/S002185961900090X

Morissette R, Jégo G, Bélanger G, Cambouris AN, Nyiraneza J, Zebarth BJ (2016) Simulating potato growth and nitrogen uptake in eastern Canada with the STICS model. Agron J 108 (5):1853–1868. https://doi.org/10.2134/agronj2016.02.0112

Munyaneza JE, Henne DC (2013) Chapter 4 – Leafhopper and psyllid pests of potato. In: Alyokhin A, Vincent C, Giordanengo P (eds) Insect pests of potato. Academic Press, San Diego, pp 65–102. https://doi.org/10.1016/B978-0-12-386895-4.00004-1

Ojeda JJ, Rezaei EE, Remenyi TA, Webb MA, Webber HA, Kamali B, Harris RMB, Brown JN, Kidd DB, Mohammed CL, Siebert S, Ewert F, Meinke H (2020) Effects of soil- and climate data aggregation on simulated potato yield and irrigation water requirement. Sci Total Environ 710:135589. https://doi.org/10.1016/j.scitotenv.2019.135589

Paredes P, D'Agostino D, Assif M, Todorovic M, Pereira LS (2018) Assessing potato transpiration, yield and water productivity under various water regimes and planting dates using the FAO dual Kc approach. Agric Water Manag 195(Supplement C):11–24. https://doi.org/10.1016/j.agwat.2017.09.011

Parent S-É, Leblanc MA, Parent A-C, Coulibali Z, Parent LE (2017) Site-specific multilevel modeling of potato response to nitrogen fertilization. Front Environ Sci 5(81). https://doi.org/10.3389/fenvs.2017.00081

Peins DR, Crawford JW, Grashoff C, Jefferies RA, Parter JR, Marshall B (1996) A simulation study of crop growth ahd development under climate change. Agric For Meteorol 79:271–887

Peiris DR, Crawford JW, Grashoff C, Jefferies RA, Porter JR, Marshall B (1996) A simulation study of crop growth and development under climate change. Agric For Meteorol 79 (4):271–287. https://doi.org/10.1016/0168-1923(95)02286-4

Pelletier Y, Michaud D (1995). Insect pest control on potato: genetically-based control. In: Duchesne RM, Boiteau G (eds) Potato insect pest control: development of a sustainable approach, Gouvernement du Que'bec. 69–79

Pinhero RG, Coffin R, Yada RY (2009) Post-harvest storage of potatoes. Advances in potato chemistry and technology. Academic Press (Elsevier), New York, pp 339–370

Rajsic P, Weersink A (2008) Do farmers waste fertilizer? A comparison of ex post optimal nitrogen rates and ex ante recommendations by model, site and year. Agric Syst 97(1):56–67. https://doi.org/10.1016/j.agsy.2007.12.001

Raymundo R, Kleinwechter U, Asseng S (2014). Virtual potato crop modeling A comparison of genetic coefficients of the DSSAT-SUBSTOR potato model with breeding goals for developing countries. Zenodo. https://doi.org/10.5281/zenodo.7687

Raymundo R, Asseng S, Prassad R, Kleinwechter U, Concha J, Condori B, Bowen W, Wolf J, Olesen JE, Dong Q, Zotarelli L, Gastelo M, Alva A, Travasso M, Quiroz R, Arora V, Graham W, Porter C (2017) Performance of the SUBSTOR-potato model across contrasting growing conditions. Field Crop Res 202:57–76. https://doi.org/10.1016/j.fcr.2016.04.012

Razzaghi F, Zhou Z, Andersen MN, Plauborg F (2017) Simulation of potato yield in temperate condition by the AquaCrop model. Agric Water Manag 191:113–123. https://doi.org/10.1016/j.agwat.2017.06.008

Rens LR, Zotarelli L, Rowland DL, Morgan KT (2018) Optimizing nitrogen fertilizer rates and time of application for potatoes under seepage irrigation. Field Crop Res 215:49–58. https://doi.org/10.1016/j.fcr.2017.10.004

Ritchie J, Griffin TS, Johnson BS (1995) SUBSTOR: functional model of potato growth, development and yield. In: Modelling and parameterization of the soil-plant-atmosphere system: a comparison of potato growth models, pp 401–435

Romanucci V, Di Fabio G, Di Marino C, Davinelli S, Scapagnini G, Zarrelli A (2018) Evaluation of new strategies to reduce the total content of α-solanine and α-chaconine in potatoes. Phytochem Lett 23:116–119

Rosenzweig C, Phillips J, Goldberg R, Carroll J, Hodges T (1996) Potential impacts of climate change on citrus and potato production in the US. Agric Syst 52(4):455–479. https://doi.org/10.1016/0308-521X(95)00059-E

Rykaczewska K (2015) The effect of high temperature occurring in subsequent stages of plant development on potato yield and tuber physiological defects. Am J Potato Res 92(3):339–349. https://doi.org/10.1007/s12230-015-9436-x

Singh U, Matthews RB, Griffin TS, Ritchie JT, Hunt LA, Goenaga R (1998) Modeling growth and development of root and tuber crops. In: Tsuji G, Hoogenboom G, Thornton P (eds) Understanding options for agricultural production, vol 7. Systems approaches for sustainable agricultural development. Springer, Dordrecht, pp 129–156. https://doi.org/10.1007/978-94-017-3624-4_7

Shillito RM, Timlin DJ, Fleisher D, Reddy VR, Quebedeaux B (2009) Yield response of potato to spatially patterned nitrogen application. Agric Ecosyst Environ 129(1):107–116. https://doi.org/10.1016/j.agee.2008.07.010

Šrek P, Hejcman M, Kunzová E (2010) Multivariate analysis of relationship between potato (Solanum tuberosum L.) yield, amount of applied elements, their concentrations in tubers and uptake in a long-term fertilizer experiment. Field Crop Res 118(2):183–193. https://doi.org/10.1016/j.fcr.2010.05.009

Stevenson WR, Loria R, Franc GD, Weingartner DP (2001) Compendium of potato diseases, 2nd edn. The American Phytopathological Society, St. Paul

Tang J, Xiao D, Bai H, Wang B, Liu DL, Feng P, Zhang Y, Zhang J (2020) Potential benefits of potato yield at two sites of agro-pastoral ecotone in North China under future climate change. Int J Plant Prod. https://doi.org/10.1007/s42106-020-00092-7

Tang J, Wang J, Fang Q, Dayananda B, Yu Q, Zhao P, Yin H, Pan X (2019) Identifying agronomic options for better potato production and conserving water resources in the agro-pastoral ecotone in North China. Agric For Meteorol 272-273:91–101. https://doi.org/10.1016/j.agrformet.2019.04.001

Tryjanowski P, Sparks TH, Blecharczyk A, Małecka-Jankowiak I, Switek S, Sawinska Z (2017) Changing phenology of potato and of the treatment for its major pest (Colorado potato beetle) – a long-term analysis. Am J Potato Res. https://doi.org/10.1007/s12230-017-9611-3

Van Der Waals JE, Korsten L, Aveling TAS (2001) A review of early blight of potato. Afr Plant Prot 7:91–102

van Oort PAJ, Timmermans BGH, van Swaaij ACPM (2012) Why farmers' sowing dates hardly change when temperature rises. Eur J Agron 40:102–111. https://doi.org/10.1016/j.eja.2012.02.005

Wahid A, Gelani S, Ashraf M, Foolad MR (2007) Heat tolerance in plants: an overview. Environ Exp Bot 61(3):199–223. https://doi.org/10.1016/j.envexpbot.2007.05.011

Wang L, Coulter JA, Palta JA, Xie J, Luo Z, Li L, Carberry P, Li Q, Deng X (2019) Mulching-induced changes in tuber yield and nitrogen use efficiency in potato in China: a meta-analysis. Agronomy 9(12):793

Woli P, Hoogenboom G (2018) Simulating weather effects on potato yield, nitrate leaching, and profit margin in the US Pacific Northwest. Agric Water Manag 201:177–187. https://doi.org/10.1016/j.agwat.2018.01.023

Application of Generalized Additive Model for Rainfall Forecasting in Rainfed Pothwar, Pakistan

15

Mukhtar Ahmed, Fayyaz-ul-Hassan, Shakeel Ahmad, Rifat Hayat, and Muhammad Ali Raza

Abstract

Climatic variations affect growers of dry regions, and so the agricultural management techniques require modification according to the timing and amount of precipitation for the optimization of yield and economic output for a specified season and location. Farm manager preparedness depending on past practices can be enhanced by long-range skilled forecasting of rainfall. The well-known modes of interannual fluctuations affecting the Indian subcontinent are the Indian Ocean Dipole (IOD) and El-Niño Southern Oscillation (ENSO). Dry regions of Pakistan, i.e., Pothwar, are facing a number of key challenges in the prediction of irregular rain. Modeling skewed, zero, nonlinear, and non-stationary data are a few of the main challenges. To deal with this, a probabilistic statistical model was used in three of the dry areas of Pothwar to predict monsoon and wheat-growing season. To find out the prospects of rainfall, occurring in the system, the model utilizes logistic regression through generalized additive models (GAMs). Our study

M. Ahmed (✉)
Department of Agricultural Research for Northern Sweden, Swedish University of Agricultural Sciences, Umeå, Sweden

Department of Agronomy, Pir Mehr Ali Shah Arid Agriculture University, Rawalpindi, Pakistan
e-mail: mukhtar.ahmed@slu.se; ahmadmukhtar@uaar.edu.pk

Fayyaz-ul-Hassan
Department of Agronomy, Pir Mehr Ali Shah Arid Agriculture University, Rawalpindi, Pakistan

S. Ahmad
Department of Agronomy, Bahauddin Zakariya University, Multan, Pakistan

R. Hayat
Department of Soil Science and Soil water Conservation, Pir Mehr Ali Shah Arid Agriculture University, Rawalpindi, Pakistan

M. A. Raza
College of Agronomy, Sichuan Agricultural University, Chengdu, People's Republic of China

M. Ahmed (ed.), *Systems Modeling*, https://doi.org/10.1007/978-981-15-4728-7_15

exploits climatic predictors (Pacific and the Indian Ocean SSTs demonstrating the status of the IOD and the ENSO) affecting rainfall fluctuations on the Indian subcontinent for their effectiveness in predicting seasonal rainfall (three rainfall intervals and the monsoon rains throughout the wheat-growing period). The outcome demonstrated that the observed area had the amount and fluctuation of rainfall determined by SSTs, so predictions can be carried out by intellect to overpass the gaps among average and potential wheat yield with a change in management practices, i.e., appropriate time of sowing and use of suitable genotypes. In addition, the forecasting ability score, i.e., R^2, RMSE (root-mean-square error), BSS (Brier skill score), S% (skill score S), LEPS (linear error in probability space), NSE (Nash-Sutcliffe model efficiency coefficient), and ROC (receiver operating characteristics, p-value), assessed validation of model for rainfall prediction to verify the effectiveness of GAM and to formulate contrast among varying validation abilities to do cross-validation of rainfall prediction. Likewise, the forecast systems present substantial benefits in enhancing general operational management when used in agriculture production across the whole value chain.

Keywords

Forecasting · GAMs · SSTs · ENSO · IOD · Management

15.1 Introduction

The most important climate element for rainfed agriculture is rainfall, and it has a great impact on the socioeconomic development of the region. Rainfall in rainfed regions of Pakistan show great variations across space and time. This might be because of complex topography and a number of different factors which also include global warming (GW). GW is among the most significant global environmental challenges, and it has strong impacts on food security, natural resources, rainfall, and droughts (Ahmed 2020; Ahmed and Stockle 2016; Klein Tank et al. 2006; Mustafa 2011; Stocker et al. 2013). Catastrophic impacts of extreme weather events have already taken global attention, and it has been now the fact that the intensity and frequency of these events have been increased significantly (Liu et al. 2005). Countries like Pakistan are more prone to negative impacts of climate change as compared to the developed countries (IPCC 2014). Changing pattern of rainfall has significant effects on agricultural production. Monsoon is the main rainfall pattern in the rainfed regions of Pakistan, and it has been observed that the pattern of monsoon is changed (Turner and Annamalai 2012). Monsoon begins its journey from the south of India around the end of May when the cross-equatorial low-level jet is present along the coast of Somalia into the near-equatorial Arabian Sea (Ding and Sikka 2006). Large-scale monsoon current with interannually fluctuation proceeds west-northwestward, and central Pakistan is the finishing point during the middle of July. Although, monsoon distribution is generally between June and September, the substantial spatiotemporal variation is observed in the region. This significant variability could be because of sea surface temperature (SST) beside orographic influence. Meanwhile, a low-pressure system is another factor which brings significant rain over the Indo-Pak subcontinent. Therefore, SST and pressure system are the one which brings rainfall variability over the subcontinent, and this variability is annual as well as seasonal.

Pothwar Plateau is the chief rainfed area of Pakistan, surrounded on the east by the Jhelum river, on the west by the Indus river, on the south by the Salt Range, and on the north by the Kala Chitta Range and the Margalla Hills. The mean height of Kala Chitta Range is 450–900 meters (3000 ft) and extends for about 72 kilometers. The Pothwar Plateau of Pakistan is an important agricultural, economic, and cultural arid region that extends between latitudes 32° 10′ and 34° 9′ N and longitudes 71° 10′ to 73° 10′ E. It covers an area of 1.82 million ha, and geography ranges from even to slightly undulating, locally broken by low hill ranges and gullies. The bedrock mainly consists of loess, narrow strips of river alluvium, residual mantle on sandstones and shale bedrocks, residual mantle on sandstones and shale bedrocks, and piedmont alluvium near the foot of mountains.

Rainfall variability is the key aspect determining crop production and threat related to the environment under the rainfed area of Pakistan. Likewise, when operational seasonal forecasting systems are used in practical farming system management, some factors are considered important, i.e., pre-sowing soil water contents, soil type, planting dates, temperature, soil fertility, rainfall intensity, and timeliness of rainfall (Meinke and Stone 2005). Rainfall is the only available source of water; therefore, the people in rainfed regions of Pakistan mainly depend on it. If the rainfall fails, agriculture of the area can be harshly disturbed. Accurate prediction of rainfall quantum and onset for a few days up to a crop season can create a distinction between agricultural success and failure. Government action and public response also need precise rainfall forecasts with sufficient lead times. Likewise, excess hardship to the people in the region can be brought by prolonged droughts and floods. These may result in life loss and property and deep economic trouble for the people and the government.

Researcher in the past has depicted a significant relationship with rainfall variability and global circulation system components (van Ogtrop et al. 2014). The most prominent component, according to Walker, was the Southern Oscillation (SO), which was further confirmed by Bjerknes as El Niño. The term El Niño is linked to the warming of the eastern equatorial Pacific, and NINO3, which indicates the sea surface temperature (SST) anomaly in the NINO3 region (90 W–150 W, 5S–5N) of the eastern equatorial Pacific, is commonly used as an index of El Niño. The Southern Oscillation is a seesawing of atmospheric mass and hence the sea level pressure (SLP), between the western and eastern Pacific. It is most frequently indexed by the Southern Oscillation Index (SOI), a normalized SLP difference between Darwin, Australia, and Tahiti. However, IOD is the dipole structure of SST which is the variation in SST between the tropical western Indian Ocean (50E – 70E, 10S – 10 N) and the tropical south-eastern Indian Ocean (90E – 110E, 10S – equator).

The aim of this study is to identify rainfall drivers for the rainfed area of Pothwar, which can be used in statistical forecasting models. The objectives of the study include (1) to identify climatic drivers of rainfall variability for three locations in Pothwar, Pakistan; (2) to evaluate relationships between these drivers of climate variability and growing season rainfall; and (3) to explore options for using knowledge on climatic drivers in seasonal climate forecasting.

15.2 Materials and Methods

15.2.1 Study Area

The Pothwar Plateau of Pakistan covers an area of 1.82 million ha and extends between 32°10'N–34°9'N and 71°10′E–73°10′E. The SST data from the *Niño1 + 2* (*Niño1.2*), *Niño3*, *Niño3.4*, *and Niño4 region* were taken from National Oceanic and Atmospheric Administration (NOAA), USA http://www.cpc.ncep.noaa.gov/data/ (Wang et al. 1999*;* Trenberth and Stepaniak 2001), while IOD data was obtained from Frontier Research Centre for Global Change, Japan http://www.jamstec.go.jp/frsgc/research/d1/iod/ (Caroline et al. 2011). *Similarly, the rainfall data (1961–2009) for the rainfed area of Pothwar,* i.e., *Islamabad, Chakwal, and Talagang, Pakistan, was obtained from the meteorology department of Pakistan.*

15.2.2 Models

Modeling rain with a zero-adjusted distribution of the type is equal to modeling zero and non-zero data discretely:

$$f(y;\theta,\pi) = \begin{cases} (1-\pi) & \text{if } \; y = 0 \\ \pi f_T(y,\theta) & \text{if } \; y > 0 \end{cases} \tag{15.1}$$

where π, $f_T(y,\theta)$, and the prospect of the happening of non-zero rainfall is the distribution of the non-zero rainfall. So, initially, the happening of monthly rainfall was modeled. Binomial distribution was utilized because the result is binary (Hyndman and Grunwald 2000). As a next step, non-zero rainfall intensities (volumes) are modeled. The generalized linear model (GLM) can be initially detailed for the binomial model of the occurrence of flow as follows:

$$g(\pi) = \log\left(\frac{\pi}{1-\pi}\right) = x'\beta \tag{15.2}$$

where π is the prospect of the happening of non-zero rainfall, $x'$is a vector of covariates, β is a vector of coefficients for$x$, and $g(\pi)$ is the logit link function$x$. Generalized additive model for location, scale, and shape (GAMLSS) was specified for contrast as follows (because GAMLSS is an extension of GLM (Rigby and Stasinopoulos 2001)):

$$g(\pi) = \log\left(\frac{\pi}{1-\pi}\right) = x'\beta + \sum_{j=1}^{J} s_j\left(w_j\right) \tag{15.3}$$

where in Eq. 15.2, $x'\beta$ is a combination of the linear estimator, s_j for $j = 1, 2, \ldots\ldots,$ J is smoothing terms, and w_j for $j = 1, 2, \ldots\ldots,$ J is the covariate. GAMLSS with added smoothing terms is very useful; for example, nonlinear covariate impacts in otherwise noisy data sets are identified (Hastie and Tibshirani 1986). In this study, penalized B-splines are supported by the smoothing (Eilers and Marx 1996). The penalized maximum likelihood in the gamlss package is used for automatic selection of the degree of smoothing (Rigby and Stasinopoulos 2005). Within the open-source program R, gamlss function in the gamlss package was used for the application of the GAMLSS models (R Development Core Team 2008; Stasinopoulos et al. 2009). A simple linear regression model was firstly used in order to build a relationship between rainfall and climatic drivers. Data sets with a lag period of 2, 6, and 12 months were used to develop line regression equations:

$$Y = \beta_0 + \beta_1 X_1 + \beta_2 X_2 + \cdots + \beta m X m \tag{15.4}$$

where Y denotes the probability of occurrence of rainfall; $\beta 0$, $\beta 1$, $\beta 2, \ldots \beta m$ are the constants; and $X1$, $X2, \ldots Xm$ are the different climatic drivers. For checking whether the resulted rains from the line regression equations were significance or not, first, the coefficients of multiple correlations are figured out, and then the F-test is applied. Seasonal variations in the data are explained with the inclusion of additional harmonic covariates like synthetic variables (*sine* and *cosine*) (Hyndman and Grunwald 2000):

$$\begin{aligned} sine &= \sin\left(\frac{2\pi S_m}{12}\right) \\ cosine &= \cos\left(\frac{2\pi S_m}{12}\right) \end{aligned} \tag{15.5}$$

where S_m is m (mod 12) and m is the month. A penalized B-spline fitted with these harmonic covariates supplemented flexibility, so higher-order harmonics were not needed. Significance of these covariates indicates strong seasonal drift in the rainfall and therefore captures seasonal climatic rain. Now the linear regression model equation becomes

$$\begin{aligned} Y = \beta_0 &+ sine + cosine + NINO1.2 + NINO3 + NINO4 + NINO3.4 \\ &+ IOD \end{aligned} \tag{15.6}$$

15.3 Results and Discussions

The annual variability in rainfall for the rainfed area of Pothwar, i.e., Islamabad, revealed that in the certain year it could reach to the peak value of 1746 mm (1981), while in another year it might go to a minimum level, i.e., 532 (1994) (Fig. 15.1). Similarly, for Chakwal medium rainfall area of Pothwar, long-term rainfall variability depicted that the maximum rainfall is recorded during 1997 (1221 mm), while lowest value is noted in 1979 (225 mm) (Fig. 15.2). However, the lowest rainfall area of Pothwar, i.e., Talagang, depicted rainfall variability with annual maximum value in 1997 (520 mm) while the minimum value in 1979 (121) (Fig.15.3). This long-timescale rainfall variability in Pothwar areas may be because of different climatic drivers like ENSO (El Niño Southern Oscillation Index), Madden-Julian oscillation (MJO) and Indian Ocean Dipole (IOD).

In the rainfed "barani" areas of Pakistan, rainfall variability is the main driver for fluctuations in agricultural productivity. These areas cover 24.4% of the total arable land; 14% of Pakistan's population depends on rainfed agriculture. In general, the rainfall pattern among the seasons in Pakistan was aggravated, implying the increased frequency of rainfall during summer and the decrease of rainfall during winter. The prediction of rainfall on the spatiotemporal pattern in rainfed areas of

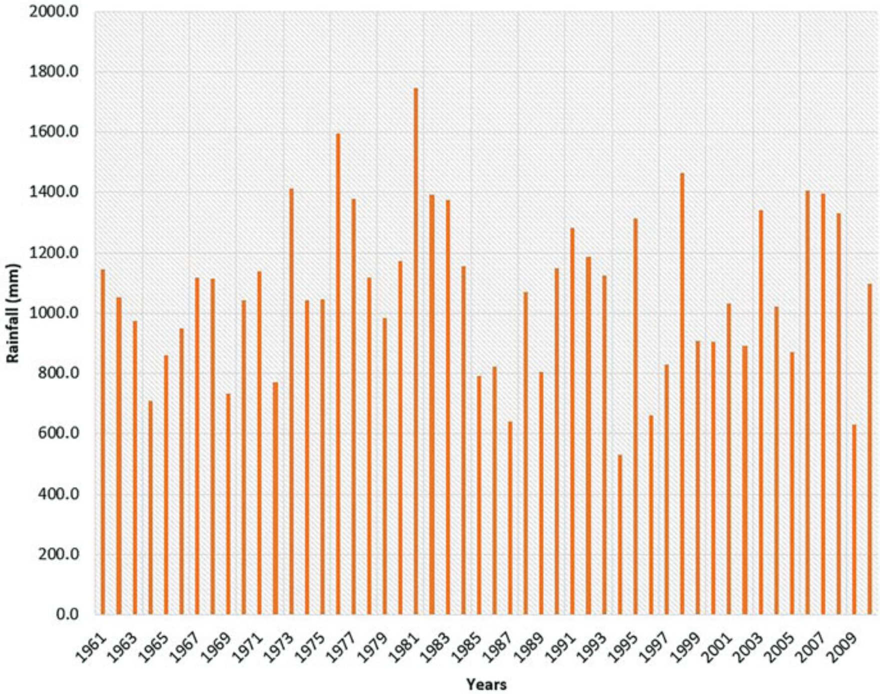

Fig. 15.1 Time series of rainfall at Islamabad (1961–2010)

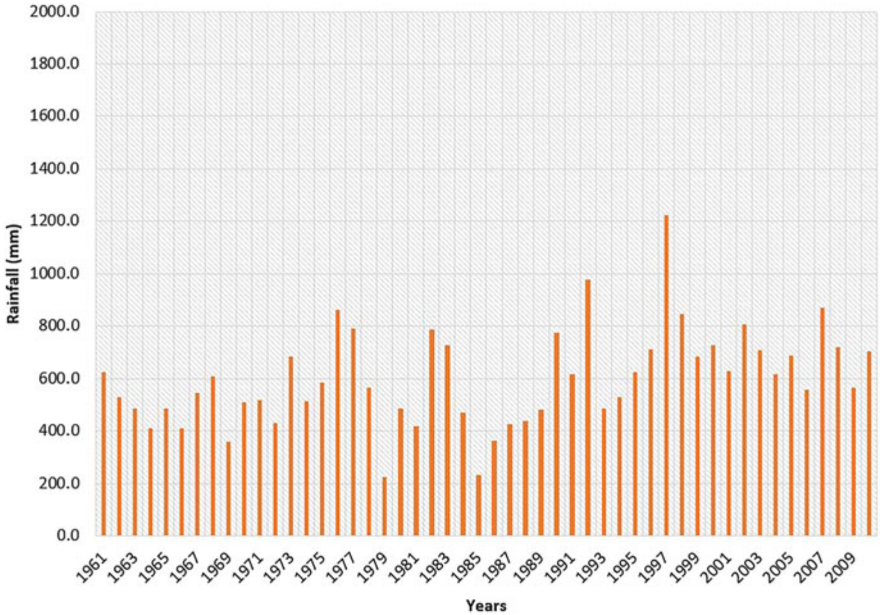

Fig. 15.2 Time series of rainfall at Chakwal (1961–2010)

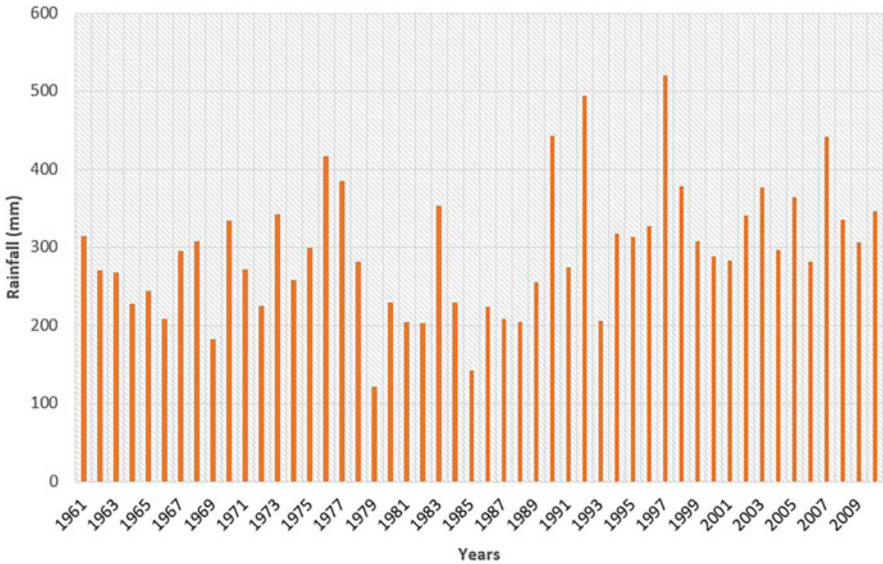

Fig. 15.3 Time series of rainfall at Talagang (1961–2010)

Pakistan can provide useful information for decision-making in the management of the wheat-based rainfed farming system. There are many factors which in combined form contribute to the difficulty of farming in Pothwar and application of agricultural innovations. The major factor is the year-to-year variability in rainfall which significantly adds to the risk of farming operations. Therefore, the long-lead forecast of precipitation could develop planning to diminish the hostile impacts of rainfall variability and to take benefit of good conditions (Ahmed 2011).

SSTs (sea surface temperatures) in the Pacific and Indian Oceans play a significant role in the rainfall variability of the summer monsoon. Similarly, rainfall during the rainfed wheat-growing season can have a significant relationship with SSTs. The correlation of ENSO with Indian monsoon rainfall reported significantly highest (at 99% significance) except for the years of 1983 and 1997, which showed that ENSO phenomenon was used to predict rainfall of Indian subcontinent. Therefore, it is essential to use the knowledge of ENSO to develop a rainfall forecasting model to utilize monsoon and growing season moisture effectively. Similarly, the SOI, which is an index of air pressure between the western and eastern tropical Pacific, has an important influence on rainfall in many regions of the world particularly monsoonal regions in relation to the onset and end of monsoon and the amount of rainfall likely to be received during the season. A frequently occurring cycle of Southern Oscillation Index reflecting the air pressure between Darwin and Tahiti was utilized for climatic forecasting, particularly rainfall up to a couple of years. It has an average cycle of 4 years, but strong negative and positive phases of SOI could occur at 3–6 years interval in terms of El Niño and La Niña actions.

The long-term rainfall data (1961–2010) of Chakwal, Talagang, and Islamabad was studied using APSIM and R model. The leading purpose of this study was to analyze the connection between SSTs and Southern Oscillation Index (SOI) phases and how these climatic drivers change climatic pattern under rainfed conditions of Pothwar. This resulted in exposing a positive connection between the rainfall variations and July SOI phases during October–November (the sowing time of wheat). Based on the long-term rainfall data (1961–2010), the study showed that the Islamabad, Chakwal, and Talagang have 44, 40, and 35% and 35, 34, and 33% prospect of exceeding median precipitation near zero and constantly negative SOI phases, respectively, during July. Likewise, the forecasting outcomes by R showed that prediction of monsoon (JAS), wheat grain filling period (FMA), wheat early growth (NDJ), and total wheat-growing season precipitation using covariates like a dry spell, IOD of different months, NINO1.2, NINO3, NINO3.4, and NINO4 have shown significant signals. The skill scores like RMSE (root-mean-square error), BSS (Brier skill score), S% (skill score S), NSE (Nash-Sutcliffe model efficiency coefficient), and ROC (receiver operating characteristics for forecasting above and below-median rainfall) have shown suitability of using SSTs to forecast rainfall (Table 15.1). The rainfall forecast for NDJ, FMA, and NDJFMA by considering

Table 15.1 Forecasting skill scores for the forecast period and p-value of covariates using generalized additive modeling (GAM) approach at three locations of Pothwar by long-term rainfall data (1961–2010)

		p-value of covariates							Forecasting skill scores						
Forecast period	SST	s (NINO1.2)	s (NINO3)	s (NINO4)	s (NINO3.4)	s(IOD)	Spell	r^2	NSE	RMSE	S %	leps.0	leps.1	BSS	ROC (p-value)
Islamabad															
JAS	May	0.003**	0.003**	0.08	0.012*	0.44	0.02*	0.56	0.18	36	13	0.27	0.1	0.28	0.07
NDJ	AugSep	0***	0.003**	0.01*	0.02*	0.001**	0.7	0.35	0.4	22	29	0.3	0.01	−0.33	0.01
FMA	Aug	0**	0.07	0.48	0.26	0.36	0.84	0.04	−3.14	33	4	0.34	−0.06	−0.5	0.73
NDJFMA	Sep	0.04*	0.11	0.45	0.57	0.52	0.34	0.09	−0.27	23	1	0.27	0.049	−0.37	0.39
Chakwal															
JAS	April	0.73	0.14	0.01*	0.18	0.54	0.07	0.12	−0.3	13	5	0.3	0.03	−0.2	0.2
NDJ	AugSep	0.33	0.002**	0.008**	0.02*	0***	0.47	0.07	1.96	11	13	0.33	0.02	−0.32	0.21
FMA	AugSep	0.14	0.06	0.01*	0.02*	0.05	0.51	0.05	−0.54	16	17	0.27	0.12	−0.16	0.06
NDJFMA	Aug	0.88	0.24	0.01*	0.08	0.04*	0.02*	0.11	−0.06	26	30	0.27	0.16	−0.06	0
Talagang															
JAS	April	0.51	0.007**	0.01*	0.19	0.09	0.02*	0.03	−0.35	13	4	0.29	0.09	−0.34	0.17
NDJ	Sep	0.38	0.4	0.08	0.45	0.18	0.86	0.07	2.64	6	13	0.36	−0.14	−0.67	0.95
FMA	AugSep	0.07	0.02*	0.002**	0.005**	0.03*	0.05	0.24	0.3	6	42	0.23	0.22	0	0
NDJFMA	Jul	0.84	0.2	0.32	0.03*	0.64	0.01*	0.07	0.94	10	16	0.3	0.02	−0.18	0.1

***$p < 0.01$, **$p < 0.05$ and *$p < 0.10$

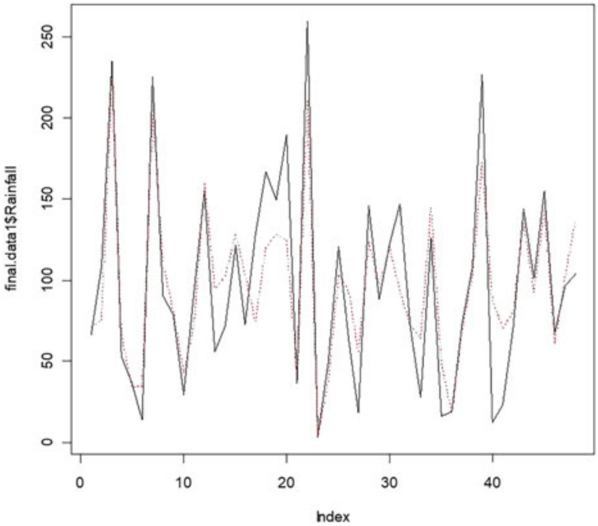

Fig. 15.4 Rainfall forecast for NDJ period at Islamabad using SST of August and September

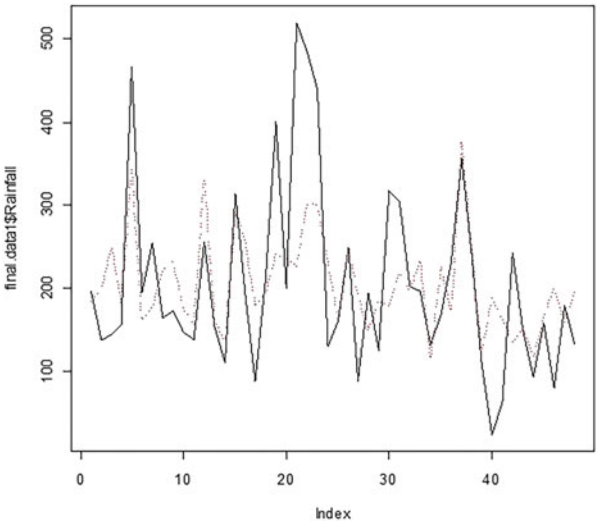

Fig. 15.5 Rainfall forecast for FMA period at Islamabad using SST of August and September

SST of August and September at Islamabad revealed a strong close association with observed and predicted rainfall (Figs. 15.4, 15.5, and 15.6).

Acknowledgment The authors are thankful to the Higher Education Commission for the financial support to complete this study.

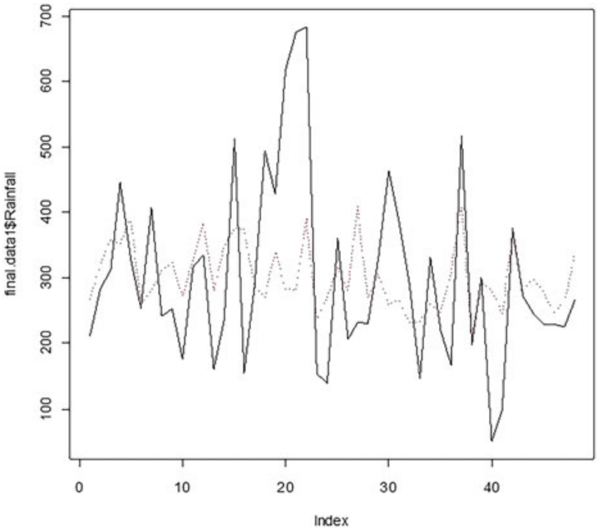

Fig. 15.6 Rainfall forecast for NDJFMA period at Islamabad using SST of August and September

References

Ahmed M (2011) Climatic resilience of wheat using simulation modeling in Pothwar. PhD thesis. Arid Agriculture University, Rawalpindi

Ahmed M (2020) Introduction to modern climate change. Andrew E. Dessler: Cambridge University Press, 2011, 252 pp, ISBN-10: 0521173159. Sci Total Environ 734:139397. https://doi.org/10.1016/j.scitotenv.2020.139397

Ahmed M, Stockle CO (2016) Quantification of climate variability, adaptation and mitigation for agricultural sustainability. Springer Nature Singapore Pvt. Ltd., Singapore, 437 pp. https://doi.org/10.1007/978-3-319-32059-5

Caroline CU, Alexander Sen G, Yue L, Andréa ST, Matthew HE (2011) Multi-decadal modulation of the El Niño–Indian monsoon relationship by Indian Ocean variability. Environ Res Lett 6:034006

Ding Y, Sikka D (2006) Synoptic systems and weather. The Asian Monsoon. Springer, Berlin, pp 131–201

Eilers PHC, Marx BD (1996) Flexible smoothing with B-splines and penalties. Stat Sci 11:89–101

Hastie T, Tibshirani R (1986) Generalized additive models (with discussion). Stat Sci 1:297–310

Hyndman RJ, Grunwald GK (2000) Generalized additive modelling of mixed distribution markov models with application to Melbourne's rainfall. Aust N Z J Stat 42:145–158

IPCC (2014) Climate change 2014: impacts, adaptation, and vulnerability. Part A: global and sectoral aspects. Contribution of Working Group II to the fifth assessment report of the Intergovernmental Panel on Climate Change [Field CB, Barros VR, Dokken DJ, Mach KJ, Mastrandrea MD, Bilir TE, Chatterjee M, Ebi KL, Estrada YO, Genova RC, Girma B, Kissel ES, Levy AN, MacCracken S, Mastrandrea PR, White LL(eds.)]. Cambridge University Press, Cambridge/New York.

Klein Tank AMG, Peterson TC, Quadir DA, Dorji S, Zou X, Tang H, Santhosh K, Joshi UR, Jaswal AK, Kolli RK, Sikder AB, Deshpande NR, Revadekar JV, Yeleuova K, Vandasheva S, Faleyeva M, Gomboluudev P, Budhathoki KP, Hussain A, Afzaal M, Chandrapala L, Anvar H, Amanmurad D, Asanova VS, Jones PD, New MG, Spektorman T (2006) Changes in daily temperature and precipitation extremes in central and south Asia. J Geophys Res-Atmos 111, n/a-n/a

Liu B, Xu M, Henderson M, Qi Y (2005) Observed trends of precipitation amount, frequency, and intensity in China, 1960–2000. J Geophys Res-Atmos 110, n/a-n/a

Meinke H, Stone R (2005) Seasonal and inter-annual climate forecasting: the new tool for increasing preparedness to climate variability and change in agricultural planning and operations. Clim Chang 70:221–253

Mustafa Z (2011) Climate change and its impact with special focus in Pakistan. Pakistan Engineering Congress, Symposium. Lahore, p 290.

R Development Core Team (2008) R: a language and environment for statistical computing. R Foundation for Statistical Computing, Vienna

Rigby R, Stasinopoulos D (2001) The GAMLSS project: a flexible approach to statistical modelling. pp 249–256

Rigby RA, Stasinopoulos DM (2005) Generalized additive models for location, scale and shape (with discussion). J R Stat Soc Ser C 54:507–554

Stasinopoulos DM, Rigby RA, Akantziliotou C (2009) gamlss: a collection of functions to fit generalized additive models for location, scale and shape. R Packag Version 2:2–0

Stocker TF, Qin D, Plattner GK, Tignor M, Allen SK, Boschung J, Nauels A, Xia Y, Bex B, Midgley B (2013) IPCC, 2013: climate change 2013: the physical science basis. Contribution of working group I to the fifth assessment report of the intergovernmental panel on climate change. Cambridge University Press.

Trenberth KE, Stepaniak DP (2001) Indices of El Niño evolution. J Clim 14:1697–1701

Turner AG, Annamalai H (2012) Climate change and the South Asian summer monsoon. Nat Clim Chang 2:587–595

van Ogtrop F, Ahmad M, Moeller C (2014) Principal components of sea surface temperatures as predictors of seasonal rainfall in rainfed wheat growing areas of Pakistan. Meteorol Appl 21 (2):431–443. https://doi.org/10.1002/met.1429

Wang C, Weisberg RH, Virmani JI (1999) Western pacific interannual variability associated with the El Nino-Southern Oscillation. J Geophys Res 104:5131–5149

Index

M. Ahmed (ed.), *Systems Modeling*, https://doi.org/10.1007/978-981-15-4728-7

X

Y